Industrial Electrochemistry

To Pamela, Heather and Steven;
Gill, Linda and Ian

Industrial Electrochemistry

SECOND EDITION

Derek Pletcher
Department of Chemistry, University of Southampton

and

Frank C. Walsh
Department of Chemistry, Portsmouth Polytechnic



Springer Science+Business Media, LLC

First edition 1982
Paperback edition 1984
Second edition 1990
Paperback edition 1993

© 1982, 1984, 1990, 1993 Derek Pletcher and Frank C. Walsh
Originally published by Blackie Academic & Professional in 1993
Typeset in 10/12pt Times by Macmillan India Ltd, Bangalore 560 025

ISBN 978-0-7514-0148-6 ISBN 978-94-011-2154-5 (eBook)
DOI 10.1007/978-94-011-2154-5

Apart from any fair dealing for the purposes of research or private study, or criticism or review, as permitted under the UK Copyright Designs and Patents Act, 1988, this publication may not be reproduced, stored, or transmitted, in any form or by any means, without the prior permission in writing of the publishers, or in the case of reprographic reproduction only in accordance with the terms of the licences issued by the Copyright Licensing Agency in the UK, or in accordance with the terms of licences issued by the appropriate Reproduction Rights Organization outside the UK. Enquiries concerning reproduction outside the terms stated here should be sent to the publishers at the Glasgow address printed on this page.

The publisher makes no representation, express or implied, with regard to the accuracy of the information contained in this book and cannot accept any legal responsibility or liability for any errors or omissions that may be made.

A catalogue record for this book is available from the British Library
Library of Congress Cataloging-in-Publication Data available

Contents

	Preface	viii
	Symbols	xi
1	**Fundamental concepts**	**1**
	1.1 Electron transfer	8
	1.2 Mass transport	18
	1.3 The interplay of electron transfer and mass transport control	30
	1.4 Adsorption	32
	1.5 Electrocatalysis	38
	1.6 Phase formation in electrode reactions	48
	1.7 Chemical reactions	50
	1.8 The properties of electrolyte solutions	51
	1.9 The assessment of cell voltage	54
	1.10 Electrochemistry at surfaces on open circuit	55
	Further reading	58
2	**Electrochemical engineering**	**60**
	2.1 General considerations	60
	2.2 Costing an electrolytic process	64
	2.3 Performance and figures of merit	70
	2.4 Electrolysis parameters	91
	2.5 Principles of cell design	95
	2.6 The additional technology of electrolytic processes	109
	2.7 Typical cell designs	141
	2.8 Laboratory data and scale-up	166
	Further reading	171
3	**The chlor-alkali industry**	**173**
	3.1 General concepts of brine electrolysis	175
	3.2 Modern technological developments	177
	3.3 Chlorine cell technologies	184

3.4 The production of potassium hydroxide 208
Further reading 209

4 The extraction, refining and production of metal 210
4.1 Electrowinning 211
4.2 Cementation 228
4.3 Electrorefining 231
4.4 Electrodeposition of metal powders 245
Further reading 247

5 Other inorganic electrolytic processes 249
5.1 Fluorine 249
5.2 Water electrolysis 256
5.3 Sodium chlorate and sodium bromate 269
5.4 Peracids and their salts 274
5.5 Potassium permanganate 275
5.6 Potassium dichromate and chromic acid 278
5.7 Hydrogen peroxide 279
5.8 Ozone 282
5.9 Manganese dioxide 288
5.10 Cuprous oxide 290
5.11 Synthesis of metal salts via anodic dissolution 291
Further reading 292

6 Organic electrosynthesis 294
6.1 The hydrodimerization of acrylonitrile 298
6.2 Other commercial electrosynthetic processes 311
6.3 Indirect electrosynthesis 326
6.4 The future of electrosynthesis 329
Further reading 330

7 Water purification, effluent treatment and recycling of industrial process streams 331
7.1 Metal ion removal and metal recovery 333
7.2 Hypochlorite and low-tonnage chlorine electrolysers 353
7.3 Electrodialysis 358
7.4 The treatment of liquors containing dissolved chromium 364
7.5 Electrolytic methods of phase separation 374
7.6 Flue-gas desulphurization 379
7.7 Other electrochemical processes 382
Further reading 384

8 Metal finishing 385
8.1 Electroplating 386
8.2 Electroless plating 424

8.3 Conversion coatings 434
8.4 Electrophoretic painting 441
8.5 Other related surface-finishing techniques 447
Further reading 448

9 Metals and materials processing **451**
9.1 Electroforming 451
9.2 Electrochemical machining 457
9.3 Electrochemical etching 468
Further reading 479

10 Corrosion and its control **481**
10.1 Fundamentals of corrosion 483
10.2 The thermodynamics of corrosion 489
10.3 The kinetics of corrosion reactions 498
10.4 Corrosion problems in practice 509
10.5 Corrosion prevention and control 518
10.6 Corrosion problems in electrolytic processing 536
10.7 Corrosion measurement and monitoring 538
Further reading 541

11 Batteries and fuel cells **543**
11.1 Battery characteristics 546
11.2 Battery specifications 551
11.3 Evaluation of battery performance 554
11.4 Battery components 555
11.5 Present battery systems 559
11.6 Batteries under development 584
11.7 Fuel cells 590
Further reading 595

12 Electrochemical sensors and monitoring techniques **596**
12.1 Electrochemical procedures 596
12.2 Polarography to anodic stripping voltammetry 596
12.3 Ion-selective electrodes 603
12.4 Portable and on-line devices 609
12.5 Electrochemical biosensors 618
12.6 Electrochemical detector cells for high-performance liquid chromatography (HPLC) 624
12.7 Miscellaneous 634
Further reading 636

Index 639

Preface

The objective of this second edition remains the discussion of the many diverse roles of electrochemical technology in industry. Throughout the book, the intention is to emphasize that the applications, though extremely diverse, all are based on the same principles of electrochemistry and electrochemical engineering. Those familiar with the first edition will note a significant increase in the number of pages. The most obvious addition is the separate chapter on electrochemical sensors but, in fact, all chapters have been reviewed thoroughly and many have been altered substantially. These changes to the book partly reflect the different view of a second author as well as comments from students and friends. Also, they arise inevitably from the vitality and strength of electrochemical technology; in addition to important improvements in technology, new electrolytic processes and electrochemical devices continue to be reported.

In the preface to the first edition it was stated:

. . . the future for electrochemical technology is bright and there is a general expectation that new applications of electrochemistry will become economic as the world responds to the challenge of more expensive energy, of the need to develop new materials and to exploit different chemical feedstocks and of the necessity to protect the environment.

The preparation of this second edition, seven years after these words were written, provided an occasion to review the progress of industrial electrochemistry. To our great pleasure, the conclusion is that despite the fact that energy has not become more expensive, the progress in terms of both improved technology and completely new processes and devices is very substantial. Improved membrane cell technology for the chlor–alkali industry, new processes for the manufacture of low-tonnage organic and inorganic chemicals, the appearance on the market of new lithium batteries and a variety of sensors, the coming of age of cathodic electropainting, many electrolytic processes for effluent treatment, the commercial availability of several families of electrochemical cells, etc. are all symptoms of a healthy technology.

Less satisfactory are the status of electrochemistry and electrochemical engineering as academic disciplines. They remain insufficiently taught at both undergraduate and postgraduate levels. Moreover, even when they appear within the syllabus, all too frequently one aspect of the subjects is covered to the exclusion of all others. It is a prime hope of both authors that this book will encourage many more teachers to take up the challenge of teaching an integrated applied electrochemistry course.

Following the two introductory chapters, we have tried to use a similar approach for the discussion of the various groups of applications. We have sought to relate the technology to the underlying principles and to discuss current thinking and practice within the industries as well as to comment on likely future trends. We would wish to emphasize, however, that it is never our purpose to compare the technologies, cells or devices available from competing companies; the examples selected are based on our personal experiences and are in the text for illustration. We have also sought to describe only technology which has already reached industrial usage. Hence, we have always tried to avoid the temptation to outline the many other processes which have only been demonstrated in the laboratory or on a small pilot scale (otherwise the book would be in many volumes). We have attempted thereby, to produce a readable account of real industrial electrochemistry, useful to both students and those already engaged in the investigation of some aspect of the subject.

In writing this book, many compromises had to be made. There have been many lively (but friendly) debates between the two authors and topics discussed have included the depth of treatment, the balance between fundamental and applied aspects and the choice of illustrative material. By far the most vexed topics were, however, those relating to signs, symbols and other conventions; throughout we were aware that the established practices of electrochemists, electroplaters, corrosion engineers, materials technologists and chemical engineers were quite different and they also depended on the country of origin. In these very unfortunate circumstances, authors are bound to offend most readers. In some desperation we decided to follow a system which will be most readily acceptable to electrochemists since we expect them to be our largest group of readers. Most of all, we have endeavoured to achieve uniformity.

Finally, it is a pleasure to thank the many who have helped us in the preparation of this book. The most obvious are those who have kindly persuaded their organizations to release the photographs which illustrate the text. There are, however, many other industrialists and academics who have provided source material. We also feel that we owe much gratitude to the many who have stimulated our interest in applied electrochemistry. In the case of one of us (D.P.) special mention should be made of Professor Martin Fleischmann (University of Southampton) and Dr Gordon Lewis (associate and guide during a survey of industrial electrochemistry carried out in 1979). The other (F.C.W.) would wish to single out Dr Des Barker (Portsmouth Polytechnic),

Dr David Gabe (University of Loughborough) and Professor Martin Fleischmann, as particularly strong influences in his training. We are both also aware of our debt to several companies who have given us practical training in the most acceptable way – they have paid us as consultants! Thanks are due to Susan Neale and David Jackson of the Frewen Library, Portsmouth Polytechnic who checked the lists of further reading at the end of each chapter. Our typists are also remembered with many thanks. Lastly, we wish to acknowledge the debt to our families, especially our wives who have suffered extra duties to allow the completion of this book, but also our parents and children for their contributions to our contented writing.

Derek Pletcher
Frank Walsh

Symbols

Symbol	*Definition*	*Typical units*
a_+	Activity of cation	Dimensionless
a_-	Activity of anion	Dimensionless
$a_\pm$	Mean ionic activity	Dimensionless
A	Electrode area	m^2
A_S	Electroactive area per unit reactor volume	m^{-1}
A_E	Electroactive area per unit electrode volume	m^{-1}
b	Cost of a unit of electrical power	£ W^{-1} s^{-1}
B	Width of flow channel	m
c_i	Concentration of species i	mol m^{-3}
c_i^∞	Concentration of species i in the bulk solution	mol m^{-3}
c_i^σ	Concentration of species i at the electrode surface	mol m^{-3}
$c_{(0)}$	Initial concentration of reactant	mol m^{-3}
$c_{(t)}$	Concentration of reactant at time t	mol m^{-3}
$c_{(IN)}$	Concentration of reactant at inlet to reactor	mol m^{-3}
$c_{(OUT)}$	Concentration of reactant at outlet of reactor	mol m^{-3}
C	Capital invested	£
C	Capacitance	$F\,m^{-2}$
C	Capacity of a battery electrode	A s
C_E	Electrolysis power cost	£
C_F	Fixed capital	£
C_I	Variable reactor investment cost	£
C_L	Land capital	£
C_S	Cost of electrolyte agitation	£
C_W	Working capital	£
C_{SCRAP}	Total scrap value of plant	£
C_P	Heat capacity at constant pressure	J kg^{-1} K^{-1}
d_e	Equivalent diameter of a flow channel	m
D	Depreciation	£ $year^{-1}$

Symbol	*Definition*	*Typical units*
D_i	Diffusion coefficient of species i	$m^2 s^{-1}$
E	Measured or applied electrode potential	V
E_e	Equilibrium electrode potential	V
$E_e^\ominus$	Standard electrode potential	V
E_e^C	Equilibrium cathode potential	V
E_e^A	Equilibrium anode potential	V
E^C	Cathode potential	V
E^A	Anode potential	V
E_{CELL}^e	Equilibrium cell potential ($E_e^C - E_e^A$)	V
E_{CELL}	Cell potential ($E^C - E^A$)	V
E_M	Membrane potential	V
E_{CORR}	Corrosion potential	V
E_{TRANS}	Potential at which transpassivity first occurs	V
$E_{p.z.c.}$	Point of zero charge potential	V
E_{tn}	Thermoneutral cell potential	V
F	Faraday constant	$A\,s\,mol^{-1}$
g	Acceleration due to gravity	$m\,s^{-2}$
G_i	Total Gibbs free energy for species i	$J\,mol^{-1}$
G_i'	Gibbs free energy for species i in the absence of a potential field	$J\,mol^{-1}$
ΔG	Gibbs free energy change	$J\,mol^{-1}$
$\Delta G_{ADS}^\ominus$	Standard Gibbs free energy of adsorption	$J\,mol^{-1}$
$\overrightarrow{\Delta G}_\pm$	Gibbs free energy of activation for the forward process	$J\,mol^{-1}$
h	Heat transfer coefficient	$W\,m^{-2}\,K^{-1}$
H	Enthalpy	$J\,mol^{-1}$
i	Current	A
i_0^C	Exchange current for the cathodic process	A
i_0^M	Exchange current for the metal dissolution reaction	A
i_{CRIT}	Critical current for the onset of passivation	A
i_{PASS}	Current in the passive range	A
i_L	Mass transport controlled limiting current	A
I	Current density; $I = i/A$	$A\,m^{-2}$
I_0	Exchange current density	$A\,m^{-2}$
I_0^H	Exchange current density for the hydrogen evolution reaction	$A\,m^{-2}$
I_0^M	Exchange current density for the metal dissolution reaction	$A\,m^{-2}$
$\vec{I}$	Reduction (cathodic) partial current density	$A\,m^{-2}$
$\overleftarrow{I}$	Oxidation (anodic) partial current density	$A\,m^{-2}$
I_L	Limiting current density (under mass transport control due to diffusion or convective diffusion)	$A\,m^{-2}$

Symbol	*Definition*	*Typical units*
I_{OPT}	Optimum current density	$A\,m^{-2}$
I_x	Current density at a distance x along the electrode	$A\,m^{-2}$
k	Rate constant for first order chemical process	s^{-1}
$\vec{k}$	Rate constant for the forward (cathodic) process	$m\,s^{-1}$
$\overleftarrow{k}$	Rate constant for the reverse (anodic) process	$m\,s^{-1}$
k_0	Rate constant for an electron transfer process at $E=0\ V$ vs. the reference electrode	$m\,s^{-1}$
$k^{\ominus}$	Standard rate constant for an electrode process	$m\,s^{-1}$
k_L	Mass transport coefficient	$m\,s^{-1}$
k_h	Averaged, overall heat transfer coefficient	$m^2\,s^{-1}$
K'	Kohlrausch constant	$ohm^{-1}\,m^{7/2}\,mol^{-3/2}$
K_i	Selectivity constant for species i	Dimensionless
l	Characteristic length	m
L	Length of a plate electrode	m
m_+	Molality of cation	$mol\,kg^{-1}$
m_-	Molality of anion	$mol\,kg^{-1}$
m	Number of moles of electroactive species	mol
m_o	Initial molar amount of reactant	mol
m_t	Molar amount of reactant at time t	mol
$m_{(IN)}$	Molar amount of reactant at the inlet to a reactor	mol
$m_{(OUT)}$	Molar amount of reactant at the outlet of a reactor	mol
m_p	Molar amount of product	mol
M	Molar mass	$kg\,mol^{-1}$
n	Number of electrons	Dimensionless
n_p	Number of moles of product	Dimensionless
N	Projected lifetime of plant	years
N_C	Chromatographic plate number	Dimensionless
N_m	Mass flow	$kg\,s^{-1}$
q	Electrical charge	A s
Q	Volumetric flow rate	$m^3\,s^{-1}$
Q	Charge density	$A\,s\,m^{-2}$
Q_n	Heat flow	W
r	Radius of disc or cylinder electrode	m
R	Gas constant	$J\,K^{-1}\,mol^{-1}$
R	Electrical resistance	ohm
R_{CELL}	Cell resistance	ohm
$R_{CIRCUIT}$	Resistance of electrical circuit, including busbars	ohm
R_p	Linear polarization resistance	ohm
s	Space–velocity	s^{-1}
s_n	Normalized space–velocity	s^{-1}

Symbol	*Definition*	*Typical units*
S	Entropy	$J K^{-1}$
S	Separation of electrodes	m
S_p	Overall selectivity	Dimensionless
t	Time	s
t'	Time to discharge battery	s
t'	Critical time in batch processing	s
t_R	Retention time	s
t_+	Transport number of cation	Dimensionless
t_-	Transport number of anion	Dimensionless
T	Temperature	K
u_i	Mobility of species i	$m^2 s^{-1} V^{-1}$
v_+	Number of positive ions	Dimensionless
v_-	Number of negative ions	Dimensionless
v	Velocity of electrolyte flow	$m s^{-1}$
v_x	Solution velocity in the x direction	$m s^{-1}$
$\bar{v}$	Mean flow velocity	$m s^{-1}$
V	Volume	m^3
V_R	Reactor volume	m^3
V_T	Reservoir volume	m^3
V_M	Molar volume	$m^3 mol^{-1}$
V_E	Electrode volume	m^3
w	Mass of material	kg
W	Power required for electrode/electrolyte movement	W
W_{CELL}	Electrolytic power requirement	W
x	Distance, thickness or penetration	m
X_A	Fractional conversion	Dimensionless
z_i	Electrical charge on species i	Dimensionless
Z	Frequency factor for an activation controlled process	$m s^{-1}$

Dimensionless Groups

Gr	Grashof Number: $Gr = \dfrac{g\Delta\rho L^3}{v^2\rho}$	Dimensionless
Re	Reynolds Number: $Re = \dfrac{vl}{v}$	Dimensionless
Sc	Schmidt Number: $Sc = \dfrac{v}{D}$	Dimensionless
Sh	Sherwood Number: $Sh = \dfrac{k_L l}{D}$	Dimensionless

Symbol	*Definition*	*Typical units*
	Greek	
α	Transfer coefficient	Dimensionless
α_A	Anodic transfer coefficient	Dimensionless
α_C	Cathodic transfer coefficient	Dimensionless
β	Inverse of the slope of a $\log\|i\|$ vs. E (or $\log\|i\|$ vs. η plot)	V
γ_G	Energy yield	Dimensionless
γ_H	Thermal energy yield	Dimensionless
γ	Effectiveness factor for mass transport control	Dimensionless
γ_+	Activity coefficient of cation	Dimensionless
γ_-	Activity coefficient of anion	Dimensionless
$\gamma_\pm$	Mean ionic activity coefficient	Dimensionless
δ_{SB}	Stefan–Boltzmann constant $= 5.67 \times 10^{-8}$	$W\,m^{-2}\,K^{-4}$
δ_N	Nernstian, concentration boundary layer thickness	m
ε	Emissivity	Dimensionless
η	Overpotential $(E - E_e)$	V
η'	Polarization $(E - E_{CORR})$	V
η_C	Overpotential at cathode	V
η_A	Overpotential at anode	V
θ	Surface coverage	Dimensionless
θ_P	Material yield	Dimensionless
κ	Electrolytic conductivity	$ohm^{-1}\,m^{-1}$
λ_o^+	Ionic conductivity of cation at infinite dilution	$ohm^{-1}\,m^2\,mol^{-1}$
λ_o^-	Ionic conductivity of anion at infinite dilution	$ohm^{-1}\,m^2\,mol^{-1}$
λ	Thermal conductivity	$W\,m^{-1}\,K^{-1}$
Λ	Molar conductivity of electrolyte	$ohm^{-1}\,m^2\,mol^{-1}$
Λ_o	Molar conductivity of electrolyte at infinite dilution	$ohm^{-1}\,m^2\,mol^{-1}$
μ	Dynamic viscosity	$kg\,m^{-1}\,s^{-1}$
ν	Kinematic viscosity; (μ/ρ)	$m^2\,s^{-1}$
ρ	Density	$kg\,m^{-3}$
$\Delta\rho$	Difference in density between solution at electrode surface and bulk	$kg\,m^{-3}$
ρ_{ST}	Space–time yield	$kg\,m^{-3}\,s^{-1}$
ρ_N	Normalized space–time yield	$kg\,m^{-3}\,s^{-1}$
σ_C^2	Peak variance	Dimensionless
τ	Detector time constant	Dimensionless
τ	Residence time	s
τ_{ST}	Space–time	s
ϕ	Peak fidelity	Dimensionless

Symbol	*Definition*	*Typical units*
ϕ	Current efficiency	Dimensionless
ϕ_M	Absolute potential at the electrode surface	V
ϕ_P	Overall conversion related yield	Dimensionless
ϕ_S	Absolute potential of the bulk solution phase	V
ϕ_2	Absolute potential at the plane of closest approach of cations	V
ψ	Potential field strength	$V\,m^{-1}$
ω	Rotation rate	s^{-1}

1 Fundamental concepts

An electrochemical reaction is a heterogeneous chemical process involving the transfer of charge to or from an electrode, generally a metal, carbon or a semiconductor. The charge transfer may be a cathodic process in which an otherwise stable species is reduced by the transfer of electrons from an electrode. Examples of such reactions which are important in electrochemical technology include:

$$2H_2O + 2e^- \longrightarrow H_2 + 2OH^- \quad (1.1)$$

$$Cu^{2+} + 2e^- \longrightarrow Cu \quad (1.2)$$

$$Na^+ + e^- + Hg \longrightarrow NaHg \quad (1.3)$$

$$2CH_2 = CHCN + 2H_2O + 2e^- \longrightarrow (CH_2CH_2CN)_2 + 2OH^- \quad (1.4)$$

$$PbO_2 + 4H^+ + SO_4^{2-} + 2e^- \longrightarrow PbSO_4 + 2H_2O \quad (1.5)$$

Conversely, the charge transfer may be an anodic process where an otherwise stable species is oxidized by the removal of electrons to the electrode and relevant examples would be:

$$2H_2O - 4e^- \longrightarrow O_2 + 4H^+ \quad (1.6)$$

$$2Cl^- - 2e^- \longrightarrow Cl_2 \quad (1.7)$$

$$Ce^{3+} - e^- \longrightarrow Ce^{4+} \quad (1.8)$$

$$Pb + SO_4^{2-} - 2e^- \longrightarrow PbSO_4 \quad (1.9)$$

$$2Al + 3H_2O - 6e^- \longrightarrow Al_2O_3 + 6H^+ \quad (1.10)$$

$$CH_3OH + H_2O - 6e^- \longrightarrow CO_2 + 6H^+ \quad (1.11)$$

Some typical cathodic and anodic processes are also shown in Fig. 1.1.

Of course, electrochemistry is only possible in a cell which contains both an anode and a cathode and, to avoid the accumulation of net positive or net

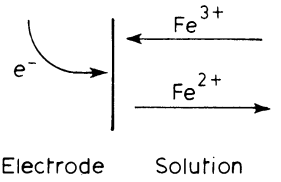

(a) Simple electron transfer,
e.g. $Fe^{3+} + e^- \rightarrow Fe^{2+}$

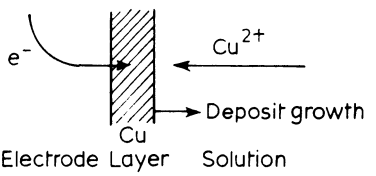

(b) Metal deposition
e.g. $Cu^{2+} + 2e^- \rightarrow Cu$

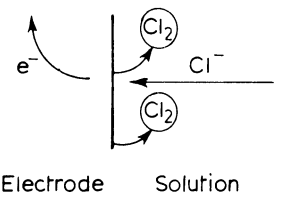

(c) Gas evolution,
e.g. $2Cl^- - 2e^- \rightarrow Cl_2$

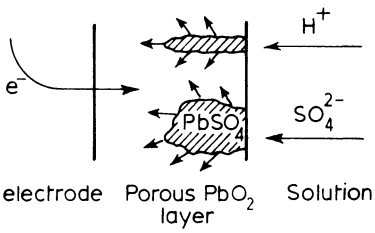

(d) Surface film transformation
e.g. $PbO_2 + 4H^+ + SO_4^{2-} + 2e^- \rightarrow PbSO_4 + 2H_2O$

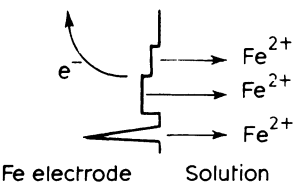

(e) Anodic dissolution
e.g. $Fe - 2e^- \rightarrow Fe^{2+}$

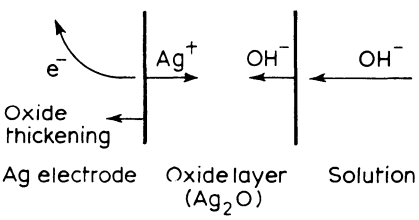

(f) Oxide formation
e.g. $2Ag - 2e^- + 2OH^- \rightarrow Ag_2O + H_2O$

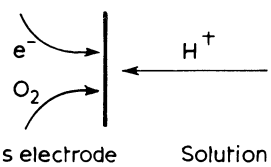

(g) Gas reduction in porous gas diffusion electrode,
e.g. $O_2 + 4H^+ + 4e^- \rightarrow 2H_2O$

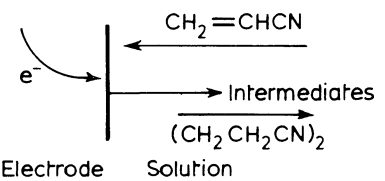

(h) Electron transfer with coupled chemistry,
e.g. $2CH_2{=}CHCN + 2H_2O + 2e^- \rightarrow (CH_2CH_2CN)_2 + 2OH^-$

Fig. 1.1 Some common types of electrode processes. For simplicity, ions of the background electrolyte (numerically in large excess) and counter ions are not shown.

negative charge somewhere in the cell, the amount of reduction at the cathode and oxidation at the anode must be equal. Moreover, the necessity to maintain charge balance throughout the cell system has other important consequences:

1. For electrolysis to occur, electrons must pass from the anode to the cathode through an external, electrical circuit interconnecting the two electrodes.
2. There must be a mechanism for charge transport between the electrodes within the cell.

In fact, the movement of ions through the solution and any separator between the electrode is responsible for maintaining charge neutrality within the electrolyte solution; anions move towards the anode and/or cations towards the cathode in sufficient quantity to maintain a charge balance. In practice, the charge may not be carried by the same ions throughout the interelectrode gap. The charge transport processes essential to electrolysis are illustrated in Fig. 1.2 for the case of a cell with a cation selective membrane as described in Chapter 3, (section 3.2.2).

The equality of electrons passing across each electrode surface and through the external circuit largely determines the way in which we seek to understand or to study electrode reactions and electrolysis cells. The current i is in fact the rate at which electrons move through the external circuit. It is also a very

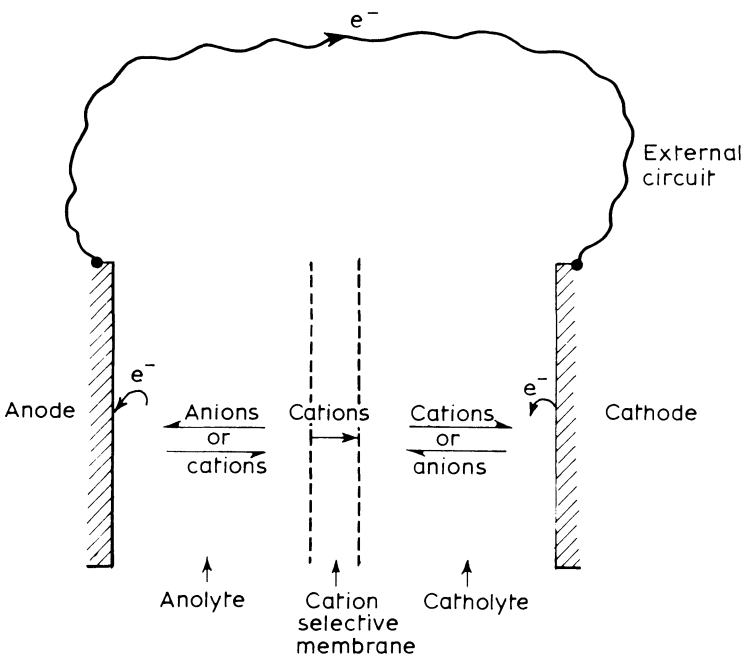

Fig. 1.2 Charge transport processes essential to electrolysis in a cell containing a cation-selective membrane as a separator.

convenient measure of the rate of the electrode reactions and also of the overall chemical change in the cell. Moreover, the charge q passing through the external circuit tells one the extent of chemical change at each electrode. The charge required to convert m mol of starting material to product in an ne^- electrode reaction is readily calculated using Faraday's laws of electrolysis, i.e.:

$$q = \int_0^t i\mathrm{d}t = mnF \tag{1.12}$$

where F is the Faraday constant (96 485 C mol^{-1}).

The total chemical change in the cell is found by adding the anode and cathode reactions; thus the chemical change in a lead–acid battery during discharge is obtained by adding reactions (1.5) and (1.9), i.e.:

$$PbO_2 + Pb + 2SO_4^{2-} + 4H^+ \longrightarrow 2PbSO_4 + 2H_2O \tag{1.13}$$

and that in a water electrolyser by adding reactions (1.1) and (1.6), i.e.:

$$2H_2O \longrightarrow 2H_2 + O_2 \tag{1.14}$$

The thermodynamics of electrochemical cells is treated in all textbooks of physical chemistry as are the conventions. The discharging lead–acid battery would commonly be written as the cell:

$$Pb|PbSO_4|\text{aqueous } H_2SO_4|PbO_2|PbSO_4|Pb \tag{1.15}$$

where phase boundaries are denoted by vertical lines. The equilibrium (or reversible) cell potential is obtained by subtracting the equilibrium potential of the anode (left-hand electrode in reaction (1.15)) from that of the cathode (right-hand electrode in reaction (1.15)) and this is related to the free energy of the overall cell reaction (as written in reaction (1.13)) by the well known equation:

$$\begin{aligned} \Delta G &= -nFE^{\mathrm{e}}_{\mathrm{CELL}} \\ &= -nF(E^{\mathrm{C}}_{\mathrm{e}} - E^{\mathrm{A}}_{\mathrm{e}}) \end{aligned} \tag{1.16}$$

Experimentally, the equilibrium cell potential for the lead–acid battery is found to be $+2.05$ V and, hence, the free energy change associated with the redox reaction between Pb and PbO_2 is -394 kJ mol^{-1}. Clearly, thermodynamics is telling us that the reaction is very favourable (or strictly that the position of equilibrium lies strongly to the side of conversion of the PbO_2 and Pb to $PbSO_4$) as is to be expected for a system which is used to supply energy, i.e. a battery. Equally, the calculation is confirming that the conversion of $PbSO_4$ to Pb and PbO_2 is very unfavourable, $\Delta G = +394$ kJ mol^{-1} and, hence, the recharging of the battery only occurs when we introduce this energy into the system by means of an external power supply.

The equilibrium cell voltage for the water electrolysis cell, with the overall cell reaction (1.14), is -1.23 V and the free energy change $+472$ kJ mol^{-1} (of oxygen). Hence, the conversion of water to hydrogen and oxygen is thermo-

dynamically unfavourable and can only occur when electrical energy is supplied. Conversely, a cell which combines the reduction of oxygen and the oxidation of hydrogen is capable of supplying energy and, indeed, O_2–H_2 fuel cells have been constructed (Chapter 11).

Hence, a thermodynamic discussion would lead to the conclusion that the overall cell reaction will occur and current will flow whenever the two electrodes of the cell are interconnected by an external electrical circuit and either: (1) the cell reaction has a negative free energy; or (2) the cell reaction has a positive free energy but a voltage larger than the equilibrium cell potential is applied across the two electrodes to drive the chemical change. These conclusions are sound but do not consider the rate at which the chemical change can take place, i.e. the current that will flow. The rate of chemical change will depend on the kinetics of the two electrode reactions. Some electrode reactions are inherently fast and give a reasonable current density (current/unit area of electrode surface) close to the equilibrium potential. In contrast, others are inherently slow and then an overpotential η ($= E - E_e$), is necessary in order to obtain any required current density. The kinetics of electrode reactions are discussed below and we shall see that η increases with current density I.

We noted above that, for the cell reaction to occur, ions must pass through the solution and separator between the electrodes. An input of energy is also essential to drive this migration process and leads to a potential drop iR_{CELL} (where R_{CELL} is the internal resistance of the cell, a function of electrolyte properties, the form of the electrodes and cell design) within the cell. Hence, the cell voltage required to observe a current i in a real cell is given by:

$$E_{CELL} = E_e^C - E_e^A - \sum|\eta| - iR_{CELL} \tag{1.17}$$

Both the η and iR_{CELL} terms increase with current density and may be regarded as inefficiencies whereby electrical energy is degraded into heat which must be taken into account in any consideration of heat balance. Indeed, the percentage energy efficiency of a cell may be defined as:

$$\% \text{ energy efficiency} = \frac{(E_e^C - E_e^A)100}{E_e^C - E_e^A - \sum|\eta| - iR_{CELL}} \tag{1.18}$$

and one reason for electrochemical technologists to be concerned with electrode kinetics, electrolyte properties and cell design can be seen.

These conclusions are understood best by considering further our two particular cells, the lead–acid battery and a water electrolyser. The properties sought in secondary batteries are discussed in detail in Chapter 11. Here, it is sufficient to note that the battery should be based on a cell reaction where the free energy is large and negative so that the equilibrium cell voltage is large. In addition, as current is drawn from the battery, the cell voltage should remain as close as possible to the equilibrium value and this requires that the over-potentials at anode and cathode are low (i.e. that the kinetics are fast) and that

the iR_{CELL} drop through the cell is small, i.e. a narrow interelectrode gap and a high electrolyte conductivity. For a secondary battery, it is also necessary for recharge to be possible; by supplying energy to the battery, it must be possible to reverse the cell chemistry occurring during discharge and the active materials (i.e. the PbO_2 and Pb in the lead–acid battery) must be reformed in a suitable state for further discharge. The lead–acid battery meets these ideals to some extent. Similarly, the performance of a water electrolyser will be enhanced if the cell potential remains close to the equilibrium potential during operation. This again requires that the η and iR_{CELL} terms are minimized.

It will already be clear that in order to understand the way in which the various experimental parameters can affect the performance of electrochemical cells and, in particular, the behaviour of the two electrode reactions, it will be necessary to have a knowledge of the thermodynamics and kinetics of electrode reactions. Thus, one purpose of this chapter is to develop the concepts and equations which will be useful for this purpose.

First, however, we need to recognize the nature of electrode reactions. Perhaps the simplest electrode reaction is one which interconverts, at an inert surface, two species O and R which are completely stable and soluble in the electrolysis medium containing an excess of electrolyte which is electroinactive:

$$O + ne^- \rightleftharpoons R \tag{1.19}$$

Even in this case, the electrode reaction is a sequence of more basic steps; to maintain a current it is essential to supply reactant to the electrode surface and to remove the product, as well as for the electron transfer reaction at the surface to occur. Hence, for example, in experimental conditions where O is reduced to R, the electrode reaction must have three steps:

$$O_{bulk} \xrightarrow[\text{transport}]{\text{mass}} O_{electrode} \tag{1.20}$$

$$O_{electrode} \xrightarrow[\text{transfer } (ne^-)]{\text{electron}} R_{electrode} \tag{1.21}$$

$$R_{electrode} \xrightarrow[\text{transport}]{\text{mass}} R_{bulk} \tag{1.22}$$

and since the rate of reduction and hence the cathodic current density is determined by the rate of the overall sequence, it must be dependent on the rate of the slowest step. Thus, to understand the characteristics of such an electrode reaction, we need to know about both mass transport and electron transfer.

An examination of reactions (1.1)–(1.11) quickly shows that electrode reactions of interest in electrochemical technology are seldom that simple. They involve multiple-electron transfers and at least three additional types of basic steps also occur: chemical reactions, adsorption and phase formation.

1. *Chemical reactions.* The species formed by electron transfer may not be stable in the electrolysis medium: it may only be an intermediate which undergoes chemical change to form the observed product. In favourable conditions, there may be a single reaction pathway leading to one product but with reactive intermediates it is common for there to be competitive reactions leading to a mixture of products. In general, the chemical reaction may be a homogeneous process occurring as the species R is transported away from the surface or a heterogeneous process occurring while the species R is adsorbed on the surface (see below). Reactions (1.4) and (1.11) are examples where such following chemical reactions are important.

   Less frequently, it is found that the electroactive species O is not the major species in bulk solution but is only formed by a chemical process, i.e. the electrode reaction is disturbing an equilibrium in homogeneous solution. An example is the reduction of acetic acid to hydrogen which proceeds via dissociation of the weak acid and reduction of the proton.
2. *Adsorption.* The sequence of reactions (1.20)–(1.22) assumes that electron transfer occurs at the electrode surface but without formation of a bond between the surface and either O or R. This may not be the case and for the reaction to proceed it may be necessary for reactants, intermediates or product to be adsorbed on the electrode.

   Moreover, adsorption has other important roles in electrochemical technology. In electrocatalytic reactions (e.g. the evolution of H_2 at Pt) adsorption of intermediates is a key step since their presence on the surface provides alternative lower energy pathways (page 39). Also, adsorption of species not directly involved in the electron transfer process is used to modify the net electrode reaction (e.g. additives used for the modification of electroplates, in the inhibition of corrosion and for the phosphating of steel).
3. *Phase formation.* The electrode reaction may involve the formation of a new phase (e.g. the electrodeposition of metals in plating, refining and winning e.g. reaction (1.2) or bubble formation when the product is a gas) or the transformation of one solid phase to another, (e.g. reaction (1.5)). The formation of a new phase is itself a multistep process requiring both nucleation and subsequent growth, and crystal growth may involve both surface diffusion and lattice growth.

Since electrode reactions commonly involve the transfer of several electrons, the complications 1–3 above occur sandwiched between, as well as preceding or following, electron transfer. Moreover, very complex situations do arise. Thus, for example, reaction (1.5) is likely to involve electron transfer, diffusion, chemical reactions (protonation and hydration equilibria as well as sulphation), phase transformation and adsorbed intermediates! In this chapter, however, we shall take the approach of considering each fundamental type of process in turn. The equations that arise must be regarded as idealistic and simplistic but it will

generally be sufficient for us to understand most cells in industrial practice provided we can recognize which of the fundamental steps in the overall electrode processes predominantly determine the cell characteristics.

1.1 ELECTRON TRANSFER

In this section, the thermodynamics and kinetics of the electrode reaction:

$$O + ne^- \rightleftharpoons R \tag{1.19}$$

will be developed. O and R are completely stable, solution-soluble species. The working electrode is totally inert and the solution has been thoroughly deoxygenated so that there are no competing electron-transfer reactions at the surface. The solution around the working electrode contains O and R, at concentrations c_O^∞ and c_R^∞ respectively (which are sufficiently low that the resulting currents do not give rise to significant iR drop) and a high concentration of an inert electrolyte. The cell for this discussion also contains a large area reference electrode which never becomes polarized (its potential remains constant even when current is passed).

As with any chemical process, it is logical first to consider the thermodynamics. Suppose the potential of the working electrode vs. the reference electrode is monitored while no current is allowed to flow. Under these circumstances no chemical change can occur at the surface and the solution composition will remain unchanged and uniform. The working electrode will take up its equilibrium (or reversible) potential E_e, which may also be calculated from the Nernst equation:

$$E_e = E_e^\ominus + \frac{RT}{nF} \ln (c_O^\infty / c_R^\infty) \tag{1.23}$$

where $E_e^\ominus$ is the formal potential for the couple O/R in the electrolyte medium. Strictly this equation should be written in terms of the activities of O and R but for simplicity it will be assumed that the ratio of activity coefficients is 1. It should be recognized, however, that in many industrial cells with high concentrations of electroactive species and maybe no additional electrolyte, such an assumption would introduce an error and it would be better to include the appropriate activity coefficients or fugacities (section 1.8). Also in general, the Nernst equation should be written in terms of activities or concentrations at the electrode surface (c_O^σ and c_R^σ) but throughout this section it is also assumed that the currents are low enough for the surface and bulk concentrations to be essentially the same. Certainly, when no current flows, no approximation is involved.

At the equilibrium potential, although no net current is observed, there will be a dynamic equilibrium at the electrode surface. Both reduction of O and oxidation of R will be taking place, but these processes will have an equal rate so

that they lead to no change in the composition of the solution. In terms of current density this may be written:

$$-\vec{I} = \overleftarrow{I} = I_0 \tag{1.24}$$

where $\vec{I}$ and $\overleftarrow{I}$ are the reduction and oxidation partial current densities. They have different signs because oxidation and reduction causes electrons to flow in opposite directions through the external circuit; by convention, oxidation is taken to lead to a positive current. I_0 is known as the exchange current density. It is a very useful parameter in the description of the kinetics of electrode reactions but is primarily a measure of the amount of electron-transfer activity in the equilibrium situation. A high value indicates that much simultaneous oxidation and reduction is taking place and is indicative of an inherently fast reaction. A small value suggests that only a small amount of electron transfer occurs at the equilibrium potential and is a symptom of a slow electrode reaction.

The equilibrium potential E_e and the exchange current density I_0 together totally characterize the equilibrium situation at an electrode.

If a potential more negative than E_e is applied to the working electrode, equation (1.23) requires that a slight change occurs to the ratio c_O^σ / c_R^σ at the electrode surface. In fact, a decrease in this ratio is necessary and this can only be achieved by the conversion of O and R by the passage of a reduction current. In general, the magnitude of the net cathodic current and the time it takes to establish the concentration ratio demanded by equation (1.23) will depend on the kinetics of the electron-transfer reaction. The net cathodic current is achieved by an increase in the partial cathodic current and a decrease in the partial anodic current compared to the equilibrium potential, i.e. at this new potential E (more negative than E_e), $-\vec{I} > I_0$ and $\overleftarrow{I} < I_0$. Conversely, if the potential of the working electrode is made positive to E_e, a similar argument will show that a net anodic current will flow (Fig. 1.3).

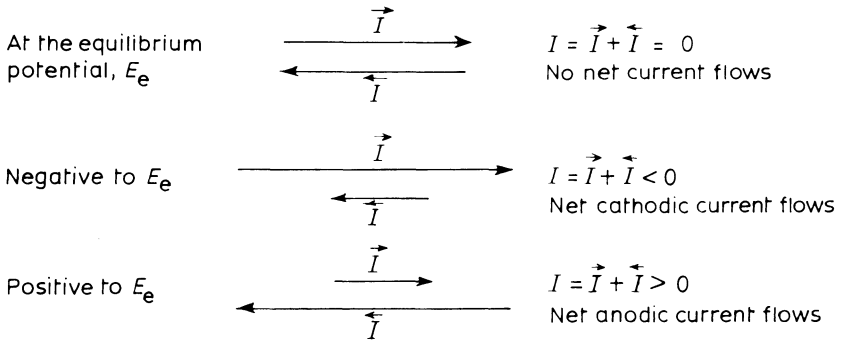

Fig. 1.3 Illustration of the way the experimental current density I varies with potential. Remember that cathodic and anodic partial current densities have opposite signs; by convention, anodic currents are taken as positive.

Now it is necessary to formulate the equations which describe the kinetics of an electron transfer reaction such as reaction (1.19). It is normal to assume that electron-transfer processes are first-order reactions and then the rate of reduction of O depends only on a rate constant and the concentration of O at the site of electron transfer (at the electrode surface). As noted above, only situations where the bulk and surface concentrations are similar will be considered for the present. This is equivalent to assuming that mass transport plays no role in determining the overall rate (see p. 30). Then we may write:

$$\text{Rate of reduction of O} = \vec{k} c_{\mathrm{O}}^{\infty} \tag{1.25}$$

and therefore the partial cathodic current density is given by:

$$-\vec{I} = nF\vec{k}c_{\mathrm{O}}^{\infty} \tag{1.26}$$

But the rate constant for a heterogeneous electron transfer process has a particular property: it is dependent on the potential field close to the surface driving the movement of electrons and hence on the applied electrode potential. We shall assume, as is generally found experimentally, that the potential dependence is of the form:

$$\vec{k} = \vec{k}_0 \exp\left(-\frac{\alpha_{\mathrm{C}} nF}{RT} E\right) \tag{1.27}$$

where α_{C} is the cathodic transfer coefficient and $\vec{k}_0$ is the rate constant for electron transfer at $E = 0$ vs. the reference electrode. Therefore:

$$-\vec{I} = nF\vec{k}_0 c_{\mathrm{O}}^{\infty} \exp\left(-\frac{\alpha_{\mathrm{C}} nF}{RT} E\right) \tag{1.28}$$

The corresponding equations for the oxidation of R, which is occurring simultaneously with the reduction of O, are:

$$\text{Rate of oxidation} = \overleftarrow{k} c_{\mathrm{R}}^{\infty} \tag{1.29}$$

$$\overleftarrow{I} = nF\overleftarrow{k}c_{\mathrm{R}}^{\infty} \tag{1.30}$$

$$\overleftarrow{k} = \overleftarrow{k}_0 \exp\left(\frac{\alpha_{\mathrm{A}} nF}{RT} E\right) \tag{1.31}$$

and:

$$\overleftarrow{I} = nF\overleftarrow{k}_0 c_{\mathrm{R}}^{\infty} \exp\left(\frac{\alpha_{\mathrm{A}} nF}{RT} E\right) \tag{1.32}$$

The observed current density at any potential is given by:

$$\begin{aligned} I &= \vec{I} + \overleftarrow{I} \\ &= nF\left[\overleftarrow{k}_0 c_{\mathrm{R}}^{\infty} \exp\left(\frac{\alpha_{\mathrm{A}} nF}{RT} E\right) - \vec{k}_0 c_{\mathrm{O}}^{\infty} \exp\left(\frac{-\alpha_{\mathrm{C}} nF}{RT} E\right)\right] \end{aligned} \tag{1.33}$$

This equation may be simplified by defining a new parameter, the overpotential η:

$$\eta = E - E_e \tag{1.34}$$

which is simply a measure of the deviation of the experimental potential from the equilibrium potential for the solution being considered. In addition, one may use equation (1.24) which applies only at $E = E_e$ and leads to:

$$I_0 = nF\overleftarrow{k}_0 c_R^{\infty} \exp\left(\frac{\alpha_A nF}{RT} E_e\right) = -nF\vec{k}_0 c_O^{\infty} \exp\left(\frac{-\alpha_C nF}{RT} E_e\right) \tag{1.35}$$

Then substitution of equation (1.34) into equation (1.33) and use of the equalities in equation (1.35) gives the Butler–Volmer equation:

$$I = I_0\left[\exp\left(\frac{\alpha_A nF}{RT}\eta\right) - \exp\left(\frac{-\alpha_C nF}{RT}\eta\right)\right] \tag{1.36}$$

This is a very useful equation in experimental and applied electrochemistry and shows that the measured current density is a function of: (1) overpotential; (2) exchange current density, I_0; and (3) the transfer coefficients, α_A and α_C. The transfer coefficients are, at least for simple electron transfer processes, not independent variables. In general:

$$\alpha_A + \alpha_C = 1 \tag{1.37}$$

and, in fact, it is common for $\alpha_A \simeq \alpha_C \simeq 0.5$. The above discussion is complicated by the number of different potentials and current densities used, and to aid understanding their definitions are summarized in Table 1.1.

Table 1.1

Symbol	Definition
$E_e^{\ominus}$	Formal electrode potential measured vs. a reference electrode
E_e	Equilibrium potential measured vs. a reference electrode
E	Experimental potential measured vs. a reference electrode
η	Overpotential – the deviation of the experimental potential from the equilibrium potential, i.e. $\eta = E - E_e$
I	Experimental current density at the overpotential, η (or actual potential, E)
I_0	Exchange current density i.e. the partial anodic and cathodic current densities (of equal magnitude but opposite sign) at the equilibrium potential
$\vec{I}$	Partial cathodic current density at the potential E
$\overleftarrow{I}$	Partial anodic current density at the potential E

It should be noted that equation (1.36) retains a form which emphasizes that the measured current density at each overpotential is the sum of the partial cathodic and anodic current densities. Moreover, this indicates useful limiting forms. Thus, as the overpotential is made more negative, $\vec{I}$ increases while $\overleftarrow{I}$ decreases and quite rapidly $-\vec{I} \gg \overleftarrow{I}$. Then the first term in the Butler–Volmer equation has become negligible compared with the second and one can write:

$$-I = -\vec{I} = I_0 \exp\left(-\frac{\alpha_C nF}{RT}\eta\right) \tag{1.38}$$

This equation applies when the overpotential is larger than about 52 mV and shows that in this potential range, the current is expected to increase exponentially with overpotential. Note also that the overpotential necessary to obtain any desired current density is largely dependent on I_0. Equation (1.38) can also be written:

$$\log -I = \log I_0 - \frac{\alpha_C nF}{2.3RT}\eta \tag{1.39}$$

which is known as the cathodic Tafel equation. Similarly, at positive overpotentials, $\eta > 52$ mV, $\overleftarrow{I} > -\vec{I}$ and this leads to the anodic Tafel equation:

$$\log I = \log I_0 + \frac{\alpha_A nF}{2.3RT}\eta \tag{1.40}$$

The two Tafel equations (1.39) and (1.40) are the basis of a simple experimental procedure for determining I_0, α_C and α_A. I–E data for the solution of O and R (note E_e, η, and I_0 all depend on c_O^∞ and c_R^∞) are replotted as $\log_{10}|I|$ vs. η and the exchange current density and transfer coefficients are obtained from the intercepts and slopes (Fig. 1.4). Since the intercepts should be the same and the slopes are related ($\alpha_A + \alpha_C = 1$), the plot is a good test of experimental data. When $\alpha_A = \alpha_C = 0.5$ the slopes are 1/120 mV at room temperature.

The Butler–Volmer equation has another limiting form which applies at very low overpotentials, say $\eta < 10$ mV. It is obtained by expanding the exponentials as series and then ignoring squared and higher terms. When $\alpha_A = \alpha_C = 0.5$, it reduces to:

$$I = I_0(nF/RT)\eta \tag{1.41}$$

and shows that in this narrow potential range close to $\eta = 0$, I depends linearly on η. This limiting form, however, has little relevance to electrochemical technology.

It can be seen, from equation (1.35), for example, that the exchange current density is a function of the concentrations of O and R in solution. Hence, it is a rather unusual kinetic parameter. It is therefore often convenient to define a kinetic parameter without such a dependence and it is common to use the

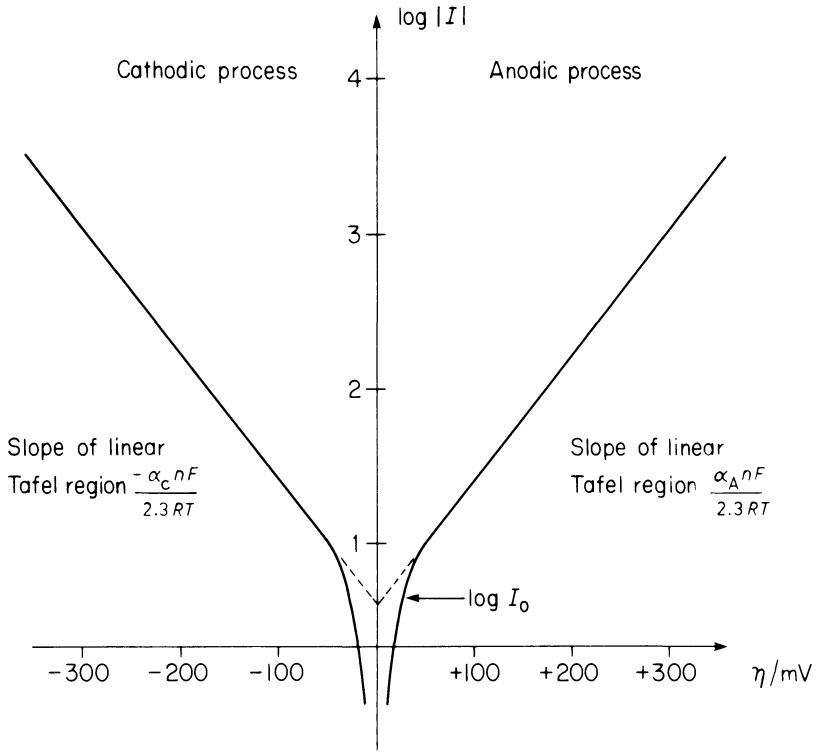

Fig. 1.4 Experimental determination of I_0, α_A and α_C using the Tafel equations (1.39) and (1.40)*.

standard rate constant, $k^\bullet$, defined by:

$$I_0 = nFk^\bullet(c_O^\infty)^{\alpha_A}(c_R^\infty)^{\alpha_C} \tag{1.42}$$

Note that the equations above are all formulated in terms of current density. Experimentally, it is current which is measured initially but this is related to current density by the trivial equation:

$$I = i/A \tag{1.43}$$

where A is the electrode area.

* Throughout this book, Tafel plots are drawn and discussed with log I as the y axis and η as the x axis. This reflects the way such data are usually recorded (i.e. using a controlled potential technique and measuring the current). A consequence is that the units of the Tafel slope are $(\text{mV})^{-1}$. Tafel originally recorded I–η data using a controlled-current technique with measurement of overpotential. Hence, he plotted log I as the x axis and overpotential as the y axis. This is a convention still followed by some technologists (e.g. many corrosion scientists) and as a result they commonly consider the units of the Tafel slope to be mV.

So far, our treatment of the kinetics of electron transfer has been rather pragmatic and gives no insight into how the act occurs on a molecular level. Our understanding of the factors which control the kinetics of electrode reactions can be increased by applying transition-state theory to the heterogeneous process occurring in a potential gradient. In general, the theory is based on the concept that the rate of reaction is determined by an activation barrier in free energy, i.e. the rate constant is given by the equation:

$$k = Z \exp\left(-\frac{\Delta G_{\ddagger}}{RT}\right) \tag{1.44}$$

where Z is the frequency factor and $\Delta G_{\ddagger}$ the energy of activation. In electrode reactions, the true driving force for electron transfer is the potential difference $\phi_m - \phi_s$ created between the electrode and the solution, and it should be emphasized that this potential drop occurs over molecular dimensions (i.e. maybe 2 V in 0.1–1 nm) at the electrode–electrolyte interface. Figure 1.5 shows the free energy curves for the initial and final states of the electrochemical reduction of $O \rightarrow R$ at two overpotentials; clearly, overpotential and $\phi_m - \phi_s$ must be related and because O and R, in general, and also the electron, are charged species, their free energies will depend on the electric potential on the phase in which they reside. In the initial state, the total free energy G_o is the sum of that for O and for the electron, i.e.:

$$G_o = G'_o + z_o F\phi_s - nF\phi_m \tag{1.45}$$

where G'_o is the free energy of the oxidized species in the absence of any potential field and takes into account all the chemical factors and z_o is the charge on O. The equivalent equation for the final state is:

$$G_R = G'_R + z_R F\phi_s \tag{1.46}$$

since only the species R is involved. Making the overpotential more negative will have the same effect on $\phi_m - \phi_s$. If one assumes that the change in potential only occurs on the solution-side of the interface, the solution potential ϕ_s will become more positive. If, for simplicity, one also considers only the case where both O and R are positively charged, the change in ϕ_s will lead to destabilization of both O and R. But O must carry a larger positive charge than R and hence, will be destabilized to a greater extent and this is recognized in Fig. 1.5 by a larger shift in the potential energy surface on changing the overpotential. It can also be seen in the figure that the free energies of activation, $\overrightarrow{\Delta G}_{\ddagger}$ and $\overleftarrow{\Delta G}_{\ddagger}$ are less sensitive than either G_O or G_R to the change in $\phi_m - \phi_s$ (or η). Hence, the free energy of activation for the forward process is given by:

$$\overrightarrow{\Delta G}_{\ddagger} = \text{const} + \alpha_C nF(\phi_m - \phi_s) \tag{1.47}$$

a statement which is equivalent to noting that only a fraction α_C of the applied

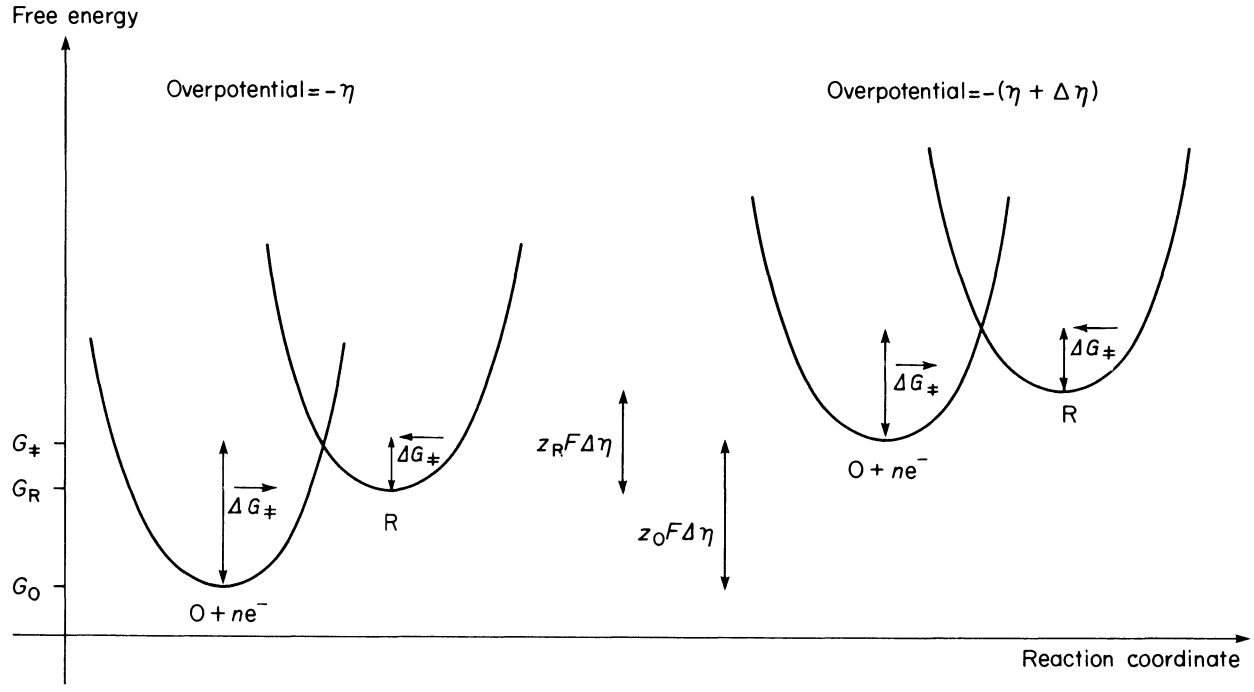

Fig. 1.5 Free-energy curves for the initial state ($O + ne^-$) and the final state (R) of a simple ne^- transfer reaction at two overpotentials. Note that: (1) the additional overpotential $-\Delta\eta$ destabilizes both O and R if both are positively charged (O is more positively charged and is destabilized to a greater extent); and (2) $\overrightarrow{\Delta G}$ decreases by less than $nF\Delta\eta$, in fact $\alpha_c nF\Delta\eta$. This diagram is drawn for the reduction of a trivalent to a divalent ion, e.g. $Fe^{3+} \rightarrow Fe^{2+}$.

overpotential will succeed in changing the rate of the electrode process. Using equations (1.26) and (1.44) one may write:

$$-\vec{I} = nFZc_O^{\infty} \exp -\left[\frac{\text{const} + \alpha_C nF(\phi_m - \phi_s)}{RT}\right] \tag{1.48}$$

which will lead to a Tafel-type equation. If similar expressions are written for the back reaction, then it is also possible to derive an equation equivalent to the Butler–Volmer equation.

The transition state theory emphasizes that the standard rate constant $k^{\ominus}$ for the couple O/R is determined by an activation energy required to form the 'activated complex' which will have a structure intermediate between O and R. Hence, it is reasonable to assume that the activation energy is associated with a rearrangement of ligands and solvent molecules around the central metal atom (if the electroactive species is a metal complex or solvated ion). Hence, it seems likely that the rate of an electrode reaction will be slow if:

1. The species O and R have different geometries.
2. The coordination numbers of O and R are different.
3. The reaction involves bond formation or cleavage.
4. The rate of ligand substitution is low.

Indeed, such correlations are observed and values of $k^{\ominus}$ between 10^{-7} and 10 cm s^{-1} are common. The fastest reactions are those where the structures of O and R are similar (e.g. anthracene/anion radical, ferrocene/ferrocinium ion, $Fe(CN)_6^{4-}/Fe(CN)_6^{3-}$) and these reactions can be considered as akin to outer sphere electron transfer processes in homogeneous solution. Typical slow couples are Cr(III)/Cr(II) where Cr(III) species are known to be substitution inert and Ce(IV)/Ce(III) in sulphuric acid solutions where the reduction of Ce(IV) requires loss of sulphate from the inner coordination sphere. Also substituents in a hydrocarbon which lead to a need for twisting within the molecule to form a planar anion radical cause a marked decrease in the standard rate constant.

To progress further in our understanding of electron transfer on a molecular level requires a more sophisticated model of the interface which recognizes the electrostatic consequences of putting a charged surface into a solution containing ions; an electrical double layer is formed, see Fig. 1.6(a) for a widely accepted model for the case where the surface is negatively charged. Cations (both electroactive species and base electrolyte cations since the interaction is completely electrostatic) are attracted to the surface, displace some solvent dipoles from the surface and form an organized layer where the cations are centred on the ϕ_2 plane, the plane of closest approach. This, then, is the inner or compact layer. Outside this highly structured layer is a further region of solution within which the ions retain some structure resulting from the electrostatic influences of the electrode surface. Hence, within this 'diffuse layer', the degree of organization is intermediate between the compact layer and the random arrangement of ions

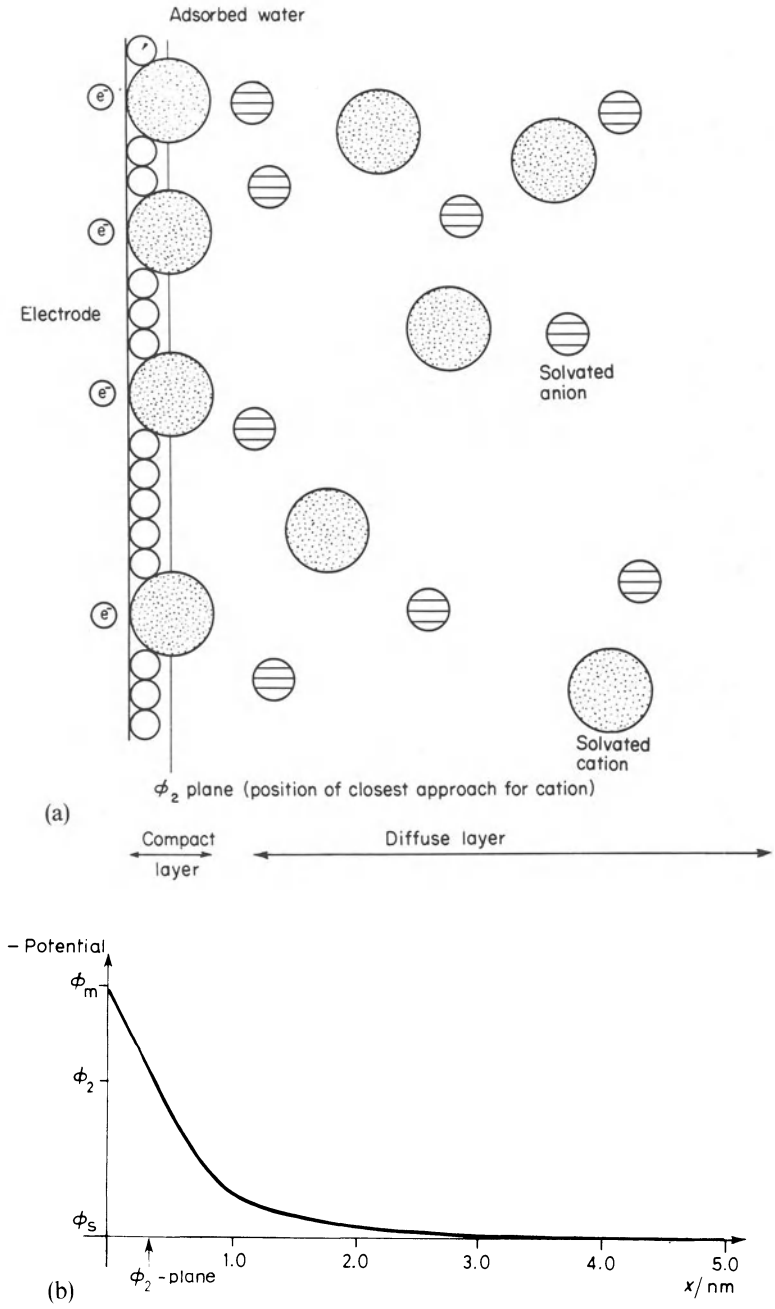

Fig. 1.6 Structure of the double layer at the electrode–solution interface. Note the highly ordered structure of the compact layer; the diffuse layer is less ordered but is not the random arrangement of the solution away from the interface. (b) Potential field resulting from this model.

within the bulk solution. The double layer causes the potential difference $\phi_m - \phi_s$ to be smeared out over several molecular dimensions (Fig. 1.6(b)). The kinetic parameters should therefore be corrected for:

1. The effect of the smeared-out potential field on the driving force for electron transfer. From the model in the figure, it can be seen that the species O is, at best, at the plane of closest approach to the electrode and at the centre of the species the potential available to drive the reaction is only $\phi_2 - \phi_s$ (which is less than $\phi_m - \phi_s$).
2. If O is charged, its concentration at the plane of closest approach differs from that in bulk solution because of the potential field.

A detailed treatment of these 'double-layer corrections' is available in the texts recommended at the end of this chapter.

The last 25 years have seen several attempts to develop a statistical–mechanical theory of electron transfer. These treatments, however, do not predict the simple linear $\log I$ vs. E relationship of the Tafel equations which seems adequate for the description of charge transfer controlled electrode reactions in electrochemical technology. Therefore, they will not be discussed here.

1.2 MASS TRANSPORT

In general, it is necessary to consider three modes of mass transport in electrochemical systems: (1) diffusion; (2) migration; and (3) convection.

1. *Diffusion.* Diffusion is the movement of a species down a concentration gradient and it occurs whenever there is a chemical change at a surface. An electrode reaction converts starting material to product (e.g. $O \rightarrow R$) and hence close to the electrode surface there is a boundary layer (up to 10^{-2} cm thick) in which the concentration of O is lower at the surface than in the bulk while the opposite is the case for R and, hence, O will diffuse towards and R away from the electrode.
2. *Migration.* Migration is the movement of charged species due to a potential gradient and it is the mechanism by which charge passes through the electrolyte; the current of electrons through the external circuit must be balanced by the passage of ions through the solution between the electrodes (both cations to the cathode and anions to the anode). It is, however, not necessarily an important form of mass transport for the electroactive species, even if it is charged. The forces leading to migration are purely electrostatic and, hence, do not discriminate between types of ions. As a result, if the electrolysis is carried out with a large excess of an inert electrolyte in the solution, this carries most of the charge, and little of the electroactive species O is transported by migration, i.e. the transport number of O is low.

3. *Convection.* Convection is the movement of a species due to a mechanical force. In practice, convection is usually induced by stirring or agitating the electrolyte solution or by flowing it through the cell. Sometimes the electrode is moved. When such forms of forced convection are present, they are normally the predominant mode of mass transport. It is possible to carry out electrochemistry in the absence of convection by using a still solution in a thermostat, but only on a short timescale, say less than 10 s. On a longer timescale, natural convection arises from small differences in density caused by the chemical change at the electrode surface.

The treatment of mass transport, more than any other aspect of the subject, highlights the differences between laboratory experiments and industrial-scale electrolyses. In the former, there is great concern to ensure that the mass transport conditions may be described precisely by mathematical equations (which, moreover, are soluble) since this is essential to obtain reliable mechanistic and quantitative kinetic information. The need in an industrial cell is only to promote the desired effect within technical and economic restraints and this permits the use of a much wider range of mass transport conditions. In particular, a diverse range of electrode–electrolyte geometry and relative movement are possible.

1.2.1 Mass transport in laboratory experiments

The investigation of the mechanism and kinetics of electrode processes is normally undertaken with solutions containing a large excess of base electrolyte (i.e. so that the migration of electroactive species is unimportant), but two types of experiment are common:

1. Using unstirred solutions and a short timescale so that natural convection does not interfere.
2. Using a form of forced convection which may be described exactly; by far the most important system is the rotating-disc electrode and it frequently provides a good but simple analogue of the mass transport conditions in industrial cells.

Electrochemical experiments in the laboratory are generally designed so that they may be described adequately by a one-dimensional mass transport model. The key dimension is always that perpendicular to the electrode surface and is here designated the x-dimension.

Fick's laws of diffusion describe the mass transport in type-1 experiments above. The electron transfer process $O \rightarrow R$ at the surface will lead to a boundary layer where the concentration of O is lower and that of R is higher than in the bulk. In this situation, Fick's first law states that the flux of any

species i through a plane parallel to the electrode surface (Fig. 1.7(a)) is given by:

$$\text{Flux} = -D_i \frac{dc_i}{dx} \tag{1.49}$$

where D_i is its diffusion coefficient. Fick's second law discusses the change in concentration of i with time due to diffusion. At a point at the centre of an element of solution bounded by two planes parallel to the electrode (Fig. 1.7(b)) the concentration will change because diffusion is occurring both into and out of the element. This leads to the equation:

$$\frac{\partial c_i}{\partial t} = D_i \frac{\partial^2 c_i}{\partial x^2} \tag{1.50}$$

Integration of equation (1.50) with initial and boundary conditions appropriate to the particular experiment is the basis of the theory of instrumental methods

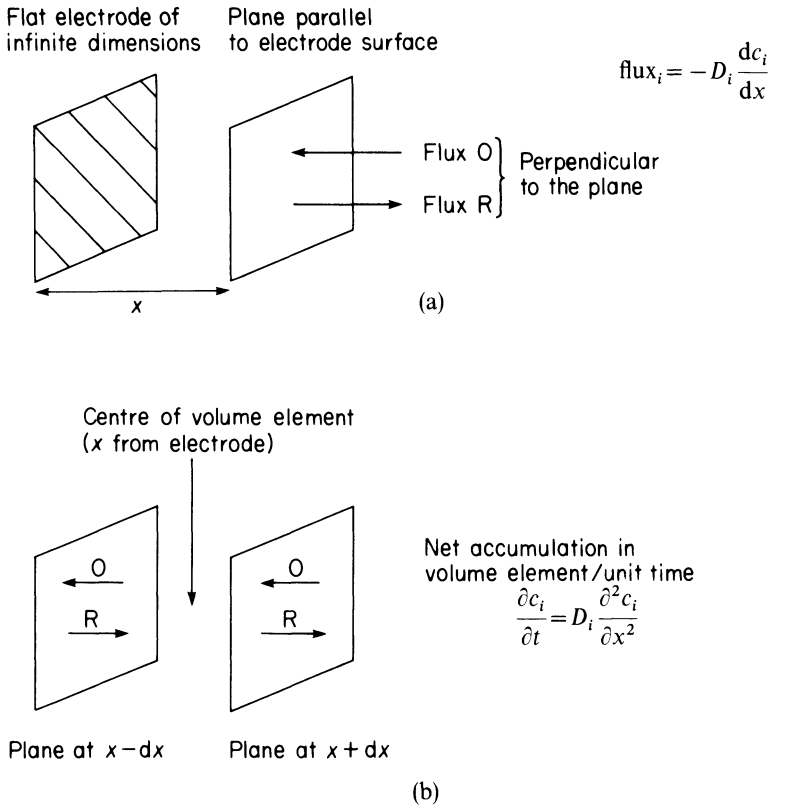

Fig. 1.7 Model used for the description of the diffusion of the electroactive species O and product R during an electroanalytical experiment. (a) Fick's first law, (b) Fick's second law.

such as chronopotentiometry, chronoamperometry and cyclic voltammetry. The solutions to equation (1.50) show that the concentrations of O and R vary with time as well as distance from the electrode. Plots of c_i vs. x are known as concentration profiles and consideration of their variation with time is an excellent way to understand non-steady-state experiments. It is important to recognize that diffusion occurs so as to minimize differences in concentration at all points in space. Hence, in the steady state the concentration profiles are linear (if the profiles are non-linear, there are some points in space where differences in concentration have not been minimized).

Fick's first law applied at the electrode surface can always be used to relate the current density to the chemical change at the electrode by equating the flux of O or R with the flux of electrons:

$$I/nF = -D_O\left(\frac{\partial c_O}{\partial x}\right)_{x=0} \tag{1.51}$$

or:

$$I/nF = D_R\left(\frac{\partial c_R}{\partial x}\right)_{x=0} \tag{1.52}$$

A rotating disc acts as a pump, pulling solution up to the disc and throwing it out across the shroud (Fig. 1.8); hence, in experiments with a rotating-disc electrode, concentration changes will arise due to both diffusion and convection. If the radius of the disc is small compared with that of the shroud, we can assume that access of the solution to the whole electrode surface is uniform. Then

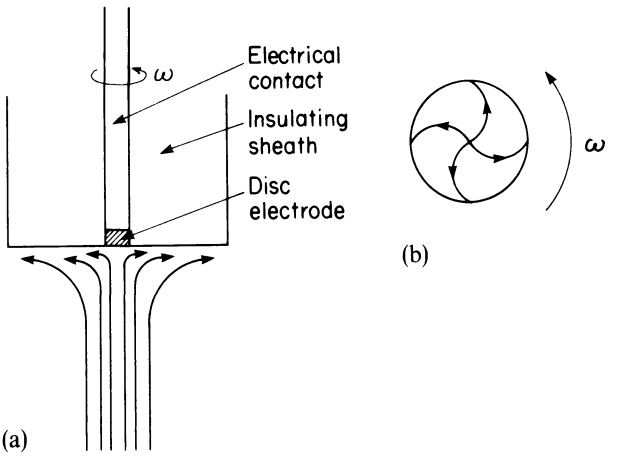

Fig. 1.8 Convection resulting from a rotating-disc electrode. Streamlines from: (a) side view. (b) below the disc.

concentration will again be a function only of the direction perpendicular to the disc surface. The equation:

$$\frac{\partial c_i}{\partial t} = D_i\left(\frac{\partial^2 c_i}{\partial x^2}\right) - v_x\left(\frac{\partial c_i}{\partial x}\right) \tag{1.53}$$

diffusion convection

includes both forms of mass transport. It refers to 'convective diffusion'. Diffusion is again expressed by Fick's second law while the changes in concentration due to convection depend on the velocity of solution movement in the x direction v_x and the concentration gradient $\partial c_i/\partial x$ in the same direction. Commonly only steady-state measurements are made in rotating disc experiments; then, $\partial c_i/\partial t$ is zero and equation (1.53) reduces to:

$$D_i\left(\frac{\mathrm{d}^2 c_i}{\mathrm{d}x^2}\right) = v_x\left(\frac{\mathrm{d}c_i}{\mathrm{d}x}\right) \tag{1.54}$$

A solution of this problem depends on knowing the relationship between v_x and x as well as other parameters, particularly the rotation rate of the disc since it is clearly the rotation which is responsible for the convection in the system. A study of the fluid mechanics (see below) of the system, leads to expression:

$$v_x = -0.51 v^{-\frac{1}{2}} \omega^{3/2} x^2 \tag{1.55}$$

where v is the kinematic viscosity (dynamic viscosity/density) of the solution and ω is the rotation rate of the disc. In fact, this expression is valid only for small x since, well away from the surface, v_x is clearly independent of x. It is, however, the basis of a very useful approximate model for rotating-disc experiments which has analogies in all systems involving convection. At the surface, the flow of solution must be zero (the solution cannot pass through the solid surface) but close to the surface, the velocity of solution flow increases rapidly ($v_x \propto x^2$). In the Nernst diffusion-layer model, one defines a hypothetical boundary layer of thickness δ_N inside which mass transport is considered to be only by diffusion. On the other hand, convection is strong for $x > \delta_N$ and maintains the concentrations at the bulk values. More precise mathematical treatments of the rotating-disc electrode are equivalent to this model with δ_N given by:

$$\delta_N = \frac{1.61 v^{1/6} D^{1/3}}{\omega^{\frac{1}{2}}} \tag{1.56}$$

Since only the steady state is being considered, the concentration profiles are linear (Fig. 1.9). Hence, the model predicts that the fluxes to the surface and, hence, the current density depend on: (1) electrode potential which determines the surface concentrations; (2) bulk concentrations; and (3) rotation rate which

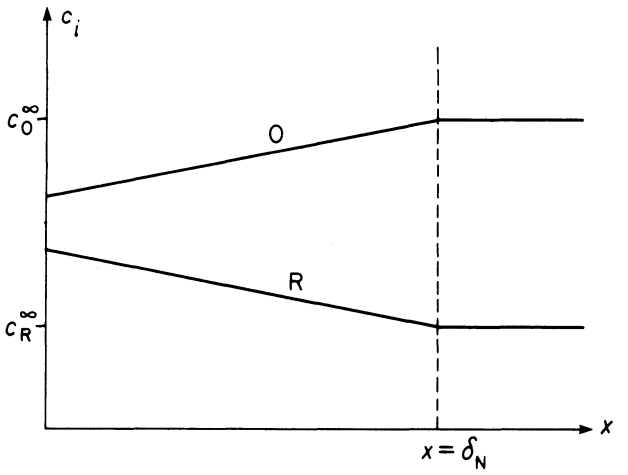

Fig. 1.9 Steady-state concentration profiles for the electrode process $O+ne^- \longrightarrow R$; solution contains $c_O^\infty = 3c_R^\infty$.

controls δ_N† i.e.:

$$-I = nFD\left(\frac{dc_O}{dx}\right)_{x=0}$$

$$= nFD\left(\frac{c_O^\infty - c_O^\sigma}{\delta_N}\right) \tag{1.57}$$

Moreover, at very high overpotentials, the electron transfer is very fast, so $c_O^\sigma = 0$. Then the mass transport limited-current density is given by*:

$$-I_L = \frac{nFDc_O^\infty}{\delta_N} = \frac{nFD^{2/3}c_O^\infty \omega^{\frac{1}{2}}}{1.61\nu^{1/6}}$$

$$= 0.62nFD^{2/3}c_O^\infty \nu^{-1/6}\omega^{1/2} \tag{1.58}$$

* The steady state limiting current can also be written in terms of a mass transport coefficient k_L i.e.:

$$-I_L = nFk_Lc_O^\infty$$

It can be seen that the mass transport coefficient is related to the thickness of the Nernst diffusion layer by $k_L = D/\delta_N$ and hence, $k_L = 0.62D^{2/3}\nu^{-1/6}\omega^{1/2}$. Engineers often prefer the use of mass transport coefficient because it avoids the discussion of the Nernst diffusion layer, a concept useful to an understanding of experiments and widely met in the electrochemical literature but, in fact, ficticious since concentration profiles are never linear.

† A comment about the relative sizes of the boundary layers discussed in electrochemistry is necessary. The dimensions of the double layer may be 5×10^{-8} cm. In contrast, the Nernst diffusion layer may have a thickness of 10^{-2} cm while the real layer effected by the electrode reaction may be an order of magnitude thicker.

As noted above, a similar model is appropriate to all systems involving stirred or flowing solutions and the problem is to relate the thickness of the 'equivalent' boundary layer to the mass transport in the system.

1.2.2 Mass transport in industrial electrolysis

In industrial practice, it is possible to find examples of cells which use unstirred solutions (e.g. electrorefining, batteries), stirred or agitated solutions (e.g. electroplating) and flowing electrolytes, e.g. synthesis, water treatment. Moreover, it is unusual for the flow of solution and the current path – which depend on cell geometry – to be parallel, and the electrode may not be a flat plate (e.g. bed electrodes, cathodes for plating); as a result, we must write our mass transport expressions in three dimensions. Nor is it always possible to assume that migration of the electroactive species is unimportant.

Thus the most general forms of the mass-transport equations are:

$$(\text{Flux})_i = \underbrace{-D_i \operatorname{grad} c_i}_{\text{diffusion}} \underbrace{- u_i c_i \operatorname{grad} \psi}_{\text{migration}} + \underbrace{c_i v}_{\text{convection}} \tag{1.59}$$

where u_i is the mobility of species i and ψ the potential field strength, and:

$$\frac{\partial c_i}{\partial t} = D_i \nabla^2 c_i - u_i \operatorname{grad} \psi \operatorname{grad} c_i - v \operatorname{grad} c_i \tag{1.60}$$

These equations may be written in the most convenient coordinates for the cell and electrode geometry but as an example, equation (1.60) in cartesian co-ordinates becomes:

$$\begin{aligned}\frac{\partial c_i}{\partial t} = D_i\left[\frac{\partial^2 c_i}{\partial x^2} + \frac{\partial^2 c_i}{\partial y^2} + \frac{\partial^2 c_i}{\partial z^2}\right] - u_i\left[\frac{\partial \psi}{\partial x}\frac{\partial c_i}{\partial x} + \frac{\partial \psi}{\partial y}\frac{\partial c_i}{\partial y} + \frac{\partial \psi}{\partial z}\frac{\partial c_i}{\partial z}\right] \\ -\left[v_x\frac{\partial c_i}{\partial x} + v_y\frac{\partial c_i}{\partial y} + v_z\frac{\partial c_i}{\partial z}\right]\end{aligned} \tag{1.61}$$

Clearly, such general expressions are intractable and we need to consider limiting cases or use other approaches.

Fluid mechanics is the study of the motion of flowing or stirred fluids, usually liquids or gases. In electrochemical technology it has two different applications: (1) to describe the movement of electrolyte solutions in a cell, since this will be a principal driving force for mass transport to the electrodes; and (2) to ensure the proper design of the pipes, valves and junctions which join the cell to the rest of the plant. Quantitative fluid mechanics is based upon the continuity equations which state that at all points in space, charge, mass, momentum and, for inviscid flow (i.e. fluids where no viscous forces operate) energy must be conserved. This section will deal mainly with the qualitative concepts because of the very complex nature of flow in most electrolysers.

We shall consider first the flow of solution over a flat plate. Two forces will be acting upon the fluid in such systems: (1) the cause of the flow (that generated by a pump or a solution head) known as the inertial force; and (2) that force which opposes the flow and results from viscous forces at the interface between the plate and the solution.

Suppose we assume that the solution may be divided into elements, then the viscous force will initially cause that element next to the stationary plate to be retarded and later each element will be slowed down by that closer to the plate. Hence, as the solution flows over the plate, a boundary layer of more slowly moving solution will develop (Fig. 1.10). In an electrolytic cell, the flat plate would normally be the electrode and therefore the formation of such boundary layers has particular importance. The electrode reaction takes place in the boundary layer in the presence of velocity gradients.

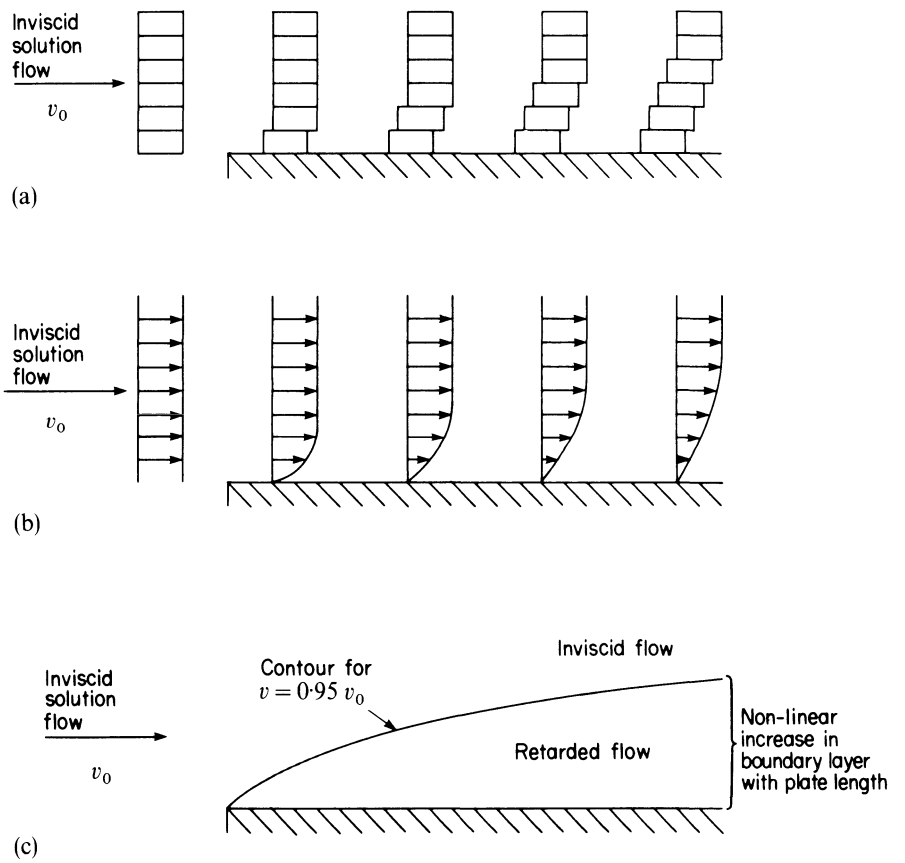

Fig. 1.10 Three different representations of the development of a boundary layer over a flat plate, e.g. an electrode.

With such a flat plate, the boundary layer will increase in thickness indefinitely, if slowly (Fig. 1.10(c)). On the other hand, if the flow is in a restricted channel (e.g. a circular-tube or a parallel-plate cell) the boundary layers at the two walls must merge at some point and beyond, a steady-state situation or 'fully developed laminar flow' will result (Fig. 1.11). Fundamental mass transport studies in electrolytic cells are usually carried out in cells with an entry length without electrodes so that the boundary-layer thickness is uniform over the current-carrying surface.

It can already be seen that the development and scale of the boundary layer will be dependent on the relative importance of the inertial and viscous forces. For this reason, the ratio of inertial : viscous forces is given a name, the Reynolds number *Re*, and it may be calculated from the formula:

$$Re = \frac{\rho l \bar{v}}{\mu} = \frac{l \bar{v}}{\nu} \tag{1.62}$$

where ρ is the density of the solution, μ its dynamic viscosity, ν its kinematic viscocity, $\bar{v}$ a mean flow velocity and l a characteristic length (in the example above, the length of the plate). In fact, the boundary layer develops in the way discussed only below a critical value of Reynolds number where the viscous damping is sufficient to suppress any perturbations which arise. At higher Reynolds number, the viscous damping is no longer predominant and turbulence commences; in effect, the high rates of shear induce rotation of the solution and small eddies are formed. This may be shown clearly by experiments where dye is injected into a solution flowing down a glass tube (Fig. 1.12). Any obstacles to fluid flow, or roughness in the channel wall will cause the commencement of turbulence at lower Reynolds number.

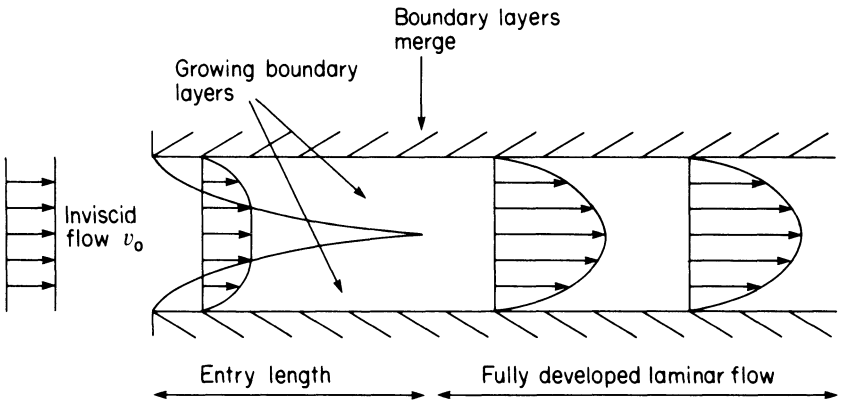

Fig. 1.11 Development of a hydrodynamic boundary layer for solution flowing through a tube.

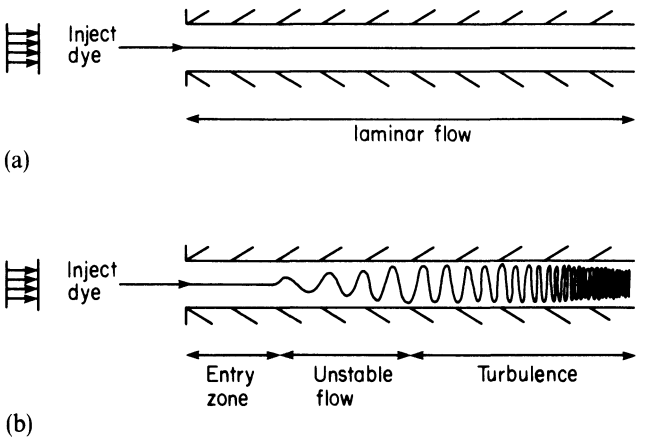

Fig. 1.12 Solution flow through a tube as shown by the dye technique. (a) Reynolds number $Re < 2000$. (b) Reynolds number $Re > 3000$.

Turbulence in electrolytic cells is usually advantageous since the eddies both increase mass transport of the electroactive species to the electrode surface and promote the exchange of species between the bulk solution and the boundary layer, minimizing local pH and other concentration changes due to the electrode reaction. Indeed, it is not uncommon to introduce insulating nets, bars or other structural features into the cell to act as turbulence promoters. In certain cases, the electrode itself may be in a form (e.g. mesh, reticulated metal, particulate bed, fibrous material) whereby it acts as a turbulence promoter.

It will be seen in the next and subsequent chapters that a wide variety of cell geometries (e.g. parallel-plate, concentric-cylinder, Swiss-roll), types of electrode (e.g. plates, beds, porous expanded metals and gauzes) and flow patterns are used in industrial electrochemistry. In most, the flow is too complex to warrant a detailed fluid–mechanical calculation. Rather, the normal approach to mass transport in electrolytic cells is to treat the cell as a unified whole and to seek expressions in terms of space-averaged quantities which permit some insight into the mass transport conditions within the cell.

Once again, considering the simplified problem of laminar flow over a flat plate, it is possible to derive an expression for the Sherwood number *Sh*:

$$Sh = 0.646\, Re^{0.5} Sc^{0.33} \tag{1.63}$$

Here, *Sh* is a measure of the rate of mass transport, which is usually calculated from the limiting current density I_L for the plate electrode (i.e. the potential of the plate is held at a value where all the electroactive species reaching the surface undergo the electrode reaction) using the relationship:

$$Sh = \frac{I_L L}{nFc_O^\infty D} \tag{1.64}$$

where L is the length of the plate. The Reynolds number, as was discussed above, compares the relative magnitudes of the inertial forces to the viscous forces in the cell. The Schmidt number Sc, defined by:

$$Sc = \mu/\rho D = \nu/D \tag{1.65}$$

compares the rate of transport by convection to that by diffusion.

In general, mass transport in electrolytic cells with flow may be discussed in terms of the expression:

$$Sh = K Re^a Sc^b \tag{1.66}$$

where the constants K, a and b many be obtained from experimental measurements of I_L under various flow conditions. For each reactor, it will be necessary to define certain average parameters. For example, if one considers a parallel-plate cell where the rectangular anode and cathode are inset in the walls of a flow channel in a position where one has fully developed laminar flow (Fig. 1.13), the appropriate equation is:

$$Sh = 1.85\, Re^{1/3} Sc^{1/3} (d_e/L)^{1/3} \tag{1.67}$$

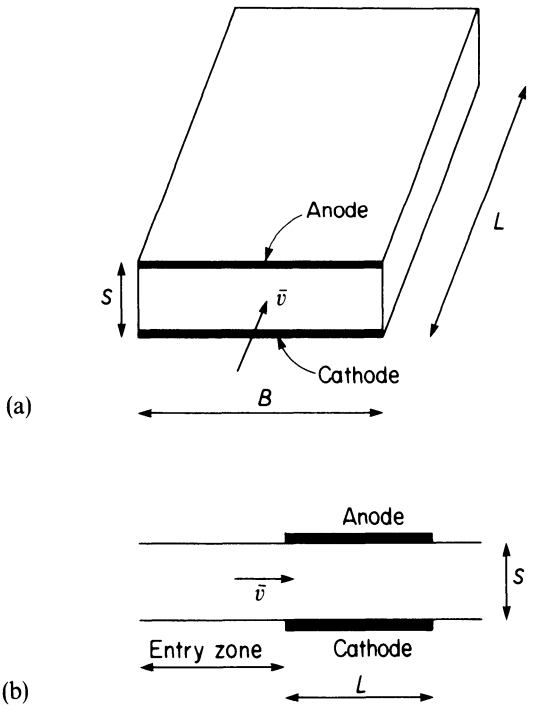

Fig. 1.13 Parallel-plate cell without separator but with fully developed laminar flow. Critical cell dimensions are $B/S > 6$ and $10 < L/d_e < 40$. (a) View along cell at the beginning of the electrodes. (b) View across cell.

where $Re = \rho \bar{v} d_e / \mu$, $Sc = \mu / \rho D$ and $Sh = \dfrac{I_L d_e}{nFc_O^\infty D}$ and d_e is the equivalent diameter (sometimes called the hydraulic diameter) which is defined by:

$$d_e = \frac{4BS}{2B+2S} = \frac{2BS}{B+S} \tag{1.68}$$

Of course, expression (1.67) is only applicable in the absence of turbulence and, hence, above a critical value of Reynolds number where turbulence is observed. For the parallel-plate cell $Re > 2000$, a different expression must be used:

$$Sh = 0.023\, Re^{4/5} Sc^{1/3} \tag{1.69}$$

It cannot be emphasized too strongly that this approach, based on dimensionless correlations, only gives an insight into macroscopic space-averaged mass transport conditions within the cell. It will not, for example, show the extent to which the flow between two parallel-plate electrodes is divided into a rapidly moving bulk phase and a slowly moving wall phase (Fig. 1.14). Nor will it demonstrate whether the electrolyte feeds and outlets to the cell are designed so as to give a uniform electrolyte flow over the whole electrode surface, an

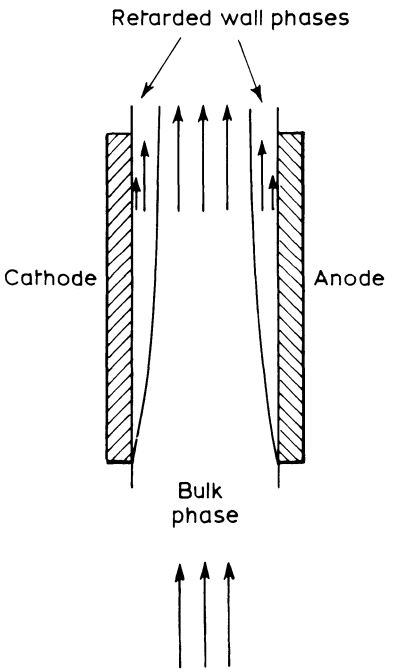

Fig. 1.14 Electrolyte flow through a parallel-plate reactor emphasizing the segregation of the flow into the rapidly moving bulk phase and slowly moving wall phases.

important factor in determining cell performance. Such questions require quite different approaches and experimental techniques may be based on:

1. Segmented electrodes.
2. Microprobes designed to measure parameters such as local current density, potential or pressure drop.
3. Marker techniques – a well defined pulse of a dye or an ion is introduced at the cell inlet and the dispersion of the species marker is measured at the cell outlet.

Such techniques are discussed further in section 2.6.1.

From the above discussion, it can be seen that the mass transport for a given electrode–electrolyte geometry and electrolyte hydrodynamics may be related to the process parameters by a suitable dimensionless group correlation, e.g., mass transport to the rotating disc in laminar flow conditions may be described by the equation (see footnote, page 23):

$$k_L = 0.62 D^{2/3} \nu^{-1/6} \omega^{1/2} \tag{1.70}$$

Multiplying by the ratio r/D, where r is the radius of the disc, gives:

$$\frac{k_L r}{D} = 0.62 r \omega^{1/2} \nu^{-1/6} D^{-1/3} \tag{1.71}$$

or:

$$\left(\frac{k_L r}{D}\right) = 0.62 \left(\frac{\omega r^2}{\nu}\right)^{1/2} \left(\frac{\nu}{D}\right)^{1/3} \tag{1.72}$$

or (in dimensionless group format):

$$Sh = 0.62 Re^{1/2} Sc^{1/3} \tag{1.73}$$

It can be seen that equations (1.58) and (1.73) are essentially equivalent (note $Sh = \frac{I_L r}{nFc^{\infty} D}$). The former is used by electrochemists, while the latter is preferred by chemical engineers since it facilitates a comparison between other cell geometries/flow conditions and allows analogies with heat and momentum transfer.

1.3 THE INTERPLAY OF ELECTRON TRANSFER AND MASS TRANSPORT CONTROL

It was noted in the introduction to this chapter that the reduction of O→R is at least a three-step process, equations (1.20)–(1.22) involving both mass transport and electron transfer, and that the rate of the overall sequence, and therefore current density, depends on the slowest step. Having considered electron transfer and mass transport independently, we can now consider the shape of a

complete I–E curve for the couple O/R (Fig. 1.15(a)). It should be noted that the rate of the electron transfer process is a function of potential (equation (1.36)) and that whatever the mass transport conditions in the cell, there will be a maximum rate at which electroactive species can reach the surface.

At the equilibrium potential, no net current flows. As the potential is made negative to E_e, a reduction current is observed. Initially, it will be very small and the surface concentration of O remains close to its bulk concentration; this potential region will lead to a linear Tafel plot (Fig. 1.15(b)). As the potential is made more negative, the rate of reduction increases rapidly, in fact exponentially

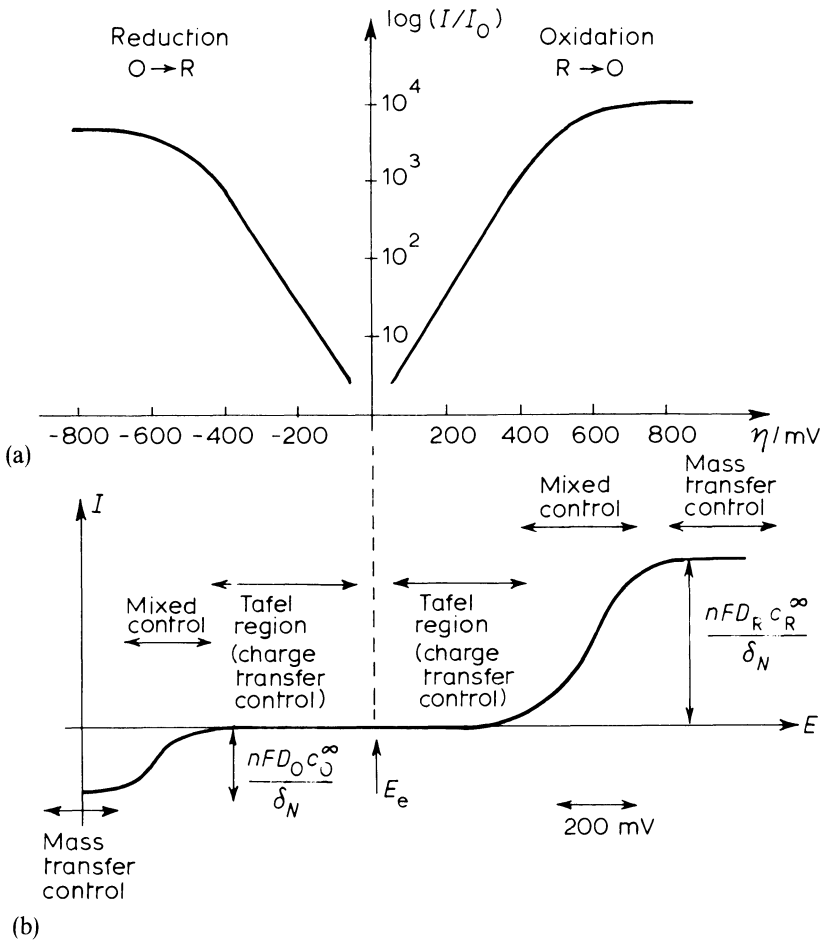

Fig. 1.15(a) Complete I–E curve. (b) Log I/I_0 vs. η curve for the couple $O + ne^- \rightleftharpoons R$ when the solution contains $c_R^\infty = 3c_O^\infty$. Case of slow electron transfer, i.e. low I_0.

(equation (1.38)), and is eventually rapid enough for c_O^s to become significantly less than c_O^∞. Then mass transport will need to occur and the current comes under mixed control; the Tafel plot is non-linear and the current density becomes sensitive to the mass transport conditions. On making the potential even more negative, the surface concentration of O decreases from c_O^∞ effectively to zero. At this point, the current density becomes independent of potential and the process is said to be mass transport controlled. The value of current density will depend strongly on the mass transport conditions in the cell and will have a characteristic variation with rotation rate, flow rate, etc, e.g. equation (1.58) for the RDE. A parallel discussion applies to the section of the I–E curve positive to E_e but relates to the oxidation of R→O.

In Fig. 1.15, the data are shown as both I–E and log I–η plots and the correlation between Tafel, mixed and mass transport controlled regions on the two figures should be noted. It is also important to note that a linear Tafel region can sometimes be observed over several orders of magnitude of current density but the range is limited by:

1. $I > 5I_0$. Below this current the back-reaction is significant (equation (1.36)).
2. $I < 0.05I_L$. Above this value, mass transport control intrudes.

Hence, it can be seen that the form of the curve depends on the kinetic parameters and the mass transport regime. Indeed, Fig. 1.15 only applies to a couple where I_0 is relatively low and significant overpotentials are necessary to drive the forward and reverse processes.

A quite different response is found for couples O/R where I_0 is large (in fact, where $I_0 > 10^{-3} I_L$ or $k^\bullet > 10^{-3}$ cm s^{-1}). Then the electron transfer reaction at the surface is rapid enough that under most mass transport conditions obtainable experimentally, the electron transfer couple at the surface appears to be in equilibrium. Then the surface concentrations may, at each potential, be calculated from the Nernst equation, a purely thermodynamic equation, and the current may be calculated, for example, from equation (1.57). The I–E curve has the form shown in Fig. 1.16; the I–E curve crosses the zero current axis steeply and there is no overpotential for oxidation or reduction. Systems with these characteristics are often termed 'reversible'. On the other hand, the limiting current densities do not depend on the kinetics of electron transfer closer to E_e. Hence the limiting current densities for 'reversible' and irreversible reactions are the same.

1.4 ADSORPTION

The electrochemistry of many industrial processes is dependent totally on the ability of the electroactive species, reaction intermediates, product or, indeed, species apparently not involved in the electron transfer process, to adsorb on the electrode surface, i.e. to form some type of bond with the electrode material. The role of the adsorbed species is to accelerate or to decrease reaction rates, and in

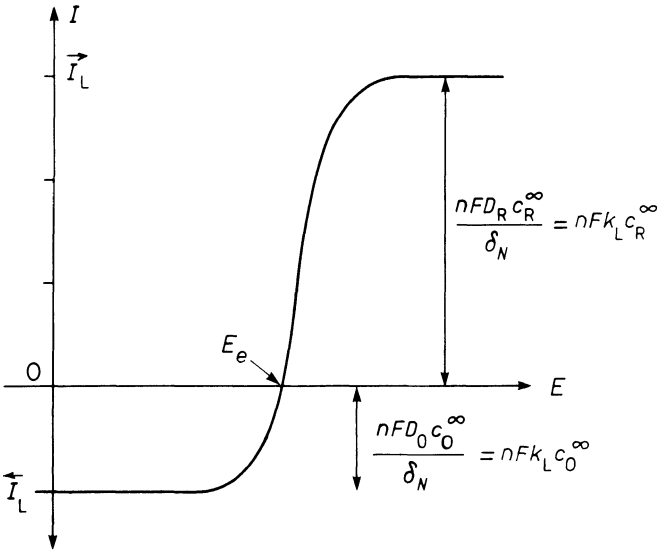

Fig. 1.16 Complete *I–E* characteristic for a reversible couple O/R (a couple where I_0 is large). The solution contains $c_R^\infty = 3c_O^\infty$. The unequal concentrations are chosen to emphasize the relation between currents and concentrations.

extreme situations this may lead to a total change in the dominant pathway and, hence, in the products of electrolysis. Important examples of the application of adsorption in electrochemical technology would include electrocatalysis, the inhibition of corrosion and the control of electroplating by organic additives, and the variation of product selectivity in organic electrosynthesis.

Adsorption results from a wide variety of interactions between the adsorbing species and the electrode surface. In some cases, the driving force for adsorption is merely dislike of the adsorbate for the electrolyte solution phase (c.f. adsorption of neutral organic molecules at the gas–liquid interface). In other cases, adsorption results from electrostatic (e.g. the adsorption of ions on a surface of opposite charge) or charge–dipole interactions, (e.g. the adsorption of thiourea, amines, aromatic molecules). The strongest interactions result from formation of a covalent bond between the adsorbate and the surface, e.g. the reduction of proton on Pt:

$$H^+ + e^- \longrightarrow H_{ADS} \tag{1.74}$$

or the dissociative adsorption of formic acid on Pt from aqueous acid solutions:

$$HCOOH \longrightarrow H_{ADS} + (COOH)_{ADS} \tag{1.75}$$

This is the first step in the complete oxidation of formic acid to carbon dioxide. Moreover, one sees great variations in the strengths of the bonds between the

electrode and the adsorbate and the degree of reversibility of the adsorption process.

1.4.1 Adsorption equilibria in the absence of electron transfer

The extent of adsorption is formally described by θ, the surface coverage or fraction of surface covered. In the absence of electron transfer processes, the value for any species will be determined by two factors: (1) the affinity or otherwise of the species for both the electrode and the solution; and (2) the ability of all other species in the solution to adsorb. Hence, the surface coverage is determined by competition between the electrode and the solution for the species under discussion and between several species for sites on the electrode surface. Adsorption is therefore, even in the simplest of situations, a displacement reaction, the adsorbate displacing molecules of solvent or ions of the base electrolyte.

At each potential, the electrode surface will carry a characteristic surface charge which depends on the electrode material, solvent and electrolyte. As the potential is made more positive, the surface charge will also become more positive while the reverse will happen when the potential is made negative. There must also be one particular potential, known as the point of zero charge or $E_{\text{p.z.c.}}$, where the surface is uncharged. When the adsorbing species is an ion or a dipole which will show a preferred orientation in the potential field, the adsorption will be strongest when the surface is highly charged and, hence, occur on one side of $E_{\text{p.z.c.}}$. In contrast, the coverage by neutral species is commonly highest at $E_{\text{p.z.c.}}$ where the competition from ions and solvent molecules (usually strong dipoles) is at a minimum.

The surface coverage overall will depend on the nature and concentration of the adsorbate as well as on the electrode potential (surface charge density), electrode material, solvent, electrolyte, pH, temperature and other possible adsorbates in solution.

The adsorption isotherms describe the dependence of the surface coverage on the concentration of adsorbate in solution and on the free energy of adsorption, the latter quantity being determined by: (1) vertical interactions between the species and the surface, $\Delta G^{\ominus}_{\text{ADS}}$; and (2) lateral interactions between adjacent adsorbed species. The extent and method of taking into account the second type of interaction give rise to a number of model isotherms.

If it is assumed that only a monolayer of adsorbate is possible, that all sites on the electrode surface are equivalent and that there are no interactions between neighbouring molecules of adsorbate (this is equivalent to assuming that the free energy of adsorption is independent of coverage), the coverage may be calculated from the Langmuir isotherm:

$$\frac{\theta}{1-\theta} = \beta c^{\infty} \tag{1.76}$$

where:

$$\beta = \exp - \left(\frac{\Delta G^{\ominus}_{\mathrm{ADS}}}{RT} \right) \tag{1.77}$$

In other isotherms, the interaction between adsorbed molecules is considered; in the Frumkin isotherm, the free energy of adsorption is considered to increase linearly with the coverage, i.e.:

$$\Delta G_{\mathrm{ADS}} = \Delta G^{\ominus}_{\mathrm{ADS}} + r\theta \tag{1.78}$$

which leads to the equation:

$$\frac{\theta}{1-\theta} \exp\left(\frac{r\theta}{RT} \right) = \beta c^{\infty} \tag{1.79}$$

The free energy of adsorption must depend on the electrode potential (see above), and the model whereby the adsorption process consists of the displacement of solvent adjacent to the electrode by a material of different permittivity leads to a quadratic dependence of the free energy of adsorption on potential, i.e.:

$$\Delta G^{\ominus}_{\mathrm{ADS}} = (\Delta G^{\ominus}_{\mathrm{ADS}})_{\mathrm{p.z.c.}} + h(E - E_{\mathrm{p.z.c.}})^2 \tag{1.80}$$

At a mercury electrode, the surface coverage is traditionally deduced from measurement of the surface tension. A more general procedure involves the measurement of the electrode capacitance. The capacitance per unit area is given by:

$$\text{Capacitance} = \frac{\partial Q}{\partial E} \tag{1.81}$$

where Q is the charge density on the electrode surface. It can be measured readily as a function of potential using a.c. techniques and at relatively low frequencies:

$$\text{Capacitance} \propto \frac{\partial \theta}{\partial E} \tag{1.82}$$

Hence, coverage by neutral substrates is readily deduced even for solid electrodes.

All the above models of adsorption, however, assume that all sites on the electrode surface are equivalent. With solid electrodes this is never entirely true; on an atomic scale, the surface cannot be flat and, unless the electrode is a single crystal, a variety of lattice orientations will be exposed to the solution. Hence, the surface is likely to contain a number of different types of sites, each with a characteristic $\Delta G^{\ominus}_{\mathrm{ADS}}$. Indeed, it is because adsorbates interact first at sites where the free energy of adsorption is most negative that organic additives may be used to control metal deposition; adsorption occurs at lattice imperfections (e.g.

screw dislocations) where otherwise the rate of deposition would be most rapid, creating an uneven thickness of the electroplated layer.

1.4.2 The effect of a neutral adsorbate on an electron transfer process

The presence of an organic molecule capable of adsorbing on the electrode surface will, in general, cause a decrease in the rate of electron transfer for a couple O/R. The explanation will depend on the most appropriate model for the electron transfer process.

Thus, if electron transfer occurs while an adsorbate layer remains on the electrode surface, the oxidation or reduction must occur by the transfer of an electron over a far greater distance. Figure 1.6 showed the potential distribution on a molecular scale close to the electrode and it was noted that only the potential difference $\phi_2 - \phi_s$ (not $\phi_m - \phi_s$) was available to drive electron transfer; the adsorbate layer will cause a substantial decrease in the potential difference available to drive the electron transfer. In the limit, the presence of an adsorbate may totally prevent electron transfer and then only a fraction $(1-\theta)$ of the electrode is available for the O/R couple. An alternative model would require displacement of adsorbate by O or R before electron transfer can occur and the extent of such a process will depend on $\Delta G^{\ddagger}_{ADS}$. Finally, the adsorbate may also be able to act as a ligand for O and R and complex formation at the electrode surface may increase or decrease the kinetic parameters for electron transfer.

These are the roles of additives for corrosion inhibition and the modification of electrodeposits. For electrode reactions where the overall sequence includes chemical steps, however, the role of the adsorbate layer may be quite different. Rather, it may be to create an environment which is more favourable than the bulk solution for a particular reaction, e.g. the proton availability may be different; it is not unusual for an adsorbate layer to be relatively aprotic compared with an aqueous electrolyte and such modifications of electrode processes have been used in the electrosynthesis of adiponitrile (Chapter 6). The presence of tetraalkylammonium ions in the electrolyte leads to the desired hydrodimerization of acrylonitrile to adiponitrile. In their absence, only propionitrile is formed. It is thought that the tetraalkylammonium ions adsorb on the cathode surface and create an environment where an intermediate is protected from protonation.

1.4.3 Adsorption in the presence of electron transfer

When the electroactive species or an intermediate adsorbs onto the electrode surface, the adsorption process usually becomes an integral part of the charge-transfer process and therefore cannot be studied without the interference of a faradaic current. In this situation, surface coverages cannot be measured directly and the role of an adsorbate must be inferred from a kinetic investigation. Tafel slopes and reaction orders will deviate substantially from those for a simple

electron transfer process when an adsorbed intermediate is involved. Moreover, the kinetic parameters, exchange current or standard rate constant, are likely to become functions of the electrode material and even the final products may change. These factors will be discussed further in section 1.5.

It is possible in a few cases to take data for the coverage by the electroactive species at potentials prior to the onset of electron transfer and to extrapolate such data into the potential region where oxidation or reduction occurs. In any case, the concept of competition between species for sites on the electrode surface, the form of the isotherms and the qualitative variation in the coverage with potential, are likely to remain valid. Hence, the earlier discussion remains a useful guide even when there is a faradaic current.

1.4.4 Dissociative adsorption

The adsorption of some molecules occurs by a more complex process where bonds are broken and the fragments adsorb at different sites on the electrode surface. In the case of small molecules, such as oxygen, this may remain a relatively simple process:

$$O_2 \longrightarrow 2O_{ADS} \tag{1.83}$$

$$H_2 \longrightarrow 2H_{ADS} \tag{1.84}$$

although the bond energies of such diatomic gases are high and few materials will have all the characteristics essential to make these steps effective in the catalysis of oxygen reduction or hydrogen oxidation. With organic molecules, however, the adsorption process, e.g.

$$CH_3OH \xrightarrow{Pt} H_{ADS} + CH_2OH_{ADS} \longrightarrow 2H_{ADS} + CHOH_{ADS}$$

$$\longrightarrow 3H_{ADS} + CHO_{ADS} \longrightarrow 4H_{ADS} + CO_{ADS} \tag{1.85}$$

must be much more complex and involve a number of bond-breaking processes. The overall reaction is unlikely to be reversible and coverages by each species will be determined by kinetic rather than thermodynamic factors. Even so, such dissociative adsorption processes are very important and are at the heart of the electrocatalysis necessary for fuel cells because the direct loss of an electron from potential fuels always requires a substantial overpotential.

The coverage by such organic fragments cannot be described in terms of isotherms (since the adsorption is not an equilibrium process) and, indeed, it is usually difficult to identify with certainty the structure of the adsorbed species. In the past, the information available has been deduced from measurement of the charges for:

1. The adsorption process.
2. The complete oxidation of all fragments on the surface; this is measured by sweeping or stepping the potential to a very positive value.

3. The adsorption of hydrogen in the presence and absence of the organic adsorbate; the ratio indicates the fraction of the total surface covered by fragments.

More recently, *in situ* spectroscopic techniques have been developed which allow the direct identification of more stable intermediates. The analysis of all data is complicated by the probable existence of a mixture of fragments on the surface and, in addition, the fractional coverage by each species may change with time. Indeed, this is the basis of the phenomenon of electrode poisoning – the poison is a fragment which is too strongly adsorbed and, hence, only oxidized very slowly. Thus, although many metals are, initially, excellent catalysts for the complete oxidation of organic fuels to carbon dioxide, few maintain their activity for an extended period because of the accumulation of a poison during the anodic oxidation of the fuel. *In situ* infra red spectroscopy has shown that with most fuels the poison is adsorbed CO.

1.5 ELECTROCATALYSIS

Many electrode reactions only occur at a measurable rate at very high overpotentials, i.e. the exchange current density is low. The art of electrocatalysis is to provide alternative reaction pathways which avoid the slow step and permit the reaction to be carried out with a high current density close to the reversible potential, i.e. to increase the exchange current density.

In general, the catalyst may be an adsorbed or a solution-free species. Although there are many examples of the latter (e.g. the epoxidation of propylene catalysed by Br^-)

$$Br^- + H_2O - 2e^- \longrightarrow HOBr + H^+ \tag{1.86}$$

$$HOBr + CH_3{-}CH{=}CH_2 \longrightarrow CH_3\underset{\displaystyle OH}{\underset{|}{CH}}{-}\underset{\displaystyle Br}{\underset{|}{CH_2}} \tag{1.87}$$

$$CH_3{-}\underset{\displaystyle OH}{\underset{|}{CH}}{-}\underset{\displaystyle Br}{\underset{|}{CH_2}} + OH^- \longrightarrow CH_3\overset{\displaystyle O}{\overset{/\backslash}{CH}}{-}CH_2 + H_2O + Br^- \tag{1.88}$$

Such reactions are probably better classified as indirect electrode reactions (Chapter 6). Only reactions catalysed by adsorbed species will be considered here. Certainly, many such reactions (e.g. Cl_2, O_2 and H_2 evolution) are very important in electrochemical technology.

1.5.1 The hydrogen evolution reaction

The hydrogen evolution reaction is historically very important since its study has contributed much towards our understanding of electrode reactions. It is

also very important in electrochemical technology and is met in corrosion, fuel cells and as a cathode reaction in water electrolysers, some chlorine cells and other oxidation processes.

In acid solution the overall reaction is:

$$2H^+ + 2e^- \longrightarrow H_2 \tag{1.89}$$

and in neutral and basic media:

$$2H_2O + 2e^- \longrightarrow H_2 + 2OH^- \tag{1.90}$$

This discussion will assume an acidic medium, although the modifications to include higher pH are obvious. The adsorbed hydrogen atom is formed by the reaction:

$$H^+ + e^- \longrightarrow H_{ADS} \tag{1.91}$$

and it plays a key role in the mechanism and kinetics of the hydrogen evolution reaction. *In situ* spectroscopic techniques and methods such as cyclic voltammetry give definitive evidence for the formation of adsorbed hydrogen atoms on some metals, particularly the platinum metals. At such metals, the exchange current density for H_2 evolution is relatively high (Table 1.2). On other metals (e.g. Hg, Cd and Hg), there is no evidence for adsorbed intermediates and the exchange current densities are low, i.e. a very large overpotential is needed in order to see significant H_2 evolution.

It should be noted that reaction (1.91) can occur more easily than H_2 gas evolution. It can occur at a potential $-\Delta G_{ADS}/F$ positive to the equilibrium potential for reaction (1.89). Also, the existence of adsorbed hydrogen atoms makes possible alternative reaction routes. Two mechanisms are generally considered:

(A) $H^+ + e^- + M \longrightarrow M\text{–}H$ (1)

$2M\text{–}H \longrightarrow 2M + H_2$ (2)

Table 1.2 Exchange current densities for the hydrogen evolution reaction in 1 mol dm^{-3} H_2SO_4

Metal	$-\log(I_0/A\ \text{cm}^{-2})$	Metal	$-\log(I_0/A\ \text{cm}^{-2})$
Ag	5.4	Ni	5.2
Au	5.5	Pb	12.2
Cd	11.0	Pd	2.3
Co	5.2	Pt	3.6
Cr	7.4	Rh	2.8
Cu	6.7	Ru	2.1
Fe	6.0	W	7.0
Hg	12.5	Zn	10.5

$$\text{(B)}\quad H^+ + e^- + M \longrightarrow M\text{–}H \tag{1}$$

$$M\text{–}H + H^+ + e^- \longrightarrow M + H_2 \tag{3}$$

where the adsorbed hydrogen is written in a way emphasizes the importance of the electrode material in determining the properties of the surface bond. It may be noted immediately that both mechanisms require the formation and then the cleavage of an M–H bond. Hence, while a variation of the cathode so as to increase the free energy of adsorption will favour the formation of the adsorbed species, it will have the opposite effect on the second step in the overall process. As a result, it is to be expected that the maximum rate of hydrogen evolution will occur at intermediate values of ΔG_{ADS} which lead to a significant, but not monolayer, coverage by adsorbed hydrogen atoms. This is, indeed, observed and Fig. 1.17 shows a 'volcano plot' of exchange current density vs. the free energy of hydrogen atom adsorption for a series of metal cathodes. Similar dependences of rate parameters on the free energy of adsorption of an intermediate are common in gas-phase catalysis. Experimental studies of hydrogen evolution at many cathodes have shown a wide range of exchange current densities as well as different Tafel slopes and dependences on proton concentration. This is typical of reactions which involve adsorbed species. In the following paragraphs the way to derive the Tafel slopes and reaction orders expected for mechanisms (A) and (B) will be outlined.

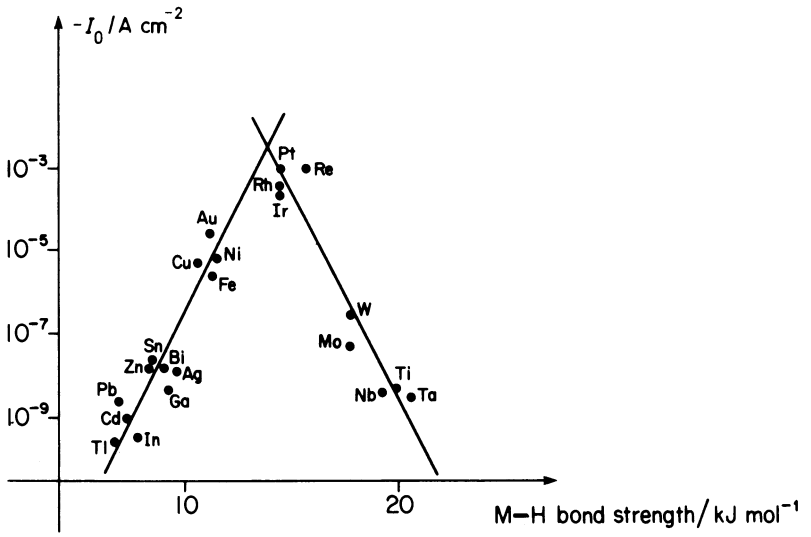

Fig. 1.17 Dependence of exchange current density for the hydrogen evolution reaction on the strength of the metal–hydrogen bond formed in the electrode reaction. (*Data from*: Trasatti, S. (1972) *J. Electroanal. Chem.* **39**, 163.

(*a*) *Reaction* (1) *as the rate-determining step*

The formation of adsorbed hydrogen as the first step is common to both mechanisms (A) and (B). Hence, when it is the rate-determining step, we cannot distinguish between the two mechanisms. The rate of reaction (1) (and, hence, of H_2 evolution if it is the slowest step in the overall reaction) may be written:

$$\vec{V}_1 = \vec{k}_{(1)} c_{H^+} (1-\theta) \tag{1.92}$$

where $\vec{k}_{(1)}$ is rate constant for reaction (1) in the forward direction, potential-dependent because the reaction involves the transfer of an electron. The rate depends on the concentration of protons in solution c_{H^+} and the free surface available for adsorption of further hydrogen atoms $(1-\theta)$. Moreover, if reaction (1) is slow compared to reactions (2) or (3), the adsorbed hydrogen cannot be present at high coverage and one can use the approximation $(1-\theta) \rightarrow 1$. Then:

$$\vec{V}_{(1)} = \vec{k}_{(1)} c_{H^+} \tag{1.93}$$

and the current for H_2 evolution is given by:

$$\begin{aligned} -I &= F\vec{k}_{(1)} c_{H^+} \\ &= F\vec{k}_{11} c_{H^+} \exp -\left(\frac{\alpha_1 F}{RT} E\right) \end{aligned} \tag{1.94}$$

where $\vec{k}_{11}$ is the value of $\vec{k}_{(1)}$ at $E=0$. Note that throughout this discussion of the H_2 evolution reaction, we shall assume that for each elementary reaction, $\alpha_A + \alpha_C = 1$ and we shall write the cathodic transfer coefficient α_n where n is the reaction concerned. Reaction (1.94) may be converted to the form:

$$\log -I = \log F\vec{k}_{11} + \log c_{H^+} - \frac{\alpha_1 F}{2.3RT} E \tag{1.95}$$

and it may be seen that the reaction is first order in proton and if $\alpha_1 = 0.5$, then the Tafel slope $\partial(\log -I)/\partial E$ is $(120\ \text{mV})^{-1}$.

(*b*) *Mechanism* (*A*), *rate-determining step reaction* (2)

In this situation, the current density for H_2 evolution is given by:

$$-I = 2F\vec{k}_2 \theta^2 \tag{1.96}$$

where $\vec{k}_2$ is a chemical rate constant, i.e. independent of potential. The coverage by H atoms θ can in the steady state be found by noting that $\partial\theta/\partial t = 0$, or:

$$\vec{V}_1 = \overleftarrow{V}_1 + \vec{V}_2 \tag{1.97}$$

If, in fact, $\vec{V}_2 \ll \vec{V}_1$ under all conditions and close to the equilibrium potential $\vec{V}_2 < \overleftarrow{V}_1$, and then we can treat reaction (1) as a pre-equilibrium. Using $\vec{V}_1 = \overleftarrow{V}_1$ gives:

$$\vec{k}_1 c_{H^+} (1-\theta) = \overleftarrow{k}_1 \theta \tag{1.98}$$

and, since both $\vec{k}_1$ and $\overleftarrow{k}_1$ are potential-dependent:

$$\vec{k}_{11}\exp\left(-\frac{\alpha_1 E}{RT}E\right)c_{H^+}(1-\theta)=\overleftarrow{k}_{11}\exp\left(\frac{(1-\alpha_1)F}{RT}E\right)\theta \tag{1.99}$$

which rearranges to:

$$\theta=\frac{K_1 c_{H^+}\exp\left(\frac{-F}{RT}E\right)}{1+K_1 c_{H^+}\exp\left(\frac{-F}{RT}E\right)} \tag{1.100}$$

where $K_1=\vec{k}_{11}/\overleftarrow{k}_{11}$. Close to the equilibrium potential $K_1 c_{H^+}\exp\left(-\frac{FE}{RT}\right)<1$ and, hence:

$$\theta=K_1 c_{H^+}\exp\left(\frac{-F}{RT}E\right) \tag{1.101}$$

which substituted into equation (1.96) gives:

$$-I=2F\vec{k}_2 K_1^2 c_{H^+}^2\exp\left(\frac{-2F}{RT}E\right) \tag{1.102}$$

and:

$$\log -I=\log 2Fk_2K_1^2+2\log c_{H^+}-\frac{2F}{2.3RT}E \tag{1.103}$$

For this mechanism, therefore, the Tafel slope is $(30\,\text{mV})^{-1}$ and the current varies as the square of the proton concentration.

(*c*) *Mechanism* (*B*), *rate-determining step reaction* (3)
The rate of reaction (3) is given by:

$$\vec{V}_3=\vec{k}_3 c_{H^+}\theta \tag{1.104}$$

since it depends on the concentration of proton and the availability of adsorbed hydrogen atoms; $\vec{k}_3$ is potential-dependent. Two limiting forms of the rate expression are possible at low and high overpotentials.

At low overpotentials, both $\vec{V}_1$ and $\overleftarrow{V}_1$ are much faster than $\vec{V}_3$ and θ can be found by an identical argument to (b) above. Then:

$$-I=2F\vec{k}_{31}\exp-\left(\frac{\alpha_3 F}{RT}E\right)c_{H^+}K_1 c_{H^+}\exp\left(-\frac{F}{RT}E\right) \tag{1.105}$$

$$-I=2F\vec{k}_{31}K_1 c_{H^+}^2\exp\left(-\frac{(1+\alpha_3)F}{RT}E\right) \tag{1.106}$$

and:

$$\log -I = \log 2F\vec{k}_{31}K_1 + 2\log c_{H^+} - \frac{(1+\alpha_3)F}{RT}E \tag{1.107}$$

when, for $\alpha_3 = 0.5$, the Tafel slope is $(40\ \text{mV})^{-1}$.

At high overpotentials, $\vec{V}_3 \gg \vec{V}_1$ and $\vec{V}_1 = \vec{V}_3$.

Therefore:

$$\vec{k}_{11}\exp\left(-\frac{\alpha_1 F}{RT}E\right)c_{H^+}(1-\theta) = \vec{k}_{31}\exp\left(-\frac{\alpha_3 F}{RT}E\right)c_{H^+}\cdot\theta \tag{1.108}$$

and if $\alpha_1 = \alpha_3$, θ is independent of potential. The rate expression for this mechanism is:

$$-I = 2F\vec{k}_{31}c_{H^+}K\exp\left(-\frac{\alpha_3 F}{RT}E\right) \tag{1.109}$$

and:

$$\log -I = \log 2F\vec{k}_{31}K + \log c_{H^+} - \frac{\alpha_3 F}{2.3RT}E \tag{1.110}$$

The reaction at high overpotentials has become first order in proton with a Tafel slope of $(120\ \text{mV})^{-1}$.

Table 1.3 summarizes the conclusions from these calculations for the mechanisms considered. The different mechanisms lead to different reaction orders and Tafel slopes, but the experimental data are not completely diagnostic because different mechanisms lead to the same values. Moreover, we have not considered all the likely possibilities, e.g. the discussion above assumes the coverage by adsorbed hydrogen follows the Langmuir isotherm; the use of other isotherms would lead to different conclusions.

From the viewpoint of electrochemical technology, however, the major point to be emphasized is that the choice of the electrode material influences exchange current density, Tafel slope and reaction order with respect to proton. Hence,

Table 1.3 Tafel slopes and reaction orders calculated for some mechanisms of the H_2 evolution reaction

Mechanism	Rate-determining step	Over-potential range	Tafel slope/mV^{-1}	Reaction order in H^+
(A) or (B)	1	All	120	1
(A)	2	Low	30	2
(B)	3	Low	40	2
(B)	3	High	120	1

the selection of cathode material can have a large effect on the observed overpotential for H_2 evolution. This conclusion is general for reactions involving adsorbed intermediates and is at the heart of electrocatalysis. The relation between electrocatalysis and cell energetics is discussed in Chapter 2.

1.5.2 Oxygen reduction

In almost all applications of the oxygen reduction reaction (but not H_2O_2 production!), it is desirable to select conditions where the complete $4e^-$ reduction occurs, i.e. in acid solution:

$$O_2 + 4H^+ + 4e^- \longrightarrow 2H_2O \tag{1.111}$$

or in basic solution:

$$O_2 + 2H_2O + 4e^- \longrightarrow 4OH^- \tag{1.112}$$

and at pH 0 and 14, the formal potentials of reactions (1.111) and (1.112) are +1.23 V and 0.39 V (vs. NHE) respectively. The formal potentials for the O_2/H_2O_2 couple are +0.68 V and −0.16 V at pH 0 and 14 respectively.

Particularly in acid solution relatively few cathode materials, capable of operating at these potentials, are available because most metals dissolve anodically at potentials well negative to the equilibrium potential for oxygen reduction. Moreover, even with the more noble metals which do not dissolve, the study of oxygen reduction is hampered by oxidation and/or reduction of their surface within the potential range of interest; this makes the experimental data for oxygen reduction less precise and perhaps also leads to a change in mechanism when the electrode surface changes from metal oxide to metal or vice versa. In this respect the oxygen evolution reaction is easier to study since it generally occurs on a fully oxidized anode surface, and for such surfaces its study gives information relevant to its reverse reaction, providing the principle of microscopic reversibility may be applied.

In any case, the oxygen electrode is a complex system and the overall reaction in either direction requires the transfer of four electrons and four protons. As a result, it is possible to write a very large number of reaction mechanisms but they are essentially of two types:

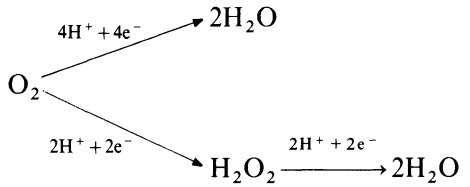

(A)

(B)

Route (A) leads to water as the first identifiable product while in route (B) the reduction to water clearly occurs in two steps with hydrogen peroxide as an intermediate. Indeed, in some conditions the reaction stops at the hydrogen

peroxide stage, (e.g. at mercury or carbon, oxygen is reduced in two well defined steps, separated by up to 1V), and in this mechanism catalysts may well have the role of ensuring the rapid and total disproportionation of the hydrogen peroxide to oxygen and water. Route (A) implies the cleavage of the O–O bond by dissociative adsorption at an early stage in the reduction whereas in route (B), the first step is the reduction of oxygen to superoxide (or HO_2^+ to HO_2^-). The two types of mechanism are most readily distinguished by an experiment with a rotating ring-disc electrode. Oxygen is reduced at a rotating disc of the active material and any hydrogen peroxide formed is monitored on a ring electrode surrounding the disc and separated from it by a thin layer of insulator; in general, the disc and ring electrode may be controlled independently. At least fourteen reaction pathways for oxygen reduction have been considered and, taking into account the various possible rate-determining steps, the anodic and cathodic Tafel slopes for 53 mechanisms for the oxygen electrode system have been established. In these circumstances, reliable kinetic parameters can seldom be obtained. Certainly, comparison between electrode materials, where the products and mechanisms may be different, is not possible. Even so, the reduction of oxygen is clearly always a slow reaction and the best of the metals platinum, requires an overpotential of over 0.3V for a reasonable current density. At other metals (e.g. Hg) and some carbons, the overpotential may need to be of the order of 1.5 V.

Route (A) offers the best chance of effective electrocatalysis and is also necessary to ensure the full free-energy output from the $4e^-$ reduction and an approach to the equilibrium potential of 1.23V. The O–O bond in oxygen is, however, strong and it is therefore not surprising that good catalysts have proved difficult to find. Recent research studies have concentrated on various mixed oxides (e.g. spinels, bronzes and perovskites) and transition-metal complexes, e.g. metal porphyrins. In general, such catalysts are mixed with, or deposited onto, a high-surface-area carbon and, even in this high-area form, it has to be admitted that they seldom approach the performance of the more active metal catalysts. The most promising materials are the oxide, $NiCo_2O_4$ and a dimeric, face-to-face porphyrin with two cobalt ions. Both these catalysts give electrodes where oxygen reduction occurs in the potential range from $+800$ to $+600$ mV in acid media. This is comparable with the performance of massive precious metal; the best practical oxygen cathode, however, remains a high-surface-area platinum.

1.5.3 The design of electrocatalytic electrodes

It is not sufficient for an electrode material to exhibit good catalytic properties under laboratory conditions. It is often essential in an industrial process for the electrode to catalyse specifically only one reaction, e.g. it is a prerequisite for an anode for a chlorine cell to oxidize chloride ion at low overpotential but it must also inhibit oxygen evolution since this is the thermodynamically preferred

reaction (Chapter 3). Furthermore, it must be possible to design and construct an electrode from the catalyst material. Since modern catalysts may not be a metal, it may be necessary to mix them with an inert conductor and a binder and press them onto a supporting grid or to develop a technique for coating them onto an inert metal. In practice the electrode may be operated as a porous-gas, or as a gas-evolving, electrode and this will also place additional restraints on the design. Certainly, under the electrolysis conditions, the electrode structure must be physically stable, resistant to corrosion and the catalyst must maintain its activity over a long period of time, i.e. it must not poison.

What factors determine the activity of electrocatalysts and are likely to introduce specificity into an electrode reaction? A complete answer to this question is not possible at the present time and we have certainly not reached the stage where it is possible to design electrocatalysts from theoretical considerations. On the other hand, a number of general principles can be set out. Thus, while metals, alloys, semiconductors (particularly oxides) and complexes have been shown to exhibit catalytic properties, invariably catalysts are based on transition metals and it seems that the design of a catalyst requires the placing of transition-metal ions or atoms in a matrix which serves to optimize their electronic configuration and position with respect to each other.

The dependence of electrocatalysis on adsorption has already been emphasized and therein lies the explanation of the success of transition metals as catalysts; they have unpaired *d*-electrons and unfilled *d*-orbitals which are available to form bonds with the adsorbate. The free energy of adsorption will, however, depend strongly on the number of unpaired electrons per atom and also on their energy levels. Hence, it is not surprising that activity varies with the transition metal and may be modified by alloying or placing in a non-metallic lattice. In the limit, the lattice and the adsorbate may be considered as ligands in a metal complex. The observation that the rate of hydrogen evolution passes through a maximum when plotted vs. free energy of adsorption is equally true of other electrocatalytic processes and, hence, the objective should be to tailor the electronic environment of the metal to obtain the free energy of adsorption which leads to the maximum current density.

In addition to electronic factors, the geometric arrangement of catalyst centres will also be important. All electrocatalytic reactions involve the formation or cleavage of bonds and it is likely that such processes will be increased in rate substantially if they can occur as concerted reactions, i.e. in the reduction of chlorine, the bond between the surface and the chlorine atoms forms at the same time as the Cl–Cl bond is broken:

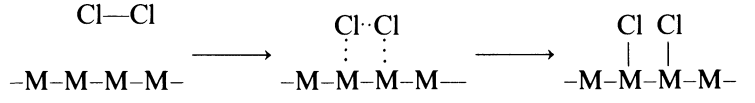

(1.113)

Such mechanisms require the correct spacing of the adsorption sites. Here, the

sites are written as the metal atoms themselves but it is also possible that adsorption occurs at interstitial positions, although the argument would remain the same. The adsorption of larger molecules may involve adsorption at more than one site and this will also require the appropriate site spacings.

The activity of electrocatalysts can be enhanced further by special sites on the surface and step, kink and edge sites, lattice vacancies, grain boundaries and dislocations have all been suggested to have a beneficial effect. This may be because they lead to sites with different free energies of adsorption or because they create unusual spacings or arrangements of potential adsorption sites.

To summarize the conclusions concerning catalyst design we shall again look at oxygen reduction: how can we set out to find the most suitable catalysts? Certainly, it is desirable to promote the dissociative adsorption of oxygen to give M–O bonds of intermediate strength so that the oxygen atom can readily be reduced to water.

These processes will require the correct spacing of catalyst sites and the optimum electronic energy levels to ensure the appropriate free energy of adsorption. In addition, it may be advantageous for the oxygen molecule to be able initially to form a π complex at the surface and the final step may be assisted by polarization of the M–O bond. The various stages in the overall process may require different properties from the transition metal and one way of facilitating this is to use transition metals where the oxidation state may readily be altered. It must be said, however, that few catalysts lead to a lower overpotential than platinum metal and this will also be the case for hydrogen evolution, the oxidation of ethylene, methanol and carbon monoxide and chlorine evolution. Hence, our search is limited largely to catalysts with similar performance but which are cheaper and/or avoid the formation of poisons on the surface. Present studies largely relate to non-stoichiometric oxides and metal complexes where inorganic chemistry would indicate that the oxide lattice or ligands may be tailored closely.

Once the catalyst is developed, it remains necessary to construct an electrode incorporating it. In electrocatalytic processes, the real surface area of the electrode is important and the measured exchange current density can be increased by preparing a rough or otherwise high-area surface (this is in contrast to mass transfer controlled reactions where only the apparent geometric area matters, provided the surface roughness is small compared with the diffusion layer thickness). Hence, a variety of procedures for obtaining high-surface-area electrodes have been developed; these include spray-coating, sputtering, thermal decomposition of solutions of a catalyst or a catalyst precursor and painting dispersions of the appropriate crystallite size, e.g. satisfactory platinum electrodes have been manufactured with very low loadings of the active metal, such as a few milligrams per gram of carbon powder.

When the reactant is a low-solubility gas it is advantageous to minimize mass-transport effects by employing a porous-gas electrode. The electrode is manufactured by compressing catalyst, conducting powder (e.g. graphite) and perhaps a

hydrophobic material (e.g. PTFE) onto a conducting grid and the gaseous reactant is passed over the back of the electrode so that the electrode reaction occurs at a three-phase interface between gas, solution and electrode material within the electrode structure. When the product is a gas it is more common to use a shaped electrode ('louvred', a mesh, or a 'cheese-grater') where the gas passes to the back of the electrode and away from the current path where it can increase cell resistance.

1.6 PHASE FORMATION IN ELECTRODE REACTIONS

Many of the electrode reactions of interest to electrochemical technology involve the formation of a new phase. This may be a metal resulting from the reduction of an ion in solution (as in electroplating or electrowinning), an oxide formed by dissolution (e.g. anodizing) or by oxidation of a solution-free species (e.g. PbO_2 from a nitrate bath), other metal salts from oxidation of an electrode (e.g. $PbSO_4$ deposition from lead during the discharge of a lead–acid negative plate) or by the reduction of another phase (e.g. $PbSO_4$ from the reduction of PbO_2 in a lead–acid positive plate) or a gas (e.g. chlorine in a chlor-alkali cell or hydrogen and oxygen in a water electrolyser).

Such electrode reactions frequently have a unique feature, namely the *I–E* characteristics before and after the formation of the new phase are quite different. For example, the *I–E* curves for a solution of copper ions at an inert electrode (e.g. carbon) and the same electrode after the formation of a thin layer of copper will be totally different, the latter being similar to a bulk copper cathode. Similarly, the *I–E* curve for a recharging lead–acid positive electrode will change dramatically once the lead sulphate paste contains microscopic centres of lead dioxide.

These features are due to the difficulties of nucleation, i.e. of forming small centres of a new phase. Throughout nature, nucleation is an improbable event; small particles have a high area : volume ratio and, hence, the positive surface-free energy exceeds the negative lattice energy and the nuclei should redissolve. Typical consequences of the difficulty of nucleation are the stability of supercooled water and the need to seed when recrystallizing many organic compounds.

The formation of a thick electrodeposit requires several stages: (1) nucleation; (2) growth of the isolated centres; (3) overlap of the centres into a continuous layer; and (4) thickening of the layer. Each step will influence the properties of the final layer.

In electrochemistry, nucleation is generally forced by the application of a large overpotential, and once centres are formed which are big enough to be stable, they grow very rapidly if such an overpotential is maintained. Each nucleus may grow two-dimensionally leading only to a monolayer, or three-dimensionally as hemispheres or cones and the rate determining step may be electron transfer or mass transport. Overlap occurs as the centres get large

enough to merge and this leads to a continuous layer. The nature of the thickening process depends on the properties of the layer.

In the deposition of a metal, thickening is a relatively simple process. The metal ion M^{n+} will be transported through the electrolyte solution to the surface of the growing layer where it will be reduced to a metal adatom. The main question of interest is how this atom becomes incorporated into the metal lattice and how the structure of the deposit depends on the rate of formation of metal atoms, i.e. current density. These questions will be discussed in detail in Chapter 8, section 8.1 and, at this stage, we shall only note that, if the equilibrium lattice is to result, it will be necessary for the discharged atoms to diffuse across the surface to special sites (e.g. edge or kink sites or screw dislocations) where the lattice can reproduce itself in an orderly way. Certainly, during this stage in the metal deposition process, the *I–E* characteristic will have the form of the Tafel equation – the current will increase exponentially with potential and be independent of time – and the phenomena occurring during nucleation and early stages of growth only affect the growth to the extent that they create the surface on which the later stages take place.

If the deposit is an oxide or an anodic film, the mechanism of the growth process is quite different and dependent on: (1) whether the film is an electronic or an ionic conductor; and (2) whether both components of the film come from the solution or, as is much more common, one lattice component is supplied by the solution and the other by the electrode.

In general, for an anodic film to grow on an electrode surface, an ion must be transported through the layer; if the mobile species is a cation, lattice growth occurs at the film–electrolyte interface, while if it is an anion the growth will occur at the electrode–film boundary. At ambient temperatures the transport of an ion through a solid phase is a very slow process and, hence, is likely always to be the rate-determining step. Two limiting growth laws, for high and low fields, are observed. In the latter case, it is assumed that the differene in electrochemical potential between two successive lattice positions is small compared with RT so that transport is essentially non-activated. The ion flux and, hence, the current, is proportional to the electrochemical potential gradient in the film and at a fixed potential; this will depend only on the thickness x of the film. Therefore the rate of growth is given by:

$$dx/dt = a/x \tag{1.114}$$

where a is a constant and it can be seen by integration that the thickness of the film will increase with the square root of time. When a high field is necessary to bring about ionic transport, the elementary ionic jumps are activation-controlled and the current will increase exponentially with field strength; as a result the thickness of the film varies with log t. Electronically conducting layers behave very differently because they cannot support appreciable rates of ionic migration. Hence, if they are coherent and protect the metal electrode completely from contact with the electrolyte solution, growth cannot occur.

1.7 CHEMICAL REACTIONS

In electrosynthesis, the electrode processes are usually complex and involve a sequence of coupled chemical reactions. In general, the role of the electron transfer process is to generate a reactive intermediate which then undergoes its normal chemistry in the environment in which it finds itself. In other words, the electrode reaction may be considered to occur in two distinct stages:

$$\text{Starting material} \xrightarrow{\pm e^-} \text{intermediate(s)} \xrightarrow{\text{chemical steps}} \text{product(s)} \qquad (1.115)$$

where the chemistry may occur in the adsorbed state on the electrode surface or in the solution phase as the intermediate(s) are being transported away from the electrode surface.

Selective and imaginative synthesis is dependent on controlling both stages and recognizing the possibilities for forming key intermediates as well as using them constructively. Electrochemical parameters such as potential influence only the first step; appropriate control will ensure the generation of a single, dominant intermediate and also the rate at which it is formed. The selectivity and rate of the second step will depend on the environment. If the chemistry is occurring in solution, then the choice of solvent and the concentration of species added to trap the intermediates are the key parameters. Typical intermediates involved in electrode reactions are radicals, carbenium ions, carbanions, ion radicals, 17 or $19e^-$ transition metal species, etc. and it is always to be expected that the products will be the same as when the intermediates are formed by alternative chemical methods in the same medium. It is commonly much more difficult to control the chemistry than the formation of the intermediate; it is possible to form very reactive intermediates but often they lead to a mixture of products.

Even if the chemistry occurs in solution and unless the intermediates are very stable, they will be consumed within a reaction layer very close to the electrode surface. This reaction layer overlaps the diffusion layer where concentrations are a function of distance from the electrode surface and also the hydrodynamic layer where the solution movement is influenced by the presence of the surface. It can therefore be important to ensure strong mixing between the reaction layer and the bulk solution so that the reactive intermediate sees a more uniform environment as it diffuses away from the electrode and to avoid large changes in, for example, pH, within the reaction layer. Such mixing is achieved by using strongly stirred solutions, high flow rates and turbulence promoters.

Syntheses via both surface and homogeneous chemistry are important in electrochemical technology. When the reactions occur on the surface, the most important factor will be the strengths of the electrode–adsorbate bonds and, thus, the electrode material. Examples of such reactions would include Cl_2, O_2 and H_2 evolution as well as the Kolbé reaction and electrocatalytic hydrogenation. There are many examples of syntheses where the chemistry occurs in solution and a selection will be discussed in Chapter 6.

1.8 THE PROPERTIES OF ELECTROLYTE SOLUTIONS

It will already be clear that the properties of the electrolyte solution within the electrolysis cell contribute to its characteristics. Most obviously, the conductivity determines the cell resistance but, in addition, the properties of the solvent and the electrolyte determine their interaction with the electroactive species and thereby influence the electrode reactions. An extensive discussion of the physical chemistry of electrolyte solutions is outside the scope of this book and this section only seeks to emphasize the most important features.

The conductivity of an electrolyte solution is a key property. It is easily measured with an a.c. device and its detailed study is responsible for much of our knowledge of electrolyte solutions. The electrolytic conductivity κ is calculated from the resistance of the solution between two electrodes, area A and separation S;

$$\kappa = \frac{1}{R}\frac{S}{A} \tag{1.116}$$

Some illustrative conductivities are shown in Table 1.4. The table reports values for electrode materials, aqueous solutions and some lithium salts in various solvents. Of course, electrode materials are partly selected because of their high conductivity. However, some values are reported here to note the variation of conductivity between the highly conducting metals, Cu and Al, and some other metals, particularly Hg, and the relatively poorly conducting graphite. Also, the large difference in conductivity between electrode materials and electrolyte solutions and between the aqueous and non-aqeuous solutions should be noted.

Water has at least three unusual features which combine to give it quite unique solvent properties: (1) water molecules are able to H bond with neighbours and this leads to highly structured solvent; (2) it self-ionizes to a small extent so that water always contains a low concentration of OH^- and H^+; perhaps, more importantly, it can act as both a proton acceptor or proton donor; and (3) water is a small molecule with a substantial dipole; hence, it tends to interact electrostatically with charged species and is able to solvate most ions. Particularly with small cation (e.g. H^+, Li^+ and Na^+) the free energy of hydration is very large. It is this final property which is responsible for the extensive dissociation of most salts in aqueous media and, hence, the high conductivities. On the other hand, at high electrolyte concentrations, the electrolytic conductance is not proportional to the concentration, and this is taken to indicate ion pairing or multiple-ion association between solvated species of opposite charges.

Non-aqueous solvents are unable to solvate ions to the same extent as water and, hence, there is commonly incomplete ionization. When comparing solvents, two factors should be considered: (1) the ability of the solvent to interact with ions; (2) the viscosity, since it determines the ease with which ions may move through the solution. It is, for example, the second factor which causes the low conductivity of propylene carbonate solutions despite its high value of dielectric

Table 1.4 Electrolytic conductivities measured at 298 K

Electrode materials (Busbars)	$\kappa/\Omega^{-1}\,cm^{-1}$	$\rho/g\,cm^{-3}$
Cu	5.6×10^5	8.9
Al	3.5×10^5	2.7
Pt	1.0×10^5	11.3
Pb	4.5×10^4	11.4
Ti	1.8×10^4	4.5
Hg	1.0×10^4	13.5
Graphite	2.5×10^2	2.3

Typical aqueous electrolytes	$\kappa/\Omega^{-1}\,cm^{-1}$		
	0.1 mol dm^{-3}	1 mol dm^{-3}	10 mol dm^{-3}
NaCl	0.011	0.086	0.247
KOH	0.025	0.223	0.447
H_2SO_4	0.048	0.246	0.604
CH_3COOH	0.0004	0.0013	0.0005

Solutions of lithium salts in various solvents	$\kappa/\Omega^{-1}\,cm^{-1}$
1 mol dm^{-3} LiCl in H_2O	0.073
1 mol dm^{-3} $LiClO_4$ in H_2O	0.071
0.66 mol dm^{-3} $LiClO_4$ in propylene carbonate	0.005
1.16 mol dm^{-3} $LiClO_4$ in dimethylformamide	0.022
1.6 mol dm^{-3} $LiAsF_6$ in tetrahydrofuran	0.016

constant. From a practical viewpoint, the low values of conductivity in non-aqueous solvents is a major reason for the preference for aqueous media.

Further advances in the analysis of conductivity data are usually made by defining a molar conductivity:

$$\Lambda = \kappa/c \tag{1.117}$$

and then plotting Λ vs. $c^{\frac{1}{2}}$. Strong electrolytes are found to give a linear plot according to Kohlrausch's law:

$$\Lambda = \Lambda_0 - K'c^{\frac{1}{2}} \tag{1.118}$$

where Λ_0 is the molar conductivity at infinite dilution and K' is the Kohlrausch constant. Weak electrolytes give non-linear plots. Clearly, the total conductivity of the solution has a contribution from both cations and anions. Hence, knowing the molar conductivities at infinite dilution which have been measured for a large number of electrolytes, it is possible to assign the molar ionic

conductivities at infinite dilution to individual ions (according to Kohlrausch's law of independent ionic migration):

$$\Lambda_0 = \nu_+ \lambda_0^+ + \nu_- \lambda_0^- \tag{1.119}$$

where ν_+ and ν_- are the number of positive and negative ions formed by dissociation of the salt. The molar ionic conductivities at infinite dilution are related to the ionic mobilities u by the expression:

$$\lambda_0 = Fu \tag{1.120}$$

where F is the Faraday constant. As with diffusion coefficients, ionic mobilities will depend on the size of the ion and the viscosity of the medium. The ionic mobilities of group (I) metals reflect the size of the hydrated ions and increase along the series Li^+, Na^+, K^+. The exception is the proton which has a special mechanism for movement in water resulting from the chain structure discussed above which facilitates 'proton-hopping'. It is found experimentally that for most salts, Λ_0 is inversely proportional to the viscosity.

It can also be of interest to define the transport numbers t_+ and t_-, which are the fraction of the current carried by the cation and anion respectively, i.e. for a solution of a single electrolyte:

$$t_+ = \frac{\lambda_0^+}{\lambda_0^+ + \lambda_0^-} \quad \text{and} \quad t_- = \frac{\lambda_0^-}{\lambda_0^+ + \lambda_0^-} \tag{1.121}$$

In practice in most aqueous electrolytes, slightly more than a half of the charge is carried by the anions; the exceptions are acid solutions because of the large value of the transport number for the proton.

Finally in this section, the errors introduced by equating concentrations and activities throughout this book will be examined. For each ion in solution, the activity is defined by:

$$a_+ = \gamma_+ m_+ \quad \text{or } a_- = \gamma_- m_- \tag{1.122}$$

where γ_+ and γ_- are the activity coefficients for the positive and negative ions respectively and m_+ and m_- are their molalities. In fact, the principle deviations from ideality for electrolyte solutions are the electrostatic interactions between ions and it is not possible to separate the effects due to cations and/or anions. Therefore, the system is discussed in terms of mean ionic activities. For the electrolyte:

$$M_{\nu_+} A_{\nu_-} \longrightarrow \nu_+ M^+ + \nu_- A^- \tag{1.123}$$

the mean ionic activity $a_\pm$ is defined by the equation:

$$a_\pm^\nu = a_+^{\nu_+} a_a^{\nu_-} \tag{1.124}$$

where $\nu = \nu_+ + \nu_-$, correspondingly, the mean ionic activity coefficient is defined by:

$$\gamma_\pm^\nu = \gamma_+^{\nu_+} \gamma_-^{\nu_-} \tag{1.125}$$

Table 1.5 Activity coefficients for some electrolytes in aqueous solution at 298 K

	Mean molal activity coefficients in H_2O				
m/mol kg^{-1}	NaCl	KCl	NaOH	H_2SO_4	$LaCl_3$
10^{-3}	0.966	0.965	—	0.830	0.853
10^{-2}	0.904	0.901	0.861	0.544	0.637
10^{-1}	0.780	0.769	0.780	0.265	0.356
1	0.660	0.606	0.680	0.130	0.583
2	0.670	0.576	0.700	0.124	0.954
4	0.780	0.579	0.890	0.171	—

where $\gamma_\pm$ describes the deviation of the electrolyte solution from its standard state – the hypothetical situation where the electrolyte exists at unit molality but has the environment of an infinitely dilute solution, i.e. no ionic interactions. Table 1.5 shows values for five electrolytes in water as a function of concentration. It can be seen that with concentrated solutions, the activity coefficients are always significantly below 1. The deviations are least with 1:1 electrolytes, but even then $a_\pm \simeq 0.65$ when $m_+ = m_- = 1\,\text{mol kg}^{-1}$. It can also be seen that the activity coefficients first decrease with increasing concentration but pass through a minimum and increase again at very high molalities. This increase is thought to be due to the effects of the solvent, much of which becomes 'tied up' by ions.

The discussion, however, would suggest an importance to the errors introduced by equating concentration and activity, which is not always confirmed in practice. This is because one is often concerned with a ratio of activities where the activity coefficients tend to cancel. Also, in some applications of electrochemistry the concentration of electroactive species is low compared with that of the total electrolyte.

In applied electrochemistry, a number of electrode reactions of interest involve gaseous reactants or products (H_2, O_2, F_2, Cl_2, CH_4). The non-ideality of gases is discussed in terms of their fugacity coefficient γ which relates the measured parameter – pressure – to the fugacity, i.e. activity of a gas.

1.9 THE ASSESSMENT OF CELL VOLTAGE

The voltage of an electrolysis cell is given by an expression of the type given in equation (1.17) above:

$$E_{\text{CELL}} = E_e^{\text{C}} - E_e^{\text{A}} - |\eta_{\text{C}}| - |\eta_{\text{A}}| - AIR_{\text{CELL}} \tag{1.126}$$

We are now in a position to see how the cell voltage may be estimated from laboratory measurements. Irrespective of the mechanistic complications which

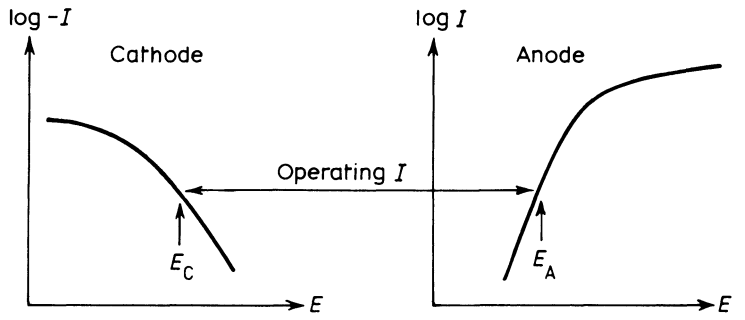

Fig. 1.18 Log *I–E* characteristics for the anode and cathode reactions of an electrolysis cell.

occur in the two electrode processes, it is possible to record an *I–E* curve for each electrode reaction (Fig. 1.18). Provided identical conditions (e.g. electrode materials, temperature, concentrations, mass transport conditions) to the real cell are used, the potentials taken up by anode, E_A, and cathode, E_C, at the operating cell current density may be read from the curves. In other words, equation (1.126) may be written:

$$E_{CELL} = E_C - E_A - AIR_{CELL} \tag{1.127}$$

$$= (E_e^C - |\eta_C|) - (E_e^A - |\eta_A|) - AIR_{CELL} \tag{1.128}$$

In addition, the cell resistance may be calculated from the electrolyte conductivity and the cell dimensions. Hence, all the terms in the cell voltage equation are readily accessible to measurement. This topic is treated in more detail in Chapter 2, Section 2.3.7.

1.10 ELECTROCHEMISTRY AT SURFACES ON OPEN CIRCUIT

So far in this chapter, only electrochemical cells where the two electrodes are clearly identifiable and separate have been considered. There is, however, another type of situation where electrolysis can occur and which is important in technology. This arises whenever a conducting surface stands in an electrolyte medium which contains appropriate electroactive species to support both an oxidation and a reduction on the surface, e.g. consider the electrode reactions occurring simultaneously on the same surface:

$$A + e^- \longrightarrow B \tag{1.129}$$

$$P - e^- \longrightarrow Q \tag{1.130}$$

so that the overall chemical change is:

$$A + P \longrightarrow B + Q \tag{1.131}$$

Clearly, reaction, (1.131) can only occur by any mechanism if it is thermodynamically favourable, i.e. there is a negative-free energy associated with it. Hence, the electrochemical mechanism will be of interest if this reaction is kinetically hindered in a homogeneous solution or if the material of the surface is one of the reactants. In the former case, the surface plays the role of a catalyst, allowing the overall chemical change to occur via a mechanism involving the transfer of electrons to and from the surface. Note that since the surface is on open circuit (there are no external electrical connections) and it cannot retain a net charge, it is essential that the rates of the two electron-transfer reactions (1.129) and (1.130) are equal.

At least in theory, the conducting surface may be completely uniform, when the anodic and cathodic sites will be intimately mixed, unidentifiable and variant with time. In reality, however, it is more common for the anode and cathode reactions to take place at different types of site, distinguishable on a macroscopic, or at least on a microscopic, scale. The differences in surface sites can: (1) arise naturally, (e.g. crystal imperfections or grain boundaries can be very favourable sites for the catalysis of one of the reactions); (2) be designed into the system deliberately, (e.g. when a surface suitable for one of the electron transfer reactions is partly covered by a catalyst for the other); (3) occur accidentally, (e.g. by scratching of a paint- or oxide-covered metal so that the bare metal is partly exposed; or (4) develop during the reaction as, for example, in the creation of pits during corrosion or the creation of nuclei during electroless metal deposition.

The situation prevailing at the conducting surface is probably best understood by considering the log I–E characteristics for the two electrode reactions on the material of the conducting surface (Fig. 1.19). The positions of the Tafel lines for each electrode reaction depend on the equilibrium potential, exchange current density and Tafel slope for that electrode reaction (section 1.1). But the conducting surface must take up the potential where the currents for the two electrode reactions are equal. This open-circuit potential is called a 'mixed potential' since it depends on the thermodynamic and kinetic characteristics of both electrode processes (this contrasts with an equilibrium potential where it is the forward and back processes for the same electron transfer couple which are equal in rate). The overpotentials for the two electron-transfer reactions are also shown in Fig. 1.19. The current density where the two Tafel lines intersect is a measure of the rate at which the overall chemical change will occur while the thermodynamic driving force for reaction (1.131) is the difference between the two equilibrium potentials. Moreover, the figure leads to an understanding of how the properties of the surface may be used to influence the rate of the chemical change in reaction (1.131). Suppose the surface is partly covered by an effective catalyst for the reduction of A to B. Then the position of the Tafel line will shift because more cathodic current will flow at each potential. The two Tafel lines must then intersect at a higher current density and, hence, the reaction A + P will take place more rapidly on the surface (also the open-circuit

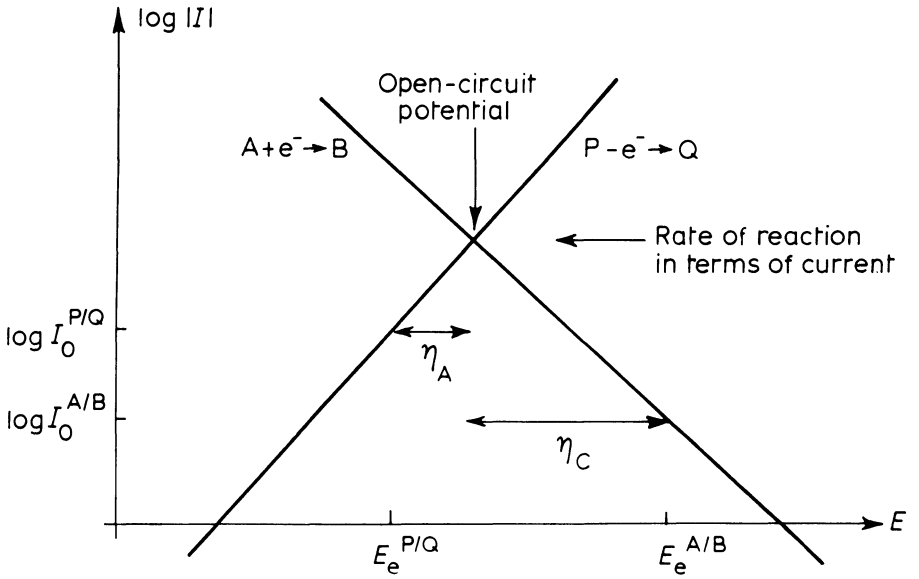

Fig. 1.19 Tafel plots for the reactions $A + e^- \longrightarrow B$ and $P - e^- \longrightarrow Q$ to show how it is possible to estimate the open-circuit potential and the rate of the reaction $A + P \longrightarrow B + Q$ on the surface.

potential will shift to a more positive value, the cathodic overpotential will be decreased but the anodic overpotential is correspondingly increased). In contrast, the addition of an inhibitor for the reduction of A to B will have the opposite effect. The Tafel line will be shifted to lower current densities and, in consequence, the rate of conversion of A + P to B + Q will decrease, the open-circuit potential will be more negative and the cathodic overpotential will get larger. There are, however, some warnings about the use of diagrams such as Fig. 1.19 which should be noted:

1. In all cases, the conversion of A + P to B + Q obviously leads to a change in the concentrations of A, B, P and Q and this leads to a shift in the equilibrium potentials and a change in exchange current densities. Hence, the figure is strictly only correct at one instant in the reaction.
2. The morphology and the catalytic activity of the surface will vary, especially if the reaction involves metal deposition or dissolution and this will again lead to the need for modification of the figure.
3. It has been assumed that mass transport is never important.

Electrolysis on a single surface at its open-circuit potential is the basis of many technologies. For example:

1. It is the concept on which the denuder in the mercury cell process is based (Chapter 3). The reaction of sodium amalgam and water is very slow in the

absence of a catalyst. Hence, the two reactants are passed over a surface which is carbon impregnated with iron or nickel. The oxidation of the sodium occurs readily on the carbon and the transition metal is able to act as a catalyst for the reduction of water to hydrogen. Hence, the conversion of sodium amalgam and water to sodium hydroxide, hydrogen and mercury, thermodynamically a very favourable reaction – is able to occur at a greatly enhanced rate.

2. Many chemical reactions, especially those which involve dissolving metals, can be envisaged to occur via such an electrolysis. For example, the reduction of a nitrobenzene with iron filings almost certainly takes place via a mechanism where the electrochemical reduction of the nitrobenzene and the anodic dissolution of the metal occur simultaneously on the iron surface.
3. Cementation (Chapter 4), is another type of chemical reaction occurring electrochemically; one metal is deposited while another is dissolving.
4. Electroless plating (Chapter 8), involves the deposition of a metal on a surface by reduction of its soluble ion by a chemical reducing agent such as formaldehyde, hypophosphite or hydrazine. Again, this overall chemical change occurs via simultaneous cathodic reduction of the metal ion and anodic oxidation of the chemical reducing agent.
5. Most techniques for the reduction of the rate of corrosion of metals are based on the recognition that corrosion has an electrochemical mechanism (Chapter 10). In this case, the metal surface itself is the anode reactant.

FURTHER READING

1 P. Delahay (1965) *Double Layer and Electrode Kinetics*, Wiley Interscience, New York.
2 J. O'M. Bockris and A. K. N. Reddy (1970) *Modern Electrochemistry*, Vol. 2, Macdonald, London.
3 W. J. Albery (1975) *Electrode Kinetics*, Clarendon Press, Oxford.
4 E. Gileadi, E. Kirowa-Eisner and J. Penciner (1975) *Interfacial Electrochemistry – An Experimental Approach*, Addison-Wesley, Reading, MA.
5 R. Greef, R. Peat, L. M. Peter, D. Pletcher and J. Robinson (1985) *Instrumental Methods in Electrochemistry*, Ellis Horwood, Chichester.
6 J. Koryta and J. Dvorak (1987) *Principles of Electrochemistry*, Wiley, Chichester.
7 J. S. Newman (1973) *Electrochemical Systems*, Prentice-Hall, Englewood Cliffs, NJ.
8 B. S. Massey (1983) *Mechanics of Fluids*, 5th Edition, Van Nostrand Reinhold, New York.
9 E. L. Cussler (1984) *Diffusion – Mass Transfer in Fluid Systems*, Cambridge University Press, Cambridge.
10 D. J. Pickett, (1979) *Electrochemical Reactor Design*, 2nd Edition, Elsevier Scientific, Amsterdam.

11 F. Coeuret and A. Storck (1984) *Eleménts de Génie Electrochimique, Techniques et Documentation*, Tecdoc, Paris.
12 J. O'M. Bockris and S. Srinivasan (1969) *Fuel Cells: Their Electrochemistry*, McGraw-Hill, New York.
13 W. J. Moore (1972) *Physical Chemistry*, 5th Edition, Longman, London.
14 P. W. Atkins (1986) *Physical Chemistry*, 3rd Edition, Oxford University Press, Oxford.

2 Electrochemical engineering

Industry exists to serve the needs of society and, while operating within a legal and social structure, seeks to maximize profits. In general, therefore, it will wish to use the cheapest raw materials and sources of energy (taking into account their projected costs and availability during the expected lifetime of the plant) and by low-cost technology convert them into the desired product. The role of the engineer is to transform the ideas of science into an industrial-scale plant; he must select from the various possible process routes and design the plant for the optimum financial return while recognizing society's concern about the environment and safety (although the cynic might say that these factors, too, are translated into costs for meeting legal specifications for effluents, insurance, etc.). Hence, one cannot discuss industrial processes without constant reference to economics. Moreover, not all processes will have the same objective; some will be designed to produce a high-quality product which will command a high price, while others will manufacture to a lower specifications because the products are used internally in the company or can be sold in large volume, albeit at a lower profit per unit. Nor are circumstances the same in all companies; some will have feedstocks available as a result of other processes when the internal price may be below the market price. Also the cost of transport and energy, particularly electricity, is widely dependent on the site of the plant.

2.1 GENERAL CONSIDERATIONS

Some possible routes for the manufacture of certain products will contain an electrolytic step. The electrolytic route will, however, be chosen only if accountants can be convinced that, in economic terms, it is the best. Furthermore, it must be recognized that the electrolysis commonly will be one stage in a complex sequence and that the economic assessment must consider the overall process, e.g.:

$$\text{Solid salt underground} \longrightarrow \text{liquid } Cl_2 + \text{50\% aqueous NaOH}$$

$$\text{Hydrocarbon} + NH_3 \longrightarrow \text{nylon}$$

$$\text{Sheet metal} \longrightarrow \begin{matrix}\text{kettle; corrosion-resistant finish} \\ \text{with a pleasant appearance}\end{matrix}$$

rather than the electrolytic step (i.e. the brine electrolysis, the cathodic hydrodimerization of acrylonitrile and the electroplating of chromium) in isolation.

Hence, one must seek to optimize the total process and it will sometimes be found advantageous to that process to run the electrolysis under conditions which are non-optimum for the cell if considered alone, e.g. a separator may be included in the cell solely to permit simple isolation of pure anode and cathode products, although the separator will increase cell resistance (hence, energy consumption) and the complexity of the cell design (section 2.6).

The design, characterization and operation of electrolytic devices and processes is the province of electrochemical engineering. This field may be regarded as a relatively young branch of chemical engineering, although inherently it is related to many other disciplines including materials technology and surface science. The electrochemical engineer must, in general, consider aspects of fundamental electrochemistry, industrial-scale electrochemistry and the essential link between them, namely electrochemical technology (Fig. 2.1).

In comparison to chemical engineering, the design, development and operation of electrolytic processes has been slow and qualitative. There are, perhaps, several contributory reason for this:

1. Traditionally, electrochemical engineering has not been a recognized, consolidated subject area for students of chemistry, chemical engineering or materials technology. Early textbooks have concentrated on descriptions of various process technologies rather than unified, quantitative treatments of cell design and performance. There is a lack of appreciation of electrochemical routes amongst chemists and process engineers.
2. Electrochemistry courses have often been limited to topics such as equilibrium-cell thermodynamics, simple redox kinetics and aspects of electroanalytical chemistry, e.g. pH electrodes and conductivity probes. Additionally, these topics are sometimes presented in a fragmented fashion, devoid of unifying principles.
3. Industrially, many of the areas of electrochemical technology have developed in isolation, with little interaction or transfer of concepts, experience or hardware, e.g. batteries, electroplating, corrosion monitoring and chlor-alkali processing are often viewed as entirely separate disciplines, each with its own technology, mythology and market.
4. Theoretical treatments of electrochemical reaction engineering, mathematical modelling of reactors and comparative performance of cells have only recently been developed.
5. The specialist knowledge, hardware and personnel for electrochemical engineering ventures are sometimes in short supply.
6. As a processing technique, electrochemical routes are strongly dependent on

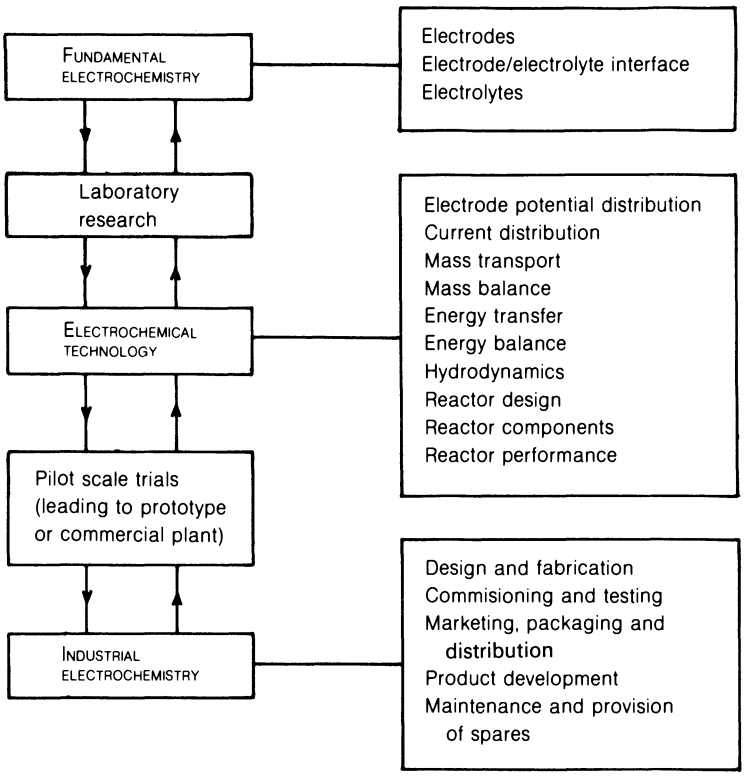

Fig. 2.1 Electrochemical engineering: its scale and endeavours. Note that the development of industrial electrochemistry involves both scaleup and scaledown procedures.

the electrode potential distribution within a reactor. The potential distribution and its interaction with cell design, will be influenced by the choice of electrode material and its form, the mass-transport (of reactants, intermediates and products), hydrodynamics and current distribution. This aspect has received inadequate treatment in the literature and is poorly appreciated; it has an important influence on, for example, selectivity and scale-up.

Whilst acknowledging the need to consider any chemical process as an integrated package, it is convenient in this chapter to focus attention on the electrochemical stage and particularly upon the key component, the electrochemical reactor.* The detailed design and characterization of such reactors may involve complex, interactive procedures. An understanding of factors such as potential and current distribution, electrolyte flow patterns, electrode ther-

* The term 'electrochemical reactor' is used to mean a purpose-built electrochemical cell (or number of cells in a common package) which performs a useful duty.

modynamics and kinetics, mass and heat transfer, together with due consideration of the cost and performance of reactor components (e.g. reactor body, electrodes and separators) and its ancillaries is an essential prerequisite. These factors are common to all chemical-engineering processes with the important exception of potential distribution.

In concept, an analytical approach to the design and characterization of an electrochemical reactor might consider a complete treatment of the following aspects:

1. Mass balance (including the electrical charge balance) for all reactants and products.
2. Heat balance across all reactor compartments and components.
3. Voltage balance across the reactor.

Hence, an exhaustive energy balance could be performed. Such a detailed treatment is seldom possible in practice and often unnecessary. Nevertheless, an appreciation of these factors is important in any reactor operation.

The reactor type may be classified according to the nature of energy transformation as indicated in Table 2.1. In this chapter, we will largely consider 'driven' (i.e. electrolytic) cells where electrical energy supplied to the reactor is used to induce the desired chemical change.

In order to describe the performance of a reactor, a mathematical model may be used, i.e. a set of quantitative relationships between the important parameters. This defines the reactor characteristics and their relationships to process conditions. Hence, the model may be used to simulate process conditions and, therefore, to predict or rationalize behaviour in practice. There are, perhaps, two extreme approaches to modelling.

1. *The fundamental approach.* A precise and detailed model is prepared from first principles using well established scientific and engineering expressions and approaches.
2. *The 'black box' approach.* Empirical relationships are established from practical observation, treating the reactor as a characterized module.

While the first approach is more detailed and intellectually satisfying, the second often provides a simpler and more appealing description of the reactor and, hence, its behaviour towards major process variables, its scale-up characteristics and attendant optimization parameters.

The reactor must fit into the overall process, and it is useful to develop 'figures of merit' which indicate cell performance and permit a discussion of its interaction with other parts of the process.

The figures of merit should also aid the selection of an appropriate cell design. For example, the optimum cell for: (1) an energy-intensive electrolysis, (e.g. Cl_2 or Al production); (2) a process requiring extensive work-up and recovery of products (e.g. an organic synthesis); (3) effluent treatment where large volumes of dilute solutions must be handled; or (4) a process which consumes little charge

Table 2.1 Classification of electrochemical cells according to the nature of energy transformation

Parameter	Self-driving cell (galvanic cell)	Driven cell (electrolytic cell)
Energy transformation	Chemical → Electrical	Electrical → Chemical
$\Delta G_{CELL} = -nFE_{CELL}$	−	+
Thermodynamic tendency for cell reaction	Spontaneous	Not spontaneous
$E_{CELL} = E^C - E^A$	+	−
Relative polarity of the electrodes		
cathode	+	−
anode	−	+
Examples of application areas (chapter or section)	Immersion plating (8.2); electroless plating (8.2); most phosphating (8.3.2) and chromating (8.3.3); corrosion cells (10); batteries on discharge (11.1–11.6) and fuel cells (11.7)	Chlor-alkali cells (3); electrowinning (4.1) and electrorefining (4.2); inorganic synthesis (5); organic synthesis (6); cells for industrial process recycling and effluent treatment (7); electroplating (8.1), anodizing (8.3) and electrophoretic painting (8.4); electroforming (9.1) and electrochemical machining (9.2); amperometric and voltammetric sensors (12.2) and (12.6)

but where the electrodes must be readily removed (e.g. electroplating or anodizing), will each be quite different.

In this chapter we will first consider briefly the factors involved in costing an electrolytic process and discuss the various figures of merit. Then, cell components and the principles of cell design will be discussed, together with selected examples of reactor geometries.

2.2 COSTING AN ELECTROLYTIC PROCESS

2.2.1 General approach

A company deciding whether to build a new chemical plant, will consider the percentage return on investment of vital importance. This is defined by the

equation:

$$\% \text{ return on capital} = \frac{\text{profit}}{\text{capital investment}} \times 100$$

$$= \frac{\text{sales values} - \text{total product cost}}{\text{capital invested}} \times 100 \qquad (2.1)$$

since this will allow the comparison of the effectiveness of using money for the chemical plant to an alternative, investing the money in a bank or starting other business activities. In the present circumstances, the percentage return on capital would need to be at least 15–25% to justify building a new plant.

The capital C invested is the total sum of money required initially to set up the plant and it is estimated from:

$$C = C_F + C_W + C_L \qquad (2.2)$$

where C_F is the fixed capital or the cost of buying and installing the plant – for an electrolytic process this will include the cell houses, cells and rectifiers, all auxiliary unit processes (e.g. distillation, crystallization, liquefaction of gaseous products, effluent treatment) and a computer system to control and continuously optimize the overall process (clearly C_F is minimized by designing a plant with a high manufacturing rate); C_W is the working capital, i.e. the cost of buying all the chemicals to start up the process (in the case of an electrowinning plant, for example, the cost of the metal to fill the cells with a concentrated solution of its ion is substantial); C_L is the cost of buying the land (minimized by packing the units as closely as safety considerations will permit and by building upwards rather than outwards).

The total product cost is computed for each working year by a consideration of the following items.

1. *Direct costs.* The costs of raw materials, utilities (effluent treatment, water and energy for heating, pumping, etc. as well as electrolysis), labour, maintenance and replacement of components (in electrolyses, particularly electrodes or electrode coatings and membranes) and royalties if the company needs to license patent rights in respect to the process.
2. *Plant overhead costs.* The costs of insurance, administration, safety, medical services, canteen and recreational facilities for the workforce, quality-control laboratories.
3. *Marketing and distribution costs.* The product must be advertised, sold and transported to the customer; technical support during and after sales must be considered.
4. *Research and development costs.* The process must repay the expenditure involved in its development and perhaps also support an R and D programme to improve its performance, e.g. to develop better electrodes or to run pilot plants under modified process conditions.

5. *Depreciation.* The capital cost of the plant must be recovered during its working life. This is usually done by charging a depreciation D each year. The simplest procedure for calculating D is:

$$D = \frac{C - C_{SCRAP}}{N} \tag{2.3}$$

where C_{SCRAP} is the total scrap value of the plant and land and N years is the projected lifetime of the plant. It is normal to be very cautious in the evaluation of both the scrap value and the life of the plant despite the probability that the value of the land and chemical inventory ($C_L + C_W$) will increase with time. Moreover, many plants are running for many years after their capital investment has been fully recovered and this is a big disincentive to the introduction of replacement technology. The absence of depreciation in the total product costs often leads to a situation where old technology can compete with apparently better processes.

Many of the items 1–5 above would be difficult to estimate from first principles and the total product cost is more likely to computed from an equation such as:

$$\text{Total product cost} = z[\text{raw materials} + \text{utilities} + (x \text{ labour}) + (yC_F) + D] \tag{2.4}$$

where x, y and z are empirical factors (typical values $x = 1.15$, $y = 0.01$ $z = 1.5$) which are based on experience and recognize, for example, that the costs of canteen and recreational facilities are related to the labour cost and the cost of component replacement is related to the fixed capital.

In order to compute the capital required to build the plant or the total product cost, the first step will be to estimate the volume of the product which can be sold, since this will determine the size of the plant. The chemical engineer will then be in a position to begin the detailed design of a possible plant; normally, he or she will commence the task by drawing-up a detailed design flow sheet (Fig. 2.2). The purposes of the flow sheet will be:

1. To allow an accurate evaluation of the number of unit processes (e.g. cells, pumps, distillation columns, crystallizers, compressors, solvent extractors, heating devices, heat exchangers, filters) which will be necessary.
2. To permit an estimate of the size of each unit process – this will require detailed performance data.
3. To allow a preliminary mass and energy balance and, hence, to show-up useful waste heat which might be used elsewhere in the process, identify by-products which might be sold and improve the process economics, etc.
4. To identify areas where further R and D might significantly improve the process and define the additional data required to optimize the overall process.

When complete, the flow sheet can be used for a preliminary economic evaluation of the process. If this shows that the process is promising, then the

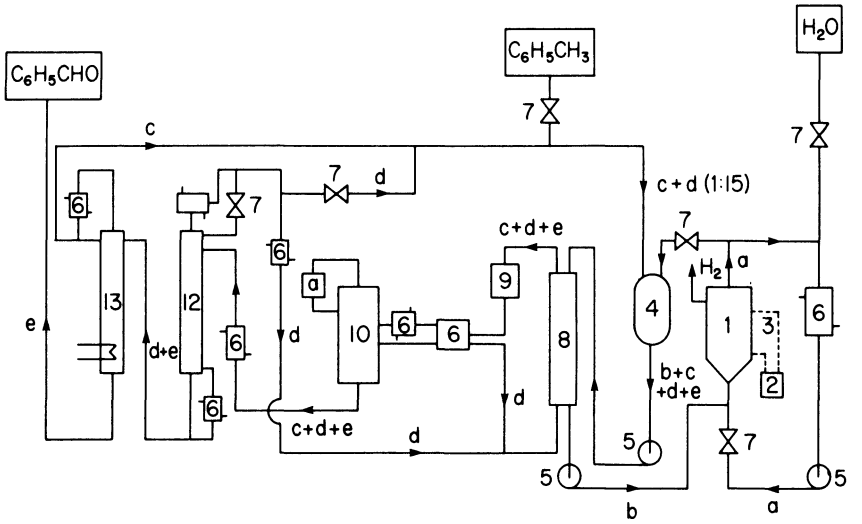

Fig. 2.2 Preliminary flow sheet for a 2000 ton year^{-1} benzaldehyde plant using electrolytic oxidation of Ce^{3-} to Ce^{4+} in $HClO_4$ and two-phase chemical oxidation, i.e. aqueous Ce^{4+} with toluene in hexane, in a second reactor. (After: K. Kramer, P. M. Robertson and N. Ibl (1980) *J. Appl. Electrochem.*, **10**, 29. Key: 1, electrolysis cells (proposed 31 undivided tubular cells, radius 91.4 cm, height 86.4 cm; $I = 113$ mA cm^{-2}): 2, rectifier; 3, busbars; 4, chemical reactor (proposed 5×20 m^3 reactors); 5, pump; 6, heat exchanger; 7, valve; 8, extraction column (with hexane); 9, electrolyte stripper; 10, solvent extractor using heat pump principle with compressor(s); 11, distillation column to remove remaining hexane; 12, condenser; 13, distillation to separate toluene and benzaldehyde. Process streams: a, aqueous $HClO_4$ with Ce^{4+} + Ce^{3+}; b, aqueous $HClO_4$ with Ce^{3+}; c, toluene, d, hexane; e, benzaldehyde.

outstanding problems will be tackled and a pilot plant will be built to confirm the conclusions. Then, as more data become available, the flow sheet will be refined until the company has sufficient confidence in the process to commence building the production plant. Even after the plant is running, however, improvement of the process technology will continue and larger processes will be supported by an active pilot-plant facility which will seek to define the optimum working parameters for the overall process to meet the various economic and market conditions which are likely to arise. Also, an R and D programme will aim to improve the weaker points in the process and the pilot plant will again test and adapt the conclusions. Hence, for a larger process, modification to improve the financial return is a continuous procedure, which may be influenced significantly by both technical and commercial factors.

2.2.2 Process optimization

Optimization of chemical processes may involve one of five targets:

1. Maximum profit.

2. Minimum product cost.
3. Maximum return on investment.
4. Desirable incremental return on investment.
5. Minimizing energy consumption.

Generally, the most important strategy for electrochemical reactors is to minimize the product cost by optimizing the current density. Productivity is greater at a higher useful current density but usually cell voltage increases and, hence, the energy efficiency per unit amount of product decreases. Non-profit considerations such as plant safety and environmental acceptability are becoming increasingly important. The associated costs are often a significant component of overall costs. It should be noted that a realistic approach to costing is often complex due to the number of interactive variables involved. Additionally, the approach is often specific to a particular organization and must consider both internal requirements of the company as well as external market forces.

We will consider a very simplified approach, assuming that the total product cost, associated with the cell alone, C_{TOTAL} may be expressed as follows:

$$C_{\mathrm{TOTAL}} = C_{\mathrm{E}} + C_{\mathrm{I}} + C_{\mathrm{S}} \tag{2.5}$$

where C_{E} is the electrolytic power cost, C_{I} is the reactor investment cost, and C_{S} is the cost of electrolyte stirring (or electrode movement). In general, all of these components will be dependent upon current density.

The electrolytic power cost C_{E} is given by:

$$C_{\mathrm{E}} = bqE_{\mathrm{CELL}} \tag{2.6}$$

where b is the cost of a unit electrical energy (e.g. £ or $ per kilowatt hour) and q is the electrical charge needed; the cell voltage E_{CELL} is given by equation (1.126):

$$C_{\mathrm{E}} = bq[(E_{\mathrm{e}}^{\mathrm{C}} - E_{\mathrm{e}}^{\mathrm{A}}) - |\eta_{\mathrm{C}}| - |\eta_{\mathrm{A}}| - iR_{\mathrm{CELL}} - iR_{\mathrm{CIRCUIT}}] \tag{2.7}$$

$(E_{\mathrm{e}}^{\mathrm{C}} - E_{\mathrm{e}}^{\mathrm{A}})$ is a thermodynamic component of the cell voltage, η_{C} and η_{A} are the cathodic and anodic overpotentials, $\mathrm{R}_{\mathrm{CELL}}$ is the resistance of the electrolyte (plus any separator) and R_{CIRCUIT} represents the resistance of electrical connections such as busbars. Equation (2.7) may be rewritten:

$$C_{\mathrm{E}} \simeq bq(E_{\mathrm{e}}^{\mathrm{C}} - E_{\mathrm{e}}^{\mathrm{A}}) - bqiR \tag{2.8}$$

The first term relates to thermodynamics and is independent of current density, while the second is due to overpotentials at the electrodes together with ohmic losses in the cell and busbars.

The reactor investment cost C_{I} (which is inversely proportional to current density) is given by:

$$C_{\mathrm{I}} = aA \tag{2.9}$$

where a is the cost per electrode area (e.g. £ or $ per square metre) and A is the

electrode area. A fixed rate is often assumed for a, which includes depreciation and interest on the capital. The cost per unit area of electrodes is assumed not to change with current density.

The cost of electrolyte stirring C_S is very dependent upon the process considered, in some cases:

$$C_S = bWt \tag{2.10}$$

where b is the cost of unit energy, W is the power required for electrolyte–electrode movement and t is the elapsed time. For mass transport controlled processes, C_S is closely related to the current density requirements.

The total cost (equation 2.5) is given by a combination of equations (2.6), (2.9) and (2.10):

$$C_{TOTAL} = (bqE_{CELL}) + (aA) + (bWt) \tag{2.11}$$

Under constant current conditions, $q = it$ and $C_E = bti^2R_{TOTAL}$, where R_{TOTAL} is the effective, overall cell resistance ($= E_{CELL}/i$).

Equation (2.11) may then be rewritten:

$$C_{TOTAL} = (bqiR_{TOTAL}) + (aA)q/it + (bWq/i) \tag{2.11a}$$

The relationship between the terms in equation (2.11a) is shown schematically in Fig. 2.3. The total cost has a minimum at the optimum current, i_{OPT} which can be calculated by differentiating C_{TOTAL} with respect to current and setting the differential equal to zero, i.e.:

$$\frac{dC_{TOTAL}}{di} = 0 = (bqR_{TOTAL}) - \left(\frac{(aA)q/t + bWq}{i^2}\right) \tag{2.12}$$

Equation (2.12) may then be rearranged to give an expression for the optimum current:

$$i_{OPT} = \left(\frac{aA/t + bW}{bR_{TOTAL}}\right)^{1/2} \tag{2.13}$$

The optimum current will therefore depend, in general, on the investment-related cost factor a, the price per unit of electrical energy b and the overall cell resistance R_{TOTAL}.

Selectivity is often an important factor in electrosynthesis; low values may result in increased reagent costs and higher downstream separation costs. Thus the running and capital costs of a process may be significantly affected by selectivity which, in turn, is a function of current density.

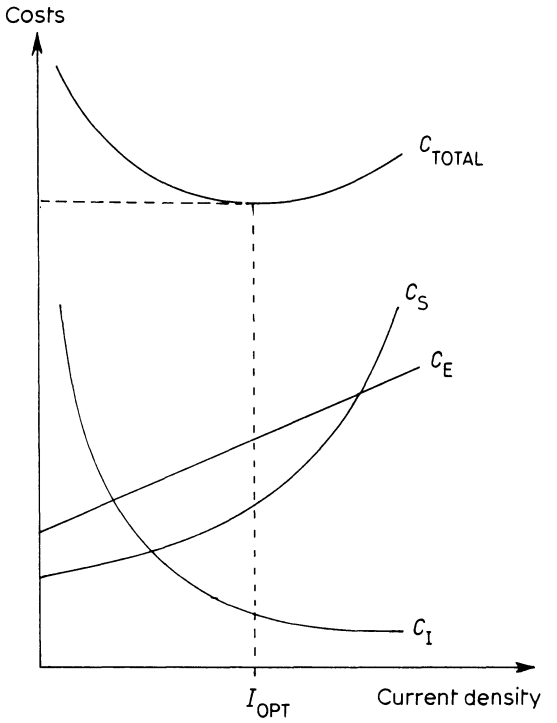

Fig. 2.3 Cost components for an electrochemical reactor as a function of current density, showing optimization of the current density according to minimum product cost.

2.3 PERFORMANCE AND FIGURES OF MERIT

While the percentage return on investment will often be the final criterion for the assessment of a process, it is a very intractable parameter for the scientist or engineer. It is more convenient to those involved in electrochemical technology, to develop other criteria or 'figures of merit' which pertain more closely to the electrolysis process and allow it to be treated as another unit process in the overall scheme.

It can be seen by perusing the later Chapter headings in this book that the applications of electrochemistry are extremely diverse. Hence, it is not surprising that the importance of, and in the limit, the relevance to, the different applications of the various figures of merit will vary substantially. Moreover, it will commonly be found that it is not possible to optimize all the figures of merit; a change in reactor design or electrolysis parameters to improve one figure of merit may be detrimental to another. Then it is necessary to trade-off the importance of the figures of merit to find the overall economic optimum. Two general points are noteworthy:

1. It is essential to consider several figures of merit and to make comparisons with values for competitive reactors.

2. Practical aspects such as safety, reliability, or convenience in operation, ease of maintenance, facility for product removal and proprietary considerations may assume overriding importance.

We will consider the general electrochemical reaction:

$$A + ne^- \longrightarrow n_p P \tag{2.14}$$

where 1 mole of the reactant A receives n moles of electrons to yield n_p moles of product P.

There are several possible ways to define each figure of merit, depending upon its relationship to processing time and reactor space. For example, if a quantity B may, in general, be time- and space-dependent, we may define B in four separate ways.*

1. Point or differential value (both time- and space-dependent):

$$B' = B(t, x) \tag{2.15}$$

2. Temporal value (time-dependent but space-averaged):

$$B_t = 1/A \int_A B(t, x)\,\mathrm{d}A \tag{2.16}$$

where here A is the electrode area

or:

$$B_t = 1/V \int_V B(t, x)\,\mathrm{d}V \tag{2.17}$$

3. Local value (time-averaged and space-dependent):

$$B_x = 1/t \int_0^t B(t, x)\,\mathrm{d}t \tag{2.18}$$

4. Overall value (both time- and space-averaged):

$$B = (1/A)(1/t) \int_A \int_0^t B(t, x)\,\mathrm{d}A\,\mathrm{d}t \tag{2.19}$$

or:

$$B = (1/V)(1/t) \int_V \int_0^t B(t, x)\,\mathrm{d}V\,\mathrm{d}t \tag{2.20}$$

Normally, the most useful version for practical reactors is the overall value; the point values are also useful in some circumstances.

* See G. Kreysa (1985) *J. App. Electrochem.*, **15**, 175

2.3.1 Fractional Conversion X_A

This is the fraction of reactant which is consumed by the electrochemical reaction.

For a batch process:

$$X_A = \frac{m_{(o)} - m_{(t)}}{m_{(o)}} = 1 - (m_{(t)}/m_{(o)}) \tag{2.21}$$

where $m_{(o)}$ is the initial, molar amount of reactant and $m_{(t)}$ is the molar amount at time t.

For a continuous flow-through reactor, the fractional conversion is related to the inlet- and outlet-concentration of reactant:

$$X_A = \frac{m_{(IN)} - m_{(OUT)}}{m_{(IN)}} = 1 - (m_{(OUT)}/m_{(IN)}) \tag{2.22}$$

If the electrolyte volume V is constant, $c_{(o)} = m_{(o)}/V$ and $c_{(t)} = m_{(t)}/V$. Equations (2.21) and (2.22) may then be written in terms of the reactant concentration.

For a batch process:

$$X_A = \frac{c_{(o)} - c_{(t)}}{c_{(o)}} = 1 - (c_{(t)}/c_{(o)}) \tag{2.23}$$

and for a continuous, flow through reactor:

$$X_A = \frac{c_{(IN)} - c_{(OUT)}}{c_{(IN)}} = 1 - (c_{(OUT)}/c_{(IN)}) \tag{2.24}$$

Since electrolysis is a heterogeneous process, the fractional conversion depends on the ratio of the active electrode area to the cell volume and to the flow rate of the electrolyte. A high conversion per pass is desirable if, for example, the starting material is not to be recycled (e.g. an effluent treatment) or the product must be extracted during each cycle, e.g. when the product is unstable. This is obtainable with most cell designs only when a slow flow rate is used which leads to a long residence time and poor mass transport conditions.

Hence, a cell with a high conversion per pass at a high flow rate is often a desirable goal and certainly provides a driving force for designing cells with a high surface area per unit volume.

2.3.2 Material yield

Material yield θ_p (which is more precisely called the 'overall operational yield') is the maximum molar amount of desired product obtained from 1 mole of reactant, taking the reaction stoichiometry into account:

$$\theta_p = \frac{\text{moles of reactant converted to product}}{\text{total moles of reactant consumed}} \tag{2.25}$$

$$\theta_p = \frac{m_p}{n_p m_{(o)}} \tag{2.26}$$

The material yield determines the annual consumption of raw material for the desired tonnage of product. In addition, however, the material yield is important, because for $\theta_p < 100\%$, it will be necessary either to accept the lower price normally associated with an impure material or to introduce additional unit processes for purifying the product and handling the by-product. The latter will inevitably increase the fixed capital.

2.3.3 Overall conversion-related yield

This is the ratio of the material yield to the fractional conversion:

$$\phi_p = \frac{\theta_p}{X_A} = \frac{m_p}{n_p(m_{(o)} - m_{(t)})} \tag{2.27}$$

2.3.4 Current efficiency

The current efficiency ϕ is the yield based on the electrical charge passed during electrolysis, i.e. it is a yield based upon the electron as a reactant:

$$\phi = \frac{\text{charge used in forming product}}{\text{total charge}} \tag{2.28}$$

From Faraday's laws of electrolysis:

$$\phi = \frac{(wnF)/M}{q} \tag{2.29}$$

or:

$$\phi = \frac{mnF}{q} = \frac{nFV}{q}\Delta c \tag{2.30}$$

We may define two convenient versions of the current efficiency, depending upon the period during which the charge is measured:

$$q = \int_0^t i\,dt \tag{2.31}$$

will lead to the overall current efficiency, and:

$$q = \int_{t_1}^{t_2} i\,dt \tag{2.32}$$

the interval current efficiency.

A value of ϕ below 100% indicates either: (1) that the back-reaction occurs to some extent in the cell; or (2) (more likely) that by-products are being formed.

These may, however, arise by electrolysis of the solvent or the background electrolyte rather than the starting material, e.g. hydrogen from electrolysis of water during many metal depositions or oxygen in chlorine from oxidation of water will lead to current efficiencies below 100% for such metal-plating processes and chlorine production respectively. Hence, a value of ϕ below 100% need not be associated with a material yield less than 100%.

2.3.5 Overall selectivity

The overall selectivity S_p is the ratio of desired product to total products:

$$S_p = \frac{\text{number of moles of desired product}}{\sum \text{moles of all products}} \tag{2.33}$$

Consider the reaction schemes 1 and 2 below.

$$1.\ A \begin{matrix} \nearrow\ n_1P_1 \rightarrow n_2P_2 \\ \searrow\ n_3P_3 \end{matrix} \tag{2.34}$$

$$2.\ A_1 \begin{matrix} \nearrow\ n_1P_1 \\ \searrow\ n_2P_2 \end{matrix} \tag{2.35}$$

$$A_2 \rightarrow n_3P_3$$

In both cases:

$$S_{p_1} = \frac{m_{p_1}/n_1}{\sum m_{p_i}/n_i} \tag{2.36}$$

In reaction scheme 1, the selectivity of P_1 has the same value as the overall conversion related yield in equation (2.27). In the case of reaction scheme 2, however, these two parameters are different, i.e.:

$$S_{p_1} = \frac{m_{p_1}/n_1}{\sum_{i=1}^{3} m_{p_i}/n_i} \tag{2.37}$$

but:

$$\phi_{p_1} = \frac{m_{p_1}/n_1}{\sum_{i=1}^{2} m_{p_i}/n_i} \tag{2.38}$$

2.3.6 (Electrical) energy consumption

The electrolytic energy costs of an electrochemical process are related closely to the energy efficiency. The energy consumption may be referred to the amount of substance on a molar, mass or volume basis.

$$\text{Molar energy consumption} = \frac{-nFE_{cell}}{\phi} \tag{2.39}$$

The more common

$$\text{Specific energy consumption} = \frac{-nFE_{\text{cell}}}{\phi M} \tag{2.40}$$

while for gaseous or liquid products,

$$\text{volumetric energy consumption} = \frac{-nFE_{\text{cell}}}{\phi V_m} \tag{2.41}$$

may be used, where V_m is the molar volume. If the Faraday constant has the units of A s mol^{-1} and E_{CELL} is in V, then E_S will take the units of J mol^{-1} as in equation (2.39), J kg^{-1} as in equation (2.40) or J m^{-3} as in equation (2.41).

It is more common to express E_S in terms of kWh mol^{-1}, kWh kg^{-1} or kWh m^{-3}. This is achieved readily upon division of the right-hand side of equations (2.39)–(2.41) by 3.6×10^6.

It can be seen that the energy consumption does not depend directly on current density (because the passage of current is essential to the conversion of starting material to product – the charge to form one mole of product is determined by Faraday's laws of electrolysis) but really only on the cell voltage and the current efficiency. Hence, the energy consumption can be minimized only by selecting the electrolysis conditions so that the current is used solely for the reaction of interest and making the cell voltage as low as practicable.

2.3.7 Cell voltage

The cell voltage is a complex quantity made up of a number of terms, i.e.:

$$E_{\text{CELL}} = E_C - E_A - iR_{\text{CELL}} - iR_{\text{CIRCUIT}} \tag{2.42}$$

$$E_{\text{CELL}} = E_e^C - E_e^A - |\eta_C| - |\eta_A| - iR_{\text{CELL}} - iR_{\text{CIRCUIT}} \tag{2.43}$$

(c.f. equation 1.1.8.) E_e^A and E_e^C are the equilibrium potentials for the anode and the cathode reactions respectively, so that $(E_e^C - E_e^A)$ may be calculated from the free-energy change for the overall cell reaction by:

$$\Delta G = -nF(E_e^C - E_e^A) \tag{2.44}$$

In the cases of self-driving cells (e.g. batteries and fuel cells), E_{CELL} is positive and the energy consumption is negative, i.e. the cell produces electrical energy. In the latter case, the energy consumption is sometimes referred to as the 'electrical energy yield'.

Electrochemical technology, with the exception of corrosion, certain metal finishing processes, batteries and other power sources, is concerned with carrying out reactions where the free energy is positive (i.e. $E_e^C - E_e^A$ is negative) and, indeed, an advantage of electrolytic methods is that they may be used to drive very unfavourable reactions, e.g. the electrolysis of molten NaCl to sodium metal and chlorine. In electrolytic processes the overpotentials and iR terms

represent energy inefficiencies and, hence, will make the cell voltage a larger negative value. The fraction of the cell voltage ($E_e^C - E_e^A$) is one that cannot be avoided. It may be reduced only by changing the overall cell reaction, and in some circumstances this is possible by changing the counter-electrode reaction, e.g. in present diaphragm or membrane chlor-alkali cells, the cathode reaction is the reduction of water so that the cell reaction is:

$$\begin{aligned} &2H_2O + 2Cl^- \longrightarrow Cl_2 + H_2 + 2OH^- \\ &E_e^C - E_e^A \simeq -2.19\,V \end{aligned} \tag{2.45}$$

but an attractive alternative would be to use an oxygen cathode. The cell reaction would then be:

$$\begin{aligned} &2H_2O + O_2 + 4Cl^- \longrightarrow 2Cl_2 + 4OH^- \\ &E_e^C - E_e^A \simeq -0.96\,V \end{aligned} \tag{2.46}$$

and although the free-energy changes for reactions (2.45) and (2.46) are both positive, from a thermodynamic viewpoint the energy required by reaction (2.46) is much less.

In equation (2.43), $|\eta_A|$ and $|\eta_C|$ are the anode and cathode overpotentials respectively. In general, these overpotentials may contain contributions from the electron transfer process and from mass transport. Many industrial cells are normally operated under conditions where the contribution from the second term is small. Then, from Chapter 1, rearranging equation (1.39) or (1.40) it can be seen, that, for a simple electron transfer reaction, the overpotential is given by the expression:

$$|\eta| = \frac{2.3RT}{\alpha nF}(\log I - \log I_0) \tag{2.47}$$

In other words, the overpotential will depend on the transfer coefficient and on the exchange current density. For more complex processes:

$$|\eta| = \beta(\log I - \log I_0) \tag{2.48}$$

and it is the measured Tafel slope rather than $2.3RT/\alpha nF$ which is important. In practice, the overpotential will increase by 30–250 mV, depending on the Tafel slope, for each decade increase in current and the major factor determining the magnitude of the overpotential will be the exchange current density, i.e. the kinetics of the electrode process. This will depend on the electrolysis conditions (electrolyte, pH, temperature), and particularly the electrode material (section 1.5).

It has to be borne in mind, however, that the requirement for the electrode material is even more specific; it should catalyse the reaction of interest but not others, e.g. the electrolysis of water which is commonly the thermodynamically preferred reaction. Thus, the anode in the chlor–alkali cell must catalyse

chlorine but not oxygen evolution and the cathode in the synthesis of adiponitrile must allow acrylonitrile reduction to be favoured, rather than hydrogen evolution.

The design of cells with minimum resistances is the first problem of electrochemical engineering. Clearly, the internal cell resistance R_{CELL} is decreased by making the interelectrode gap smaller and using a highly conducting electrolyte (molten salts or water with a high concentration of electrolyte are particularly favourable media in this respect). Moreover, any separators will cause substantial increases in cell resistance although they may be essential for a good current and material yield, for safety reasons or to extend anode lifetime. The final term in equation (2.43) recognizes that there will be a potential drop in the electrodes themselves and the busbars which carry the current, in the various connectors and in the other parts of the electrical circuit, and the total potential drop in the cell house must be apportioned between the cells.

In the general case and for a divided cell, it is possible to restate equation (2.42) as follows:

$$E_{CELL} = E_e^C - E_e^A - |\eta_C| - |\eta_A| - iR_{CATHOLYTE} - iR_{SEPARATOR} - iR_{ANOLYTE} - iR_{CIRCUIT}^C - iR_{CIRCUIT}^A \quad (2.49)$$

or

$$E_{CELL} = -(iR_{CIRCUIT}^C) - (E_e^C + |\eta_C|) - (iR_{CATHOLYTE}) - (iR_{SEPARATOR}) - (iR_{ANOLYTE} - (E_e^A + |\eta_A|) - (iR_{CIRCUIT}^A) \quad (2.50)$$

Figure 2.4 illustrates equation (2.50) in a schematic form, and shows certain sloping, straight lines indicating ohmic behaviour, i.e. the current is linearly dependent on potential (and, hence, on the interelectrode distance x). In the case of an electrode and its busbar (the pair constituting $iR_{CIRCUIT}$ for each electrode) electronic conduction occurs, while in solution (and through the separator) ions transport the current. The nearly vertical lines, representing the anode and cathode potentials, reflect the fact that these potential drops occur over very small distances, corresponding to the electrode interface (for activation overpotentials) and the hydrodynamic boundary layer (for concentration overpotentials). Horizontal lines represent (idealistic) zero voltage components. Several points may be made concerning the cell voltage:

1. It has many components.
2. The practical situation is more complex than the above suggests, e.g. gas evolution at one of the electrodes may cause an appreciable ohmic potential drop, due to the hold-up of (poorly conducting) gas bubbles; in such cases, problems may be minimized by using open, porous electrodes (which allow gas to escape from their back surface) or by suitable electrolyte–electrode movement, e.g. an increased electrolyte flow. Alternatively, electrodes may produce poorly conductive (e.g. polymeric or oxide) films, or separators may be fouled (by, for example, deposition of organic films or metals hydroxides).

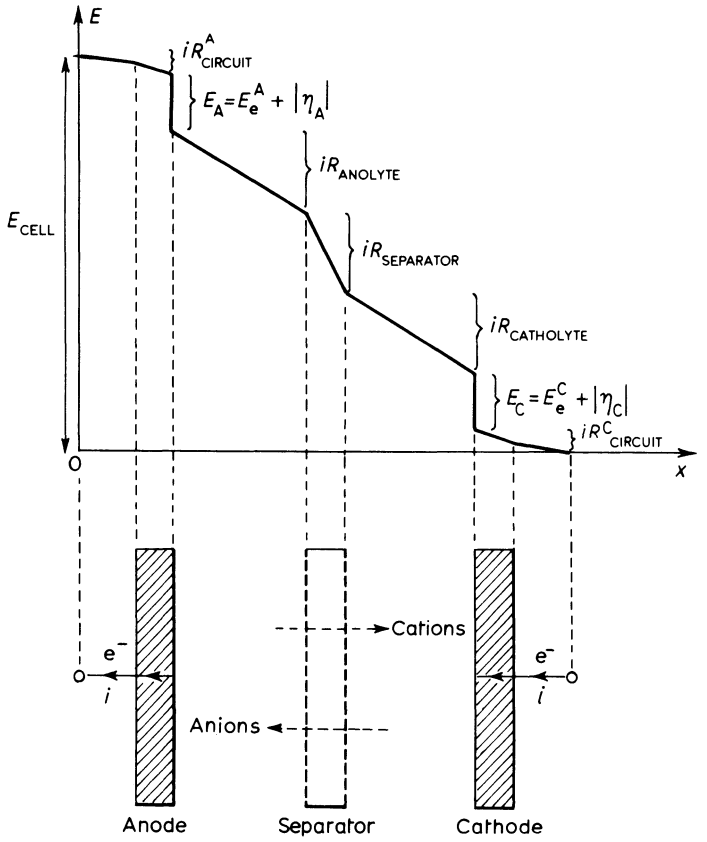

Fig. 2.4 Schematic voltage components in a divided cell, illustrated by a plot of potential versus distance x in the interelectrode direction.

3. Each of the components may be time- and position-dependent, i.e. Fig. 2.4 represents a simple, one-dimensional 'snapshot' of the voltage distribution.
4. The measured cell voltage is therefore a complex parameter, being space-averaged and time-dependent.
5. The cell voltage may be influenced by many process parameters including temperature, electrolyte composition, electrolyte flow, electrode material, form and surface condition.

It will be appreciated that the cell voltage is therefore a difficult parameter to predict analytically, and it may not readily be used as a primary control parameter. In practice, constant cell voltage operation is sometimes adopted for convenience, but constant electrode potential (potentiostatic) or, more realistically, constant cell current (galvanostatic) control is preferable.

The important contribution of cell voltage to the overall power costs should always be considered in driven cells:

$$E_{CELL} = iR_{TOTAL} \tag{2.51}$$

where R_{TOTAL} is the overall effective cell resistance (equation 2.7) which is a function of the electrode overpotentials, the electrolyte (plus any separator) resistance and the resistance of electrical connections. The overall electrolytic power costs are then given by:

$$W_{CELL} = iE_{CELL} \tag{2.52}$$

It should be remembered that the electrolytic power consumption W_{CELL} increases as the square of the cell current, i.e.:

$$W_{CELL} = i^2 R_{CELL} \tag{2.53}$$

2.3.8 Energy efficiency

Two parameters used to indicate efficiency of cells with respect to their use of energy are the energy yield:

$$\gamma_G = \frac{\Delta G\phi}{E_{CELL}nF} = -\frac{(E_e^C - E_e^A)\phi}{E_{CELL}} \tag{2.54}$$

and the thermal energy yield:

$$\gamma_H = \frac{\Delta H\phi}{E_{CELL}nF} = -\frac{E_{tn}\phi}{E_{CELL}} \tag{2.55}$$

where E_{tn} is the thermoneutral cell voltage, i.e. the cell voltage which permits isothermal operation*

$$E_{tn} = -(\Delta H/nF) \tag{2.56}$$

2.3.9 Electroactive area per unit volume A_S

Since the overall rate of any electrochemical process at a fixed current density is directly proportional to the electroactive area A, it is obviously important to calculate simple, area-related parameters. Unfortunately, determining A is not always straightforward, either by calculation or from experimental determinations, e.g. the active area of many porous electrodes (e.g. particulate-packed beds or foam materials) depends strongly on the flow conditions (e.g. flooded- or trickle-flow), the extent of gas evolution, the degree of solid product build-up on the electrode and the cell geometry (i.e. the potential distribution).

The need to design a cell with a high active surface area per unit volume of electrolyser is an important challenge to electrochemical engineers. In heterogeneous catalysis – where the requirement is only to have a high surface area of catalyst – the problem is relatively simple, but in electrolytic cells there is the additional restriction that the local electrode potential must be suitable if the

* See B. V. Tilak, P. W. Lu, J. E. Colman and S. Srinivasan (1981) *Comprehensive Treatise of Electrochemistry* (Eds J.O.'M. Bockris, B. E. Conway, E. Yeager and R. E. White), Vol. 2, p. 15, Plenum Press.

reaction is to occur. Moreover, for the desired situation of a uniform rate of reaction over the whole electrode area, the current density and, hence, the potential must be uniform over all the electrode surface. This will only be the case if all the electrode surface is equivalent geometrically with respect to the other electrode, e.g. Fig. 2.5 shows four electrode geometries. In (a) the parallel-plate cell and (b) the rotating-cylinder cell, the current distribution will be uniform (provided the electrode operates at low η so that the electroactive species is not depleted markedly as the solution flows through the cell). On the other hand, in cells (c) and (d) the current distribution cannot be even. In cell (c) the backs of the electrodes are not insulated (cf. cell (a)) and clearly the back and the front of the electrodes are not equivalent; the additional iR drop will ensure

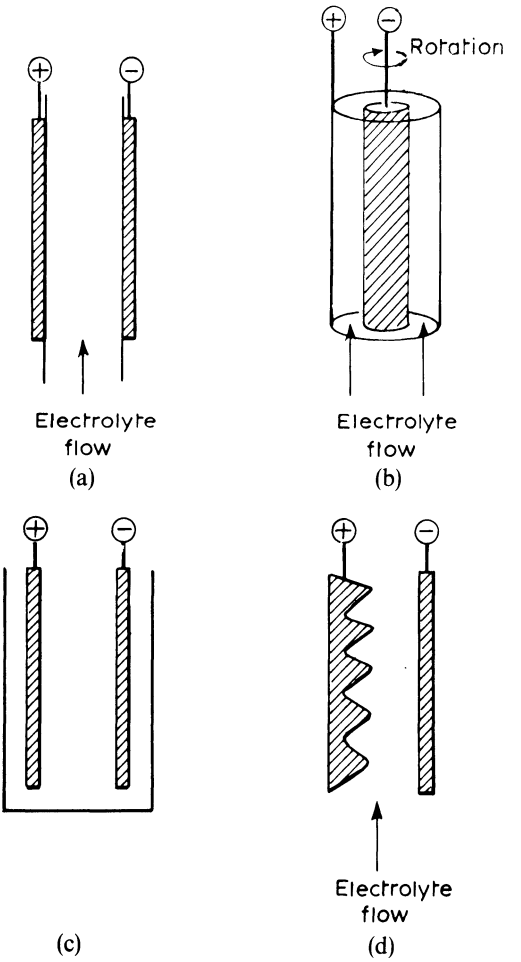

Fig. 2.5 Elementary reactor geometries. (a) Parallel-plate cell. (b) Concentric rotating-cylinder cell. (c) Plate-in-tank cell. (d) Plate cell with non-parallel electrodes.

that little current flows through the backs of the electrodes (although the situation would change totally if auxiliary electrodes were placed facing the back of the electrodes). In cell (d) the non-uniformity of the current distribution will be less dramatic but less current will flow through the depressions than at the tips of the projections because the electrode surface in the depressions is further from the other electrode.

The electroactive area per unit volume A_S should be stated whenever possible (this is frequently and incorrectly* called the the 'specific' electrode area):

$$A_S = A/V_R \tag{2.57}$$

There are three possible volume terms which may be used in the denominator. V_R may refer to the *overall* reactor volume (i.e. the amount of space occupied by the reactor) V_R^{EXT}:

$$A_S^{EXT} = A/V_R^{EXT} \tag{2.58}$$

It is sometimes convenient to consider the effective inventory of electrolyte within the reactor V_R^{INT}

$$A_S^{INT} = A/V_R^{INT} \tag{2.59}$$

It is sometimes more useful to consider the electrode volume V_E particularly in those cases where the electrode occupies a major part of the cell volume or is expensive – when:

$$A_E = A/V_E \tag{2.60}$$

It is obviously attractive to maximize A_S and A_E in order to produce a compact, high performance reactor and this has been a major driving force for the many 'high-surface-area' cells developed over the last two decades.

It is remarkably difficult in practice to obtain a high A_S value whilst maintaining a uniform reaction rate over the entire electrode surface, e.g. porous- and packed-bed electrodes often suffer from poor potential, and current, distributions (section 2.6.3). Often, the adoption of a three-dimensional electrode involves a trade-off between increased electroactive area and diminished selectivity.

2.3.10 Mass transport coefficient

For a process under mass transport control (via convective diffusion) the limiting current i_L expresses the duty of the reactor:

$$i_L = k_L AnFc^{\infty} \tag{2.61}$$

Equation (2.61) follows from the definition of the mass transport coefficient:

$$k_L = i_L/(AnFc^{\infty}) \tag{2.62}$$

* Specific means 'divided by unit mass'.

This may be considered as a limiting current which has been normalized with respect to electrode area and bulk concentration of the electroactive species.

A common practical situation is one where the electrode reaction of interest is only partly mass transport controlled and there is a significant competing reaction. The fraction of the limiting current attained is then:

$$\gamma = \phi i / i_L \leqslant 1 \tag{2.63}$$

$$\gamma k_L = \gamma i_L / AnFc^\infty \tag{2.64}$$

Here, γk_L becomes a modified figure of merit. γ is sometimes called the mass transport 'effectiveness factor'.

In the general case, for a mass transport controlled reaction, the values of both k_L and the electrode area A will contribute to performance. Therefore, it is often useful to calculate their product:

$$k_L A = i_L / (nFc^\infty) \tag{2.65}$$

This is a particularly useful approach in circumstances when these parameters are interrelated strongly, and perhaps time-dependent, e.g. if cathodic deposition of metal is carried out in the reactor near limiting-current conditions (Chapter 7), the rough deposit obtained may not only increase the electroactive area, but also provide effective turbulence promotion, so increasing k_L. On the other hand, the use of a porous, insulating mesh next to an electrode may significantly improve k_L via turbulence promotion, but it may obscure part of the electrode, i.e. A will be decreased.

2.3.11 Mass transport coefficient, electroactive area and volume

One of the most useful figures of merit is the product of mass transport coefficient and electroactive area per unit volume*.

$$k_L A_S = \frac{k_L A}{V_R} \tag{2.66}$$

It is common to utilize the internal reactor volume, when:

$$k_L A_S^{INT} = \frac{k_L A}{V_R^{INT}} \tag{2.67}$$

expresses the performance of the reactor normalized with respect to its size*. In cases where the active electrode area is referred to electrode volume (and particularly in the case of three-dimensional, porous electrodes such as packed beds, reticulated materials and stacked meshes) A_e is preferred in place of A_S:

$$k_L A_e = \frac{k_L A}{V_E} \tag{2.68}$$

* Such factors are sometimes termed 'volumetric' mass transport coefficients.

It will be seen in section 2.5 that a consideration of expressions relating fractional conversion X_A to k_L and A provides two further figures of merit. For a simple batch reactor, which is used to process a volume V_R, the factor:

$$k_L A_S / V_R = \frac{k_L A}{V_R} \tag{2.69}$$

is important. In the case of continuous-flow reactors, an important index is $(k_L A)/Q$, where Q is the (steady) volumetric flow rate of electrolyte.

2.3.12 Space–time and space–velocity

The parameters described in this and the following two sections are important statements which describe the investment costs for an electrochemical process.

The space–time τ_{ST} is defined by:

$$\tau_{ST} = V_R / Q \tag{2.70}$$

as the ratio of reactor volume to volumetric flow rate. If V_R is the effective volume of electrolyte in the reactor, then τ_{ST} is equivalent to the mean residence time of electrolyte in the reactor τ. If V_R has units of m^3 and Q is in $m^3 s^{-1}$, τ_{ST} will be in seconds.

The space–velocity s is defined as the ratio of volumetric flow rate to reactor volume:

$$s = Q / V_R \tag{2.71}$$

and is therefore the reciprocal of space–time:

$$s = 1 / \tau_{ST} \tag{2.72}$$

The space–velocity describes the investment costs per unit volume of electrolyte. Such a parameter is important when the electrolyte has an intrinsically high value (e.g. concentrated solutions of precious metals) or if the reactor duty primarily involves the treatment of electrolyte (as in the recycling of industrial process liquors, including waste water treatment, Chapter 7).

The space–velocity is effectively the volume of electrolyte which may be processed in unit reactor volume in unit time, e.g. the units of $m^3 m^{-3} h^{-1}$ are obtained if the right-hand side of equation (2.71) is multiplied by 3600.

It is useful to relate the space–velocity to other simple models of practical reactor performance. Expressions describing conversion in model reactors are provided later (section 2.5). It is convenient to summarize expressions for the (well-stirred) simple batch reactor and the single-pass, plug flow reactor here, considering a reaction under complete mass transport control. For the batch reactor, the limiting current is given by:

$$i_L = \frac{nFc_{(o)} V_R}{t} [1 - \exp - (k_L A / V_R)] \tag{2.73}$$

where V_R is the effective volume of electrolyte within the reactor, $c_{(o)}$ is the initial concentration of electroactive species, t is the batch processing time and k_L is the mass transport coefficient. Equation (2.73) may be rewritten:

$$i_L = \frac{nFc_{(o)}V_R}{t}[1-\exp-(k_L A_S t)] \tag{2.74}$$

where A_S is the electroactive area per unit reactor volume.

For the, plug flow reactor:

$$i_L = nFc_{(IN)}Q[1-\exp-(k_L A/Q)] \tag{2.75}$$

or:

$$i_L = nFc_{(IN)}Q[1-\exp-(k_L A_S \tau)] \tag{2.76}$$

where $c_{(IN)}$ is the inlet concentration to the reactor, Q is the steady volumetric flow rate and τ is the mean residence time. The fractional conversions (section 2.3.1) are defined as follows.

For the simple batch reactor:

$$X_A = 1-\exp-(k_L A_S t) \tag{2.77}$$

and for the single-pass plug flow reactor:

$$X_A = 1-\exp-(k_L A_S \tau) \tag{2.78}$$

So, for the batch reactor, coupling equations (2.74) and (2.77) gives:

$$i_L = \frac{nFV_R c_{(o)} X_A}{t} \tag{2.79}$$

which allows i_L to be related to the initial concentration and the fractional conversion per pass at various times.

Similarly, for the plug flow reactor, coupling equations (2.76) and (2.78) gives:

$$i_L = nFQc_{(IN)}X_A \tag{2.80}$$

allowing i_L to be related to the fractional conversion for a given inlet concentration and known volumetric flow rate. From equations (2.21) and (2.22), the concentration changes may also be written. For the simple batch reactor:

$$c_{(o)} - c_{(t)} = X_A c_{(o)} \tag{2.81}$$

and for the plug flow, and continuously stirred tank reactors:

$$c_{(IN)} - c_{(OUT)} = X_A c_{(IN)} \tag{2.82}$$

Substituting the concentration difference expressions from equation (2.81) into equation (2.79) and equation (2.82) into equation (2.80) gives for the simple batch reactor:

$$i_L = \frac{nFV}{t}(c_{(o)} - c_{(t)}) \tag{2.83}$$

and for the plug flow reactor:

$$i_L = nFQ(c_{(IN)} - c_{(OUT)}) \tag{2.84}$$

Recalling equation (2.72) and coupling it to equation (2.84) we may write:

$$s = 1/\tau = i_L/[nFV\Delta C] \tag{2.85}$$

where $\Delta C = (c_{(o)} - c_{(t)})$ for the batch reactor (and $\tau = t$) while $\Delta c = (c_{(IN)} - c_{(OUT)})$ (and $\tau = V_R/Q$) for the plug flow reactor. Equation (2.85) clearly shows that the space–time is strongly dependent on the concentration change and, hence, on the inlet concentration.

Substituting X_A from equation (2.81) into equation (2.77) and rearranging gives the following expressions:

For the batch reactor:

$$\log (c_{(o)}/c_{(t)}) = \frac{k_L A_S t}{2.3} \tag{2.86}$$

and for the plug flow reactor:

$$\log (c_{(IN)}/c_{(OUT)}) = \frac{k_L A_S \tau}{2.3} \tag{2.87}$$

For the continuously stirred tank reactor, substituting X_A from equation (2.82) into:

$$X_A = 1 - \frac{1}{1 + k_L A_S \tau} \tag{2.88}$$

gives:

$$c_{(IN)}/c_{(OUT)} = (1 + k_L A_S \tau) \tag{2.89}$$

Equations (2.86), (2.87) and (2.89) enable the conversion to be predicted from known reactor parameters (k_L and A_S) at a given batch time (equation (2.86)) or residence time (equations (2.87) and (2.89)).

Rearrangement gives:

For the batch reactor:

$$k_L A_S = \frac{2.3 \log(c_{(o)}/c_{(t)})}{t} \tag{2.90}$$

and for the plug flow reactor:

$$k_L A_S = \frac{2.3 \log(c_{(IN)}/c_{(OUT)})}{\tau} \tag{2.91}$$

For the continuously stirred tank reactor:

$$k_L A_S = \frac{[(c_{(IN)}/c_{(OUT)})] - 1}{\tau} \tag{2.92}$$

Equations (2.90)–(2.92) enable the figure of merit $k_L A_S$ (section 2.3.11) to be related to process conditions.

2.3.13 Space–time yield

The space–time yield ρ_{ST} is one of the most valuable statements of reactor performance. It expresses the mass of product per unit time w/t which can be obtained in a unit cell volume V_R, i.e.:

$$\rho_{ST} = (w/t)/V_R \tag{2.93}$$

It can be seen that the space–time yield is related to the space–velocity s as follows:

$$\rho_{ST} = s\Delta C\mathrm{M} = \Delta C\mathrm{M}/t \tag{2.94}$$

where ΔC is the concentration change and M is the molar mass of material. From Faraday's laws of electrolysis:

$$w/t = (\phi i\mathrm{M})/nF \tag{2.95}$$

enabling equation (2.75) to be rewritten as:

$$\rho_{ST} = (\phi i\mathrm{M})/nFV_R \tag{2.96}$$

or:

$$\rho_{ST} = (\phi IA\mathrm{M})/nFV_R \tag{2.97}$$

Recognizing that $A/V_R = A_S$ is the electrode area per unit reactor volume as shown in section 2.3:

$$\rho_{ST} = (A_S I\phi\mathrm{M})/nF \tag{2.98}$$

and it can be seen that the space–time yield is directly proportional to the useful current density ($=I\phi$) and to A_S. If I is in $\mathrm{A\,m^{-2}}$, M in $\mathrm{kg\,mol^{-1}}$, A_S in $\mathrm{m^{-1}}$ and F in $\mathrm{A\,s\,mol^{-1}}$, ρ_{ST} takes the units of $\mathrm{kg\,m^{-3}\,s^{-1}}$. It is often more practical to multiply the right-hand side of equations (2.97) or (2.98) by 3.6 to obtain the units of $\mathrm{kg\,dm^{-3}\,h^{-1}}$.

Under mass transport controlled conditions and in the absence of competing reactions, equation (2.98) becomes:

$$\rho_{ST} = (A_S I_L\mathrm{M})/nF \tag{2.99}$$

or in terms of the mass transport coefficient k_L:

$$\rho_{ST} = A_S k_L c^{\infty}\mathrm{M} \tag{2.100}$$

It can also be seen that the space–time yield is proportional to the effective current through the cell per unit volume of reactor and, hence, to the current

density. The space time yield depends on the concentration of electroactive species and the mass transport regime and the current efficiency.

Hence, electrode geometry is paramount in obtaining the high surface area per unit volume essential to a good space–time yield. Indeed, it is perhaps not surprising that, in comparison with other chemical reactors (particularly catalytic heterogeneous reactors), electrolytic cells have poor space–time yields; the expectation for many chemical reactors is a space–time yield of 0.2–1 $kg\,h^{-1}\,dm^{-3}$ while that, for example, for a typical copper electrowinning cell is only 0.08 $kg\,h^{-1}\,dm^{-3}$. As a result, much academic electrochemical engineering has sought to increase this figure of merit by revolutionary changes in cell design, e.g. the introduction of fluidized-bed electrodes.

It should also be noted that it is not possible to optimize both the space–time yield and energy yield. The former requires the use of the highest possible current density which is certain to affect the energy consumption adversely because of the increased iR_{CELL} term in equation (2.43).

It is often desirable to relate the space–time yield to the conversion in, or over, a reactor. We will once again consider a process which is under complete mass transport control. As in section 2.3.12, the cases of a simple batch reactor and a single-pass, steady-state plug flow reactor will be discussed.

For the batch reactor, the batch-process time is given by a rearrangement of equation (2.86) as:

$$t = \frac{2.3}{k_L A_S} \log(c_{(o)}/c_{(t)}) \tag{2.101}$$

The mass of material produced is:

$$w = V_R \mathrm{M}(c_{(o)} - c_{(t)}) \tag{2.102}$$

The rate of material production on a mass basis is given by equations (2.101) and (2.102) as:

$$w/t = \frac{k_L A_S V_R \mathrm{M}(c_{(o)} - c_{(t)})}{2.3 \log(c_{(o)}/c_{(t)})} \tag{2.103}$$

$$w/t = \frac{k_L A \mathrm{M}(c_{(o)} - c_{(t)})}{2.3 \log(c_{(o)}/c_{(t)})} \tag{2.104}$$

The averaged space–time yield is then given by equation (2.93), after inserting w/t from (2.103):

$$\rho_{ST} = \frac{k_L A_S \mathrm{M}(c_{(o)} - c_{(t)})}{2.3 \log(c_{(o)}/c_{(t)})} \tag{2.105}$$

For the plug flow reactor, the electrolyte volume in the reactor V_R is given by equations (2.70) as:

$$V_R = \tau Q \tag{2.106}$$

From equation (2.80):

$$\frac{c_{(\mathrm{OUT})}}{c_{(\mathrm{IN})}} = \exp(-k_{\mathrm{L}} A_{\mathrm{S}} \tau) \tag{2.107}$$

which, upon rearranging gives:

$$\tau = \frac{2.3}{k_{\mathrm{L}} A_{\mathrm{S}}} \log(c_{(\mathrm{IN})}/c_{(\mathrm{OUT})}) \tag{2.108}$$

Combining equations (2.108) and (2.106):

$$V_{\mathrm{R}} = \frac{2.3Q \log(c_{(\mathrm{IN})}/c_{(\mathrm{OUT})})}{k_{\mathrm{L}} A_{\mathrm{S}}} \tag{2.109}$$

The mass of material per unit time is:

$$w/t = Q\mathrm{M}(c_{(\mathrm{IN})} - c_{(\mathrm{OUT})}) \tag{2.110}$$

So the space–time yield is given by equation (2.93), inserting w/t from equation (2.110) and V_{R} from equation (2.109):

$$\rho_{\mathrm{ST}} = \frac{k_{\mathrm{L}} A_{\mathrm{S}} \mathrm{M}(c_{(\mathrm{IN})} - c_{(\mathrm{OUT})})}{2.3 \log(c_{(\mathrm{IN})}/c_{(\mathrm{OUT})})} \tag{2.111}$$

It may be noted that equation (2.111) is identical to equation (2.105) if the following identities are made: $c_{(t)} \equiv c_{(\mathrm{OUT})}$; $c_{(\mathrm{o})} \equiv c_{(\mathrm{IN})}$. These expressions provide a convenient method of calculating space–time yield from an observed conversion and known reactor parameters k_{L} and A_{S}.

It will be clear from the above that the space–velocity (equation (2.85)) and the space–time yield (equations (2.105) and (2.111)) are dependent upon the degree of conversion and upon the initial (batch reactor) or inlet (plug flow reactor) concentrations. In order to compare the performance of reactors involving different X_{A}, $c_{(\mathrm{o})}$ or $c_{(\mathrm{IN})}$ values, it is therefore useful to define normalized s and ρ_{ST} parameters (sections 2.3.14 and 2.3.15).

2.3.14 Normalized space velocity*

This is defined by:

$$s_n = \frac{i\phi}{(c_{(\mathrm{o})} - c_{(t)}) V_{\mathrm{R}} nF} \log(c_{(\mathrm{o})}/c_{(t)}) \tag{2.112}$$

for a batch process, or:

$$s_n = \frac{i\phi}{(c_{(\mathrm{IN})} - c_{(\mathrm{OUT})}) V_{\mathrm{R}} nF} \log(c_{(\mathrm{IN})}/c_{(\mathrm{OUT})}) \tag{2.113}$$

* These normalized parameters are particularly useful in the wastewater treatment industries. They have been formalized by G. Kreysa (1981) *Electrochimica Acta*, **26**, 1693.

for a plug flow reactor. Under complete mass transport control, and the condition $c_{(OUT)} = 0.1\, c_{(IN)}$:

$$s_n = \frac{k_L A_S}{2.303} \tag{2.114}$$

s_n means the volume of electrolyte for which the concentration of the key reactant can be reduced by a factor of 10, during unit time in a unit volume reactor.

If i is in A, V_R in m^3 and F in A s mol^{-1}, and c is in mol m^{-3}, s_n will take the units of ($m^3\, m^{-3}\, s^{-1}$). The more useful, practical unit of $m^3\, m^{-3}\, h^{-1}$ results if the expression is multiplied by 3.6×10^3.

2.3.15 Normalized space–time yield*

This is the amount of key reactant which can undergo a conversion of 0.9 during unit time in a unit volume reactor.
For a batch process:

$$\rho_n = \frac{i\phi M 0.9}{V_R n F X_A} \log (c_{(o)}/c_{(t)}) \tag{2.115}$$

and for a continuous process:

$$\rho_n = \frac{i\phi M 0.9}{V_R n F X_A} \log (c_{(IN)}/c_{(OUT)}) \tag{2.116}$$

As the fractional conversion has a strong influence on the costs of raw materials and the need for further processing, ρ_n is generally more useful than ρ_{ST}.

2.3.16 Practical considerations

(a) Cost and lifetime of cell

While this is another figure of merit which, away from totally specific circumstances is difficult to quantify, it is clear that the cost, performance and lifetime of all cell components will affect the design of the electrolysis cell, e.g. the benefit of catalytic electrodes will depend on the initial cost and their lifetime, which in turn will depend on current density; certainly the saving in electricity consumption during the lifetime of the electrodes must exceed the difference in cost between the catalytic and poorer electrode materials. Cells are usually taken off-stream on a routine cycle because of the inconvenience and cost of failure of components such as electrodes and separators (although in successful processes this may be once in several years) and the components replaced or, at least, inspected closely, e.g. the thickness of a precious metal coating may be deter-

* See footnote on p. 88.

mined by perhaps X-ray fluorescence; hence, ease of dismantling the cell and replacement of cell components are important factors in cell design.

Also, in selecting materials for the construction of cells it must be remembered that the concentrated electrolyte solutions used for electrolysis are corrosive and even pumps, pipework and cell bodies must be selected with corrosion resistance in mind. Indeed, whenever it is feasible, non-electrode components should be fabricated from (or coated with) an electrically insulating material (usually a polymer but possibly a ceramic). In particular, it is wise to avoid the problem of 'bipolar corrosion' (Chapter 10) which may arise if a conductive material interrupts the usual current path between anode and cathode. It is essential to test all components in the system for corrosion resistance, with the cell on load and under open-circuit conditions.

(*b*) *Product quality and form*

Product quality often cannot be defined quantitatively. In some processes, however, product quality and its reproducibility are paramount. Examples would include surface finishing, where it is of overriding importance that the surface has the desired appearance or properties, and drug manufacture, where even trace amounts of some impurities can be critical.

In other cases, the nature and form of the product may be paramount, e.g. a cell selected to recover metal directly from a process liquor may be designed for continuous extraction of the metal in powder form (Chapter 7). In such cases, the residence time and electrolyte flow characteristics within the cell may have significant effects on product quality, e.g. redissolution of a metal may occur.

(*c*) *Convenience and safety in operation*

A number of practical considerations may be listed.

1. Many electrolytic processes have to operate routinely with little attention or maintenance; skilled manpower may not be available.
2. Start-up *and* shut-down must be straightforward and controllable. One of the advantages of electrochemical processing is the ease with which a cell may be turned on and off.
3. It may be necessary to monitor the electrochemical process continuously and perhaps use sensor signals as a feedback source for the purpose of automatic control.
4. Flexibility and versatility may be important, e.g. the duties of certain reactors may be altered relatively easily, within certain limits by, for example, increasing the rotational speed of a rotating electrode or incorporating an extra number of elements in a filterpress, plate cell geometry. Alternatively, it may be desirable in small batch systems to switch a reactor rapidly from one process to another, with minimal cleaning and downtime.
5. Safety should be paramount, e.g. it may be necessary to design the reactor to withstand extremes of temperature or pressure. Care must be taken to avoid

electrical sparking which may induce local overheating and damage or else ignition of flammable or explosive electrolytes, reactants and products. It may be required to separate cathodically generated hydrogen and anodically produced oxygen by means of a separator; in certain cases, explosive conditions may be avoided by diluting the product gas with air (section 5.8) or an inert gas, e.g. N_2 (section 5.2).

The amount of available head space or floor space for the electrochemical reactor and its ancillaries may be limited in certain cases; the reactor may need to be both compact and of a suitable shape. An additional consideration is that crowded process environments receiving an electrochemical reactor may necessitate it being sited in a position where access is restricted somewhat, e.g. the reactor and its power supply may be well separated, involving increased iR_{CIRCUIT} losses in the long busbars or tanks may be located at some distance from the cell, resulting in greater pumping requirements. Such a physical separation may be necessary if the cell operates in a flameproof, classified area, while the transformer rectifier and associated monitoring and controlling equipment operate outside the zoned area. In these circumstances, consideration must be given to the need for longer periods between maintenance.

2.4 ELECTROLYSIS PARAMETERS

As was discussed above, each of the figures of merit depends on a number of experimental variables. Hence, the overall cell performance will be determined by a complex interplay of these factors and it seems appropriate at this stage to summarize the various parameters which may be used to optimize an electrolytic process. The main electrolysis parameters are as follows.

2.4.1 Electrode potential

The electrode potential determines which electron transfer reactions can occur and also their absolute (and relative) rates, i.e. current densities. The potential, or current density is in many cases a major factor controlling the current efficiency, the space–time yield and the product quality.

2.4.2 Electrode materials and structure

The ideal electrode material for most processes should be totally stable in the electrolysis medium and permit the desired reaction with a high current efficiency at low overpotential. In a few processes, the anode reaction is the dissolution of a metal (e.g. plating or refining) and then this reaction should occur with the same current efficiency as the cathodic deposition so as to maintain the electrolyte composition constant; again, the overpotential should be as low as possible.

We remain, in practice, far from meeting these apparently trivial requirements: so-called 'inert' electrodes have a finite lifetime due to corrosion and physical wear while it is common, even normal, to accept an overpotential of several hundred millivolts. Only in the chlor-alkali process and, to a lesser extent, in water electrolysis and electrowinning has significant progress towards improved electrode materials been made. Generalizations concerning electrode materials are probably unwise and the choice of electrodes for particular industrial processes will be discussed in subsequent chapters; Table 2.2, however, lists some common anode and cathode materials.

The present trend is away from massive electrodes. The better materials are frequently expensive and it is therefore more common for the active material to be a coating on a cheaper, inert substrate (titanium or carbon for anodes, steel for cathodes). Dispersed electrodes, where the catalyst is pressed with a conducting powder (carbon), perhaps with additives (e.g. PTFE to decrease wetting), have also been discussed in Chapter 1. The coated electrodes are produced by several techniques including electroplating, spraying, vacuum sputtering and pyrolysis of solutions containing one or more metal ions. These electrodes, in addition to cheapness, have the advantage that they have high real-surface areas (i.e. they are microrough) and can be produced with different structures (e.g. various crystallite sizes) in order to improve activity.

The form of the electrode is also modified to meet the needs of particular processes. Thus, for example, electrodes are constructed commonly from meshes, expanded metal and related materials, in order to maximize surface area,

Table 2.2 Common electrode materials

Cathodes	Anodes
Hg, Pb, Ni	Pt, Pt/Ti, Ir/Ti, Pt–Ir/Ti (Pt/Nb, Pt/Ta)
Graphite and other forms of C sometimes treated thermally with organics or polymers (e.g. PTFE) to modify porosity, density, corrosion resistance, wettability	Graphite or other forms of C (treated)
	Pb in acid-sulphate media
	PbO_2 on Ti, Nb or C
Steels	Ni in alkaline media
Stainless steels	
Coatings of low-H_2 overpotential materials on steel, e.g. Ni, Ni/Al, Ni/Zn	Dimensionally stable anodes i.e. a mixed Ru-Ti oxide on Ti for Cl_2, IrO_2 on Ti for O_2
Hastelloys (Ni–Mo–Fe or Ni–Mo–Cr alloys)	Magnetite: $Fe_{3-x}O_4$
TiO_x	Conducting ceramics e.g. Ti_4O_7

reduce cost and weight and also enhance the release of gaseous products. It will also be seen in the later discussion of cell design that various types of particulate-bed electrodes have been proposed and the possibilities for porous-gas electrodes, which reduce mass transport restrictions for gaseous reactants, must also be considered.

The shape and form of the electrode may be modified to meet the needs of a particular process or a specific reactor geometry, e.g. electrodes constructed from perforated or expanded metal, those pressed into a louvred configuration, foams or nets having a very high porosity, may all facilitate the release of gaseous products or reduce weight. An increasingly diverse range of porous three-dimensional electrodes is available including stacked meshes, beds of carbon granules or fibre, and microporous felt or cloth. Such materials have high electroactive areas per unit electrode volume (section 2.3.9) but can present the following problems in practice:

1. A high pressure drop.
2. Plugging by solid products.
3. Difficulty in securing an electrically conductive contact (i.e. feeder) to the electrode.
4. Relatively high cost.
5. Restricted availability regarding material and porosity.
6. Incomplete wetting of, for example, microporous cloth materials.

As in the case of ion exchange membranes, it is difficult to justify economically the tailoring of an electrode to a particular process or reactor. Rather, electrode materials are often transferred from other, existing (and often high tonnage) technological fields of application. Examples include microporous metal or carbon cloths intended for fine filtration, porous metal meshes supplied as strainers and filters, and carbon felt and fibre designed as reinforcing media for carbon-reinforced–polymer composites.

One of the newest types of porous, three-dimensional materials to receive attention is reticulated (foam) metal (e.g. Ni, stainless steel, Cu) or carbon, e.g. reticulated vitreous carbon (RVC). The open-cell (alveoli-like) porous structure of these materials confers a range of interesting properties:

1. Reasonable isotropy of electrical conductivity, porosity and flow characteristics.
2. Reasonable electrical conductivity.
3. High porosity and, hence, low electrolyte pressure drop.
4. Low effective density.
5. Possibility of coating the material to provide a surface-modified electrode.

Practical drawbacks include:

1. The brittle, fragile nature of RVC (which means the electrode materials require adequate support in the reactor and suitable care in handling).

2. Difficulties in making feeder connections (although certain metal foams may be locally compressed to facilitate this).
3. Relatively high cost.
4. Restricted range and availability of materials.

2.4.3 The concentration of electroactive species

The concentration of the electroactive species is the major parameter that determines the maximum feasible current density and, hence, the optimum space–time yield. This current normally is proportional to concentration and therefore the concentration of electroactive species will also be as high as possible in most systems, being limited only by cost, solubility or post-electrolysis process requirements.

2.4.4 Electrolysis medium

The properties of the electrolysis medium will be determined by the choice of solvent, electrolytes and pH and perhaps also complexing agents, additives (i.e. species present in relatively low concentrations to modify the properties of the electrode–electrolyte interface) and reagents present to react with intermediates produced in the electrode reaction. The concentration of each constituent will also be important.

Although the last 30 years have seen much academic research on electrochemistry in non-aqueous solvents, its impact on industrial processes has been small because of the lower conductivity of such solvents and doubts concerning their long-term stability under electrolysis conditions. Water with a high concentration of electrolyte is certainly the medium of choice for an industrial electrolytic process, with molten salts a second best if their use is essential to a process. Some of the achievements in aprotic solvents (e.g. acetonitrile, dimethylformamide, propylene carbonate) as well as solvents such as methanol and acetic acid, are, however, impressive (e.g. non-aqueous batteries, electroplating baths and as media for certain organic syntheses) and electrochemical engineers continue to seek cell designs which utilize non-aqueous solvents.

The other constituents of the electrolysis medium are chosen on the basis of cost and their effectiveness in meeting the needs of a particular process. Their selection will be discussed in subsequent chapters.

2.4.5 Temperature and pressure

Electrolysis at elevated or reduced pressures is generally to be avoided because of the complexity of cell design; in practice, the large-scale examples of electrochemistry much above atmospheric pressure are mainly limited to special water electrolysers and battery systems. However, if volatile solvents are utilized, an

increased pressure may be desirable to minimize solvent loss, with its attendant cost, health and safety problems.

On the other hand, temperature is a parameter frequently employed. Temperatures above ambient are used frequently because of their beneficial effects on the kinetics of all steps in an electrode process. The diffusion coefficient, the exchange current density and the rates of chemical reactions are generally all increased. The decrease in viscosity and increase in diffusion coefficient both serve to enhance mass transport rates. In any case, the passage of current through most cells leads to Joule heating and extensive cooling may be necessary to maintain the cell at room temperature. Again, in the case of volatile solvents or thermally unstable reactants/products, forced cooling of the electrolyte may be essential.

2.4.6 Mass transport regimes

The mass transport regimes used in industrial processes range from natural convection and diffusion in unstirred electrolytes to highly turbulent conditions produced by rapid stirring, or pumping or using turbulence promoters such as a bed of particles. A high Reynolds number is commonly favourable since it increases mass transport and, hence, both increases the current density at any potential and leads to a greater uniformity of concentration in the reaction layer adjacent to the electrode surface. All forms of pumping and stirring, however, cost money (section 2.2) and in undivided cells can produce problems of interaction of anode and cathode products, e.g. aluminium electrolysis.

2.4.7 Cell design

The design of the cell will affect all the figures of merit for an electrolytic process. Cell design will be considered in detail in section 2.5 but it should be noted here that the principal factors determining the electrolysis performance will be the presence or absence of a separator and its type (porous diaphragm or ion-selective membrane), the mass transport regime, the arrangement and form of the electrodes (hence, the anode–cathode gap and potential distribution at both electrodes) and the materials of construction.

2.5 PRINCIPLES OF CELL DESIGN

2.5.1 Classical types of chemical engineering reactor

Chemical engineering recognizes three broad types of reactor (Fig. 2.6). These are now described and design equations are developed in a simplified manner, using the principle of mass balance over the reactor.

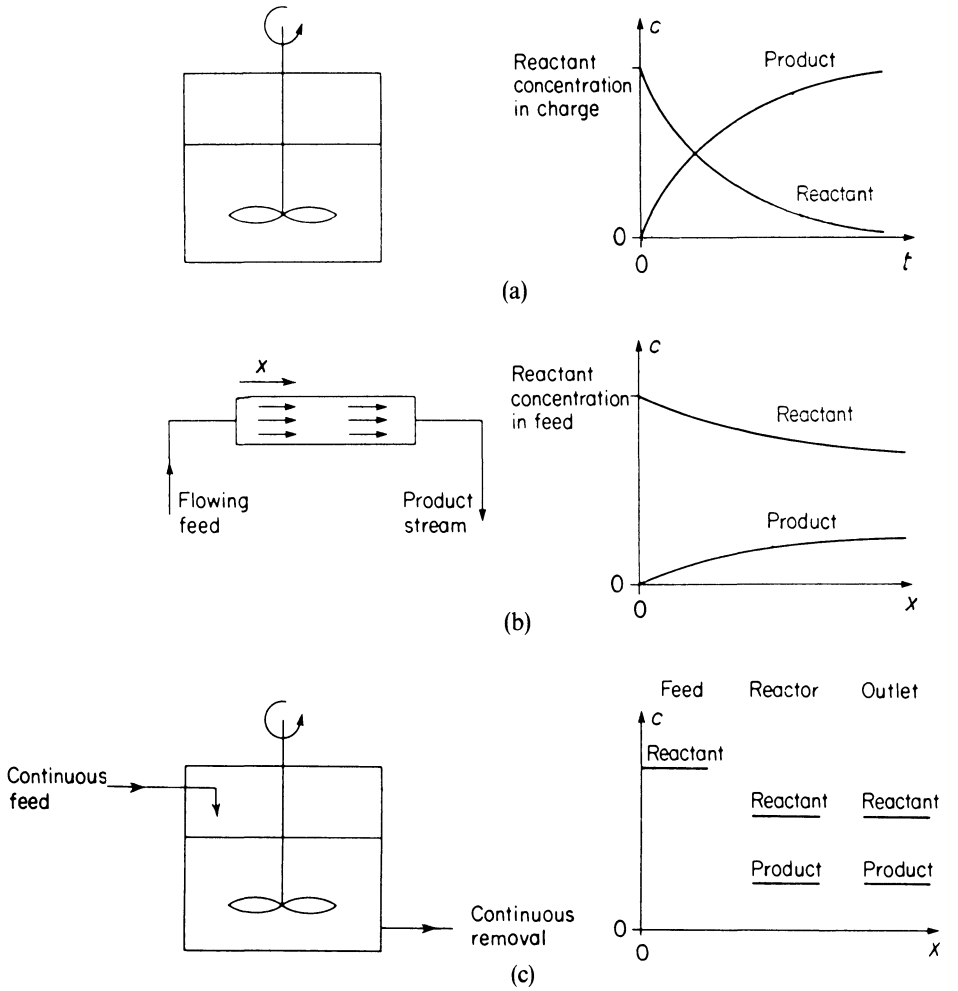

Fig. 2.6 The three ideal types of chemical reactor and their characteristic concentration versus time or concentration versus distance behaviour for the reactant and product. (a) Simple-batch reactor. (b) Plug flow reactor (PFR). (c) Continuously stirred tank reactor (CSTR).

(*a*) *The simple batch reactor*

The simple batch reactor is charged with the reactants which are then well mixed and left for a period for the reaction to occur to some predetermined extent. The resulting solution is then discharged from the reactor and worked-up to isolate the product. The concentration of reactants and product will change smoothly with time (in a way dependent on the reaction kinetics) but the composition is uniform throughout the reactor volume and the residence time is well defined, i.e. the same as the reaction time.

Batch processing is clearly labour intensive and better suited to small-scale operations or those requiring intermittent supplies of product.

(*b*) *The plug flow reactor (PFR) or tube reactor or piston-flow reactor*
This is a continuous and steady-state reactor. The reactant mixture is flowed through the reactor (e.g. a tube filled with catalyst) and the product is extracted from the mixture leaving the reactor. Ideally, a plug flow reactor is characterized by a flow of fluid where no element overtakes or mixes with that preceding or following it; hence, it is equivalent to a train passing through a tunnel with the carriages proceeding in a perfectly orderly manner. The composition of the mixture changes with distance through the reactor and the residence time is the same for all species.

(*c*) *The continuously stirred tank reactor (CSTR) or back-mix reactor*
The continuously stirred, or back-mix reactor consists of a well-stirred tank so that the composition is uniform but reactant is added continuously and a product stream removed at the same rate. The exit stream will have the same composition as the fluid in the reactor.

There are a number of 'modes of operation' for reactors, with respect to the electrolyte manifolds and reactant feed–product withdrawal schedules. Here, we will consider the design equations for four common modes of operation (Fig. 2.7), expressions being written in terms of *reactant* concentration for a process under complete mass transport control.

2.5.2 The simple batch reactor (Fig. 2.7(a))

Consider a constant volume of electrolyte V_R which is well mixed within the reactor at all times. The reactant will decay from an initial concentration of $c_{(o)}$ to a value $c_{(t)}$ at time t. Effective stirring makes the concentration spatially uniform. We may assume, for simplicity, that the reaction displays first-order kinetics with respect to the reactant; the rate of change of reactant concentration is then:

$$\frac{dc_{(t)}}{dt} = -kc_{(t)} \tag{2.117}$$

A mass balance in the reactor may be written by relating the rate of decrease of concentration to the cell current, in terms of Faraday's laws of electrolysis:

$$-\frac{dc_{(t)}}{dt} = i_{(t)}/(nFV_R) \tag{2.118}$$

where $i_{(t)}$ is the instantaneous current at time t. Under complete mass transport control, and by definition of the mass transport coefficient:

$$i_{(t)} = i_L = k_L AnFc_{(t)} \tag{2.119}$$

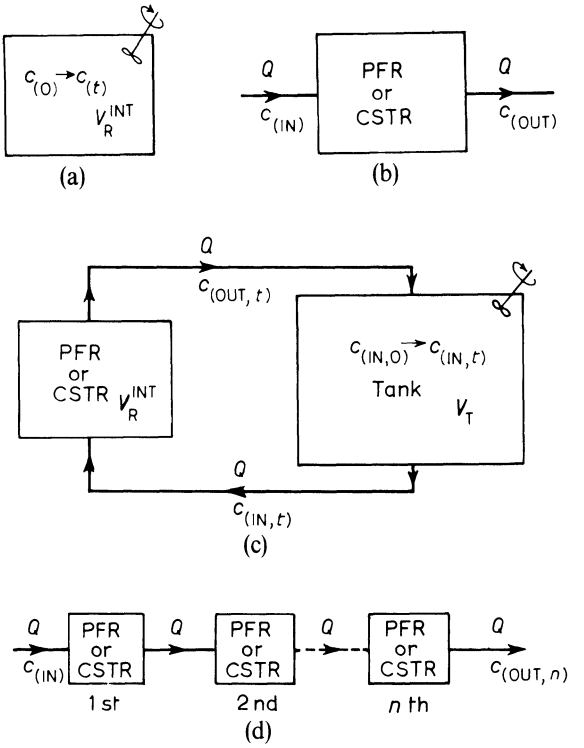

Fig. 2.7 Definition sketch showing common modes of operation for reactors. (a) Simple-batch reactor. (b) Single-pass reactor. (c) Batch-recirculation reactor. (d) Cascade of n identical reactors. PFR, plug flow reactor; CSTR, continuously stirred tank reactor.

Substituting $i_{(t)}$ from equation (2.119) into equation (2.118):

$$\frac{-\mathrm{d}c_{(t)}}{\mathrm{d}t} = \frac{k_L A c_{(t)}}{V_R} \tag{2.120}$$

Comparison of equations (2.120) and (2.117) shows that the apparent rate constant in equation (2.117) is given by:

$$k = \frac{k_L A}{V_R} \tag{2.121}$$

Integration of equation (2.120) gives:

$$c_{(t)} = c_{(o)} \exp\left(-\frac{k_L A}{V_R} t\right) \tag{2.122}$$

which describes the reactant concentration as a function of time, showing that the rate of decay is enhanced by increasing k_L or A (or both) for a given

electrolyte volume V_R within the reactor. The ratio A/V_R is A_S^{INT}, giving:

$$c_{(t)} = c_{(o)} \exp(-k_L A_S^{INT} t) \tag{2.123}$$

The fractional conversion in a simple batch reactor may be stated via equation (2.122) as:

$$X_A = 1 - (c_{(t)}/c_{(o)}) = 1 - \exp\left(-\frac{k_L A}{V_R} t\right) \tag{2.124}$$

By its very nature, the simple batch reactor operates in an unsteady state; the reactant (and product) concentration are time-dependent.

There are several variants of the simple batch reactor, e.g. the electrolyte may be treated batchwise, but product may be withdrawn continuously in order to prevent redissolution, blockage of the cell (causing high-pressure drops or stirrer problems), interelectrode shorting or electrode erosion.

2.5.3 The single-pass reactor (Fig. 2.7(b))

Consider the general case of a single-pass reactor, where a steady volumetric flow rate Q of electrolyte passes through the reactor. The inlet concentration of reactant $c_{(IN)}$ is reduced to $c_{(OUT)}$ at the outlet. Both $c_{(IN)}$ and $c_{(OUT)}$ are time-independent in the case of a steady-state reactor.

A mass balance over the reactor (on a molar basis) gives, via Faraday's laws:

MASS IN − MASS OUT = MASS REMOVED BY ELECTROLYSIS

$$Qc_{(IN)} - Qc_{(OUT)} = i/nF \tag{2.125}$$

or in terms of the concentration change:

$$\Delta c = c_{(IN)} - c_{(OUT)} = i/nFQ \tag{2.126}$$

(a) The plug flow reactor

The reactant concentration decreases continuously along the length x of the electrode (measured from the inlet end of the electrode, where $x = 0$). The total current flowing to the electrode may be obtained by integration of the local current $i_{(x)}$:

$$i = \int_0^x i_{(x)} \mathrm{d}x \tag{2.127}$$

If the entire electrode supports a reaction under mass transport control via convective diffusion of the reactant or product, then the local current density is given by:

$$I_x = I_L = k_L nF c_{(x)} \tag{2.127a}$$

where $c_{(x)}$ is the local concentration at a distance x from the inlet side of the

electrode. If longitudinal dispersion of flow due to diffusion is negligible, the concentration gradient along the reactor may be described via equation (2.126) as:

$$\frac{-\mathrm{d}c_{(x)}}{\mathrm{d}x} = \frac{i_{(x)}A'}{nFQ} \tag{2.128}$$

where A' is the electrode area/unit length of reactor.

Substituting $i_{(x)} = i_L$ from equation (2.127):

$$\frac{-\mathrm{d}c_{(x)}}{\mathrm{d}x} = \frac{k_L A'}{Q} c_{(x)} \tag{2.129}$$

where k_L is a spatially-averaged mass transport coefficient (cf. equation 2.120).

Equation (2.129) may be integrated over the reactor length to give:

$$c_{(OUT)} = c_{(IN)} \exp\left(-\frac{k_L A}{Q}\right) \tag{2.130}$$

which describes the reactant concentrations at the inlet and outlet of the reactor at a given volumetric flow rate in terms of the averaged mass transport coefficient and electrode area.

For a given flow rate Q and inlet reactant concentration $c_{(IN)}$ the outlet concentration may be decreased by raising k_L or A. The fractional conversion over the plug flow reactor may be stated from equation (2.120) as:

$$X_A = 1 - \frac{c_{(OUT)}}{c_{(IN)}} = 1 - \exp\left(-\frac{k_L A}{Q}\right) \tag{2.131}$$

The limiting current may be expressed in terms of the inlet concentration by combining equations (2.126) and (2.130):

$$i_L = nFQc_{(IN)}X_A = nFQc_{(IN)}\left[1 - \exp\left(-\frac{k_L A}{Q}\right)\right] \tag{2.132}$$

Recalling that the residence time $\tau = V_R^{INT}/Q$, equation (2.130) may be rewritten:

$$c_{(OUT)} = c_{(IN)} \exp\left(-\frac{k_L A}{V_R^{INT}}\tau\right) \tag{2.133}$$

which is identical to equation (2.122) for the simple-batch reactor, with $t = \tau$.

In terms of fractional conversion over the plug flow reactor,

$$X_A = 1 - \exp\left(-\frac{k_L A}{V_R^{INT}}\tau\right) \tag{2.134}$$

i.e. for a given k_L, A and V_R^{INT}, the plug flow reactor and simple-batch reactors will give an identical conversion if the residence time of the plug flow reactor is equivalent to the batch-processing time. An alternative way to regard this is that the plug flow reactor and simple batch reactor will each have an identical electrolyte volume in the reactor V_R^{INT} for a given conversion, as long as the reactors have the same $k_L A$ value.

(b) The continuously stirred tank reactor

The major features for this reactor are that the outlet concentration $c_{(OUT)}$ is identical to that inside the reactor, and the concentration is uniform throughout the reactor. These features are a consequence of perfect back-mixing.

The limiting current density and mass transport are therefore time, and spatially, invariant, being related by:

$$i_L = k_L n F A c_{(OUT)} \tag{2.135}$$

A mass balance over the reactor via equation (2.125) and consideration of equation (2.135) gives:

$$\Delta c = c_{(IN)} - c_{(OUT)} = \frac{k_L A}{Q} c_{(OUT)} \tag{2.136}$$

or:

$$c_{(OUT)} = \frac{c_{(IN)}}{1 + (k_L A/Q)} \tag{2.137}$$

which relates the concentrations at the reactor manifolds to k_L, A and Q. From equation (2.137), the fractional conversion over the reactor:

$$X_A = 1 - \frac{c_{(OUT)}}{c_{(IN)}} = 1 - \left[\frac{1}{1 + (k_L A/Q)}\right] \tag{2.138}$$

which again shows the importance of maximizing k_L and A in order to achieve a high conversion.

The limiting current may be related to the inlet concentration by a consideration of equations (2.126) and (2.138):

$$i_L = nFQc_{(IN)}\left[1 - \frac{1}{1 + (k_L A/Q)}\right] \tag{2.139}$$

Equations (2.138) and (2.139) may be compared to the analogous equations (2.131) and (2.132) for a plug flow reactor. It then becomes evident that, for given values of k_L, A and Q, a smaller fractional conversion is achieved in a continuously stirred tank reactor than a plug flow reactor. For a given $c_{(IN)}$ value, the limiting current is also higher in a plug flow reactor. However, a controlled high value of k_L may be maintained by vigorous agitation in a moderate size of reactor, whereas a plug flow reactor having the same k_L may be physically larger in order to maintain a high averaged k_L. If the agitation conditions are sufficiently good in a continuously stirred tank reactor, the value of k_L may become largely independent of Q, which makes process design simpler. This situation is approximated well by a rotating cylinder electrode in turbulent flow (Chapter 7).

In practice, the fractional conversion over a single-pass reactor is often limited, e.g. if the flow rate is reduced in an attempt to achieve a higher

conversion, then the k_L may be reduced and adverse build up of heat or product accumulation may occur. A recycle loop on the reactor (Fig. 2.8) may:

1. Help to aid cooling, mixing or to stabilize k_L.
2. Provide an opportunity to locate sampling and injection points, and sensors for process monitoring and control.
3. Allow the reactor to operate or be controlled about a set point, e.g. a constant outlet concentration for slight variation in $c_{(IN)}$.

It is noteworthy that a true continuously stirred tank reactor is perfectly mixed; a recycle loop cannot be used to further improve agitation or the value of k_L.

In practice, particularly useful methods of improving the overall fractional conversion are: (1) batch recirculation of the electrolyte through the reactor from a storage tank (section 2.5.4); or (2) the use of a number of reactors in hydraulic series, i.e. a cascade arrangement (see section 2.5.5).

2.5.4 Batch recirculation (Fig. 2.7(c))

Batch recirculation is a particularly flexible and convenient mode of operation. The provision of a reservoir external to the reactor may serve several useful purposes. In addition to increasing the electrolyte inventory, it may: (1) help to correct pH (via addition of reagents); (2) stabilize temperature (by suitable heat exchangers); (3) facilitate sampling; (4) act as a gas disengagement vessel or a solid–liquid separator; and (5) provide a convenient, well-stirred zone for reactant preparation and mixing prior to electrolysis.

The system as a whole (i.e. cell plus reservoir) approximates to continuously stirred tank reactor behaviour if the reservoir volume is much greater than that

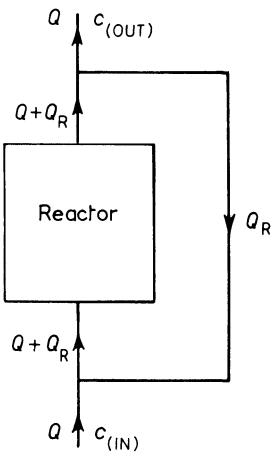

Fig. 2.8 A recycle loop on a reactor may be used to control the outlet concentration of reactant.

of the reactor ($V_T \gg V_R^{INT}$) and the reservoir residence time τ_T is high. Unlike the single-pass case (section 2.5.3), both the inlet and outlet reactor concentrations are time-dependent.

In the general case, it is necessary to consider mass balances over the reactor and the reservoir. For the well-mixed reservoir:

$$V_T \frac{dc_{(IN)}}{dt} = Q(c_{(OUT)} - c_{(IN)}) \tag{2.140}$$

For a plug flow reactor, substitution of $c_{(OUT)}$ from equation (2.130) into equation (2.140), followed by integration, gives:*

$$c_{(IN,\,t)} = c_{(IN,\,o)} \exp\left[-\frac{t}{\tau_T}\left(1 - \exp\left(-\frac{k_L A}{Q} \right) \right) \right] \tag{2.141}$$

or:

$$c_{(IN,\,t)} = c_{(IN,\,o)} \exp\left(-\frac{t}{\tau_T} X_A^{PFR} \right) \tag{2.142}$$

where X_A^{PFR} is the fractional conversion for a single-pass plug flow reactor.

The overall fractional conversion for the system is then:

$$X_{A,\,t}^{PFR} = 1 - \left[\frac{c_{(IN,\,t)}}{c_{(IN,\,o)}} \right] = 1 - \exp\left(-\frac{t}{\tau_T} X_A^{PFR} \right) \tag{2.143}$$

For the continuously stirred tank reactor in batch recycle, a simple approach using equations (2.137) and (2.140) gives:*

$$c_{(IN,\,t)} = c_{(IN,\,o)} \exp\left[-\frac{1}{\tau_T}\left[1 - \frac{1}{1 + (k_L A/Q)} \right] \right] \tag{2.144}$$

Recalling the fractional conversion for a single-pass reaction in equation (2.138):

$$c_{(IN,\,t)} = c_{(IN,\,o)} \exp\left(-\frac{t}{\tau} X_A^{CSTR} \right) \tag{2.145}$$

The overall fractional conversion for the continuously stirred tank reactor in batch recycle is therefore:

$$X_{A,\,t}^{CSTR} = 1 - \frac{c_{(IN,\,t)}}{c_{(IN,\,o)}} = 1 - \exp\left(-\frac{t}{\tau_T} X_A^{CSTR} \right) \tag{2.146}$$

There are many variants on the batch-recycle mode. A practical example is shown in Fig. 2.9. Semi-batch operation allows for continuous or intermittent addition of reactant.

* These approximate solutions are usually adequate for modelling practical reactor systems. (A. T. S. Walker and A. A. Wragg (1977) *Electrochimica Acta*, **22**, 1129.)

2.5.5 A cascade of reactors (Fig. 2.7(d))

A cascade of reactors is capable of achieving a high overall conversion with a continuous flow of electrolyte. In order to minimize investment and maintenance costs, the reactors (n in number) are usually identical and in certain cases may be assembled in a common package.

For the plug flow reactor, successive application of equation (2.130) gives:

$$c_{(\mathrm{OUT},n)} = c_{(\mathrm{IN})} \exp(-nk_{\mathrm{L}}A/Q) \tag{2.147}$$

or

$$X_{\mathrm{A},n} = 1 - \frac{c_{(\mathrm{OUT},n)}}{c_{(\mathrm{IN})}} = 1 - \exp(-nk_{\mathrm{L}}A/Q) \tag{2.148}$$

For the continuously stirred tank reactor, successive application of equation (2.137) gives:

$$c_{(\mathrm{OUT},n)} = c_{(\mathrm{IN})}(1 + k_{\mathrm{L}}A/Q)^n \tag{2.149}$$

or:

$$X_{\mathrm{A},n} = 1 - \frac{c_{(\mathrm{IN})}}{c_{(\mathrm{OUT},n)}} = 1 - \frac{1}{(1 + k_{\mathrm{L}}A/Q)^n} \tag{2.150}$$

In practice, the reactor system may be more complex than the simple modes considered. It is possible to introduce partial or complete recycles of the outlet stream, to consider the use of multistage set-ups with reactors in series or parallel or to introduce feed or heat management between stages. The principles

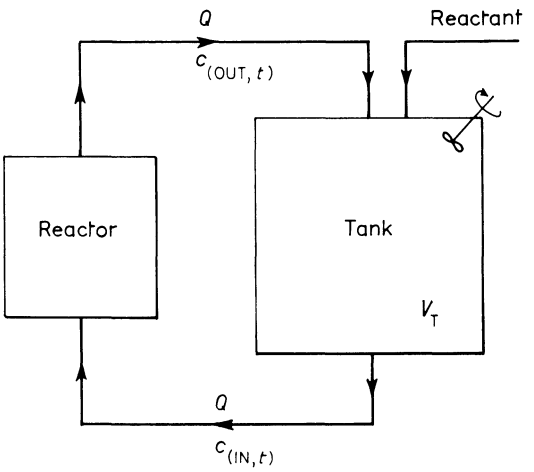

Fig. 2.9 An example of semi-batch operation: batch recycle with continuous addition of reactant to the tank.

for the discussion of such systems are, however, the same. Practical reactors usually show behaviour which is intermediate between that of an ideal batch, plug flow, or continuously stirred tank reactor. However, an adequate description of practical reactor performance is usually possible via assumption of one of these models.

It may be necessary to consider many non-idealities for more rigorous modelling exercises, e.g.:

1. Poor mixing or volume changes in a simple batch reactor.
2. Flow dispersion (and, hence, mixing) in the longitudinal direction of a plug flow reactor.
3. By-passing (channelling) of flow from inlet to outlet in a continuously stirred tank reactor.

The problem of current density distribution and the need to control electrode potential distribution, in comparison to chemical reactors, is an additional problem in electrochemical reactors. This aspect and some additional factors relevant to electrolytic processes will be reviewed in section 2.5.6 as a prelude to the discussion of cell design.

2.5.6 Kinetics of the batch reactor in practice

The overall kinetic behaviour of an electrochemical reactor may be illustrated by considering the example of a simple batch reactor.

In the general case of constant current i electrolysis, the reactant concentration change Δc is given by Faraday's laws of electrolysis as:

$$\Delta c = c_{(o)} - c_{(t)} = \frac{\phi i t}{nFV} \tag{2.151}$$

where ϕ is the overall current efficiency after time t.

Rearranging:

$$c_{(t)} = c_{(o)} - \frac{\phi i t}{nFV} \tag{2.152}$$

or:

$$\phi = (c_{(o)} - c_{(t)}) \frac{nFV}{it} \tag{2.153}$$

Taking natural logarithms in equation (2.152)

$$\ln c_{(t)} = \ln\left(c_{(o)} - \frac{\phi i t}{nFV}\right) \tag{2.154}$$

The behaviour of the reactor with time during constant current i electrolysis depends upon the value of i compared to the mass transport controlled limiting

current i_L. Extreme cases may be distinguished as current limited control and mass transport control.

(*a*) *Current-limited control*

There is abundant reactant for all the current to be used in electrochemical reduction or oxidation in the early stages of electrolysis ($t < t'$; $c_{(t)} < c'$), $i < i_L$ and the rate of decrease of concentration is constant, as is the current efficiency $\phi = \phi'$. Equation (2.152) becomes:

$$c_{(t)} = c_{(o)} - \frac{\phi' it}{nFV} \tag{2.155}$$

or:

$$\phi' = (c_{(o)} - c_{(t)}) \frac{nFV}{it} \tag{2.156}$$

Taking natural logarithms of equation (2.155):

$$\ln c_{(t)} = \ln\left(c_{(o)} - \frac{\phi' it}{nFV} \right) \tag{2.157}$$

The fractional conversion is given by equation (2.155) as:

$$X_A = \frac{c_{(o)} - c_{(t)}}{c_{(o)}} = \frac{\phi' it}{nF c_{(o)}} \tag{2.158}$$

As ϕ', i and $c_{(o)}$ are constants, the fractional conversion rises linearly with time. The space–time yield is:

$$\rho_{ST} = \frac{M(c_{(o)} - c_{(t)})}{t} \tag{2.159}$$

and from equation (2.156):

$$\rho_{ST} = \frac{M\phi' i}{nFV} \tag{2.160}$$

which shows that ρ_{ST} is a constant.

(*b*) *Mass transport control*

The above behaviour persists until a limiting time t', when the applied current is larger than the limiting current corresponding to reactant in solution:

$$t \geqslant t';\ c_{(t)} \leqslant c';\ i \geqslant i_L$$

The current efficiency now falls with time. As the reaction is now mass transport controlled, the concentration decay becomes exponential with time and is described by equation (2.122) with $c_{(o)} = c'$, the critical concentration of reactant

which is just able to maintain the current i_L:

$$c_{(t)} = c' \exp\left[-\frac{k_L A}{V}(t-t')\right] = \frac{i_L}{nFAk_L} \exp\left[-\frac{k_L A}{V}(t-t')\right] \tag{2.161}$$

and from equations (2.29) and (2.65), the current efficiency is now given by:

$$\phi = \frac{k_L A c_{(t)} nF}{i_L} \tag{2.162}$$

Combining equations (2.161) and (2.162):

$$\phi = \frac{k_L AnF}{i_L} c' \exp\left[-\frac{k_L A}{V}(t-t')\right] \tag{2.163}$$

Taking natural logarithms of equation (2.161):

$$\ln c_{(t)} = \ln c' - \left[\frac{k_L A}{V}(t-t')\right] \tag{2.164}$$

The increase in fractional conversion for $t > t'$ is:

$$X_A = 1 - c_{(t)}/c' = 1 - \exp\left[\frac{-k_L A}{V}(t-t')\right] \tag{2.165}$$

which is a non-linear relationship for $t > t'$.

The space–time yield at $t > t'$ is a function of time, being given by:

$$\rho_{ST} = \left[\frac{M(c' - c_{(t)})}{t}\right] \tag{2.166}$$

or:

$$\rho_{ST} = \frac{M\phi i}{nFV} \tag{2.167}$$

ρ_{ST} falls with time as ϕ decreases (equation (2.163)).

The overall kinetic behaviour of this simple batch reactor is illustrated in Fig.2.10. Even with a constant volume and a given cell, this schematic behaviour may be modified in practice by several effects:

1. The transition between current- and mass transport-limited control is gradual, rather than sharp, due to a region of mixed control.
2. Adsorption phenomena at the electrode or chemical reactions may alter the kinetics significantly.
3. At the start of electrolysis, the behaviour may take some time to stabilize due, for example, to electrode conditioning, e.g. to formation or removal of surface films.
4. At long times, the concentration may tend to a low but finite value, as chemical reactions become more important than mass-transport restrictions.

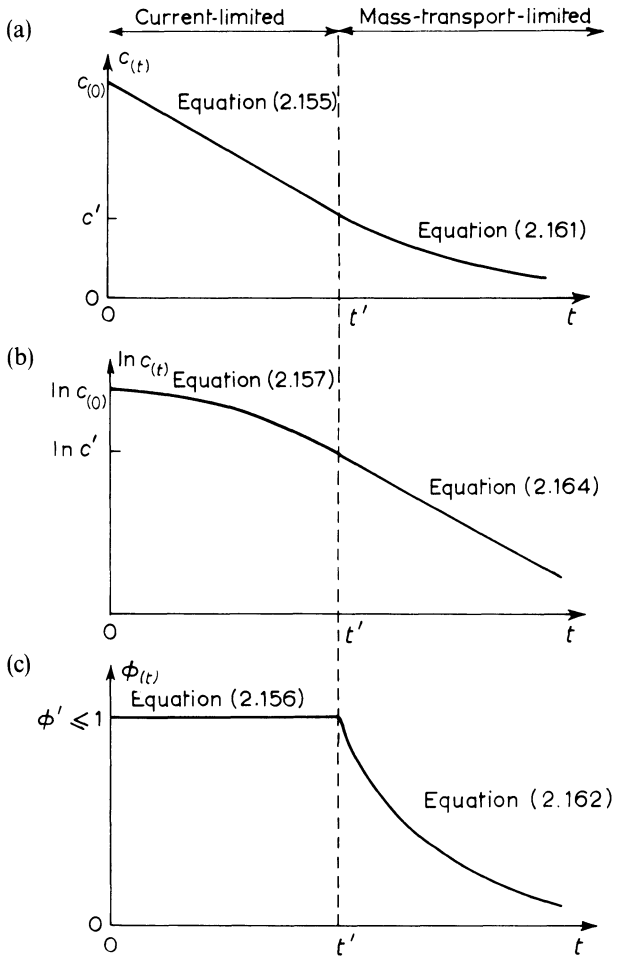

Fig. 2.10 The time-dependence of (a) reactant concentration, (b) logarithm of reactant concentration, (c) overall current efficiency during batch processing using a constant current where initially $i < i_L$.

5. The active electrode area or the mass transport may change with time due, for example, to adsorption onto the electrode, deposition of product, surface roughening or changes in flow conditions.

Despite these complicating factors, the procedure of obtaining reactant concentrations vs. time curves under appropriate galvanostatic conditions followed by the approach outlined above provides a convenient and practical method. Not only can ϕ' and $k_L A/V_R$ be determined, but the time and concentration dependence of ϕ, X_A and ρ_{ST} can be determined over a wide range of $c_{(t)}$, in a single experiment.

2.6 THE ADDITIONAL TECHNOLOGY OF ELECTROLYTIC PROCESSES

The similarities between the design and characterization of electrolysis cells and other chemical reactors and the need to integrate the cell with the other unit processes in the plant, have been emphasized. On the other hand, there are some notable differences which need also to be recognized, e.g. the fact that in a comparison of an electrolysis cell with a reactor for a more familiar heterogeneous process, such as gas-phase catalysis, there are two outstanding differences:

1. Mass transport processes in the liquid phase are always very slow in comparison with those in the gas phase. This will cause both mass transport limitations on the rate of chemical changes in the reactor and the creation of reaction layers at the solid–fluid interface to be much more troublesome.
2. While, in both types of reactor, it is desirable to maximize the surface area per unit volume, the designer of an electrolytic cell has to concern himself with the problems of non-uniform current distributions, since the electrode surface will only be active if there is an appropriate local potential difference; it was noted above that the geometric arrangement of anode and cathode is the key factor.

It is the purpose in this section to review these problems and then to discuss those technological features which are unique to electrolytic processes.

2.6.1 The importance of mass transport in electrolytic reactors

An obvious strategy in electrochemical process engineering is to operate the reactor under mass transport controlled, limiting-current conditions, as the production rate should then be maximized. There are cases, however, when operation at or near the limiting current may not be optimal or even desirable as below:

1. A consideration of overall process costs (section 2.2), such as the trade-off between energy consumption and space–time yield may result in an optimum current below i_L.
2. Chemical or other electrochemical steps may influence significantly the yield and selectivity (sections 2.3.2–2.3.5). These reactions may be sensitive to the electrolyte flow conditions; however, it may be necessary to adjust their rates such that $i \ll i_L$.
3. The quality of the product may be inferior near limiting-current conditions, e.g. in the case of electroplating, $i < i_L$ in order to avoid roughened deposits (section 8.1.2) or problems due to codeposition of metal oxide–hydroxide. The maximum current for acceptable electrodeposition is, however, strongly linked to i_L and enhancement of mass transport will often permit an increase in the rate of electroplating (or else a reduced time to obtain a given deposit

thickness). Additionally, the metal powder deposits often obtained near i_L are often removed easily from the electrode and reactor (Chapter 7) which permits a continuous metal product recovery when removing dissolved metal from process liquors.

4. The limiting current density may exceed the capability of permissible or readily available electrode materials or membranes particularly when the concentration of electroactive species is high. Operation at high currents may also cause overheating due to Joule heating in the electrolyte and iR drop within the electrode material, leading to an uneven potential distribution (section 2.6.4).
5. At i_L, a small change in reactor or electrolyte conditions may alter significantly the material yield, selectivity or current efficiency, e.g. during constant current ($i = i_L$) electrolysis, a decrease in the level of electroactive species at the reactor inlet (or initially in the case of a simple batch reactor) will reduce i_L such that $i > i_L$. The incidence of side reactions may then be problematic.

Despite these provisos, it is common to design reactors to operate at or near i_L. Indeed, the electrochemical engineer's interest in mass transport relates to three different aspects of cell performance:

1. The advantage to be gained from a high current density; it has been seen in section 2.5 that the reactor performance (as evidenced by, for example, the fractional conversion, mass-transport coefficient, space velocity and space–time yield) is enhanced at higher currents.
2. The desire for a uniform current density over all the electrode surface (section 2.6.2) in order to minimize secondary reactions and, hence, maintain the current efficiency, materials yield and selectivity at high levels.
3. The need in certain processes to maintain the composition of the reaction layer at the electrode close to that in the bulk solution, in order to prevent unwanted chemical reactions which may, for example, hinder the kinetics of the desired process, foul the electrode or decrease product quality.

Commonly, the cell designer will be concerned with concentration variations in two directions, e.g. in most parallel plate cells the concentration variations parallel to the electrolyte flow and also perpendicular to the electrode surface will be of concern. As the solution flows up the electrode, the electrode reaction is occurring and, hence, the concentration of the electroactive species must decrease. Whether this depletion is significant will depend on the electrode potential (and hence on the ratio i/i_L), length of the electrode, flow rate, and the ratio of electrode area to electrolyte volume. There must also be a layer next to the electrode surface where there is a concentration gradient in the electroactive species. The variation of the concentration within this reaction layer and its thickness will again depend on the ratio i/i_L via the surface concentration and the Reynolds number respectively. In some electrolyses, particularly those

involving complex chemistry, there will be concentration gradients in reagents other than the electroactive species within the reaction layer (where almost all the chemistry will occur because of the relatively high concentration of intermediates), e.g. in electrolysers for the production of hypochlorite from sea water, a problem can arise at the cathode. The electrode reaction is hydrogen evolution but it also generates hydroxide ion and, unless there is efficient mixing between the reaction layer and the main body of electrolyte, the pH of the solution will rise to a value where the magnesium in the sea water precipitates as magnesium hydroxide. The maintenance of uniform conditions in the reaction layer is greatly assisted by turbulence or tangential shear forces, since the small eddies enter the reaction layer.

Fluid mechanics is also important in the design of electrolytic plant. The pipework between cells and between the cells and other units must be designed to minimize pumping costs, requiring the correct choice of pipework diameter and the avoidance of unnecessary pressure drops caused by obstructions or restrictions, incorrectly designed entries, sharp turns or rapid changes in pipe diameter. More importantly, however, the electrochemical engineer must pay particular attention to the fluid entry into the cell and ensure that there are no dead zones within the interelectrode gap and that the flow becomes uniform as quickly as possible. This requires correct distributor design.

It is normal to characterize the mass transport regime within a reactor as a function of flow rate and cell and/or electrode dimensions. This is generally done in terms of average parameters derived from measurements of the total cell current when the cell voltage is such that all the electroactive species reaching the surface are oxidized or reduced. These experimental data are cast into equations in terms of dimensionless parameters which indicate the relative importance of inertial/viscous forces and convection/diffusion, etc. (section 1.2). Some typical equations for common electrode geometries are given in Table 2.3. Considering industrial scale reactors, it is often not possible to obtain the same dimensionless group correlations as in laboratory cells. There are several reasons for this:

1. Flow transitions may occur in the velocity range of interest.
2. The electrode–reactor geometry may not be uniform.
3. Part of the electrode near the inlet may be in the developing hydrodynamic boundary region; it is unusual for an industrial reactor to have a 'calming' section to condition the flow.
4. There may be a significant iR_{CIRCUIT} drop within the electrode itself, particularly if it is fabricated from a relatively poor conductor (e.g. titanium), if it is very thin or porous (e.g. packed-bed electrodes) or if the electrode particles are in poor, intermittent contact, as in active fluidized bed electrodes.
5. There may be a significant iR_{CELL} drop due to a low electrolyte conductivity or a necessarily large gap between the electrode of interest and the reference electrode in certain experiments.

Table 2.3 Average mass transfer correlation equations for some simplified electrode geometries*

Cell- and flow-type	Schematic	Conditions	Correlation equation	Definitions
1. Vertical plate:	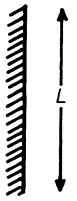			
(a) Natural convection, laminar flow		$Gr \times Sc < 10^{12}$	$Sh = 0.45\, Gr^{0.25} Sc^{0.25}$	
(b) Natural convection, turbulent flow		$4 \times 10^{13} < Gr \times Sc < 10^{15}$	$Sh = 0.31\, Gr^{0.28} Sc^{0.28}$	
(c) Gas evolving electrode		$a = 1.38$ for spherical bubbles	$Sh = a(1-\theta)^{0.5} Re^{0.5} Sc^{0.5}$	$Re = \dfrac{L v_g}{\nu}$
		$a = 1.74$ for hemispherical bubbles		
2. *Horizontal, channel flow; parallel plates*:	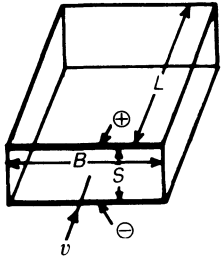			
(a) Fully developed laminar flow		$Re < 2000$, $B > S$, $L/d_e < 35$	$Sh = 1.85 Re^{0.33} Sc^{0.33} (d_e/L)^{0.33}$	$l = d_e = 2BS/(B+S)$
(b) Turbulent flow		$Re > 2300$ $L/d_e > 10$	$Sh = 0.023 Re^{0.8} Sc^{0.33}$	$l = L$
3. *Rotating disc*:	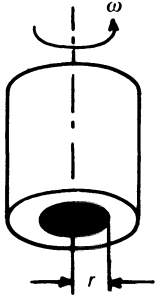			
(a) Laminar flow		$10^2 < Re < 10^4 - 10^5$	$Sh = 0.62 Re^{0.5} Sc^{0.33}$	$Re = \dfrac{r^2 \omega}{\nu}$
(b) Turbulent flow		$Re > 10^6$	$Sh = 0.011 Re^{0.87} Sc^{0.33}$	$Re = \dfrac{r^2 \omega}{\nu}$

4. *Concentric cylinders*:

(a) Fully developed laminar flow ($\omega = 0$) through an annulus

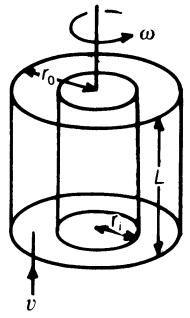

$Re < 2000$, inner electrode $\quad Sh = 1.61\phi Re^{0.33} Sc^{0.33}(d_e/L)^{0.33}$

$$\phi = \frac{r-1}{r}\left(\frac{0.5+[r^2/(1-r^2)]\ln r}{1+[(1+r^2)/(1-r^2)]\ln r}\right)$$

$r = r_i/r_0$

$l = 2(r_0 - r_i)$

$Re > 2000$, inner electrode $\quad Sh = 0.023 Re^{0.8} Sc^{0.33}$

(b) Rotating cylinder, turbulent flow around the inner cylinder ($v = 0$)

$100 < Re < 1.6 \times 10^5 \quad Sh = 0.079 Re^{0.7} Sc^{0.36}$

$$Re = \frac{2r_i\omega}{v}$$

$l = 2r_i$

5. *Bed electrodes*:

(a) Packed

(b) Fluidized

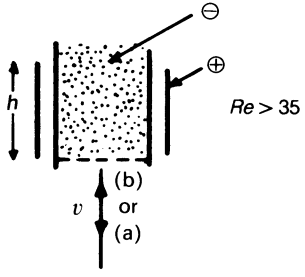

$Sh = 1.52 Re^{0.55} Sc^{0.33}$ $\quad l$ = ave particle diameter

$$Sh = \frac{(1-\varepsilon)^{0.5}}{\varepsilon} Re^{0.5} Sc^{0.33}$$ $\quad l$ = ave particle diameter

ε = bed voidage

---

*The dimensionless parameters, the Reynolds number Re, the Grashof number Gr, the Schmidt number Sc and the Sherwood number Sh are defined by

$$Re = \frac{v.l}{\nu} \qquad Gr = \frac{g\Delta\rho L^3}{\nu^2\rho} \qquad Sc = \frac{\nu}{D} \qquad Sh = \frac{k_L l}{D}$$

where v = flow velocity, l = characteristic length parameter, ν = kinematic viscosity, $\Delta\rho$ = difference in density between solution at electrode surface and the bulk, D = diffusion coefficient, and k_L = average mass transfer coefficient, θ = surface coverage, v_g = volume of gas per unit electrode area per unit time

2.6.2 The determination of limiting current

The most generally applicable method of measuring the limiting current is to obtain a steady-state i vs. E (or polarization) curve. This is usually performed for a model reaction–electrode combination in the presence of a high level of inert electrolyte (which means the contribution of migration to mass transport may be ignored, as discussed in Chapter 1). In practice, the two most useful reactions are the cathodic deposition of copper from copper sulphate and the reduction of ferricyanide to ferrocyanide. The former is often preferred for electrowinning cells but entails periodic copper removal from the electrodes; a soluble copper anode or suitable flow and concentration conditions may be used to maintain a constant Cu^{2+} level in the electrolyte. The reduction of ferricyanide generally gives better results than oxidation of ferrocyanide, although problems arise from the chemical stability of both of these anions, including their sensitivity to light. If a divided cell configuration is used, a useful technique is to employ a common reservoir for the anolyte and catholyte and a high ratio of ferrocyanide to ferricyanide, e.g. 10:2. The anode reaction is then under electron transfer control and the oxidation of ferrocyanide to ferricyanide will occur efficiently. The loss of ferricyanide (at the cathode) is also balanced by its anodic production, as long as $i \leqslant i_L$ at the cathode. In an undivided cell, anodic oxygen evolution should be avoided as it may affect the hydrodynamics near the cathode and provide an additional cathodic reaction, i.e. oxygen reduction. This may be achieved by using an electrolyte containing a high ratio of ferrocyanide to ferricyanide. Even so, air is usually removed and excluded from the electrolytes by nitrogen bubbling or blanketing. This is often difficult or even impractical for large volumes and, in such cases, allowances must be made for the (constant?) background current primarily due to oxygen reduction (Fig. 2.12).

It is convenient to employ an electrolyte and conditions (c, T) which have established transport properties (ν and D), in order to facilitate calculation of dimensionless groups. Figure 2.11 shows a steady-state, cathodic i–E curve. Three overpotential regions may be distinguished:

1. $0 < \eta < \eta_1$; $i \leqslant i_L$: only the model reduction occurs, $O + ne^- \rightarrow R$. At η_1, the reaction reaches complete mass transport control.
2. $\eta_1 < \eta < \eta_2$; $i = i_L$: the limiting current region is ideally a plateau (the slope of the curve, $di/dE = 0$). There is often, in practice, a significant slope, as shown in Fig. 2.12.
3. $\eta > \eta_2$; $i > i_L$: an additional, side reaction occurs, typically hydrogen evolution due to reduction of the solvent; this process is usually under electron transfer control (Chapter 1) and occurs at a rate equivalent to $(i - i_L)$.

In practice, several factors may complicate the appearance of the limiting current curve, as indicated in Fig. 2.12. The limiting current plateau should be long (i.e. $\eta_1 - \eta_2$ should be large) and of small slope (Fig. 2.11), but it may tilt (Fig. 2.12(a)), be influenced by background reactions (Fig. 2.12(b)) or reduce in

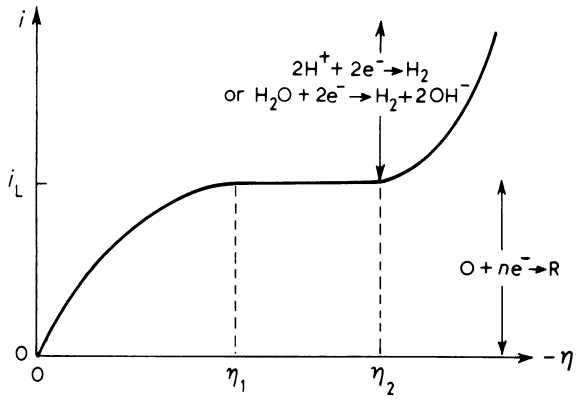

Fig. 2.11 Schematic current versus overpotential curve for a cathodic reaction $O + ne^- \longrightarrow R$, showing a mass transport controlled current i_L as a plateau in the overpotential range $\eta_1 \rightarrow \eta_2$. At overpotentials more negative than η_2, an additional reaction, hydrogen evolution, takes place.

size to a mere inflection (Fig. 2.12(c)), i.e. $\eta_1 - \eta_2 \rightarrow 0$. This latter effect may be caused by changes in the bulk concentration, increasing surface roughness or non-uniform current distribution.

In the general case, i_L may be determined over a wide range* of each of the experimental variables, e.g. Fig. 2.13 shows the separate effects of electrode area, concentration of electroactive species and relative velocity at a constant temperature.

It is also useful, in appropriate cases, to control the electrode potential at a value η_1 and incrementally step the relative velocity or concentration (Fig. 2.14(b)). There are various techniques available to obtain i_L. The common potential-sweep method, may be slow and, hence, result in electrode surface changes or concentration changes in a divided cell, particularly if the fractional conversion is large. If the i vs. E behaviour is well established, a rapid and convenient alternative is the potential step method, where E is stepped from its open-circuit value to a value in the range $\eta_1 - \eta_2$ (Fig. 2.14(a)). The current decreases rapidly due to non-faradaic charging, then relaxes to the steady i_L value with time. It may be necessary to suppress the rapid initial transient to, for example, avoid damage to power supplies. The potential-step technique is particularly useful for natural convection systems (where steady-state currents are only established slowly) for cases where rapid surface roughening occurs (due, for example, to etching or electrodeposition) and when rapid depletion of the reactor concentration occurs, i.e. when the fractional conversion is high.

* It is particularly important in the case of dimensionless group correlation, in order to provide a meaningful value of the constants K, a and b in the expression $Sh = KRe^aSc^b$, where Re is the Reynolds number, Sc is the Schmidt number and Sh is the Sherwood number.

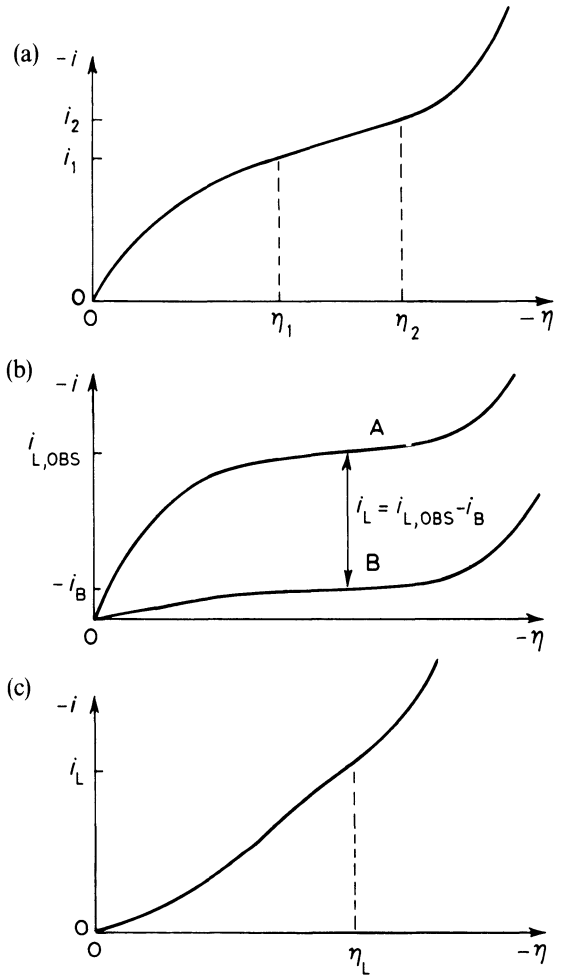

Fig. 2.12 Typical current versus overpotential curves, showing difficulties which may arise during the determination of the limiting current i_L. (a) The curve has an appreciable slope near i_L. The limiting current may be determined graphically, using one of the following criteria: (i) $i_L = (i_1 + i_2)/2$; (ii) i_L corresponds to a minimum in the slope $di/d\eta$; (iii) i_L corresponds to i at $(\eta_1 + \eta_2)/2$. (b) A: Indifferent electrolyte + electroactive species; B: Indifferent electrolyte only. Curve B shows an appreciable background current i_B in the region of the observed limiting current region of curve A. i_B also varies with η. The true limiting current i_L is obtained as the difference between the observed value and the corresponding background current. (c) The limiting current is barely discernable as an inflection due to domination of the overall reaction kinetics by electron transfer (in the range $0 < \eta < \eta_L$) and by the side reaction (for $\eta > \eta_L$).

It should be noted that, with industrial-scale reactors, it is often difficult (or impossible) to achieve potentiostatic control, i.e. control of the electrode potential. In such cases, the usual route to i–E curves is to adjust the current incrementally and record the steady E value by incorporating a reference

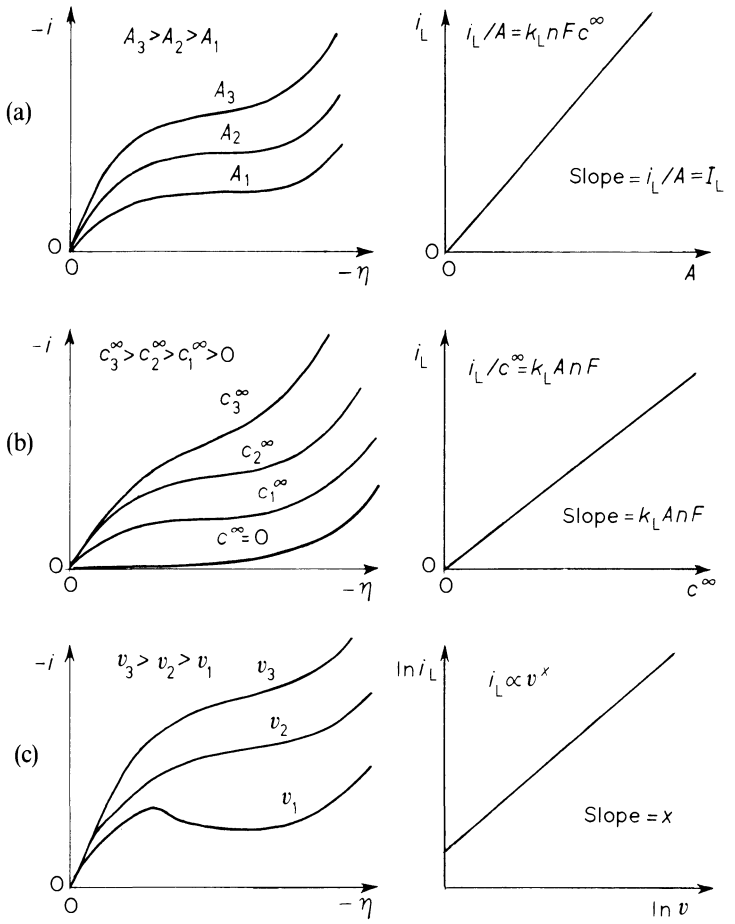

Fig. 2.13 Current versus overpotential curves showing the effect of experimental parameters in the presence of forced convection, according to the relationship $i_L = k_L A n F c^\infty$. (a) Electrode size (and shape). Ideally, in the presence of a uniform current-density distribution, $i_L \propto A$. Deviations may be due to edge effects, non-uniformity of flow (e.g. entrance length effects) or contributions from natural convection. (b) Concentration of electroactive species in the reactor. i_L should be proportional to c^∞. It is sometimes convenient to test this by incremental increases in c^∞. The background curve is represented by $c^\infty = 0$. (c) Relative velocity of the electrolyte or electrode. $i_L \propto v^x$ where x is a constant which depends upon the geometry and flow conditions. x may vary slightly over different ranges of Reynolds number. The limiting-current plateau may shorten and tilt as velocity increases, due to the increasing importance of electron transfer to the overall reaction kinetics. The maximum on the v_1 curve may arise due to unsteady-state mass transport and is akin to a peak in linear sweep voltammetry, i.e. it may arise due to an excessive rate of potential change.

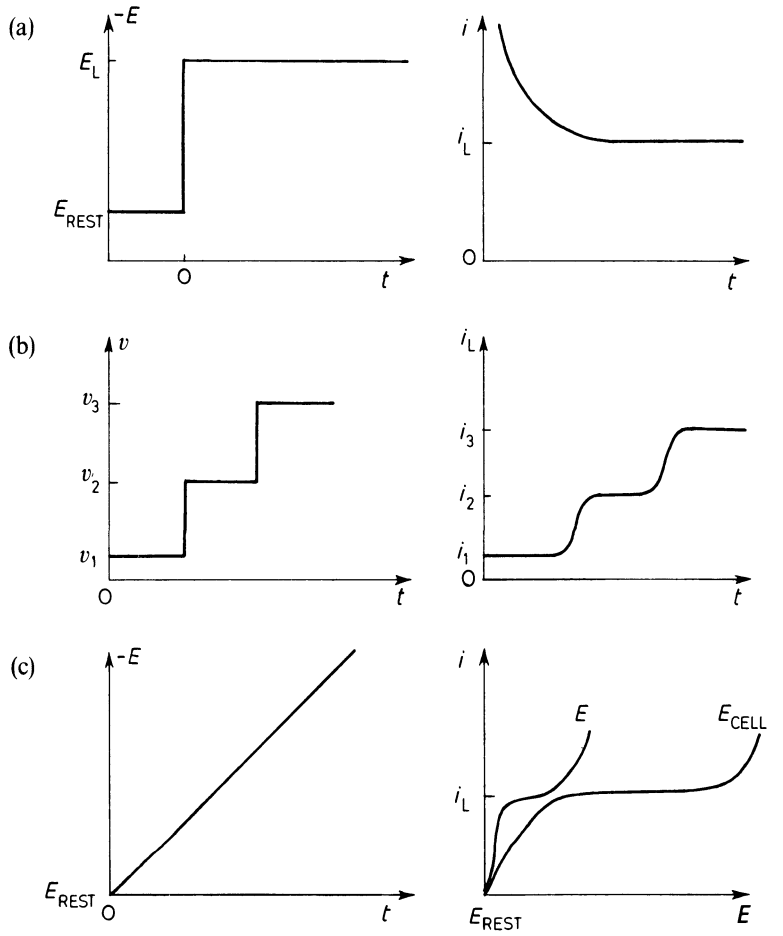

Fig. 2.14 Electrochemical techniques for limiting current measurement. (a) The electrode potential is stepped to a potential in the limiting current region, while the current is monitored. (b) The electrode–electrolyte velocity is stepped while the current is monitored. (c) In special cases, the cell voltage E_{CELL} may be recorded as a function of current, allowing use of a two-electrode cell (i.e. precluding need for a reference electrode).

electrode into the reactor. Unfortunately, the retrofitting of a reference electrode probe in a suitable position (adjacent to the electrode) is often difficult. In addition, it may well have to withstand more arduous conditions than its laboratory counterpart. In certain, favourable, circumstances it may be possible to record well-defined limiting currents by incrementally adjusting the cell current (or voltage) and monitoring cell voltage (or current) as indicated in Fig. 2.14(c).

The direct electrochemical methods discussed above readily give the mass-transport coefficient, if the electroactive area is known. Alternative methods of

finding k_L include its calculation from: (1) established dimensionless group correlations; and (2) measured fractional conversion over a reactor, using the approach outlined in section 2.5. Other techniques for measurements of an averaged k_L include:

1. Chemical dissolution of a solid material such as benzoic acid in order to determine an averaged, chemical mass-transport coefficient.
2. Weight change of the electrode (or analysis of the concentration change in the electrolyte) followed by application of Faraday's laws of electrolysis.
3. Optical techniques such as interferometry.

So far, we have considered bulk or 'macroscopic' mass transport measurements which involve an averaged value of i_L and hence k_L for the entire electrode. However, all practical electrodes will have a non-uniform distribution of i_L, due to factors such as:

1. Flow variation due to natural convection or variations in the local hydrodynamics due to turbulence, flow segregation, gas evolution or secondary flows (such as jetting or vortexing).
2. A non-uniform surface roughness due to, for example, fabrication and pretreatment history, corrosion or deposition of films.
3. Non-uniform potential distribution as, for example, in porous electrodes.

In such cases, the local or 'microscopic' distribution of the mass-transport coefficient may be established using a variety of techniques. Direct i_L measurements may be made using:

1. An array (one- or two-dimensional) of microelectrodes embedded into the electrode surface.
2. Segmented electrodes (usually one-dimensional) which provide locally averaged i_L over a strip of the electrode.

The local (limiting) current may be plotted as a function of position and flow conditions. In either case, the individual electrode currents may be monitored as the voltage drop over a series of (low) resistances or, preferably, using a number of current followers. The advent of low-cost operational amplifiers and cheap, high-speed microcomputers has greatly facilitated these measurements. It is particularly important to ensure that the localized electrodes are flush with the bulk electrode surface, as any step may generate local turbulence or a modified potential distribution.

Indirect, *in situ* methods of determining the k_L distribution have usually been restricted to electrowinning, e.g.:

1. In a Cu electrowinning cell operating below i_L for copper deposition, the rate of codeposition of Ag from trace amounts of Ag^+ added to the electrolyte, may be found by localized stripping of the deposit, followed by chemical analysis.

2. A radioactive tracer, e.g. $^{110}Ag^{+}$ may be added to the electrolyte, followed by (non-destructive) autoradiography of an electrodeposit containing ^{110}Ag.

These two techniques are interesting; although the tracer is present at very low levels, it deposits in a smooth matrix of another metal, e.g. Cu or Ni.

Further information about the mass-transfer conditions in flow cells may be deduced by the analysis of marker experiments; in such experiments, a well-defined pulse of a dye or an ion (formed by anodic dissolution of a metal) is introduced at the inlet to the reactor. The solution with the marker is allowed to pass through the cell (with no current flowing) and the concentration of marker as a function of time is monitored at the outlet. Ideally, for plug flow, the marker concentration vs. time at the outlet should have the same shape as that at the inlet. In practice, some solution will be slowed down by its proximity to solid surfaces (Chapter 1, Fig. 1.14) during the passage of the solution through the cell and this flow segregation leads to dispersion of the marker pulse (Fig. 2.15). Analysis of the response at the outlet gives information about flow conditions in the cell. In general, the response may be used to characterize the reactor according to a model such as:

1. A plug flow reactor with dispersion in the longitudinal direction of flow.
2. A backmixed reactor with a degree of flow bypassing the manifolds.

As mentioned above, a common situation is the occurrence of two phases: a fast bulk phase and a slower-moving wall phase with a degree of interchange between them. The reaction engineering behaviour is complex; electrochemical reaction takes place in one of the phases and chemical reaction often occurs in both.

2.6.3 Potential distribution and current distribution

An important objective of cell design is to obtain a uniform potential distribution and often also a uniform current distribution. The current distribution is a function of the local concentration of electroactive species (section 2.6.2) as well as the potential distribution.

The potential distribution will depend on the relative positions of the anode and cathode and their surface profiles. The reason for this may not be obvious since, if the electrode is made of a highly conducting metal, it must have an equipotential surface. But while, in Chapter 1, the kinetics of electron transfer were discussed mainly in terms of overpotential, it was pointed out that the current is, in fact, determined by the potential difference between the metal and the solution (i.e. $\phi_M - \phi_S$ (or more correctly $\phi_2 - \phi_S$)) and $\phi_M - \phi_S$ is a potential difference in the solution phase. Moreover, it is a local property since the potential field in the solution depends on the arrangement of electrodes, their profile, the solution conductivity, the electrode conductivity, and the applied voltage between the electrodes. Indeed, overpotential is usually used in kinetic

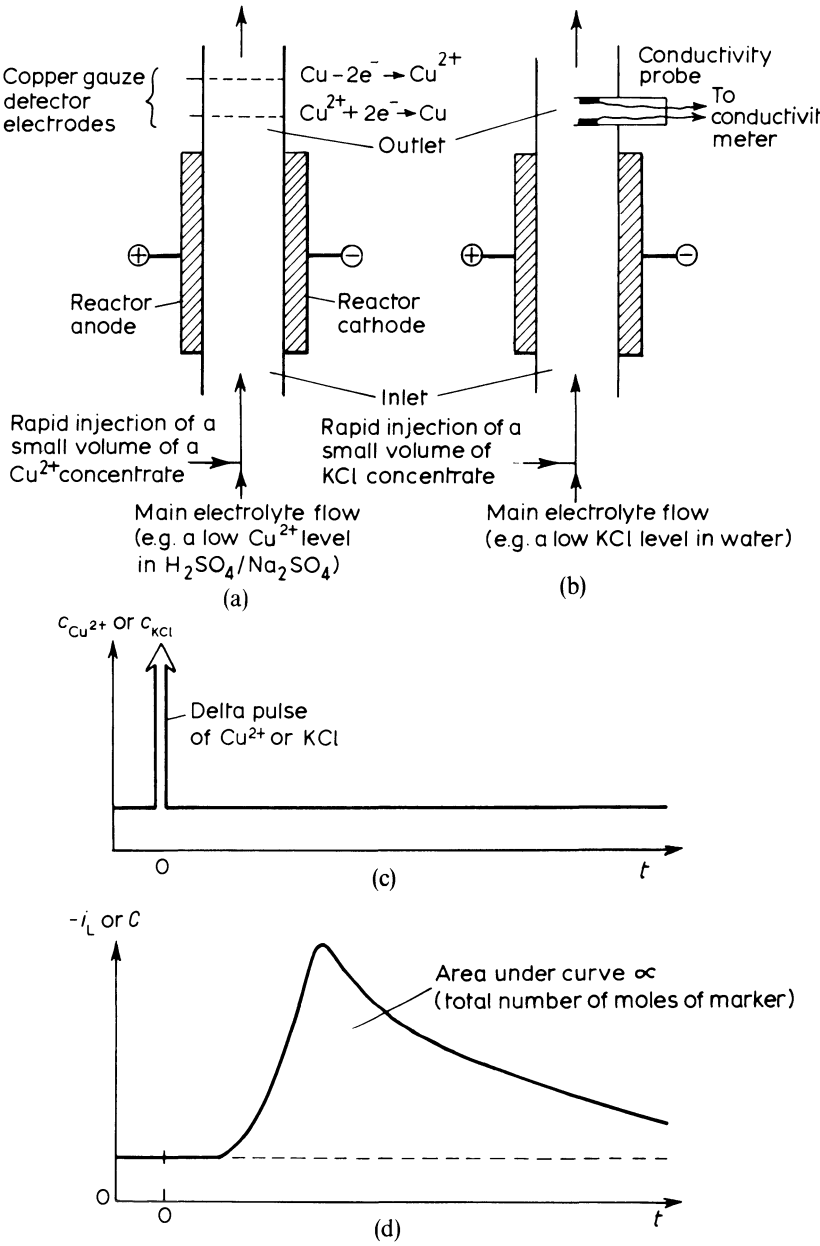

Fig. 2.15 The stimulus–response technique for investigation of flow dispersion in an electrochemical reactor. (a) Injection of a marker pulse of Cu^{2+} ions at the reactor inlet, followed by cathodic detection of the limiting current at the reactor outlet; $i_L \propto c_{Cu^{2+}}$. (b) Injection of a marker pulse of KCl at the reactor inlet, followed by conductimetric detection at the outlet. The conductance of the KCl electrolyte C_{KCl}, is proportional to the KCl concentration c_{KCl}. In the case of (a) and (b), the δ-function marker pulse shown in (c) gives rise to the response indicated in (d). The response at the reactor outlet is measured via the time dependence of limiting current i_L in the case of Cu^{2+} or the electrolyte conductance in the case of KCl.

equations only because of its ease of measurement and because it is proportional to $\phi_M - \phi_S$. The general factors affecting the potential distribution can be rationalized by rearranging equation (2.42) in terms of, for example, the cathode potential:

$$-E_c = -E_{CELL} - E_e^A - |\eta_A| - iR_{CELL} - iR_{CIRCUIT} \tag{2.168}$$

Any local change in the values of the parameters on the right-hand side of this equation will result in a change in the local value of the cathode potential.

The current distribution is related closely to that of the potential, and depends upon the same factors, i.e.:

1. The geometry of the electrodes and reactor.
2. Electrolyte conductivity.
3. Electrode conductivity.
4. Overpotentials at each electrode due to charge transfer (and, hence, on the electrode material) or mass transport effects (and, hence, on the local hydrodynamics).

In addition, the current distribution depends on the local concentration of electroactive species. The technological importance of current distribution is evidenced by the effects of a non-uniform distribution, e.g.:

1. Reduced current efficiency, which may in turn result in unwanted by-products, non-uniform wear of electrodes and decreased space–time yield in the case of reactors for electrosynthesis.
2. Uneven use of battery electrodes, resulting in poor utilization of active material, and reduced energy efficiency.
3. Selective corrosion may be promoted, leading to rapid, localized attack (section 10.4.2).
4. Electrodeposits may show an uneven thickness or localized excessive current density effects such as dendrite formation, ($i \simeq i_L$) or oxide/hydroxide formation due to localized pH increases. (These effects may be examined in devices such as the Hull cell, (section 8.1.1) which exhibits a deliberate variation in cathode current density.)

It is possible conceptually to distinguish three types of current distribution, depending upon the nature of the overpotential (Table 2.4).

The primary current distribution is calculated assuming that the current density is low so that there is no significant overpotential and no depletion of the electroactive species over the electrode surface. The variation of the solution potential ϕ_S in found by solving, analytically or numerically, Laplace's equation:

$$\frac{\partial^2 \phi_S}{\partial x^2} + \frac{\partial^2 \phi_S}{\partial y^2} + \frac{\partial^2 \phi_S}{\partial z^2} = 0 \tag{2.169}$$

with boundary conditions appropriate to the electrode geometry, e.g. at the electrode surface, ϕ_M = constant (the resistivity of the electrode is ignored

Table 2.4 The types of current distribution

Type of current distribution	Nature of the overpotential			Important parameters				
	Charge transfer	Mass transfer	Others*	Cell/electrode geometry	Charge transfer over-potentials	Electrode and electrolyte conductivity	Mass transfer overpotential	Others*
Primary	×	×	×	✓	×	×	×	×
Secondary	✓	×	×	✓	✓	✓	×	×
Tertiary	✓	✓	×	✓	✓	✓	✓	×
Practical	✓	✓	✓	✓	✓	✓	✓	✓

* Due to, for example, chemical reaction, adsorbed films on the electrode or partial blinding of the electrode by gas bubbles, solid products or an insoluble phase

compared to that of the electrolyte) and at an insulating surface, $d\phi/d\eta = 0$ (as no current can flow). From a map of ϕ_S immediately adjacent to the electrode surface, the variation in $\phi_M - \phi_S$ and, hence, current density, can be calculated. However, this equation is often difficult to solve; indeed, the parallel plate- and disc-electrode geometries are two of the few cases where analytical solutions exist.

As was shown in Fig. 2.5, the primary current distribution is only uniform when all points on the electrode surface are strictly equivalent and the current density is low. This is possible only with two reactor designs, a parallel-plate reactor having electrodes of equal area and occupying opposite walls and the concentric-cylinder reactor. There will be a variation of potential and current density over the surface for all other electrode arrangements; an example is shown in Fig. 2.16(a) where the broken lines join equipotential points and the current densities are inversely proportional to the lengths of the arrowed lines. The highest current density is between the points closest together on the two electrodes and almost no current flows on the reverse side of the anode.

Such simple calculations do not correspond to the real conditions in electrolytic cells. There will be a significant current in the electrolysis cell and, hence, there is likely to be a substantial overpotential associated with electron transfer. The calculation must now consider the way in which the local current density will affect ϕ_S and, hence, $\phi_M - \phi_S$ in the electrolyte. The result is the secondary current distribution and, in general, it shows that the variation in current over the electrode surface is not as great as indicated by the primary current distribution (Fig. 2.16(b)). A simplified treatment of secondary current distribution is possible by combining the important experimental parameters together as a dimensionless group. The Wagner number is defined by:

$$Wa = (\kappa \, d\eta/dI)/L \tag{1.170}$$

where κ is the electrolyte conductivity, $d\eta/dI$ is the reciprocal slope of an I–η curve and L is a characteristic length. The Wagner number may be written

$$Wa = \frac{(d\eta/dI)}{(L/\kappa)} \tag{2.171}$$

and regarded as the ratio of a 'polarization resistance per unit area' to the electrolyte resistance per unit area. When $Wa \to 0$, the primary current distribution prevails.

According to similarity theory, systems having the same Wa will have similar secondary current distributions. In general, the secondary current distribution will be more uniform at higher Wa, i.e. for higher $d\eta/dI$, larger κ and smaller L. This has several implications for practical cells operating under charge transfer-controlled electrode kinetics:

1. The current distribution depends upon electrolyte composition. An inert electrolyte will increase κ while additives may be added to the electrolyte to increase $d\eta/dI$ (as in electroplating, section 8.1.4).

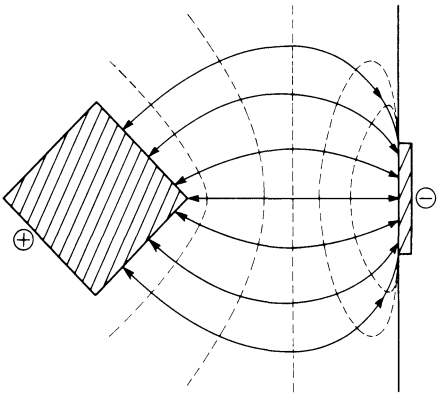

(a)

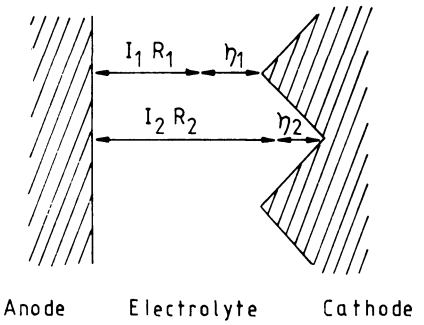

(b)

Fig. 2.16(a) Primary current distribution for the electrode geometry shown. The broken lines show equipotential contours. The current density is inversely proportional to the length of the arrows. Note that almost no current flows to the anode surface which faces away from the cathode.

(b) Primary- and secondary-current distributions on a serrated profile cathode.

Primary-current distribution:

$$\eta_1 = \eta_2 = 0, \qquad I_1 R_1 = I_2 R_2, \qquad I_1 > I_2$$

i.e. the current density is higher at the peaks than in the valleys.

Secondary-current distribution:

$$\eta_1 > \eta_2 > 0; \quad |\eta_1| + I_1 R_1 = |\eta_2| + I_2 R_2 \quad \text{and} \quad I_1 R_1 < I_2 R_2; \quad I_1 > I_2;$$

i.e. the current density is still higher at the peaks than in the valleys, but the difference is smaller, resulting in a more uniform current distribution.

2. Many industrial electrolytic processes (e.g. electroplating (section 8.1), chlor-alkali (Chapter 3), water electrolysis (section 5.2) and fluorine evolution (section 5.1)) operate primarily under charge-transfer control. Any increase in the average current density is expected to cause a less uniform current distribution.
3. Electrode and cell geometry are very important parameters. Scale-up (or scale-down) exercises should therefore consider the size of the characteristic length, e.g. for a parallel plate geometry, there are two: the electrode length L and the interelectrode gap S.

The tertiary current distribution also takes into account the variation of current density when there are significant changes in the concentration of electroactive species across the surface; the largest variation must occur when the overpotential is so high that the current is mass transfer controlled.

An example, Fig. 2.17 is a sketch of the various current distributions for a parallel-plate cell with electrodes of length L and of infinite width, and with fully developed laminar flow. The primary current distribution shows the current to be uniform over most of the electrode but with a considerable edge effect at $x = 0$ and $x = L$; the current goes to a very high value at these ends. The secondary distribution is similar but is even closer to the ideal while the limiting tertiary distribution shows that in these conditions the current density drops sharply along the electrode.

We have considered so far the overall electrode geometry. However, the electrode surface profile must also be noted (Fig. 2.18). If the electrode surface roughness is large in comparison to the Nernst diffusion layer thickness (Fig. 2.18(a)), the latter follows the surface profile, giving rise to a uniform limiting-current density distribution. When the roughness is small (Fig. 2.18(b)), a non-uniform tertiary-current distribution arises, as the high points are favoured with a larger limiting current density. This case is important in several technological areas, including:

1. Electroplating, where solution additives promote 'good microthrow', producing a more level deposit, by increasing the overpotential at a given current density.
2. Electropolishing, when high points are removed selectively by anodic dissolution via a viscous Nernstian diffusion layer.
3. Electrodeposition of metal powders (section 4.4) provides an interesting case; under certain conditions, not only is growth favoured at the high points, but the increased surface roughness may act as a turbulence promoter. The result (Fig. 2.18(c)) is a severe thinning of the Nernst diffusion layer.

Three-dimensional electrodes generally give rise to more problems with potential and current distributions than their two-dimensional counterparts; this is primarily due to the anisotropy of porous- and packed-bed electrodes, with respect to electrode conductivity, electrolyte flow and concentration of the

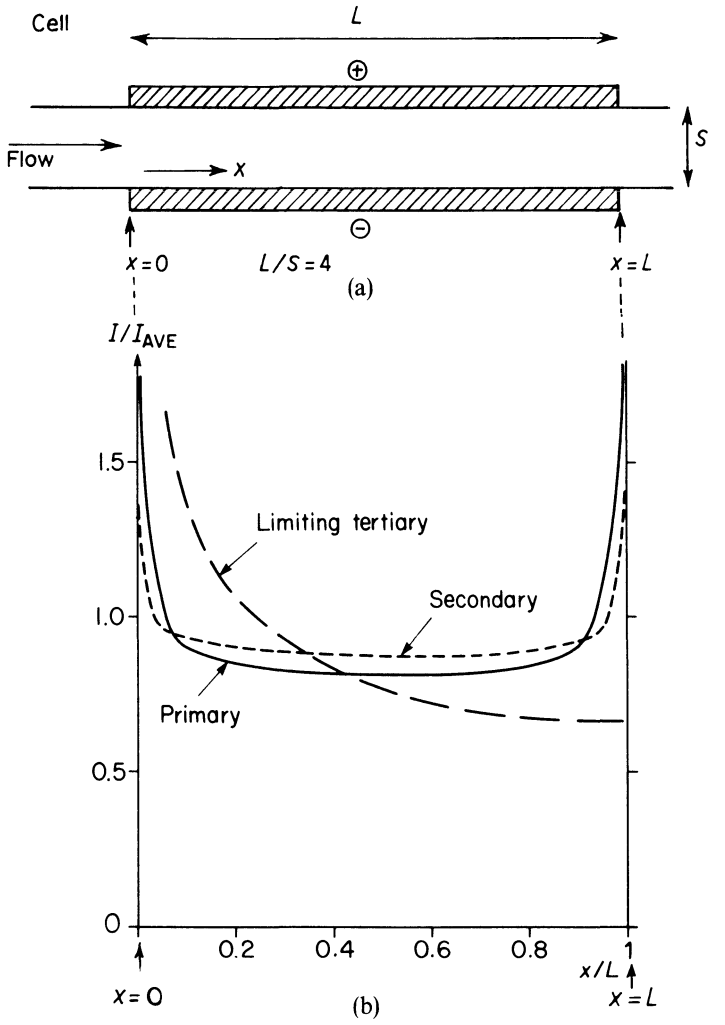

Fig. 2.17 Current distributions for a parallel-plate reactor in fully developed laminar flow. (a) Definition sketch. (b) Normalized current as a function of dimensionless distance along the electrode.

electroactive species. There are, in particular, two extreme configurations with respect to the directions of electrolyte flow and current flow (Fig. 2.19). The 'flow-through' arrangement (Fig. 2.19(a)) is often convenient in laboratory studies; the bed depth is limited by the potential drop over its length but this results in a low fractional conversion and, hence, a relatively uniform reactant concentration within the reactor. On the other hand, scale-up is severely limited.

The vast majority of porous- and packed-bed electrodes in practice, utilize variations of configuration shown in Fig. 2.19(b): the 'flow-by' configuration.

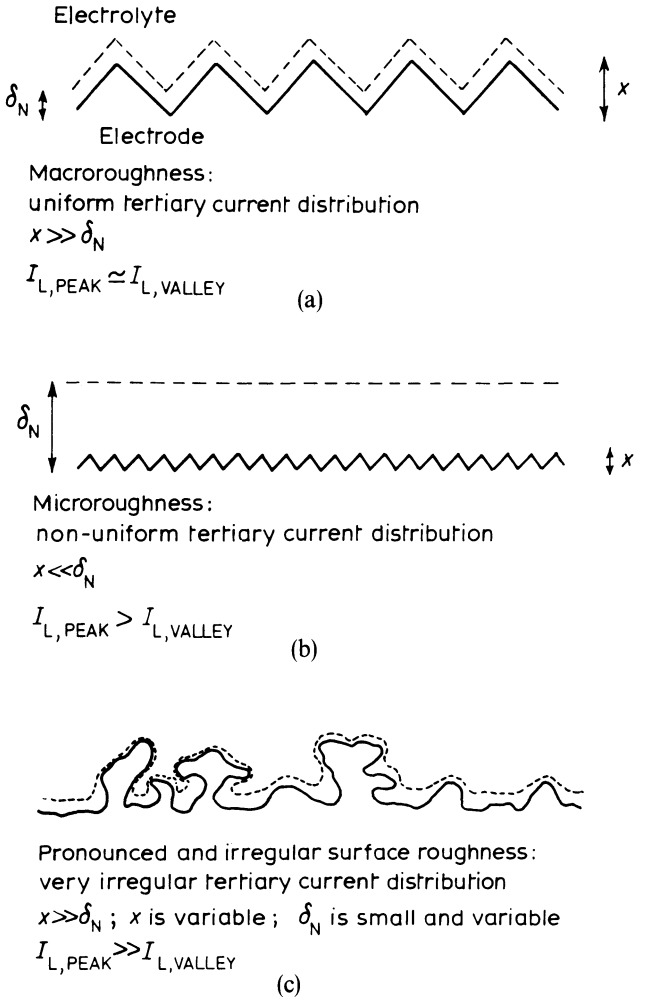

Fig. 2.18 The effect of electrode surface profile on the tertiary current distribution showing the size of the surface roughness x compared to the Nernstian diffusion layer thickness δ_N and the relative limiting-current density I_L on the peaks and valleys.

The fractional conversion is varied readily by altering the bed height. The ideal operating condition for such a cell is to achieve the limiting current density over the entire width of the bed by ensuring that the overpotentials at the cathode feeder and membrane correspond to the start and end of the limiting current plateau (Fig. 2.20). The potential drop in the bed in practical terms may be larger than $\eta_2 - \eta_1$ and the practical value of η_1 may be reduced. Such a strategy should maximize current efficiency and fractional conversion.

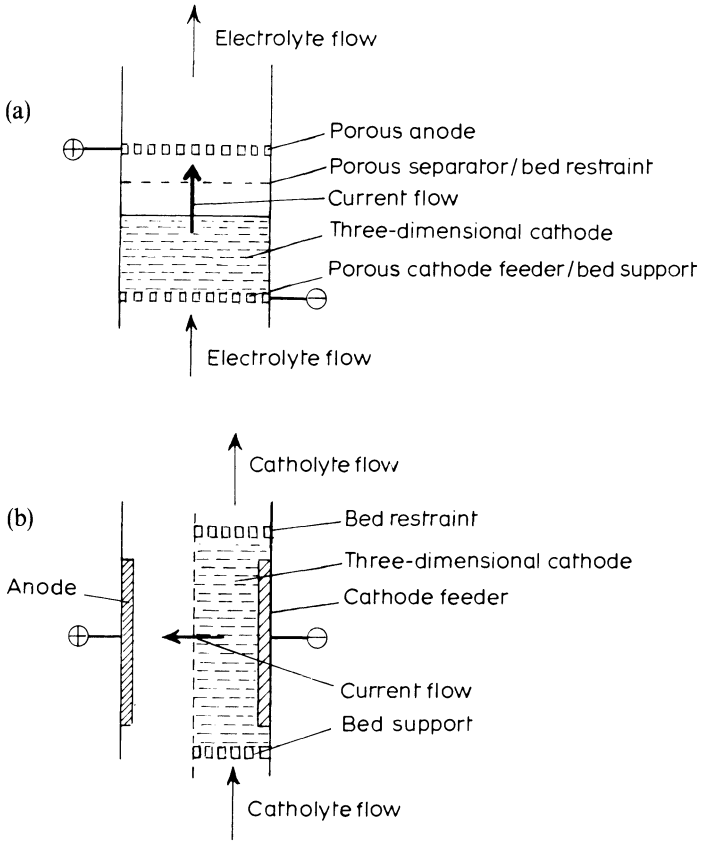

Fig. 2.19 Configurations for three-dimensional electrodes. Only the cathode is shown as three-dimensional. If the electrolyte flow is sufficiently high, fluidization of a particulate cathode bed may occur. (a) Current flow parallel to electrolyte flow. (b) Current flow perpendicular to electrolyte flow.

The overall kinetic behaviour of practical three-dimensional electrodes is dominated by the non-uniform electrode potential and, hence, current, distribution within the bed, along with the dimension parallel to current flow. The practical potential, and current, distributions are shown in Fig. 2.21 (packed-bed electrode) and Fig. 2.22 (fluidized-bed electrode). Consider the packed-bed electrode case. In the case of a thin bed, ϕ_M falls slowly (and linearly) with distance due to the small ohmic drop within the electrode (Fig. 2.21(a)); the solution phase potential ϕ_S varies with distance due to iR drop in solution. The result is that the driving force for electron transfer ($\phi_M - \phi_S$) reduces towards the feeder electrode. This, in turn, means that the current density decreases towards the feeder (Fig. 2.21(b)). For a thicker bed, $\phi_M - \phi_S$ may reduce, at a certain bed depth, to a value so low that the reaction rate is negligible (Fig. 2.21(c)). In terms

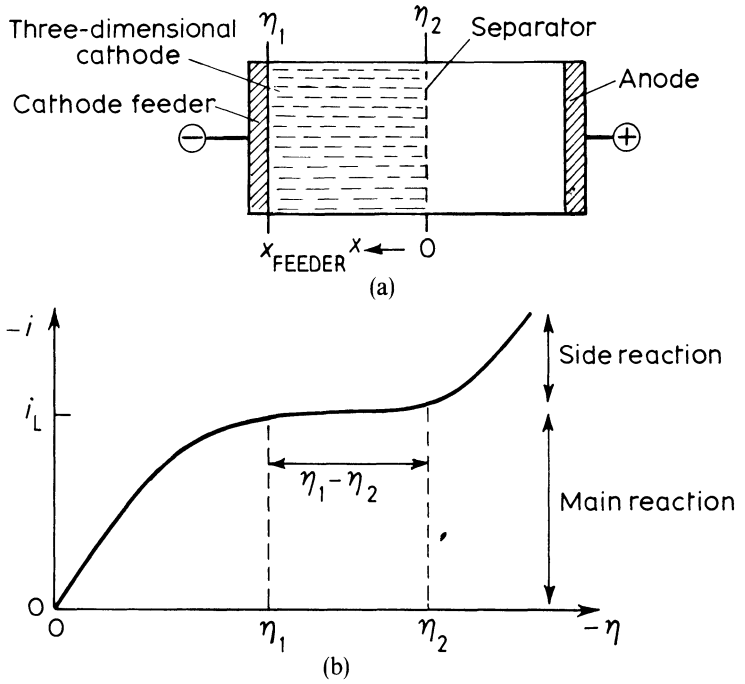

Fig. 2.20 An idealized strategy for operation of a three-dimensonal electrode (assuming that the entire electrode operates under mass transport control). (a) Definition sketch. (b) Current versus overpotential curve.

of the current distribution, that part of the bed beyond the 'effective bed depth' has a negligible current (Fig. 2.21(d)).

For the fluidized-bed electrode (Fig. 2.22), the behaviour is further complicated by bed expansion. An increase in fluid velocity may increase mass transport but result in a poor electroactive area and a poor potential distribution due to a lowered interparticle and particle–feeder contact. Particular features of Fig. 2.22 may be highlighted. The intermittent contact between bed particles and the complex solution flow results in a non-uniform ϕ_M and ϕ_S, particularly in the case of a thick or highly expanded bed (Fig. 2.22(c) and 2.22(d)). The current density may be relatively uniform for a thin bed of small expansion (Fig. 2.22(b)). However, thick, highly expanded beds may result in large inactive zones (Fig. 2.22(d)), where the reaction rate is negligible due to the exceedingly low $\phi_M - \phi_S$ (Fig. 2.22(c)).

From the standpoints of potential, and current, distribution in three-dimensional electrodes, the following comments may be made:

1. If $\eta_2 - \eta_1$ is not too large, a greater current efficiency may be achieved using fluidized-bed-electrodes rather than porous electrodes, due to the more uniform potential distribution.

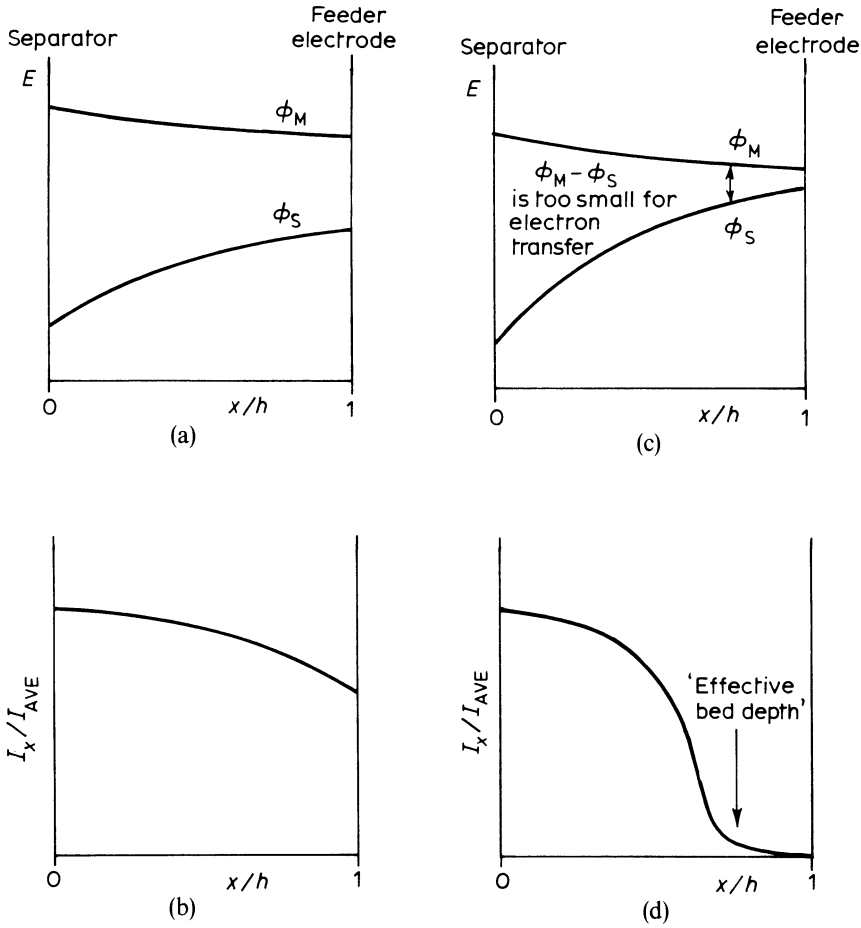

Fig. 2.21 Distribution of electrode potential and normalized current in a porous electrode. (a) and (b) Thin bed electrode. (c) and (d) Thick-bed electrode. I_x = local current density at point x; I_{AVE} = averaged current density over all x; x = distance measured from the separator towards the feeder electrode; h = depth of bed parallel to the direction of current flow; ϕ_m = electrode (metal) potential; ϕ_s = electrolyte (solution) potential; and $\phi_m - \phi_s$ is effectively a driving force for reaction.

2. The fluidized-bed electrode will require a higher cell voltage than the packed-bed electrode for a given current density.
3. During the design of packed-bed electrode reactors it is important that the actual bed depth is not greater than the effective bed depth, in order to maintain A_S and ρ_{ST}.
4. The hydrodynamics, electrode movement and complex current distribution of fluidized-bed electrodes must all be considered. In particular, inactive zones must not appear as A_S and ρ_{ST} will be reduced.

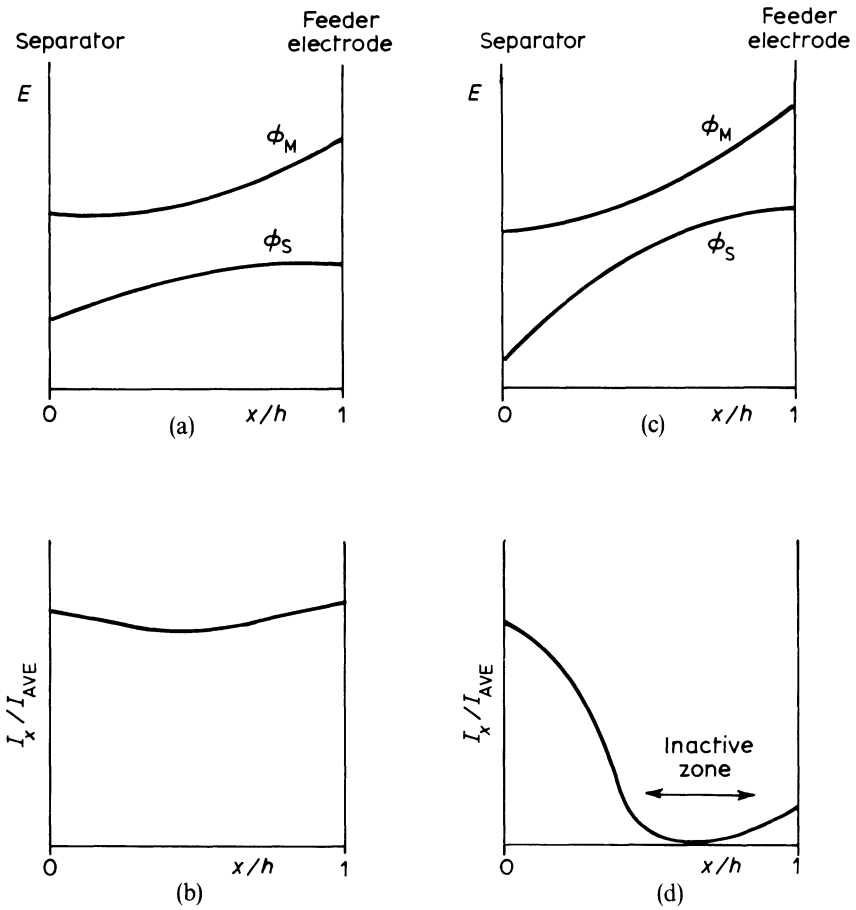

Fig. 2.22 Potential and current distributions in a fluidized-bed electrode (a definition of terms is given in the caption to Fig. 2.21). (a) and (b) thin beds. (c) and (d) thick beds.

5. The deposition of a conductive product, typically metal inside bed electrodes, may further complicate the potential, current and flow distributions, in time as well as space. In extremely adverse cases (e.g. high current densities and low bed voidage) packed beds may be completely 'plugged' with metal in their interstices, while fluidized beds may suffer agglomeration of the electrode particles with themselves and the feeder.

The above discussion has shown how the current distribution may be affected by an increasing number of influences, primary → secondary → tertiary. In practical cells, the behaviour may be complicated further by factors such as those indicated in Table 2.4. As an example, gas evolved at the counter-electrode may

introduce a complex (time and spatially dependent) iR drop in the electrolyte, which is also sensitive to the prevailing hydrodynamics. The suspension, fluidization or creeping of a solid-phase product may also affect significantly the electrode potential, whether it is conductive or not.

It is also noteworthy that, in divided cells, the membrane current distribution may also be important. In adverse cases, the membrane may partly foul due to deposition of an insulating film of an organic or a solid-cell product, distorting the current distribution. Alternatively, a solid, conductive material may locally increase the membrane current density, possibly leading to 'burn out' of the separator.

The conclusion for practical cell design is clear: normally, the electrode geometry must be simple. The exceptions to this rule will be when the current distribution is not important (e.g. in low-current devices for removing dilute metal ion from solution) or when, by necessity, one electrode must have a complex shape, e.g. electroplating or electrochemical machining. In the latter case, it is often necessary to use auxiliary counter-electrodes, shields of insulating materials to guide the current paths, or counter-electrode shapes of very careful design in order to obtain the desired current distribution (Chapter 8, Fig. 8.21).

2.6.4 Heat transfer

The cell voltage E_{CELL} during electrolysis exceeds the reversible value $E_e^C - E_e^A$ due to the presence of electrode overpotentials η_C and η_A together with various iR drops (iR_{CELL} and iR_{CIRCUIT}) as described by equations (2.43) and (2.49).

A portion E_D of the cell voltage in excess of the thermoneutral voltage (equation 2.56):

$$E_D = E_{\text{CELL}} - E_{tn} \tag{2.172}$$

provides an electrical power loss W_D:

$$W_D = iE_D = i(E_{\text{CELL}} - E_{tn}) \tag{2.173}$$

This results in Joule heating of the cell. The heat flow:

$$Q_{\text{HEAT}} = i(E_{\text{CELL}} - E_{tn}) \tag{2.174}$$

provides an important input to the heat balance over the reactor (Fig. 2.23) and must be considered at the design stage.

The individual heat-flow components, in principle (corresponding to the potential drops in equation (2.43)), may be calculated if an analysis of cell voltage (section 2.3.7) is available. The major factor in many cases is R_{CELL}, i.e. the combined resistance of the electrolyte and any separator present; R_{CIRCUIT} may also provide a contribution. The importance of minimizing these parameters and, hence, minimizing the electrolytic power cost has already been stressed in section 2.3.7.

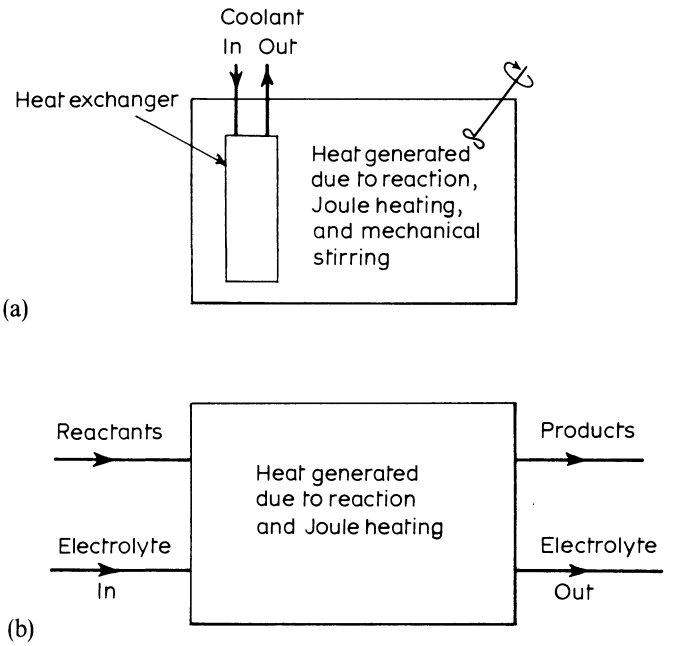

Fig. 2.23 Simplified heat balance over electrochemical reactors. (a) Simple batch reactor with electrolyte cooling via an internal heat exchanger. (b) Flow-through reactor with the electrolyte acting as a heat-exchanging medium.

We may consider, for simplicity, the case of a steady-state heat balance across an electrochemical reactor:

$$\sum Q_h^{IN} = -\sum Q_h^{OUT} \tag{2.175}$$

The relevant heat flows are due to:

1. The electric current flow (via equation (2.174)).
2. Heat transfer via conduction, convection and radiation.
3. Mass flow of reactants and products:

$$Q_h^{R,P} = A\sum_i n_i M_i C_{p,i}, T \tag{2.176}$$

where A is the cross-sectional area for mass flux, M and n are the molar mass and molar mass flux, C_p is the heat capacity at constant pressure and T the temperature of the reactants or products.

4. Mass flow of the heat exchanger medium (i.e. the coolant or heating fluid):

$$Q_n^{EX} = N_m C_p \Delta T \tag{2.177}$$

where N_m is the mass flow, C_p is the specific heat capacity at constant pressure and ΔT the temperature difference over the heat exchanger.

The three fundamental modes of heat transfer are conduction, convection and radiation (cf. mass transport (section 1.2.2)). In the general case, all of these modes must be considered. However, radiation is generally significant only for very hot reactors such as those used for fused-salt electrolysis.

(*a*) *Conduction*

Fourier's law of heat transfer expresses heat flow across a flat wall:

$$Q_h = -A\lambda\Delta T/x \tag{2.178}$$

The heat flow is proportional to the contact area A and the temperature difference across the wall ΔT and inversely proportional to thickness x, the characteristic constant of proportionality being known as the thermal conductivity λ.

Rewriting equation (2.178) in differential form as a heat flux:

$$Q_h/A = -\lambda(dT/dx) \tag{2.179}$$

shows that λ is the constant of proportionality between heat flux and temperature gradient.*

(*b*) *Convection*

Heat transfer at phase boundaries such as solid electrode–liquid electrolyte or solid electrode–gaseous product is complex, being dependent on flow conditions, electrode geometry and electrode profile (as in the case of mass transfer). In a simple approach, we may consider a temperature boundary layer, by analogy with the concentration boundary layer (Chapter 1, section 1.2). The heat flow is then:

$$Q_h = Ah\Delta T \tag{2.180}$$

where A is the cross-sectional area for heat transfer, and ΔT is the temperature difference between the two phases. The constant h is the heat transfer coefficient (cf. equation (2.178)).

(*c*) *Radiation*

The Stefan–Boltzmann law describes heat flow for a grey body (1) radiating into a large enclosed space (2):

$$Q_h = A_1\delta_{SB}\varepsilon_1(T_1^4 - T_2^4) \tag{2.181}$$

where δ_{SB} is the Stefan–Boltzmann constant, ε_1 is the emissivity of the grey body which has a temperature T_1 and an area A_1.

Radiation is negligible for many low-temperature systems, and many practical heat-transfer problems reduce to a combined consideration of convection

* Equation (2.179) is analogous to equation (1.49), the latter relating mass flux to concentration gradient via a diffusion coefficient.

and conduction (cf. convective diffusion (Chapter 1, section 1.2). It is often convenient in such cases to consider an averaged, overall heat-transfer coefficient k_h by combining equations (2.178) and (2.180):

$$Q_h = Ak_h\Delta T \tag{2.182}$$

k_h will, in general, have contributions from the electrolyte, the electrodes, the cell wall and the heat exchanger.

There are many practical implications of heat transfer in industrial electrolysis; the following considerations serve as examples:

1. Heat transfer is likely to be most important for cells operating at extremes of temperature. Indeed, it may be a dominant factor in cell design.
2. Under start-up or shut-down conditions, it may take a significant time for the reactor to reach the normal operating temperature.
3. Steady state, isothermal operation may not occur.
4. Joule heating may serve two useful purposes; (a) it can provide or contribute to initial electrolyte heating during start-up conditions; and (b) charge and/or mass transport will be enhanced if the temperature is allowed to rise, possibly leading to higher reaction rates.
5. In quiescent reactors (e.g. simple, unstirred, plate-in-tank reactors) heat transfer may be poor due to the lack of convection and the Joule heating may be high due to a large interelectrode gap.
6. In flow-through cells, the electrolyte conveniently acts as a heat-exchanger fluid.
7. In open-topped cells, the rate of electrolyte evaporation may be high, resulting in a relatively large heat transfer to the surroundings.

In practice, it is often difficult to predict the heat transfer quantitatively due to the variety of materials used in cell construction and the (sometimes) complex cell geometry. In such cases, pilot-plant studies may provide useful opportunities to measure heat transfer and, hence, establish an operational heat balance (Fig. 2.23).

2.6.5 Electrical connections to cells

Electrical power, whether generated in a slave power station on site or bought from a national grid, almost always becomes available as high-voltage alternating current. It is, first rectified then transformed to give d.c. current at the required voltage prior to transmission around the cell house with the minimum energy loss. The developments in rectification which occurred during the 1950s led to substantial improvements in electrolytic processes. Before this period, rectifiers were very bulky and gave the highest conversion efficiencies, then only about 85–90%, for high voltages and low currents. The silicon semiconductor rectifiers were much more compact and for the first time permitted economic production of high currents at lower voltages; even at 200 V the efficiency was

about 95%. Silicon rectifiers are universally used as a result and now rectification and transmission is cheapest in the range 200–700 V. Cell rooms are arranged electrically so that the voltage requirement falls within this range; a common arrangement is for the cells to be connected in series so that the total voltage requirement is about 450 V; the centre of the cell stack is earthed and the two ends are at +225 V and −225 V, larger voltages being avoided for safety reasons. The current requirement will depend on the scale of the process and the size of the cells but at this time it is not unusual for the plant to use $1–5 \times 10^5$ A.

The transmission of power around the cell room also requires thought once it is at the appropriate voltage and current. The current is transmitted along busbars, normally constructed from copper or aluminium because of their exceptional conductivity, and the busbar dimensions are calculated carefully because of the considerable investment in the metal. Moreover, the connectors to the cells must be designed to avoid energy loss even at the very high currents and there must be switches which permit individual cells to be isolated for maintenance without disturbing the rest of the cell house. In certain cases, quick-release contacts or flexible cables to the cell may facilitate maintenance or troubleshooting operations.

The arrangement of cells is also important. The plant must be electrically and chemically safe and, although it is common for each cell to have a number of pipes for electrolyte feed and effluent and for gaseous products, the connections must again be made so that individual cells may be isolated for cleaning, maintenance and the replacement of cell components. The high currents in larger plants create substantial magnetic fields and it is therefore necessary to lay out the cells to minimize these.

When a cell or cell stack contains more than two electrodes, there are two ways of making the electrical connection: (1) the cell may be monopolar (Fig. 2.24(a)); or (2) bipolar (Fig. 2.24(b)). There is an external electrical contact to each electrode in the monopolar cell and the cell voltage is applied between each cathode and anode. It can be seen that in the cell shown, anodes and cathodes alternate and both faces of each central electrode are active, with the same polarity. Monopolar connection requires a low-voltage, high-current supply. Bipolar connection requires only two external electrical contacts to the two end electrodes and it recognizes that the cell reaction will occur wherever there is an appropriate potential difference. The voltage field caused by the bipolar connection is shown in Fig. 2.25 and demonstrates how the six electrodes of the cell in Fig. 2.24(b) can lead to five electrolysis cells. The voltage distributes itself between the end electrodes with the electrical contacts, most of the potential drop occurring in the solution phase because of the high conductivity of the metal electrodes. Hence, if the total applied voltage is sufficient to drive current through the structure, then a potential difference equivalent to one monopolar cell voltage will exist between electrodes (1) and (2), (2) and (3), etc. In the bipolar cell, the opposite face of each electrode will have different polarities. The bipolar cell, in addition to simplicity of electrical connection, has the

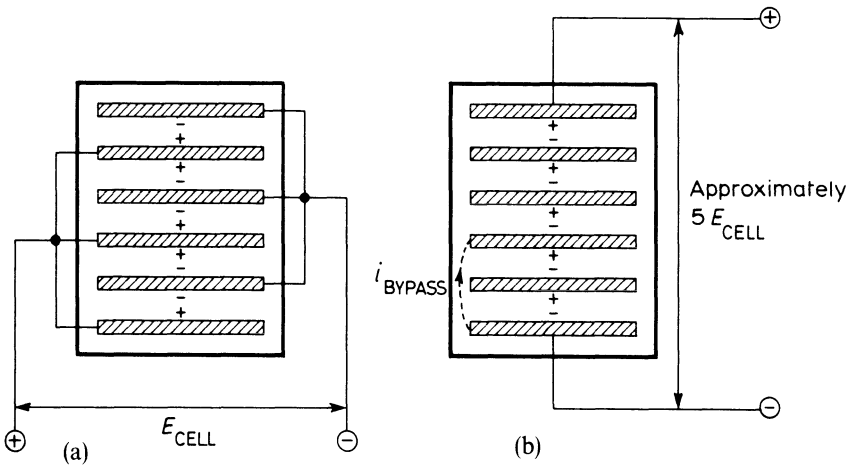

Fig. 2.24 Electrical connections in multielectrode cells. (a) Monopolar connections. (b) Bipolar connections showing the possibility of 'bypass' or leakage currents.

advantage that it produces the equivalent amount of product to monopolar cells using a lower current and a higher voltage (note that, effectively, the current is used many times) and this can be a more economic way of using power.

Bipolar connection, however, poses an additional problem if the cell body is metal or there is an electrolyte path between neighbouring cells, e.g. common feeds or exhausts. This is the electrical leakage current – also known as the 'bypass' or 'shunt current'. The electrical leakage current is a current not between the electrodes of the same cell but between electrodes in neighbouring cells; this arises because, in a bipolar cell, there is a voltage difference between such electrodes and current can flow if there is a current path. A leakage current not only causes a loss in current efficiency (which can be 4%), but it also can lead to corrosion, since cathodes will have 'anodic' zones, and to products which are impure (and may be safety hazards, e.g. H_2 in Cl_2). The leakage current can best be avoided by using an insulating cell body and introducing a break (e.g. a weir) or a barrier, such as an insulating paddle, which isolates the electrolyte flow from neighbouring cells. Leakage currents may also occur in cellrooms where a common electrolyte feed connects an array of monopolar cells.

It is also possible to operate three-dimensional electrodes in a bipolar manner, as in the case of the bipolar trickle tower reactor (Fig. 2.26) where each electrode layer is separated from its neighbour by an insulating mesh. The potential distribution along the height of each layer is non-uniform (Fig. 2.26(b)) and the packing conditions, electrolyte composition and electrolyte flow must be controlled to minimize the bypass current flowing past each layer, within the reactor envelope. Hence, such reactors are best suited to poorly conducting electrolytes.

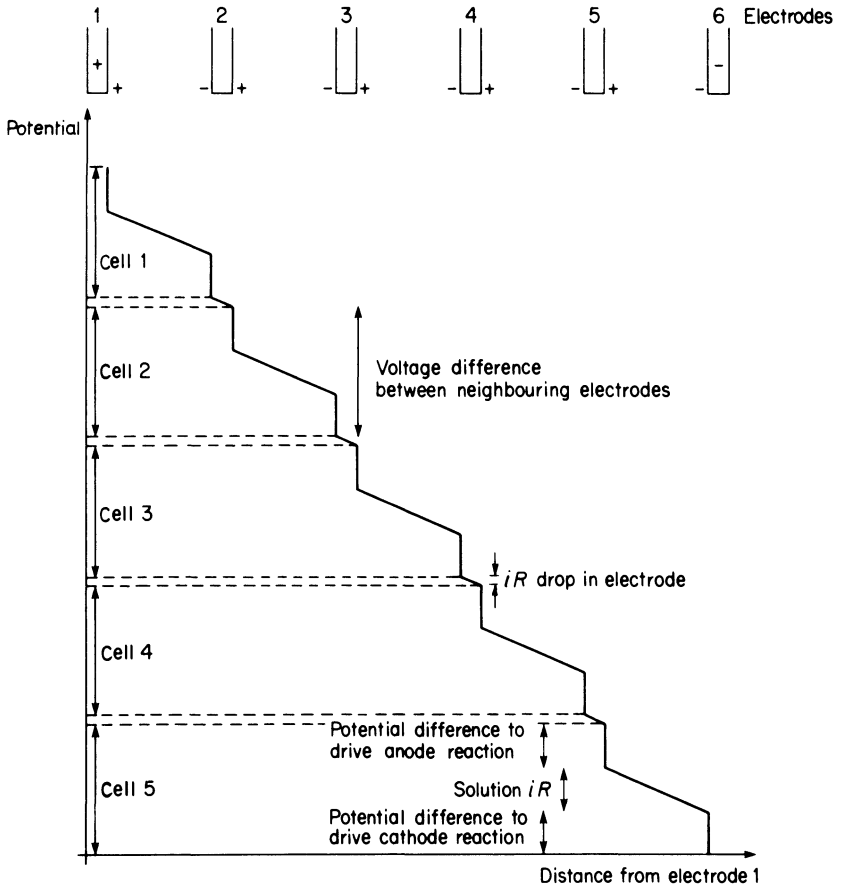

Fig. 2.25 Voltage distributions across a reactor having bipolar electrodes.

Much greater sophistication in process control has become possible with the advent of cheaper computers. They have made it possible both to monitor routinely characteristics from each cell (and, hence, to locate problem cells) and to vary control parameters (E_{CELL}, i, feed rates) to optimum values for the prevailing conditions, e.g. cost of power and feed composition. Certainly, in the UK, where power is cheaper at night, it is routine practice to increase current for this period.

The electrodes and the separator are the only components in an electrolytic cell which are not to be found in other chemical reactors. Electrode materials have been discussed thoroughly in earlier sections but some comments should be made about separators. In the first place, it is clear that a cell should only have a separator if one is entirely necessary. Quite apart from cost, the inclusion of a separator restricts the electrode geometry and the practically feasible mass

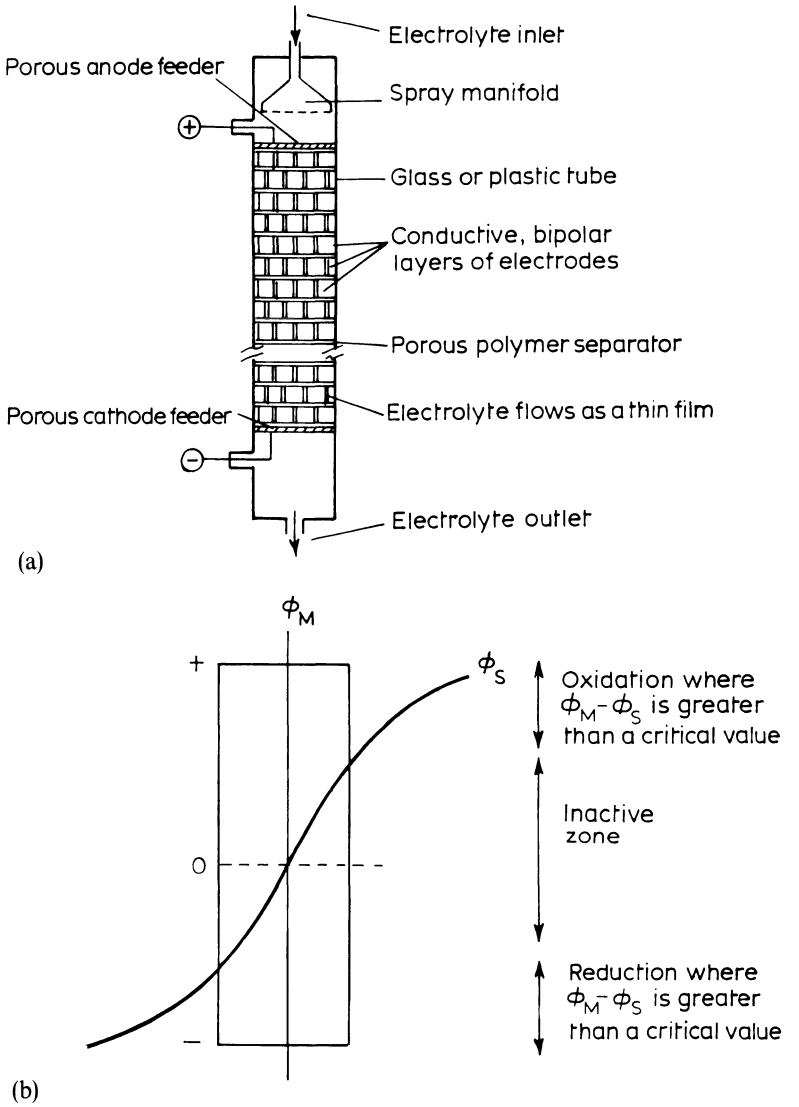

Fig. 2.26 The bipolar trickle-tower reactor. (a) A schematic. (b) The potential distribution over a single bipolar layer. The electrode is assumed to have a constant potential, ϕ_M while the solution potential, ϕ_S varies with distance down the layer. The driving force for reaction ($\phi_M - \phi_S$) varies with position, being largest near the ends of each electrode layer.

transport conditions, increases the cell resistance substantially and certainly makes the cell design more complex; the separator must be gasketed to avoid leaks, there must be separate anolyte and catholyte chambers, and therefore twice the number of pipe connections to the cell. In many electrolyses, a

separator is, however, unavoidable and two types of material have been used for the purpose:

1. A porous material (e.g. asbestos, porous plastic, a glass frit, porcelain and other porous pottery) which acts purely as a physical barrier, slowing down transport between the anode and cathode compartments. Such materials do not distinguish between species; all will pass through the separator in time if there is a concentration gradient.
2. Ion-selective membranes, e.g. Nafion, Flemion, Na-β-alumina. These materials are highly selective, permitting the transport only of either cations or anions and accompanying solvent.

Recent years have seen great advances in membrane materials both in terms of such selectivity, increasing chemical stability and decreased resistance. Their cost, however, remains high. Moreover, all the new perfluorinated membranes have been developed for chlor-alkali processing (they are discussed further in Chapter 3). Other processes now require the use of these membranes but without modifications which might improve the membrane's performance. Indeed, relatively little is known about the performance of these materials in non-chlor-alkali electrolytes; factors such as stability in non-aqueous solvents and selectivity between different cations remain largely uninvestigated. It should also be noted that transport of ions through a membrane is always accompanied by solvent transport; hence, the solvent balance must be considered. Presently, cation membranes show a marked superiority, in all respects, to their anion counterparts.

The question of materials for electrolysis cells has also been mentioned. It should be emphasized again, however, that concentrated solutions of electrolytes in water can be highly corrosive media. This restricts the choice of materials of construction and in later chapters there will be many examples of cell bodies made from unusual materials such as concrete, asbestos, alumina, carbon and nickel as well as more normal structural materials, e.g. steel, polymers and suitable composites.

2.7 TYPICAL CELL DESIGNS

In a discussion of fundamental electrochemistry, the unity of the subject matter is very clear; however, this is not always the case when dealing with electrochemical technology. Nowhere is this more evident than in a discussion of cell design. The cells used for the different industrial applications of electrochemistry look quite different, ranging from the rectangular open tanks common in electroplating, through the highly optimized parallel-plate cells used in the chlor-alkali industry, to the sometimes complex designs used in metal-ion removal from effluent or organic electrosynthesis; for electrochemical machining or grinding there is no cell in the sense of a reactor body. This should not be unexpected because, in the different applications, the relative importance of the

various figures of merit will be quite different. Thus, in electroplating, the quality of the product is of key importance and energy efficiency is less important because the charge used in plating is so small. On the other hand, in the large, power-intensive processes such as chlor-alkali or aluminium production, energy yield and space–time yield are the important figures; in organic synthesis, selectivity and ease of product extraction must be added.

2.7.1 General considerations

Despite this diversity there are clearly some general rules in cell design; these might include the following:

1. *Simplicity.* The cell design should meet the process requirements in the simplest way. This will usually lower capital and running costs and may render the technology more attractive to users. This is an important consideration which influences a number of decisions (Table 2.5).
2. *Operational convenience and reliability.* The cell must facilitate routine process operations including product extraction (batchwise or continuously) and maintenance (e.g. inspection of electrodes and separators followed by cleaning or replacement when necessary). Depending upon the process environment and provision of labour, the cell may have to operate automatically for long periods without attention with a high degree of reliability, safety and security.
3. *Integration and versatility.* The reactor must integrate easily and directly into the overall process. In some cases, it may be necessary to use it intermittently, with different feedstocks or for various reactions. It is sometimes advantageous to carry out other operations (e.g. solid product or gas separation or solvent extraction) within the reactor body. The shape and space requirements of the reactor and its ancilliaries must be considered, in view of the available floor space or headroom. If process expansion is envisaged, the reactor must be capable of facile scale-up (by increasing the size of the reactor, the number of cells within it or the number of modules). If there is a significant degree of uncertainty about the projected reactor performance, provision must be made for increasing performance during commissioning.
4. *Reaction engineering parameters.* The achievement of a correct rate and selectivity of production requires control and uniformity of the potential and current distribution. In turn, very high rates will usually involve a uniformly high mass transport over the electrode, achieved by provision of the required hydrodynamics. The electroactive area per unit reactor volume may need to be high if the available current density is low and a compact design is required. Adequate heat transfer must be available between the reactor and its environment.
5. *Running costs.* These will be minimized by several factors including:
   (a) low cost, reliable cell components;

(b) a small cell voltage and, hence, suitable choice of the electrode material and shape; the counter electrode reaction (to minimize cell voltage, via E_e and η for the counter electrode reaction); a small interelectrode gap; adequate electrolyte conductivity; where possible, an undivided cell, and conductive electrical contacts;
(c) absence of high-power mechanical devices for electrolyte stirring or electrode movement;
(d) a low pressure drop over the reactor, in order to reduce pumping costs.

The above considerations often provide conflicting requirements of a cell design; the skill and experience of the design engineer must be applied to grade the process needs and achieve a suitable final design.

The factors in Table 2.5 may be reviewed briefly. The mode of operation may involve a batch (simple batch or batch recycle) or a continuous (plug flow, stirred tank or cascade) reactor, with respect to electrolysis (as detailed in section 2.4). The mode of operation must also be considered with regard to product extraction from the cell, which may be batch or continuous. In the simplest case, the products are removed via the exit flow from the reactor.

In other cases, the method of removal depends upon the nature of the product, e.g. gases may be: (1) vented from the reactor, possibly via a slight reduction in pressure; (2) displaced from the electrolyte via inert gas sparging; (3) segregated via a solid polymer electrolyte (section 5.2) or recirculated via a gas–liquid separator. Liquid products may be: (1) separated by flotation or settlement if they are immiscible and have a markedly different density to the electrolyte; or (2) emulsified by mixing, then swept out of the reactor. Solid products can be separated via: (1) flotation or settlement; (2) fluidization or tangential shear to remove them from the reactor; (3) solvent extraction or incorporation into a mercury phase, e.g. amalgamation of metals.

Table 2.5 Some decisions in the process of cell design

Choice A	Factor	Choice B
Batch	Mode of operation	Continuous
Single	Number of cathodes or anodes	Multiple
Static	Electrode movement	Moving
Two-dimensional	Electrode geometry	Three-dimensional
Monopolar	Electrode connections	Bipolar
Moderate	Interelectrode gap	Capillary*
External	Electrolyte manifolding	Internal
Undivided	Division of cell	Divided
Open cell	Sealing of cell	Closed cell

Choice B often entails a greater effort in design, higher costs or a more complex design; it may however provide important technological advantages.
* Or the so-called zero gap cell, where the electrodes are in contact with the membrane

It is possible to classify cell designs according to the electrode type (Table 2.6). This is a useful rationalization, though somewhat arbitrary due to the many variants of a particular design and the many interrelationships. Electrode movement may improve mass transport or promote the mixing of reactants and products or facilitate solid product removal, albeit with additional maintenance needs. Three-dimensional electrodes may provide very high areas for reaction, improve gas disengagement or enhance mass transport; the problems of potential and current distribution were discussed in section 2.6.

The relative merits of bipolar vs. monopolar electrical connection have been discussed in section 2.6.5.

Narrow-gap or even capillary-gap cells may be required to maintain a moderate cell voltage while processing electrolytes of poor conductivity. The need to maintain a uniform capillary gap over large electrodes or multiple electrode stacks requires precise engineering, however, particularly in the case of rotating electrodes or divided cells. In the energy-intensive processes, such as chlor-alkali production and water electrolysis, the trend is towards the so-called zero gap cells where the electrodes actually contact the membrane.

Table 2.6 Classification of cell designs according to the type of electrode

Electrode movement	Electrode Geometry	
	Two-dimensional	Three-dimensional
Static	Parallel-plate –plate-in-tank –filter press	Porous electrodes –stacked mesh –reticulated –cloth
	Concentric cylinder –Eberson cell	Packed-bed electrodes –fibre
	Stacked Discs –capillary gap cell –perforated-plate trickle tower	–granules –spheres/rods –flakes
		Particulate trickle-tower
	Chemelec cell (inert fluidized bed)	Swiss-roll cell
Dynamic	Moving sheet or wire: –reciprocating plate –vibrating electrode	Active fluidized beds
	Rotating disc (e.g. pump cell)	Moving beds –moving-bed electrode –slurries –tumbled-bed cell
	Rotating cylinder (e.g. Eco-Cell)	

The electrolyte inlets and outlets must be designed to give a low pressure drop over the reactor and the required flow characteristics (for mixing or mass transport reasons) with due regard for the nature of the reactants and products. In the case of a filterpress, parallel-plate reactor, internal manifolding provides a neat, compact method of distributing the catholyte and anolyte flows but it requires precise sealing and offers little control over bypass currents in bipolar cells.

Division of a cell by means of a separator is often practised, despite the additional costs, the need for additional seals and possible maintenance problems. A separator may: (1) allow a more independent choice of anode/anolyte or cathode/catholyte; (2) enable current efficiency to be maintained due to the exclusion of redox shuttles; (3) help to isolate electrode products; (4) enable electrodialysis to be practised; or (5) prevent the formation of explosive or toxic mixtures, e.g. H_2/O_2 or H_2/Cl_2.

Reactors may be operated at atmospheric pressure wherever possible and remain open to the environment for ease of inspection, maintenance or reactant charging and product removal needs. However, sealing a reactor may permit: (1) the safe and rapid removal of products; (2) an increased operational pressure; (3) reduced splashing or vortexing of electrolyte; (4) a higher electrolyte flow to enhance mass transport; or (5) the exclusion of air.

We will now discuss some typical examples of these principles of cell design. Each subsequent chapter will deal with cell design in the more specific context of the particular application.

2.7.2 Tank cells

The tank cell is the classical batch or semi-batch (reactants added and products removed at intervals) reactor of electrochemical technology. The battery is perhaps the best example of a batch reactor; the electrodes, electrolyte and electroactive species are sealed into the cell during manufacture and the 'reactor' is either discarded or recharged when the stored energy has been used. Electroplating is also often a batch process carried out in an open rectangular tank; the items to be plated are placed in the tank together with the soluble anodes and, depending on the complexity of the cathode shape, various degrees of care will be taken with the anode–cathode geometry and the placing of auxiliary anodes and/or shields. Moreover, tank cells operated in a semi-batch manner are used in electrolytic processes, e.g. in aluminium extraction, fluorine generation and older-style electrolysis. The choice of a tank cell for aluminium extraction is determined by the extremely aggressive nature of the cryolite electrolysis medium and the materials problem it poses. The same is largely true for the acidic fluoride melt used for fluorine generation, but in water electrolysers, the selection of a tank design is more because of the simple construction and cheap materials which may be used.

In the usual Hall–Heroult cell for aluminium production (Chapter 4), the electrodes are horizontal, the cathode being the molten metal and the anode being

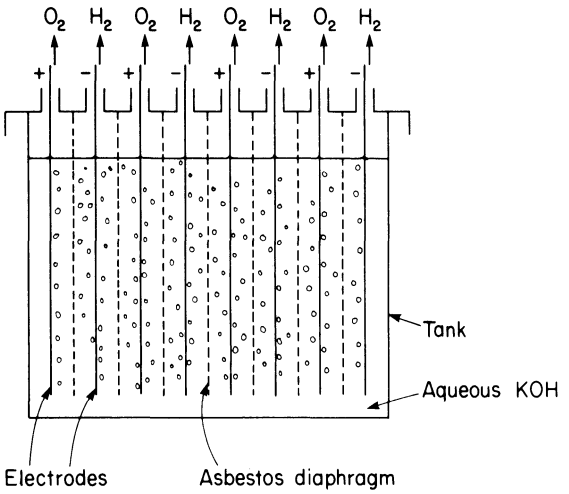

Fig. 2.27 A monopolar plate-in-tank reactor for water electrolysis.

carbon blocks mounted from the top of the cell so as to give parallel-plate electrode geometry. In most tank cells, however, the electrodes are vertical and made from sheet, gauze or expanded metal. The cell is arranged with parallel lines of alternate anodes and cathodes, the electrodes extending across and to the full depth of the tank. The anode–cathode gap is made as small as possible to maximize the space–time yield and to reduce the energy consumption. In fact, the minimum interelectrode gap is usually determined by a practical limitation, i.e. the need to prevent shorts in electrowinning cells or the need to separate anode and cathode gases in a fluorine cell. In some cells (e.g. some water electrolysers, Fig. 2.27, and lead–acid batteries), there is a separator (asbestos sheet and porous plastic respectively), although this is not usually sealed to prevent the passage of liquid around the outside; the asbestos diaphragm in a water electrolyser is only to prevent mixing of the oxygen and hydrogen while allowing the interelectrode gap to be quite small. It is unusual in tank cells to induce convection by mechanical means, although gas bubbles evolved at electrodes stir the electrolyte strongly. Moreover, the electrical connection may be monopolar or bipolar.

The great advantage of the tank cell is the simplicity of construction and the wide range of materials which can be used for the manufacture of the simple components required. It is, however, limited in space–time yield and poorly suited to large-scale operation or to a process where control of the mass transport conditions is necessary.

2.7.3 Parallel-plate flow cells

Most industrial flow cells are based on the parallel-plate electrode configuration and again the electrodes may be horizontal or (more commonly) vertical.

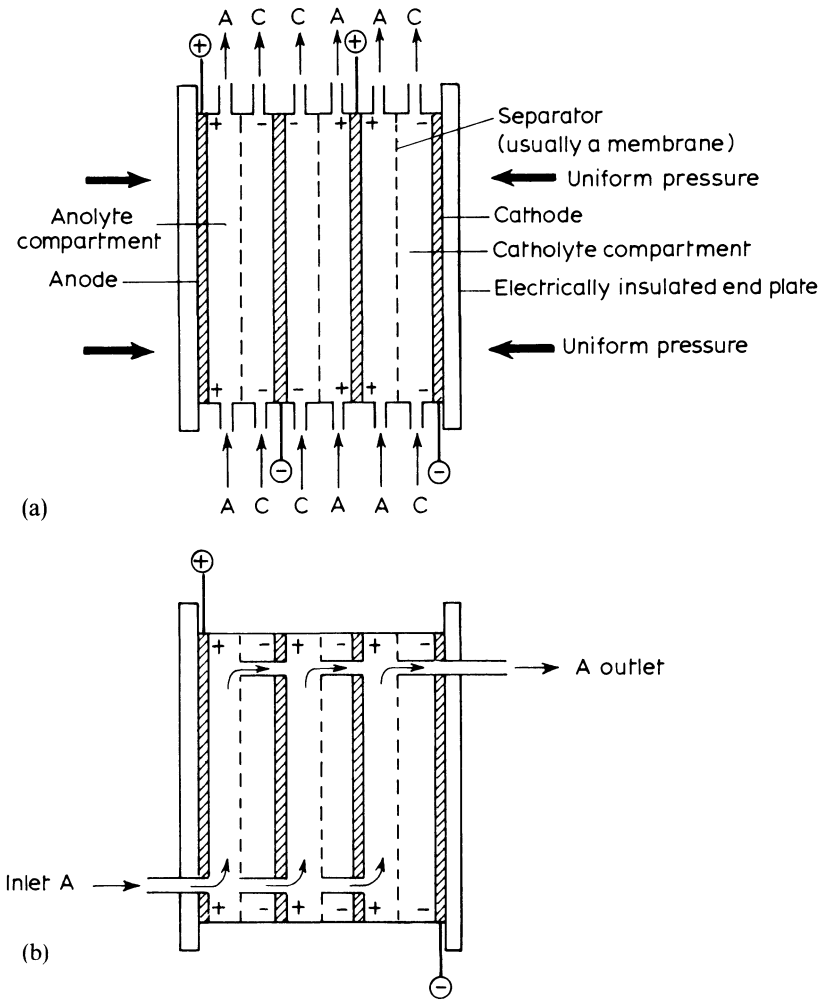

Fig. 2.28 Plate-and-frame cells. Typically, these cells are mounted in a filterpress with suitable gasket materials between components to seal the assembly. Compression may be applied via a screwpress, a hydraulic press or tiebars. A = anolyte; C = catholyte. (a) Monopolar electrodes; external manifolding. (b) Bipolar electrodes; internal manifolding. Only the anolyte flow is shown, for clarity. The cells are shown in the divided mode.

The most common cell with horizontal electrodes is the mercury cell from the chlor-alkali industry (section 3.3.1). The mercury cathode flows down the slightly sloping baseplate of the cell and many rectangular dimensionally stable anodes (of gauze, expanded metal-type structures, blades, or rods to allow the chlorine gas to rise with only minimum restriction) are mounted from the top of the cell so that they cover the surface area of the mercury and give an

interelectrode gap of a few centimetres. Recently, a number of very large electrode size chlorine cells have been introduced by several manufacturers. These bipolar cells contain electrodes as large as 5 m^2. The cell may be as large as 70 m^2. The brine is, however, passed through the cell at a relatively low velocity and, because of the considerable mixing caused by the evolving chlorine gas, the cell shows intermediate behaviour between a plug flow and a back-mix reactor. Diaphragm cells used in chlor-alkali production are also effectively a parallel-plate flow reactor but they are constructed in a very different way; they will be discussed in section 3.3.2.

With vertical electrodes the cell is usually constructed in a plate-and-frame arrangement and mounted on a filterpress. The electrodes, electrolyte chambers, insulating plates to separate cells electrically and, where used, membranes or separators, are constructed individually and mounted with suitable gasketing materials between each component; the filterpress is then used to seal the cells with up to 100 cells in each unit (Fig. 2.28). It is difficult generally to manufacture the cells with an individual electrode area greater than 1 m^2. Again, the electrical connection may be bipolar instead of monopolar (effectively by removing the intercell insulation) and in a series of cells the electrolyte feeds to the cells may be connected so that the cells are in series or parallel so far as the electrolyte is concerned. The minimum attainable gap in mercury cells is approximately 1 mm; typically modern cells utilize a gap in the range 1–3 mm.

In plate-and-frame cells it is normal to reduce the interelectrode gap to 0.5–5 cm and the electrolyte flow rates are often high. The electrolyte entry ports must be designed to give a uniform distribution of electrolyte into the cell and an adequate linear velocity. The flow within the cell can be made more turbulent by a variety of methods, e.g. a number of strategically placed (insulating) baffles may force the electrolyte to adopt a serpentine flow pattern, increasing its effective contact time in the reactor and reducing channelling of flow. Perhaps the most common method of turbulence promotion is the use of electrodes which each have a definite texture and/or insulating plastic meshes next to the electrode. Such devices are used in the majority of general-purpose electrosynthesis cells which are now available.

The parallel-plate geometry is a popular and convenient choice of reactor for a diverse range of processes. Reasons for this include:

1. Simplicity of construction with regard to features such as cell frames, electrode connections and membrane sealing.
2. Wide availability of electrode materials and separators in a suitable (or readily adaptable) form.
3. The potential distribution is reasonably uniform.
4. Mass transport may be enhanced and adjusted using a variety of turbulence promoters and control of the linear electrolyte velocity.
5. Scale-up readily achieved by a suitable combination of:
   (a) increased electrode size;
   (b) using more electrodes;

(c) duplicating the cell stack.

6. Versatility, with respect to monopolar or bipolar operation and the possibility of modifying the fundamental unit cell (Fig. 2.29)
7. The construction and appearance of the filterpress cell has similarities with

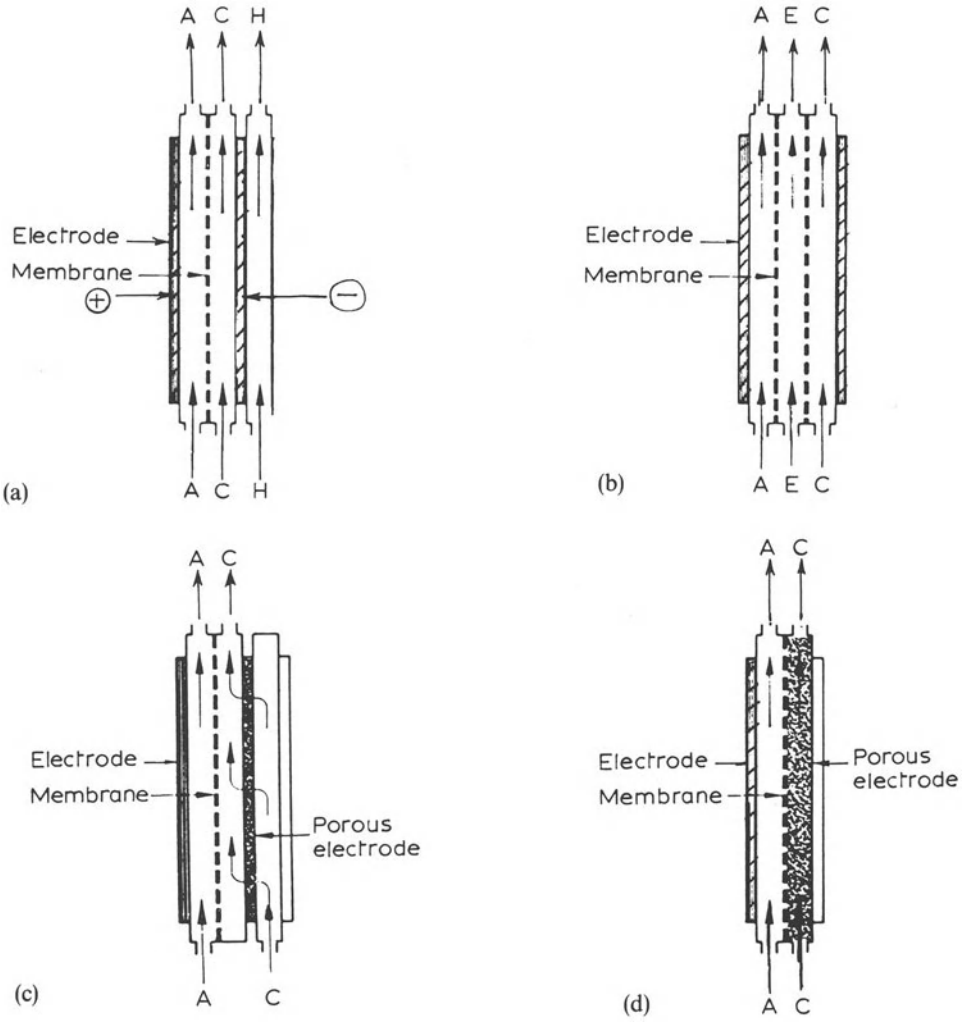

Fig. 2.29 Modifications to the fundamental electrolyte path of a filterpress cell. (a) A third compartment which could act as a heat exchanger. (b) A third compartment which could act as an electrodialysis compartment. (c) Three-dimensional electrodes may be incorporated in the 'flow-across' electrolyte mode. (d) Three-dimensional electrodes may be incorporated in a 'flow-through' electrolyte mode. A = anolyte; C = catholyte; H = heat exchange fluid; E = electrodialysis compartment. (Courtesy: ElectroCell AB, with modifications).

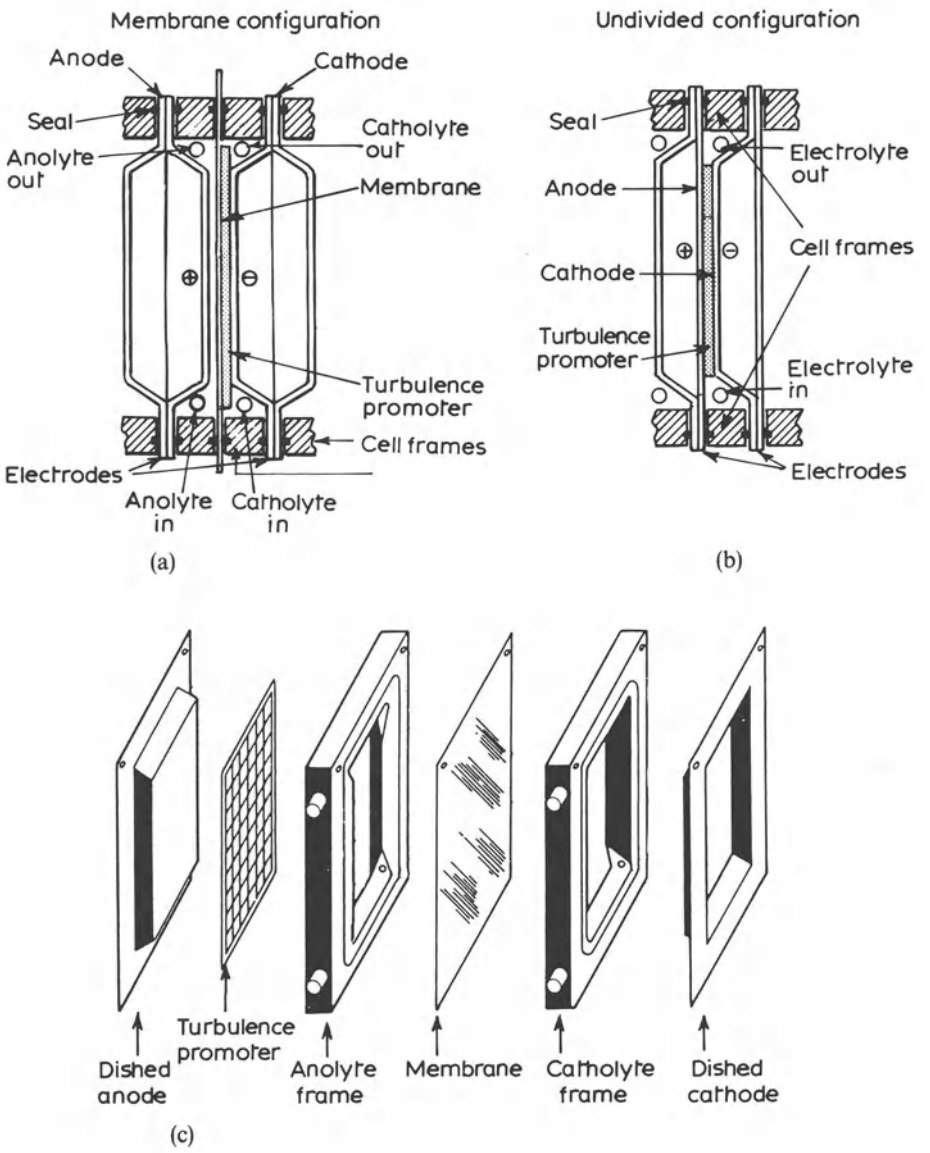

known examples of chemical engineering hardware such as heat exchangers and dialysis units.

8. The success of the filterpress cell has been demonstrated for a diverse range of electrolytic applications, including large-scale water electrolysis and synthesis of adiponitrile.

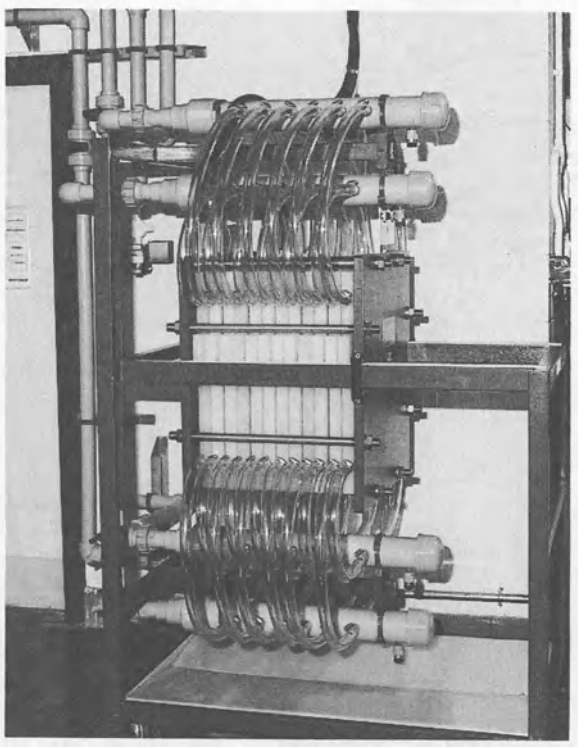

(d)

Fig. 2.30 The dished electrode membrane (DEM) cell. (a) Section of the divided unit cell. (b) Section of the undivided unit cell. (c) Exploded view of a divided unit cell. (d) An intermediate size reactor, comprising six unit cells, which is used for pilot-plant and small-scale production of, for example, pharmaceuticals. A larger cell stack, incorporating 34 l m^2 unit cells is shown in Fig. 7.26. (Courtesy: Electricity Council Research Centre).

There were, until recently, few general-purpose filterpress cells available in a range of sizes. This situation has fortunately changed; a number of cells are now available from various manufacturers and distributors as illustrated in Figs 2.30–2.32.

The Dished Electrode Membrane cell (Fig. 2.30) uses specially shaped electrodes in order to provide a small interelectrode gap over the active electrode, while maintaining adequate peripheral space at the bottom and top of the electrodes for a conventional pipe manifold. When bipolar operation is used, the use of relatively long external manifolds (Fig. 2.30(d)) minimizes bypass currents.

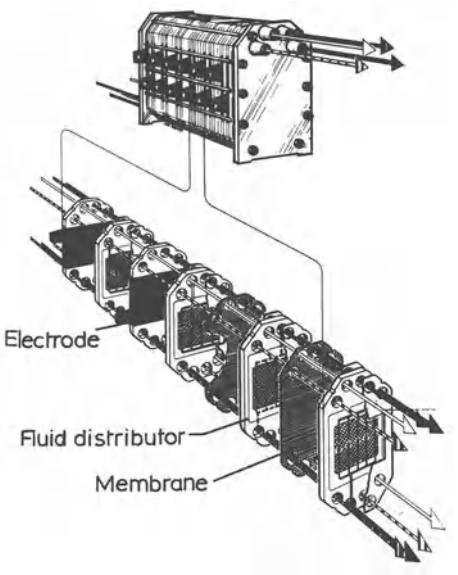

(a)



(b)

Fig. 2.31 The ElectroCell AB family of cells. (a) An exploded view of the Electro MP cell, which provides up to four different electrolyte or gas flows using internal manifolding. The cell is a small, multipurpose reactor for laboratory trials and process development. (b) The ElectroCell AB family of cells. From left to right: Electro MP cell, ElectroSyn cell, hand-held micro-flow cell and ElectroProd cell.

Table 2.7 The ElectroCell AB family of cells

Parameter	Microflow cell	ElectroMP cell	ElectroSyn cell	ElectroProd cell
Electrode area/m^2	0.001	0.01–0.2	0.04–1.04	0.4–16.0
Current density/kA m^{-2}	<4	<4	<4	<4
Interelectrode gap/mm	3–6	6–12	5	0.5–4
Electrolyte flow per cell/dm^3 min^{-1}	0.18–1.5	1–5	5–15	10–30
Linear flow velocity/m s^{-1}	0.05–0.4	0.03–0.3	0.2–0.6	0.15–0.45
Number of electrode pairs	1	1–20	1–26	1–40

The ElectroCell concept (Fig. 2.31) utilizes internal manifolding to distribute the electrolyte, in the manner of some plate-and-frame heat exchangers (Fig. 2.31(a)). Such an arrangement helps to provide a compact reactor. In special cases, individual compartments with external manifolds may be incorporated into the cell stack (Fig. 2.29).

The recently introduced FM21 SP cell (Fig. 2.32) represents a general-purpose design which is a development from FM21 chlor-alkali cells (section 3.3.3). This reactor utilizes a monopolar connection to the electrodes which may be, for example, a flat plate, lantern blade electrodes or an expanded mesh, with provision for additional turbulence promoters if required. This design does not utilize cell frames as such; rather, electrode spacing is achieved via a shaped gasket which is moulded to provide secure sealing. The electrolyte flow is via internal manifolding, each electrode incorporating an inlet and outlet port to distribute flow over its surface (Fig. 2.31(a)).

While the potential distribution in a parallel-plate cell is good and the mixing conditions can be made to meet most requirements, the space–time yield leaves much to be desired, and it is often difficult to reduce the interelectrode gap sufficiently to give the required space–time yield and energy efficiency. Extraction of solid production may be difficult. These problems have led to the development of many novel cell designs, but few have survived through a pilot-plant scale and even fewer have thrived in a commercial environment. The diversity of novel designs is particularly evident in the field of metals removal from industrial process liquors (Chapter 7), but here we will consider certain cell designs which have proved successful on a pilot scale or small commercial, industrial application.

FM21 SP

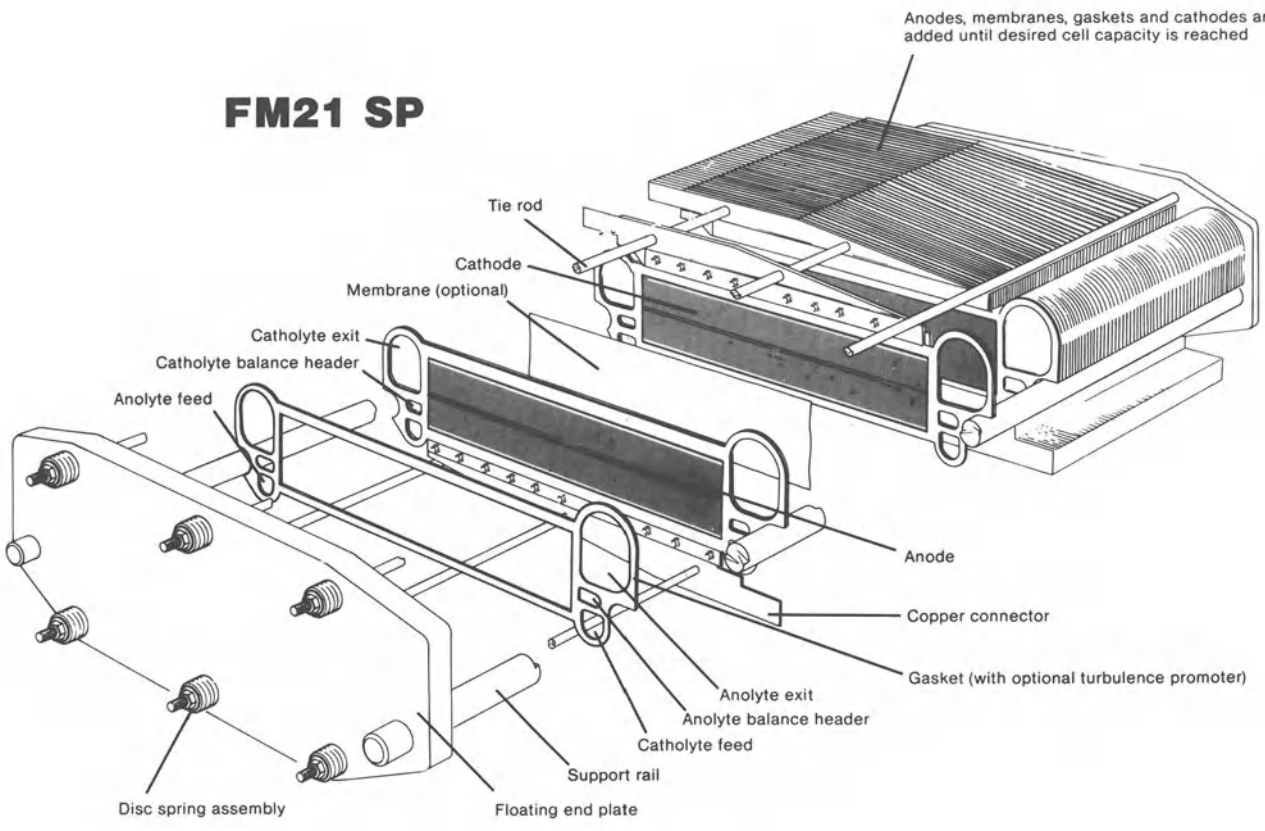
Anodes, membranes, gaskets and cathodes are added until desired cell capacity is reached
Tie rod
Cathode
Membrane (optional)
Catholyte exit
Catholyte balance header
Anolyte feed
Anode
Copper connector
Gasket (with optional turbulence promoter)
Anolyte exit
Anolyte balance header
Catholyte feed
Support rail
Floating end plate
Disc spring assembly

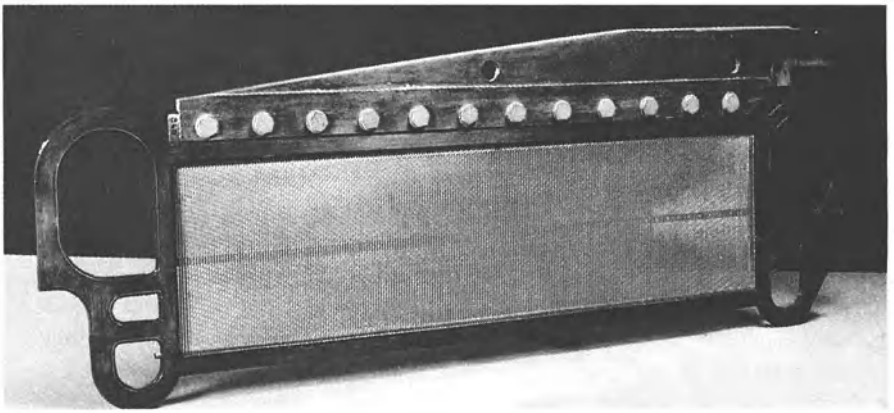

(b)

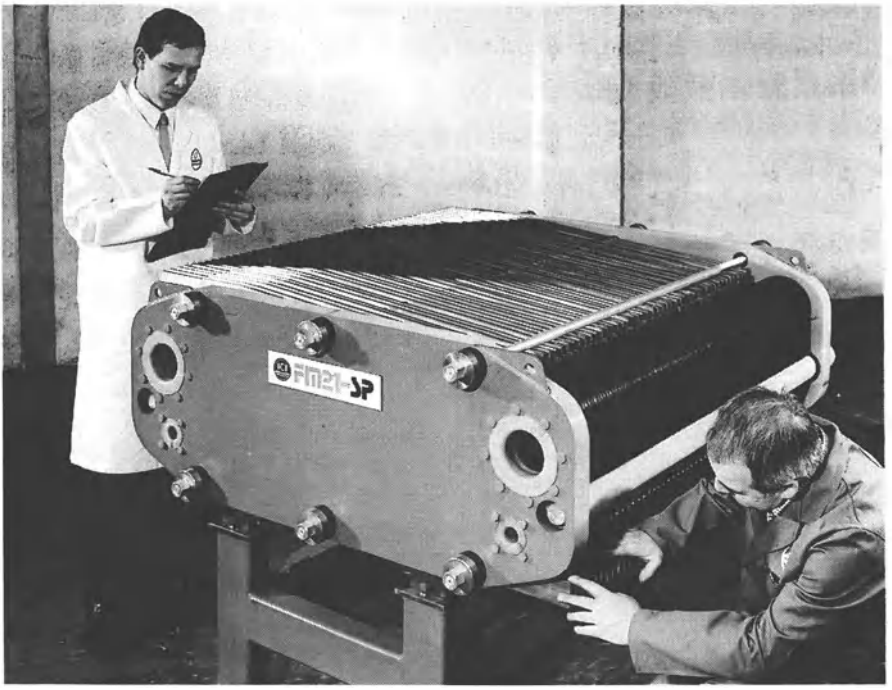

(c)

Fig. 2.32 The FM21 SP Electrolyser. (a) The overall construction. (b) A single electrode, which has a nominal projected area of 0.21 m^2 on each face. The photograph shows the electrolyte ports and the current feeder busbar. A symmetrical lantern blade electrode is shown complete with its compression-moulded gasket. (c) An assembled, multi-electrode reactor, showing the electrolyte manifolds and the end plate. The electrolyser unit is capable of taking up to 60 electrode pairs, which would provide a projected cathode or anode area of up to 25 m^2. A double-pack version utilizes a central plate extending, the capacity to a maximum of 120 electrodes (50 m^2). The construction of FM21 electrolysers for chloralkali production is considered in Chapter 3. (Photographs supplied by ICI Chemicals and Polymers Ltd.)

2.7.4 Capillary gap and thin film cells

Thin electrolyte films and small interelectrode gaps are advantageous in the processing of poorly conductive electrolytes, as the iR_{CELL} component in equation (2.43) is minimized.

The bipolar trickle tower reactor has already been mentioned (Fig. 2.26). Here, the electrolyte falls, under gravity, down a packed column containing a bipolar array of electrodes. In order to maintain trickle flow (and, hence, minimize bypass currents) the flow rate is restricted. High flow rates cause flooding while low values result in incomplete wetting of the electrodes.

Figure 2.33(a) shows the capillary gap cell first developed in order to reduce the energy consumption for an organic electrosynthesis in a poorly conducting organic solvent. The cell is cylindrical and the electrodes are a stack of discs kept apart by insulating spacers, $\simeq 1$ mm thick. The cell is bipolar and the electrolyte is pumped through the interelectrode gaps from the centre outwards. Several modifications have been proposed, including the pump cell (section 2.7.5). The cell shown in Fig. 2.33(a) is a laboratory unit and larger-scale versions are often

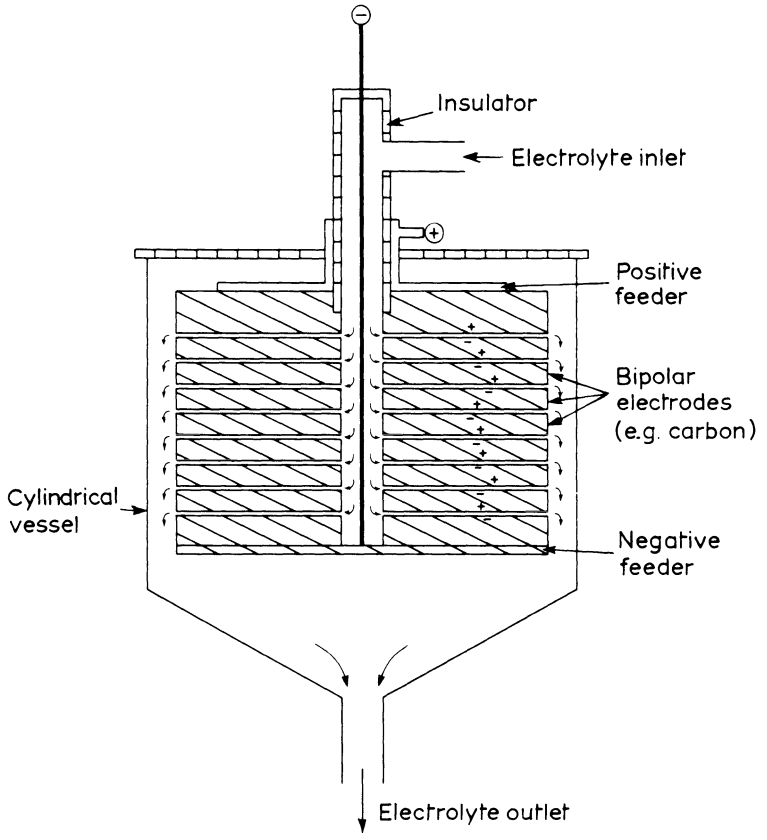

(a)

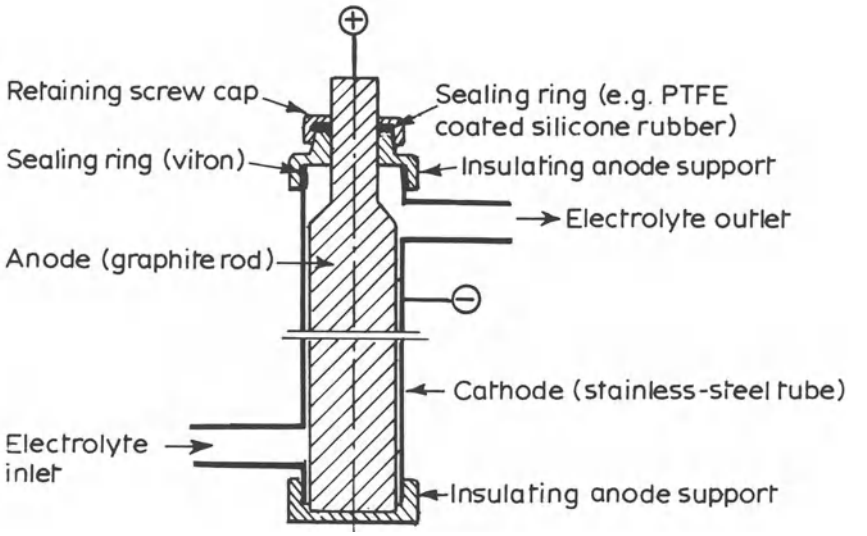

(b)

Fig. 2.33 Capillary gap ($\simeq$ 1 mm) cells. (a) The bipolar capillary gap cell. The electrodes are a stack of closely spaced discs. Electrolyte flows radially outwards in each inter-electrode gap. (*After*: Beck, F. and Guthke, H. (1969) *Chem.-Ing.-Tech.*, **41**, 943). (b) The monopolar capillary gap cell. The inner cylindrical electrode is concentrically mounted in a confirming tube. (*After*: Eberson, L., Nyberg, K. and Sternerup, H. (1973) Chemica Scripta, **3**, 12).

based on vertical, rectangular electrodes, which represent a more practical geometry.

Concentric cells provide another method of maintaining a uniform and small interelectrode gap. The cell shown in Fig. 2.33(b) was developed as a simple annular-flow tubular reactor for laboratory and pilot-scale organic electrosynthesis. While the space–time yield is relatively low (due to the use of essentially two-dimensional electrodes and a dead space within the inner electrode) the reactor is robust and a separator may be incorporated much more readily than for the stacked-disc cell. The resulting reactor provides a convenient modular, flow-through cell, which has been utilized for industrial-scale processes.

2.7.5 Rotating electrodes

Rotating the electrode enhances mass transfer directly without recourse to external pumping, i.e. the current density can be controlled to a high degree independently of the residence time and, hence, conversion in the reactor. This is

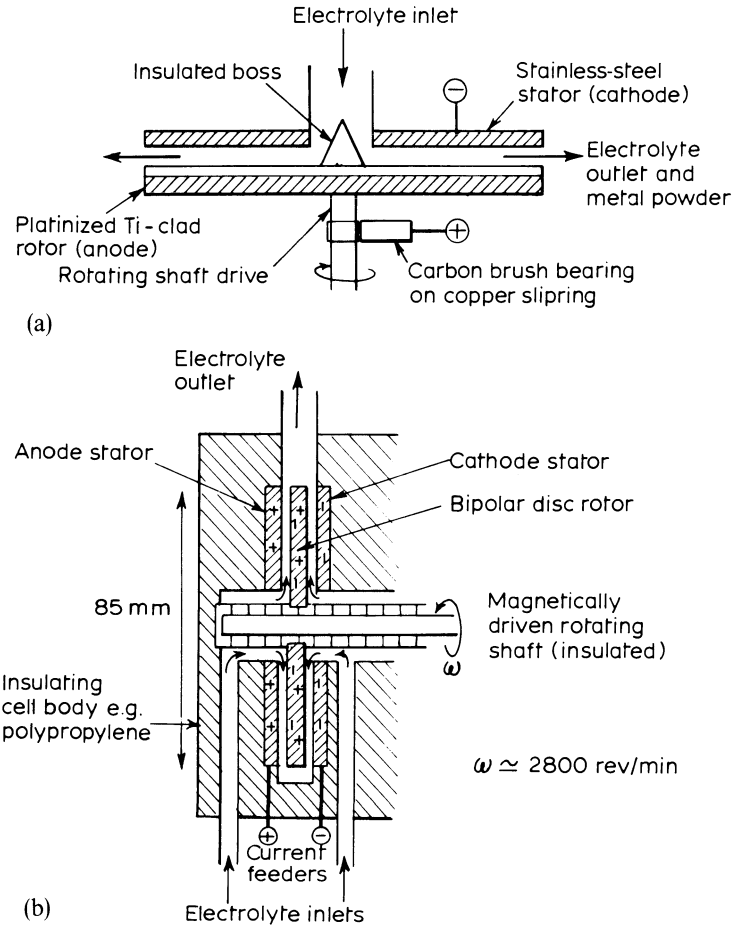

not usually of primary importance in soluble product synthesis. In cases where solids are produced, however, tailoring the shear stress of the electrode via rotation is a useful way in which to obtain powders of requisite size which are readily removable from the electrode. Three principal mechanisms have been successful: (1) direct scraping; (2) shearing of dendritic deposits; and (3) chemical reaction of short-lived intermediates scavenged from the electrode surface. The option of rotating the electrode has led to well-characterized cell designs; the pump cell (Fig. 2.34) and a rotating cylinder (Chapter 7) provide important examples.

The pump cell in its simplest form is shown in Fig. 2.34(a). Electrolyte entering the capillary gap (typically 0.5–1 mm) is accelerated tangentially, which gives rise to high mass transfer rates and the cell becomes self-pumping. The

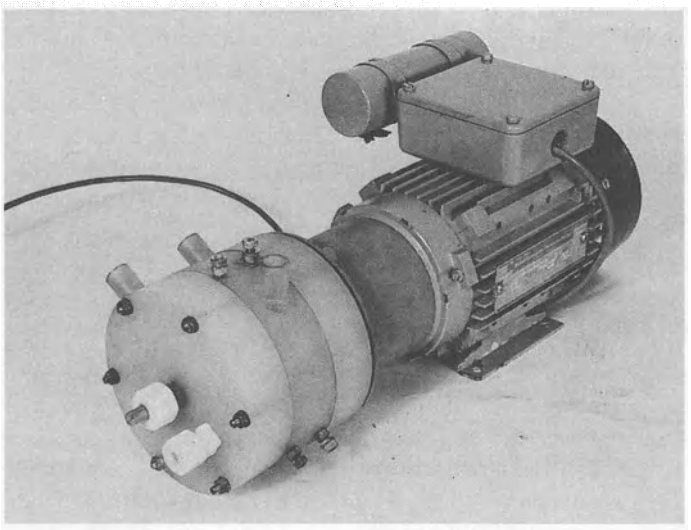

(c)

Fig. 2.34 The electrochemical pump cell. (a) A monopolar cell for production of metal powders. (*After*: Jansson, R. E. W. and Ashworth, G. A., (1977) *J. Appl. Electrochem.*, **7**, 309). (b) Bipolar rotor cell for electrosynthesis. (*After*: Jansson, R. E. W., Marshall, R. J. and Rizzo, J. E. J., (1978) *J. Appl. Electrochem.*, **8**, 281). (c) An improved version of (b) which incorporates facilities for adjustment of the rotor position, a reference electrode probe and enhanced mass transport. The bipolar rotor has a diameter of 10 cm and rotates at 2800 rev min^{-1}.

monopolar pump cell (Fig. 2.34(a)) has been exploited for the continuous production of metal powders.

A more convenient engineering design not requiring current connection through brush contacts is the bipolar pump cell shown in Fig. 2.34(b). This arrangement has been made available commercially (Fig. 2.34(c)) primarily as a modular bench-top cell as a unit driven by magnetic coupling to a pump motor for electrosynthesis reactions. The pump cell is most conveniently scaled-up as a multiplate bipolar stack, and in this case there is sequential radial inflow and outflow of electrolyte. The self-pumping facility is lost in this case, but this is of minor importance in larger-scale designs. A device of this type has been tested successfully on the 3 kW scale for the production of solid metal oxide products. Despite the superficial similarities between the capillary gap cell and the pump cell, the mass transport conditions are quite different. The pump cell permits higher Reynolds number in the thin gaps between the electrodes and, although in both cells the electrolyte must decelerate as it flows radially outwards, in the pump cell the tangential shear increases. The net effect in the pump cell is for the

rate of mass transport to increase continuously as the fluid moves outwards; in contrast, in the capillary gap cell it reaches a maximum value and then declines. Hence, the current density in the pump cell is higher. Moreover, as the rotational speed increases, the pump cell behaves increasingly as a plug flow reactor in the radial direction but with the tangential shear producing intense mixing across the gap. In practice, the particular advantages of the pump cell are the ability to remove solid products continuously from the reactor (with a minimum residence time for the products) and the strong mixing within the gap.

2.7.6 Porous and packed-bed electrodes

It has already been mentioned that three-dimensional, porous, electrodes offer particularly high values of the electroactive area per unit reactor volume A_S whilst also giving a moderate increase in the mass transport coefficient k_L. The result is a significantly increased performance from a given volume of reactor, compared to two-dimensional electrode materials, due to the high value of $k_L A_S$. This performance may be utilized in various ways including:

1. A compact reactor for a given duty.
2. The capability of providing a high fractional conversion per pass, given a sufficiently large residence time.
3. The ability to maintain a reasonable production rate and current efficiency when processing solutions which contain low levels of the electroactive species (Chapter 7).

There are several compromises to achieve this performance, however, and the following factors must be considered.

1. The range of available electrode materials is much lower for three-dimensional packed-beds than for the case of two-dimensional parallel-plate reactors.
2. Potential distribution may be non-uniform within the electrode matrix (section 2.6.3) leading to low current efficiency and poor selectivity.
3. Similarly, a non-uniform current distribution may result in a variable rate of reaction within the electrode. In the case of metal-removal cells (Chapter 7), this may result in premature blocking of the matrix or excessive build-up of metal near the membrane (section 2.6.3).
4. The potential, current, and mass transport distributions may also be affected in time and space by gas evolution.
5. The performance of porous, three-dimensional electrodes is often difficult to predict and scale-up may be less predictable than for two-dimensional electrodes.
6. Too low an effective porosity (either initially or for reasons stated in (3) and (4)) may result in a high-pressure drop over the reactor, with attendent design problems and higher pumping costs.

The term 'porous, three-dimensional electrode' covers an unusually broad range of materials, e.g. the matrix may be:

1. A packed bed of numerous discrete particles, e.g. carbon spheroids, or granules.
2. A packed bed of numerous, intermeshing elements, e.g. carbon fibre or steel wool.
3. A regular array of (essentially two-dimensional) electrodes, e.g. meshes or perforated plates.
4. A continuous, porous matrix, e.g. reticulated materials.
5. A semi-regular array of elements, as in the bipolar trickle-tower reactor (Fig. 2.26).

Traditional electrode materials have included lead spheres and carbon particles, e.g. the Nalco cell* for production of lead tetraalkyls utilized a number of vertical, steel anode tubes containing consumable lead shot, in a 'shell-and-tube' arrangement. Due to the recent trend towards lead free petrol, this process is no longer operating.

More recent electrode materials include metal and carbon foams (reticulates), carbon granules, fibre and cloth, and a range of metal meshes.

The major application of porous, three-dimensional electrodes has been in metal removal from dilute process liquors (Chapter 7) although inorganic and organic electrosynthesis applications continue to be explored (see, for example, the Dow–Huron cell for H_2O_2 production in Chapter 5). Many battery and fuel cell electrodes utilize an active material which is (or is supported by) a porous, three-dimensional matrix (Chapter 11), while miniature porous electrodes have found use in electrochemical detector systems for high-pressure liquid chromatography analysis (Chapter 12).

As in the case of other types of reactor geometry, many variations are possible in practice, depending upon the operational mode (Table 2.5). The following factors, for example, may be varied:

1. Electrolyte flow may trickle through the porous electrode (as in the trickle-tower reactor (Fig. 2.26(a)) or be pumped upwards through a flooded-bed electrode, e.g. Fig. 2.35(b)).
2. The current flow may be parallel or perpendicular to the electrolyte flow (section 2.6.3), the latter being more practical.
3. The counter-electrode may be two-dimensional, or three-dimensional (as in the trickle tower, Fig. 2.26).
4. The overall reactor geometry may utilize parallel-plate feeders, a concentric cylinder or a packed column.
5. Electrical feeder connections may be monopolar or bipolar.

* See *Industrial Electrochemistry*, First Edition

Two contrasting examples of porous three-dimensional electrodes are shown in Fig. 2.35. The Swiss-roll cell (Fig. 2.35(a)) consists of an electrode–separator or spacer–electrode sandwich spirally wound, usually with axial flow through the mesh electrodes. The mass transport is promoted by textured electrodes and/or plastic mesh turbulence promoters which also serve as membrane–electrode spacers. The interelectrode gap is small (0.2–2 mm), providing a low cell voltage

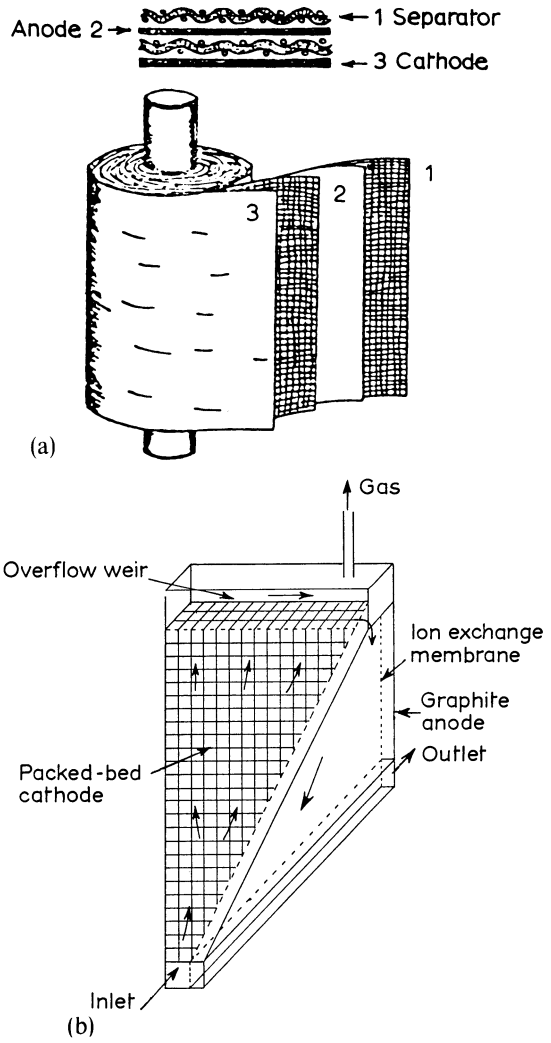

Fig. 2.35 Examples of porous three-dimensional electrodes. (a) The Swiss-roll cell, showing its sandwich-and-roll structure. The electrodes may be single or multiple sheets or nets. The separator is selected from cloths, porous polymers or ion-exchange membranes. (b) The Enviro-Cell, which incorporates a profiled bed of carbon particles. In this manner, the current density is deliberately decreased towards the reactor outlet.

and promoting uniform flow, and electrode potential distributions. The design is cartridge-orientated, and electrode or separator changes are best made via a replacement module.

The EnviroCell (Fig. 2.35(b)) has primarily been developed as a modular design for metal removal from industrial process streams. A major design feature is the provision of a cathodic bed which increases in active area with the direction of flow to compensate for the effects of depletion. This is achieved by a combination of a larger cross-sectional area and a smaller particle size towards the low concentration (exit) end of the cell. A wide range of metals has been recovered from diverse solutions; various modes of operation are possible for metal recovery including direct exchange of the granular graphite bed (by means of a suction tube, for example) and anodic redissolution to produce a concentrate. An obvious driving force in the commercialization of this device was the specialized tailormade material for both the cathode bed and the graphite, anodic feeder plate. This can be contrasted with many other designs which have necessarily relied on available electrode materials, often borrowed from other technologies.

2.7.7 Dynamic, three-dimensional electrodes

When the upward electrolyte flow through an unrestrained particulate bed is sufficiently high, fluidization of the electrode particles may occur, the electrode–electrolyte combination behaving like a single fluid.

A fluidized electrode phase provides several possible advantages:

1. The dispersed nature of the electrode provides a large A_S value.
2. Mass transport is higher than for static-bed electrodes.
3. The electrical and physical contact between particles may help to provide an active electrode surface.
4. Under suitable conditions, the potential and current distribution may be more uniform than for packed-bed electrodes (section 2.6.3).
5. In the case of metal extraction from industrial process liquors (by far the most important application), the product may be extracted continuously from the reactor (Fig. 2.36).

In practice, control of the fluidization can be a problem, due to a non-uniform reactor geometry, particle agglomeration, unwanted metal deposition on the feeder electrode and separator damage due to erosion or electrical shorting caused by metal particles lodging near the membrane. The potential distribution can be complex, being time-dependent and affected by the shape and dimensions of the bed, positioning of the feeder and counter electrode(s), the degree of bed expansion, electrolyte composition and gas evolution.

One of the most successful designs for fluidized-bed electrodes was developed by AKZO Zout Chemie (Fig. 2.36). The technology has been acquired by Billiton

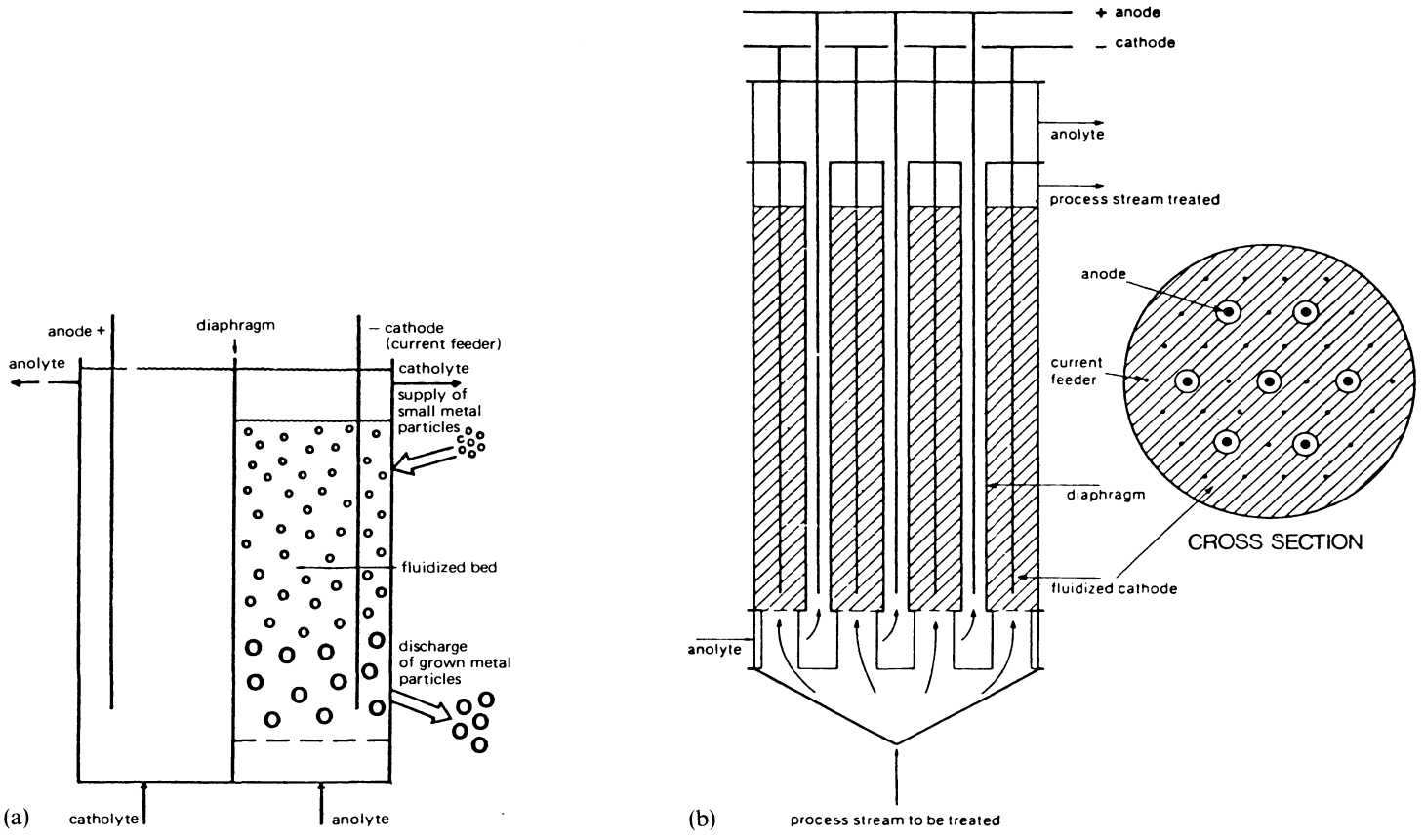

Fig. 2.36 The AKZO/Billiton fluidized-bed electrode reactor. (a) The concept of continuous withdrawal of metal product. (b) The reactor, which resembles a shell-and-tube heat-exchanger.

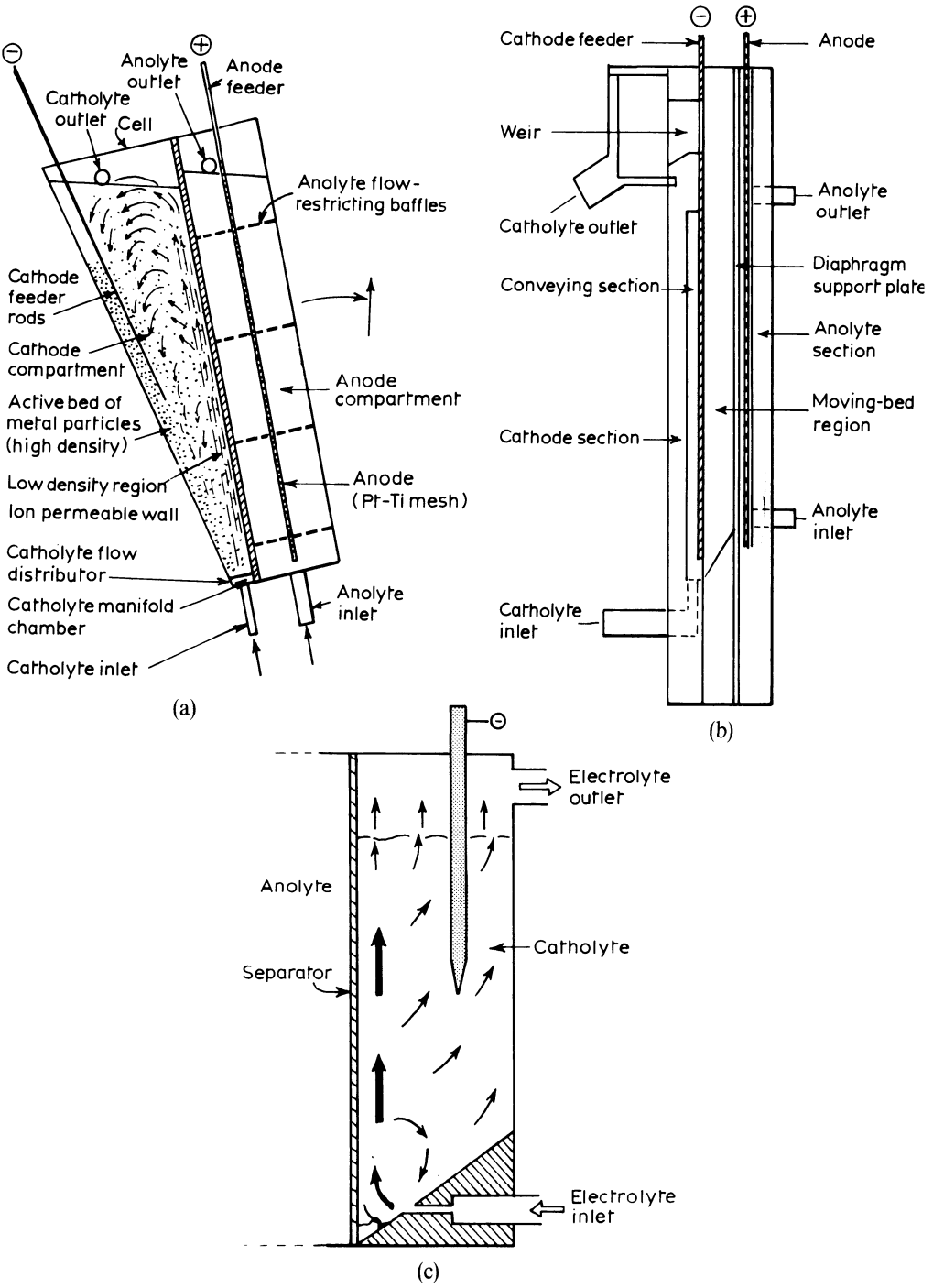

Fig. 2.37 Dynamic, particulate-bed electrodes. (a) The inclined two-phase Parel fluidized-bed electrode reactor. (b) The moving-bed electrode in a rectangular configuration. (c) The spouting-bed electrode, showing the circulation of a light, rapidly ascending, and a dense, slowly descending, solid phase.

Research b.v. who have further developed the reactor for extraction and reclamation of metals. This reactor has a geometry which resembles a shell-and-tube heat exchanger. Possible advantages over previous fluidized-bed reactors might include:

1. Rounded corners and smoothed surfaces together with improved flow distribution help to provide uniform fluidization without particle agglomeration.
2. The geometry facilitates a relatively uniform potential, and current, distribution, due to the number and placement of cathode feeders.
3. Problems of membrane damage are precluded by the use of cylindrical ceramic diaphragms.

Many variants of fluidized or moving-bed electrodes have been proposed and operated at pilot or small commercial plant level. Such reactors have largely attempted to reduce the problems of bed agglomeration, poor bed–feeder contact and feeder deposition by controlling the dynamics of the mobile electrode phase. Several such cases are shown in Fig. 2.37, while Chapter 7 provides further examples.

2.8 LABORATORY DATA AND SCALE-UP

The successful commercialization of an electrochemical reaction depends upon a sufficient knowledge of the process gained at the laboratory bench and in a pilot plant. This is particularly true with a new electrochemical process. In general, a critical amount of data will be required in order to:

1. Choose the type and size of the reactor.
2. Integrate the reactor into the overall process.
3. Predict the needs for a satisfactory scale-up.
4. Provide the basis for modifying an existing process to suit another feedstock or a different operating point (which may be dictated by a change in overall production needs or else by economic constraints). In such cases, a working reactor may be scaled down to a convenient laboratory pilot-plant scale.

The number of reactor sizes used in a development programme and the range of operational parameters studied (and, hence, the number of experiments on each reactor) will depend on the nature of the process together with economic, time and personnel constraints. The general compromise exists that a scale-up using a few, large steps may allow a rapid development. However, failure to provide a sufficient range of data at a number of intermediate reactor stages may result in unwanted surprises (or even shocks).

In some cases, a certain amount of data may be available from the literature or experience but the majority of development work will start at a small laboratory scale, in order to check existing information or to extend its scope.

The use of a small laboratory cell for early studies is attractive for several reasons:

1. Low capital and running costs.
2. Speed and convenience in changing experimental parameters.
3. Few supply and disposal costs for cell components, electrolytes, reactants and products.
4. The cell requires minimal space.
5. Parametric control is facilitated, e.g. temperature, pH, stirring rates, etc.
6. Routine laboratory equipment may be used, e.g. power supplies, glassware, stirrer hotplates, thermostat baths, etc.
7. An electrolyte pump may be avoided.

While the type of laboratory cell will depend very much on the precise circumstances, we will consider a glass 'H' cell (Fig. 2.38). This type of cell is useful for several experiments (although the relatively large interelectrode gap may result in high value of iR_{CELL}):

1. It may be used to examine the current density vs. overpotential characteristics of an electrode.
2. Parametric studies are possible by systematically changing, for example, temperature, pH, electrolyte composition, electrode materials, separators, etc.

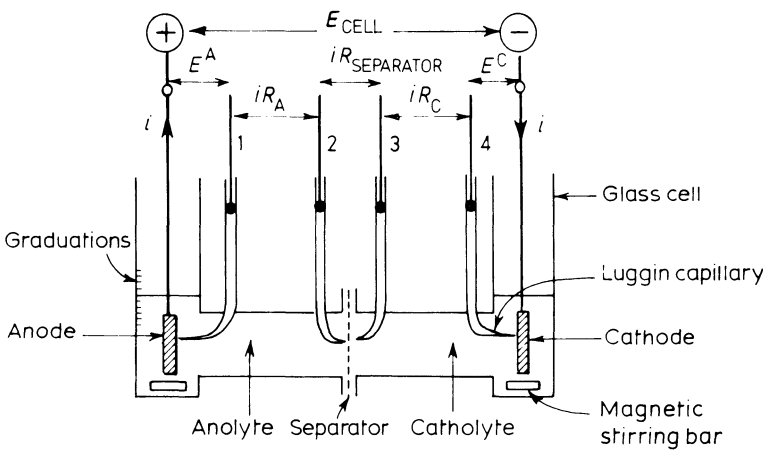

Fig. 2.38 Schematic laboratory cell used to analyse the components of cell voltage. 1, 2, 3 and 4 are identical reference electrodes. Operation may be galvanostatic (i.e. constant current i) or potentiostatic, i.e. constant cathode- or anode-potential E^C or E^A. For simplicity, facilities such as temperature measurement and control, sampling points, nitrogen gas inlet and outlet, etc. are not shown.

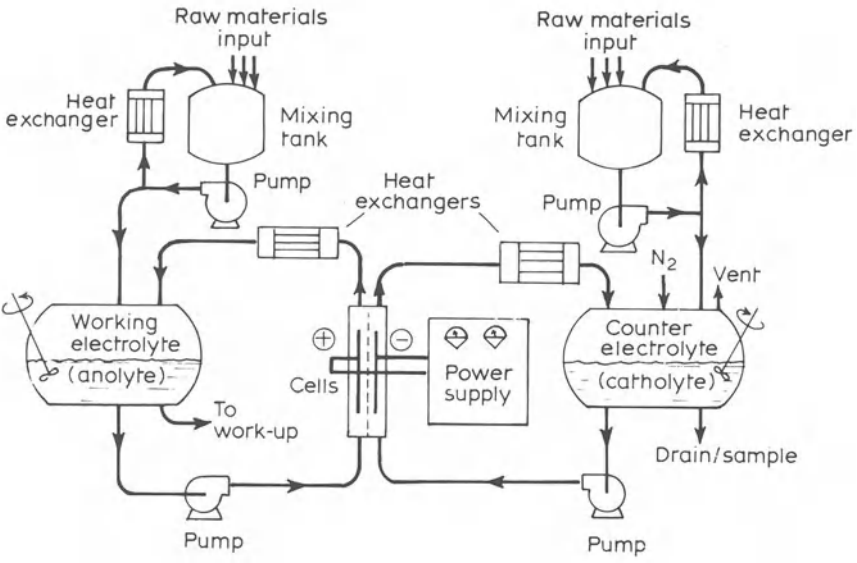

(a)

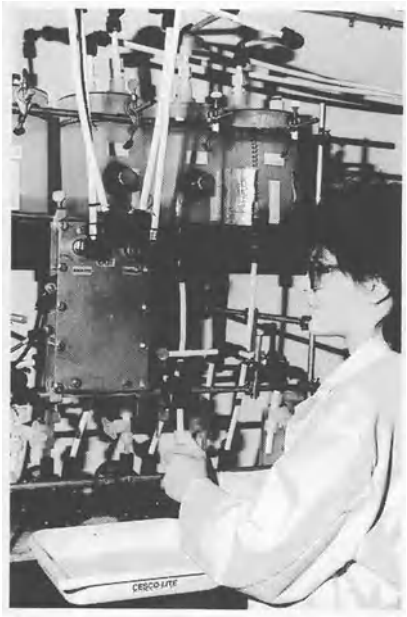

(b)

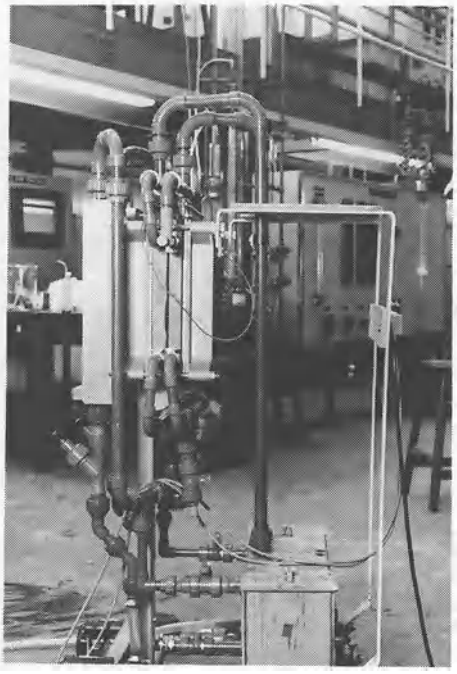

(c)

Fig. 2.39 Typical laboratory pilot-scale facilities using divided, parallel-plate cells. (a) The major components of a flow system for anodic electrosynthesis. (*After*: Reilly Tar and Chemical Corp.) (see also Fig. 6.7) (b) A small laboratory pilot facility based on the MP ElectroCell. Here, an electrodialysis process is being performed. The facility is also used for electrosynthesis by means of simple modification of the cell components and process streams. (Courtesy: Electrosynthesis Co., Inc.). (c) A DEM cell for synthesis. (Courtesy: Electricity Council Research Centre and University of Strathclyde.)

3. The voltage components of the cell may be determined.
4. The influence of stirring may be (qualitatively) established. More precise studies might then utilize a rotating disc (or cylinder) electrode.
5. It may be treated as a simple batch reactor to produce small amounts of product, in order to establish preliminary figures of merit.

Such a laboratory cell might typically involve an electrode area of 1–10 cm^2 and a current of 0.1–1 A. Following definition of a reasonable range of operating conditions, the process may then be scaled-up to a laboratory pilot plant. We will consider the common case of a parallel plate geometry, which might involve a unit cell (i.e. one cathode, one anode, one separator if required) which may be designed with a further scale-up in mind, e.g. it might easily be expanded by the addition of further elements into a filterpress arrangement. This reactor might involve a single electrode size of 100–1000 cm^2 and a current of 10–100 A. This scale usually involves: (1) flow circuits for the anolyte and catholyte; (2) a heat exchanger to stabilize temperature; and (3) facilities for product removal and recovery and perhaps the continuous or semicontinuous addition of reagents (Fig. 2.39). This type of reactor can be used to establish:

1. Long-term stability of the cell components and the reactor integrity.
2. Mass and heat balances.
3. Optimum flow conditions, in terms of volumetric flow rate and suitable turbulence promoters in the cell.
4. Larger amounts of product for quality-assurance tests.
5. Figures of merit over a range of experimental parameters.
6. Reasonable methods of product extraction and work-up.
7. Pressure drops over the reactor (and, hence, pumping costs).
8. Cell voltage components under realistic conditions.

Expansion of such a laboratory pilot cell to several plates in a filterpress arrangement may be used to check bipolar operation or the use of internal manifolds.

In common with all chemical process engineering, the reactor is only one (key) component in a process plant. This is illustrated in Fig. 2.40 which shows an example of an integrated laboratory pilot plant for electrosynthesis at the laboratory bench scale (Fig. 2.40).

Further scale-up may involve a quarter-, half- or full-size pilot plant with a total electrode area of perhaps 10 m^2 and currents up to 10 kA. Following suitable testing, this scale may already prove adequate as an operational plant. Indeed, it should be realized that the size of commercial reactors is extremely diverse: a precious-metal or high-cost pharmaceutical process may operate at only 1–100 A, while large cell rooms for synthesis of bulk chemicals or electrowinning may involve currents up to 500 kA.

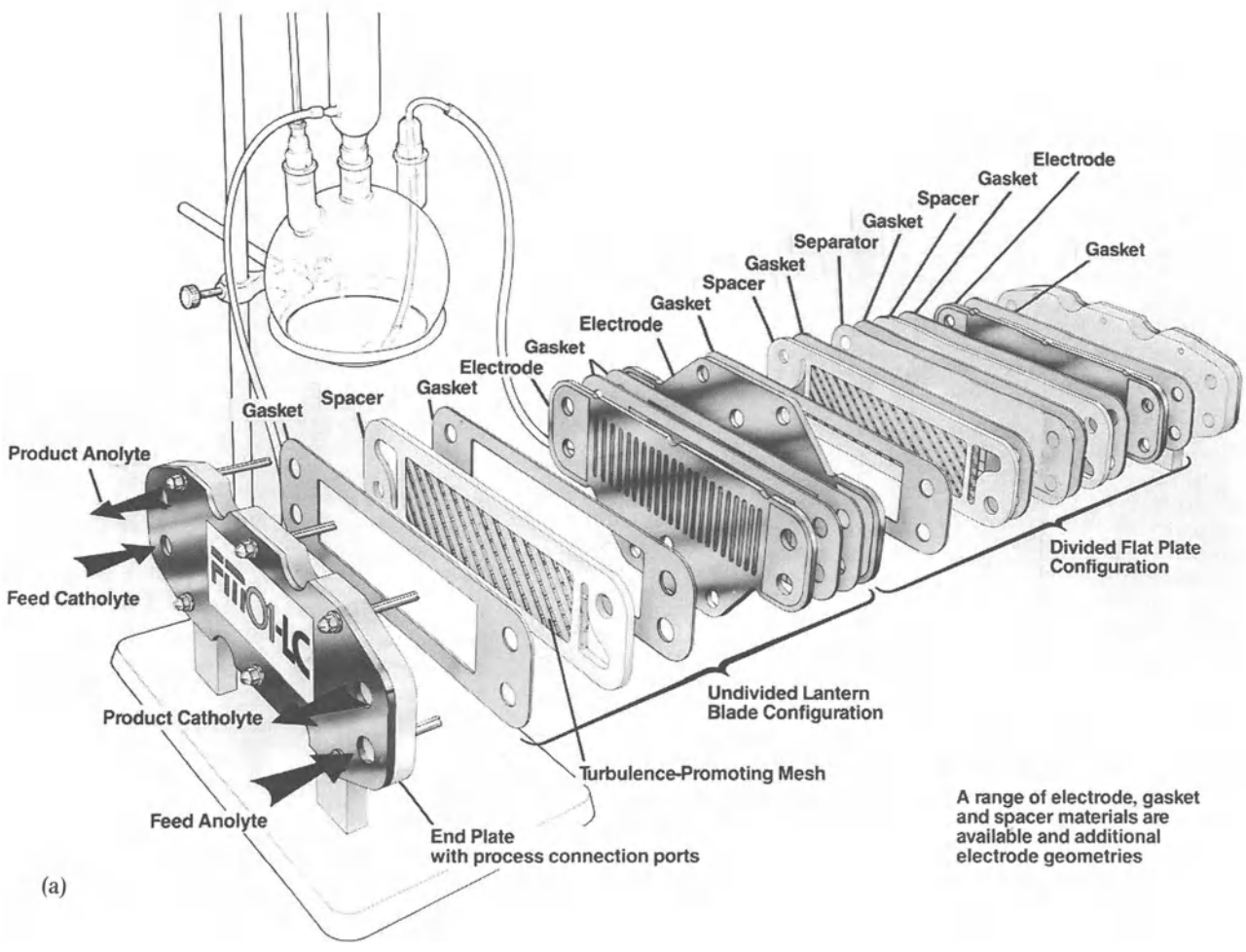
Electrode
Gasket
Spacer
Gasket
Separator
Gasket
Spacer
Gasket
Electrode
Gasket
Electrode
Gasket
Spacer
Gasket
Gasket
Product Anolyte
Feed Catholyte
Product Catholyte
Feed Anolyte
FM01-LC
Divided Flat Plate Configuration
Undivided Lantern Blade Configuration
Turbulence-Promoting Mesh
End Plate with process connection ports
A range of electrode, gasket and spacer materials are available and additional electrode geometries
(a)

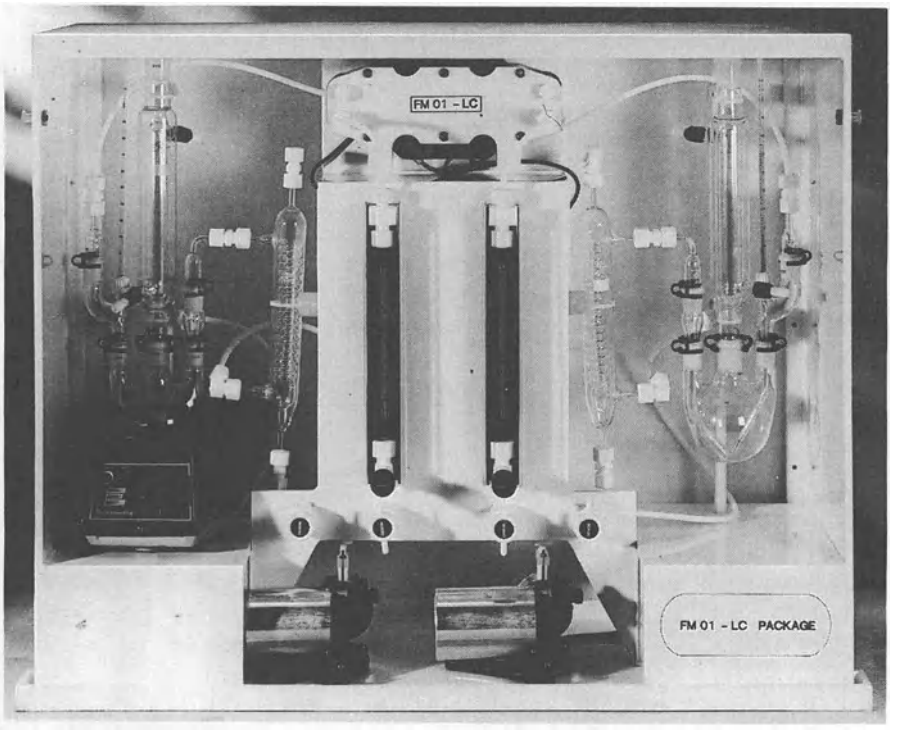

(b)

Fig. 2.40 An example of an integrated package for electrosynthesis in the laboratory. (a) Exploded view of the FM01-LC reactor. The cell is of monopolar construction and is configured in the filterpress arrangement, with internal manifolding of the feed and product streams. In the undivided configuration, the interelectrode gap may be as low as 1 mm. Other electrode types and cell arrangements are possible. Each electrode has a projected area of *c.* 0.0064 m^2, on each face. (b) A laboratory package utilizing the above electrolyser. Facilities are provided for heating/cooling and control of the anolyte and catholyte flows. Temperature measurement is also provided. All non-electrolyser components in contact with the electrolyte streams are manufactured in glass or fluorocarbons such as PTFE. (Photograph, courtesy: ICI Chemicals and Polymers Ltd.)

FURTHER READING

1 O. Levenspiel (1972) *Chemical Reaction Engineering*, 2nd Edition, Wiley, New York.
2 D. J. Pickett (1979) *Electrochemical Reactor Design*, 2nd Edition, Elsevier, Amsterdam.
3 J. S. Newman (1973) *Electrochemical Systems*, Prentice-Hall, Englewood Cliffs, N.J.

4 C. L. Mantell (1960) *Electrochemical Engineering*, 4th Edition, McGraw-Hill, New York.
5 A. Schmidt (1976) *Angewandte Elektrochemie*, Verlag Chemie, Weinheim.
6 F. Beck (1974) *Elektroorganische Chemie*, Verlag Chemie, Weinheim.
7 P. Gallone (1973) *Trattato di Ingegneria Electrochimica*, Jamburini, Milan.
8 J. O'M. Bockris, B. E. Conway, E. Yeager and R. E. White (Eds) (1981) *Comprehensive Treatise of Electrochemistry*, Vol. 2, Electrochemical Processing, Plenum Press, New York.
9 E. Heitz and G. Kreysa (1977) *Grundlagen der Technischen Elektrochemie*, Verlag Chemie, Weinheim.
10 E. Heitz and G. Kreysa (1986) *Principles of Electrochemical Engineering*, VCH Publishers, Weinheim.
11 T. Z. Fahidy (1985) *Principles of Electrochemical Reactor Analysis*, Elsevier, Amsterdam.
12 F. Coeuret and A. Storck (1984) *Eléments de Génie Électrochimique*, Tecdoc, Paris.
13 Tutorial Lectures in Electrochemical Engineering and Technology, AIChE Symposium Series **204** (1981) and **229** (1983).
14 R. J. Marshall and F. C. Walsh (1985) 'A Review of Some Recent Electrolytic Cell Designs', *Surface Technol.*, **24**, 45.
15 G. Kreysa (1985) 'Performance Criteria and Nomenclature in Electrochemical Engineering', *J. Appl. Electrochem.* **15**, 175.
16 I. Rousar, K. Micka and A. Kimla (1986) *Electrochemical Engineering*, Vols 1 and 2, Elsevier, Amsterdam.

3 The chlor-alkali industry

The electrolysis of aqueous sodium chloride, normally brine obtained directly from natural salt deposits, to yield chlorine, sodium hydroxide and hydrogen is the largest of the electrolytic industries. In 1986, the world's annual production of chlorine was a little under 3.5×10^7 ton. The USA was the largest producer at 10.4 million ton, followed by Western Europe (9.5 million ton), and Japan (3 million ton).

The electrode reactions are, at the anode:

$$2Cl^- - 2e^- \longrightarrow Cl_2 \tag{3.1}$$

and at the cathode either, directly:

$$2H_2O + 2e^- \longrightarrow H_2 + 2OH^- \tag{3.2}$$

or indirectly as in a mercury cell where the cathode reaction is:

$$Na^+ + e^- + Hg \longrightarrow NaHg \tag{3.3}$$

and the sodium amalgam is decomposed in a separate reactor to give the desired products:

$$2NaHg + 2H_2O \longrightarrow 2Hg + 2Na^+ + 2OH^- + H_2 \tag{3.4}$$

Both chlorine and sodium hydroxide (normally traded as a 50%w/v aqueous solution) must be considered to be main products; the one in greater demand varies with time. Their major uses are summarized in Table 3.1. The hydrogen is also used, where possible, as a chemical (e.g. for the hydrogenation of fats), otherwise as a fuel (e.g. at the power station which is inevitably on site at any large chlor-alkali facility).

The chlor-alkali industry should be particularly interesting to the student of electrochemical technology. Firstly, it is by any standards, a process carried out on a very large scale and at many sites and it is central to the chemical industry as a whole. In addition, three different electrolytic technologies based on mercury, diaphragm and membrane cells are all currently used. Moreover,

although it is a mature industry – the first electrolytic cells having been introduced in the 1890s – the last 25 years have seen extensive and notable advances in the technology resulting both from scientific innovation and the economic and social pressure for energy conservation, pollution control and higher safety standards. In consequence, we shall see that membrane-cell technology, almost unknown in 1970, has advanced to the point where it is increasingly considered superior in performance. In 1987, it was responsible for about 10% of the total world production and by the year 2000, it is expected to be the dominant, and perhaps the only, technology within the chlor-alkali industry.

The majority of the chlorine produced is used internally within the chemical industry for the manufacture of polyvinyl chloride, chlorinated hydrocarbons, propylene oxide, etc. (Table 3.1). Hence, it is common to find chlor-alkali plants as part of very large, integrated chemical complexes and the capacity of such plants may be 0.5×10^6 tons Cl_2/year. On the other hand, concern about the transport and storage of liquid chlorine has led to a different trend towards smaller plants sited close to the user. This is particularly attractive when there is an almost balanced requirement for both chlorine and sodium hydroxide, e.g. in pulp and paper mills (Table 3.1). A typical plant in this application may have a capacity of 10^4 tons Cl_2/year. On an even smaller scale, the same concerns lead to a need for plants, for example, to provide Cl_2 to prevent biological growth on

Table 3.1 Major uses of chlorine and sodium hydroxide*

Chlorine:
Manufacture of polyvinylchloride (20)
Preparation of chlorinated organic solvents, e.g. methylene chloride, chloroform, carbon tetrachloride, *per-* and *tri*-chloroethylene, 1,1,1-*tri*-chloroethane (26)
Preparation of propylene oxide (8)
Synthesis of other organic compounds, e.g. chlorobenzenes, alkyl chlorides (particularly methyl chloride for lead alkyls), herbicides (7)
Preparation of fluorocarbons (4)
Pulp and paper manufacture (14)
Preparation of inorganic compounds, e.g. sodium hypochlorite, titanium tetrachloride, iodine chlorides (12)
Water treatment (4)
Sodium hydroxide (Caustic soda):
Synthesis of many organic compounds (38)
Manufacture of textiles and rayon (5)
Soap and detergent production (5)
Oil refining (5)
Paper and pump manufacture (20)
Aluminium extraction (4)
Manufacture of inorganic compounds, e.g. sodium cyanide, sodium salts (11)

* Figures in brackets are percentages of US production (taken from E. Spore and B. V. Tilak (1987)) *J. Electrochem. Soc.*, **134**, 179c.

water-intake pipes at power stations or to service a single swimming pool (0.1–10 tons Cl_2/year). Clearly, there is great diversity in the size of plant demanded by customers. The markets may be met either by purpose-built units for each application or using a modular concept where cell units can be built together to give the required capacity. Both approaches have been used. In this chapter, however, emphasis is placed on the discussion of the larger-scale plants.

3.1 GENERAL CONCEPTS OF BRINE ELECTROLYSIS

A discussion of the electrolytic production of chlorine and sodium hydroxide requires an understanding of the very large scale of the industry. The annual world production of chlorine was noted above as 3.5×10^7 tons. It is difficult to comprehend the enormity of this scale but it can be put into different terms, e.g. this chlorine production rate requires some 2 km^2 (or almost a square mile) of anode and the consumption of 10^8 MWh of electricity (say 1–2% of the electricity generated or the output of more than ten very large power stations). Even in the absence of a discussion of the economics of the process, it can be seen that we are dealing with an energy-intensive process requiring many cell units. Therefore, we shall be looking for:

1. Simple and cheap cell design.
2. High current densities to minimize capital investment in plant.
3. Cell components which are reliable, readily available and have a long lifetime, so as to minimize downtime.
4. Good current efficiency and material yields for both the anode and cathode reactions. Parasitic reactions not only lower the energy consumption and increase the use of materials but also lead to impurities in the products.
5. Low power consumption (kWh ton^{-1}). This is determined by the current efficiency and the cell voltage. The latter was discussed in Chapter 2 and it was shown that the cell voltage is made up of a number of terms, i.e.:

$$E_{CELL} = E_e^C - E_e^A - |\eta_A| - |\eta_C| - iR_{CELL} - iR_{CIRCUIT} \tag{3.5}$$

and good energy efficiency will be obtained only if attention is paid to minimizing each component voltage.

Table 3.2 lists the equilibrium potentials for the four electrode reactions which must be considered in brine electrolysis. The data are given for 25% brine and at pH values important to an understanding of the chemistry of a chlor-alkali cell. Even so, the data do not correspond to the exact conditions of industrial cells, since activity coefficients have been assumed to be 1 and the values are presented for room temperature and pressure. In fact, slightly elevated temperatures and pressures, 60–95°C and 1–10 atm. respectively would be more normal. But the equilibrium potentials in Table 3.2 form a sensible basis for discussing the cell chemistry.

Chloride ion is usually oxidized in a slightly acid solution to prevent hydrolysis of the chlorine to hypochlorite and also to minimize the oxygen evolved in competing water oxidation at the anode. The pH at the cathode in a diaphragm and membrane cell will be about 14 as the electrode reaction generates hydroxide. Two factors emerge immediately:

1. In a mercury cell, where the electrode reactions are A and D in Table 3.2, the term $(E_e^C - E_e^A)$ of equation (3.5) is -3.16 V, a value much larger than the corresponding minimum cell voltage for a diaphragm or membrane cell, -2.15 V, where the electrode reactions are A and C(ii). Hence, a mercury cell is only competitive because some other terms in equation (3.5) are favourable, e.g. a mercury cell does not require a separator between the electrodes and, hence, R_{CELL} is lower.
2. The potential advantage of a membrane cell with an oxygen cathode, i.e. a cell where the reactions are A and B(ii), can readily be seen. The equilibrium cell voltage is reduced to -0.92 V.

It can also be seen that kinetics play an important role in a chlor-alkali cell. A mercury cell is only possible because the hydrogen evolution overpotential is very large at both mercury and sodium amalgam. Table 3.2 shows that reaction C(i) is thermodynamically more favourable than reaction D by 1.6 V, yet the formation of sodium amalgam occurs without significant hydrogen evolution. At the anode, in all cells, it is necessary to form chlorine with a very low oxygen content; yet, again, in Table 3.2 it can be seen that thermodynamics indicates that reaction B(i) and not A is the preferred reaction. Hence, it is necessary to seek electrode materials where the overpotential for the desired reaction is low but, in addition, the selected material must also have a high overpotential for possible competing reactions. We shall see in section 3.2 that the development in anode and cathode materials has contributed much to the changes in the chlor-alkali industry over recent years.

Table 3.2 Equilibrium potentials for the electrode reactions occurring in chlor-alkali cells. The values are given for the pH met in such cells and are calculated assuming 25% brine, that all activity coefficients are 1 and gases are at atmospheric pressure (temperature 298 K)

Reaction	pH	E_e/V vs. *NHE*
A $2Cl^- - 2e^- \rightleftharpoons Cl_2$	4	+1.31
B (i) $2H_2O - 4e^- \rightleftharpoons O_2 + 4H^+$	4	+0.99
(ii) $O_2 + 2H_2O + 4e^- \rightleftharpoons 4OH^-$	14	+0.39
C (i) $2H^+ + 2e^- \rightleftharpoons H_2$	4	−0.24
(ii) $2H_2O + 2e^- \rightleftharpoons H_2 + 2OH^-$	14	−0.84
D $Na^+ + Hg + e^- \rightleftharpoons NaHg$	4	−1.85

Equation (3.5) also shows that in order to reduce energy consumption, the iR terms should be minimized. This can partly be achieved by the development of components, e.g. membranes with low resistance and electrode materials without significant resistance and designed to minimize gas bubbles in the interelectrode gap. In addition, the energy consumption can be reduced by decreasing the interelectrode gap and this has led to the so-called 'zero gap technology'.

An understanding of the developments within the chlor-alkali industry clearly depends on being aware of the new electrode materials and separators which have been developed specifically for this industry. Hence, the section 3.2 is devoted to cell components.

The last few pages have very much stressed the importance of energy consumption in the chlor-alkali industry. This is appropriate but it is perhaps important to remind ourselves that other factors, particularly purity of the products, environmental factors and ease of management of the cell house, are probably equally important.

3.2 MODERN TECHNOLOGICAL DEVELOPMENTS

3.2.1 Electrode materials

With the exception of the cathode in a mercury cell, there is freedom to select the anode and cathode materials according to performance. The two requirements are:

1. An anode material which evolves chlorine at low overpotential while not supporting the oxidation of water to oxygen, the latter being the thermodynamically preferred reaction.
2. A cathode which evolves hydrogen at low overpotential in alkaline solution.

It should be noted, however, that the operating environments for the electrodes are not identical in the three technologies, e.g. in a diaphragm cell the anode operates in a more alkaline medium (due to diffusion of hydroxide from cathode to anode) than in membrane or mercury cells. Also, it is only in a diaphragm cell that the cathode sees significant chloride ion in solution and this can increase corrosion problems, particularly when the cell is open-circuited. These particular difficulties will be discussed in section 3.3.2.

The general concepts of electrocatalysis and the H_2 evolution reactions were discussed in some detail in Chapter 1. Here, we should notice the similarity in the chlorine and hydrogen evolution reactions. Both involve the electrode reaction of an ion in solution to give a product which is dimeric and a gas. Hence, the mechanisms which should be considered will be similar, and it is to be expected that a critical property is the strength of adsorption of hydrogen or chlorine atoms on the surface of the electrode material.

Where surface intermediates are important, the apparent current density will depend on the real surface area (i.e. the roughness of the electrode surface) and

some of the catalysis observed with many materials may be due partly to a very high surface area. Other properties, particularly stability, are essential in a potential electrode material, since a chlor-alkali cell will be expected to run for months or even years without extensive renovation or replacement of components. Moreover, the availability of the electrode material in diverse forms is helpful to innovative cell design, e.g. since mercury is a liquid, the designs of cell are restricted; in contrast, titanium can be machined into many forms broadening the shapes, sizes and form of electrodes which may be used. Hence, it is helpful if either the electrode material can be machined or worked readily, or can be coated readily onto a convenient base metal such as steel, nickel or titanium.

Throughout most of the history of the chlor-alkali industry, the anode material has been graphite or some related form of carbon. The overpotential for Cl_2 evolution was as high as 500 mV and the wear rate 2–3 kg of anode carbon per ton chlorine. The high rate of anode loss predetermined the design of cell and also the management of the cell house; it was essential that anodes could be replaced easily. In an attempt to improve the anode performance, precious-metal-coated anodes (e.g. Pt on Ti) were first developed and, indeed, they did reduce the anode overpotential to about 100 mV. Such anodes are, however, expensive and not entirely stable; platinum in concentrated chloride medium is lost at a rate of 0.2–0.4 g per ton of chlorine. Hence, it was the development in the early 1960s of materials which have become known as dimensionally stable anodes (DSAs)* which has led to the change from carbon to metal anodes; DSAs are now a family of coatings which are applied to titanium and their name arises because they are inert and very stable to corrosion and their service life can be many years. In addition, they are excellent catalysts for chlorine evolution, the overpotential commonly being < 50 mV. The coatings are based on ruthenium dioxide but they may also contain valve metal, precious metal or transition metal oxides to improve performance. Generally they are prepared by spraying a mixture of chlorides in an alcohol, commonly isopropanol, and then heating in air. Many different coating compositions of DSA have been developed, e.g. for mercury cells an intermediate TiO_2 layer is used to reduce damage from shorting when the Hg and anode occasionally come into contact, while special coatings to minimize the O_2 content of the Cl_2 are also available. In fact, the requirements for low Cl_2 overpotential and high O_2 overpotential are not particularly difficult to meet and, largely for reasons associated with patent rights, other companies have developed anode coatings, e.g. those based on PdO_2 and the spinels, $M_xCo_{3-x}O_4$ $(0<x<1,\ M=Cu, Mg, Zn)$. The more difficult requirements concern anode lifetime in operating conditions, although the O_2 content of the Cl is also important (some low percentage of O_2 is always observed). It is in these areas that the materials may differ in performance and

* DSA is a registered trademark of Diamond Shamrock Technologies S. A. but has become used by the scientific community as a term which includes a wide range of very corrosion-resistant anode coatings.

are the key targets during development programmes. All these anode coatings must be used in carefully controlled conditions since, for example, decreasing temperature or sulphate in solution can increase oxygen evolution markedly.

The almost universal replacement of carbon by metal anodes has led, by itself, to a reduction of the energy consumption by 10–15% (the cell voltage is changed by 0.45 V in −2.5 to −5 V). But, in addition, the chlor-alkali industry has benefited because anode replacement is no longer an important factor in the way the cell house is run and because the titanium to be coated may be fabricated in many forms. This has helped to revolutionize cell design.

The cathode in diaphragm cells was traditionally mild steel, which was very stable to corrosion but gave rise to an overpotential of 300–500 mV. It is only since the increase in energy costs following the oil crisis of 1973 that much consideration has been given to better catalysts. A number of high area nickel alloy coatings have been described but none has been totally successful in diaphragm cells. In membrane cells, the design of catalysts is easier both because of the absence of chloride in solution and the way the cathode is used (it is not coated with asbestos which must periodically be replaced). Hence, precious-metal coatings on a nickel base and high area nickel coatings are both available and overpotentials may be as low as 50 mV. Again, this represents a further 10% energy saving.

In addition to the material of the electrode, its physical structure can also be important. At electrodes where gas is evolved, the design must permit rapid bubble release, otherwise the bubbles will contribute an additional iR loss. Hence, it is common to employ expanded metal or plates with louvres (Fig. 3.1) to release gas in the desired direction. The design of such structures, however, must ensure that there is no iR drop in the electrode itself and this may require the inclusion of additional current-carrying bars (Fig. 3.1).

3.2.2 Membranes

The perfect separator in a chlor-alkali cell would:

1. pass sodium ions (but no protons) from anolyte to catholyte without the co-transport of chloride ion (leads to Cl^- contamination of the NaOH) or hydroxide ion from catholyte to anolyte (causes loss of NaOH and O_2 contamination of the Cl_2).
2. have a low resistance.
3. be stable to wet chlorine and 50% sodium hydroxide over a long period of time.

Moreover, these properties should be maintained even when the catholyte is 50% sodium hydroxide as ideally it would be when leaving the cell.

A diaphragm is porous and cannot discriminate between species. All will diffuse through its pores where there is a concentration difference. Hence, equal amounts of Na^+ and Cl^- diffuse through a diaphragm from anolyte to catholyte

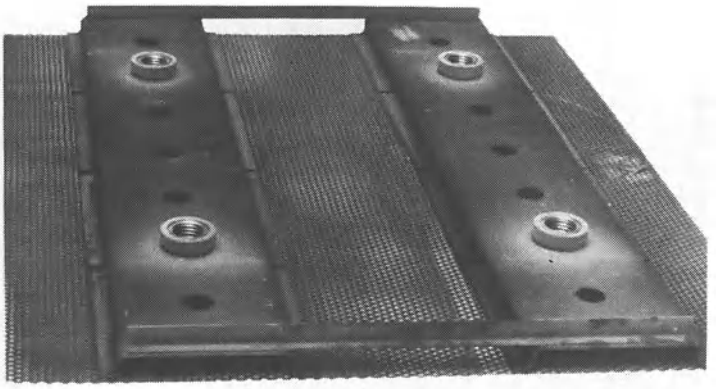

(a)

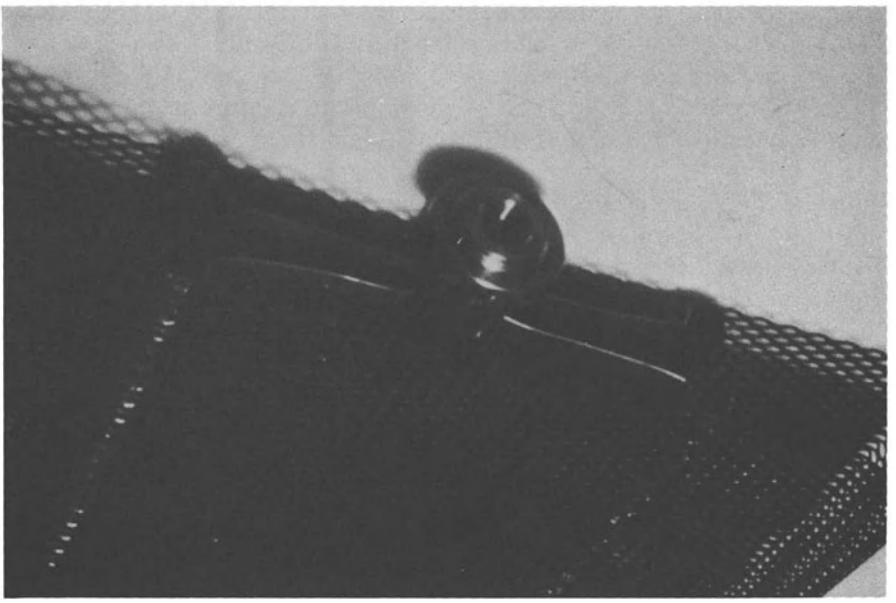

(b)

Fig. 3.1 Modern anodes for chlorine cells. (a) Horizontal dimensionally stable anodes for a mercury cell. (b) Vertical dimensionally stable anode for a diaphragm cell. (Courtesy: OxyTech Systems, Inc.)

in a diaphragm cell and the caustic soda produced must therefore be contaminated heavily with chloride ion. Also, the catholyte leaving the cell cannot contain more than 10% sodium hydroxide since otherwise hydroxide-ion diffusion to the anode becomes significant and oxygen as well as chlorine is evolved. Thus, prior to sale, the sodium hydroxide produced in a diaphragm cell must be concentrated by evaporation to a 50% solution.

On the other hand, cation exchange membranes are theoretically capable of meeting all the criteria set out above. It is, however, only in the last 20 years that membranes with properties approaching those required have become available and they have been the basis for the development of membrane cell technology in general. The chemical stability is obtained by manufacturing the membranes from perfluorinated polymers while the ionic conductivity results from using monomers with side chains with terminal acid groups. The polymers have been shown to have a structure with hydrocarbon-like zones and the acid groups collect together so as to form channels through which cations can pass. The cation selectivity may arise from the size of these channels. Two basic types of membrane were developed, based on strong-acid and weak-acid functions and typical structures are shown in Fig. 3.2. Their physical and chemical properties are compared in Table 3.3. In many respects, the strong acid membranes have superior properties. The key drawback is, however, their inability to permit the production of high caustic soda concentrations ($> 15\%$). This results from back-diffusion of sodium hydroxide through the membrane from catholyte to anolyte when the catholyte is very concentrated sodium hydroxide, a property arising because of the high water content of this hydrophilic polymer. In contrast, the weak acid membrane allowed the direct production of 30–40% caustic soda without significant loss of current efficiency. But these membranes have a rather high resistance, particularly if they are in contact with an acidic solution so that the carboxylate groups become protonated. Hence, it is not possible to use an acidified anolyte with the weak acid membranes and this leads to an increase in oxygen evolution (and, hence, O_2 contamination of the Cl_2) as well as reducing the lifetime of anode coatings. Clearly, with either type of polymer, the electrical

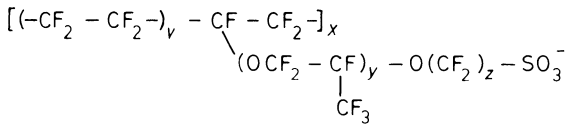

$v = 5\text{-}15 \quad x = 1000, \quad y = 1\text{-}3 \quad z = 1\text{-}4$

(a)

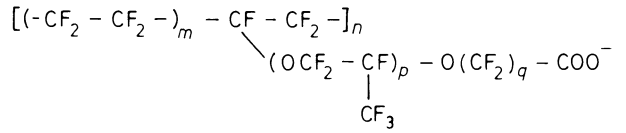

$m = 6\text{-}8, \quad n = 700, \quad p = 0\text{-}1, \quad q = 1\text{-}5$

(b)

Fig. 3.2 Structures of typical perfluorinated polymers used for ion-permeable membranes in the chlor-alkali process. (a) Strong acid. (b) Weak acid membranes.

Table 3.3 Comparison of membrane properties of importance in the chlor-alkali process

	Strong Acid Membrane	Weak Acid Membrane
Ion-exchange group	$-SO_3H$	$-COOH$
pK_A	<1	3
Water content	High	Low
Current efficiency at high NaOH concentration	Low	High
Electrical conductivity	High	Low
Maximum current density	High	Low
Chemical stability	Very good	Good

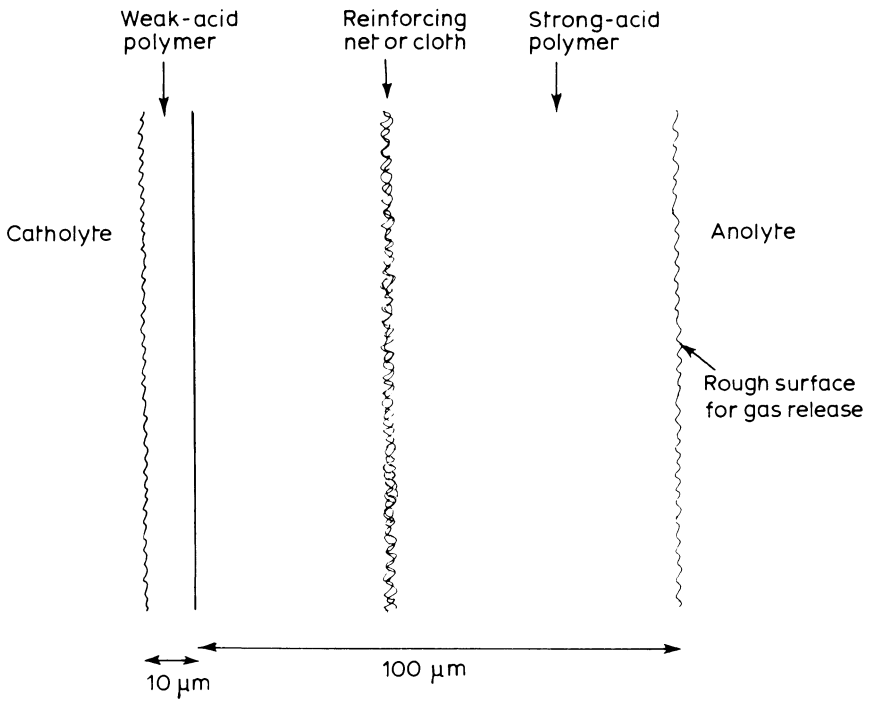

Fig. 3.3 Modern bilayer membrane for the chlor-alkali process.

resistance is minimized by manufacturing the membrane as a very thin sheet (*c.* 0.1 mm) and in order to impart physical strength, the membranes are reinforced with fine plastic nets.

Neither the weak- nor strong-acid membranes had all the properties desired by the industry. Hence, further development work was carried out and led to the bilayer membranes (Fig. 3.3) where a strong acid membrane is coated on the

catholyte side with a thin layer of weak-acid membrane. This combination gives a good sodium ion conductivity, only strong-acid membrane is exposed to the anolyte so that acid may be added to the anolyte, while the weak-acid layer imparts a barrier to sodium hydroxide transport from catholyte to anolyte. Several American and Japanese companies now market such bilayer membranes and they permit the production of 30–40% sodium hydroxide and low O_2 content Cl_2 with good current efficiency (section 3.3.3). The bilayer membranes are produced by several techniques including lamination, grafting and chemical conversion of some of the sulphonic acid groups to carboxylate groups. This latter technique is probably to be preferred since it allows good control of the gradient of the change in chemical composition. A further sophistication now introduced is surface roughening and/or modification to allow ready gas release from the membrane in a zero gap configuration.

As with the electrode coatings, the membranes only operate to specification under tightly controlled conditions. In particular, the brine and catholyte feeds must be highly purified. Sulphate and group II metals lead to precipitation within the membrane while heavy metals (and iron from corrosion) complex the carboxylate groups and cause an increase in membrane resistance.

3.2.3 Engineering and control equipment

As in all chemical engineering, a major trend has been towards the complete utilization of all raw materials and energy and, for example, all heat from exothermic reactions or Joule heating is used elsewhere in the plant. Moreover, the plants have had to change in order to comply with the legal requirement to monitor and control emissions of possible pollutants; in the chlor-alkali industry the major concerns have been mercury and chlorine itself. Normally, both the atmosphere and the effluent will be monitored for Hg and Cl_2 and the hazards have been much reduced.

Although, as noted above, the fear over the transportation and storage of chlorine has led to a trend towards many smaller, on-site plants, the majority of the chlorine and sodium hydroxide is manufactured in large plants. Here, the tendency has been to build larger plants and to intensify their operation. In particular, current densities have been increased and cellrooms have become larger. This has required the design of very heavy current rectifiers and switchgear; mercury cells operate at up to 500 kA. The cellroom will thus require equipment to operate at this rating and to rectify grid a.c. to d.c. Perhaps the first step in the modern era was the introduction of silicon rectifiers which improved the conversion efficiency from 86 to 99%; they can produce d.c. current at 240 V and it is normal to arrange the cellroom so that the centre of a series of cells is earthed. Then there is a 240 V drop on either side of the earth making the total voltage drop available in the cellroom 480 V. Subsequently, the electronics revolution has had a substantial impact on the organization and control of a chlor-alkali plant. It is now possible to measure and record on a computer, data

from each cell, flow and reactor. The aim is to detect problems as they arise and to have a measure of automatic control, e.g. of anode–cathode gaps in a mercury cell.

The computer has a second and larger control function. The optimum conditions in the cellroom are time dependent, e.g. in the UK the cost of power from the national grid is less at off-peak times, when it will be economic to run the cellroom on a high load and current density. On the other hand, the load should be reduced when power is expensive, and the computer is programmed to make these changes automatically while ensuring the desired daily production rate.

3.3 CHLORINE CELL TECHNOLOGIES

3.3.1 Mercury cells

In a mercury cell the electrode reactions are:

$$2Cl^- - 2e^- \longrightarrow Cl_2 \tag{3.6}$$

$$Na^+ + Hg + e^- \longrightarrow NaHg \tag{3.7}$$

and the sodium amalgam is hydrolysed:

$$2NaHg + 2H_2O \longrightarrow H_2 + 2Na^+ + 2OH^- + 2Hg \tag{3.8}$$

in the presence of a catalyst in a separate reactor known as the denuder. The reversible cell potential is -3.16 V and, provided the anodes are DSA, the overpotentials associated with the electrode reactions are very low. The normal cell voltage is about -4.50 V and the additional voltage is required to drive the current through the Hg–DSA gap, the electrodes and the cell connections and busbars.

A typical mercury cell is shown in Fig. 3.4. It consists of a large, shallow trough, dimensions $15 \times 2 \times 0.3$ m, with a steel base which slopes slightly from end to end so that the mercury can flow along the bottom of the cell. The coated, expanded titanium dimensionally stable anodes (DSA) (Fig. 3.1), each of approximate dimensions 30×30 cm, enter the cell from the top and are arranged parallel to the Hg surface with an anode–cathode gap of less than 1 cm. The cell will have about 250 such anodes so that most of the mercury is covered by anode; the cell approximates to a horizontal parallel-plate configuration. The brine – concentration 25% and temperature 60°C – flows through the cell and leaves at 17% either to be recycled through the salt deposit or, after treatment, to be discharged. The chlorine gas leaves the cell at the top while the sodium amalgam (approximately 0.5% sodium) leaves at the base, passes through two washing weirs to remove all the sodium chloride solution and enters the denuder.

The denuder is a cylindrical reaction vessel packed with graphite balls impregnated with a transition metal (e.g. Fe or Ni) to catalyse the amalgam

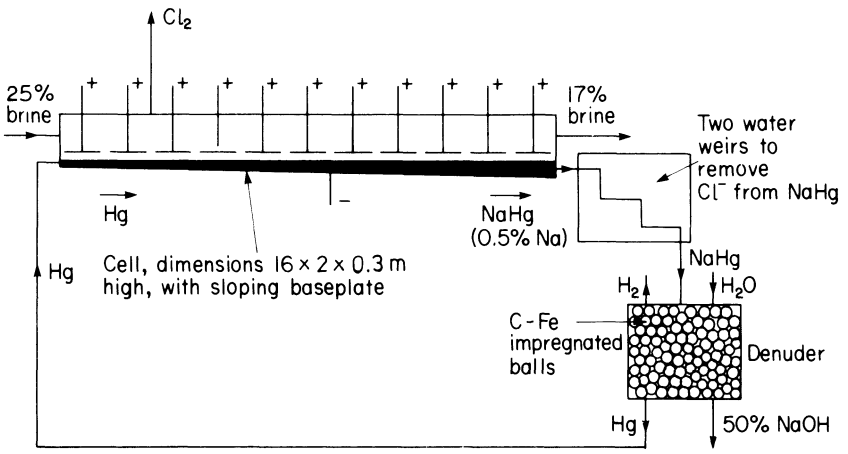

Fig. 3.4 A sketch of a mercury cell design and the coupled Hg circuit.

decomposition. The sodium amalgam and a controlled volume of pure water flow down the graphite and react. It was noted above that the sodium amalgam water reaction is kinetically hindered; on the other hand, the reaction occurs rapidly in the denuder and is highly exothermic, because the transition metal provides an alternative surface to mercury for the hydrogen evolution reaction. The reaction in the denuder thus occurs by a type of corrosion mechanism, i.e. the reactions:

$$NaHg - e^- \xrightarrow{C} Na^+ + Hg \tag{3.9}$$

$$2H_2O + 2e^- \xrightarrow[\text{metal}]{\text{transition}} H_2 + 2OH^- \tag{3.10}$$

occur on different parts of the impregnated graphite surface but at equal rates so that no net current flows. The hydrogen gas leaves from the top of the denuder, and the mercury for recirculation to the cell and the aqueous sodium hydroxide separate at the bottom. Hence, by controlling the water feed rate, it is possible to produce 50% caustic soda directly.

A typical cellroom (Fig. 3.5) consists of a large number of cells in electrical series so as to make use of the available 480 V, i.e. about 100 cells. Mercury cells operate at current density in the range 0.8–1.4 A cm^{-2} so that the total cell current will vary between 180 and 315 kA and the cellroom power requirement will be 80–160 MW. It may also be noted that such a cellroom will be somewhat larger than a soccer pitch and be capable of producing about 250 000 ton of chlorine each year.

Many of the world's major chlor-alkali companies have developed their own mercury cells and the designs will differ in the way they seek to obtain the

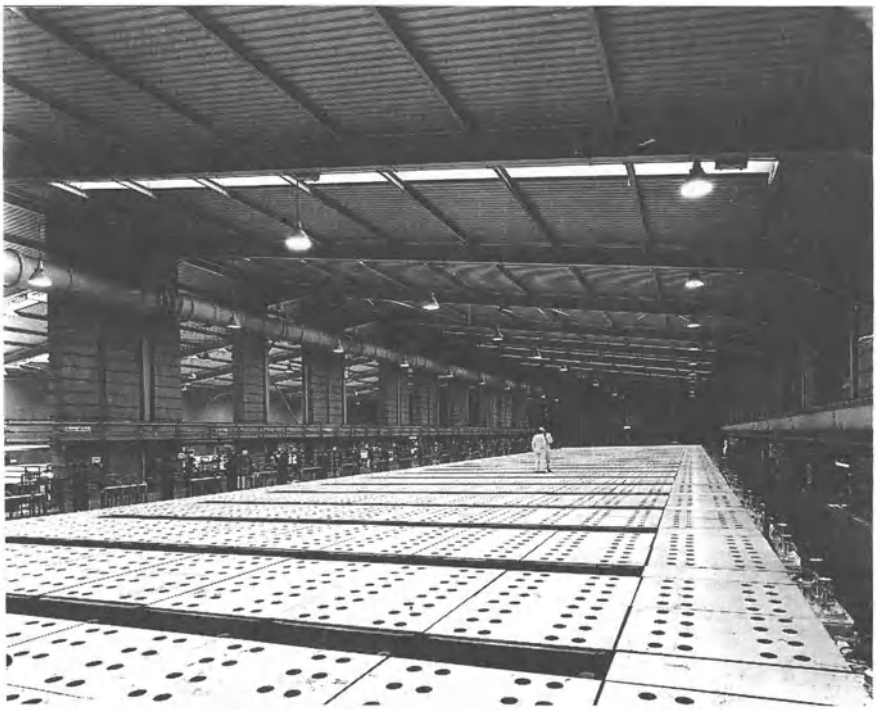

Fig. 3.5 A general view of a mercury cell room. The facility contains 106 cells, each of 25 m^2 and a current rating of 225 kA. (Courtesy: ICI Chemicals and Polymers Ltd.)

maximum electrode area and in the arrangement of the auxiliary equipment. The development of the cells during almost a century of electrolytic chlorine and caustic soda production, and the variation in the cells recently available, are described in the texts listed at the end of the chapter.

The cellroom is only part of the plant necessary for conversion of brine into chlorine and caustic soda and the complete process is shown in Fig. 3.6. Most chlor-alkali plants are sited above, or close to, a saltdome and the brine is made by pumping water through the salt deposit. The resulting solution is not, however, pure sodium chloride and, prior to electrolysis, the group II metals must be removed since they give rise to a phenomenon known as thick mercury or mercury butter, where solid amalgam is formed in the mercury leading to shorts and possible anode coating damage as well as impurities in the sodium hydroxide. The purification process is usually by precipitation of the group II metals as hydroxides by increasing the pH with sodium hydroxide although ion-exchange methods are also available. The brine is then acidified, to avoid hydrolysis of the chlorine, heated to 60° using heat from the denuder and passed to the cell.

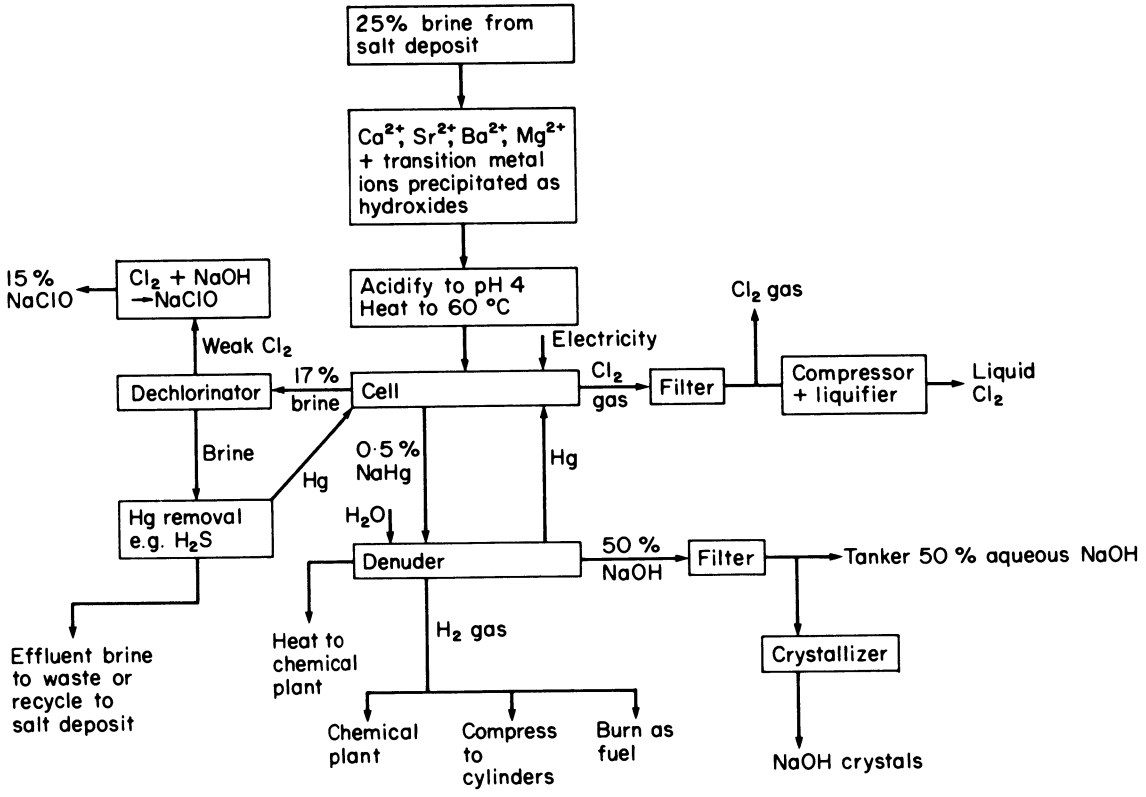

Fig. 3.6 The complete mercury cell process for the conversion of salt deposits into chlorine and 50% caustic soda.

After electrolysis and decomposition of the sodium amalgam in the denuder, all three products – chlorine, hydrogen and sodium hydroxide, must be filtered and transformed to forms required for sale. The sodium hydroxide is sold as 50% solution or pellets, and the chlorine is compressed and liquefied for storage and transport or used directly in an adjacent chemical plant. The hydrogen gas is used, if possible, as a chemical feedstock or sold as compressed gas since this gives the best financial return; otherwise, it is burnt as a fuel in the power station. The effluent brine must be treated with a stream of air to remove the residual chlorine (which is generally used to manufacture hypochlorite) and also for the removal of both finely dispersed mercury metal and mercury compounds and ions. Whether it is then recycled to the salt deposits or discharged into natural waterways will depend partly on the proximity of the boreholes and local effluent discharge practices.

3.3.2 Diaphragm cells

A diaphragm cell has a separator based on asbestos with various polymers added to improve its performance and the electrode reactions generate chlorine and sodium hydroxide directly (reactions A and C(ii) of Table 3.2).

The principle of a diaphragm cell is sketched in Fig. 3.7. The asbestos is deposited directly onto a steel gauze which also acts as the cathode. The anode is placed close to the diaphragm and the 30% brine is passed into the anode compartment; chlorine is formed on the anode. A fraction of the brine diffuses through the porous diaphragm and the H_2 gas and sodium hydroxide are formed on the opposite side of the separator. The anodes will nowadays be a catalyst-coated titanium (e.g. DSA) and in modern cells, the steel cathode may

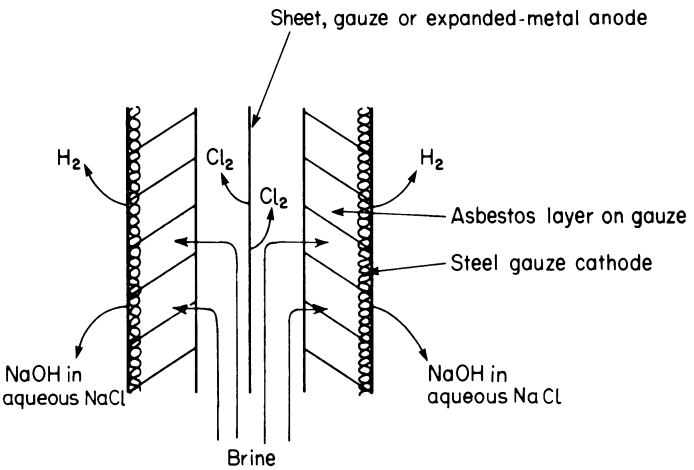

Fig. 3.7 The principle of the diaphragm cell.

also be coated with a catalyst (e.g. high-area Ni) to minimize the overpotential for H_2 evolution. The cathode coatings for diaphragm cells are not as good as those available for membrane cells; the difference arises because of the high chloride ion concentration at the cathode in a diaphragm cell.

The use of an asbestos diaphragm has several problems associated with it:

1. It is purely a physical barrier and all ions and other species are equally able to diffuse through it when there is a concentration gradient. As required for the cell chemistry, Na^+ are transported rapidly through the diaphragm from anolyte to cathode by diffusion, convection and migration. But an almost equal quantity of Cl^- accompanies the Na^+ ions into the cathode region so that the caustic soda formed must contain a high chloride content. Moreover, the concentration of hydroxide ion formed at the cathode must be restricted to below 12%, otherwise diffusion of hydroxide ion from the cathode into the anolyte becomes significant. This leads to loss of chlorine by hydrolysis to hypochlorite and formation of oxygen at the anode and, hence, contamination of the chlorine. Low oxygen DSA were developed to minimize the latter problem.

   The limitation of the sodium hydroxide concentration to 12% means that an additional step must be introduced into the process if this product is to be traded in its normal form, i.e. 50% solution. The evaporation of water (note, to get from 10 to 50% solution, about 80% of the water must be removed) is an energy-intensive process which also requires additional plant. The evaporation stage does, however, reduce the problem from Cl^- contamination since, on cooling, much of the sodium chloride crystallizes-out from the 50% sodium hydroxide solution. Even so, the chloride level remains about 1% and this is unacceptable in many applications, for example it increases corrosion problems in any situation where the sodium hydroxide contacts metals. Certainly, diaphragm plants are most attractive, if the sodium hydroxide can be used as a 10% solution containing the sodium chloride.
2. The *iR* drop in the diaphragm is considerable. While the reversible potential for the cell is about -2.2 V, diaphragm cells operate in the range -3.2 to -3.8 V and much of the additional voltage is associated with the asbestos separator. Moreover, the *iR* drop in the cell increases with time because of the deposition of calcium and magnesium hydroxides in the pores of the diaphragm and, to minimize this effect, very highly purified brine must be used. The brine purification process must be more rigorous than for mercury cells.
3. The asbestos does not last indefinitely and its lifetime is the factor determining the management of the cell and its design. The diaphragm must be replaced every few months and the cell design must permit the washing-off of old asbestos and its replacement by new. The cell must be readily dismantled and reassembled and the change of diaphragm is carried out on a routine cycle. Recently, diaphragm performance has been improved by addition of various polymers to the asbestos base.

Because the resistance of a diaphragm cell is high, the energy penalty of operating at high current density is economically unacceptable and the optimum current density is usually only in the range 0.15–0.20 A cm^{-2}. Hence, in designing the cell, there is an overriding need to arrange for the maximum

(a)

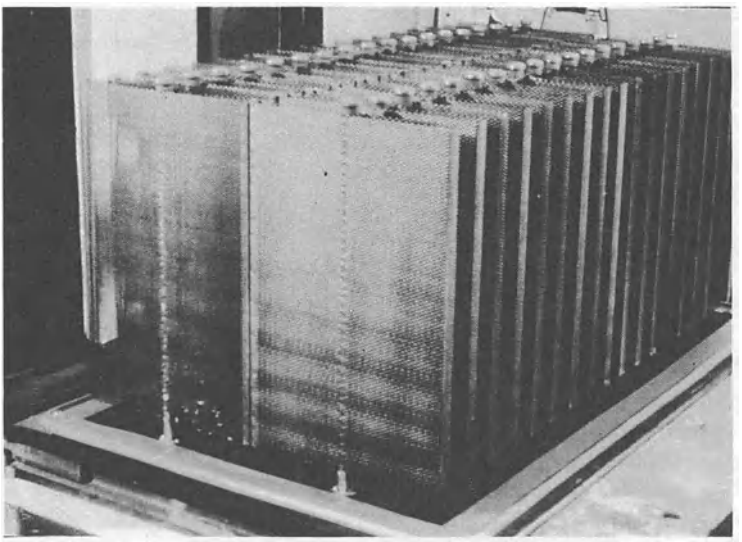

(b)

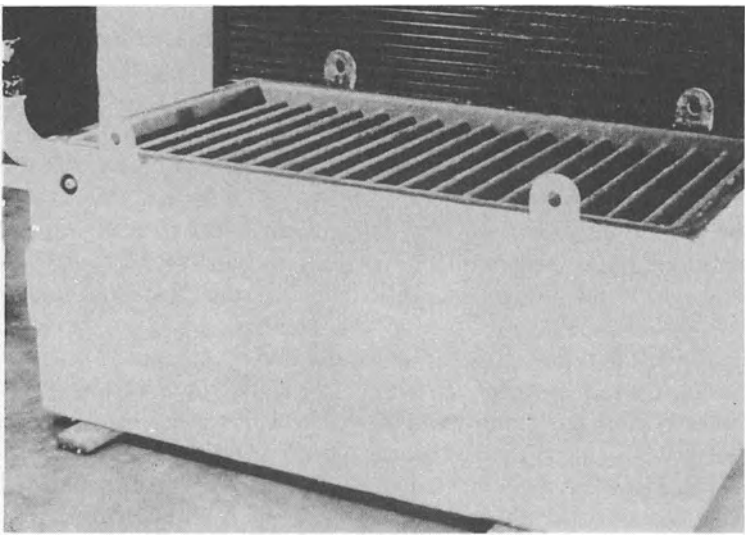

electrode area per unit volume of the cell. With this in mind, a number of electrode configurations have been developed and these will be illustrated here with two examples.

1. The first is the OxyTech Systems Inc. MDC cell, which is typical of many cells designed on the 'electric toaster' principle (Figs 3.8 and 3.9). Figure 3.8(a) shows the DSA anodes ('the toast') bolted to the base of the cell, while Fig. 3.8(b) shows the cell body containing the cathode assembly, a series of asbestos-covered steel gauze fingers extending across the cell body. The cathode assembly is dropped by crane over the cell base with fixed anodes so that each of the anodes is surrounded by cathode (Fig. 3.8(c)). The cell is sealed at the base by the weight of the cathode assembly on a polymer gasket. The cell is completed (Fig. 3.9), by attachment of electrical connections, electrolyte feeds and product take-off pipes. The cell shown has eighteen pairs of anodes and seventeen cathode fingers. The cathode tubes (Fig. 3.10), shows

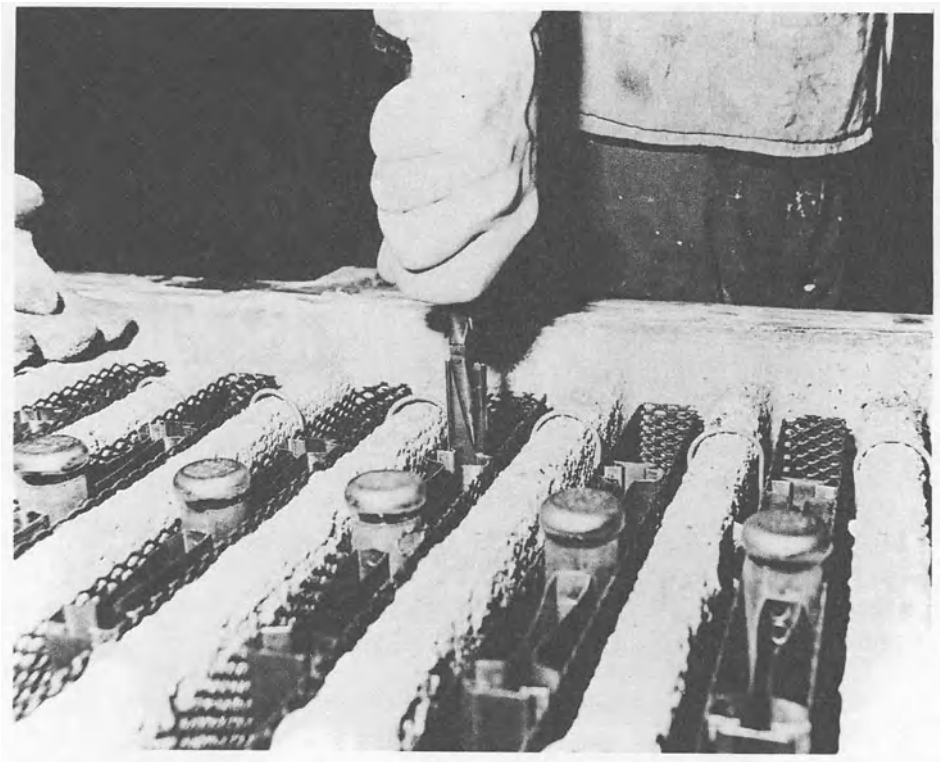

(c)

Fig. 3.8 The arrangement of a chlor-alkali diaphragm cell. (a) Anode assembly, see Fig. 3.1(b). (b) Cathode box. (c) Anode–cathode arrangement. (Courtesy: OxyTech Systems, Inc.)

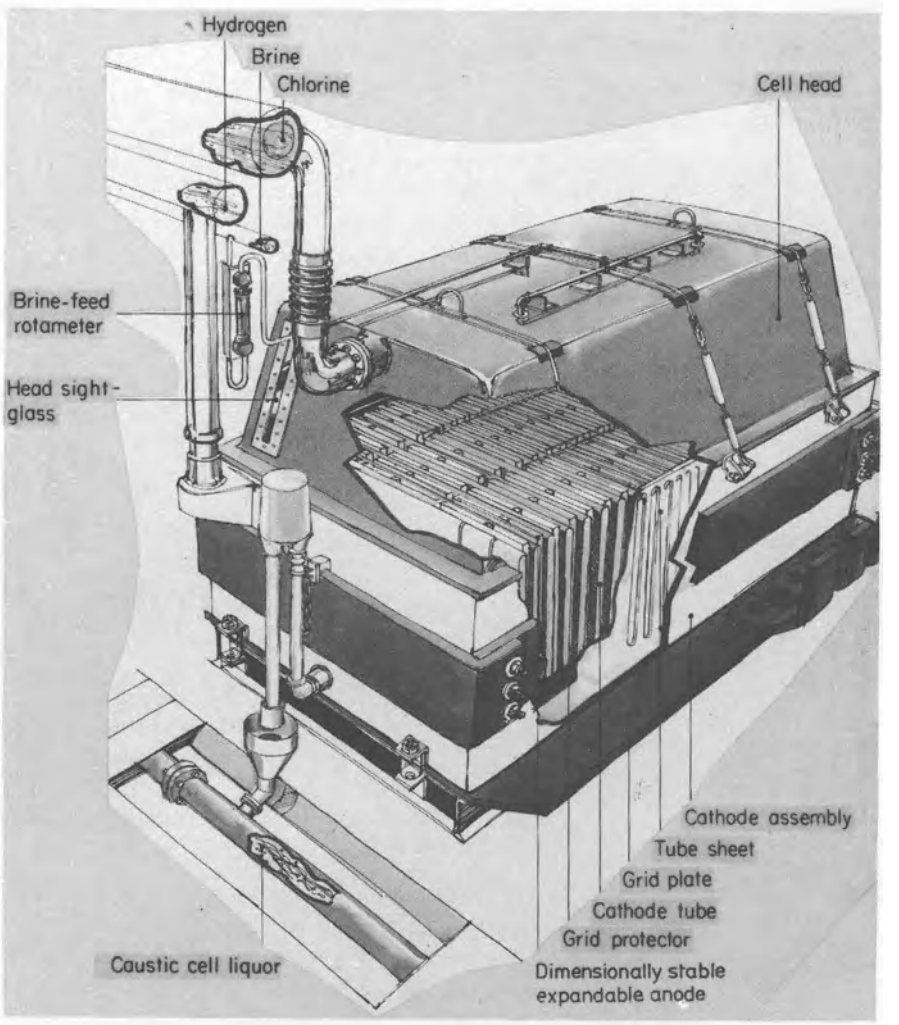

Fig. 3.9 A cutaway diagram of a complete diaphragm cell, type MDC 55. (Courtesy: OxyTech Systems, Inc.)

the view from the side, and the internal faces of the cell body are all constructed from steel mesh (possibly covered by catalyst) and the asbestos-based diaphragm is deposited onto the mesh by dipping the whole assembly into an asbestos slurry. The caustic soda and hydrogen are collected from inside the cathode assembly. The MDC 55 cell has the dimensions 3×1.6 m $\times$ 2 m and its dry weight is almost 7 ton. It is operated in a monopolar mode

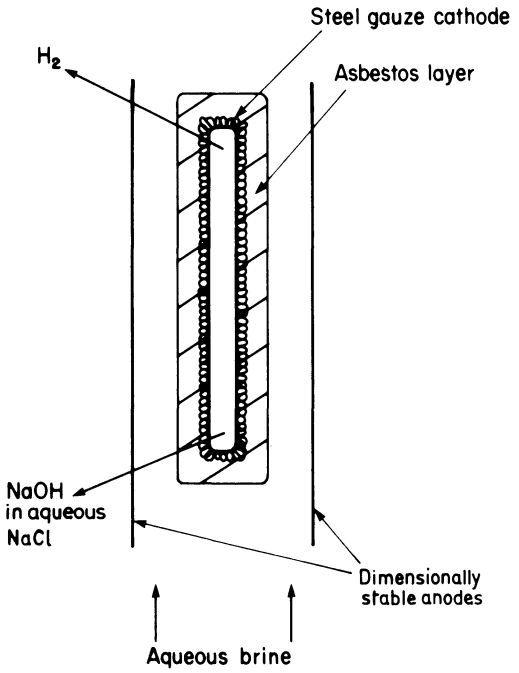

Fig. 3.10 The side view of cathode fingers in the OxyTech Systems MDC 55 cell.

and with a total cell current of 120 kA and a cell voltage of 3.4 V; it produces about 3.5 ton of Cl_2 per day.

2. A quite different approach to packing a high electrode area into unit volume of cell is used in the PPG Industries electrolyser, model V-1161. The electrolyser is a bipolar unit with eleven cells. In each cell, the expanded metal anode and asbestos-covered cathode mesh are arranged as two sets of thirty interlocking fingers. The arrangement of interlocking fingers and that of cells is shown as a view from above the electrolyser in Fig. 3.11. The cell has a good space–time yield and has advantages in assembly and management. The electrolyser is made up of individual cathode and anode units which are clamped together on the rods between end elements. The design allows selection of optimum materials and is easily gasketed. Moreover, when disassembled, the asbestos is readily hosed from the cathode unit and replaced (there is better access to all points of the cathode surface than in the 'toaster' design) and in operation the diaphragm is more readily supported. The V-1161 model has an operating current of 72 kA and a voltage of 3.1 V per cell, i.e. 34 V is applied across the end plates. It produces approximately 27 ton of Cl_2 per day.

The need to reduce energy consumption and to extend the lifetime of diaphragms has led to developments in the technology. These relate to improved diaphragm materials, electrode catalyst coatings and changes in cell design, e.g.

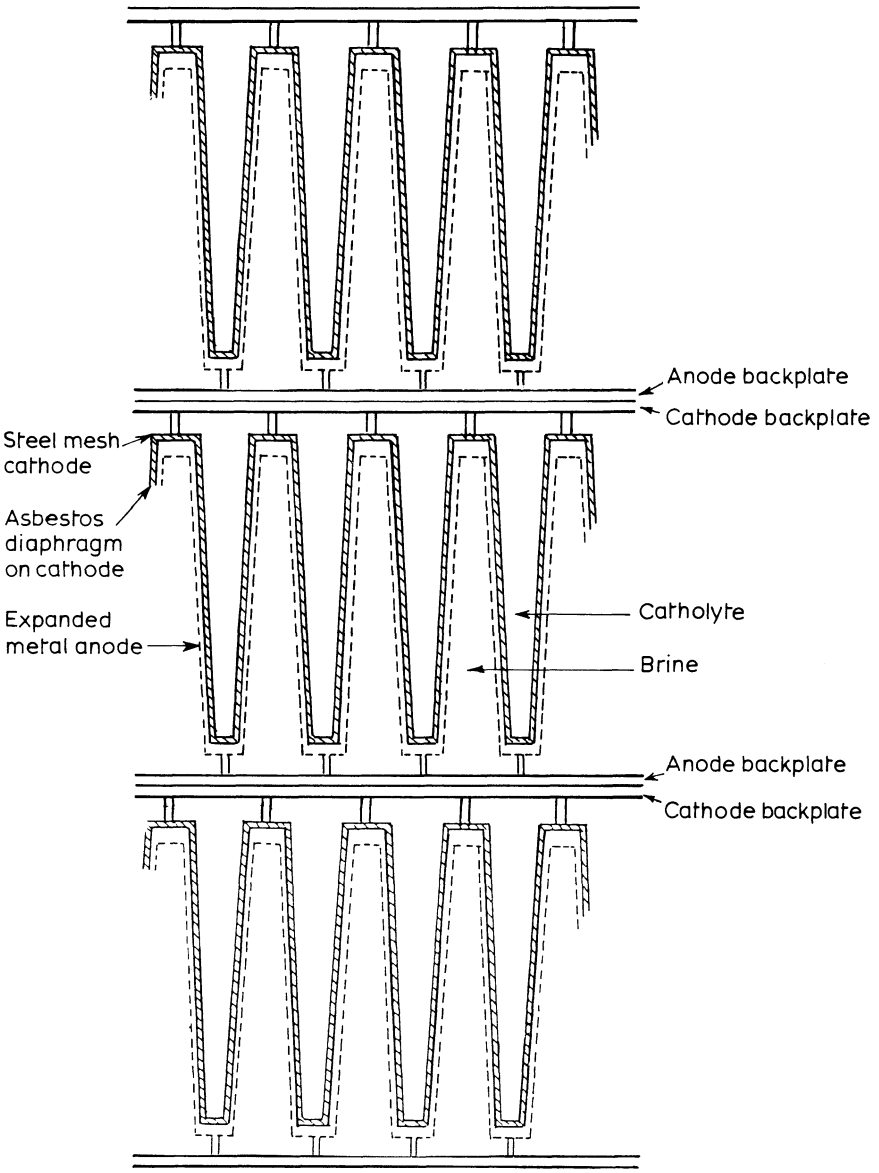

Fig. 3.11 The view from above of a PPG V1161 electrolyser unit to show arrangement of electrodes. The sketch shows three of the *n* cells in the bipolar stack.

reductions in the interelectrode gap. The improvement in diaphragms results from the addition of polymers to the asbestos during formulation. These lead to lifetimes of 2–3 years as well as a lower energy consumption. This latter point is illustrated by data for the OxyTech Systems Inc. cell in Table 3.4. The improvement in diaphragm lifetime is most helpful to the process economics but

Table 3.4 Potential distribution in recent diaphragm cells, $I = 250\ \text{mA cm}^{-2}$

Cell type	$E^C - E^A$/V	iR_{CELL}/V	$iR_{DIAPHRAGM}$/V	$iR_{CIRCUIT}$/V	E_{CELL}/V
1. DSA box anode, steel cathode + standard asbestos diaphragm	−2.48	−0.53	−0.71	−0.27	−3.99
2. DSA expanded anode, steel cathode + polymer modified diaphragm	−2.48	−0.27	−0.46	−0.27	−3.48
3. DSA expanded anode, Ni catalyst coated cathode + polymer modified diaphragm	−2.36	−0.27	−0.46	−0.27	−3.36

Data taken from OxyTech Systems Inc leaflet, *Modified Diaphragm Cells*

it should be noted that the lifetime of catalyst coatings is estimated as 5–10 years and so it is still the diaphragm which determines cell replacement schedules.

3.3.3 Membrane cells

The electrode reactions in a membrane cell are the same as those in a diaphragm cell but the separator is now a cation-permeable membrane. The development of modern membrane cell technology dates only from about 1970 when it was recognized that the perfluorinated membranes (section 3.2.2) had the properties essential to the chemistry of a chlor-alkali cell.

Because of the ability of the membrane to discriminate between cations and anions and to a lesser extent between sodium ions and protons, the cell is, in principle, able directly to produce 50% sodium hydroxide free of chloride ion. In fact, the membranes presently available do not quite have the necessary resistance to hydroxide ion transport and this limits the sodium hydroxide concentration which may be produced directly to below 40%; hence, an evaporation step is still necessary. The energy consumed in evaporation to produce a 50% NaOH solution is, however, much less than in the case of a diaphragm cell. For example, the concentration of 35% to 50% sodium hydroxide requires in the order of 12% the energy needed to concentrate a 10% solution. Moreover, since the membrane is designed not to permit the transport of either chloride or hydroxide ion, the chloride contamination of the sodium hydroxide is low and the oxygen content of the chlorine should be reduced compared to a diaphragm cell. The cell can be operated at a higher current density and the optimum is in the range 0.25–0.40 A cm^{-2}.

The development of membrane cell technology has coincided with the rapid increase in energy costs and, therefore, in the relative importance of energy consumption. Fortunately, good catalysts are available for both electrode reactions (see section 3.2.1). Since the resistance of the membrane is also low, the search for further energy savings has been concentrated on minimizing the interelectrode gap. This has led to the so-called 'zero gap' cells where the two electrodes are in contact with the opposite sides of the membrane. This mode of operation requires further modification of the membrane surface, often by a porous inorganic coating, to ensure gas bubble release from the membrane.

More than a dozen companies throughout the world offer membrane cell technology and only two types of cell will be used to illustrate here the important features of the designs. Most membrane cells are based on a filterpress containing a series of plate and frame cells. Both monopolar and bipolar electrical connection is used. The basic structure of this type of cell is illustrated in Fig. 3.12 (note that the relative dimensions are not correct – membrane areas may be up to 2 × 2 m, although more normally 1 × 1 m, while the thickness of the electrolyte chambers is usually much less than 1 cm). The electrodes are vertical and constructed with louvres or from expanded metal so that the gases formed at the electrodes are directed to the back of the electrodes and do not stay in the

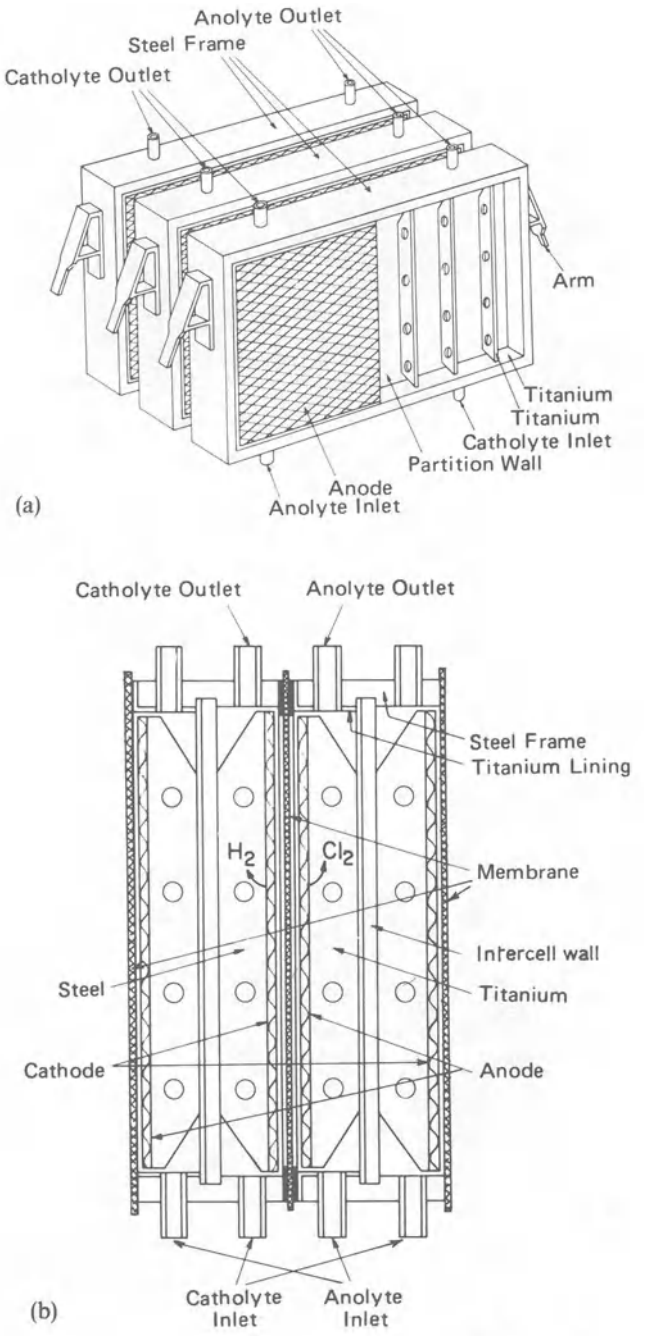

Fig. 3.12 The construction of the Asahi membrane cell. The complete cell is made by repeating this unit. (*Courtesy*: Asahi Chemical Co.)

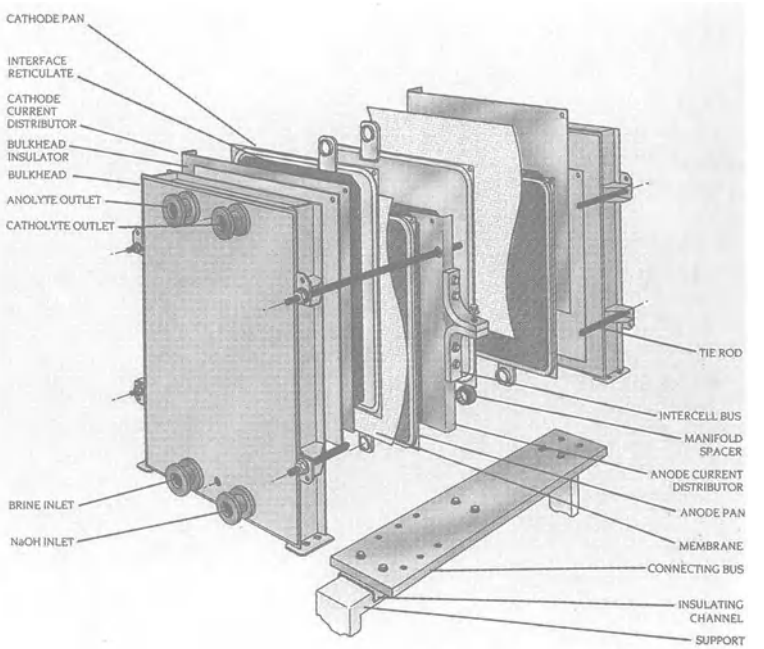

Fig. 3.13 The components and construction of the MGC electrolyser. (Courtesy: Oxy-Tech Systems, Inc.)



Fig. 3.14 The construction of an MGC electrolyser. (Courtesy: OxyTech Systems Inc.)



Fig. 3.15 A membrane cell house in the USA using the MGC electrolyser. (Courtesy: OxyTech Systems Inc.)

interelectrode gap where they would increase cell resistance. The anode and cathode compartments are fed with 25% brine and dilute sodium hydroxide respectively, and the main electrolyte flow is behind the electrodes; hence, the electrolysis largely occurs at the three-way interface between membrane, electrode and electrolyte. Figures 3.13 and 3.14 show the different constructions of this type of cell, while Figs 3.15 and 3.16 show complete cell units.

ICI in England have developed a different approach to zero-gap membrane cell technology where the gasketing essentially also fulfils the role of cell body. Figure 3.17 shows the components to each cell and the way the cell units are put together in an electrolyser. The key components are the electrodes made by pressing sheet metal into a structure with two sets of 'fingers'. The gasket then fits around this electrode structure, to give a good seal and the membrane lies flat on the electrode and gasket. The electrode and gasketing are shown in more detail in Fig. 3.18 and the complete cell unit is shown in Fig. 3.19. The cell must be operated with monopolar connections and is short but wide (area 0.21 m^2) in order to minimize iR drops in the electrode structures.

A complete filterpress stack of membrane cells will contain typically 50–100 cells and will be capable of producing up to 10 000 tons of chlorine per year. It can also be seen that it is straightforward to vary the number of cells in

(a)

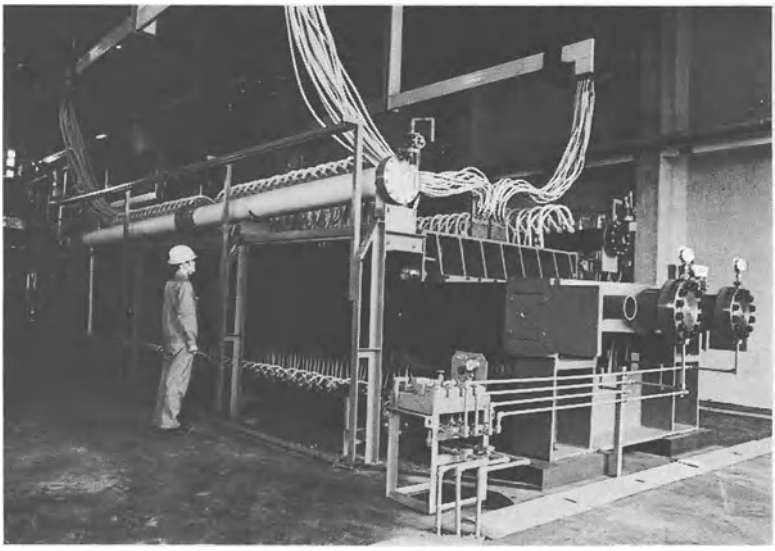

(b)

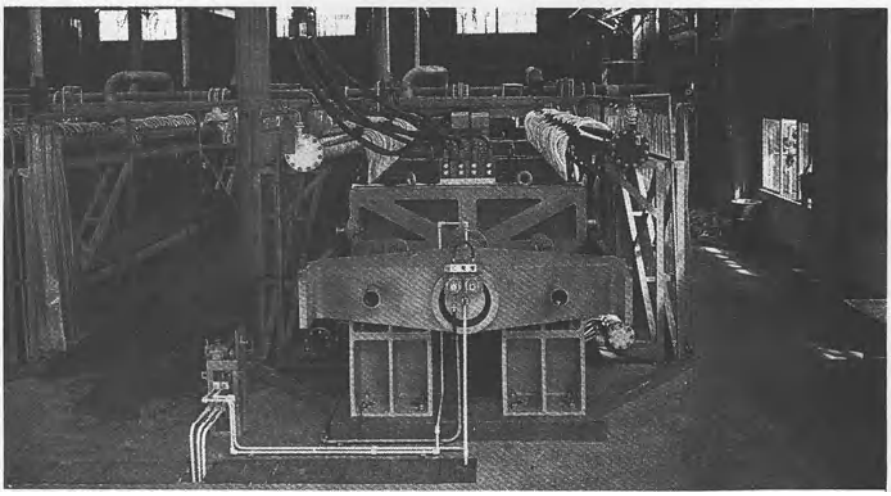

Fig. 3.16 A filterpress membrane cell facility in Japan. (Courtesy: Asahi Chemical Co.)

each electrolyser unit and, hence, to build plants with various capacities. Indeed, the present membrane cell technology has been adopted most readily for plants of about 10^4 tons per year and a number of such plants are operational at papermills in remote locations; there is no waste, as both Cl_2 and NaOH are used in paper manufacture, and the H_2 may be used as a fuel. On the other hand, very large chlor-alkali plants using membrane technology have been constructed and are operational, e.g. a 270 000 ton per year plant in Holland.

The cell voltage can be as low as -2.7 V in membrane cells with coated cathodes and anodes, giving an energy consumption of only 2200 kWh ton^{-1} NaOH. Such performance does, however, require operation under carefully controlled conditions. The temperature commonly is as high as 90°C and certainly the brine must be of a very high purity to avoid problems at both anode and membrane; hence, it is normal to include an ion exchange treatment in addition to precipitation of impurities. Under optimal operational conditions, membrane lifetime is now more than 3 years and the electrode coatings have a much longer lifetime. As noted at the beginning of the chapter, a further substantial energy saving is potentially possible using oxygen reduction as the cathode reaction. It is only in a membrane cell that the technology would be conceivable but even then the current view is that the additional complexity resulting from the porous cathode in a cell would not be justified.

3.3.4 A comparison of cell technologies

A comparison of the relative merits of the three electrolytic routes for the production of chlorine and caustic soda must be based on economics, although there are social and policy factors which must also be taken into account. It is the intention here to discuss the factors determining the economics of the processes only in qualitative terms because the uncertainties in a more exact calculation are too great. It might be noted, however, that recent published calculations would indicate that the costs of chlorine and caustic soda produced by the processes are very similar and this must be the case since mercury, diaphragm and membrane cells are all presently operated and, until recently, were all considered when new plant was to be purchased. The improvements in the membrane cell discussed above have, however, led to a situation where it is expected that membrane cells will be the preferred technology of the future. It is only lack of operational experience which, in most situations, prevents their automatic adoption when new plant is required. Certainly, the percentage of world chlorine produced in membrane cells is rising rapidly.

Typical data for the three cell technologies is summarized in Table 3.5.

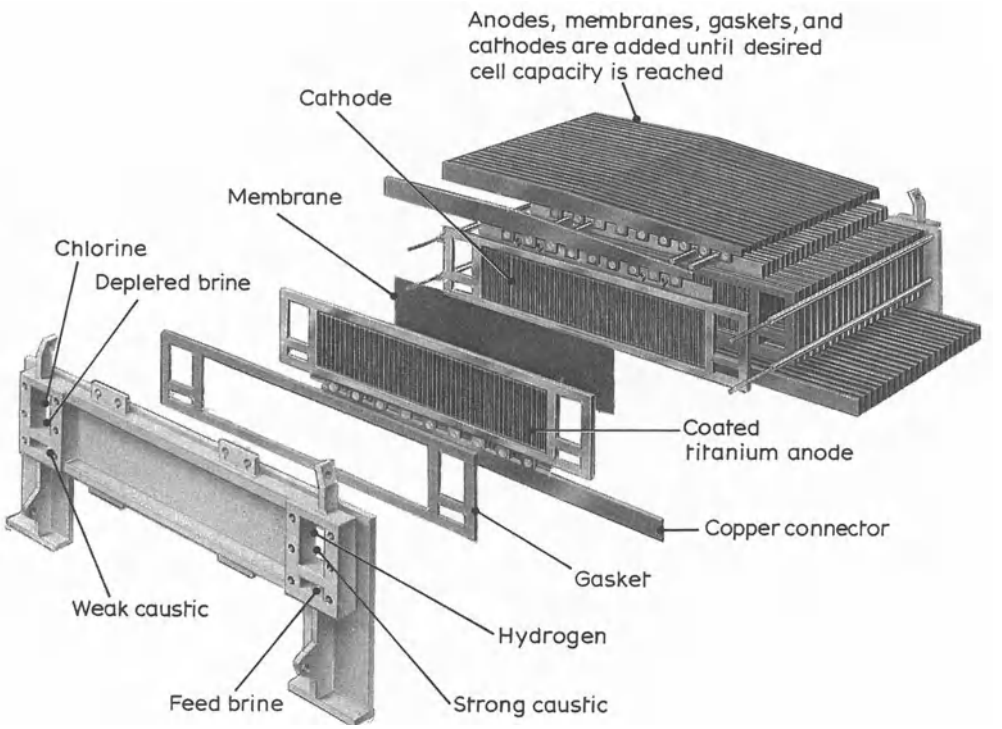

Fig. 3.17 The design concept for the FM series of ICI electrolysers. The module shown is the original FM21 HP electrolyser (the present SP series is shown in Figure 2.32). (Courtesy: ICI Chemicals and Polymers Ltd.)

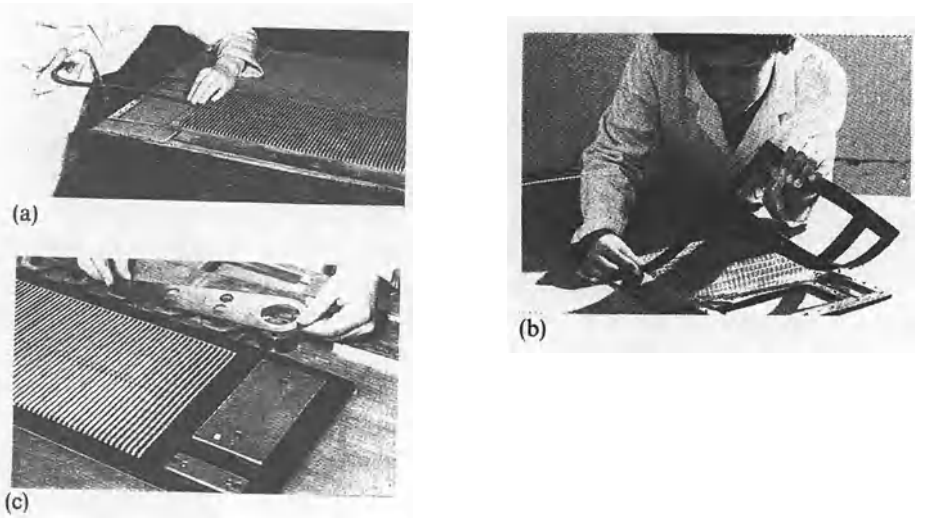

Fig. 3.18 Construction of the FM series of electrolysers. (a) spacer being inserted between the blades of the electrode. (b) fitting gasket to the electrode panel. (c) complete electrode unit. (Courtesy: ICI Chemicals and Polymers Ltd.)

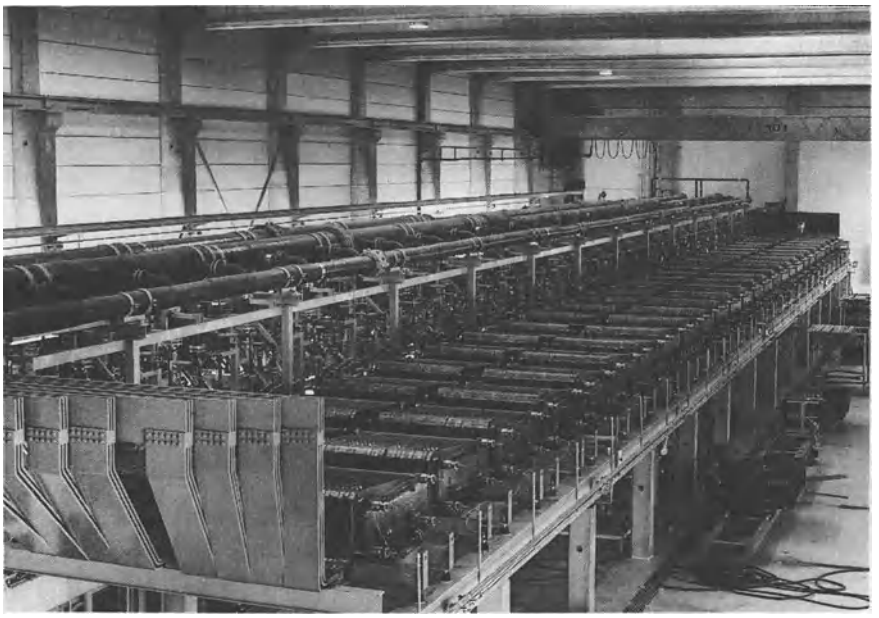

Fig. 3.19 Chlor-alkali cell room based on FM21 SP electrolysers. (Courtesy: ICI Chemicals and Polymers Ltd.)

Table 3.5 Typical data for recent commercial chlor-alkali cells

	Mercury cell	Diaphragm cell	Membrane cell
Cell voltage/V	−4.4	−3.45	−2.95
Current density/A cm^{-2}	1.0	0.2	0.4
Current efficiency for Cl_2/%	97	96	98.5
Energy consumption/kWh per ton of NaOH			
(a) Electrolysis only	3150	2550	2400
(b) Electrolysis + evaporation to 50% NaOH	3150	3260	2520
Purity Cl_2/%	99.2	98	99.3
Purity H_2/%	99.9	99.9	99.9
O_2 in Cl_2/%	0.1	1–2	0.3
Cl^- in 50% NaOH/%	0.003	1–1.2	0.005
Sodium hydroxide concentration prior to evaporation/%	50	12	35
Mercury pollution considerations	Yes	No	No
Requirement for brine purification	Some	More stringent	Very extensive
Production rate per single cell/tons NaOH per year	5000	1000	100
Land area for plant, of 10^5 tons NaOH per year/m^2	3000	5300	2700

(a) The initial cost of the plant

This will include the purchase of the cells, control equipment and all the ancillary equipment for purifying the brine, liquefaction of the gases, concentration of the sodium hydroxide to a 50% solution, effluent treatment, etc.

The cells are constructed from expensive materials. The electrolyte chambers are commonly titanium in order to avoid corrosion problems, while both membranes and electrode coatings are costly components. It is, hence, desirable to minimize the number of cells and to seek operating conditions for extending the cell lifetime. In electrochemical processes, it is the current density which determines the size and number of cells necessary for the required annual production and, hence, is a key factor determining the cost of the cellrooms. It has been recorded in the preceding sections and is noted in Table 3.5 that the normal working current density for a mercury cell is very much higher than for a membrane or diaphragm cell, and the effect of this parameter combined with the easier scale-up of such cells may be seen in the comparison of the annual production rates.

Only with a mercury cell can 50% NaOH be produced directly. Diaphragm cells, since only producing 12% NaOH, must be combined with extensive evaporation plant; membrane cells require considerably less. Mercury cells also require the least stringent brine purification since they can tolerate relatively high concentrations of Ca^{2+} and Mg^{2+}. Membrane cells require very highly purified brine and, hence, more plant, e.g. ion exchange columns as well as alkaline precipitation. On the other hand, in order to meet legal requirements, mercury cell facilities must have plant to treat the effluent for the removal of mercury, and the presence of large quantities of mercury increases monitoring requirements in the plant. Finally, the cost of the mercury and pumping it are not negligible!

(b) Operating costs

Operating costs include labour, replacing components and the rent and taxes on the land. A comparison of the latter is very unfavourable to diaphragm cells where almost twice as much land is necessary because of the low current density and the need for evaporation plant. Membrane and mercury cells have similar land requirements because the former are packed together closely in a filterpress and to some extent the electrodes scale vertically. All the processes are largely automated and, hence, the difference in labour costs is likely to arise because of a variable incidence of component and pipework failure. The need to replace diaphragms on a routine cycle certainly increases the labour costs for the diaphragm cell process; improved diaphragms may operate for 2–3 years. The lifetime of membranes is very sensitive to operating conditions but operation for upwards of 3 years can be achieved. Electrode coatings, in general, have much longer lifetimes. The replacement of membranes is now an easier operation than replacement of diaphragms.

(*c*) *Value-added during the process*

The value-added depends on both the cost of the raw materials and the value of the products. The raw materials for all three processes are similar but differences in the purity of the products will affect the price which may be obtained for them. The diaphragm cell process again comes a poor third since the sodium hydroxide is high in chloride ion and the chlorine contains a higher content of oxygen. Hence, the diaphragm cell becomes much more favourable if the sodium hydroxide is not to be sold on the open market and the internal use can tolerate the chloride ion impurity. The most favourable situation is when the sodium hydroxide may be used as a 10% solution, direct from the cell, thus avoiding the need for concentration. This is often possible when the sodium hydroxide is used to neutralize acid during organic synthesis.

(*d*) *The cost of energy*

Figure 3.20 shows current density-cell voltage plots for cells of all three technologies, the full lines indicating the normal operating regions. The plots are all linear and this indicates the total predominance of the iR_{CELL} term in equation (3.5). The cell voltage is, however, only important in so far as it

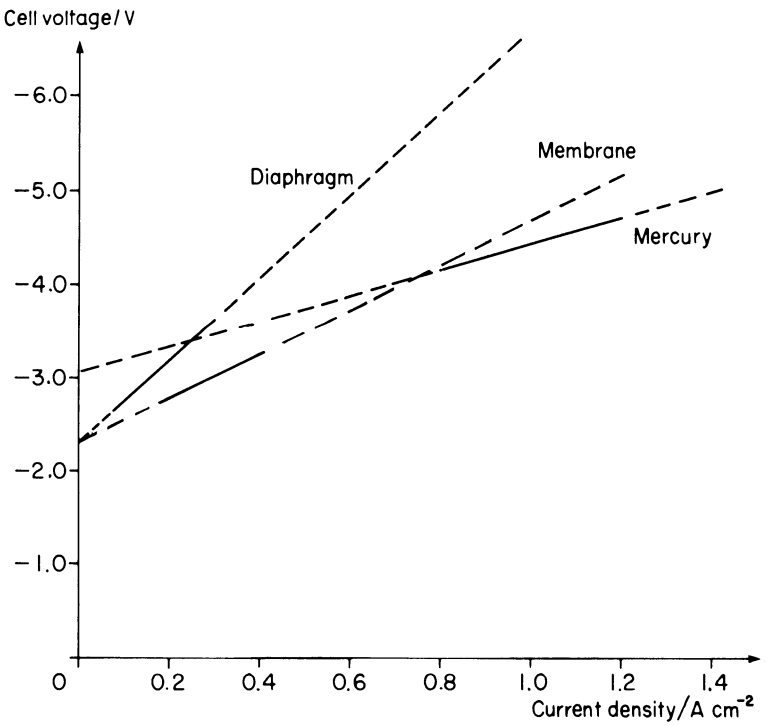

Fig. 3.20 Cell voltage versus current-density plots for the three types of chlor-alkali cell. The full lines indicate the normal operating regions.

determines the energy consumption of the cell and Fig. 3.21 therefore shows the relationship between energy consumption and current density; both the energy consumed in the electrolysis and the total energy to form chlorine and 50% aqueous sodium hydroxide are included, the latter being the normal basis for comparison.

In seeking the conditions for operating the cell, both the absolute energy consumption and the slope of the lines (essentially the cell resistance), are important since there will be a trade-off between energy consumption and the rate of production (i.e. current density) when the total cost is considered; the slopes indicate the additional energy which must be consumed to permit a faster production rate. It is the low resistance of the mercury cell which allows the use of high current densities without an unreasonable voltage penalty.

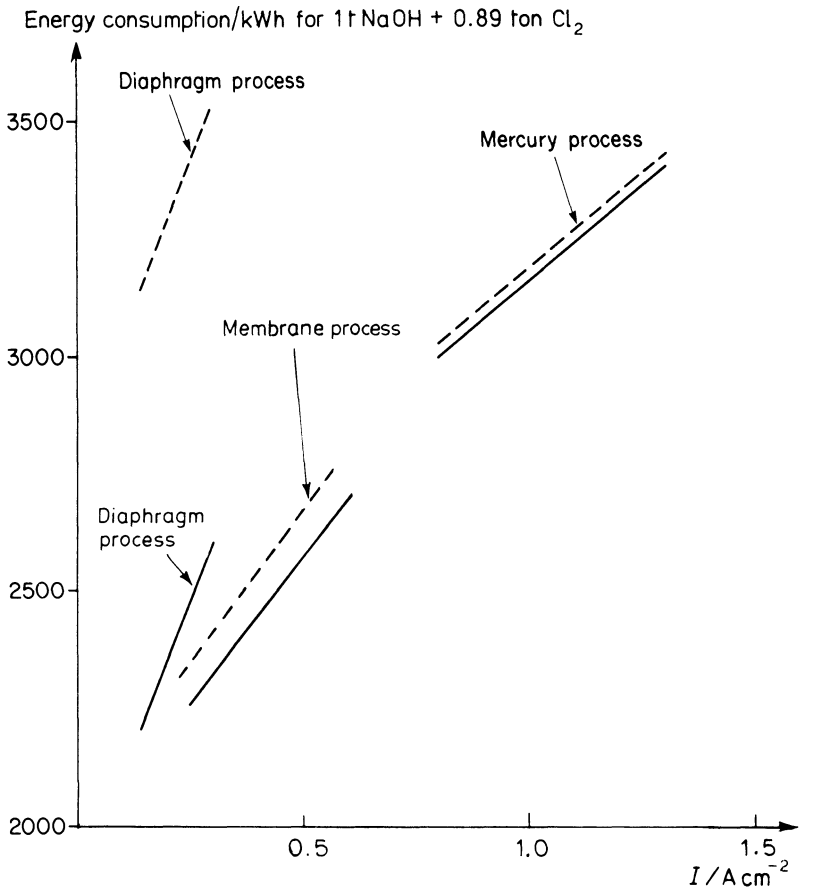

Fig. 3.21 A comparison of the energy consumption in the three cell technologies for chlor-alkali production. The full lines represent electrolysis only; the broken lines, total energy consumption, including evaporation and heating the electrolyte.

It will be seen that the energy consumptions of the three cells are not dissimilar before concentration of the NaOH. Until now it has been considered worthwhile to increase current density (i.e. production rate) rather than conserve energy as cell technology has been improved. This decision is changing as electric power becomes more expensive and it is conceivable that current densities might even be reduced to decrease the energy requirement. Moreover, the improvement in the energy consumption of membrane cells is a key factor in their increasing share of the market. The necessity for evaporation and, hence, the market for the NaOH, has a large influence on any decision to install a diaphragm plant.

(*e*) *The choice*

The choice of cell technologies has not been made on the basis of an economic assessment alone. It is clear from the above that the mercury cell, despite being the oldest of the technologies, has many substantial advantages. It has, however, come under strong pressure because of the fear of mercury pollution. The dangers of the industrial use of mercury became fully recognized following several deaths due to mercury poisoning at Minimata in Japan in the 1950s. Two responses to the problem of potential mercury poisoning are possible: (1) to control carefully the use of mercury in the plant and ensure that effluent does not contain harmful amounts of mercury, or (2) to discontinue completely using mercury. The USA has decided to replace mercury cells as rapidly as possible, the Japanese government has banned them, while in Europe the tendency has been to control the cellroom environment, perform continuous health checks on the workers by regularly monitoring Hg levels in blood and to carry out careful effluent treatment to remove mercury. It is claimed in the UK that the mercury in effluent from chlor-alkali plants does not significantly increase the mercury level of the local water environment. This diversity of action largely resulted from a difference in the market response to chloride-contamined sodium hydroxide; European customers insisted on the continued supply of chloride-free sodium hydroxide and diaphragm cells were not able to meet this requirement.

The developments in membrane cell technology have changed the situation markedly. The product quality is, at least, comparable with that from mercury cells and there is no possibility of mercury pollution. Moreover, there are bonuses to the operator in terms of energy consumption and cellroom management. Membrane cells have already largely replaced mercury cells in Japan. In Europe, the performance of the membrane cells is now sufficient and certainly, when combined with pressure from environmental groups, it is probable that all future new cellrooms will be based on membrane cells. In the USA, the predominance of diaphragm cells results from an early switch from the mercury cells and the continued market for weak sodium hydroxide containing chloride ion.

Table 3.6 An estimate of the split between cell technologies in 1987 (% of total Cl_2 production)

	Mercury	Diaphragm	Membrane
UK	94	5	1
W. Europe	67	27	6
Japan	0	43	57
USA	20	75	5
World	40	50	10

Thus, it is to be expected that the industry will move to membrane cells, although perhaps most slowly in the USA. Two factors retard the change: (1) although there is much pilot-plant and even small-plant experience, there are few very large membrane cell plants in operation and, hence, some suspicion remains about real operational performance; (2) the market for chlorine and sodium hydroxide is not strong enough to demand additional plant, and the driving forces for replacement of existing cellrooms is insufficient until they have reached the end of their natural lifespan. Table 3.6 presents an estimate of the split between the three cell technologies in 1987.

The past 25 years have seen continuous change and improvement in the technology of the chlor-alkali industry. As a result, modern cells are able to produce high purity products while the cell components, designs and control strategies have reached a stage where further improvements in, say, energy consumption, can only be small and will be very difficult to achieve. The only major change which might be envisaged would be a conversion to oxygen cathodes. This, in principle, could reduce energy consumption by a further 60%, but requires the development of catalysts with an acceptable performance and could be achieved only at an expense in terms of more complex cell design because of the need for a gas-fed electrode. Where there is a market for H_2 and, hence, its value influences favourably the process economics, there appears to be no reason to switch to oxygen cathodes. In some circumstances, however, the H_2 can even be a nuisance and then the energy savings from an oxygen cathode look attractive. Indeed, it is believed that some companies now operate large pilot-scale processes using fuel-cell-type cathodes. The oxygen reduction catalyst is dispersed Pt on carbon and the large-area cathodes are constructed from smaller 'tiles' of the porous carbon cathodes.

3.4 THE PRODUCTION OF POTASSIUM HYDROXIDE

Potassium hydroxide is considerably more expensive than sodium hydroxide because the feedstock is refined, crystalline, potassium chloride. It is only used when it has a particular advantage, and the production of potassium hydroxide is only 2–3% that the sodium hydroxide. Potassium hydroxide can be produced

by each of the electrolytic routes described in section 3.3 above; the only major difference is that the potassium chloride electrolyte is always recycled, the solution leaving the cell being resaturated and passed back to the cell.

FURTHER READING

1 C. L. Mantell (1960) *Electrochemical Engineering*, 4th Edition, McGraw-Hill, New York.
2 A. Schmidt (1976) *Angewandte Elektrochemie*, Verlag Chemie, Weinheim.
3 D. L. Caldwell (1981) 'Comprehensive Treatise of Electrochemistry', in Vol. 2, *Electrochemical Processing*, (Eds J. O'M. Bockris, B. E. Conway, E. Yeager and R. White), Plenum Press, New York.
4 M. Coulter (Ed.) (1980) *Modern Chlor-Alkali Technology*, Vol. 1, Ellis Horwood, Chichester.
5 C. Jackson (Ed.) (1983) *Modern Chlor-Alkali Technology*, Vol. 2, Ellis Horwood, Chichester.
6 K. Wall (Ed.) (1986) *Modern Chlor-Alkali Technology*, Vol. 3, Ellis Horwood, Chichester.
7 P. Schmittinger, L. C. Curlin, T. Asawa, S. Kotowski, H. B. Beer, A. M. Greenberg, E. Zelfel and R. Breitstrade (1986) in *Ullmann's Encyclopedia of Industrial Chemistry*, Vol. A6, 5th Edition, VCH Verlag, Weinheim.

4 The extraction, refining and production of metal

This chapter will describe those electrolytic processes which are used in the manufacture of metals from their ores (i.e. electrowinning) and for the purification of metals, (i.e. electrorefining) and the production of metals in powder form.

The extraction of a metal from its ore will always include a reduction step from whichever oxidation state is most stable in our oxygen-rich natural environment to the zero oxidation state. In principle, this reduction can almost always be accomplished by electrolysis and many metals are, at least on a small scale, isolated by an electrolytic route. Commonly, however, routes based on carbon or sodium reduction are preferred for economic reasons. On a large scale, electrolysis is only used for the manufacture of the very electropositive elements (aluminium, sodium, lithium and magnesium) where the electrolysis medium is a molten salt and for elements where the chemical route has environmental problems or the electrolytic route has advantages in terms of the purity of the metal. This latter group includes particularly copper, zinc and perhaps nickel. Cobalt, chromium, manganese, gallium, rare earths, tantalum and niobium are examples of other metals where electrolysis has been used, at least on a small scale, for their extraction. Large electrolytic plants for metal extraction are heavy consumers of electrical power and it is therefore common for them to be sited close to cheap sources of electricity, e.g. hydroelectric power stations.

The objective in electrorefining is to remove unwanted elements from impure metals. The impure material will be the anode and the process seeks to deposit pure metal at the cathode, the other metals being left as anode sludge (i.e. solids) or as ions in the electrolyte solution. Where very pure metal is essential (e.g. copper for certain electronics applications) the electrorefining process may be part of the overall extraction procedure but it is more common for electrorefining to be employed to assist the recycling of metals. Recycling metals is increasingly necessary as the world reserves become depleted and electrorefining is a powerful process for the separation of the complex mixtures found in scrap. Many metals are now electrorefined but perhaps the most important are copper, tin, lead, nickel, cobalt, aluminium, silver and gold.

4.1 ELECTROWINNING

4.1.1 Aluminium extraction

In terms of scale of production (around 2×10^7 ton year^{-1} worldwide) aluminium electrolysis is second in importance only to the chlor-alkali industry. This is because aluminium is both light and strong and therefore suitable for many engineering and construction applications, may readily and cheaply by treated by anodizing (section 8.3.1) to retard corrosion and is the principal alternative to copper as a conductor of electricity. Moreover, the known reserves of aluminium ores are relatively high.

Aluminium is normally produced from the ore, bauxite, which is a hydrated aluminium oxide containing silica and other metal oxides, particularly iron. It is converted to a pure alumina using the equilibrium:

$$Al_2O_3.3H_2O + 2NaOH \rightleftharpoons 2NaAlO_2 + 4H_2O \qquad (4.1)$$

The ore is first treated with sodium hydroxide under pressure. The aluminium largely dissolves as the aluminate, the iron oxide is insoluble and the silica also remains in the form of a sodium aluminium silicate, which leads to a loss of aluminium. Hence, the best bauxites are those low in silica. After filtration, the hydrated aluminium oxide is reprecipitated by seeding and the sodium hydroxide solution may be reused. The alumina is washed and then heated at 1200° C to remove water. The final step in the production of aluminium metal has to be electrolytic since the reduction of alumina with carbon is only possible at very high temperatures and the reverse reaction occurs on cooling. Moreover, because of the chemistry of aluminium, the electrolysis medium cannot be water; in fact, almost all commercial production of aluminium during the last 90 years has used an electrolysis in molten cryolite, Na_3AlF_6.

The process is based on the observation made concurrently and independently in 1886 by Hall in the USA and Héroult in France that, whereas alumina melts at 2020° C to give a non-conducting liquid, it will dissolve to the extent of 15 wt% in molten cryolite at 1030° C to give a conducting medium. Two years later, the second important step towards a viable process of aluminium extraction was made by Bayer who developed a method for leaching sodium aluminate to produce alumina. The high solubility of alumina in molten Na_3AlF_6 results from the near equality of size of fluorine and oxygen atoms in the aluminium complexes in the melt and, hence, facile formation of oxyfluoride ions on addition of the oxide to the Na_3AlF_6. Indeed, the aluminium is probably present as a mixture of several related species, although the exact chemistry of the system is not known and it is therefore difficult to write complete electrode reactions. Clearly, however, the cathode reaction is the reduction of an aluminium (III) species to the metal which is molten at the electrolysis temperature; the cathode is effectively a pool of liquid aluminium. Ideally, the anode reaction would be the oxidation of oxide ion to oxygen but it is difficult to

find an anode material which is inert under the electrolysis conditions. Hence, the electrolysis has always been run with consumable carbon anodes so that the overall cell reaction is:

$$2Al_2O_3 + 3C \longrightarrow 4Al + 3CO_2 \tag{4.2}$$

The carbon anode is consumed in a stoichiometric amount but the free energy for this reaction is 340 kJ mol^{-1} Al (at 1000° C) compared with 640 kJ mol^{-1} for the reaction:

$$2Al_2O_3 \longrightarrow 2Al + 3O_2 \tag{4.3}$$

i.e. the overall cell reaction if oxygen was evolved at the anode. In consequence, the sacrifice of the carbon anode leads to a much reduced cell voltage and energy consumption. Thus, the reversible cell voltage is −1.18 V compared with −2.21 V if the cell reaction was (4.3).

A cell for the Hall–Héroult process is shown in Fig. 4.1, and a block diagram of the whole process is shown in Fig. 4.2. Cell design is determined largely by the need to contain molten cryolite at high temperatures and to withstand attack by molten aluminium and also by sodium and fluorine formed as minor products at the cathode and anode respectively. Hence, the cell is a strong steel box lined first with alumina to act as a refractory, thermal insulator and then with carbon.

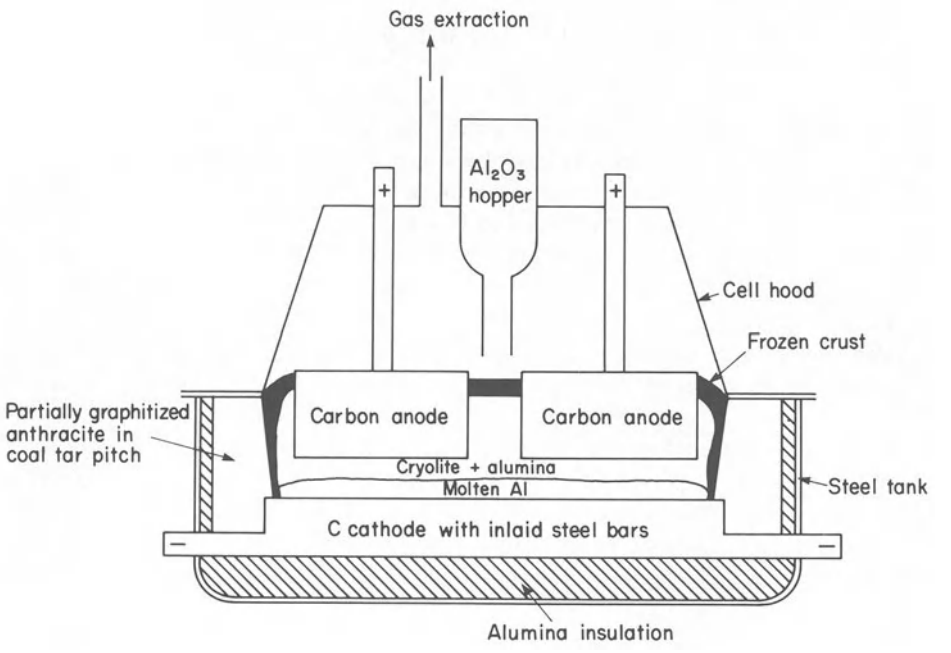

Fig. 4.1 Cell for the Hall–Heroult process for aluminium extraction.

In fact, the base of the tank is lined with prebaked carbon blocks which are inlaid with steel bars to reduce their electrical resistance and which act as current carriers to the molten aluminium cathode. The sides are lined with partially graphitized anthracite in coal-tar pitch. The process is then run so that there remains a layer of solid cryolite and alumina at the sides of the cell and a solid crust on the surface. This acts as a further barrier to corrosion and also to reduce the heat loss from the cell. The cell also has facilities for the periodic addition of alumina through the crust and for the removal of aluminium metal by suction. It is hooded with an extractor to vent the anode gases, mainly carbon dioxide, but also containing carbon monoxide from the unwanted back chemical reaction:

$$2Al + 3CO_2 \longrightarrow Al_2O_3 + 3CO \tag{4.4}$$

and particulate matter as well as in some cases fluorine or hydrogen fluoride. Reaction (4.4), of course, reduces the current efficiency for the electrolysis.

The carbon anodes are manufactured from a carbon source such as anthracite and a pitch binder mix. Two types have been used:

1. Prebaked carbon blocks of dimensions approximately $80 \times 100 \times 50$ cm deep.
2. Self-baking anodes (known as Soderberg anodes) usually one per cell and therefore of much larger dimensions. Such anodes are fed at the top with the ground carbon and pitch binder and this bakes *in situ* as it gradually descends into the molten electrolyte to form a hard, dense material which acts as the anode surface.

In both cases the anode is consumed and therefore must be lowered regularly (approximately 2 cm day^{-1}) to maintain a constant anode–cathode gap. Soderberg anodes were common in the late 1940s and the 1950s because they removed the anode-manufacturing step and, hence made the overall process cheaper to operate. Prebaked anodes were used in earlier cells and are again employed almost universally because they give a better energy performance and lead to less difficult environmental problems; the *in situ* baking causes fumes which are more difficult to control.

Except for the anodes, cell design has changed little since the introduction of the process in the last century. The cells have become larger, however, as the materials and construction techniques have improved, and typically a cell will now be $3\ m \times 8\ m \times 70$ cm deep with eighteen prebaked anodes. The inter-electrode gap must be rather wide, about 5 cm: (1) to prevent shorting because the small difference in density between the melt (2.1 g cm^{-3}) and the molten aluminium (2.3 g cm^{-3}) leads to an unstable cathode–electrolyte interface; and (2) to minimize the chemical reaction of the electrolysis products (reaction (4.4)) which causes loss in current efficiency.

While the electrolyte is essentially molten cryolite, certain additions are made and a typical electrolysis medium also contains excess aluminium trifluoride

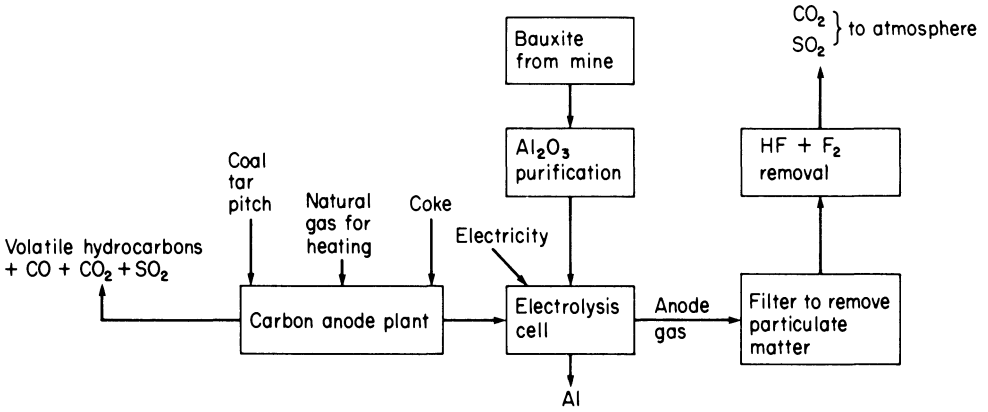

Fig. 4.2 Steps in the Hall–Heroult process for aluminium extraction.

(4–6%) and calcium fluoride (4–6%). These additives increase the conductivity of the medium and lower the melting point of the cryolite to 960–980° C. A reduction in the operating temperature has the advantages of decreasing energy consumption and lowering the extent of the back reaction (4.4) (by about 1%/10° C). On the other hand, by both decreasing the operating temperature and diluting the cryolite, the additives cause a decrease in the solubility of the alumina and this limits their total concentration.

Alumina must be added to the cell periodically and this is done through a hopper which breaks through the surface crust. In the normal electrolysis conditions, i.e. cryolite with calcium fluoride and excess aluminium fluoride and an operating temperature of 970° C, the alumina is only soluble to 6 wt %. During electrolysis its concentration drops, and if it is allowed to fall below about 2%, the electrolysis cell undergoes a sudden and major operational failure known as an 'anode effect'. The cell voltage increases rapidly from −4.5 V to a value in the range −40 to −60 V, and this is thought to be due to an insulating gas film, fluorine or carbon tetrafluoride, across the anode surface. To return the cell to its normal operating conditions, alumina must be added and the bath stirred to remove the gas film. The anode effect is, however, not regarded as totally unhelpful since sparking across the gas film burns off macroscale surface roughness to produce a better anode and provides a simple, if unusual, *in situ* analysis of alumina concentration in the electrolyte. Overfeeding of the cell causes problems by precipitation of alumina on the molten aluminium cathode. Hence, it is common to permit an anode effect to occur at regular intervals.

A typical cell house will contain about 200 cells arranged in series on two lines, each 3 × 8 m cell having a total anode area of 15 m^2. The optimum current density is around 1 A cm^{-2}, giving a total cell current of 150 kA and this requires a cell voltage in the range from −4.0 to −4.5 V. The cell voltage, of course, depends on alumina concentration since this determines the concentration of electroactive species at both electrodes. It drops to just below −4 V

after addition of alumina to 6% and rises to about −4.5 V before the onset of an anode effect. All cell houses have a strong magnetic field due to the large currents used and it is particularly important to take this into account in the design of aluminium electrolysers because of the turbulence the magnetic field can produce at the aluminium/electrolyte interface due to the small difference in their densities. Hence, the cells are arranged in the cell house to produce the minimum magnetic field.

Reaction (4.4) always leads to some loss in current efficiency and in most cells the aluminium current efficiency is only 85–90%. From these data the energy requirement may be estimated to be 14 000–16 000 kWh per ton of aluminium and we can also calculate that the cell house described would produce 70 000 ton year^{-1}.

It can be seen that the energy consumption of the aluminium electrolyser is very high (cf. 3000 kWh per ton of Cl_2). This is partly because the production of aluminium requires 3 F, partly because of its low atomic mass and finally because of very substantial inefficiencies in the cell. Table 4.1 shows how the cell voltage is made up. The reversible potential is calculated from thermodynamic data and it can be seen that it represents only a small fraction of the observed cell voltage. Similar calculations for a cell where the reaction (4.3) occurs, i.e. where the anode reaction is oxygen evolution and the electrode is inert, show that the reversible potential would be −2.21 V. An anode which is stable in the molten salt and able to evolve oxygen at low overpotentials would, however, be advantageous since it would remove the need to manufacture carbon anodes and, hence, remove considerable environmental problems. Moreover, the penalty of a higher reversible potential may be more than outweighed if the anode overpotential and resistance were less than those shown in Table 4.1.

In view of the high temperature, it is to be expected that the kinetics of the electrode reactions will be rapid and this is certainly the case at the cathode. A

Table 4.1 Estimate of voltage distribution in the Hall–Héroult cell

	−Voltage/V
Reversible cell potential	1.2
Overvoltages	
anode	0.5
cathode	0.0
iR drop in electrodes	
anode	0.5
cathode	0.6
iR drop in the electrolyte	1.5
Total cell voltage	4.3

substantial overpotential has been found at the anode but it must be remembered that the oxidation of an oxyanion at carbon to give carbon dioxide is probably an unknown reaction at room temperature.

The *iR* drops in the cell are large. Those in the electrodes arise because of their size and the relatively low conductivity of carbon, particularly the form used in this electrolysis; the carbon cathode has inlaid steel bars to decrease its resistance. The substantial electrolyte *iR* drop is due to the need for a large ($\simeq 5$ cm) interelectrode gap. This overpotential is, however, used to some extent since it gives rise to heat which maintains the electrolyte in a molten state.

If the energy required to maintain the cell at 970° C is taken into account, the energy efficiency of the process is only 33%. Even this relatively poor performance has only been achieved as a result of a careful examination of the physical chemistry of the electrolyte and electrodes and of the cell technology. Moreover, the process has several environmental problems associated with both the curing of the carbon anodes and the anode gases, which must be treated to remove both fluoride and particulate matter. Hence, it is not surprising that considerable effort has gone into developing an alternative technology.

While some of this effort has gone into inert anodes, the major emphasis has been to develop a process in a chloride medium. Much of the work has been unsuccessful, but Alcoa in the USA have recently operated a small plant based on a chloride electrolyte. The cell reaction is:

$$2AlCl_3 \longrightarrow 2Al + 3Cl_2 \tag{4.5}$$

and the electrolysis is carried out at C electrodes in a 3:2 mixture of sodium and lithium chloride containing 2–15% aluminium trichloride. The temperature is 700° C, almost 300°C below that of the Hall–Héroult process but above the melting point of aluminium (this greatly simplifies the process). The process requires the prior conversion of alumina to aluminium trichloride by the chemical reaction:

$$2Al_2O_3 + 3C + 6Cl_2 \longrightarrow 4AlCl_3 + 3CO_2 \tag{4.6}$$

The cell for the electrolysis consists of a bipolar stack of horizontal carbon anodes with an interelectrode gap of 1.5 cm. The electrodes and electrolyte flow is designed to ensure the minimum contact between the electrolysis products, since the molten aluminium and gaseous chlorine would otherwise react rapidly. The aluminium falls to a pool below the electrodes while the chlorine is pumped out the top of the cell to be used in the reaction with alumina. A simplified cell is shown in Fig. 4.3. It may be noted that the overall process again uses carbon in at least stoichiometric quantities although now in a chemical step. Overall the process run at 1 A cm^{-2} has an energy efficiency which is currently claimed to be about 10% better than that for the Hall-Héroult process.

Aluminium is regarded as a strategic material, i.e. it is essential for military applications. Bauxite is, however, not found in large quantities in the developed Western world; rather it comes from Africa, South America, Australia and Asia

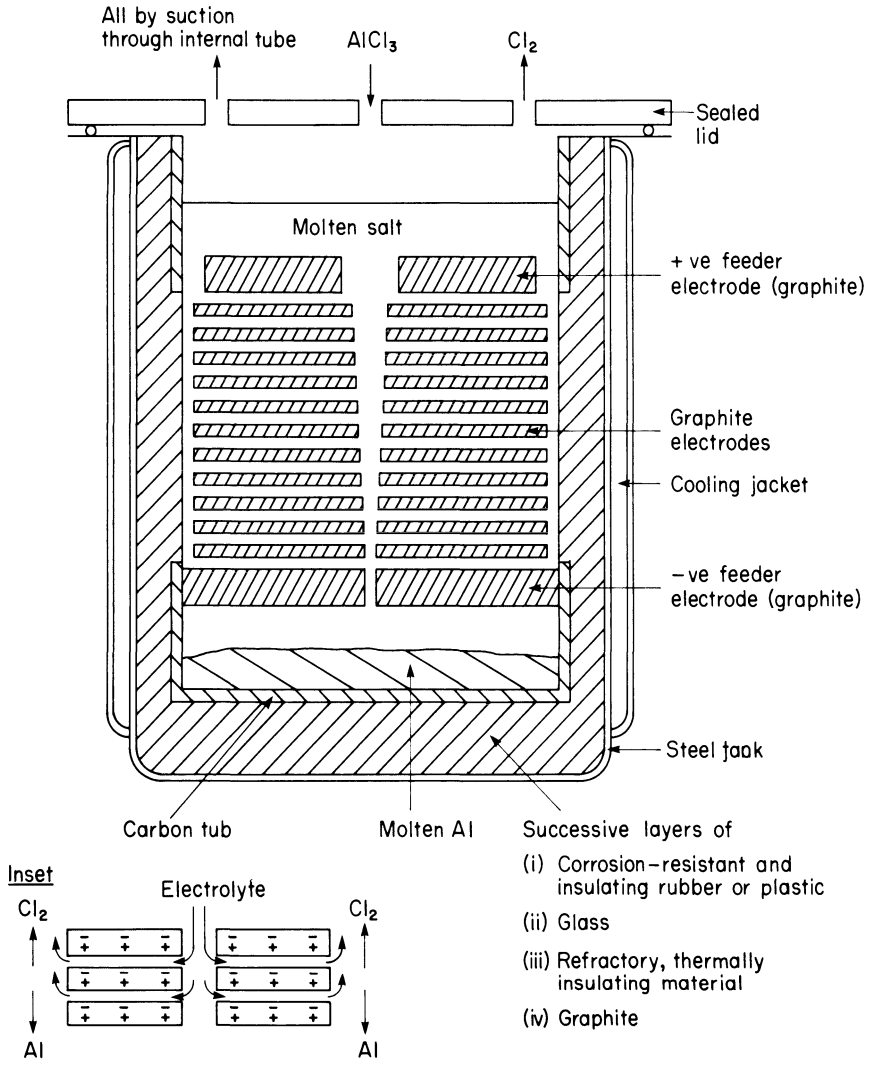

Fig. 4.3 Cell for aluminium extraction by the Alcoa process.

and is transported in the form of purified alumina. On the other hand, aluminium is the most abundant metal in the Earth's crust and is found everywhere, although in a less concentrated form than in bauxite, in common clays. Hence, a further objective of R and D activity is to develop processes for the extraction of aluminium metal from clay.

Aluminium production will always be a highly energy-intensive industry. Table 4.2 shows a breakdown of the costs in a typical Hall–Héroult plant and it can be seen that electrical power is the second largest item; hence, the importance of energy conservation cannot be overemphasized.

Table 4.2 Cost breakdown for aluminium metal production

	% of total cost
Alumina	30
Anodes	7
Other materials	7
Electricity	23
Labour	16
Capital cost	17

4.1.2 Sodium, magnesium and lithium manufacture

These metals are all produced by electrolysis of a mixture of molten metal chlorides; the electrolyte composition is selected to minimize the process temperature and to ensure that it is the desired metal that is discharged at the cathode. The estimated annual world production of sodium and magnesium is a few hundred thousand tons while that for lithium is only a few thousand tons. The major uses are: (a) sodium–manufacture of lead alkyls, isolation of titanium metal, production of several organic and inorganic substances; (b) magnesium–organic synthesis, metal alloys; (c) lithium – polymer initiation, organic synthesis and batteries.

The general technology may be illustrated by the example of sodium production in the Down's cell. The electrolyte is a molten mixture of sodium chloride (40%) and calcium chloride (60 wt % requiring a process temperature of about 600° C. The principle of cell design is shown in Fig. 4.4, although more modern cells have four anodes and cathodes in each cell. The design and materials of construction are again determined by the electrolysis medium. The electrode reactions are simple; at the cylindrical graphite anode:

$$2Cl^- - 2e^- \longrightarrow 2Cl_2 \tag{4.7}$$

and at the steel cathode surrounding the anode:

$$Na^+ + e^- \longrightarrow Na \tag{4.8}$$

Some separation of the products is necessary to prevent the back-reaction and a steel gauze diaphragm ensures that the chlorine gas and the liquid sodium are guided to different collection reservoirs. The sodium is much less dense than the melt and readily rises up a pipe into a reservoir; indeed, this is the basis of its separation from the small quantity of calcium which also forms at the cathode. The calcium is more dense and sinks back into the electrolyte where the equilibrium:

$$Ca + 2NaCl \rightleftharpoons CaCl_2 + 2Na \tag{4.9}$$

ensures that its concentration remains constant and low. The operation of the

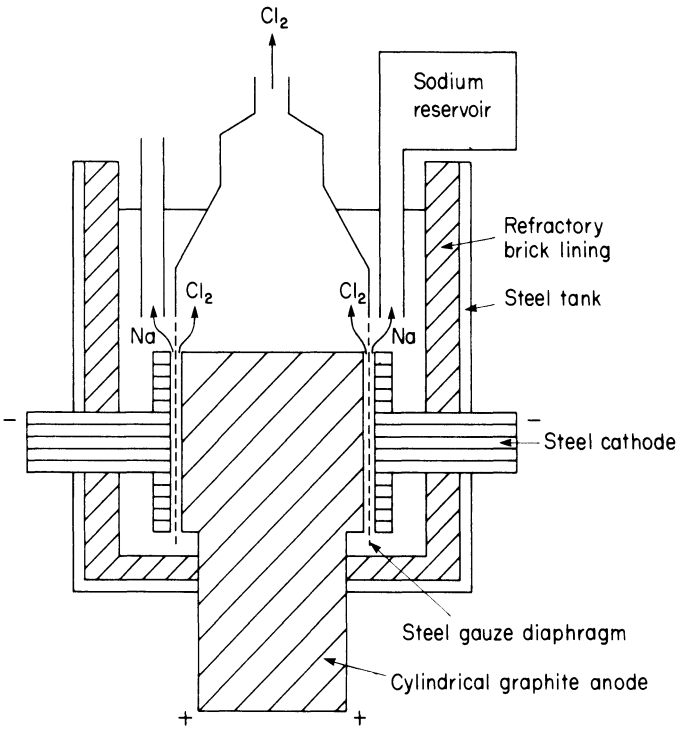

Fig. 4.4 Down's cell for the extraction of sodium metal via electrolysis of molten NaCl or $CaCl_2$.

cell is controlled by the rate of anode corrosion; in the presence of some trace water or oxide ions in the molten chloride medium, the graphite anode is oxidized to carbon monoxide and carbon dioxide, and, hence, precautions are necessary to minimize the rate of loss of graphite.

Down's cells operate at about 1 A cm^{-2} with a cell voltage of approximately -7 V. This compares with a reversible cell voltage of approximately -3.6 V, the difference being almost entirely iR drop in the electrolyte and the electrodes since overpotentials for the electrode reactions will be small at the operating temperature. The current efficiency is about 80%, indicating that significant back reaction occurs, and the energy consumption is in the range 9000–10 000 kWh ton^{-1}.

4.1.3 Hydrometallurgical processes

Hydrometallurgical processes may be used when the metal ion is readily reduced to the parent metal and, hence, the electrolytic reduction may be carried out in aqueous solution. Such chemistry, however, implies that other routes from the ore to the metal must be possible and, indeed, smelting techniques are always applicable. Hence, the choice between smelting and electrolysis will depend on

the quality and type of ore available and local economic factors, particularly the cost of various forms of energy, labour supply and environmental discharge restrictions.

Copper and zinc are the principle metals extracted by electrolysis in aqueous solution; the total world production of both approaches 10^7 tons per year although the electrolytic route accounts for only 10% of the copper and 50% of the zinc produced. Moreover, the large electrolytic plants are limited to sites in Africa, Australia and Canada where hydroelectric power is available close to the mines. Cobalt, nickel, chromium, manganese, cadmium, gallium, thallium, indium, silver and gold have also been reported to have been extracted by a hydrometallurgical process but, since these metals are only produced in a low tonnage, the electrolytic processes are on a smaller scale.

The processes of electrorefining and electrowinning utilize broadly similar process-plant design. The required cathode reaction, considered simply, is in both cases the deposition of metal from a soluble, electroactive species:

$$M^{n+} + ne^- \longrightarrow M \tag{4.10}$$

while, particularly in acid solutions, hydrogen evolution is the most important competing reaction:

$$H^+ + e^- \longrightarrow \tfrac{1}{2}H_2 \tag{4.11}$$

The anode reactions are, however, different. In electrorefining, a soluble anode is used, dissolution occuring at high current efficiencies:

$$M_A - ne^- \longrightarrow M^{n+} \tag{4.12}$$

Ideally, the overall cell reaction in electrorefining is simply the transfer of metal from the impure anode into a purified cathode deposit:

$$M_A \longrightarrow M_C \tag{4.13}$$

It is important to consider the selectivity of both electrode reactions in electrohydrometallurgy cells. Ideally, at the cathode only deposition of the metal required occurs, other metals remaining in solution. However, codeposition of contaminants may be favoured by their low deposition potentials and formation of a true solution in the refined metal. The more noble metals will normally codeposit readily at the cathode. However, in some electrorefining cells, these impurities do not dissolve significantly from the anode due to nobility, formation of resistant intermetallics (e.g. Ag_2Se) or production of insoluble compounds via reaction with the electrolyte (e.g. AgCl, $PbSO_4$).

If the cathode and anode selectivities are good, a simple, undivided electrorefining cell may suffice as in the case of Cu, Pb, Ag or Au. In the presence of poorer selectivities (e.g. in Ni cells), a divided cell serves to localize less noble impurities (e.g. Co, Fe, Zn) in the anolyte. The anolyte may then be purified prior to transfer to the catholyte.

In electrowinning, an insoluble anode is used, oxygen evolution being the major reaction:

$$2H_2O - 4e^- \longrightarrow O_2 + 4H^+ \tag{4.14}$$

Here, the overall cell reaction is achieved by summing reactions (4.10) and (4.14):

$$M^{n+} + n/2H_2O \longrightarrow n/4O_2 + nH^+ + M \tag{4.15}$$

Electrowinning is usually one of the final steps in a complex extraction procedure.

The complete extraction process will have the following (greatly simplified) stages:

1. Mining the ore, which is commonly a sulphide or an oxide or a mixture of both and will contain several metals ions.
2. If the ore is a sulphide, it is roasted in air to convert it to an oxide:

   $$2MS + 3O_2 \longrightarrow 2MO + 2SO_2 \tag{4.16}$$

   which is then leached with acid (normally H_2SO_4) to give an acidic metal sulphate solution:

   $$MO + H_2SO_4 \longrightarrow MSO_4 + H_2O \tag{4.17}$$

   The first step inevitably produces large quantities of sulphur dioxide and, hence, environmental problems. In addition, it is energy-intensive, particularly if the metal to be isolated is not the major constituent and large quantities of crude ore must be heated. For these reasons, oxide ores which may be leached directly are preferred, although their supply is usually insufficient for the demand. To reduce the energy requirement in the roasting process, the crude ore is sometimes purified, e.g. by flotation, and completely different approaches to metal removal from the ore, e.g. direct electrolytic leaching:

   $$MS - 2e^- \longrightarrow M^{2+} + S \tag{4.18}$$

   have been considered.
3. The acidic metal sulphate solution is purified and all metal ions which are reduced more readily than the element of interest must be removed. The principal methods of purification are:
   (a) precipitation with hydroxide or sulphide ion;
   (b) solvent extraction. Chelating agents are used to make the metal ions soluble in an organic solvent. Much recent research effort has gone into designing chelating agents which are highly selective for single transition-metal ions;
   (c) cementation, i.e. the solution containing M^{n+} ions is passed through a reactor containing a more electropositive metal, M_1, in powdered form so

that the reaction:

$$M^{n+} + M_1 \longrightarrow M + M_1^{n+} \tag{4.19}$$

can occur.

4. The electrolysis.
5. The liquor from the electrolysis cells may contain a relatively high percentage of elements which were originally minor constituents (e.g.arsenic containing liquor from Cu cells) and such elements are often extracted. In any case, the effluent liquors must be treated to remove transition-metal and heavy-metal ions before they are discharged into the environment.

The technology of these electrowinning processes is very simple. The cells are open concrete tanks lined with rubber or plastic and the lines of anode and cathode plates are placed alternatively with a separation of 5–15 cm; the cells are connected monopolar and one arrangement is shown in Fig. 4.5. The anodes are lead alloy sheets which in the sulphate medium form a lead oxide coating; the metal additions to the lead (e.g. silver) are to catalyse oxygen evolution and therefore reduce the anode overpotential. The starter sheets for the cathodes are aluminium or titanium and the metal is deposited until there is a layer 3–5 cm thick, at which point the cathodes are removed from the cell. The metal is then stripped from the starter sheets and these are reused. The electrodes are typically 0.3–0.5 m^2 in area but the anodes are always larger than the cathodes to prevent

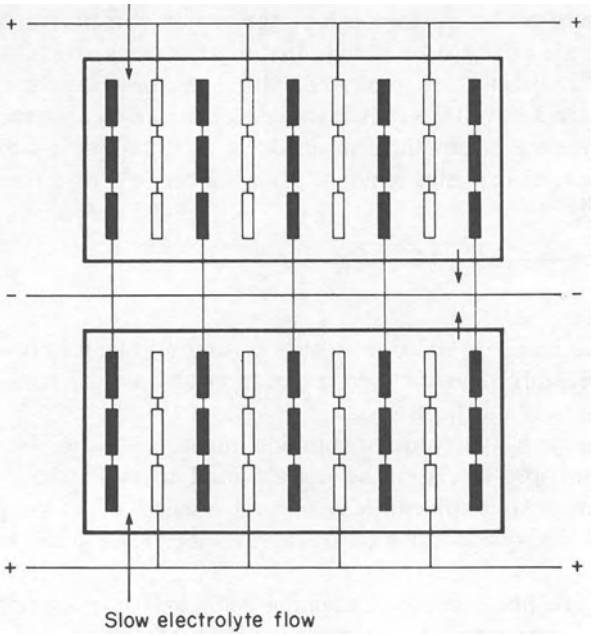

Fig. 4.5 General layout of a copper electrowinning cell house.

deposition edge effects and, hence, obtain an even deposit. The electrolyte is flowed slowly through the cells and there is often no attempt to introduce convection since this can lead to contamination of the cathode deposits by solids which form in the cell. On the other hand, air sparging of the cathode surface (i.e. passing air through a series of nozzles below the cathode) can increase the current density by a factor of 5–10.

For copper electrowinning, the electrolyte feed is sulphuric acid (2 mol dm^{-3}) with copper sulphate (0.5–1 mol dm^{-3}) together with various additives (e.g. glue, thiourea, gelatin) in low concentrations to improve the quality of the copper deposit by increasing crystallinity and avoiding dendrites and gas occlusions (Chapter 8). The operating conditions depend critically on the impurity content of the electrolyte but typically these would be electrolyte temperature (40–60° C) current density (15–150 mA cm^{-2}) cell voltage (from -1.9 to -2.5 V) and current efficiency (80–96%). Commonly, the purity of the copper deposit exceeds 99.5% and the energy consumption is in the range 1900–2500 kWh per ton of copper. Thus, for a production rate of 10^4 ton $year^{-1}$, a cell house might contain twelve tanks each with 100 sets of parallel anode and cathode pairs and a total cathode area of 100 m^2.

For zinc the electrolyte is sulphuric acid and zinc sulphate (0.5–1 mol dm^{-3}) and the usual additives are silicate or animal glue. The current density is 30–75 mA cm^{-2}, requiring a cell voltage of about -3.3 V and an energy requirement of 3000–3500 kWh t^{-1}.

The present cell houses are designed for ease of operation and the absence of shorts and it is clear that they have a number of shortcomings, namely:

1. The cells are not designed for energy efficiency. The interelectrode gaps are large and the oxygen overpotential at the anode is considerable.
2. The productivity of the cell house is poor; the low current density and the cell design combine to give a low space–time yield. Not only does this lead to large cell rooms but also to large quantities of metal being tied up in the cell house; the residence time of a metal atom may be up to a month, and this represents a considerable investment at present prices.
3. The concentration of the metal ion must be high. The leaching of low-grade ores leads to dilute solutions which must be concentrated and it would be advantageous to have cells which could handle more dilute leach solutions directly.
4. Care must be taken to control the build up of soluble redox species; e.g. significant levels of dissolved iron may reduce the anode and cathode current efficiencies via a parasitic redox shuttle:

$$Fe^{3+} + e^- \underset{\text{anode}}{\overset{\text{cathode}}{\rightleftharpoons}} Fe^{2+} \qquad E^\circ = 0.77 \text{ V} \tag{4.20}$$

These limitations have encouraged developments in two directions. Improvements in conventional plate-in-tank cells have included:

1. Enhanced and more uniform mass transport (via air-sparging, forced electrolyte circulation, ultrasonics and tapered anodes) which permits higher current density operation (Fig. 4.6).
2. Reduced anode overpotential via the addition of, for example, Co(II) ions to an acid copper sulphate electrolyte ($>10\ mg\ dm^{-3}$) involves the following

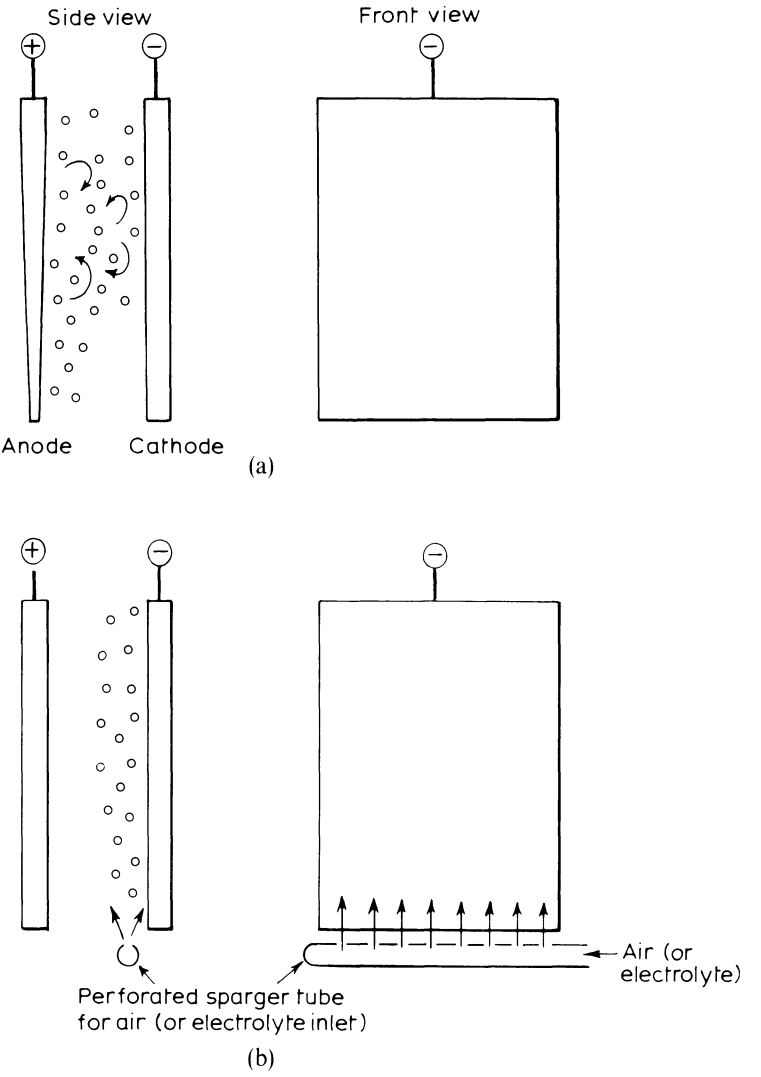

Fig. 4.6 Methods of improving mass transport in vertical plate-in-tank electrowinning cells. (a) Tapered anode with mass transport improved by oxygen evolution at the anode (cathodic hydrogen evolution may also enhance mass transport). (b) Air-sparging (electrolyte jetting may also be used; electrolyte outlet is not shown.)

reactions. At the anode:

$$Co^{2+} - e^- \longrightarrow Co^{3+} \tag{4.21}$$

which is followed by:

$$4Co^{3+} + 2H_2O \longrightarrow 4Co^{2+} + 4H^+ + O_2 \tag{4.22}$$

Reactions (4.21) and (4.22) serve to reduce the overpotential for oxygen evolution. An additional benefit of the Co(II) is a reduced dissolution rate of Pb–Sb anodes, leading to a lower lead contamination of the copper deposit (to a level $< 10\ mg\ kg^{-1}$).

3. Alternative anodes may be used, particularly the various dimensionally stable anodes (DSA) coatings based on precious metals and their oxides. The correct choice of such materials may allow a longer anode lifetime and low oxygen overpotentials.
4. Alternative anodic reactants include Fe^{2+} (reaction (4.20)) and SO_2.

Both of the anodic reactions:

$$Fe^{2+} - e^- \longrightarrow Fe^{3+} \tag{4.23}$$

$$SO_2 + 2H_2O - 2e^- \longrightarrow SO_4^{2-} + 4H^+ \tag{4.24}$$

have appreciably lower electrode potentials than that of oxygen evolution (reaction (4.15)) allowing a reduction in overall cell voltage, e.g. a thermodynamic comparison of the overall cell reactions for conventional and SO_2-modified procedures may be made:

$$Cu^{2+} + H_2O \longrightarrow Cu + \tfrac{1}{2}O_2 + 2H^+ \tag{4.25}$$

$$\Delta H = 221\ kJ\ mol^{-1}\ Cu$$
$$\Delta G = 172\ kJ\ mol^{-1}\ Cu$$

$$Cu^{2+} + SO_3^{2-} + H_2O \longrightarrow Cu + 2H^+ + SO_4^{2-} \tag{4.26}$$

$$\Delta H = -77\ kJ\ mol^{-1}\ Cu$$
$$\Delta G = -32\ kJ\ mol^{-1}\ Cu$$

Thus, the cell reaction involving SO_2 oxidation has a much more favourable cell voltage, enthalpy change and Gibbs free energy change. However, reaction (4.24) has rather slow kinetics, especially at high current densities, and this reduces the advantages in practice.

A very strong effective anodic depolariser is Fe^{2+}, but its presence may handicap the overall cell efficiency via the incidence of parasitic redox shuttles (reaction (4.20)).

Several attempts have been made to regenerate Fe^{2+} from anodically produced Fe^{3+} by SO_2 sparging (which also seems to improve mass transport):

$$2Fe^{3+} + SO_2 + 2H_2O \longrightarrow 2Fe^{2+} + 4H^+ + SO_4^{2-} \tag{4.27}$$

$$2Fe^{2+} + SO_2 + O_2 \longrightarrow 2Fe^{3+} + SO_4^{2-} \tag{4.28}$$

The behaviour of the system depends upon the SO_2 level in the air feed. At $<5\%$, SO_2 reaction (4.28) occurs; and at $>5\%$ reaction (4.27) predominates.

5. Smaller interelectrode gaps may be achieved by air agitation, a more rigorous control of deposit uniformity and more careful positioning of electrodes.
6. A higher metal quality (in terms of harder, more dense and finer-grained deposits) may be achieved by improved solution agitation and the judicious control of electrolyte composition. (Under adverse flow conditions, and in the absence of anode bags or rapid filtration, particulate matter may be entrained in the deposit.)
7. Anode quality is vital; in particular, insoluble particulate matter (from soluble Cu anodes) in copper electrorefining or $PbSO_4$ (from inert Pb–Ag or Pb–Sb) in copper or zinc electrowinning may cause deleterious deposits. Metallurgically homogeneous, fine-grained soluble anodes are usually preferred via, for example, rolled fabrication techniques.
8. In order to provide particularly low anode overpotentials, a recent development has been the use of hydrogen diffusion anodes. Hydrogen gas is continuously passed through a porous, catalytic anode matrix, to facilitate hydrogen oxidation. Hydrogen anodes have already been introduced into some zinc electrowinning tank houses.

While each of these techniques has been tried at the pilot scale, very few have reached and survived full plant-scale operations for extended periods. It may be argued that in terms of low investment and running costs, rapid plant modification and relatively marked technical improvements, air agitation is the single best improvement.

An alternative approach is the development of different types of cell design, particularly those utilizing three-dimensional electrodes. This strategy is an attractive one for the treatment of dilute (say $<2\ g\ dm^{-3}$) metal-containing liquors, where the increased mass transport and electroactive area of the three-dimensional cathodes is very important in order to sustain a reasonably high current (and, hence, production rate of metal), e.g. cells with packed, 'spouting' or fluidized beds of carbon or metal particles have been operated on a pilot plant and full plant scale. Such cells are described in detail in Chapters 2 and 7.

Particulate electrodes, however, have difficulties: (1) there is an uneven potential distribution and, hence, current distribution along the direction of current flow; and (2) the bed tends to coalesce during electrowinning, particularly on a long timescale and with concentrated metal ion solution – this destroys the favourable properties of such electrodes. Hence, at the present time, cells with particulate electrodes are considered more likely to have an impact in metal recovery from industrial process liquors and effluents (Chapter 7) than in large-tonnage electrowinning.

4.1.4 Electrowinning of gold

While many types of cell design are currently in use, the Zadra type of cell (Fig. 4.7(a)) has been favoured by industry since its inception in 1952.* The design

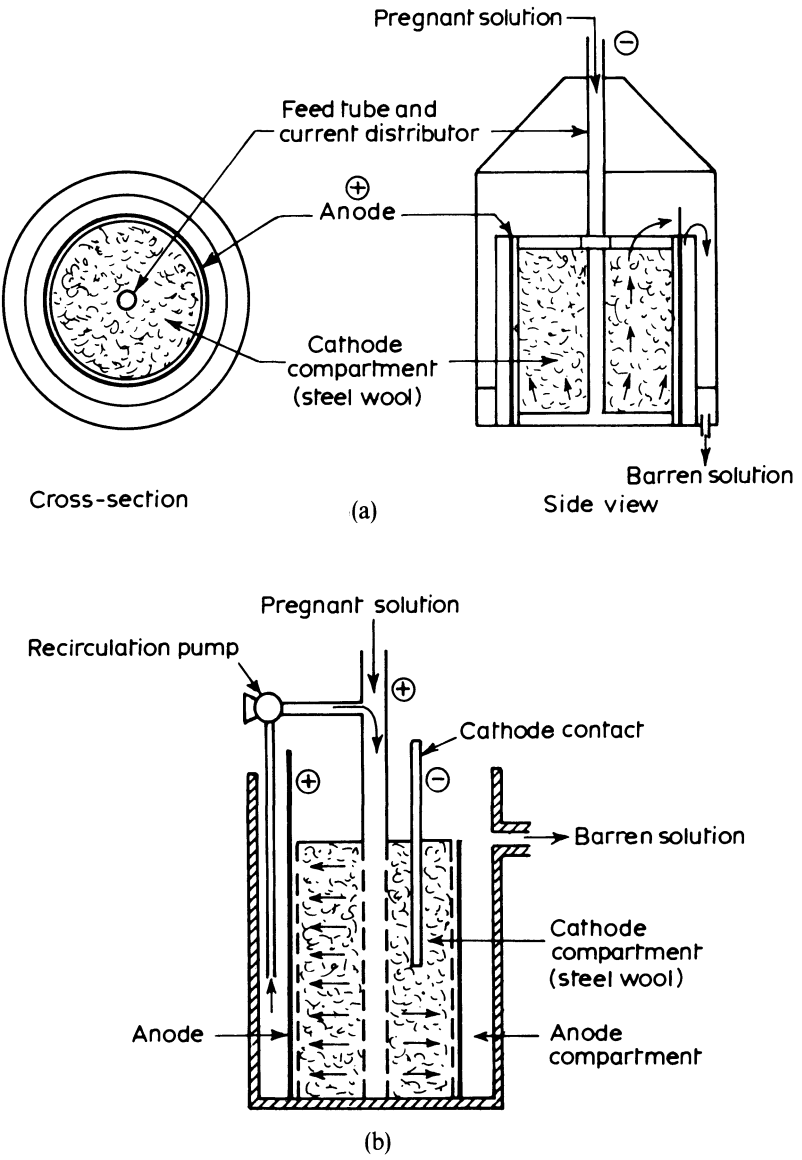

Fig. 4.7 Gold electrowinning cells. (a) The traditional Zadra cell design. (b) A modified Zadra cell, the improved mass-transfer cell. (After: US Bureau of Mines.)

* J. B. Zadra, A. L. Engel and H. J. Heinen, US Bureau of Mines Report 4843 (1952)

utilizes three concentric cylinders. The inner one, which serves as the cathode compartment, is a perforated polymer containing a central feed tube, current distributor and steel wool cathode. The anode – a circular stainless steel mesh – lies outside the cathode. Pregnant, gold-rich, liquor enters the cell from the bottom of the central feed tube and flows upwards, distributing radially through the steel wool. Electrolyte temperatures are usually maintained at 70–85° C. Typically, at a relatively low electrolyte flow rate of 10 $dm^3 min^{-1}$, the nominal residence time in the cell is approximately 5 min. Depending on the electrolysis conditions and electrolyte composition, gold deposits in the steel wool matrix as a sponge, compact layer or powder. In any case, the Fe–Cr stainless steel wool may be removed from the gold by fluxing and melting followed by extraction of the Fe–Cr oxides from the slag.

The Zadra cell, however, suffers from several drawbacks:

1. Electrolyte flow is unevenly distributed throughout the porous cathode; the resulting non-uniform mass transport gives rise to uneven deposition and wastage of electrode area.
2. The effective interelectrode spacing is excessive, resulting in a relatively high cell voltage.
3. The volume of the cell is not utilized effectively.

The circular improved mass transport cell (Fig. 4.7) has recently been designed to overcome these problems. The solution-distribution tube is stainless steel and serves as a second anode, decreasing the effective interelectrode spacing and improving current distribution. The cell hydrodynamics are rendered more uniform by rapid internal recirculation of electrolyte. Gold deposition rates are increased by a factor of up to 2. Prototype work was conducted using a circular cell, typically operating at ambient temperatures (20–21° C), a cell voltage of −3.0 V and a cathode packing density of 0.018 $g cm^{-3}$, with an internal circulation rate of 2 $dm^3 min^{-1}$. The cathode volume is 888 cm^3 and operating currents are *c.* 1A. (Rectangular designs, which have improved scaling features, are currently being used for full-scale electrowinning.) A combined Ag–Au feed yields a cathode current efficiency up to 7% for Au and 25% for Ag at deposition rates of 8 and 16 mg min^{-1} respectively.

4.2 CEMENTATION

The removal of a metal M from solution by chemical displacement (i.e. cementation of a metal onto a more base metal M_1 substrate) is widely used in hydrometallurgy:

$$M^{n+} + M_1 \longrightarrow M_1^{n+} + M \tag{4.19}$$

Both metals are in finely divided powder or flake form.

The overall process may be subdivided into the individual electrode reactions (which take place under open-circuit conditions on the surface of M_1):

Cathode: $$M^{n+} + ne^- \longrightarrow M \tag{4.10}$$

Anode: $$M_1 - ne^- \longrightarrow M_1^{n+} \tag{4.12}$$

The major secondary cathode process is typically H_2 evolution:

$$nH^+ + ne^- \longrightarrow n/2H_2 \tag{4.11}$$

which gives rise to loss of reactant by corrosion. Coupling reactions (4.12) and (4.11):

$$M_1 + nH^+ \longrightarrow M_1^{n+} + n/2H_2 \tag{4.29}$$

Another parasitic cathodic reaction is possible if the base metal dissolves (or is oxidized) to give an active redox species, e.g. iron may dissolve as Fe^{2+} which chemically oxidizes to Fe^{3+}. Then:

$$M_1 + nFe^{3+} \longrightarrow M_1^{n+} + nFe^{2+} \tag{4.30}$$

For efficient cementation, reaction (4.19) must progress nearly to completion at a rapid rate. In practice, the cemented metal M is not pure; contamination with residual, undissolved M_1 occurs. Reaction (4.19) also becomes restricted by mass transport of M^{n+} to, and M_1^{n+} from, the reaction sites, particularly during the processing of more dilute liquors.

Cementation is usually carried out in stirred tanks. Sluggish kinetics necessitate relatively large reactors and the metal particles must be disturbed continuously to reveal fresh substrate metal and maintain a high active area.

Several types of cementation reactor have been developed including ones employing hydraulic agitation, rotating-drum reactors, oscillating chamber reactors, and fluidized beds.

More recently, a process has been developed which utilizes a fluidized bed of iron particles subjected to an external, pulsating magnetic field (Fig. 4.8). The particles are given a higher velocity and an increased frequency of collision by the magnetic field. The cemented material (e.g. copper) is readily detached and entrained in the liquid flow, being separated by decantation or filtration. Iron particles are retained and confined to the active magnetic zone of the reactor, where the metal is fully consumed. Replenishment may be achieved continuously by the addition of fresh iron particles. This process has several possible advantages over conventional cementation:

1. Increased mass transport and higher rate of reaction due to enhanced particle movement and collision rate.
2. Higher utilization of starting material due to continuous exposure of active material.

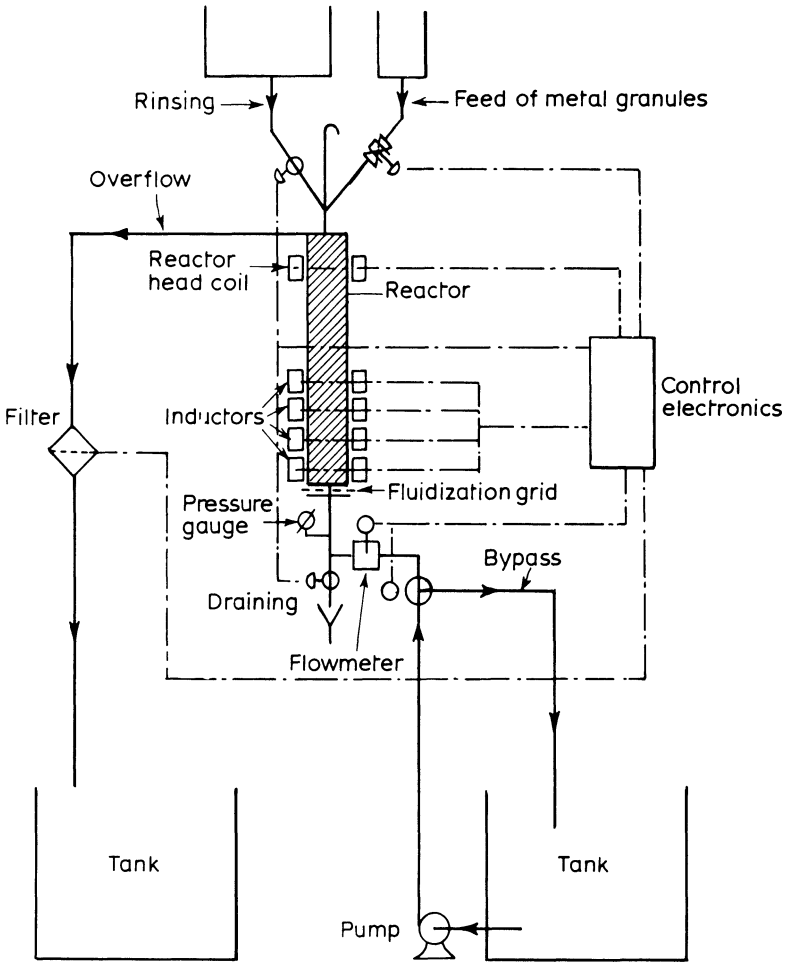

Fig. 4.8 A fluidized-bed cementation process enhanced by a pulsed magnetic field – the Actimag process. (Courtesy: Darcy Products Ltd.)

As an example of the performance of this process, a reactor of diameter 0.25 m and bed height 3 m may be used to treat a liquor containing Cu (5 g dm^{-3}) in H_2SO_4 (pH 3). With a volumetric flow rate of 20 $m^3 h^{-1}$, the outlet concentration of copper is typically 100 mg dm^{-3} (equivalent to a copper recovery of 99%). The iron consumption under these conditions is 0.95 kg Fe/kg Cu, equivalent to 93% utilization of iron according to:

$$Fe + Cu^{2+} \longrightarrow Fe^{2+} + Cu \tag{4.31}$$

The copper cement is obtained after drying, as a red powder in the size range

5–400 μm, depending on the operating conditions. The copper purity can be >98.5% wt Cu, falling to 97% wt Cu as iron is consumed in the reactor at longer times. The major impurities are 0.8–1% wt C (from the steel-feed particles), 0.5–1.5% wt oxygen and 0.1–0.2 % maximum Fe. Following the remelting of dried and compacted cement, >99% Cu is obtained.

4.3 ELECTROREFINING

In an electrorefining process, the anode is the impure metal and the impurities must be lost during the passage of the metal from the anode to the cathode during electrolysis, i.e. the electrode reactions are, at the anode:

$$M - ne^- \longrightarrow M^{n+} \tag{4.12}$$

and at the cathode:

$$M^{n+} + ne^- \longrightarrow M \tag{4.10}$$

Electrorefining is a much more common process than electrowinning and such plants occur throughout the world on scales between 1000–100 000 ton year^{-1}. Usually they are part of a larger operation to separate and recover pure metals from both scrap and primary ores. Therefore, the process must be designed to handle a variable-quality metal feed and lead to a concentration of all the metals present in a form which can be treated further. Electrorefining often provides a particularly high purity of metal.

Electrorefining processes using a molten salt or non-aqueous electrolyte are used (e.g. see aluminium refining in section 4.3.3) and, indeed, are the subject of further development. This is due to the possibilities they offer for increasing current densities and refining via lower oxidation states not stable in water (e.g. refining of copper via Cu^+ would almost halve the energy requirement). However, aqueous processes presently predominate due to their ease of handling, more developed chemistry and familiarity with aqueous process liquors and electrolytes.

4.3.1 Aqueous electrorefining

The conditions used for the refining of five metals are summarized in Table 4.3. The electrolyte and other conditions must be selected so that both the anodic dissolution and the deposition of the metal occur with high efficiency while none of the impurity metals can transfer from the anode to the cathode. Certainly there must be no passivation of the anode (Chapter 10) and the objective is to obtain a good-quality, often highly crystalline, deposit at the cathode. Where necessary, additives are added to the electrolyte to enforce the correct behaviour at both electrodes. Chloride ion is a common addition to enhance the dissolution process and, where essential, organic additives are used to modify the cathode deposit. Since, however, organic compounds can be occluded to some extent and reduce the purity of the metal, their use is avoided when possible.

Table 4.3 Parameters for electrorefining processes

Metal	Concentration of components in electrolyte/g dm^{-3}	I/mA cm^{-2}	−Cell voltage/V	T/°C	Current efficiency/%	Impurity metals	
						Slime	Solution
Cu	$CuSO_4$ (100–140) H_2SO_4 (180–250)	10–20	0.15–0.30	60	95	Ag, Au, Ni, Pb, Sb	Ni, As, Fe, Co
Ni	$NiSO_4$ (140–160) NaCl (90) H_3BO_3 (10–20)	15–20	1.5–3.0	60	98	Ag, Au, Pt	Cu, Co
Co	$CoSO_4$ (150–160) Na_2SO_4 (120–140) NaCl (15–20) H_3BO_3 (10–20)	15–20	1.5–3.0	60	75–85	—	Ni, Cu
Pb	Pb^{2+} (60–80) H_2SiF_6 (50–100)	15–25	0.3–0.6	30–50	95	Bi, Ag, Au, Sb	—
Sn	Na_2SnO_3 (40–80) NaOH (8–20)	5–15	0.3–0.6	20–60	65	Pb, Sb	—

The process for electrorefining copper is typical of those carried out in aqueous solution. The electrolyte is copper sulphate ($0.7\,mol\,dm^{-3}$) and sulphuric acid ($2\,mol\,dm^{-3}$) and the way in which the purification of the copper occurs can be seen by considering the metals likely to be found as impurities:

1. Ag, Au and Pt are more noble than copper and therefore will not dissolve anodically. They will be found as metals in the anode slime.
2. Sn, Bi and Sb dissolve anodically but will precipitate in the electrolyte as oxides or hydroxides which will be found in the anode slime.
3. Pb is oxidized anodically but will form insoluble lead sulphate in this electrolyte. Again, this will fall to the slime in the base of the cell.
4. Fe, Ni, Co and Zn all dissolve anodically and in the sulphate medium form species which are soluble in the electrolyte. The species formed, however, only reduce at potentials more negative than that at which the copper deposits and therefore remain in the electrolyte.

Hence, the impurities accumulate in either the electrolyte or the cell slime and these can be processed further to recover the significant metals.

The electrolytic cells are generally of a very simple open-tank and parallel-plate electrode design, similar to that described above for copper winning except that the anodes are now of the impure copper. The copper anodes must have the correct size and geometry (i.e. flat plates larger than the starter sheets of aluminium, titanium or steel for the cathodes to avoid heavy edge deposits) and have a homogeneous composition. The flow rate of the electrolyte through the cells is low so that the slime drops to the base of the cell and does not come into contact with the cathode.

Figure 4.9 summarizes the total process. Normally, the sludge removal is by filtration of the electrolyte, although in some cases (e.g. Pb) the sludge collects on the anode which periodically must be removed from the cell and scraped. Before recycle, the electrolyte must be purified and the concentration of metal ion, electrolytes and addition agents adjusted to the correct values. The purification normally involves cementation or precipitation (by addition of hydroxide or sulphide ion or by change of oxidation state, e.g. Sn(II) → Sn(IV)). The exact procedure will depend on the level and type of impurities in the electrolyte.

It can be seen from the data in Table 4.3 that in order to obtain pure metals at the cathode, the current density is always low. On the other hand, with the exception of tin, the current efficiencies are good and the cell voltages can be low. In electrorefining the cathode reaction is the reverse of that at the anode and therefore, in the ideal case, the cell voltage is only required to drive the current through the electrolyte. In practice, there may also be overpotentials associated with the anode and cathode reactions, and in the cases of nickel and cobalt these are considerable because the M/M^{2+} couples are very irreversible. The energy consumptions are relatively low, in the range 200–1500 $kWh\,ton^{-1}$ of metal, and to the present time this has led to the use of cells with relatively large interelectrode gaps (5–15 cm) which minimizes the labour costs for checking

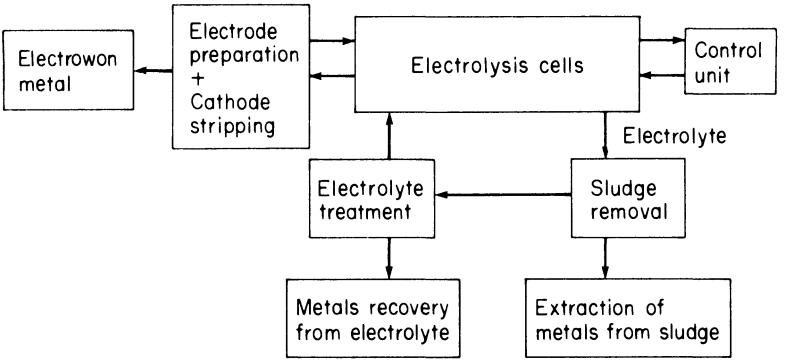

Fig. 4.9 Hydrometalurgical process including an electrolysis step for the refining of a metal and the recovery of the minor elements.

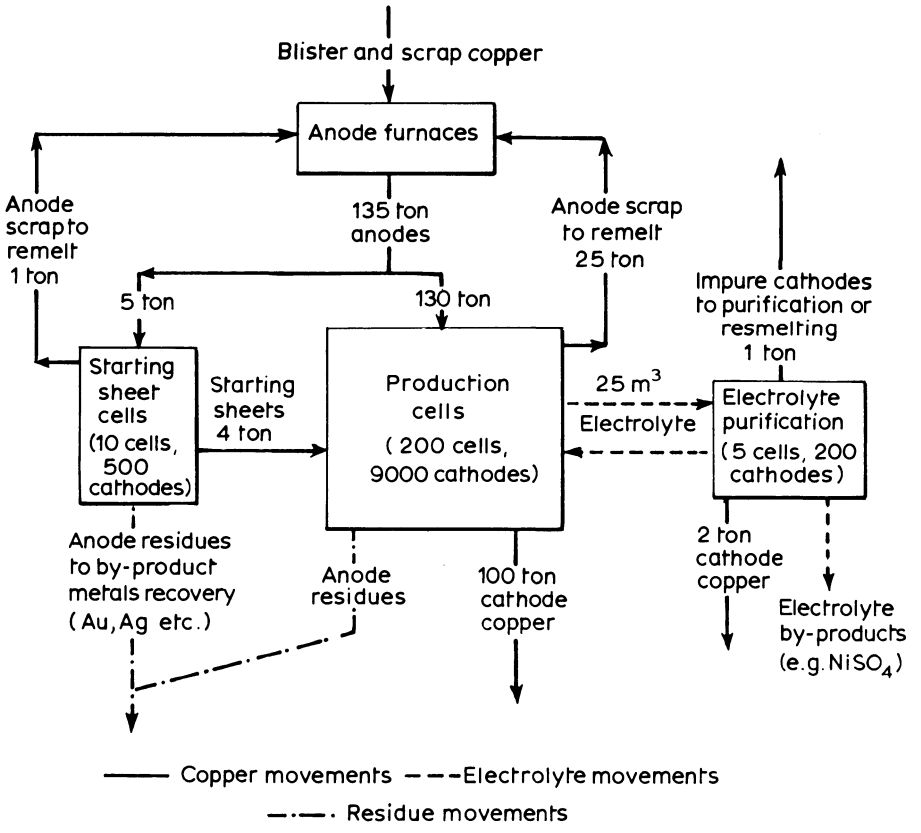

Fig. 4.10 A flow sheet for a copper refinery. The approximate weights or volumes of intermediates 100 tonnes of cathode copper are indicated. (A portion of the electrolyte goes to purification.)

cells to prevent shorts and to handle electrode changes. The low current densities contribute to the low energy consumption (the iR term is small) but causes the cell houses to be large and, more importantly, the inventory of metal tied up in the cell house is large. The residence time of the metal in the cell is often 21–28 days and this is expensive, particularly in the case of silver, gold and the platinum group metals. Hence, increased current densities without loss in purity of the refined metal would be advantageous.

As an illustration of large-scale electrorefining, the process for Cu may be considered in more detail. Virtually all copper produced from ore receives an electrolytic treatment at some stage either via electrorefining from impure anodes or electrowinning from leach or solvent-extraction liquors. Electrorefining produces the majority of cathode copper *c.* 95% as opposed to *c.* 5% from electrowinning). The electrorefining step serves two purposes:

1. Elimination of unwanted impurities; cathode copper typically has a purity $>99.9\%$ wt Cu, with $<0.005\%$ total metallic impurities.
2. Separation of valuable impurities which can be recovered in other processes (section 4.2).

Figure 4.10 shows a general flowsheet of the copper refining operation.

The major technical factors in electrorefining are the cathode purity, the production rate and the specific energy consumption. These factors are influenced primarily by anode quality, electrolyte conditions and cathode current density.

Typical electrolyte conditions are shown in Table 4.4. The electrolyte additionally contains organic additives which serve to control copper electrocrystallization at the cathode (levellers and brighteners) and help prevent insoluble

Table 4.4 Typical electrolyte conditions for copper electrorefining

Component	Concentration/g dm^{-3}
Cu	40–50
H_2SO_4	170–200
	Upper limits
Ni	20
As	10
Fe	2
Sb	0.5
Bi	0.2
Cl	0.03
Specific gravity	1.25 ± 0.03
Temperature	60–65° C

particulates from codepositing (surfactants). Temperature is usually maintained via steam-heating at 60–65° C (inlet to cell), falling to 55–60° C (cell outlet). Circulation rates are typically 0.01–0.03 $m^3 min^{-1}$, a cell achieving a nominal change of electrolyte every 4–6 h. This circulation helps to control temperature, gently increase the mass transport, prevent compositional gradients, replenish addition agents and serve as a convenient stream for bleeding-off impurities. The electrolyte composition is maintained by purification of the bleed stream in three sequential steps:

1. Removal and recovery of copper, usually by electrowinning in stage-1 'liberator' cells (Table 4.5).
2. Removal of As, Sb and Bi via electrowinning them onto an impure Cu deposit.
3. Evaporation of water and precipitation of Ni, Fe and Co as sulphides.

In order to achieve high production rates, high current densities are obviously desirable. However, an excessive current density causes at least two problems: (1) increased impurity levels in the cathode deposit; an increased roughness promotes occlusion of anode residues and electrolyte; and (2) anode passivity occurs at current densities above 25–28 mA cm^{-2}.

In modern refineries, cathode current efficiency is 90–97%, anode curent efficiency being slightly higher. Inefficiency results from strong currents to ground (1–3%), anode–cathode short circuits (1–3%) and loss of copper deposit by air (or Fe^{3+}) oxidation (*c.* 1%). Ground leakage currents are minimized by the avoidance of electrolyte spillage. Short-circuiting is predominantly caused by nodular or dendritic growth which must be removed or restricted by suitable addition agents. A range of modern aids is available to monitor and identify shorts including computer monitoring of current distribution and infrared detection of 'hot spots'.

Table 4.5 Liberator cell stages in the removal of copper from bleed streams

Stage	Approximate change in copper concentration/g dm^{-3}	Cathode product
1	45–15	Commercial purity cathodes
2	15–8	Cathodes may require remelting in the anode furnace and re-refining
3	8–0.2 (requires hooding as poisonous arsine (AsH_3) gas may be evolved)	Very impure, especially high in As and Bi. Cathodes require purification prior to remelting in the anode furnace

The typical voltage components are shown in Table 4.6. Specific electrolytic energy consumption is around 0.22 kWh kg^{-1} cathode copper, which is increased to *c.* 0.31 kWh kg^{-1} by additional power components. (Table 4.7)

Perhaps the most significant recent development in copper refining has been periodic current reversal which permits an increase (of $<15\%$) in production rates via two effects: (1) the anodic current density at which passivations occur may be increased; and (2) selective removal of Cu high spots (e.g. nodules) during the reverse current gives smoother cathode deposits.

Optimum conditions of periodic current reversal permit cathode current densities of up to 36 mA cm^{-2}. The preferred ratio of forward-current time: reverse-current time is 20 or 30 to 1, with identical forward and reverse currents, for a cycle time of 0.5–3 min.

Table 4.6 Typical voltage components in a copper electrorefining cell

	−Voltage/V
Voltage drop in the electrolyte	0.11–0.13
Cathode overpotential due to organics and polarization	0.04–0.08
Anode and cathode electrical connections	0.03–0.06
Busbar and lead losses	0.01–0.02
Anode polarization	0.0–0.01
Cell voltage	0.23–0.27

Table 4.7 Typical contributions to specific energy required for copper electrorefining

Component	Specific energy required/kWh ton^{-1}
Electrowinning energy (production and starting sheet cells)	220
Electrowinning ('liberator') cells, purification section	25
Lead and busbar losses	15
Total d.c. energy	260
Conversion loss at 95% energy-conversion efficiency	15
Total a.c. energy for deposition	275
Auxiliary equipment	35
Grand total a.c. energy	310 kWh ton^{-1} of cathode

4.3.2 Precious metals

Several additional factors serve to distinguish precious metals (mainly Ag, Au and the Pt group) from others which are treated by electrometallurgical routes:

1. Their restricted amounts and availability.
2. The high costs involved.
3. The need to treat dilute solutions in some cases.
4. The requirement to process rapidly an impure metal to produce a pure, presentable and saleable commodity in a fluctuating market.

These factors have several possible implications for cell design, including a tendency for: (1) batch operation; (2) rapid (and substantially complete) electrolysis; (3) a small inventory of (possibly dilute) electrolyte; (4) high security against process failure, e.g. by leakage of electrolyte, theft or fraud; and (5) process design for, and rapid recycling of by-products such as slimes.

The selection of a particular cell has usually followed empirical, traditional or proprietary designs. This trend has been aggravated by the reduced importance of electricity costs in comparison with more base, larger-tonnage metals. One result is that a large number of broadly similar and dated cells are used routinely. Another consequence is that some 'novel' cell designs have been adopted in an empirical, unoptimized fashion.

The adoption of a particular electrorefining process or cell depends to an extent on the purity and form and, hence, the source of the metal. The case of dilute process liquors is considered in more detail in Chapter 7, as are some of the more recent cell designs.

(*a*) *Silver*

The anode material for silver electrorefining is mainly derived from anode slimes from copper, lead, nickel and zinc electrorefining processes together with diverse contributions from the secondary recovery and scrap-recovery processes.

The first industrially accepted process for silver refining was patented by Moebius in 1884 who used an acidic silver nitrate electrolyte. An industrial plant was commissioned in 1885 and the modern refining of silver still follows this pioneering work quite closely.

The general requirements of a silver electrorefining process are:

1. Production of silver, usually in a crystalline form, which can be removed from the cathode, washed and dried as pure metal.
2. Uniform dissolution of the impure anodes (which are normally cast) at a high current efficiency.
3. Closely comparable anode and cathode efficiency such that the silver level in the electrolyte may remain relatively constant.
4. Consideration of the consequences of production of anode silver slime due to insoluble impurities. The anodes must remain active and precious metals must be continuously reclaimed from the slime. The cathode product must not be affected detrimentally by inclusions.

5. Ease of replacement of used anodes.

The above requirements lead to the need for relatively simple geometries usually based on 'tank' cells where the anodes are surrounded by porous bags, baskets or membranes to contain anode debris and slime. There are two traditional cell designs which, with modern improvements in engineering design and constructional materials, persist today. The Moebius cell uses a vertical electrode arrangement, while the Balbach cell (later improved by Thum) uses horizontal electrodes.

Anode slimes collected from the mud of copper refining cells are leached, roasted, fire-refined and cast into anodes (Fig. 4.11), the composition being known as Doré metal (Table 4.8).

In the Moebius cell (Fig. 4.12), the anodes are cast, drilled, then bolted to hanger bars. A woven cloth or polymer bag of controlled porosity surrounds the anodes to catch slime. The cathodes are usually stainless-steel plates which

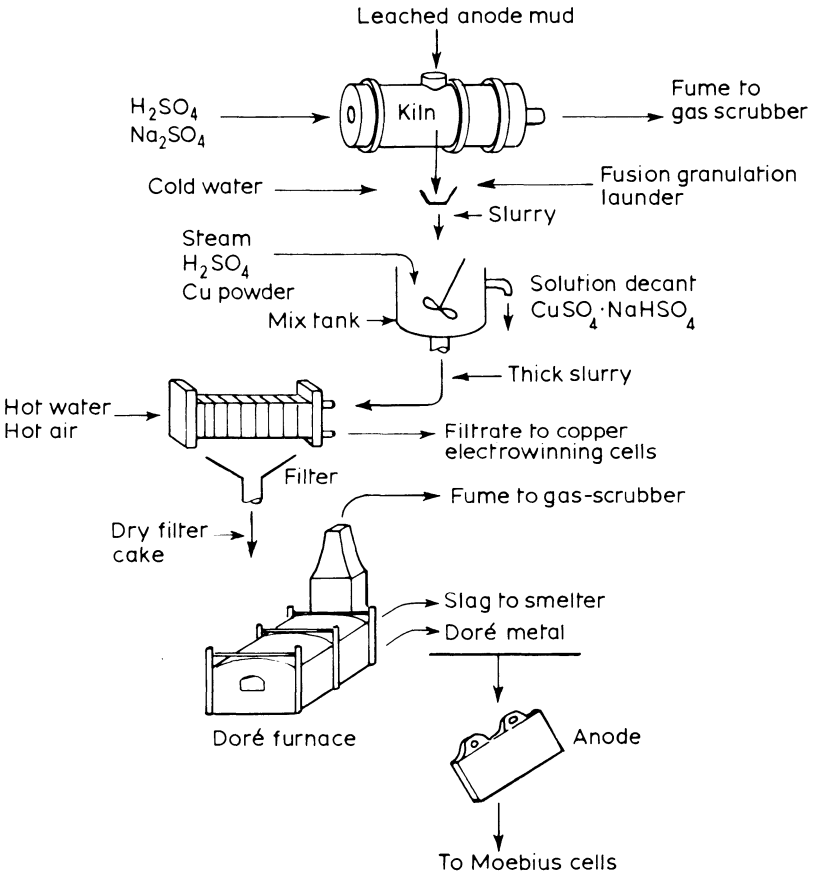

Fig. 4.11 Simplified flow sheet for the treatment of anode slimes from copper electrorefining cells.

Table 4.8 Typical composition (% wt) of anode mud and Doré metal obtained from copper electrorefining cells

Element	Anode mud	Doré metal
Au	0.8	8–9
Ag	8	86–92
Cu	30	0.5–1.0
Pd	0.0064	0.16–0.19
Pt	0.00056	0.004–0.009
Pb	2	0.02
Te	3	0.003
Se	12	0.00002
As	2	—
Sb	0.5	—

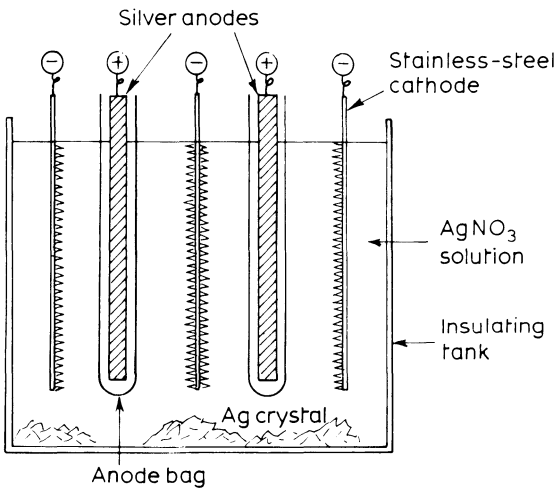

Fig. 4.12 Sectional view of a Moebius cell for electrorefining of silver.

facilitate removal of silver crystals by scraping (which may be manual and intermittent or automatic and continuous via reciprocatory wiper blades). In the latter case, the silver falls to the bottom of the cell from where it is periodically removed. Certain designs incorporate catchment trays to aid product recovery.

A wide variation is found in the detailed design and operating parameters of Moebius-type cells, but the typical range of conditions may be summarized. A 'cell' may have between four and twenty cathodes, operating at 100–500 A and from -1.5 to -2.8 V. The cells are usually operated near ambient temperature with a cathode current density of 20–40 mA cm^{-2}. While the cathode silver purity is dependent upon anode quality, electrolyte purity and operating conditions, >99.9% wt Ag is usually obtained, with 99.99% wt being realized in some cases.

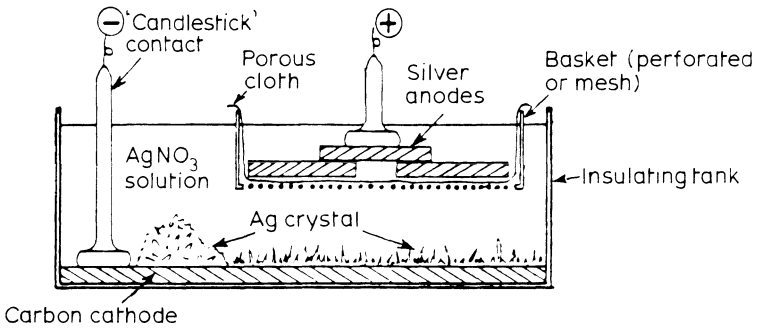

Fig. 4.13 A Balbach–Thum cell for electrorefining of silver.

The Balbach–Thum cell (Fig. 4.13) is designed around a rectangular trough containing a thick, solid carbon plate cathode which covers the cell bottom. An anode basket is suspended in the top of the cell; the basket is fabricated so as to support a number of silver anodes. The anodes are usually cast plates, but smaller, more irregular, pieces of silver scrap can be used. Woven cloth or polymer mesh inside the tray serves to contain insoluble anode material. Recovery of silver is usually by manual scraping, following cathode removal.

Balbach–Thum cells with their higher anode–cathode gap usually operate at a significantly higher cell voltage (from -3.5 to -5.5 V) than Moebius cells. Both cells tend to utilize silver concentrations in the range 30–150 g dm^{-3}. The $AgNO_3$ electrolyte often has free HNO_3 and $CuNO_3$ is occasionally present to help produce large, well-separated, non-adherent crystallites of silver facilitating removal, washing and drying operations. The recovered silver is normally melted and cast into bars for resale, or transformed into pure silver nitrate or other speciality silver chemicals.

There are many advantages and drawbacks to each type of cell (Table 4.9). The Moebius type of design is perhaps best suited to modern automated processing, while the Balbach–Thum cell is preferred for smaller use in low-technology markets. There are many modifications and indeed hybrids of the two cell designs.

A number of rotating cylinder cathode cells have been used as an alternative to the above outdated designs. Figure 4.14 shows one version of such a cell. While a membrane-divided rotating cylinder electrode cell facilitates automatic scraping, provides the convenience of a single cathode and gives a uniform silver product, there are several possible disadvantages which must be considered in cell design:

1. Increases in maintenance levels due to the rotational drive and electrical brushgear.
2. Increased catholyte stirring, if excessive may entrain any insoluble impurities into the deposit or increase the rate of codeposition of any soluble, noble metals present.

Table 4.9 Comparison of silver refining in the Moebius and Balbach–Thum cells

Feature	Moebius cell	Balbach–Thum cell
Anode scrap	Leaves stumps which must be remelted	Consumes all anode material
Cathode scraping	May be almost continuous and automatic	Needs manual scraping at intervals
Anode slimes	Anodes must be bagged individually and carefully positioned; relatively intolerant to anode slimes	A removable one-piece filter cloth may be used with a permanent, coarse mesh; tolerant to anode slimes
Electrolytic power requirements	Closely spaced electrodes lead to a low cell voltage	Larger interelectrode spacing gives a high cell voltage
Floor space	Small	Large (up to 5 times that of a Moebius cell)
Electrolyte inventory	Small	Large, but impurity levels (e.g. Cu) may be lower, allowing more anodes of lower purity to be used
Current density	High	Low (but this may give a lower codeposition of noble metals)
Maintenance	Moving scrapers may give maintenance problems	No moving parts gives fewer maintenance problems

3. Increased Joule heating and maintenance problems of a membrane, e.g. silver may lodge against the membrane, causing early membrane failure due to locally high current densities.

(*b*) *Gold*

Insoluble, black gold residues are recovered from the anode slimes of silver refining cells and are combined with gold collected from the cleaning of anode scrap. This material is water washed on a filter to remove nitrates, boiled with H_2SO_4 to dissolve silver, then washed with water to remove soluble silver. The resulting yellow gold sand is dried, melted and cast into anodes, which typically have a composition: Au 99.2%, Pd 0.5%, Ag $<0.1\%$ and Pt $<0.08\%$ wt.

An acceptable industrial process for the electrorefining of gold was first developed and implemented at the Norddeutsche Affinenie, Hamburg, 1878, by Wohlwill. The Wohlwill cell is broadly similar to the Moebius cell for silver, as it

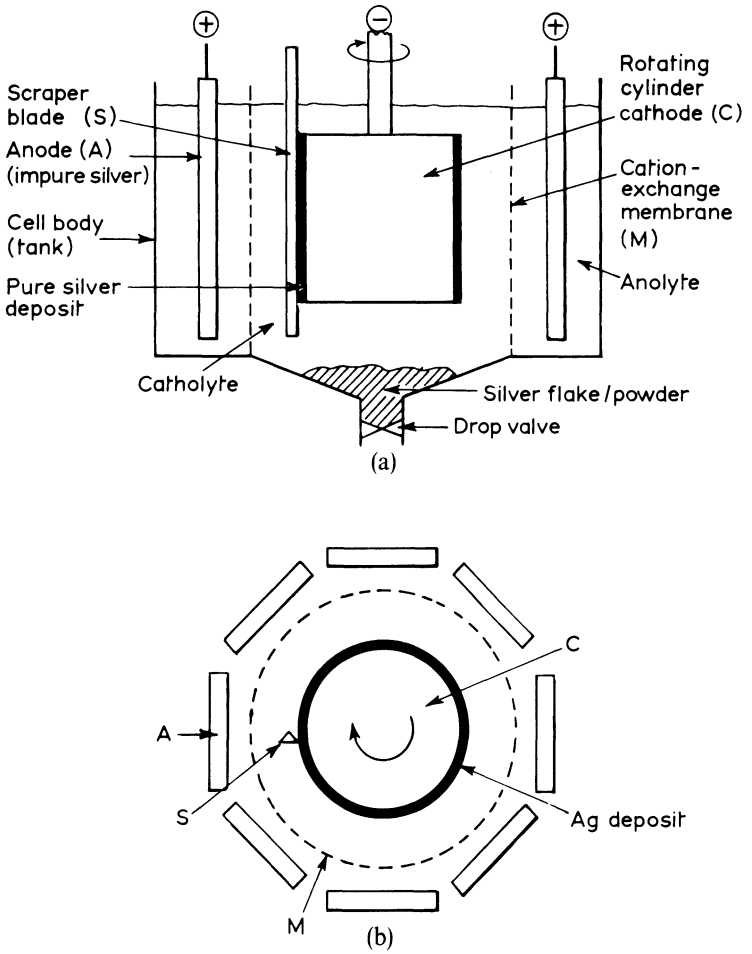

Fig. 4.14 A rotating-cylinder electrode cell for electrorefining of silver. (a) Sectional view. The metal grows as flake, is dislodged continuously by a wiper blade and may be withdrawn at the cell bottom. (b) Plan view. (Compare the metal-extraction cell shown in Fig. 7.7.)

uses vertical electrodes in a tank cell. The gold cells tend to be smaller to minimize the 'lock up' of the precious metal and to utilize an acid auric chloride electrolyte. Older cells utilized thin gold sheet as a cathode but modern practice uses titanium.

Gold dissolves as stable anionic chloro-complexes:

$$Au + 4Cl^- - 3e^- \longrightarrow AuCl_4^- \tag{4.32}$$

$$Au + 2Cl^- - e^- \longrightarrow AuCl_2^- \tag{4.33}$$

These complexes are reduced at the cathode to yield a pure gold deposit:

$$AuCl_4^- + 3e^- \longrightarrow Au + 4Cl^- \quad (4.34)$$

$$AuCl_2^- + e^- \longrightarrow Au + 2Cl^- \quad (4.35)$$

At the anode, metal impurities form chlorides; those of copper and zinc are soluble and gradually build up in solution, while silver and lead chlorides are left as an insoluble slime. Platinum and rhodium also dissolve and are recovered at intervals from the electrolyte when their combined concentration exceeds, say, 75 g dm^{-3}. Significant silver levels may cause problems of anode passivation due to AgCl formation; the coating must then be removed.

In 1908, Wöhlwill modified his process by the use of a pulsed current, in fact a low-frequency a.c. superimposed on the normal d.c. supply. This pulsing allowed insoluble chloride films to flake off the anode, facilitating the treatment of higher silver content gold at elevated current densities.

Wöhlwill cells are usually operated at a relatively high temperature, 60–75°C with significant stirring (usually by air agitation) in order to achieve acceptable gold deposits. Fume extraction to remove HCl/Cl_2 gas is essential at a cathode current density of 10–120 mA cm^{-2}. Cell voltage is typically from -0.9 to -2.5 V. The deposited gold has a purity $>99.9\%$ and following extraction, washing and drying it is melted and cast into marketable bars.

The gold concentration in the electrolyte varies considerably from one installation to another, but values of 140–200 g dm^{-3} are encountered, with a free HCl content of 100–150 g dm^{-3}.

The agitation conditions are important in gold refining cells, an air-lift being the traditional method. Excessive agitation tends to stir up insoluble slime which then codeposits with the gold.

While the Wöhlwill type of process is still applied in small installations and for secondary refining, its large-scale use in primary refining has been superseded by other process routes which allow a smaller 'lock-up' of metal. In particular, the Miller chlorination process involves chemical dissolution of gold as a chloro-complex via Cl_2 gas bubbled through the liquor.

4.3.3 Molten salt electrorefining

The principal metal refined in a molten salt medium is aluminium. Something approaching 2% of the total aluminium produced is refined by a process based on the principle illustrated in Fig. 4.15. The density of the impure aluminium is increased by the addition of copper (25–30%) and that of a cryolite melt by the addition of barium fluoride so that three distinct layers – pure aluminium, melt and aluminium/copper, are formed in the cell. The aluminium is transferred on electrolysis from the anode of impure aluminium to the top layer while the major impurities: (1) Na, Mg, Ca and Sr are oxidized from the anode pool to the melt but do not reduce at the cathode and therefore accumulate in the melt; and

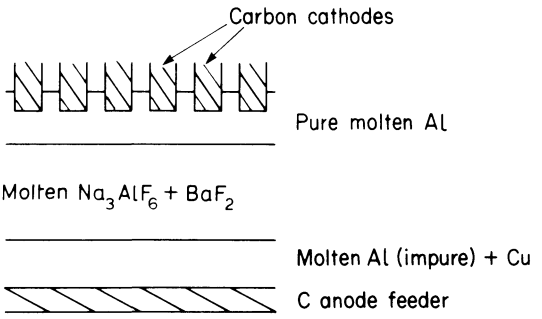

Fig. 4.15 Principle of the molten salt-refining process for aluminium.

(2) Fe, Si, Mn, Zn (and Cu) are oxidized less readily than aluminium and, hence, remain in the anode pool. The aluminium obtained is very pure, being in the range 99.99–99.999%.

Molten salt processes for refining metals as diverse as lead, beryllium, magnesium, molybdenum and uranium have been described but are seldom used commercially.

4.4 ELECTRODEPOSITION OF METAL POWDERS

In most areas of technology, the electrodeposition of metal is carried out under electrolysis and electrode conditions which promote the formation of a smooth, compact film. Important examples include electroplating (Chapter 8, Section 8.1) and electroforming (Chapter 9, Section 9.1).

As the current density is increased, however, the deposit generally becomes rougher in texture and higher in the active area (Chapter 8, Fig. 8.10) as mass transport control begins to exert an influence. Under conditions of significant mass transport control, the roughened deposit may become loosely adherent and disperse, i.e a metal powder is formed. This is the direct electrolytic method for metal-powder formation. Alternatively, for certain metals, the electrolysis conditions may be chosen to give a relatively coherent but brittle deposit which may be transformed to a powder by mechanical comminution.

Empirically, it is well established that powder formation is usually encouraged by:

1. A decrease in the concentration of dissolved metal in the electrolyte.
2. An increase in the concentration of indifferent electrolyte.
3. A decrease in the degree of agitation.
4. An increase in current density.
5. A decrease in temperature.
6. An increase in viscosity.

The above factors are all consistent with the theory that powder deposition is a

mass transport controlled phenomenon. The structure of the metal deposit is also very dependent upon the individual metal and the electrolyte composition, e.g. copper, nickel and iron yield dense, compact deposits at low-current densities, whereas silver, lead and cadmium tend to form flakes or needles from uncomplexed solutions and smooth deposits only from heavily complexed liquors, e.g. cyanides. The deposit quality and adhesion may be changed markedly by surfactants, electroactive additives, passivation of the cathode or incorporation of codeposited species.

4.4.1 Production techniques for metal powders

Technologically, electrodeposition competes with other preparation techniques including: (1) chemical reaction; (2) mechanical comminution; and (3) atomization.

The choice of technique is important not only from the standpoints of economics and convenience but also the properties of the metal powder are very dependent upon the production method. Chemical reactions generally yield cheap, porous, readily-compressible powders but alloy production is not possible. Mechanical comminution is a convenient technique for brittle metals but results in an irregular particle shape.

The most useful technique – atomization – gives a spheroidal particle size which is often preferred for subsequent processing, especially by the powder metallurgy industry.

In principle, electrodeposition offers a versatile and elegant production method having several advantages:

1. Not only can a wide range of metals be produced, but codeposition of metals as an alloy powder is possible.
2. A high purity product.
3. Favourable scale-up costs.
4. The powder quality may be varied, to an extent, by modifying both the conditions of electrolysis, electrolyte composition and the nature of the electrode surface.
5. The product has a high specific surface area (and occasionally enhanced catalytic activity).
6. Production may be rendered continuous and automatic, e.g. soluble anodes may be utilized in a flow-through reactor. The metal powder may be continuously removed from the cathode by scraping (Chapter 7) followed by extraction from the reactor via settling or fluidization (Chapter 2).

In practice, however, there are several drawbacks which limit more widespread application of the electrolytic method:

1. The particle size and shape may be irregular (e.g. dendritic) which presents problems for some applications, e.g. compaction of metal to produce sintered compacts.
2. The high, active surface area may present problems in extracting the metal

from the reactor, storage or handling. In the reactor, rapid dissolution (via corrosion) may occur. Oxidization may take place during storage or handling, rendering the powder less pure or passive. In certain cases (e.g. very finely dispersed precious metals or aluminium powders) the high reactivity may even manifest itself as pyrophoric behaviour. The uses of metal powders include catalysts, pigments for conductive paints, formation of speciality alloys and production of pressed metal components.

4.4.2 Electrolytic cell design

A remarkably wide range of electrode and cell geometries has been used to produce industrial metal powders. Traditionally, vertical, static, flat-plate electrodes have been employed in a tank cell with electrolyte agitation, the product being removed periodically and scraped from the cathode. This is not only a labour-intensive, messy and costly operation, but the product is time-dependent, as growth of the metal powder takes place on the cathode. The non-uniform hydrodynamics may also produce non-uniform growth. These facts have encouraged the development of continuous cells and reactors, e.g. the rotating cylinder is often used for small, modular operations.

Removal of the metal-powder product is a problem which has received considerable attention in the literature, and methods include:

1. Periodic current reversal.
2. Vibrating the cathode.
3. Amalgamating with mercury.
4. A moving-band cathode with product removal outside of the cell.
5. A two-layer bath, with a horizontal rotating cathode. This cathode moves through, and is passivated by, an organic solvent containing a surfactant; it then travels into the aqueous electrolyte. A fine powder is deposited at unpassivated sites, and the particles, being lyophobic, disperse in the organic solvent.
6. Mechanical scraping which may be divided into static scraping of a moving electrode, or a static electrode with moving scrapers.
7. Use of solution additives (although this may have a deleterious effect on the powder).

Cells for metal-powder production may utilize soluble replaceable anodes, as in electrorefining, and the anode be installed inside a porous container to prevent anode sludge contaminating the catholyte or the powder deposit. In the case of cells utilizing very insoluble anodes, the metal concentration in the cell may be maintained by solution flow.

FURTHER READING

1 C. L. Mantell (1960) *Electrochemical Engineering*, 4th Edition, Ch. 15, McGraw-Hill, New York.

2 A. T. Kuhn (Ed.) (1971) *Industrial Electrochemical Processes*, Ch. 7, Elsevier, Amsterdam.
3 A. Schmidt (1976) *Angewandte Elektrochemie*, Verlag Chemie, Weinheim.
4 The Open University, *The Production of Aluminium*, Materials Processing Unit T. 352, The Open University, Milton Keynes.
5 The Open University (1975) *Zinc: A Case Study*, Science and Technology Unit ST. 294, The Open University, Milton Keynes.
6 M. Sittig (1956) *Sodium, Its Manufacture, Properties and Uses*, Van Nostrand Reinhold, New York.
7 K. Grjotheim and B. J. Welch (1980) *Aluminium Smelter Technology*, Aluminium Verlag, Dusseldorf.
8 US Bureau of Mines (1986) *Precious Metals Recovery from Low-Grade Resources*, National Western Mining Conference, Denver, Colorado, Information Circular No. 9059, US Bureau of Mines, Pittsburgh.
9 A. K. Biswas (1980) *Extractive Metallurgy of Copper*, Pergamon, Oxford.
10 A. Calusaru (1979) *Electrodeposition of Metal Powders*, Elsevier Scientific, Amsterdam.
11 N. Ibl (1962) Ch. 3, 'Applications of Mass Transfer Theory: The Formation of Powdered Metal Deposits', in C. W. Tobias (Ed.) *Advances in Electrochemistry and Electrochemical Engineering*, Vol. 2, Wiley, New York.
12 A. R. Burkin (Ed.) (1987) *Production of Aluminium and Alumina*, Wiley, Chichester.

5 Other inorganic electrolytic processes

In this chapter, the electrolytic preparation of inorganic compounds other than chlorine, alkalis and metals will be discussed. The processes are, in general, low-tonnage but have an established or developing position in industrial practice. The compounds prepared by electrolytic processes are: (1) the strong oxidizing agents (e.g. $KMnO_4$, $NaClO_3$, $K_2Cr_2O_7$, $Na_2S_2O_8$, F_2, H_2O_2 and O_3; the electrolytic generation of hypochlorite is considered in Chapter 7); (2) metal oxides which are particularly active when prepared anodically (e.g. MnO_2 and Cu_2O); (3) a variety of metal-ion redox species in solution (e.g. Cr(II), Ce(IV), Ti(III) (see also Chapter 6)); (4) hydrogen/oxygen by water electrolysis; and (5) metal salts via anodic dissolution of the metal.

5.1 FLUORINE

Electrolysis is the only method for the isolation of the element fluorine. Although the reaction was described in the nineteenth century,* the first commercial production of fluorine did not occur until 1946 in the USA and 1948 in Europe. The process was first developed to produce the fluorine required for ^{238}U processing; the enrichment of ^{238}U is based on a diffusional separation of $^{235}UF_6$ and $^{238}UF_6$ and one step in the conversion of uranium ores to UF_6 is the oxidation of UF_4 either by elemental F_2 or by ClF_3. The nuclear industry remains a major producer of fluorine for this purpose but on a smaller scale, fluorine is also used in the chemical industry for the production of SF_6 (a gaseous dielectric which is non-toxic and non-inflammable) and fluorinated organic compounds. The total world production of fluorine is probably between 15 000 and 20 000 ton $year^{-1}$. All commercial electrolyses employ an electrolyte which is close in composition to the eutectic KHF_2 (melting point 82° C), because of the low vapour pressure of hydrogen fluoride above such melts. In the electrolysis, the overall cell reaction is:

$$2HF \longrightarrow F_2 + H_2 \tag{5.1}$$

* H. Moissan, *C.R. Acad. Sci.* **102**, 1534 (1886); **103**, 202, 256 (1886).

and, hence, the composition changes with time. Normally, the hydrogen fluoride content is kept in the range 38–42% by periodic addition and the electrolysis is operated at 90–110° C.

The aggressive, acidic nature of the electrolysis medium and the chemical reactivity of fluorine limit the choice of materials and determine the simple and sealed cell design based on a mild steel tank, with a volume of the order of 1 m^3. A number of cell designs are operational, and Table 5.1 provides a broad comparison of several commercial processes.

Figures 5.1 and 5.2 show cell designs due to ICI and Union Carbide. The ICI cells, rated at a nominal 5 kA, are utilized by British Nuclear Fuels; upscaled 11 kA cells are regularly used and a 15 kA pilot has been evaluated. The cell body (Fig. 5.1) consists of a welded mild-steel tank, jacketed on its sides and the bottom. Steam heating is applied to the side jackets when the cells are not in production or operating at low currents to prevent the electrolyte solidifying. Twenty-four coils connected to inlet and exit headers divide the cell transversely and function as water-cooled cathodes. The cell lid has twelve rectangular openings into which anode assemblies fit, so that they are interposed between pairs of cathode coils. Each assembly consists of a flat plate of mild steel to the underside of which is attached a rectangular monel gas-separating skirt inside which are located a pair of anode blocks. The anodes are insulated from the skirt assembly and the cell top by means of Neoprene or fluoro-elastomer gaskets, depending on the duty, and in order to ensure that no mixing of the gaseous products, each skirt protrudes a short distance into the electrolyte, thus dividing the cell into twelve fluorine compartments and one hydrogen compartment. Fluorine from the anode assemblies is collected in a common manifold while the hydrogen leaves at an offtake located at one end of the cell. A solid electrolyte layer is formed by deliberately cooling the base of the cell. This prevents hydrogen being generated on the cell base, which might otherwise enter the anode compartment. Provision is made in the cell lid for a liquid hydrogen fluoride feed pipe, electrolyte sample dip pipe, electrolyte thermocouple wells, and a nitrogen purge to both the hydrogen side and each individual anode compartment. Electrical contact to each anode is provided by a mild steel–nickel hanger secured to the block by means of an oversprayed nickel coating. The cell body is electrically connected to the cathodes.

The majority of modern American cells are based on two designs – the C-type and E-type – developed over many years by the Union Carbide Nuclear Company for the American Atomic Energy Commission. The E-type cell body (Fig. 5.2) consists of a welded monel tank with a monel water jacket for cooling and heating, incorporated to overcome the corrosion problems encountered with the steel jacket of the C-type cell. Additional heat-transfer capacity is provided by baffles in the water jacket and water recirculation tubes in the centre of the tank.

The cell lid consists of a steel plate with fluorine and hydrogen compartments, monel gas-separating skirts, externally threaded packing glands for the anode

Table 5.1 Operating and materials data for four types of commercial fluorine cell (*After*: J. F. Ellis and G. F. May (1986) Modern Fluorine Generation, in *Fluorine: The First Hundred Years* (Eds R. E. Banks, D. W. A. Sharp and J. C. Tatlow) Elsevier Sequoia, S.A. Lausanne.)

	ICI	Union Carbide	Pierrelatte	Montecatini
Operating data				
Nominal current capacity/A	5000	6000	<6000	5000
F_2 output/kg h^{-1}	3.3	3.47	3.7	3.3
Current efficiency/%	95	90–95	95	90–95
Cell voltage at normal load/V	10–11	12	8.5–10	8.5–9.5
Anode current density/A cm^{-2}	0.18	0.10–0.15	0.13	0.07
Electrolyte temperature/° C	80–90	88–104	85–100	95–105
HF concentration/% wt	39–41.5	40–42	$\simeq 40$	39–41
Constructional details				
Cell body dimensions/m	$3.10 \times 0.71 \times 0.59$	$2.26 \times 0.97 \times 1.04$	—	$2.00 \times 1.00 \times 0.60$
Cell body material	Mild steel	Monel	Monel	Monel
Cathode	Mild steel	Mild steel	Steel	Fe
Anode	Porous carbon	Graphite-free carbon	Carbon	Amorphous carbon
Gas separation skirt	Monel	Monel	—	Monel
Diaphragm	None	Monel	Monel	Monel
Anodes in cell	24	32	32	32

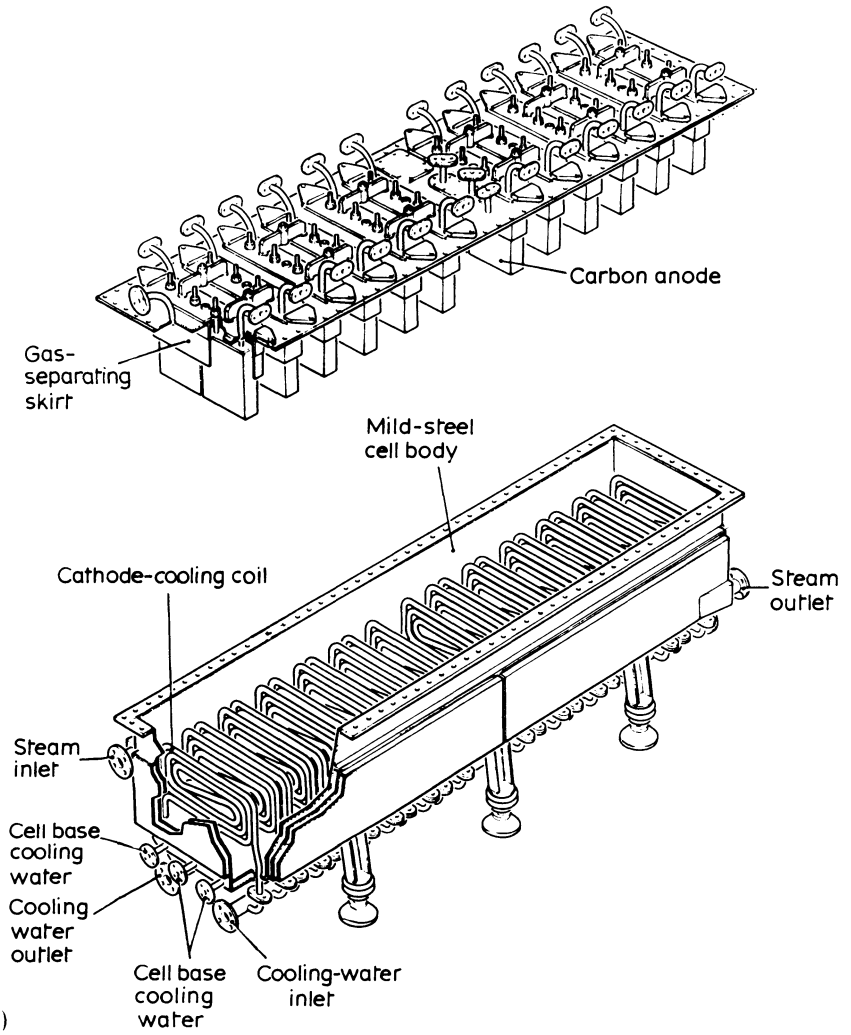

Fig. 5.1 The ICI-type of cell design for fluorine production. (a) The cell construction. (b) An industrial-scale (5 kA) cell for fluorine production. The facility is currently in use at BNFL, Springfields Works, Preston, UK. (Photograph Courtesy: BNFL plc.)

and cathode supports, fluorine and hydrogen offtake pipes, nitrogen purge and hydrogen fluoride feed lines, and electrolyte thermocouple and sampling wells. The lid is attached to the cell body with a bolted flange and sealed with a synthetic rubber gasket.

The anode assembly contains 16 anodes arranged in two parallel rows of eight each. Two assemblies totalling 32 anodes are used in each cell. A recessed bolt sealed with a carbon plug fastens the anodes to a copper support bar. This design

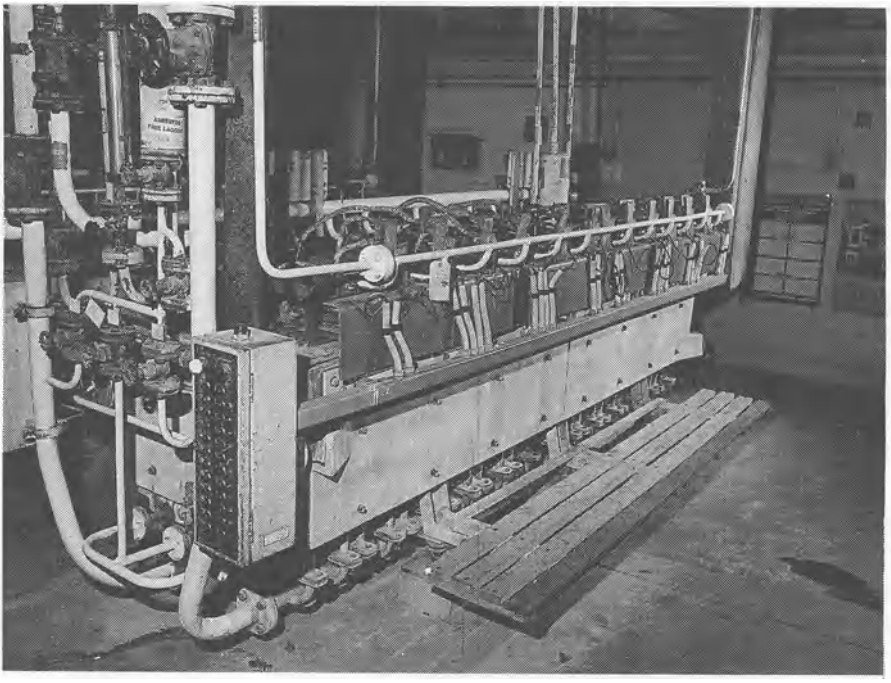

(b)

gives improved cell life over the C-type design which uses a copper pressure plate and steel anode support bar. Copper rods are projected through insulating packing glands in the cell lid to serve as electrical connectors.

The cathodes comprise three vertical parallel steel plates welded to cross-members at the end and suspending through the cell cover by steel rods which pass through insulating packing glands. A six-mesh, woven monel diaphragm is attached to an angle frame and bolted to the gas separation skirt through a Teflon gasket. The diaphragm acts to divert the hydrogen gas into the hydrogen compartment of the cell and also prevents broken anodes shorting-out the cell. The maximum current rating of this cell design is 6 kA. Alternative US cells, developed by Allied Chemical Corporation, utilize a magnesium alloy lid or skirt and do not have a diaphragm.

5.1.1 Anode effects

It is not possible to use a metal anode because of corrosion and, hence, in practice, the choice of material is limited to carbon. Even with carbon, however, a careful choice of type and grade is necessary since the properties of the carbon will determine the current efficiency, energy efficiency and the lifetime of the

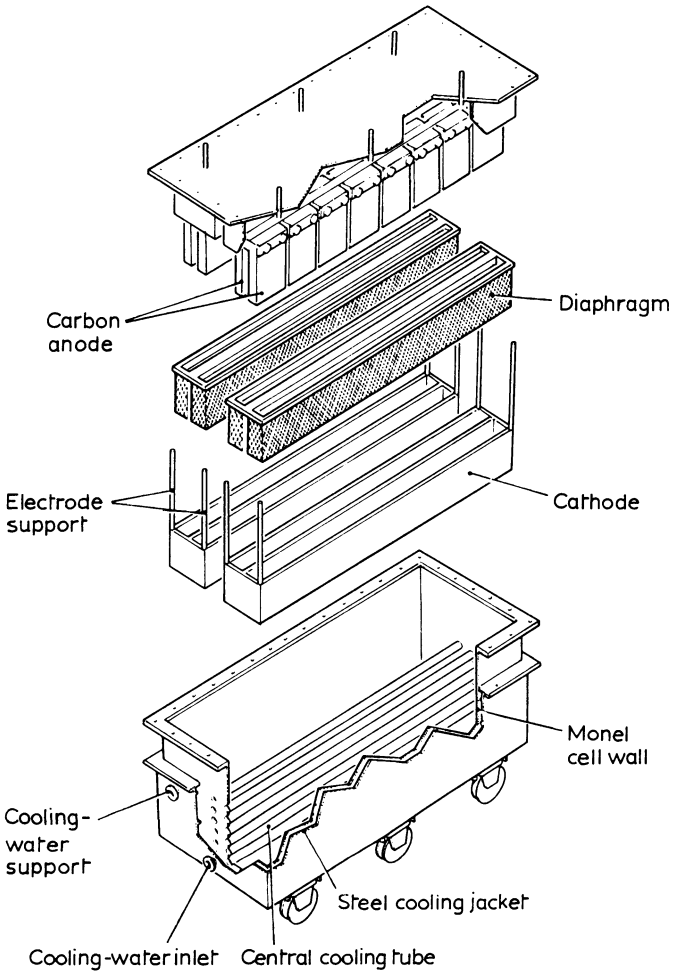

Fig. 5.2 The Union Carbide-type of cell design for fluorine production.

electrodes. The behaviour of the anode is dominated by a phenomenon known as 'polarization'; in this context, 'polarization' is not just a relatively small overpotential caused by slow kinetics; rather, it is an increase in cell voltage, maybe of several volts, and it is thought to arise because of non-wetting of the anode by the electrolyte. The fluorine gas is consequently not released from the surface and collects as a barrier to electron transfer. In the limit, 'polarization' becomes an 'anode effect' and the cell voltage increases to maybe 40–60 V, when sparking across the gas layer and incandescence are observed (compare aluminium extraction cells section 4.1.1). The cause of the non-wetting of the surface by the electrolyte is probably a layer of $(CF)_n$ polymer formed *in situ* by reaction of the anode carbon with fluorine.

Clearly, polarization must be minimized and two approaches are used:

1. A fairly permeable carbon is chosen for the anode. The objective is to allow the fluorine gas to enter the pores without them flooding with electrolyte. Then the fluorine leaves the cell by passing through the pores in the electrode, which also assists the separation from hydrogen formed at the cathode, and contact between the carbon and the electrolyte is maintained.
2. The use of a hard non-porous carbon and additives to control polarization. These may be Na^+, Li^+ or Al^{3+} or, more effectively, nickel in a higher oxidation state. Dissolved nickel exists in the electrolyte anyway, because of corrosion of the skirt used to separate the anode and cathode gases. Water, in addition to leading to oxygen in the fluorine, also promotes polarization and it is therefore normal to specify hydrogen fluoride with a very low water content. Moreover, when a new cell is set up it is often necessary to pre-electrolyse with a low current density to remove most of the water. Another impurity to be avoided is sulphate since this leads to erosion of the anode. Certainly, the period between servicing of the cell is determined either by disintegration of the anode or by corrosion of the anode contact. Downtime is a constant problem with fluorine cells.

The fluorine leaving the cell contains a high percentage of hydrogen fluoride and this is removed by passing the gas over trays of powdered sodium fluoride. The hydrogen fluoride may be recovered and recycled back to the cell by periodic heating.

Polarization can be controlled to some extent, but it is never fully overcome and this, combined with the anode–cathode gap of about 5 cm necessary to avoid reactions between the electrolysis products in undivided cells, causes the cell voltage to be from -8.5 to -13 V for the working current density of 70–200 mA cm^{-2} (Table 5.2). This compares with the calculated reversible cell voltage of -2.9 V so it is clear that fluorine manufacture cannot be described as energy-efficient! The total energy consumption for a cell with a 95% current efficiency (i.e. with a small amount of back chemical reaction between F_2 and H_2)

Table 5.2 Typical voltage components in a modern fluorine producing cell

	$-$voltage/V
Reversible cell voltage	2.9
Anode overpotential	3.0
Cathode overpotential	1.0
Total *iR* drop	3.0
Operating cell voltage	9.9

Anode current density, 150 mA cm^{-2}; temperature, 85° C; current efficiency, 95%

is about 15 000 kWh ton^{-1} of fluorine, a very high figure which is only acceptable because of the high sale price of this halogen, and the absence of competitive production methods and the need to produce fluorine on-site.

5.2 WATER ELECTROLYSIS

5.2.1 General considerations

Water electrolysis is a route to both very pure hydrogen and very pure oxygen, although in most applications it is the hydrogen which is considered the principal product. The overall cell reaction is:

$$2H_2O \longrightarrow 2H_2 + O_2 \tag{5.2}$$

From thermodynamic considerations, this reaction requires, at room temperature, a potential of -1.23 V at all pH. (The reversible potentials for both hydrogen evolution and oxygen formation shift by 60 mV pH unit towards negative potentials as the pH is increased.

Water electrolysis plants are used for the production of hydrogen for use as a chemical for the hydrogenation of organic molecules (particularly in the food industry where edible oils and fats produce margarine and shortening), in the manufacture of semiconductors, in producing and refining high-purity metals and even in the synthesis of ammonia. Generally, however, it is an expensive route for large quantities of hydrogen compared with the separation of CO and H_2 from synthesis gas produced by coal gasification:

$$C + H_2O \xrightarrow{1000^\circ C} CO + H_2 \tag{5.3}$$

or the degradation of natural gas or light oils, e.g.:

$$-CH_2- + \tfrac{1}{2}O_2 \longrightarrow CO + H_2 \tag{5.4}$$

and/or:

$$-CH_2- + H_2O \longrightarrow CO + 2H_2 \tag{5.5}$$

Therefore, water electrolysis is used particularly where high purity is essential (e.g. for foodstuffs or where catalyst poisoning is a problem) and/or cheap hydroelectric power is available. Moreover, it should be remembered that hydrogen is a by-product in the chlor-alkali industry.

Even if the economics of large-scale water electrolysis are not always favourable, the process on a small scale finds many diverse applications because of the convenience of obtaining high-purity gases at a controllable rate. These would include the supply of oxygen and/or hydrogen to industry at remote sites, hydrogen to cool electric generators in power stations, hydrogen to fill meteorological balloons, gases to laboratories and oxygen to life-support systems in

submarines and spacecraft. Another use is the provision of a reducing atmosphere for metallurgical heat-treatment operations. Hence, water electrolysis plants range from one designed to produce 2×10^{-3} $m^3 h^{-1}$ H_2 for a gas–liquid chromatograph detector to one to produce 10^4 $m^3 h^{-1}$ H_2 for a synthetic ammonia plant.

Small cells are utilized to electrolyse deuterium or tritium containing water. There are two applications for these cells: (1) they may be operated in a similar fashion to conventional water electrolysers but producing deuterium or tritium gas (in place of pure hydrogen) from D_2O, DHO or HTO; (2) (and more commonly), the cells may be used to concentrate the amount of deuterium or tritium in the electrolyte (DTO, DHO, HTO or D_2O). This is made possible by kinetic factors which determine that hydrogen is evolved more rapidly than deuterium or tritium, e.g. hydrogen is evolved from 2 to 10 times faster than deuterium. The natural abundance of deuterium in water is very low (*c.* 150 mg dm^{-3}). Hence, extensive electrolysis is required to produce a significant level of 'heavy' (deuteriated) water.

Cell designs used for deuterium and tritium containing water tend to involve: (1) a low electrolyte inventory; (2) enhanced secondary sealing facilities; and (3) a large number of cells arranged in hydraulic series, i.e. the 'cascade' mode. In terms of the nominal reactor current per electrolyte volume, these cells typically operate at 0.3–0.5 kA dm^{-3}, a magnitude higher than for most light-water electrolysers. This reflects the specialized nature of the operation; the enriched electrolytes are extremely expensive, particularly in the case of tritiated water!* Stringent attention to construction and sealing further reflects the high electrolyte costs, together with concern over the level and inventory of the tritium isotope. Indeed, some tritium cells have only one long-life gasket; tritium is not only radioactive but extremely toxic in its oxidized state (DTO or THO) due to its ability to exchange with H_2 (as H_2O) within the human body.

There are two typical types of design for deuteriated or tritiated water electrolysis: the filterpress and specialized low-volume cells. Examples are shown in Fig. 5.3.

In the long term, a growing demand is expected for hydrogen (including electrolytic hydrogen) production due to several likely trends. Supplies of lighter crude oils will diminish, resulting in the need to process heavier petroleum feedstocks which require upgrading by hydrogen; this situation may be accelerated by a declining availability and increasing price of natural gas. The additional interest in coal liquefaction to produce synthetic fuels would also involve large quantities of hydrogen.

A much larger exploitation of water electrolysis as part of the 'hydrogen economy' has been predicted for the distant future; hydrogen would be produced using 'cheap' electricity from nuclear power stations or solar collectors and be used as a method of storing and transporting energy. At urban sites, fuel cells

* Estimated prices: D_2O, $US 300–500 per litre; T, $US 30 000 per gram.

(a)



(b)

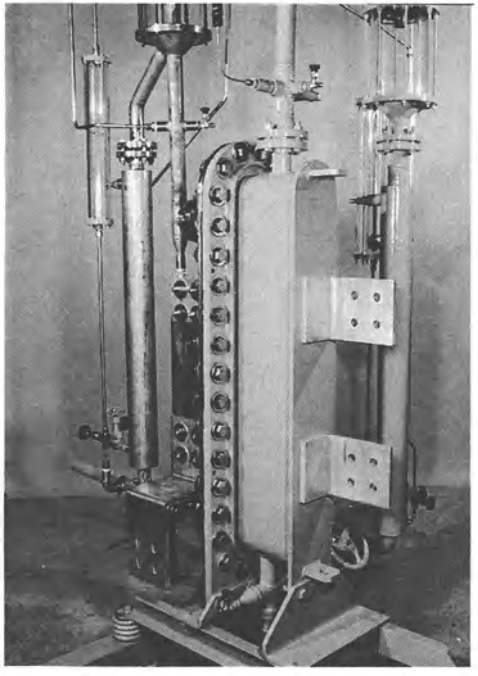

Fig. 5.3 Small modular cells for specialized water electrolysis. (a) The EI MiniCell: a lightweight, prototype, filterpress design, which provides an alternative supply of H_2 and O_2 to bottled gases. (b) The EI-003 low-inventory cell for electrolysis of heavy and tritium-containing water (developed by Atomic Energy of Canada Ltd and Ontario Hydro). The nominal design is based upon 3 dm^3 electrolyte per kiloamp of current. Construction involves a high-integrity design in order to contain the expensive and radioactive water. (Courtesy: Electrolyser, Inc.)

would be used to reconvert the hydrogen to electricity. At the present time, 'cheap' electric power is not available and there remain problems with the energy efficiency of both the water electrolyser and the fuel cell. A major requirement here is the development of improved electrocatalysts.

Several recent research programmes have sought to reduce the electricity consumed in water electrolysis by supplying some of the energy required to split water either thermally or photochemically. An example of the former is the following scheme for the production of hydrogen; the electrolysis step is:

$$H_2SO_3 + H_2O \longrightarrow H_2SO_4 + H_2 \tag{5.6}$$

a reaction theoretically requiring a cell voltage of only -0.17 V. The sulphuric acid is then decomposed thermally at 875° C and the resulting sulphur dioxide dissolved in water to give further sulphurous acid, i.e.:

$$2H_2SO_4 \longrightarrow 2SO_2 + 2H_2O + O_2 \tag{5.7}$$

$$H_2O + SO_2 \longrightarrow H_2SO_3 \tag{5.8}$$

The cell, however, requires a separator since sulphurous acid would otherwise reduce to sulphur at the cathode. There are also problems at the anode since, with presently available electrode materials, the oxidation of sulphurous acid to sulphuric acid requires an overpotential of several hundred millivolts. Hence, the advantage compared with direct water electrolysis is yet to be realized. Currently, the most promising examples of photochemically assisted water electrolysis are photovoltaic cells which use a semiconductor electrode, e.g. it is possible to construct a cell with an anode made from an optically transparent material covered with a thin layer of an *n*-type semiconductor, an aqueous electrolyte and a cathode which has a low overpotential for hydrogen evolution. When the anode is illuminated, photons of energy greater than the energy gap of the semiconductor will excite electrons from the filled levels to the conduction band leaving a hole in the filled band:

$$h\nu \longrightarrow p^+ + e^- \tag{5.9}$$

In the potential field, the electron and hole can separate, the electron passing through the external circuit to the cathode and the hole moving to the surface of the anode where the reaction:

$$2H_2O + 4p^+ \longrightarrow O_2 + 4H^+ \tag{5.10}$$

can take place; hydrogen evolution occurs at the cathode so that, overall, the absorbed photons lead to oxygen and hydrogen. Indeed, in these systems all the energy for water-splitting may be supplied photochemically and then the cell behaves as a fuel cell, i.e. it is a power source rather than requiring the input of electrical energy. The most successful cell to date has *n*-type GaAs anode with surface states modified by adsorption of a Ru(III) complex onto the surface and a polyselenide electrolyte; this system gives a solar to electrical efficiency of 12%.

5.2.2 Commercial water electrolysers

The scale of industrial water electrolysis is extremely wide, ranging from small portable devices (e.g. 5 kW) through to process installations of 7 MW. Three types of water electrolyser based on tank cells, filterpress designs and the use of elevated pressure are presently manufactured in a range of sizes to meet the various markets described above. In addition, solid electrolyte cells are now becoming available. These variants are described below.

The cells currently available have a number of common features, largely because each design aims principally to minimize the cell voltage and to avoid problems from corrosion. In older cell designs, the cathode was steel and the anode, nickel; now more care is taken to reduce the overpotentials at both electrodes. It has long been realized that platinized platinum was a superior material for both electrodes but it was too expensive. It took longer to develop economic alternatives but now the anode is more likely to be nickel plated onto steel in conditions to give a high surface area deposit or nickel oxide and cobalt oxide on nickel substrates. The anode coating may also contain precious metals to enhance further the rate of oxygen evolution. The cathodes are also catalytic coatings, e.g. high-surface-area nickel alloys (including Raney nickel), cobalt and sulphided nickel. Both electrodes are shaped to enhance gas release and to direct the gases away from the current path. The electrolysis is typically conducted at 70–80° C, partly to reduce the electrode overpotentials.

The electrolyte is potassium hydroxide or sodium hydroxide because the alkaline medium causes fewer corrosion problems with the cheaper structural and electrode materials. Their concentration is 20–25 wt% since such values give close to optimum conductivity at the operating temperature. It is also necessary to use very pure water since this is consumed during the electrolysis, causing impurities to accumulate; in particular, chloride ion, a common impurity in water may cause pitting of the passive films formed on the metal surfaces in alkali (Chapter 10).

The separator has traditionally been asbestos, often with a nickel gauze support. It should be remembered that the only role of the separator in a water electrolyser is to keep the gaseous products apart. It was noted above that the equilibrium potential for the cells is -1.23 V. In fact, no discernible gas evolution is observed until the cell voltage is from -1.65 to -1.79 V, and for the operating current densities of 100–600 mA cm^{-2} the cell voltage is generally from -1.9 to -2.6 V, giving an energy efficiency of 45–65%. The energy requirements usually lie within the range 4.2–4.6 kWh m^{-3} H_2.

Tank cells, which are usually operated in a monopolar manner, have the advantages of simplicity, reliability and flexibility; they do not require a rigorous gas–liquid separator or electrolyte circulation as do the filterpress designs. Figure 5.4 shows a typical version of the monopolar tank cell (the Stuart cell). A rectangular tank (e.g. nickel plated steel) contains alternate anodes and cathodes, which are made of rigid metal, closely spaced and parallel. All electrodes having

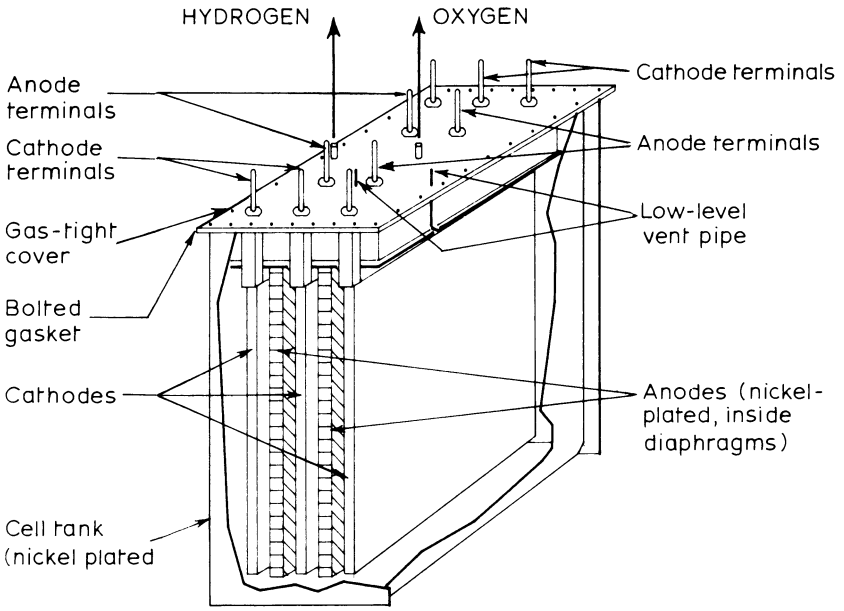

Fig. 5.4 The components and construction of a monopolar water electrolysis cell (the Stuart cell).

the same polarity are connected in parallel, such that the cell voltage (equivalent to that of a cathode–anode pair) is from -1.7 to -2.0 V. Cells are connected in series in order to provide a total voltage drop suitable to the rectifier output (from -100 to -500 V). Flexibility is inherent, e.g. higher currents (and, hence, a greater H_2 output) can be achieved by increasing the number of electrodes per tank or the number of tanks. The simple construction of many monopolar tank cells is illustrated by the use of a single gasket to seal the electrolyser tank. The Stuart cell typically has a nominal power rating of 200 kW, with the specifications listed in Table 5.3. Such tank cells have been utilized for installations rated up to 7 MW, and this technology has an extensive track record, with over 750 installations in 85 countries during the last 50 years.

For large-scale hydrogen production ($\geqslant 2$ tons per day) by water electrolysis, improved monopolar tank cells such as the one shown in Fig. 5.5 have been developed. The EI 250 cell has been operated on a scale up to 100 kA, with a current density of 0.25 A cm^{-2}. Each cell is capable of producing 42 $m^3 h^{-1}$ of H_2 and 21 $m^3 h^{-1}$ of O_2.

Filterpress cells are structurally more complex and require electrolyte circulation and gas–electrolyte separators external to the cell but they give enhanced space–time yields. Typically, bipolar filterpress units with various sizes give hydrogen delivery rates between 3 and 50 $m^3 h^{-1}$. The important components are the anodes and cathodes based on perforated steel (perforated

Table 5.3 Specifications of a modern 200 kW monopolar water electrolyser

Cell current	10 kA
Cell voltage	−1.85 V
Energy efficiency	⩾80%
Energy consumption	4.4 kWh/m^{-3}H$_2$
Current density	0.25 A cm^{-2}
Temperature	70° C
Hydrogen output	42 m^3 h^{-1}
Oxygen output	21 m^3 h^{-1}
Specific plant area	0.15 m^2/m^3 h^{-1} H$_2$

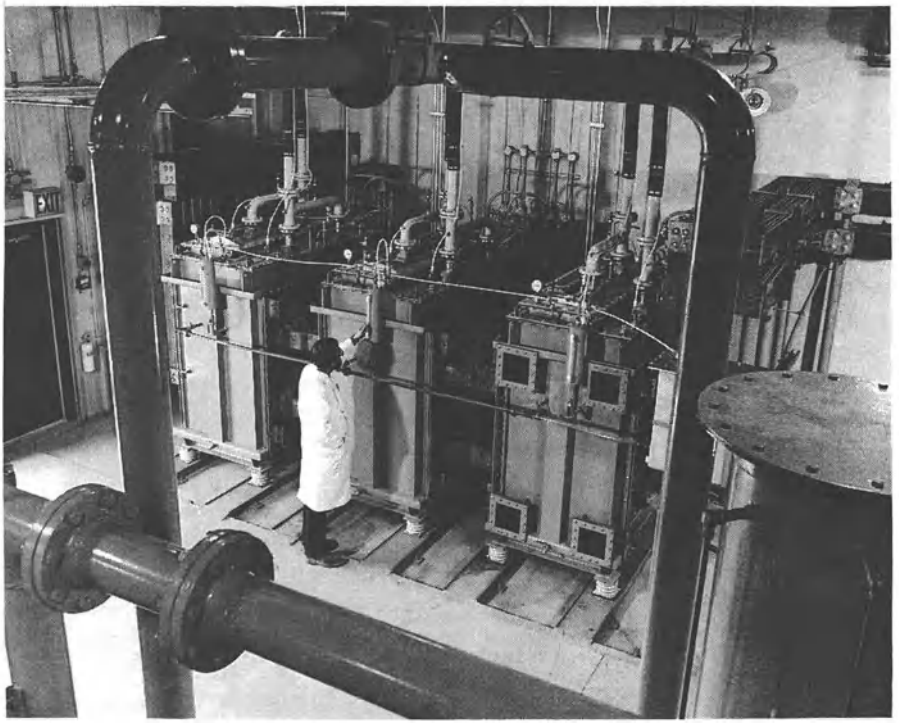

Fig. 5.5 A monopolar tank electrolyser for large-scale hydrogen production using EI 250 cells. The cell assemblies carry up to 100 kA with an energy efficiency greater than 80% and a nominal power rating of up to 200 kW. The three cells shown produce a combined output of up to 126 m^3 h^{-1} H_2 and 63 m^3 h^{-1} O_2. Each cell measures approximately 2.1 m long, 1.1 m wide, 1.8 m high. (Courtesy: Electrolyser, Inc.)

so that much of the evolving gas passes to the back of these electrodes) placed very close to either side of an asbestos diaphragm strengthened with nickel gauze. The other cell components ensure stable and leak-free operation and effective circulation of the electrolyte. The increase in hydrogen delivery rate may be achieved by increasing both the area of the diaphragm and electrodes and the number of cells in the filterpress stack. A modern bipolar filterpress unit operates at a current of 2.5 kA and a power consumption of *c.* 4.6 kWh m^{-3}, the total electrolysis capacity being 250 kW. The total floor space and energy requirements for monopolar tank cells and bipolar filterpress units are quite comparable. The major difference lies in the construction and operation and the bipolar cells require careful control of bypass currents and extensive sealing arrangements. At the present time, the trend is away from bipolar water electrolysis.

The elevated-pressure cells operate at about 30 atm. In such cells, the bubbles of gas are reduced in size, decreasing the *iR* drop between the electrodes, and it is also possible to place the electrodes closer to the membrane. The energy efficiency is, however, not significantly better than the ambient-pressure cells and the design and manufacture is more difficult. Designs are normally based on a filterpress cell.

Compact high-pressure water electrolysers have been utilized to produce oxygen on board nuclear-powered submarines as part of the life-support system; the hydrogen by-product, while flammable, is non-toxic and easily handled. Moreover, water and electrical power are the only utilities required. Since 1966, over 1 million running hours have been accumulated in service by such high-pressure electrolysers (Fig. 5.6(a)).

Each cell stack is assembled from a number of bipolar cells comprising an electrode assembly and a cell frame which contains the asbestos diaphragm (Fig. 5.6(b)). A pressure vessel is used to enclose the cell stack. An important feature of the design is the elimination of gaskets between cells which necessitates precision machining of the cell frames. A simplified flow sheet of the electrolysis is shown in Fig. 5.6(c). Electrolyte containing the entrained gas (O_2 or H_2) exits from the cell to a gas separator. Hydrogen is discharged overboard from a gas-control valve during normal operation; oxygen flows via a gas-control valve to the submarine's ventilation system. After filtration, the electrolyte returns to the cell stack via heat-exchangers. Demineralized water is fed into the hydrogen separator to replace water which has been electrolytically converted to gas. Normally, the plant is operated automatically. An important safety feature upon start-up or shutdown is to pressurize the system to 35 bar with inert N_2 gas to purge the system and avoid flammable atmospheres.

High levels of service reliability and performance have been achieved with high-pressure electrolysers but the devices are inherently complex and require precision engineering, together with sophisticated control. Additionally, the units operate with a corrosive, alkaline electrolyte. Currently, the high-pressure electrolysers are gradually being replaced by a new generation of cells based on solid polymer electrolytes, which are more compact, lighter and capable of

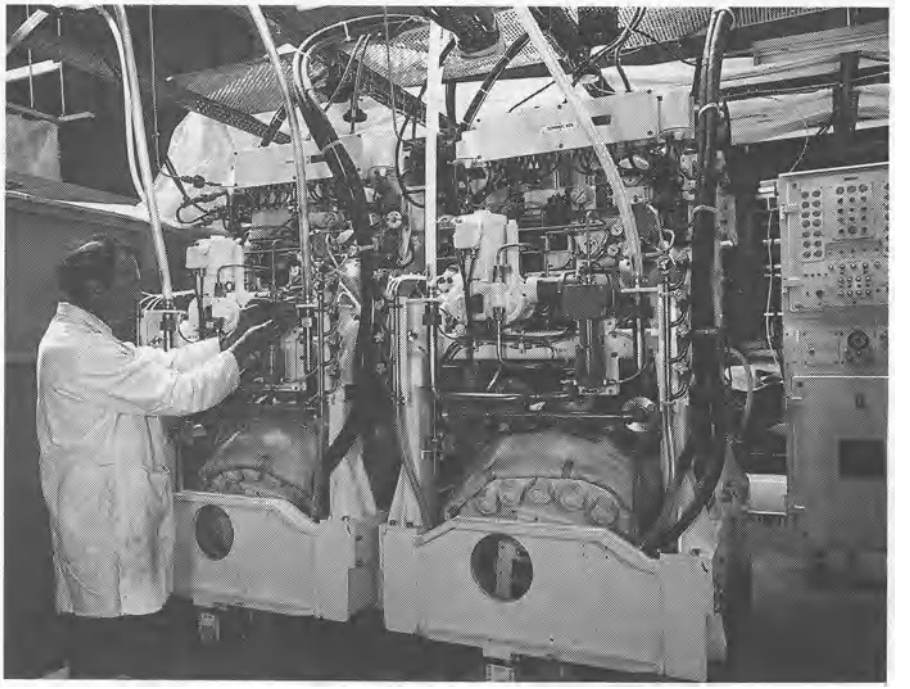

(a)

producing higher oxygen purities. Operation at low pressure allows the use of relatively simple control systems together with faster start-up and shutdown procedures.

The first solid polymer electrolysers were developed by the General Electric Company as fuel cells for the NASA space programme. Subsequently, small-scale solid polymer water electrolysers were used for military and space applications in the early 1970s (the active cathode area of each cell being only 0.02 m^2). In 1975, a development programme was established to scale-up the technology: it was targeted towards large-scale, commercial applications such as energy storage. Cells with an active cathode area of 0.093 m^2 were developed and 0.23 m^2 cells (involving a 200 kW module capable of producing 55 $m^3\ h^{-1}\ H_2$) are now in operation.

In solid polymer electrolyte cells (Fig. 5.7) the electrolyte is a thin perfluorinated sulphonic acid (Nafion) membrane (*c.* 0.25 mm thick) having a structure which promotes conduction of hydrated protons. The schematic cell reactions are shown in Fig. 5.7(a). Pure water is supplied to the anode where it is oxidized to oxygen and protons; the latter pass through the polymer electrolyte to the cathode where hydrogen gas evolves. In fact, excess water is circulated through the anode compartment to remove waste heat.

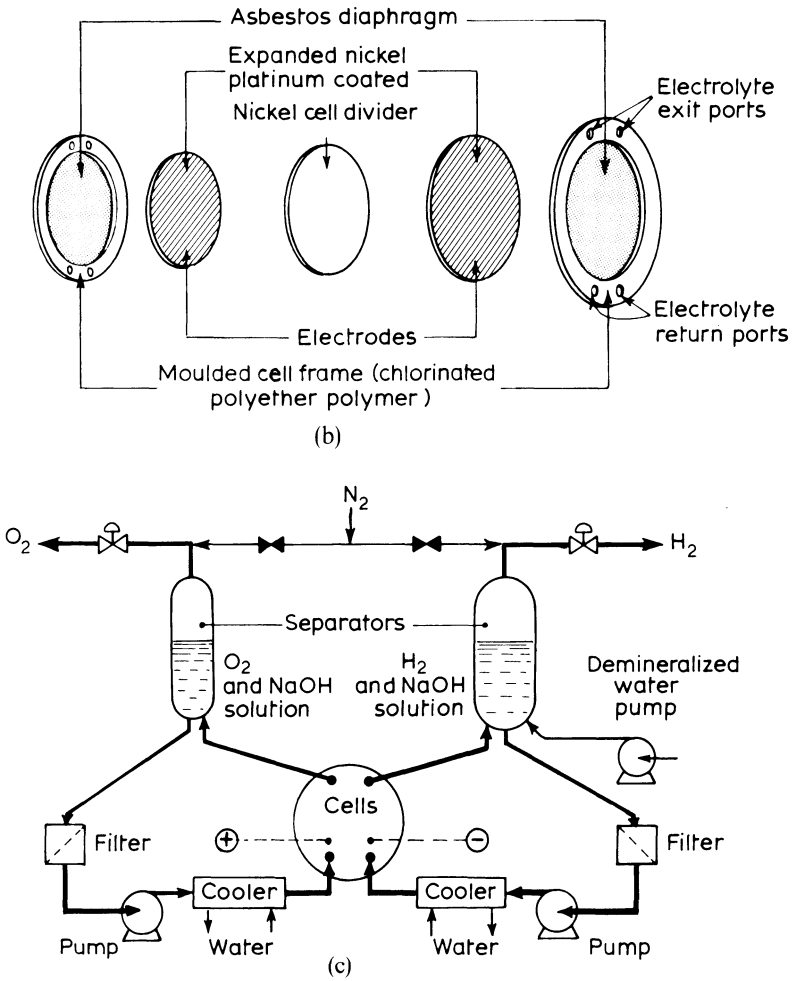

Fig. 5.6(a) A high-pressure water electrolyser. (b) Exploded view of cell. (c) A simplified flow sheet. (Photograph courtesy: CJB Developments Ltd.)

The solid polymer electrolyte cell tends to be slightly larger than corresponding high-pressure cells, and requires a compressor to remove the hydrogen gas. However, it has a number of important advantages compared to other water electrolysers:

1. The electrolyte is stable and the cell design is simple.
2. The absence of a corrosive electrolyte promotes a high reliability with low maintenance.
3. The membrane prevents mixing of the product gases, facilitating safety and high gas purities.

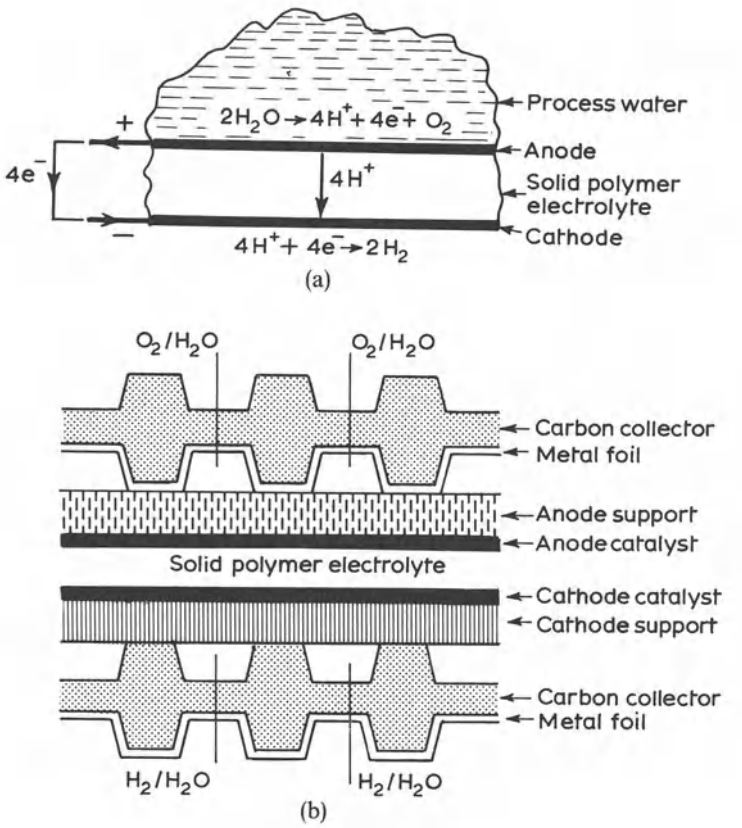

As shown in Fig. 5.7(b), the solid polymer electrolyte cell comprises a membrane, fuel cell type, porous electrodes and three further components: a carbon collector, a platinized titanium anode support and a cathode support made from carbon-fibre paper. The collector is moulded in graphite with a fluorocarbon polymer binder. A 25 μm thick platinized titanium foil is moulded to the anode side to prevent oxidation. The purpose of the collector is to ensure even fluid distribution over the active electrode area, to act as the main structural component of the cell, to provide sealing of fluid ports and the reactor and to carry current from one cell to the next. Demineralized water is carried across the cell via a number of channels moulded into the collector. These channels terminate in recessed manifold areas each of which is fed from six drilled ports. The anode support is a porous conducting sheet of platinized titanium having a thickness of approximately 250 μm. The purpose of the support is to distribute current and fluid uniformly over the active electrode area. It also prevents masking of those parts of the electrode area which would be covered by the

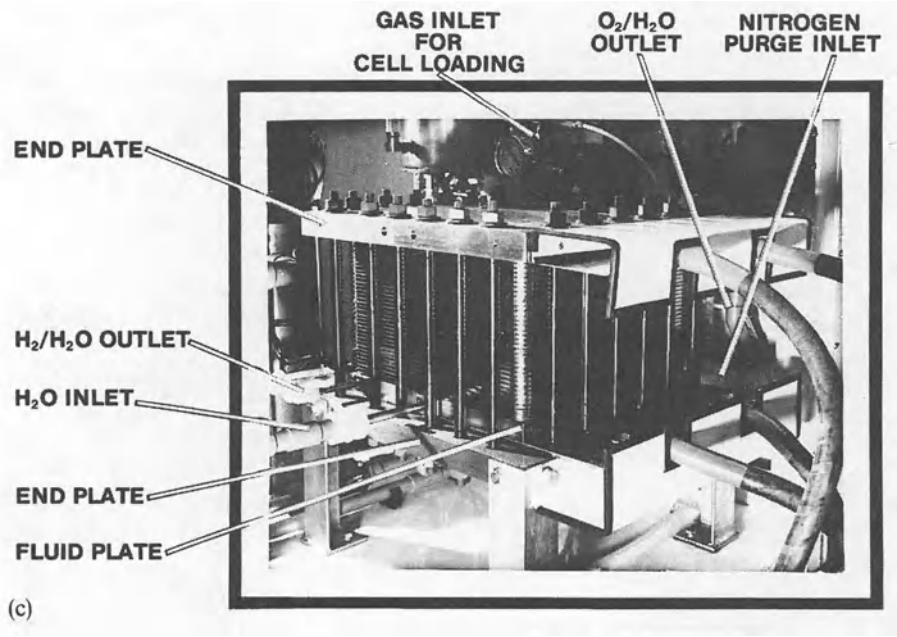

Fig. 5.7 Solid-polymer electrolyte cells for water electrolysis. (a) Reactions. (b) The cell arrangement. (c) A demonstration electrolyser module which incorporates 34 cells and will generate up to 14 $m^3 h^{-1}$ of hydrogen. (Courtesy: CJB Developments Ltd.)

carbon collector. The cathode support comprises a layer of carbon-fibre paper having a thickness of 300–330 μm. The present electrode compositions have not been fully disclosed but it is believed that the cathode is a PTFE/graphite-based porous structure with precious metal (probably Pt) catalyst, of loading 0.1–0.25 mg cm^{-2}, and the anode has a similar base but with ruthenium dioxide mixed with transition-metal additives as the catalyst. In practice, the solid polymer electrolyte cells are mounted in a bipolar stack. Figure 5.7(c) shows a 34 cell module, the cells being mounted horizontally with the anode uppermost, ensuring that the demineralized water is always in contact with the membrane.

The cells, fluid manifold plate and positive and negative terminals are sandwiched between upper and lower endplates which are linked by peripheral tie rods. The tie rods provide the compressive load to contain the structure. However, to ensure the load is distributed evenly over the complete cross-sectional area of the module, the upper endplate incorporates a sealed flexible bladder which is pressurized to 20.7–22.4 bar (2.07–2.24 MPa) with nitrogen gas. This ensures that electrical continuity is maintained within the cell module and prevents leakage of gases or liquids either within the module or to the surrounding atmosphere. Typical operating characteristics of the cell stack are

given in Table 5.4, while Fig. 5.8 indicates the cell voltage–time relationship, both for a module of fourteen 0.093 m^2 cells.

Overall, the performance of solid polymer electrolysers is impressive, particularly regarding their high operating current densities and relatively low cell voltages. Further improvements are being made and active development includes the following:

1. Increased size of the cell area; 0.92 m^2 cells are now being considered.
2. A reduced membrane thickness would provide a lower potential drop in the polymer electrolyte; 125- and 175-μm thick membranes have been tested.
3. Higher current densities (up to 2.1 A cm^{-2}) are now being used, providing an increased space–time yield.
4. Higher operating temperatures (up to 150° C) promote electrolyte conductivity and help reduce overpotentials, facilitating a lower cell voltage.

Table 5.4 Typical performance of a solid polymer electrolyte cell

Parameter	Value
Cell module:	
Cell active area	0.093 m^2
Number of cells	> 7–51
Current density	1.075 A cm^{-2}
Maximum current	1000 A
Initial cell voltage	−2 V/cell
Gas production:	
Hydrogen gas flow rate	0.42 $m^3 h^{-1}$/cell
Oxygen gas flow rate	0.21 $m^3 h^{-1}$/cell
Hydrogen gas purity	H_2 > 99.995% by volume O_2 < 0.005% by volume Halogens and halides < 4 v.p.m.* Total impurities < 50 v.p.m.
Oxygen gas purity	O_2 > 99% by volume H_2 < 1% by volume Total impurities < 500 v.p.m.
Maximum differential pressure (H_2 over O_2)	7 bar
Process water:	
Demineralized water conductivity	< 0.25 μS cm^{-1}
Inlet temperature	50° C
Outlet temperature	65° C

*Volumes per million (volumes)

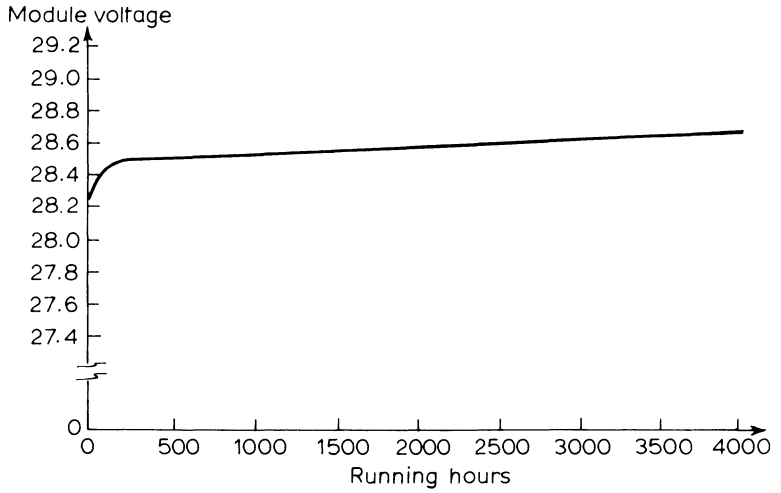

Fig. 5.8 Module voltage as a function of time for a solid-polymer electrolyte cell stack (cf. Fig. 5.7). Each module consists of 14 cathodes, each of area 0.093 m^2 operating at 1.075 A cm^{-2} and 55° C.

5.3 SODIUM CHLORATE AND SODIUM BROMATE

5.3.1 Sodium chlorate

Sodium chlorate is used in papermaking – where demand for it is increasing – in the textile industry, and as a cheap, if unselective, weedkiller. There are many electrolytic plants for its production, usually on the 5000–20 000 ton $year^{-1}$ scale and, because of the proximity of both wood and hydroelectric power, it is common in Scandinavia, Japan and North America for plants to be close to the papermills.

The electrolytic formation of chlorate is dependent on complex solution chemistry coupled to a simple electron-transfer process. In simplified terms, the overall cell reaction is:

$$NaCl + 3H_2O \longrightarrow NaClO_3 + 3H_2 \tag{5.11}$$

which is obtained via anodic evolution of chlorine:

$$6Cl^- - 6e^- \longrightarrow 3Cl_2(aq) \tag{5.12}$$

and reduction of water at the cathode:

$$6H_2O + 6e^- \longrightarrow 3H_2 + 6OH^- \tag{5.13}$$

The chlorine is hydrolysed to yield hypochlorous acid and hypochlorite:

$$3Cl_2(aq) + 3H_2O \rightleftharpoons 3HCl + 3HOCl \tag{5.14}$$

$$HOCl \rightleftharpoons H^+ + OCl^- \tag{5.15}$$

which react together, in the bulk electrolyte, to produce chlorate:

$$2HOCl + OCl^- \longrightarrow ClO_3^- + 2HCl \qquad (5.16)$$

This route consumes 6F in order to produce 1 mol of chlorate. There is a second route to the formation of chlorate which involves direct anodic oxidation of hypochlorite. This has the stoichiometry:

$$6OCl^- + 3H_2O - 6e^- \longrightarrow 2ClO_3^- + 4Cl^- + 6H^+ + 3/2O_2 \qquad (5.17)$$

and is best avoided as it consumes 9F, the additional 3F being consumed in oxygen evolution. Hence, the energy consumption can be optimized by using a cell with a high Reynolds number and turbulence so that the hypochlorite is removed from the anode surface before reaction (5.17) can occur. Since reaction (5.16) is rather slow, the process is best carried out with circulation of the electrolyte, either to a zone away from the electrode but within the cell or to an external reservoir where reaction (5.16) can go to completion before electrolyte re-enters the interelectrode gap. With such a process design, the hypochlorite concentration in the cell does not build up; not only is the further oxidation of hypochlorite avoided but a separator to stop its reduction at the cathode becomes unnecessary and the cathode reaction may be used to maintain the pH of the electrolyte constant (one proton per electron transferred is formed at the anode and removed at the cathode). Careful control of the pH is essential because the hydrolysis of chlorine requires a pH above 6 while the disproportionation of hypochlorite requires some of the anion to be in the protonated form. It is also important to control temperature in order to minimize the contribution of reaction (5.17) to chlorate production.

It is conventional to add Cr(VI) to the electrolyte (usually in the form of $Na_2Cr_2O_7$) in order to improve the current efficiency for chlorate production. This additive is believed to prevent electroreduction of OCl^- and ClO_3^- generated at the anode and to provide buffering at a (near optimum) pH of *c.* 6.6. The electrolysis is usually performed in an undivided cell, often using a bipolar stack of parallel electrodes to provide simplicity of construction and a reasonable space–time yield. The cathode faces are usually steel. Traditionally, graphite anodes were used, but modern reactors utilize platinized titanium or other precious metal–metal oxide coatings (RuO_2, dimensionally stable anodes, etc.). As in the case of chlorine cells, graphite anodes show problems of a high overpotential and relatively high loss rates (4–8 kg ton^{-1} ClO_3^-). Typical current densities are 200–300 mA cm^{-2} for platinized Ti (cf. graphite at 20–80 mA cm^{-2}) with a cell voltage in the range from -2.8 to -4 V. With a current efficiency of 80–98.5%, the specific energy consumption lies in the range 4500–6500 kWh ton^{-1}.

The electrolyte is circulated rapidly through the cell but is held in a reservoir for the disproportionation to go to completion; once formed, the chlorate is totally stable and the electrolyte may be recirculated to obtain maximum chloride consumption. In general, the electrolyte is initially NaCl (3.3 mol dm^{-3})

plus $NaClO_3$ (3 mol dm^{-3}) and the electrolysis is terminated when the chlorate concentration reaches 5.5 mol dm^{-3}. There are several types of cell design and process strategy for chlorate production; it is apparent that no single cell or process design is optimum and, indeed, several different designs compete effectively in industry.

Figure 5.9 shows one type of chlorate cell using internal recirculation of electrolyte, induced by H_2 gas lift of the solution. The mixture of H_2–NaCl, NaClO and $NaClO_3$ flows upwards towards a 'chimney' section near the top of the reactor. Hydrogen gas disengages and may be removed for purification and recovery. Addition of saturated brine is made at the top of the reactor. The $NaClO_3$ product is removed in aqueous NaCl and crystallized externally. A wide

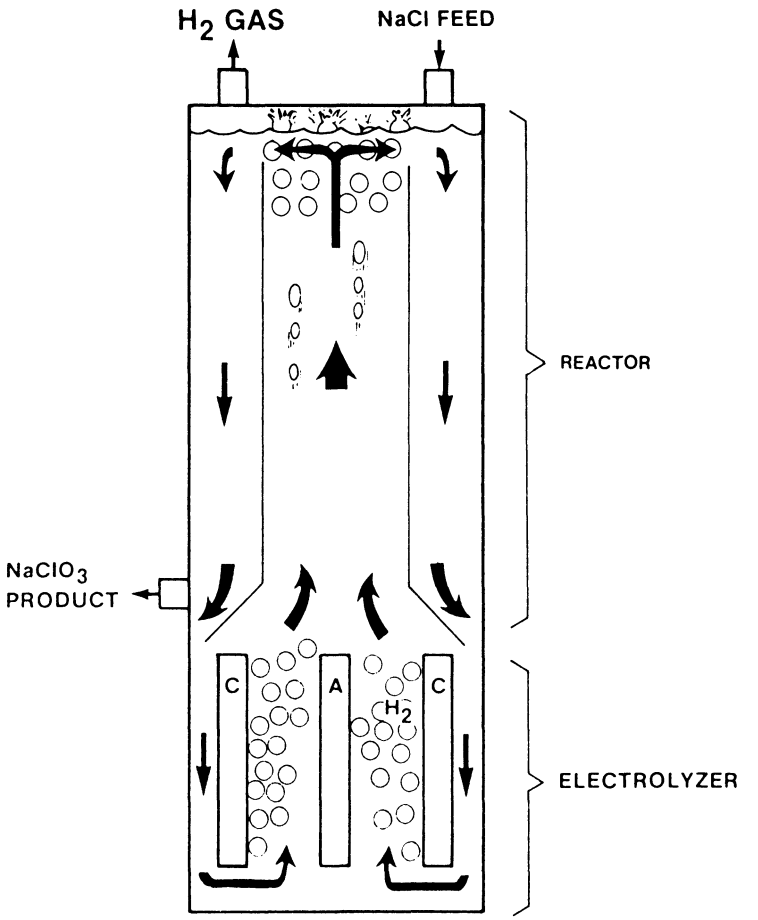

Fig. 5.9 A chlorate production cell which utilizes internal recirculation of electrolyte. The figure illustrates the Occidental Chemical Corporation LCD Mk II cell. (Courtesy: Occidental Chemical Corp.)

Table 5.5 Typical operating conditions and voltage components for the LCD Mk-II chlorate cell

Current	100 kA
Current density	230 mA cm^{-2}
Current efficiency	95%
Brine feed	310 g dm^{-3} NaCl
	25° C
Product stream	120 g dm^{-3} NaCl
	450 g dm^{-3} $NaClO_3$
Temperature	90°C
Off gases	2.2% O_2
	0.8% Cl_2

	Potential/V
Busbars	−0.080
Interelectrode gap *iR*	−0.13
Cathode overpotential	−0.84
Anode overpotential	−0.03
Reversible cell potential	−1.67
Total cell voltage	−2.76

variety of constructional materials have been used for reactor design, but the trend towards relatively high operating temperatures of *c.* 80° C means that titanium is often a favoured material. Table 5.5 summarizes operating conditions and the voltage components of a modern chlorate cell which utilizes internal recirculation of electrolyte, (the LCD Mk-II from Occidental Chemical Corporation).

The majority of chlorate cells involve a relatively high external circulation rate of electrolyte. The Krebs cell technology provides one example of this type of cell, as does the Albright and Wilson (Americas) process which is illustrated in Fig. 5.10.

5.3.2 Sodium bromate

Electrolysis of aqueous bromide liquors is one of the principal methods for production of sodium and potassium bromate. The initial reaction products are bromine at the anode and hydroxyl ions at the cathode. In an undivided cell, mixing of these species within the interelectrode gap results in hypobromite formation. This species then decomposes to bromate. The chemistry is complex and analogous to the reactions for chlorate (section 5.3.1). Loss of the hypobromite by cathodic reduction may be minimized by the addition of alkali metal



Fig. 5.10 An industrial plant for the production of sodium chlorate (the Erco process). Production is typically up to 42 000 tons per year of sodium chlorate. The process operates at a current density of 0.21–0.28 A cm^{-2} and a temperature of 80–90° C. The electrolyte, which has pH 6.4–7, contains 1.5–5 g dm^{-3} $Na_2Cr_2O_7 . 2H_2O$. Typical raw-material consumption per tonne of product are: NaCl, 550 kg; HCl, 15 kg; NaOH, 10 kg; $Na_2Cr_2O_7 . 2H_2O$, 2.5 kg. (Courtesy: Albright and Wilson Americas.)

dichromates (which are thought to produce a film on the cathode) or by dividing the cell. In the latter case, the anolyte and catholyte are allowed to react outside of the cell. The electrolyte is typically maintained at a temperature of 60–70° C. Cathode materials include stainless steels or copper sheets, often in perforated form, while anodes may be fabricated from carbon, platinized titanium or (particularly) lead dioxide which has been deposited on impregnated graphite, stainless steel or titanium. Depending on the electrode materials, the anode current density lies in the range 100–250 mA cm^{-2}, with a cell voltage of from

-2.4 to -4.3 V. Initially, the electrolyte typically contains 260 g dm^{-3} sodium bromide, together with sodium bromate (80 g dm^{-3}) and may be prepared by addition of bromine to the alkali metal hydroxide. Following electrolysis, the electrolyte is filtered, then cooled, and the bromate is precipitated by addition of NaOH or KOH. The crystallized product is filtered or centrifuged from the mother liquor, washed with water to remove bromide and chromate, then dried. The mother liquor may then be recycled.

A recent development has been the introduction of more efficient, flow-through filterpress cells as replacements for the traditional tank cells.

5.4 PERACIDS AND THEIR SALTS

Electrolysis is used to manufacture sodium, potassium or ammonium salts of several peracids including persulphates, perchlorates, periodates, and perborates by anodic oxidation of sulphate, chlorate, iodate and borax respectively and, indeed, electrolysis is the only commercial route to several of these anions. All are now very small-scale processes although in the past persulphate has been a medium-tonnage process because it was an intermediate in the manufacture of hydrogen peroxide; now hydrogen peroxide is mainly produced via a homogeneous catalytic route with anthraquinone as the catalyst. This method requires only 10–20% of the energy consumed in the electrolytic process and also is capable of producing 37% aqueous solutions directly (cf. electrolytic method with only 5%). Presently, the major interest in the electrolytic production of hydrogen peroxide is the production of strongly alkaline solutions by the reduction of oxygen (section 5.7).

The electrochemical formation of all these peroxyanions requires a high positive potential and to facilitate such conditions, it is normal to use an acidic medium and either a Pt or PbO_2 anode. Because platinum is often superior it is usual to use a platinized titanium, tantalum or niobium surface or a thin platinum foil spread on a base-metal support.

The largest of these processes remain those for ammonium and sodium persulphate and there are several plants operating on the 2000–10 000 ton $year^{-1}$ scale. The processes involve the oxidation of the sulphate in a sulphuric acid medium at a Pt-based anode and the medium must be free of heavy-metal ions which catalyse the decomposition of persulphate. The current density is high – about 1 A cm^{-2} – and the current efficiency 60–80%. Two cell technologies are used: (1) a cell with an asbestos diaphragm; and (2) an undivided concentric tube cell. To avoid reduction of the persulphate at the cathode, the conversion per pass is kept low and the persulphate is crystallized between passes through the cell.

Perchlorate is always made as the sodium salt; potassium and ammonium perchlorate are then prepared by double decomposition. The electrolyte is sodium chlorate (300–700 g dm^{-3}) at a pH between 0 and 1 and sodium perchlorate is also often present in the cell feed to ease isolation of the product.

The anode is a platinized titanium or platinum-covered base metal and the cathode is steel or another cheap metal; a separator is not necessary as the reduction of perchlorate is strongly kinetically hindered and the cathode reaction is hydrogen evolution. Reported energy consumptions lie in the range 2400–3500 kWh ton^{-1}. The energy efficiencies are as low as 20–40%, suggesting that cell designs could well be improved.

5.5 POTASSIUM PERMANGANATE

Potassium permanganate is widely used as an oxidizing agent, especially for oxidation in the fine-organic-chemicals industry. World production is about 40 000 ton $year^{-1}$, by far the largest plant being 15 000 ton $year^{-1}$ sited in the USA. The electrochemical step is the oxidation of manganate:

$$MnO_4^{2-} - e^- \longrightarrow MnO_4^- + OH^- \tag{5.18}$$

which is carried out in a strongly alkaline aqueous medium; the cathode reaction is always hydrogen evolution. Hence, the overall cell reaction is:

$$MnO_4^{2-} + H_2O \longrightarrow MnO_4^- + \tfrac{1}{2}H_2 + OH^- \tag{5.19}$$

The starting point for the manufacture of permanganate is pyrolusite ore which contains about 60% manganese dioxide. The ore is ground and suspended in 50–80% potassium hydroxide and oxidized by air to the manganese(VI) state, either in the liquid phase or by evaporating the solution and roasting the resulting solids in air-filled rotary kilns. In either case, the oxidation is carried out in two stages and the conditions must be controlled carefully in order to obtain a pure manganate solution.

The electrochemical oxidation is carried out with an electrolyte containing potassium hydroxide (1.4 mol dm^{-3}) and potassium manganate (100–250 g dm^{-3}) at 60°C at an anode made from nickel or monel (Ni–Cu). The cathode is iron or steel. The anode reaction requires an unusually low current density between 5 and 15 mA cm^{-2}. Even so, some oxygen evolution occurs and the current yields are only between 60 and 90%; the material yield generally exceeds 90%.

With such a low current density, there is a premium on packing the maximum electrode area into the cell volume in order to obtain an acceptable space–time yield. There are, however, several types of cell design used in the manufacture of permanganate. The early and smaller processes are based on batch cells. Figure 5.11 shows an example of such a cell used in Germany. The cell body is a cylindrical rubber vessel jacketed to allow steam-heating or water-cooling and it is fitted with a stirrer; a series of concentric nickel sheet tubes (anodes) alternate with a ring of steel rod cathodes, each surrounded by a porous polyvinylchloride bag to decrease the transport of permanganate to the cathode. The electrical connection is monopolar with 2.5 V applied between anode and cathode and the anode current density is 10 mA cm^{-2}. The cell is charged with a solution

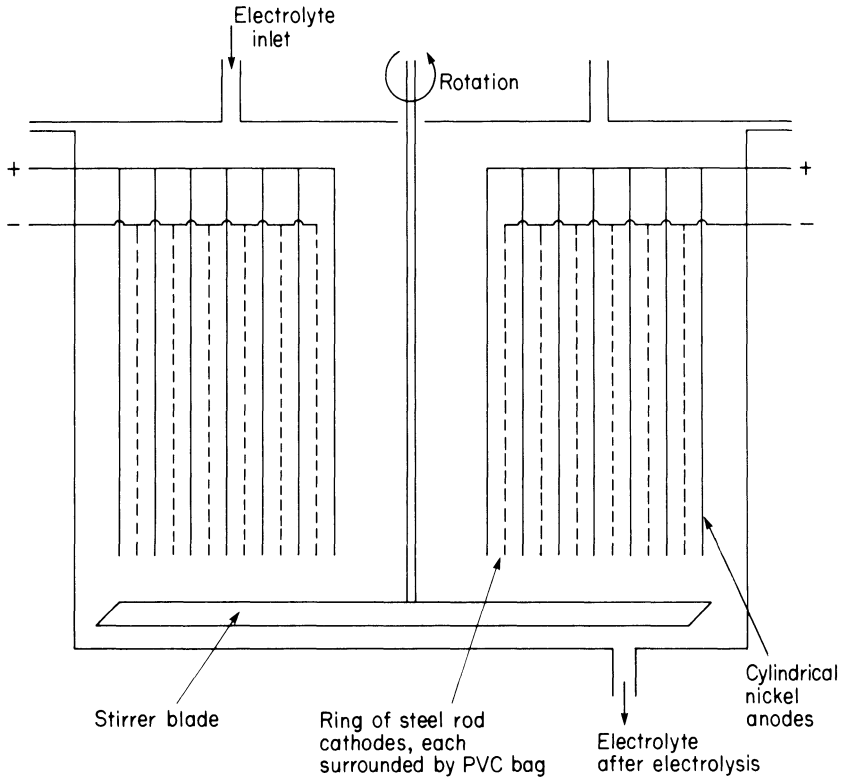

(a)

containing potassium hydroxide (2 mol dm^{-3}) and potassium manganate (250 g dm^{-3}) and the electrolysis is continued until the manganate concentration has dropped to about 10% of the original level. The current efficiency is 80% with an energy consumption of 600 kWh ton^{-1}.

The larger-scale American process is continuous and fully automated. The electrolysis unit is arranged as a bipolar filterpress containing three groups of twenty cells. The electrolyte feed to the three groups of cells is parallel but within each of the groups there are openings for electrolyte flow between the individual cells so that the feed passes serially through the twenty cells (Fig. 5.12(a)). Each of the bipolar electrodes is manufactured on a steel baseplate. On the anode side is welded a monel gauze (about 8 mesh) while onto the cathode side is welded a steel sheet with small perpendicular projections. The space between the projections is filled with an insulator (e.g. polystyrene) so that only the ends of the projections are in electrical contact with the solution. This gives a cathode of low surface area compared with that of the anode (1:150) but one where the active area is uniformly distributed over the face opposite the anode. Such low-surface-area counter-electrodes avoid the use of a separator because, even if the

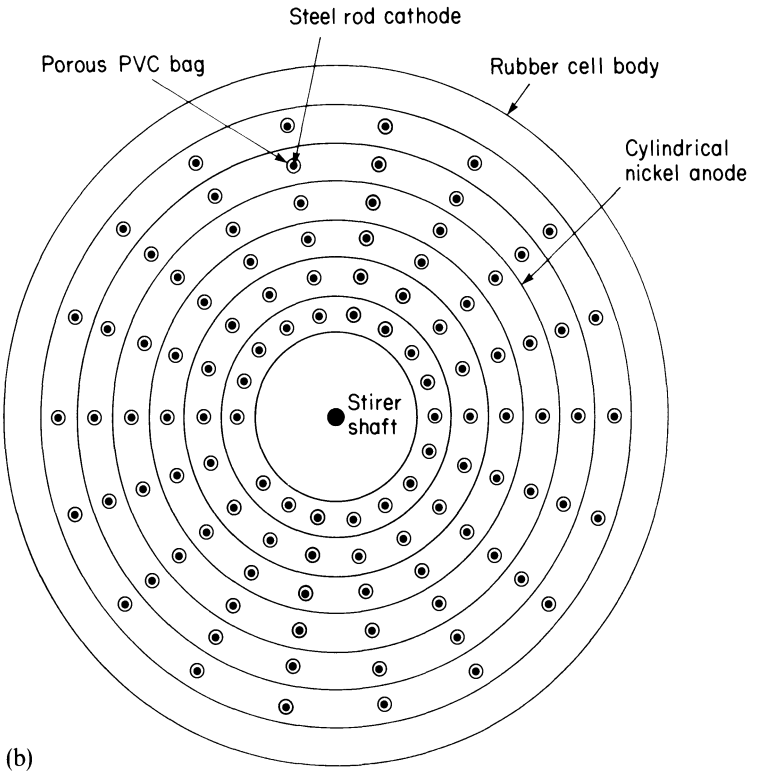

Fig. 5.11 A batch cell for the production of potassium permanganate (Neue Bitterfelder cell). (a) Side view. (b) View from above.

reduction of permanganate is diffusion-controlled, the flux of permanganate is totally insufficient to maintain the essential, very high current density and most of the cathode current therefore must go into hydrogen evolution. There is a penalty in the cell voltage for this trick, however, since both the cathode overpotential and the cell resistance must be increased. The edges of the electrodes are insulated and the spacing between the electrodes is 22 mm.

The electrolyte is pumped through the cell with a high Reynolds number since turbulence minimizes the crystallization of the product in the cells. The electrolyte feed contains potassium hydroxide (120–150 g dm^{-3}), potassium manganate (50–60 g dm^{-3}) and potassium permanganate (30–35 g dm^{-3}) and in the effluent from the cell the permanganate concentration has almost doubled. The current efficiency is about 90%, so the effluent also contains oxygen and hydrogen (from the cathode) and to assist the escape of gas the cell unit may be at a slight angle.

In this cell the current density is 8.5–10 mA cm^{-2} at the anode and the cathode current density is 1.3–1.5 A cm^{-2} with an undivided cell voltage of from -2.3 to

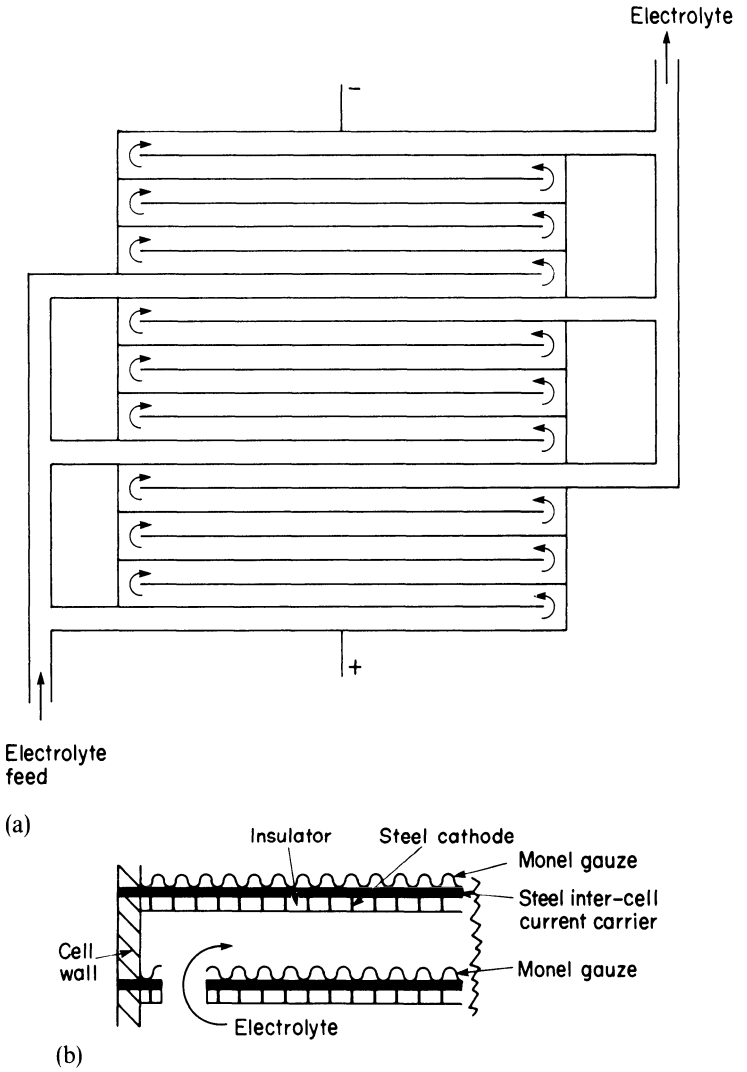

Fig. 5.12 Electrolysis cell used by the Carus Chemical Co. for the production of potassium permanganate. (a) Electrolyte-flow pattern. (b) Design of the bipolar electrodes.

−2.8 V. The total voltage across the sixty-cell stack is 140–170 V with a cell current of 1200–1400 A. The energy consumption is 500 kWh ton^{-1} although the energy required for pumping must, in this process, be high.

5.6 POTASSIUM DICHROMATE AND CHROMIC ACID

The oxidation of the chromic ion:

$$2Cr^{3+} + 7H_2O - 6e^- \longrightarrow Cr_2O_7^{2-} + 14H^+ \qquad (5.20)$$

in acidic media has been used for the manufacture of potassium dichromate but more commonly the reaction has been used to regenerate spent chromic acid solutions from the oxidation of organic compounds (e.g. anthracene, pyrene, montan wax) etching and polishing baths and for conditioning chromium plating baths (Chapter 7). As part of processes for the indirect oxidation of organic compounds, several such chromic acid electrolyses operate on a 1000 ton $year^{-1}$ scale; in the other applications the scale is always small.

Invariably, the electrolysis medium contains sulphuric acid but the concentrations of both the acid and the chromium(III) vary widely depending on the source of the solution; from the oxidation of organic compounds, a typical solution may contain 1 mol dm^{-3} Cr(III) and 3 mol dm^{-3} H_2SO_4, while from a plating bath to be conditioned, the chromium(III) may be as dilute as 0.02 mol dm^{-3} with 0.005 mol dm^{-3} H_2SO_4 and a large excess of chromium(VI).

The only common anode material with which it is possible to obtain a high current efficiency is lead dioxide and, although it is subject to slow corrosion in the electrolysis conditions, lead dioxide formed *in situ* on lead or a lead alloy (e.g. Pb–5% Sb) is the only practical choice as anode material. The oxidation of chromium(III) to chromium(VI) at a lead dioxide anode requires a high positive potential, so it is always likely that some oxygen evolution will occur as a competing reaction. With concentrated solutions of chromium(III), it is possible early in the electrolysis to obtain current efficiencies above 95% with a current density of 50–200 mA cm^{-2}. The current efficiency drops as the chromium(III) concentration diminishes and, with solutions containing very low concentrations of chromium(III) and less acid, a figure of 30–50% at 30 mA cm^{-2} is more likely. It is also well known that organic molecules in the anolyte poison the lead dioxide surface causing oxygen evolution to occur at a dramatically enhanced rate. Hence, solutions from organic reactions must be scrubbed before they are passed to the electrolysis cell.

The old design of cell is based on a lead-lined tank filled with aqueous sulphuric acid, and the spent chromic acid solution in porous ceramic pots was placed in the tank. The anodes were lead rods dipped into the ceramic pots and the cathode was the lining to the tank. The plant was obviously operated totally as a batch process. More modern and economic cells are now available; they are often based on a bipolar filterpress concept with lead alloy anodes, steel cathodes and a Nafion proton-conducting membrane. The energy consumption and space–time yields with such cells are clearly likely to be superior. Moreover, such cells can be operated as continuous or semi-continuous processes.

5.7 HYDROGEN PEROXIDE

Peroxide solutions find use as oxidizing or bleaching agents in many sectors of industry.

An on-site electrolytic process offers particular advantages for the pulp and paper industry where peroxide mixtures are used to brighten and bleach pulp

and then bleach the secondary fibre. Typically, mechanical pulp bleach liquors contain 20–30 g dm^{-3} NaOH, 40–70 g dm^{-3} Na_2SiO_3 and 15–25 g dm^{-3} H_2O_2, while chemical pulps contain 10–15 g dm^{-3} NaOH, 15–20 g dm^{-3} Na_2SiO_3 and 5–10 g dm^{-3} H_2O_2, both liquors containing stabilizers.

The cathodic reduction of dissolved oxygen to peroxide was first demonstrated by Traube in 1882. Commercialization of an electrolytic process for hydrogen peroxide has been retarded by several factors related to the complex electrochemistry of oxygen reduction, together with a poor understanding of the influence of electrode materials and cell design on the process efficiency. There has been a gradual awareness of the desirable factors for a successful process over the last 10–15 years, which include:

1. An alkaline electrolyte.
2. Carbon- or graphite-based electrodes.
3. Pure electrolytes, free from transition-metal ions which may decompose the peroxide and drastically reduce current efficiency.
4. High-surface-area electrodes due to the sluggish kinetics and mass transport restrictions due to the low solubility of oxygen.
5. Porous electrodes which help prevent $NaHO_2$ precipitation and facilitate a three-phase reaction site (electrode/O_2/H_2O).

Many pilot-scale cells have utilized fuel-cell type electrodes (Chapter 11), in particular, porous, PTFE-bonded carbon surfaces. Here, a dispersed carbon surface provides high electroactive area and the reaction zone is limited to the electrolyte side of the electrode. Such electrodes are, however, prone to $NaHO_2$ precipitation which blocks the micropores, hindering flow distribution, lowering the mass transport and blinding active cathode area.

Some of the more successful pilot cells have incorporated trickle flow, packed beds of particulate carbon (e.g. crushed graphite) with a relatively high porosity, together with high electrolyte and oxygen flow rates to prevent $NaHO_2$ precipitation, control bed flooding, and elevate the mass transport. High gas-flow rates can be economically justified only by extensive recycling. An additional problem is the need for the gas to displace electrolyte in the bed, leading to a significant pressure drop.

Most recently, cells developed by the Dow Chemical Company, operating at ambient temperature and pressure, have been based on a trickle-bed cell in which the trickle catholyte flow is achieved by controlled seepage of anolyte through a diaphragm (Fig. 5.13). The catholyte flow is controlled such that the desired concentration of peroxide is obtained in a single pass through the reactor. The porous nature of the bed ensures rapid drainage, such that only the portion of the bed adjacent to the separator is wet. The oxygen is introduced at the top of the reactor, and is dispersed by the dry portion of the bed prior to entering the wet, active cathode region near the separator. The pressure drop through the bed is kept low (< 210 N m^{-2} cm^{-1} of bed height) by the dry and porous nature of the bulk cathode.

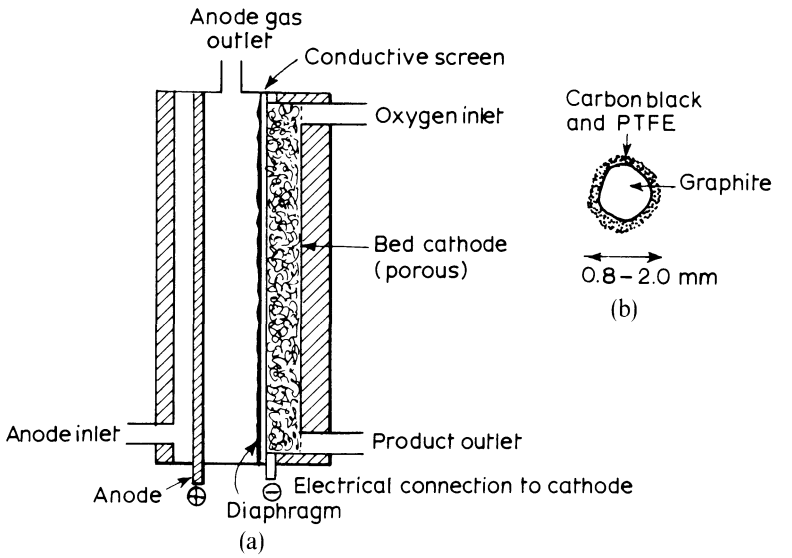

Fig. 5.13 A diaphragm-controlled, trickle-flow, packed-bed cell for hydrogen peroxide production. (a) The unit cell. (b) The 'composite chip' particles which constitute the packed-bed cathode (active area $\leqslant 3\ m^2\ g^{-1}$). (Courtesy: Dow Chemical Co. and Huron Chemicals.)

One of the best cathode materials has been found to be 'composite' PTFE–carbon chips (*c.* 0.8–2 mm) manufactured with a PTFE latex to surface-coat carbon black onto the graphite particles (Fig. 5.13(b)).

In an alkaline electrolyte (typically 0.5–1 mol dm^{-3} NaOH)* the major reactions are:

$$\text{Anode:} \qquad 2OH^- - 2e^- \longrightarrow \tfrac{1}{2}O_2 + H_2O \tag{5.21}$$

$$\text{Cathode:} \qquad O_2 + H_2O + 2e^- \longrightarrow HO_2^- + OH^- \tag{5.22}$$

$$\text{Overall cell:} \qquad OH^- + \tfrac{1}{2}O_2 \longrightarrow HO_2^- \tag{5.23}$$

In practice, OH^- is added to the anolyte as NaOH, O_2 is pumped into the top of the cathode compartment, and HO_2^- (plus some unreacted O_2) is collected at the catholyte outlet. The anode must be an efficient O_2 evolving material and must not give rise to soluble or insoluble impurities which catalyse peroxide decomposition. In practice, suitable anode materials include platinized titanium.

* Lower NaOH concentrations provide a conductivity which is too low for economic operation, as the cell voltage becomes unacceptably high, e.g. −4.6 V in 0.25 mol dm^{-3} NaOH.

There are two major reactions which result in loss of product or a lowering of observed current efficiency. Electrochemical oxidation or reduction of peroxide may occur:

$$\text{Anode:} \quad HO_2^- + OH^- - 2e^- \longrightarrow O_2 + H_2O$$

$$E^\ominus = 0.08 \text{ V} \tag{5.24}$$

(which is the reverse of reaction (5.18)) and:

$$\text{Cathode:} \quad HO_2^- + H_2O + 2e^- \longrightarrow 3OH^-$$

$$E^\ominus = 0.88 \text{ V} \tag{5.25}$$

In addition, it is well known that peroxide solutions can be catalytically decomposed by trace-metal ions:

$$2H_2O_2 \longrightarrow 2H_2O + O_2 \tag{5.26}$$

This reaction may occur homogeneously (in bulk solution) or heterogeneously (at the electrode surface).

At high cathode current densities (i.e. more negative potentials) the rate of reaction (5.25) increases significantly, resulting in a marked fall in current efficiency. In practice, current efficiencies are typically 60–67% (15.5 mA cm^{-2}), 50–58% (30 mA cm^{-2}) and 20–28% (60 mA cm^{-2}) with a 1 mol dm^{-3} NaOH feed at 25°C and 1.07 cm^3 min^{-1} catholyte flow. Reaction (5.25) is thermodynamically favoured, but kinetically sluggish such that cathodic loss of peroxide is significant but bearable.

Electrolyte temperature is maintained by an external cooler, while liquid flow rate is carefully controlled to provide a suitable combination of trickle flow, relatively high mass transport and high fractional conversion per pass.

Within the last 2 years, Dow-Huron (known as DH Tech Inc.) have built a sizeable (approximately 1 ton day^{-1}) facility for H_2O_2 in the Great Lakes area of Canada. Based upon the technology described above, this plant is installed in a paper and pulp plant in order to provide bleaching solution to the mill's requirements.

5.8 OZONE

The possibility of anodic synthesis of ozone has been known since 1840; indeed, electrolysis is the method by which ozone was first discovered.*

In simple terms, ozone may be formed by the direct anodic oxidation of water:

$$3H_2O - 6e^- \longrightarrow O_3 + 6H^+$$

$$E^\ominus = 1.51 \text{ V} \tag{5.27}$$

* Schonbein (1840) *Pogg. Ann.* **50**, 616.

The major competing process is oxygen evolution, which occurs at a much lower potential:

$$2H_2O - 4e^- \longrightarrow O_2 + 4H^+$$

$$E^\ominus = 1.23 \text{ V} \tag{5.28}$$

and is, therefore, thermodynamically favoured. A minor contribution to ozone production may also arise from anodic oxidation of the evolved oxygen:

$$O_2 + H_2O - 2e^- \longrightarrow O_3 + 2H^+$$

$$E^\ominus = 2.07 \text{ V} \tag{5.29}$$

Oxygen evolution (reaction 5.28) is always an important competitive reaction and must be inhibited in order to achieve a reasonable anode current efficiency for ozone synthesis. Therefore, much of the technology of electrolytic ozone generation has concerned the fabrication and preparation of anodes having a high oxygen overvoltage. Additionally, anions in the chosen electrolyte must be stable to oxidation. The anode must also be stable to the relatively high current density as well as the oxidizing and highly acidic conditions at the interface during active ozone production, be highly conductive and also thermally and mechanically stable. There are two main strategies for electrolytic generation of ozone. The first uses solid polymer electrolyte technology. In this approach, ozone may be produced directly as a solution by passing a stream of relatively pure water down the reverse side of a three-dimensional porous anode (e.g. PbO_2) in contact with a solid polymer (e.g. a perfluorosulphonic acid membrane) electrolyte. This method is capable of producing a high level of ozone in water. Relatively high current densities (> 1 A cm^{-2}) may be realized but the current efficiency can be low ($< 14\%$). In this approach, hydrogen evolution is the usual cathode process. An interesting advantage of this process is that no ionic contamination of the water occurs, due to the use of a solid polymer electrolyte and pure water.

Alternatively, ozone may be evolved in a more conventional cell geometry using specialized electrolytes, e.g. HBF_4. The preferred cathodic reaction is usually oxygen reduction. The use of an air cathode precludes hydrogen management problems. Advances in the electrocatalytic properties and stability of cathode materials are likely to provide an increasing incentive to adopt this approach. Special fluorocarbon-impregnated vitreous carbon anodes have shown a relatively high current efficiency for ozone generation and are unusually stable to corrosion. The majority of laboratory and pilot-scale studies have employed lead dioxide anodes in H_2SO_4, $HClO_4$ or H_3PO_4 electrolytes. However, results have been disappointing in several respects:

1. Anode stability is problematic.
2. Current efficiency for O_3 is low (generally $\ll 15\%$).
3. The process is very dependent on the type of PbO_2 ($\alpha-$ or $\beta-$) its morphology and preparation, the substrate and time.

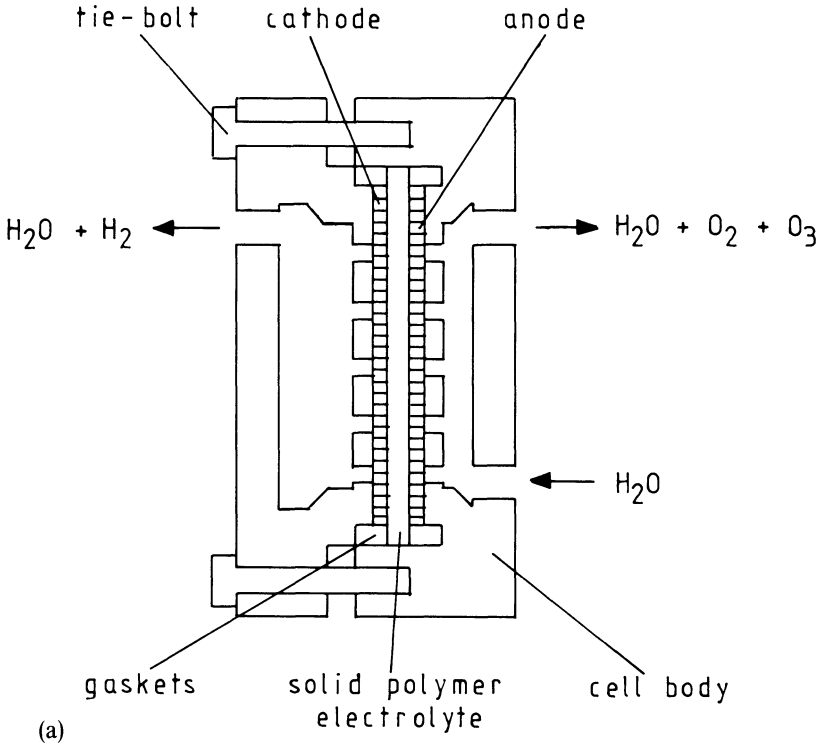

(a)

More recently, attention has been focused upon carbon anodes which have been prepared specially with a fluorocarbon binder or coating. Such electrodes have shown relatively high current efficiencies (>35%) when evolving ozone at 35% volume concentration at 10°C in 48% *w/v* HBF_4 at 400 mA cm^{-2}. Ozone collected above the anodes must be immediately diluted by air to lower the ozone concentration below explosion limits. Normally, a concentration of 15% wt is considered safe.

5.8.1 Three-dimensional PbO_2 anodes

The MEMBREL cell is shown in Fig. 5.14(a). A solid, perfluorinated cation-exchange membrane is used as the electrolyte. When immersed in water, this membrane serves both as an ionic conductor and an electrode separator. The membrane is sandwiched between two porous, three-dimensional electrodes; the anode material is PbO_2 while the cathode surface is platinum. Current is applied to the electrodes via two latticed, textured collectors which form part of the cell housing. Electrolysis typically involves a cell voltage of from −3 to −5 V typically with a current density of 0.5–2 A cm^{-2}. During electrolysis, hydrogen generated at the cathode–membrane interface is released to the atmosphere. The pure process water fulfils several functions. It acts as a source of oxygen for ozone generation, a solvent for ozone and a cooling medium. By operating the cell

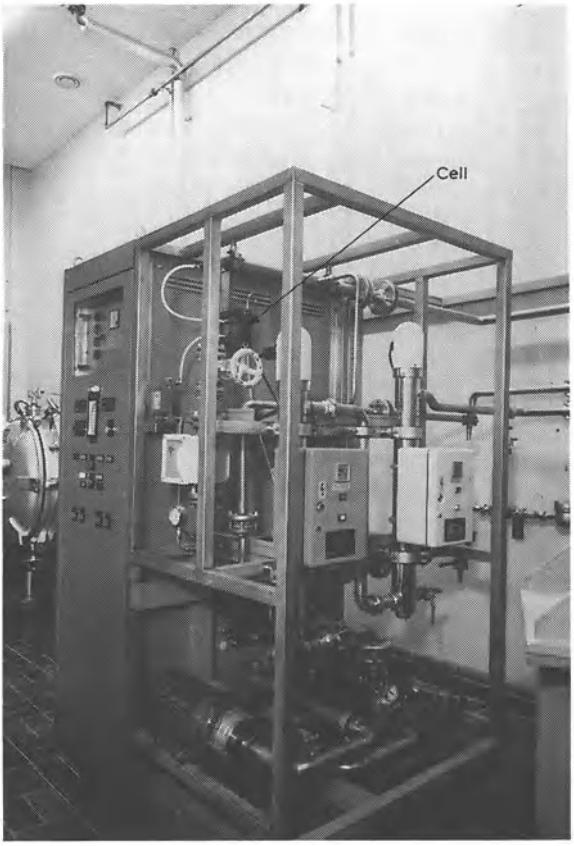

(b)

Fig. 5.14 The ABB-Membrel process for electrolytic generation of ozone using a solid polymer electrolyte. (a) Schematic of the 'Membrel' cell. (b) A complete ozone treatment unit including a circulating system, UV lamps, control panel and power supply. The system is used to deliver up to 2 $m^3 h^{-1}$ ultrapure water to a pharmaceutical production plant. Ozone is produced by a single Membrel cell of 30 cm^2 active electrode area. The cell is shown by an arrow. (Photographs courtesy: Asea Brown Boveri Ltd.)

under pressure, a highly concentrated solution of >100 mg dm^{-3} O_3 in (ultra pure) water may be produced directly. The water quality for this process is critical, demineralized water having a low conductivity (<20 μS cm^{-1}) is considered essential for trouble-free operation. Therefore, adequate pretreatment of the water is essential.

Many modern ultra-pure water systems are designed on a closed-loop basis, periodic ozone generation serving to continuously sterilize the system and prevent microbial growth. As ozone disintegrates to oxygen with a half-life of some 20 min, it is not possible to produce an overconcentration of ozone. For critical applications where residual ozone is unwanted, ultraviolet radiation may be used to decompose the ozone.

In practice, such ozone cells are extensively automated to control the process cycle (Fig. 5.14(b)) and may incorporate ultraviolet facilities. Current applications include those sectors of the pharmaceutical and fine-chemicals industry which require ultra-pure water for critical synthetic steps or to meet stringent purity limits. In such applications, the electrolytic route to ultra-pure water, via ozone generation, is competing against the more traditional methods of sterile filtration (e.g. ultra-filtration), ultraviolet irradiation and the use of conventional air-phase corona-discharge ozonizers.

5.8.2 Two-dimensional carbon-based anodes

Figure 5.15 shows a unit cell used commercially for electrosynthesis of ozone. A hollow cylindrical, fluorocarbon-impregnated carbon anode is used, refrigerated

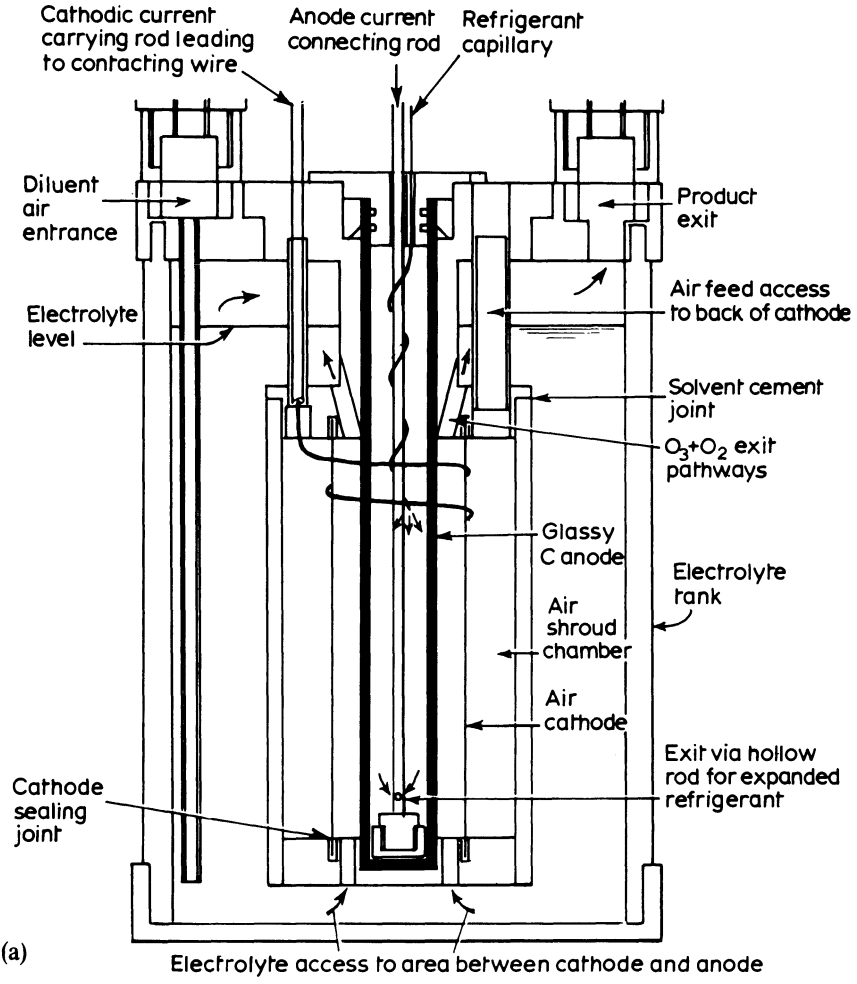

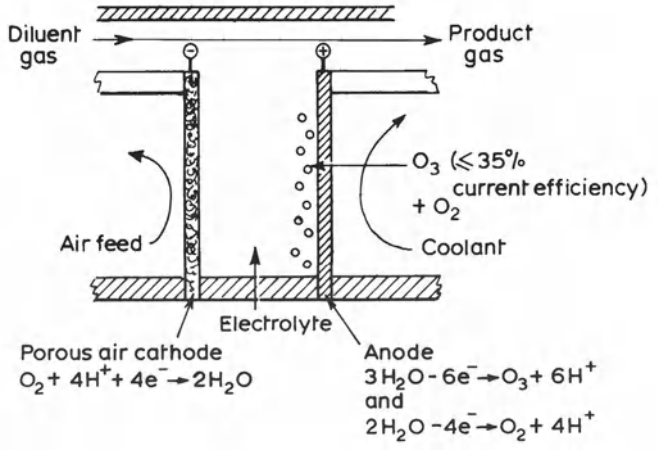

(b)

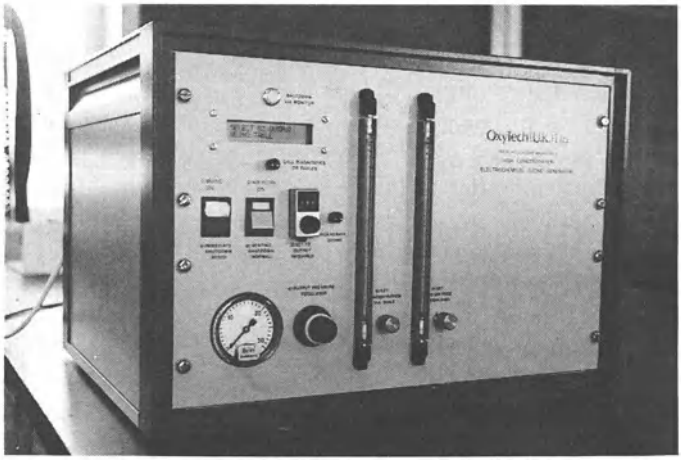

(c)

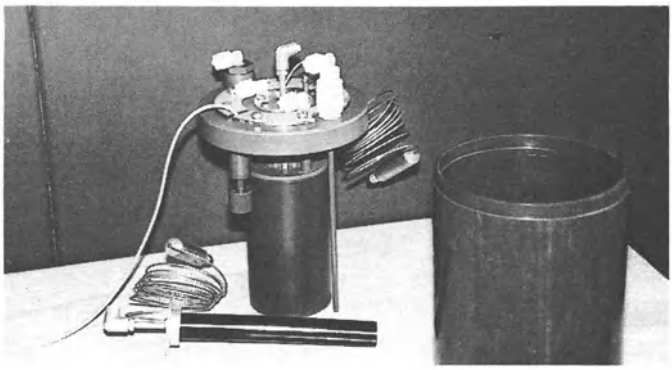

(d)

Fig. 5.15 A microprocessor-controlled electrolysis unit for ozone production. (a) The principles. (b) The concentric cell (a planar cell is under development for larger scale applications). (c) The micro-processor-controlled unit. (d) The cell components. (Photographs courtesy: OxyTech (UK) Ltd.)

Table 5.6 Data relevant to conventional and electrochemical ozonisers (*After*: Foller and Goodwin, personal communication)

O_3 source	% wt O_3	Specific energy requirement/kWh kg^{-1}	Partial pressure of O_3 in air p/mg dm^{-3}	Concentration* in water, c/mg dm^{-3}
Air-fed corona	1	26	12.1	4.7
Air-fed corona	2	44	24.2	9.4
Electrochemical	Diluted to 15	55–66	181.5	70.5

* Calculated from Henry's law. $p = Hc$ where H is the Henry's law constant at 20° C.

cooling water passing internally. Cooling is required at the approximate level of 0.9 W cm^{-2} external anode surface. It is usual to employ an 'air cathode' of the type used in fuel cells (Pt catalysed, high-surface-area carbon which has been sintered with a PTFE dispersion) which operates at *c.* 220 mA cm^{-2}.

The major application of electrochemical ozone cells is in the oxidation of water-based species (in order to provide sterilization) and the oxidation of industrial process liquors containing cyanides or organics, e.g. phenols, dyes and pesticides. In such applications it is environmentally more desirable than Cl_2 or OCl^- treatment (Chapter 7) as the latter chemicals may leave a range of undesirable species. Ozone treatments may be advantageously coupled with ultraviolet treatments in order to remove certain persistent chemicals (such as certain pesticides or polychlorinated biphenyls). In the case of sterilization of potable water, the cells are likely to remain small, modular designs (Fig. 5.15(b)). While the O_3 required is very dependent on inlet-water quality, a cell of 100 cm^2 anode area may service up to 1000 m^3 day^{-1} of water at the 1 mg dm^{-3} O_3 dose level.

Continued success of electrochemical ozonizers relies upon demonstrable advantages over the traditional gas phase, air-fed, corona-discharge devices. The latter cannot compete with electrosynthesis for high-level (> 5% wt) O_3 generation (Table 5.6) for use in chemical-waste treatment or industrial chemical processing. Other applications for electrochemical O_3 generation include cooling-tower water treatment and small, swimming pools at remote sites. The high specific energy consumption (Table 5.6) of ozonizers tends to mitigate against their wider use but devices such as the one shown in Fig. 5.15 are likely to have important selective applications.

5.9 MANGANESE DIOXIDE

The performance of Leclanché and related batteries (Chapter 11) depends critically on the source or method of manufacture of the manganese dioxide because the activity and properties of the oxide vary with crystallite size, density

of lattice imperfections and the extent of hydration. The manganese dioxide produced by the anodic oxidation of manganese(II) in solution is particularly active although it is also more expensive, perhaps by a factor of four compared with natural pyrolusite. As a result, electrolytic manganese dioxide is manufactured largely to be used in high-quality Leclanché cells or alkaline manganese batteries. More recently it has been recognized that the higher activity of electrolytic manganese dioxide extends to its chemical reactions with other species, especially if the manganese dioxide is used directly after its preparation. Hence, electrolytic manganese dioxide is increasingly considered as an oxidizing agent in the fine chemicals and pharmaceutical industries. The anodic oxidation of a manganous salt to MnO_2 dates back to 1830, while battery applications were not recognized until 1918. Over the last 20 years, the manufacture of manganese dioxide by electrolysis has expanded rapidly and the current world annual production probably exceeds 100 000 ton; most of the capacity is in Japan.

The manganese dioxide is formed by the electrode reaction:

$$\text{Anode:} \quad Mn^{2+} + 2H_2O - 2e^- \longrightarrow MnO_2 + 4H^+ \tag{5.30}$$

which is usually balanced by evolution of hydrogen:

$$\text{Cathode:} \quad 2H^+ + 2e^- \longrightarrow H_2 \tag{5.31}$$

The overall process is therefore:

$$Mn^{2+} + 2H_2O \longrightarrow MnO_2 + 2H^+ + H_2 \tag{5.32}$$

The additional acid formed may be recycled into an earlier stage of the manganese processing cycle, where solid $MnCO_3$ or MnO-based materials may be leached to produce the $MnSO_4$ solution. The MnO_2 deposits onto an inert anode such as graphite, lead dioxide or titanium. In fact, the anodic reaction is complex, involving hydrolysis and disproportionation of an adsorbed manganese species and its rate is limited by the kinetics of these chemical processes. Hence, the current density is always low. An undivided cell may be used as the manganese dioxide either remains on the anode surface (in traditional cells) or is rapidly removed from the cell by electrolyte pumping or suitable electrode movement. A typical electrolysis medium is manganese sulphate (0.5–1.2 mol dm^{-3}) in aqueous sulphuric acid (0.5–1 mol dm^{-3}) at 90–100° C and the electrolysis will be carried out at 5–15 mA cm^{-2}, requiring a cell voltage of from −2.2 to −3 V. Current yields of manganese dioxide are reported to be 75–95%, oxygen evolution and (to a lesser extent) Mn^{3+} formation being secondary reactions. Traditional cells are broadly similar to those described in Chapter 4 for copper winning and aqueous refining; they are based on an open tank with parallel and alternating lines of anodes and cathodes. The manganese dioxide layer is allowed to grow until it is 20–30 mm thick before the anodes are removed and the deposit removed mechanically. The manganese dioxide for batteries is normally dried at *c.* 80° C.

Such cells do not permit continuous operation and have a very low space–time yield. This has led to the study of cells where the MnO_2 is formed as a slurry in the anolyte in which case the manganese dioxide may be formed in a flow system, e.g. a filterpress. Usually such systems use a lower temperature and a higher pH; although successful in the laboratory and at the pilot-plant level, flow-through, parallel-plate or rotating-electrode designs have not seen widespread, full-scale use.

5.10 CUPROUS OXIDE

Copper(I) oxide finds a range of industrial applications; it is used as a precursor for a range of copper chemicals, a reducing agent in agricultural chemicals for vines and tropical crops, and as a pigment (particularly for marine antifouling paint, but also for ceramics). The scale of manufacture is relatively small; several plants around the world produce 150–700 ton $year^{-1}$. By suitable alteration of the electrolyte and electrolysis conditions, a wide range of colours, particle sizes and reducing capabilities may be achieved. The majority of processes, however, provide red cuprous oxide in powder form, with an average particle size of 3–4 μm. Purity varies, but for routine applications, a minimum Cu_2O level of 97% wt is allowed, the principle impurities being metallic copper (<0.5% wt), chlorides (<0.5% wt) and CuO (<0.5% wt).

A wide range of process conditions are used so that only an illustrative example is given here. The cell technology resembles that of an electrowinning tank house (Chapter 4), in that simple, undivided, monopolar cell is used; the parallel-plate electrodes are immersed in open (rubber-lined steel or polypropylene) tanks. Both anode and cathode are copper, some being cast material obtained from furnace refining of scrap material; the electrodes may conveniently be cast with an integral contact 'ear' to rest on the electrical busbars. The electrolyte is usually NaCl (140–180 g dm^{-3}) at pH 8–10 and a temperature of 65–75° C. Current densities are in the range 10–30 mA cm^{-2}, with a cell voltage of from −2.0 to −2.6 V.

The actual electrode processes are complex; in simple terms the main reactions may be described by:

$$\text{Anode: } 2Cu + 2OH^- - 2e^- \longrightarrow Cu_2O + H_2O \tag{5.33}$$

$$\text{Cathode: } 2H_2O + 2e^- \longrightarrow H_2 + 2OH^- \tag{5.34}$$

$$\text{Cell: } 2Cu + H_2O \longrightarrow Cu_2O + H_2 \tag{5.35}$$

At frequent intervals during the electrolysis the cell polarity is automatically reversed, such that each of the copper electrodes is the anode for half of its lifetime in the cell. This strategy prevents passivation of the anodes and helps provide a more uniform product. In some cells, manual scraping of the electrodes is also used.

The cells are operated on a batch basis; cuprous oxide falls from the anodes to the bottom of the tanks. At suitable intervals, the electrolysis is stopped, the residual electrodes removed for remelting, and the Cu_2O–NaCl slurry is agitated and pumped out of the cell for external separation of Cu_2O.

The anodic current efficiency for Cu_2O is typically 60–90%.

5.11 SYNTHESIS OF METAL SALTS VIA ANODIC DISSOLUTION

There is a growing awareness that electrochemical methods of synthesis may be used to achieve controlled purity compounds which are difficult to produce by chemical or thermal methods. A general strategy for the synthesis of metal salts or complexes is controlled anodic dissolution of the pure metal in a suitable electrolyte. In a simple case, the anode process may be the formation of a soluble, hydrated metal ion (as in electrorefining, section 4.3):

$$M - ne^- \longrightarrow M^{n+} \tag{5.36}$$

In electrorefining, the metal ion yields pure metal at the cathode. However, there are many specialized cases where the dissolved metal ion, a related metal salt, a coordination complex, or an organometallic have a premium value. Examples include $AgNO_3$ liquors for chemical processing, photographic materials and analytical reagents and potassium stannate $K_2Sn(OH)_6$ for tin and tin-alloy electroplating baths. In these cases, cathodic metal deposition or reduction of the complex may be prevented by a separator. Silver nitrate liquor may be readily obtained by anodic dissolution of pure silver into nitric acid; a divided cell prevents deposition of silver at the cathode. The metal may be in the form of discrete anodes or as suitably supported crystals. While the silver dissolves under open-circuit conditions (via corrosion) anodic processing allows a much faster and controlled rate of dissolution; the purity of the $AgNO_3$ solution is limited only by the quality of the Ag anode and the HNO_3 electrolyte.

In the potassium stannate process shown schematically in Fig. 5.16 the anode is a steel basket filled with solid tin bars or pellets immersed in KOH solution. Under suitable conditions, the tin dissolves as stannite:

$$Sn + 4OH^- - 2e^- \longrightarrow Sn(OH)_4^{2-} \tag{5.37}$$

The anolyte is sparged with air, which instantaneously oxidizes stannite to stannate:

$$Sn(OH)_4^{2-} + H_2O + \tfrac{1}{2}O_2 \longrightarrow Sn(OH)_6^{2-} \tag{5.38}$$

which is continuously withdrawn as a $K_2Sn(OH)_6$ solution from the anolyte chamber. K^+ ions transport from the anolyte to the catholyte compartment via the cation-exchange membrane. At the steel cathode, hydrogen evolution occurs:

$$2H_2O + 2e^- \longrightarrow H_2 + 2OH^- \tag{5.39}$$

The KOH effectively formed in the catholyte is metered back to the anolyte.

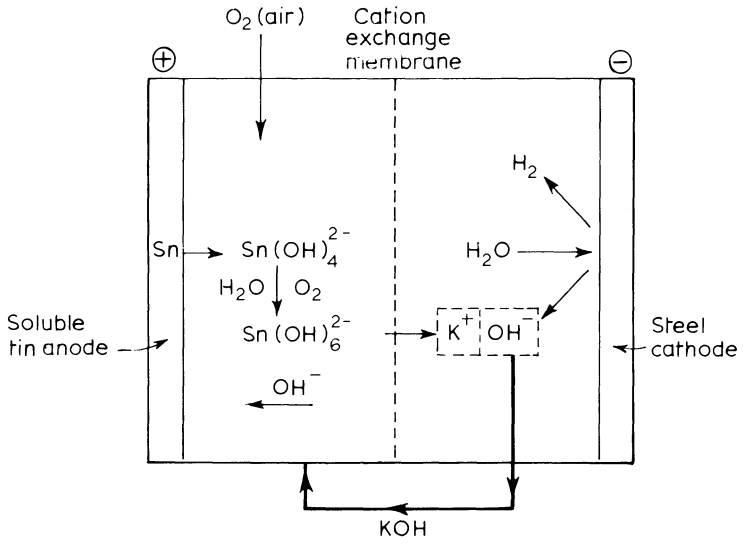

Fig. 5.16 A divided tank cell for the anodic synthesis of potassium stanate liquor. The unit process. (Courtesy: DuPont Co. and Electrochem International, Inc.)

The overall cell process may therefore be described by:

$$Sn + 2OH^- + 3H_2O + \tfrac{1}{2}O_2 \longrightarrow Sn(OH)_6^{2-} + H_2 \qquad (5.40)$$

The anodic process is restricted to a $2e^-$ change in order to minimize energy requirements, and the cell operates continuously at ambient temperature (in contrast to the rival chemical processes which generally involve an effective $4e^-$ change in a high temperature, batch process at *c.* 315° C).

FURTHER READING

1 C. L. Mantell (1960) *Electrochemical Engineering* (4th Edition of *Industrial Electrochemistry*), McGraw-Hill, New York.
2 A. T. Kuhn (Ed.) (1971) *Industrial Electrochemical Processes*, Elsevier, Amsterdam.
3 A. Schmidt (1976) *Angewandte Electrochemie*, Verlag Chemie, Weinheim.
4 *Ullmann's Encyklopadie der Technischen Chemie* (1978) Verlag Chemie, Weinheim.
5 Kirk Othmer (1978) *Encyclopaedia of Chemical Technology*, 3rd Edition, Wiley, New York.
6 R. E. Banks, D. W. A. Sharp and J. C. Tatlow (Eds) (1986), *Fluorine: The First Hundred Years*, Elsevier Sequoia, S.A. Lausanne.
7 R. L. le Roy (1983) 'Industrial Water Electrolysis: Present and Future', *Int. J. Hydrogen Energy*, **8**, 401.

8 G. Imarisio and A. B. Strub (Eds) (1983) *Hydrogen as an Energy Carrier*, Reidel, Dordrecht.
9 Z. E. Jolles (Ed.) (1966). *Bromine and Its Compounds*, Ernest Benn, London.
10 K. Wall (Ed.) (1986) *Modern Chlor-Alkali Technology*, Vol 3, Chapters 29–30. Ellis Horwood, Chichester.
11 C. Jackson (Ed.) (1983) *Modern Chlor-Alkali Technology*, Vol. 2, Chapter 18, Ellis Horwood, Chichester.
12 H. Wendt and G. Imarisio (1988) 'Nine years of Research and Development on Advanced Water Electrolysis. A Review of the Research Programme of the Commission of European Communities', *J. Appl. Electrochem.*, **18**, 1.

6 Organic electrosynthesis

In this chapter we shall consider the role of electrolysis in the manufacture of organic compounds.

Modern society requires the chemical industry to produce a very wide range of compounds used, for example, in the manufacture of polymers and plastics, pharmaceutical preparations, dyestuffs, agrochemicals and food additives. It should, however, be recognized that most organic compounds are manufactured on a relatively small scale; thus in 1975 in the USA, about 200 organic compounds were made on a scale exceeding 10 000 ton $year^{-1}$ but many, many thousands were made on smaller scales. Moreover, the market for a low-tonnage chemical may be dependent on a single final product with a limited or uncertain appeal to the customer. This is quite different from a chemical such as sodium hydroxide which has many established markets and has been manufactured for over 100 years on a very large scale.

For most organic processes, the natural feedstocks are crude oil, coal or plant extracts. Large-tonnage organic products are generally relatively small molecules and then it is common for their preparation to take only a few steps from cheap starting materials, usually derived by the cracking or reforming of oil. Indeed, where possible, such compounds are manufactured by gas-phase catalysis or 'hot tube chemistry' because such technology is well established and cheap. Since gas-phase catalytic reactions of organic compounds with oxygen, ammonia, etc. have now reached a high level of sophistication and are very successful, it is not surprising that most large-tonnage organic chemicals are manufactured by such routes. As a result, only one such large-tonnage organic chemical is currently made by electrolysis. This is adiponitrile and the process will be discussed in detail in this chapter. In contrast, the low-tonnage organic products are frequently large, polyfunctional molecules and usually result from multistep reaction sequences. These steps may involve oxidation, reduction, substitution, addition and cleavage and will be achieved by a variety of technologies including homogeneous solution chemistry, catalysis at solution–solid interfaces, fermentation and other biocatalytic reactions and, maybe,

electrolysis. Certainly, it is for the synthesis of low-tonnage organic products that electrolysis has had, and will continue to have, the greatest impact. This is clearly shown by Table 6.2 later in the chapter. The synthesis of low-tonnage organic products is considered in sections 6.2 and 6.3.

Electrolysis is a technique for the addition or removal of electrons from molecules. In organic chemistry, however, the anion and cation radicals formed by single electron transfer are seldom stable. It is normal for their formation to initiate more complex reaction sequences involving both chemical transformations (either in the solution close to the electrode surface or while species are adsorbed on the electrode surface) and further electron transfer. The net result may be the oxidation or reduction of a functional group, substitution, bond cleavage, cyclization, etc. and the possibilities are, indeed, only limited by the human imagination. In the laboratory, almost all organic reactions involving electron transfer have an electrochemical analogue. It is, of course, economic and policy factors which determine which processes are successful in industrial practice. Moreover, it should be recognized that there are normally several possible ways to carry out any transformation and maybe also a choice of starting materials for the synthesis of the desired product. Hence, the economic assessment will need to consider the relative merits of all possible syntheses and the electrolysis will generally only be selected if it is the cheapest route (and sometimes only when electrolysis is a technology familiar to the company).

It will be shown below that many factors can be important in the assessment of organic electrosyntheses but they will commonly include:

1. The availability and cost of starting material.
2. The material yield of the desired product; this is particularly important when the starting material is expensive.
3. The type and quantity of by-products – by-products always increase the cost of isolation of 'pure' product but the presence of trace impurities may completely rule out the use of the product in the application envisaged, e.g. very low levels of impurities can be critical in pharmaceutical preparations.
4. The cost of isolating pure product from the electrolysis medium. Process strategies which reduce the number of unit processes in the product isolation stage can be very advantageous to the economics of an electrolytic process.
5. The maximum cell current, since this determines the product output from the cell and, hence, the number of cells which must be purchased. The cell current depends on the total effective electrode area and the current density. The latter, in single-phase systems is, in turn, determined by the solubility of the substrate and the mass transport conditions. Hence, it is a useful rule of thumb to remember that a solubility of 1–10% for the electroactive species will be necessary to achieve a current density > 0.1 A cm^{-2}.
6. Energy consumption – this will be important for large-scale processes but generally insignificant for low-tonnage chemicals.
7. The availability of a non-interferring counter-electrode reaction. This can be a

particularly difficult problem in aprotic solvents. An attractive solution would be to carry out a synthesis at each electrode; unfortunately, it is often difficult to find conditions suitable for both reactions and the loss of yield and increase in cell complexity as well as in product isolation procedures often nullifies any advantage of this approach.

8. The chemical and electrochemical stability of the electrolysis medium.
9. The availability and stability of performance of electrodes, membranes and other cell components. It should be noted that no organic process is large enough to warrant the development of optimized cell components and the process designer can usually only select from the best available. This is in marked contrast to the chlor-alkali industry.

The relative importance of these factors varies strongly with the nature of the process, particularly its scale.

Several reasons can be cited for the development of organic electrosynthetic processes: (1) many inorganic redox reagents, e.g. Na, K, Zn, Cl_2, $Cr_2O_7^{--}$, $S_2O_8^{--}$ are themselves prepared electrochemically and their replacement in organic synthesis by direct or indirect electrode reactions would reduce the overall number of steps; (2) unlike most redox reagents, electrode reactions do not present toxicity, fire or explosion hazards and do not lead to large volumes of toxic effluent which must be treated prior to discharge; (3) electrode reactions are capable of interesting and selective chemistry; (4) compared on a mole basis, the electron is surely the cheapest available redox reagent; and (5) the electron is a versatile reagent while electricity can be produced from a variety of fuels including oil, gas and coal, as well as nuclear, solar, wind or water power. Electrolytic processes are already most attractive close to sources of hydroelectric power and cheap nuclear or solar power would markedly improve the outlook for electrosynthetic processes.

On the other hand, what are the difficulties which prevent the universal exploitation of organic electrosynthesis? Firstly, one must recognize that electrosynthetic processes are *chemically* much more complex than any other processes considered in this book. Already, it has been noted that the overall chemical change at the electrode results from a sequence of both electron transfers and chemical reactions. Indeed, it is often convenient to think of electrode reactions occurring in two distinct steps: (1) the electrode reaction converts the substrate into an intermediate (e.g. carbenium ion, radical, carbanion, ion radical) by electron transfer; and (2) the intermediates convert to the final product. Controlling the electrode potential will influence only the nature of the intermediate produced and its rate of production. The electrode potential does not influence the coupled chemistry directly, particularly if it occurs as the intermediates diffuse away from the electrode. Rather, the reaction pathways followed by the intermediate are determined by the solution environment and it is often difficult to persuade reactive intermediates to follow a single pathway. This problem is magnified in electrochemistry because all the chemistry occurs in

a thin reaction layer close to the electrode surface and the chemistry itself must lead to changes in this layer (e.g. a change in pH) and a non-uniform reaction environment (the concentration of several species will vary as a function of distance from the electrode surface). Certainly, selective electrode reactions are observed only when the conditions are favourable to both the electron transfer and chemical steps. Key experimental parameters include:

1. Electrode potential.
2. Electrode material.
3. Solvent and electrolyte.
4. Concentration of electroactive species.
5. The pH and the concentration of all species capable of reaction with the intermediates.
6. Temperature and pressure.
7. The mass transfer regime which influences maximum current density, the rate of production of intermediates and the extent of mixing between the reaction layer at the surface and the bulk solution. The mass transport regime is determined by the electrolyte flow rate, movement of the electrodes or turbulence promoters.
8. Other cell-design features, including the form of the electrodes and the presence or absence of a separator or a membrane.

The choice of solvent for organic electrosyntheses requires compromise; electrochemistry is best suited to aqueous solutions with high concentrations of electrolyte while this is seldom the preferred medium for organic reactions. Usually, organic solvents are more fitted to organic reactions, giving higher selectivity as well as allowing the use of higher substrate concentration.

There is no doubt that, in the past, electrosynthetic processes have also suffered from a failure to develop the technology essential to successful operation. As noted above, no organic process is large enough to warrant the development of electrode material or membranes with properties targeted to the particular process, and only in the case of the hydrodimerization of acrylonitrile to adiponitrile have there been studies of the influence of cell design on a large scale. This has adversely affected the performance and therefore the reputation of electrolysis. Fortunately, however, during the last 5 years, several families of cell designs (e.g. the ElectroCell AB family, the Electrocatalytic Inc. 'dished electrode membrane' cells, the FM21 range from ICI and the cells from Reilly Tar and Chemicals (Chapter 2)), suitable for general organic purposes, have become available. In addition, with their wider application, there is much greater experience available as to the choice of electrode materials and membranes. Hence, it is becoming much easier to design electroorganic processes with an acceptable, even if non-optimum, performance.

We shall first discuss in detail the one very large-scale process – the Monsanto process – for the hydrodimerization of acrylonitrile to adiponitrile. Then we shall

consider in a less detailed manner, some of the smaller-scale processes which are currently practised.

6.1 THE HYDRODIMERIZATION OF ACRYLONITRILE

Nylon 66 is a polymer manufactured by the condensation of adipic acid with hexamethylenediamine, and in excess of 1 million ton year^{-1} are manufactured in the USA alone. Adiponitrile is a convenient intermediate for the production of both hexamethylenediamine and adipic acid, the former by hydrogenation and the latter by hydrolysis. In addition, acrylonitrile is available from the gas phase, catalytic oxy-amination of propylene. Hence, to complete the manufacture of nylon from propylene and ammonia, a procedure for the conversion of acrylonitrile to adiponitrile is required (Fig. 6.1).

The electrochemical route for the conversion of acrylonitrile to adiponitrile is a cathodic hydrodimerization:

$$2CH_2{=}CHCN + 2H_2O + 2e^- \longrightarrow \begin{matrix} CH_2CH_2CN \\ | \\ CH_2CH_2CN \end{matrix} + 2OH^- \qquad (6.1)$$

and it is this reaction which was first investigated by Baizer at Monsanto in 1959. Even then, there were other chemical routes to adiponitrile, namely:

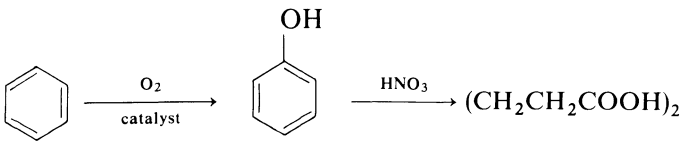

(6.2)

$$CH_2{=}CH{-}CH_2{-}CH_3 \xrightarrow[\text{catalyst}]{-H_2} CH_2{=}CH{-}CH{=}CH_2$$

$$\xrightarrow[\text{catalyst}]{HCN} (CH_2CH_2CN)_2 \qquad (6.3)$$

but the nitric acid oxidation is difficult to control while the route in Fig. 6.1 has the advantage over that in reaction (6.3) that the feedstocks (propylene, ammonia and air) are cheaper than the larger hydrocarbon, butene, and hydrogen cyanide. On the other hand, the route from butene involves only gas-phase catalysis and it is also used on a very large scale.

6.1.1 Basic chemistry

The programme at Monsanto was commenced in 1959 by following up an observation by a Russian group that the reaction of acrylonitrile with potassium

$$CH_2{=}CHCH_3 + O_2 + NH_3 \xrightarrow{\text{catalyst}} CH_2CHCN$$

$$2CH_2CHCN + 2H_2O + 2e^- \longrightarrow (CH_2CH_2CN)_2 + 2OH^-$$

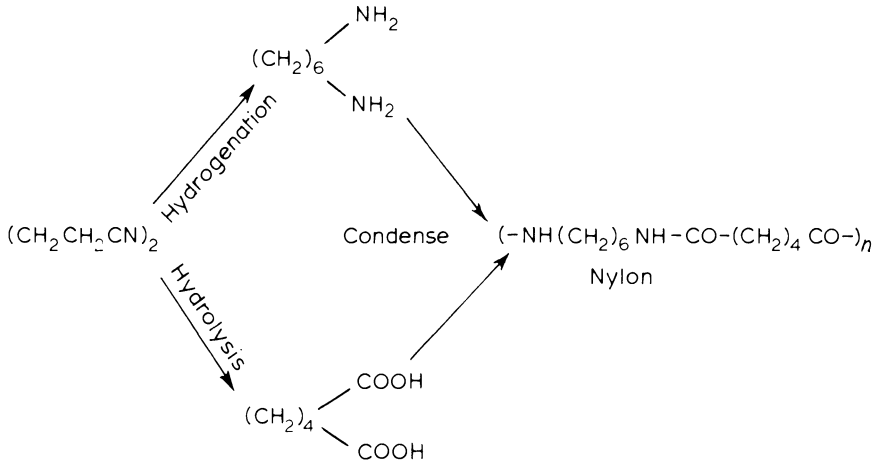

Fig. 6.1 A route for the manufacture of nylon from basic feedstocks. In practice, there are probably cheaper routes to adipic acid and all the adiponitrile is now converted to hexamethylenediamine.

amalgam led to a 60% yield of adiponitrile. The first experiments on the cathodic reduction using aqueous solutions containing a sodium or potassium salt led only to propionitrile via an anion radical:

$$CH_2{=}CHCN \xrightarrow{+e^-} [CH_2{=}CHCN]^{-\cdot} \xrightarrow[+e^- + H^+]{H^+} CH_3CH_2CN \qquad (6.4)$$

On the other hand, when the electrolyte was a neutral solution of a tetraalkylammonium salt, adiponitrile was, indeed, formed (it was later shown that such ions also greatly increased the yield from the amalgam reduction). The formation of adiponitrile also depended on the use of a high concentration of acrylonitrile and a cathode with a high hydrogen overpotential. In some electrolyses the yield of adiponitrile then exceeded 90%.

It was soon clear, however, that the conditions had to be controlled carefully. On the addition of acid, propionitrile again became the major product while the presence of base led to by-products by the route:

$$CH_2{=}CHCN \xrightarrow{OH^-} HOCH_2\bar{C}HCN$$

$$\xrightarrow{H_2O} HOCH_2CH_2CN + OH^- \qquad (6.5)$$

$$\begin{aligned}
&HOCH_2CH_2CN \xrightarrow[-H_2O]{OH^-} {}^-OCH_2CH_2CN \\
&\xrightarrow{CH_2{=}CHCN} O\!\left\langle \begin{matrix} CH_2\bar{C}HCN \\ CH_2CH_2CN \end{matrix} \right. \\
&\xrightarrow{H_2O} O\!\left\langle \begin{matrix} CH_2CH_2CN \\ CH_2CH_2CN \end{matrix} \right. + OH^-
\end{aligned} \tag{6.6}$$

These reactions are catalytic with respect to hydroxide (the OH^- is always regenerated). They probably represent the major difficulty with the process since the hydrodimerization reaction (6.1) itself depends on protonation steps and leads to the formation of hydroxide ion if a neutral solution is employed. In addition, any water reduction at the rather negative potential necessary for the reduction of acrylonitrile (about -1.8 V) will also lead to hydroxide ion.

Further byproducts observed under some conditions are trimers and polymers. The first step in the reduction of acrylonitrile is the addition of an electron to give an unstable anion radical; two possible pathways to adiponitrile (see section 6.1.5 for a more detailed discussion of the mechanism) are:

$$\begin{aligned}
&\qquad\qquad\qquad\qquad (CH_2{-}\bar{C}HCN)_2 \\
&\qquad\qquad\qquad\quad \nearrow^{\text{dimerization}} \qquad \searrow^{2H_2O,\ -2OH^-} \\
&CH_2{=}CHCN \xrightarrow{+e^-} [CH_2{=}CHCN]^{-\cdot} \qquad\qquad (CH_2CH_2CN)_2 \\
&\qquad\qquad\quad \searrow^{CH_2CHCN} \qquad \nearrow^{e^-,\ +2H_2O,\ -2OH^-} \\
&\qquad\qquad\qquad\quad CH_2\bar{C}HCN \\
&\qquad\qquad\qquad\quad CH_2\dot{C}HCN
\end{aligned} \tag{6.7}$$

and trimer and polymer could arise by side reactions such as:

$$\begin{aligned}
&(CH_2\bar{C}HCN)_2 \xrightarrow{CH_2{=}CHCN} \begin{matrix} CH_2\bar{C}HCN \\ | \\ CH_2CHCN \\ | \\ CH_2\bar{C}HCN \end{matrix} \\
&\xrightarrow[-2OH^-]{2H_2O} \begin{matrix} CH_2CH_2CN \\ | \\ CH_2CHCN \\ | \\ CH_2CH_2CN \end{matrix}
\end{aligned} \tag{6.8}$$

The occurrence of reactions such as (6.4), (6.5), (6.6) and (6.8) leads to a decrease in material yield/selectivity, while reactions (6.4) and (6.8) also cause a loss in

current efficiency. Any hydrogen evolution further decreases the current efficiency.

The key conclusions from the study, prior to the design of the first commercial process, were that the concentrations of both acrylonitrile and the tetraalkylammonium ion should be as high as possible. Certainly if the concentration of acrylonitrile fell below a critical level – around 5% – propionitrile started to form. It was suggested that the role of the tetraalkylammonium ion was to adsorb onto the cathode surface and, hence, to form a hydrophobic layer which avoids the immediate protonation of the acrylonitrile anion radical. It was also recognized that it was essential to control the local pH of the reaction environment so as to avoid reactions (6.4), (6.5) and (6.6).

At the time of this work, all electrosyntheses were carried out in single-phase media. Hence, it was necessary to define a system where water, a high concentration of acrylonitrile and also a tetraalkylammonium salt were miscible. This was achieved by the use of a tetraalkylammonium salt with an organic anion, *p*-toluenesulphonate or ethylsulphate. But the mixtures developed had little buffer capacity and undesirable swings in the pH of the reaction layer at the cathode surface could only be avoided by the design of cells with turbulent mixing of this reaction layer with the bulk solution.

6.1.2 The early Monsanto process

The main features of the cell for the Monsanto process brought on stream in 1965 are shown in Fig. 6.2. The following points should be noted:

1. The catholyte is a complex mixture consisting of 40% tetraethylammonium ethylsulphate and 28% water, the remainder being substrate and product. In fact, the process is run with a catholyte tank using both continuous removal of a fraction for work-up and continuous addition of starting material. Hence, the cell and reservoir run as a continuous stirred tank reactor and the catholyte remains close to equal concentrations of acrylonitrile and adiponitrile.
2. The cathode material must have a high hydrogen overpotential. Several metals gave satisfactory yields of adiponitrile but lead was selected. During the early operation of the process, the current efficiency for adiponitrile was found to drop with time. This problem was traced to an increase in hydrogen evolution as nickel deposited onto the cathode surface. One of the feedstocks contained nickel ion as an impurity. This therefore had to be removed.
3. Organic components of the catholyte were found to decompose anodically and, hence, it was necessary to use a separator. After considerable difficulties, a cation-permeable membrane was identified as suitable in the electrolysis conditions. The process, however, predated the developments in modern perfluorinated membranes (Chapter 3) and for many years the performance of the membrane was a problem. Indeed, this factor determined the manage-

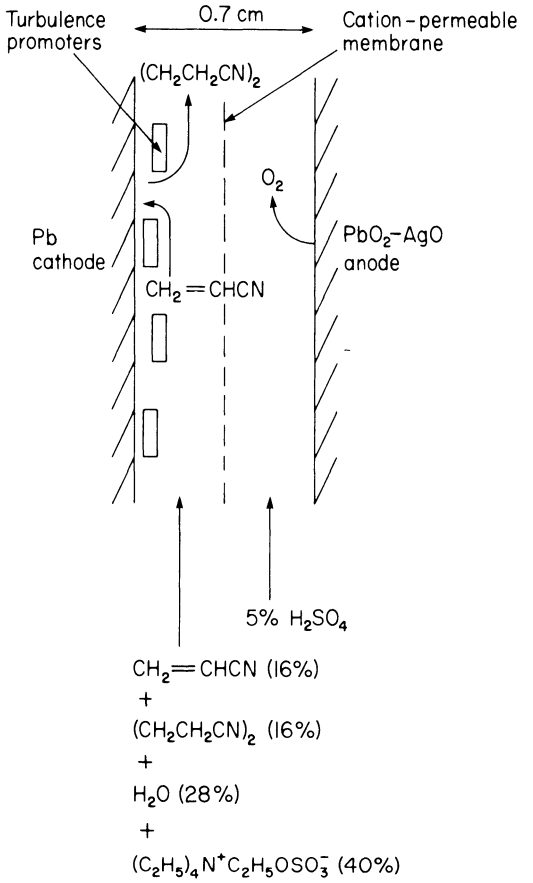

Fig. 6.2 The early Monsanto process for the hydrodimerization of acrylonitrile.

ment of the process, since the membranes had to be replaced at frequent intervals.

4. It was decided to use the simplest anode reaction, namely oxygen evolution. The membrane conducted protons and therefore sulphuric acid was a natural choice for the anolyte. The anode was a lead–silver alloy, the silver reducing the oxygen overpotential and increasing the corrosion resistance.
5. To avoid the formation of substantial amounts of β-hydroxypropionitrile and *bis*-dicyanoethylether by reactions (6.5) and (6.6), it is essential to control the build-up of hydroxide ion in the reaction layer at the cathode surface. Since the catholyte is not buffered, this can only be achieved by rapidly dispersing the hydroxide ion into the bulk catholyte. The only solution was to employ a fast catholyte flow rate (1–3 m s^{-1}) and fastening polyethylene strips to the cathode to act as turbulence promoters. In these conditions the yield of adiponitrile was in excess of 90% with proprionitrile and oligomers as the major by-products.

The electrolysis was performed in stacks of 24 cells mounted in a filterpress (Fig. 6.3) and the anolyte and catholyte flows were each in parallel from single reservoirs. Each cell is a relatively complex structure with lead cathode, catholyte chamber, turbulence promoter, membrane, anolyte chamber and lead alloy anode. The cell must be gasketed and each electrolyte chamber must have pipework attached at inlet and outlet and a flow distributor to give an even electrolyte flow. Even so, the cell had to be designed to minimize the inter-electrode gap since energy consumption was a consideration and the catholyte and membrane had relatively high resistances. Moreover, rapid dismantling and replacement of membranes was essential.

The electrical connection was bipolar, with 300 V applied across the stack, i.e. about 12 V per cell, which gave a cathode current density in the range 0.4–0.6 A cm^{-2}. The total cell current was 2870 A and the annual production of each stack about 900 tons.

Owing to the fast catholyte flow rate necessary to avoid side reactions, the conversion of acrylonitrile to adiponitrile per pass of the cathoylte through the cell was only 0.2%. This necessitated the use of an external reservoir and determined the mode of operation of the process, i.e. batch recycle. A fraction of the reservoir was bled continuously into the extraction plant and further

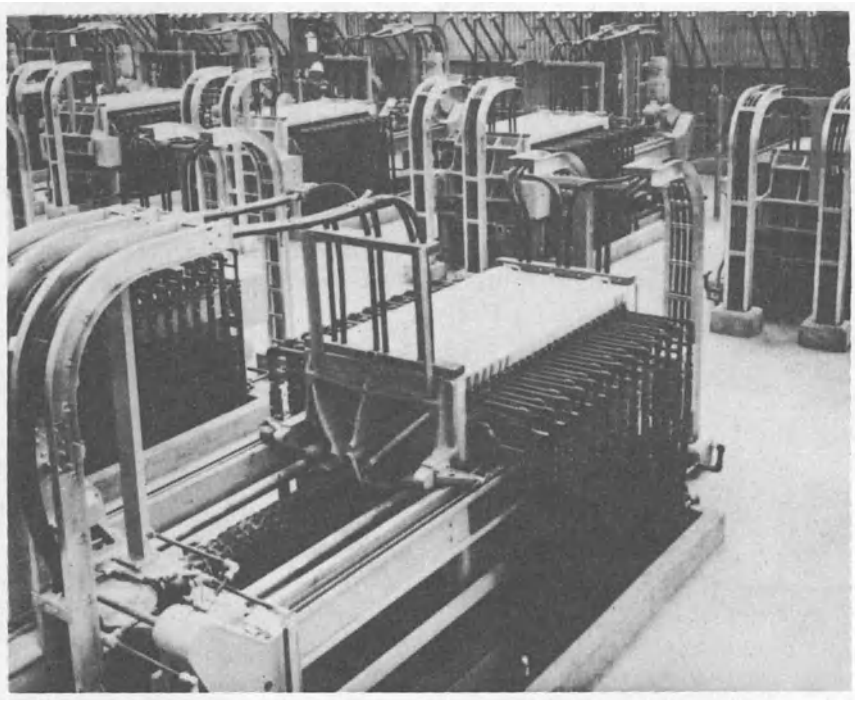

Fig. 6.3 The Monsonto adiponitrile synthesis cell house at Decatur, Alabama. The cell stacks are placed in a filterpress arrangement. (Courtesy: Monsanto Corp.)

acrylonitrile added to the reservoir. The extraction plant was very complex since it is essential to the economics of the process that the quaternary ammonium salt was recovered and the unused acrylonitrile recycled as well as pure adiponitrile isolated. The sidestream from the catholyte reservoir was cooled and the adiponitrile and unreacted acrylonitrile was extracted with further acrylonitrile in a sieve tray column. The organic phase from this unit was extracted countercurrently with water to separate remaining quaternary ammonium salt and the acrylonitrile was then removed by distillation. The final stage was a vacuum distillation of the adiponitrile. The total process is shown in Fig. 6.4.

In the 1965 process, the cellhouse contained 16 stacks of 24 cells and was designed to produce 14 500 ton year^{-1}. The energy consumption in the electrolysis alone was 6700 kWh ton^{-1} of adiponitrile. While the process must be regarded as an outstanding technological achievement for its time and was economically comparable with other methods for the manufacture of adiponitrile, it had a number of obvious shortcomings:

1. The energy consumption was high. This resulted from the poor catholyte conductivity (the water content was low and the organic content high), the interelectrode gap which could not be reduced below 7 mm and the presence of a membrane. The membrane was an early material and it was being asked to perform in less than ideal conditions. Since the reversible cell potential was unlikely to exceed -3 V, 75% of the cell voltage was iR drop.
2. The cell design was complex and costly.
3. The product isolation process was likewise complex and expensive.
4. The replacement of the membranes reduced the product output and was labour-intensive.

As a result, several groups over the next 15 years sought to modify the process and, indeed, several improvements were identified. These are discussed in section 6.1.3. It is also clear that Monsanto maintained a strong R and D group active in this area and in the late 1970s introduced a modified process which is described in section 6.1.4.

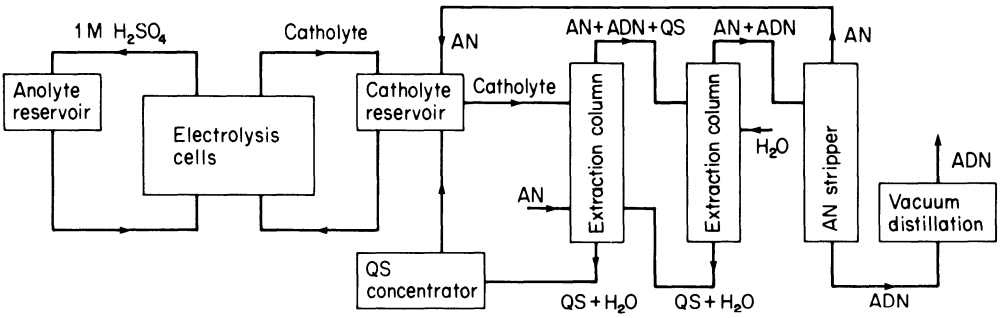

Fig. 6.4 A flow sheet for the Monsanto hydrodimerization of acrylonitrile → adiponitrile. AN is acrylonitrile; ADN is adiponitrile; QS is tetraethylammonium ethylsulphate.

6.1.3 Developments from the early Monsanto process

Asahi Chemicals Industries in Japan in the early 1970s introduced a commercial process which also uses a lead cathode in a membrane cell. The catholyte stream is, however, an emulsion of acrylonitrile and 12% ethyltributylammonium bisulphate in water. As a result, the aqueous solution is saturated with acrylonitrile (about 7%) and the product – adiponitrile – extracts back into the excess acrylonitrile within the cell. In this process the number of unit processes in the product isolation is much reduced; the tetraalkylammonium salt remains in the aqueous phase and the organic products can be separated by distillation. Moreover, the cell voltage is much reduced. The catholyte is quite acidic, and the major by-product is propionitrile.

The early attempts to use an undivided cell were based on the concept of a sacrificial anode reaction. A lead dioxide anode was used and isopropanol was added as an anode depolarizer. The reaction:

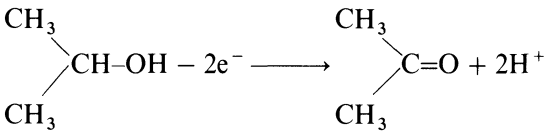

$$\begin{matrix} CH_3 \\ \diagdown \\ \quad CH\text{–}OH \\ \diagup \\ CH_3 \end{matrix} - 2e^- \longrightarrow \begin{matrix} CH_3 \\ \diagdown \\ \quad C{=}O \\ \diagup \\ CH_3 \end{matrix} + 2H^+ \qquad (6.9)$$

was expected to occur more readily than the oxidation of acrylonitrile or simple tetraalkylammonium salts and would also form protons at a rate to maintain a constant pH in the electrolyte ($1H^+$ per e^- is involved in both anode and cathode reactions). This proved to be the case but typically the current efficiency for reaction (6.9) was only about 70% because overoxidation to carbon dioxide and other products occurred; BASF in Germany recommended an electrolyte which was acrylonitrile (55%) isopropanol (28%), water (16%) and tetraalkylammonium salt (1%). The yield of adiponitrile exceeded 90%. The isopropanol also acted as a cosolvent and, at least in principle, the acetone could be reduced catalytically back to isopropanol and recycled. A bipolar capillary gap cell was proposed for this electrolysis. This cell has been discussed in Chapter 2 (see Fig. 2.33(a)) and consisted of a stack of carbon discs closely spaced by 0.2 mm strips of insulator. The electrolyte is pumped through the interelectrode gaps and a voltage is applied between the end plates. Such a cell is cheap to construct and the close spacing of the electrodes combined with the absence of a membrane certainly reduced the cell voltage and energy consumption. A value below 3000 kWh ton^{-1} was claimed, i.e. less than half that in the 1964 Monsanto process. The major by-products are formed by the addition of isopropoxide to acrylonitrile in reactions analogous to (6.5) and (6.6). The chief disadvantage of this process was the very complicated product extraction and electrolyte recycle loops.

As early as 1965 a Russian group described a one-compartment cell process with an electrolyte consisting of an aqueous phosphate buffer. The cells had graphite cathodes and magnetite anodes and had to be operated at room

temperature or below. This technology was developed in conjunction with the German company UCB and has probably been operated commercially in Russia. It is believed, however, that electrode corrosion was a problem and the need to cool the electrolyte did not make the process attractive.

By the mid 1970s it was clear that the hydrodimerization of acrylonitrile could be run very effectively with only a low concentration of tetraalkylammonium ion and that a saturated solution of acrylonitrile in an aqueous buffer was an appropriate medium. In such circumstances, it seemed likely that the electrolysis could be run in an undivided cell without the additional complication of an anode depolarizer. Such a system was first reported by Phillips Petroleum. They ran a pilot plant with an undivided cell consisting of a lead cathode and a steel anode; a very simple electrolyte, 6% acrylonitrile and 0.03% tetrabutylammonium salt in aqueous dipotassium hydrogen phosphate, was employed and the anode reaction was oxygen evolution. The yield of adiponitrile remained above 90% and the chief by-products were propionitrile and trimer. No base-initiated chemistry was observed due to the use of an effective buffer.

Overall, considerable improvements in performance over the 1964 Monsanto process could be demonstrated. In the late 1970s, Monsanto introduced new technology which incorporated the best features of most of these advances.

6.1.4 The new Monsanto process

The second-generation adiponitrile process is based on an undivided cell. It combined simpler cell design, less complex product extraction and reduced energy consumption to give a much improved process. It was selected for the expansion of adiponitrile production in both the USA and the UK and the world output of adiponitrile by electrolysis now exceeds 200 000 ton $year^{-1}$.

The modified process is summarized in Fig. 6.5 and employs an emulsion of acrylonitrile and 15% disodium hydrogen phosphate in water containing a low concentration of quaternary ammonium salt (0.4%). Thus, the concentration of the starting material in the aqueous phase is 7% (i.e. saturated) and the adiponitrile will extract back into the acrylonitrile within the cell. The quaternary ammonium ion used is hexamethylene-*bis*(ethyldibutylammonium); it is prepared on the site by quaternization of hexamethylenediamine, an intermediate between adiponitrile and the nylon. It is therefore cheap but it is also convenient because traces are readily washed from the organic phase with water. Hence, the product isolation is straightforward and the aqueous and organic phases can be treated separately. The organic phase is merely washed with water and distilled.

Electrode performance and stability were problems with the undivided cell. It was desired to evolve oxygen at the anode but lead dioxide was found to decompose acrylonitrile while transition and precious metals were found to corrode. Such anode corrosion is a problem, not only because of replacement costs, but also because it leads to metal ions in solution followed by deposition

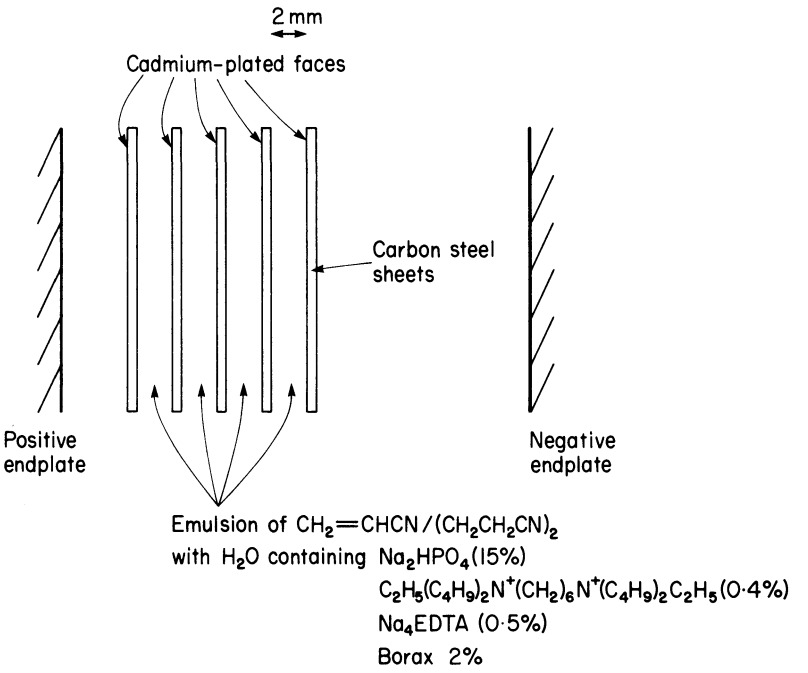

Fig. 6.5 The new Monsanto process for the hydrodimerization of acrylonitrile.

onto the cathode and catalysis of hydrogen evolution (with loss of current efficiency and also the hazard from mixtures of O_2–H_2). A carbon steel was chosen as the anode but it was necessary to investigate corrosion inhibitors. In the process, borax (2%) and EDTA (0.5%) were used as additives and reduced anode corrosion by over 95%. The EDTA also has a role at the cathode; it complexes metal ions in solution and thereby reduces the rate of cathodic metal deposition and also leads to slow corrosion of the cathode surface, further minimizing the build-up of hydrogen evolution catalysts. Cadmium is the preferred cathode material and in the absence of EDTA, hydrogen evolution increases over a 48 h period until it consumes 10–15% of the charge passed. With EDTA, hydrogen evolution remains at less than 5%. The aqueous electrolyte is, however, also periodically processed for the removal of transition metal ions.

The cell is of a very simple design. It consists of a bipolar stack of carbon steel sheets whose cathode faces are smoothly electroplated with cadmium to a thickness of 0.1–0.2 mm. The anode–cathode gap is fixed with spacers at about 2 mm and the steel sheets are surrounded by insulating skirts to reduce the bypass currents. The electrolyte is fed uniformly across the parallel interelectrode gaps to give a flow velocity of 1–2 m s^{-1}. The emulsion is recycled through the cell from a reservoir and a fraction of the organic phase is removed continuously for extraction of the product. The process is run so that the organic phase in

Table 6.1 Comparison of the Monsanto 1965 divided cell process with the recent Monsanto undivided cell process

	Divided cell	Undivided cell
Adiponitrile selectivity/%	92	88
Inter-electrode gap/cm	0.7	0.18
Electrolyte resistivity/Ω cm	38*	12
Electrolyte flow velocity/m s^{-1}	2	1–1.5
Current density/A cm^{-2}	0.45	0.20
Voltage distribution/V		
estimated reversible cell voltage	−2.50	−2.50
overpotentials	−1.22	−0.87
electrolyte *iR*	−6.24	−0.47
membrane *iR*	−1.69	—
total	−11.65	−3.84
Energy consumption/kWh t^{-1}	6700	2500

* Catholyte.

equilibrium with the aqueous solution is 55% adiponitrile and 45% acrylonitrile. A fraction of the aqueous electrolyte is also treated continuously to counter the build-up of organic by-products and metal ions.

The two Monsanto processes are compared in Table 6.1. It must be emphasized that the undivided cell stack is very much cheaper than the plate and frame cells in a filterpress. The need for membranes, electrolyte chambers, gasketing and much connecting pipework has been removed and, in fact, the cost of the cell per unit area of cathode has been reduced by more than a factor of 10. This decreases the capital cost of the plant to such an extent that (when both capital and energy costs are taken into account) the optimum current density is lower for the undivided cell.

It is also clear from the table that the absence of a membrane, the decrease in the interelectrode gap and the increase in the electrolyte conductivity combine to have a dramatic effect on the cell voltage. The change from −11.65 to −3.84 V reduces the energy consumption by almost two-thirds. Moreover, the extraction of the product within the cell reduces the number of unit processes in the product-isolation procedure. This also improves the process economics substantially. Overall, the undivided cell process is a very significant advance.

6.1.5 Reaction mechanism

Despite many attempts to determine the mechanism for the hydrodimerization of acrylonitrile, surprisingly little is known with certainty. The study of the mechanism presents several difficulties:

1. The concentration of acrylonitrile is too high for most laboratory experiments. Most electroanalytical experiments to investigate the mechanism and

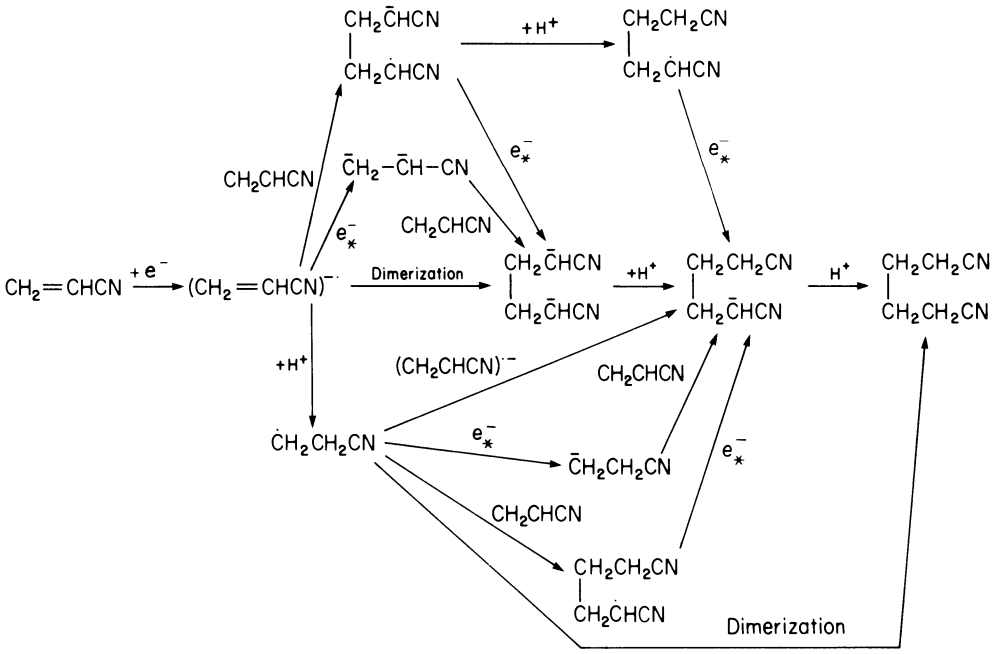

Fig. 6.6 Possible reaction pathways for the hydrodimerization of acrylonitrile → adiponitrile. The asterisks indicate that electron transfer can be from the cathode or from $[CH_2CHCN]^{-}\cdot$ in homogeneous solution. $H^+ \equiv$ to protonation by a species such as water.

kinetics of coupled chemical reactions are carried out with solutions where the concentration of electroactive species is well below 10 mmol dm^{-3}. At this acrylonitrile concentration, its electrochemical reduction always involves two electrons and leads to propionitrile and, hence, conclusions from such experiments cannot be directly relevant to the hydrodimerization reaction.

2. There are many possible reaction pathways between acrylonitrile and adiponitrile (Fig. 6.6) and in each there are several possible rate determining steps.
3. None of the reaction intermediates have been detected by electrochemical or spectroelectrochemical techniques and therefore it must be concluded that one is dealing with rapid chemistry with intermediates of half-lives $< 10^{-5}$ s. Even so, some comments about the mechanism are possible and desirable.

First, we should consider further the role of the tetraalkylammonium ion. Certainly, such ions are essential to obtain good yields of adiponitrile; in their absence the major product is propionitrile. Only a critical concentration of the tetraalkylammonium ion is necessary to give the desired product and this critical concentration decreases as the size of the cation increases. With tetrabutylammonium ion it is as low as 0.01%. There is no doubt that tetraalkylammonium ions suppress hydrogen evolution and are also corrosion inhibitors. These observations are good evidence that the cations

adsorb on the cathode surface and, indeed, there is direct experimental evidence for their adsorption. Thus, it seems that the tetraalkylammonium ions act by modifying the electrode–solution interface and it has been postulated that they create a hydrophobic layer where the protonation of anionic intermediates is slow compared to the bulk solution.

A study of the dependence of the steady state *I–E* curves on the electrolysis conditions leads to some mechanistic information, e.g. in the case of a lead cathode in mixtures of acetonitrile, water, acrylonitrile and tetraethylammonium tosylate, the Tafel slope observed is $(120\ \text{mV})^{-1}$ while the current was shown to be first order in acrylonitrile and water. This would indicate a rate-determining step of the type:

$$CH_2{=}CHCN + H_2O + e^- \longrightarrow {}^{\bullet}CH_2CH_2CN + OH^- \qquad (6.10)$$

followed by fast reactions leading to adiponitrile. Similar conclusions were drawn from a series of slow, linear sweep experiments at mercury ultramicroelectrodes. Using solutions close to those preferred in the new Monsanto process, well-formed reduction waves were observed for acrylonitrile; shape analysis showed the rate-determining step to be the first electron transfer while the change from $1e^-$ to $2e^-$ reduction on diluting the acrylonitrile could clearly be seen from the limiting currents as a function of concentration.

In another approach to the study of the mechanism, many investigators have looked at the hydrodimerization of other activated olefins, particularly those with two or more substituents (e.g. methyl cinnamate, diethyl fumarate) whose anion radicals, are much more stable. With such olefins the mechanism of hydrodimerization may be studied by cyclic voltammetry or with a rotating ring-disc electrode. It is, however, never clear whether the chemistry of stable anion radicals will be analagous to the unstable acrylonitrile anion radical.

Finally, synthetic studies using a wide range of activated olefins provides evidence about mechanism, e.g. it is possible to prepare mixed hydrodimers by the electrolysis of two olefins, ethyl acrylate and acrylonitrile, for example, at a potential where only one of the olefins reduces. This might be taken to indicate that the coupling step occurs between an anionic intermediate and a molecule of the neutral olefin, e.g.:

$$[CH_2{=}CHCOOC_2H_5]^{-\bullet} + CH_2{=}CHCN \longrightarrow \begin{matrix} CH_2\dot{C}HCOOC_2H_5 \\ | \\ CH_2\bar{C}HCN \end{matrix}$$

$$\xrightarrow[-2OH^-]{e^- + 2H_2O} \begin{matrix} CH_2CH_2COOC_2H_5 \\ | \\ CH_2CH_2CN \end{matrix} \qquad (6.11)$$

although a radical-ion–radical-ion coupling cannot be ruled out if the

electron transfer:

$$[CH_2{=}CHCOOC_2H_5]^{-\cdot} + CH_2{=}CHCN \rightleftharpoons CH_2CHCOOC_5H_5 + [CH_2CHCN]^{-\cdot} \quad (6.12)$$

is possible in the reaction layer. This will be the case if the formal potentials for the olefin–anion radical couples are not too different.

The mechanism of hydrodimerization is, however, likely to vary with both the electrolysis conditions and the structure of the olefin. Hence, it may be inappropriate to seek similarities in mechanism, particularly between acrylonitrile and the more substituted molecules which give stable anion radicals. The high selectivity of the hydrodimerization of acrylonitrile would indicate that the desired reaction route is very favourable compared to all competitive pathways.

6.1.6 Other hydrodimerization reactions

While the hydrodimerization of acrylonitrile to adiponitrile is the only example to have been exploited commercially, it should be recognized that hydrodimerization is a general reaction for activated olefins, i.e. olefins with an electron-withdrawing group on the double bond. Moreover, they have considerable scope in synthesis. The reactions:

$$2CH_2{=}CHY + 2H^+ + 2e^- \longrightarrow \begin{matrix} CH_2CH_2Y \\ | \\ CH_2CH_2Y \end{matrix} \quad (6.13)$$

$$Y = -CN, -COOC_2H_5, -COCH_3, -PO(OC_2H_5)_2, -\langle\bigcirc\rangle\text{-}N$$

have all been reported with yields between 60–100%, without extensive optimization. Disubstituted olefins can also be coupled. Similarly, a C–C bond can be formed intramolecularly if the substrate is a diolefin; yields are particularly good if five or six membered rings are formed in the reaction, e.g.:

$$\begin{matrix} CH{=}CHCOOC_2H_5 \\ (CH_2)_3 \\ CH{=}CHCOOC_2H_5 \end{matrix} + 2H^+ + 2e^- \longrightarrow \begin{matrix} CH_2COOC_2H_5 \\ \\ CH_2COOC_2H_5 \end{matrix} \quad (6.14)$$

Mixed coupling of two different olefins was mentioned in section 6.1.5. Synthetically, it is not a very satisfactory procedure because three hydrodimers are always formed. Highest yields of mixed hydrodimer, (about 60%) are obtained in conditions where only one olefin is reduced on the cathode but the other is present in large excess.

6.2 OTHER COMMERCIAL ELECTROSYNTHETIC PROCESSES

The past 25 years have seen an explosion of academic interest in organic electrochemistry and a very large number of chemical transformations at

electrode surfaces has been reported. The resulting literature is very well-discussed in a number of books and reviews listed at the end of this chapter. The same period has also seen a steady increase in the number of organic electrosynthetic processes within all parts of the fine-chemicals industry. The authors believe that the total may now exceed a hundred and a selection of these processes is listed in Table 6.2. Because of the needs and outlook of some parts of the fine-chemicals industry, details of the synthesis of many products are never reported and, hence, any contribution of electrosynthesis remains speculation.

As was noted at the beginning of this chapter, energy consumption and even the initial investment in electrolysis cells are seldom very important factors in the assessment of the process economics. The more crucial factors are usually the availability and cost of the starting materials, material yield, a simple product isolation, the stability of the electrolysis medium and the achievement of an acceptable current density. It cannot, however, be stressed too strongly that an electrolytic route only stands a chance if a research scientist within the fine chemicals company recognizes at a very early stage, that electrolysis might offer a solution to a step within a synthesis perceived to be important to future business by the management of the company. Because of the very high cost of the testing programmes to which, for example, pharmaceutical and agrochemical products are exposed, the chances of displacing any step in the synthesis once the programme is complete are very small indeed. Furthermore, it should be emphasized that the economic assessment can be influenced greatly by local circumstances, e.g. the availability of cheap hydroelectric power or the starting material close to the site as a by-product from another process can improve dramatically the chances of success. Another situation favouring electrolysis occurs in the less industrialized countries such as India. This is the small requirement for many chemicals. Several compounds produced elsewhere by catalytic hydrogenation are then better produced by electrolysis; catalytic hydrogenation is economically viable only above a critical scale of operation.

The reactions in Table 6.2 again illustrate the wide range of chemistry which may be achieved at an electrode surface. The examples include the oxidation and reduction of functional groups, hydrogenation, substitution, cleavage, dimerization and rearrangement. Moreover, the processes make use both of direct and indirect electrode reactions and include several examples of chemistry involving large, polyfunctional molecules. A number of general features can be highlighted. Firstly, there is a preponderance of reactions in aqueous solutions (in sharp contrast to the journal literature) and several oxidations in methanol, while aprotic solvents only appear in a few reactions as mixtures with water. The major reason for this is associated with the stability of the electrolysis medium especially with respect to the counter-electrode reaction. The oxidation/reduction of water leads only to $O_2 + H^+$ and $H_2 + OH^-$ and the reduction of methanol to H_2 and CH_3O^-. Hence, these reactions may conveniently be used to maintain the pH of the electrolyte at a constant level while leading to no contamination of the system. In contrast, the oxidation/reduction of aprotic

Table 6.2 Some commercial and major pilot plant organic electrosynthetic processes

Reaction	Commercial or pilot	Country	Estimated scale/ton year^{-1}	Conditions	Comments
1. *Hydrodimerization*:					
$2CH_2CHCN \xrightarrow{2e^-} (CH_2CH_2CN)_2$	C	USA, Europe, Japan	3×10^5	Two-phase aqueous phosphate buffer + acrylonitrile. Undivided bipolar parallel-plate cell. Cd cathode, steel anode, $I = 0.2$ A cm^{-2}	Monsanto Mark I process operated since 1964. Mark II on-line during 1970s. Several related processes known to operate
2. *Hydrogenation of heterocycles*, e.g.:					
(a) 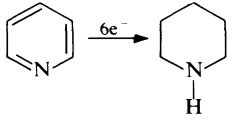	C	Europe	100	Pb cathode in H_2SO_4 medium. Divided cell	Process over 50 years of continuous operation
(b) 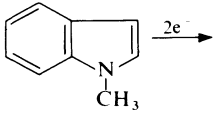 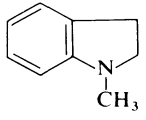	C	Europe	(20)	Pb cathode in H_2SO_4 medium. Filterpress-divided cell	

Table 6.2 (*continued*)

Reaction	Commercial or pilot	Country	Estimated scale/ton year^{-1}	Conditions	Comments
3. *Hydrogenation of nitriles*: 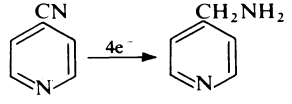	C	USA	30	Pb cathode in acid sulphate medium. Divided cell including high-area cathode $I = 5–20\ mA\ cm^{-2}$	Process developed by Reilly Tar. 2-isomer needs Fe^{3+} salt catalyst
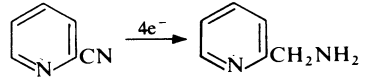	C	USA	70		
4. *Reductions of carboxylic acids*:					
(a) 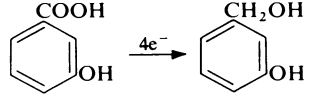	C	Japan	(100)	Pb cathode in aqueous acid	Intermediate for *m*-phenoxybenzyl alcohol and then an insecticide
(b) 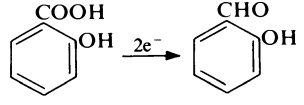	C	India	(20)	Pb cathode in acid media	
(c) 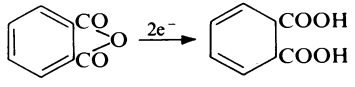	C	Europe	(100)	Pb cathode in H_2SO_4. Dioxan as cosolvent. Divided filterpress cell	Process probably discontinued due to loss of product market

(d) 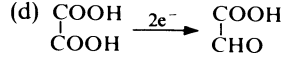	P	Europe, Japan	—	Pb cathode in aqueous solution without added electrolyte. Divided cell	Product traded as aqueous solution
(e) 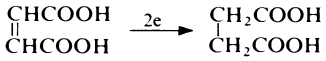	C	India	30	Pb cathode in H_2SO_4	
5. *Pinacolizations*:					
(a) $2HCHO \xrightarrow{2e^-} (CH_2OH)_2$	P	USA	—	Neutral solution with R_4N^+. Modified graphite cathode. Divided cell. High I, e.g. $>0.5A\ cm^{-2}$	Potentially, very large-scale process
(b) $2CH_3COCH_3 \xrightarrow{2e}$ 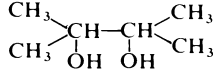	P	USA, Japan, Europe	—	Acid medium, Pb cathode	
6. *Cathodic cleavages*:					
(a) 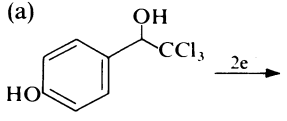	C	Japan	120	Acidic CH_3CN/H_2O. Pb cathode. Divided filter-press cell. $I=0.15\ A\ cm^{-2}$	Intermediate to *p*-hydroxy-phenylacetic acid.

Table 6.2 (*continued*)

Reaction	Commercial or pilot	Country	Estimated scale/ton year^{-1}	Conditions	Comments
(b) 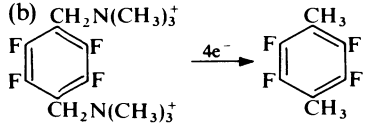	C	Europe	200	H_2O – no electrolyte. Product precipitates. Zn cathode. 0.1 A cm^{-2} Divided FM21 cell	
(c) $ArCHOHR \xrightarrow{2e^-} ArCH_2R$	P	Europe	—	Acid sulphate. Indirect using Cr^{3+}/Cr^{2+} couple. Pb cathode	
(d) 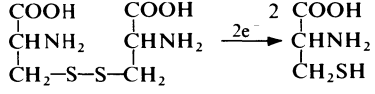	C	Europe, Japan	(30)	Pb cathode in acid. Divided cell	
(e) 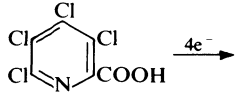	C	USA	—	Roughened Ag cathode in aqueous acid	
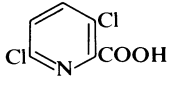					

(f) 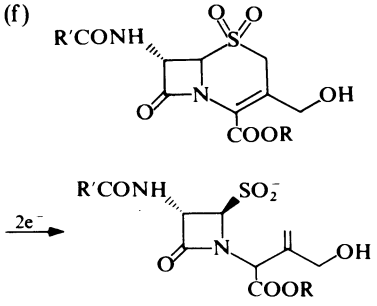	P	USA	—	—	Intermediate to cephalosporin

7. *Nitrogroup reduction*, e.g.:

(a) 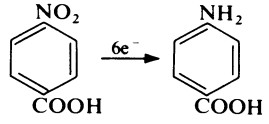	C	India	3	Pb cathode in acid medium	Many pilot-scale studies on such reactions. Not generally considered economic in USA or Europe
(b) 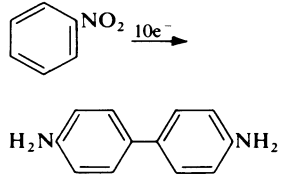	C	India	30	Stronger acid	Reaction occurs via coupling of nitrosocompound + hydroxylamine, further reduction and benzidine rearrangement
(c) 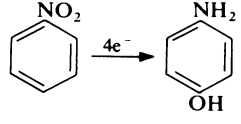	P	USA, Europe, Japan, India	—	Very strong acid. Cu or monel cathode	Reduction to phenyl-hydroxylamine and H^+ catalysed rearrangement. Process has problems with by-products. Use as a drug intermediate impossible

Table 6.2 (*continued*)

Reaction	Commercial or pilot	Country	Estimated scale/ton year^{-1}	Conditions	Comments
8. *Base generation*:					
$(CH_3)_4NCl \xrightarrow{e^-} (CH_3)_4NOH$	C	Japan, USA	24	Chlor-alkali membrane cell and conditions	
9. *Selective hydrogenation*, e.g.: (a) Steroids	P	Europe	—	High-area Ni cathode	Reactions possible without high-pressure hydrogen
10. *Sugar chemistry*: (a) Protected sorbose $\xrightarrow{-4e^-}$ corresponding acid	P	Europe	—	Ni anode in aqueous base. Undivided Swiss roll cell	Route to ascorbic acid. Process may be used in the future
(b) Glucose $\xrightarrow{-2e^-}$ gluconic acid	C	Europe, India	(10^3)	Indirect oxidation via Br_2. Acid precipitated as Ca^{2+} salt	
(c) Glucose $\xrightarrow{2e^-}$ sorbitol	C	USA, India	—	Pb cathode in aqueous acid	Probably discontinued. Renewed interest because of safety problems with catalytic hydrogenation

(d) Starch $\xrightarrow{-4e^-}$ dialdehyde starch	C	USA, India	—	Indirect oxidation via IO_4^-	No longer used
11. *Lead alkyl production*:					
$Pb + 4RMgCl \xrightarrow{-4e^-} PbR_4$ $R = CH_3$ or C_2H_5 Mixed alkyl also possible	C	USA	$>10^4$	Pb shot anode in steel tube cathode. Mixed ether solvent RMgCl partly regenerated at cathode	Discontinued since PbR_4 no longer added to USA petrol (gas)
12. *Fluorinations*: (a) Perfluorination of: RCOOH, e.g. $R = C_8H_{17}$ RSO_3H, e.g. $R = CH_3$	C	USA, Japan, UK	$>10^2$	Simons process. Ni anode in liquid HF	Always mixture of products. High value of products permit separation
(b) Partial or perfluorination of small hydrocarbons, chlorocarbons, acids, ethers, ketones	P	USA	—	Phillips process. Porous C anode in HF/KF eutectic (82° C)	Still, may be commercialized
13. *Methoxylations* (a)					
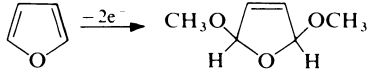	C	Europe	100	$NaBr/CH_3OH$ in narrow gap, bipolar C disc cell. $I = 0.15A\ cm^{-2}$	Indirect via Br_2

Table 6.2 (*continued*)

Reaction	Commercial or pilot	Country	Estimated scale/ton year^{-1}	Conditions	Comments
(b) 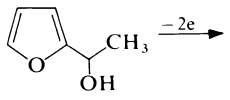 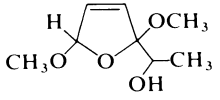	C	Japan	150	$NaBr/CH_3OH$. C cylinder anode in steel pipe cathode 1 mm gap. $I = 0.1\ A\,cm^{-2}$	Indirect via Br_2. Part of maltol synthesis
(c) 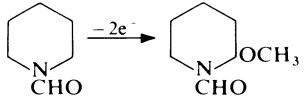	C	Europe	25	Undivided bipolar parallel plate reactor	Direct oxidation
14. *Oxidation of polynuclear aromatic hydrocarbons* (a) 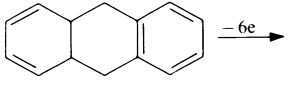 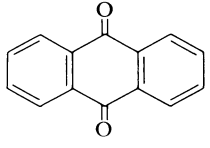	C	Europe, USA	100	Indirect via $Cr_2O_7^{2-}$. Pb anode in divided parallel plate reactor	Ex-cell oxidation carried out solid to solid. Also pyrene oxidized similarly.

(b) 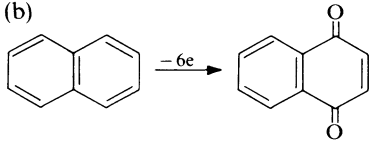	P	Canada, Europe	—	Indirect via Ce^{4+}	Ex-cell oxidation
(c) 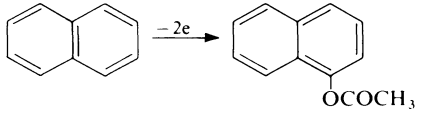	C	Europe		Undivided bipolar, narrow gap, C disc cell. $HOAc/(CH_3)_3N$ medium. $I = 40–120\ mA\ cm^{-2}$	PTFE-modified graphite anode. Distillable electrolyte
15. *Benzene oxidation*: 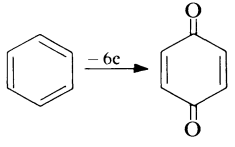	P	Europe	—	PbO_2 anode in H_2SO_4. Benzene as second phase	Current density very low
16. *Oxidation of methyl aromatics*: (a) 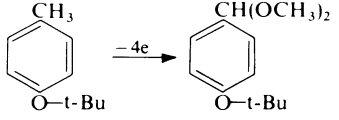	C	Europe	(1000)	CH_3OH/1% KF. Undivided C disc cell. $I = 40–100\ mA\ cm^{-2}$	Product hydrolysed to *p*-hydroxybenzaldehyde. *t*-butoxy chosen at protecting group as readily recycled
(b) 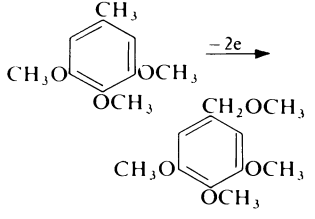	C	Japan	120	$NaOH/CH_3OH$. C tube in steel pipe cell	Product hydrolysed and air oxidised to aldehyde

Table 6.2 (*continued*)

Reaction	Commercial or pilot	Country	Estimated scale/ton year^{-1}	Conditions	Comments
(c) 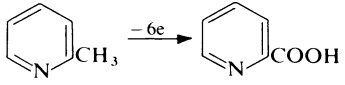	C	USA, Europe	10	PbO_2 anode in H_2SO_4/H_2O. Pb shot anode	
(d) 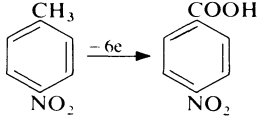	C	India	30	Indirect via $Cr_2O_7^{2-}$	
17. *Epoxidation of olefins*:					
(a) $CH_3CH{=}CH_2 \xrightarrow{-2e} CH_3\overset{O}{\overset{/\backslash}{C}}H{-}CH_2$	P	USA, Europe, Japan	—	Indirect oxidation via BrO^- or ClO^-. Aqueous Na^+ electrolyte	
(b) $CF_3CF{=}CF_2 \xrightarrow{-2e} CF_3\overset{O}{\overset{/\backslash}{C}}F{-}CF_2$	C	Europe	5	PbO_2 anode in $HOAc/HNO_3$. $I = 10$–40 mA cm^{-2} depending on pressure. Tube cell with membrane	Cost of starting material determines selectivity as priority in economics

(c) 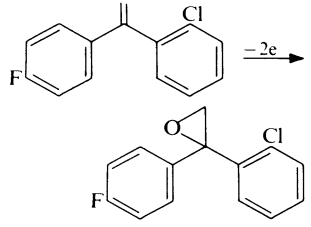	P	Europe	—	Indirect via BrO^- in aqueous DMF. FM21 cell	Insecticide product not marketed
18. *Kolbé coupling of half esters*: 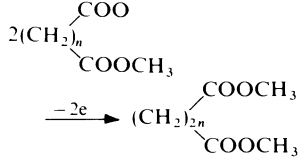 n = 3, 4, 6	C	Europe, India, Japan	—	Pt anode in methanol. Acid partially neutralized but no electrolyte added	

solvents or, indeed, the oxidation of methanol, commonly lead to a complex mixture of products which will build up in the electrolyte and also lead to loss of expensive solvent. As a result, substrates with a high solubility in water are advantageous and a number of processes involve the oxidation or reduction of pyridines in sulphuric acid solution. Examples of processes improved by a simple product isolation would include: (1) the reduction of oxalic acid to glyoxilic acid where the electrolyte contains no added salt and the product is sold as an aqueous solution; (2) the reduction to 2,3,5,6-tetrafluoroxylene which, unlike the substrate, is insoluble and precipitates; (3) the acetoxylation of naphthalene which employs a distillable electrolyte, triethylammonium acetate; and (4) processes where the product may be extracted into a second immiscible solvent within the cell.

It is not the intention to discuss each of the reactions in Table 6.2 and only a few illustrative examples of recent processes will be presented. In Germany, BASF identified 4-hydroxybenzaldehyde as a key intermediate for the synthesis of several products and *p*-cresol as the likely feedstock. They were aware that

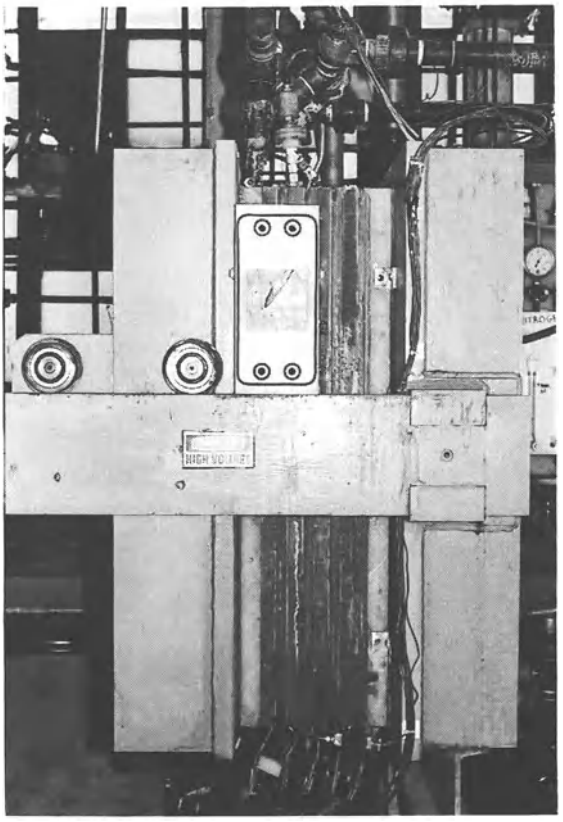

(a)

oxidation of the methyl group without protection of the phenol group was unlikely. Hence, the direct and indirect electrochemical oxidation of alkoxytoluenes was investigated. A procedure involving direct oxidation in methanol was selected. It was found that a $4e^-$ oxidation of the toluene led to dimethoxylation of the methyl group and this product was readily hydrolysed to the aldehyde. The conditions selected involved a 10–15% solution of the substrate in methanol with 2% KF as the electrolyte. The temperature was 40° C and the current density 0.04–0.1 A cm^{-2} while the cell was an undivided bipolar stack of carbon electrodes with a narrow interelectrode gap. The cathode reaction is effectively used to maintain the pH of the electrolyte constant. The organic yield is 95% and the current efficiency 70% under these conditions. The *t*-butoxy group was selected as the protecting group for the phenol; *t*-butanol readily reacts with *p*-cresol in the presence of an acidic ion-exchange resin as catalyst, while after electrolysis the *t*-butoxy group hydrolyses easily and it is possible to recover efficiently the *t*-butanol for recycle. Hence, the electrode reactions in the cell are:



(6.15)

$$2CH_3OH + 2e^- \longrightarrow 2CH_3O^- + H_2 \qquad (6.16)$$

(b)

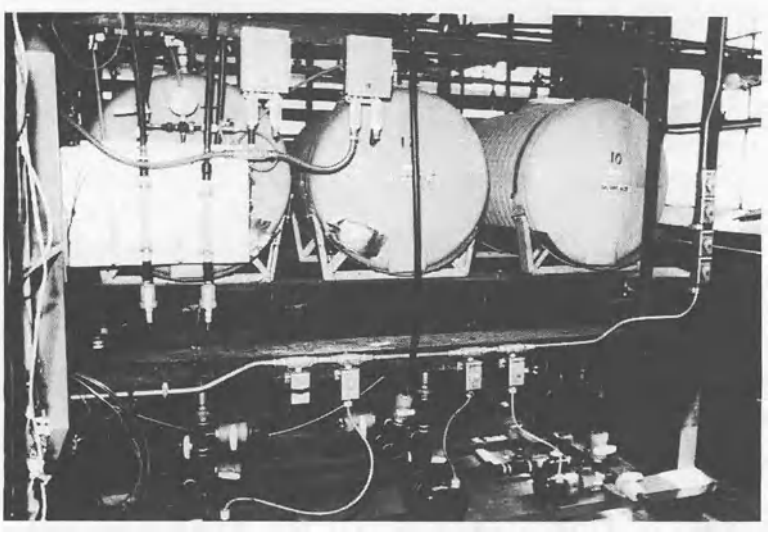

Fig. 6.7 A small-scale electrosynthetic plant. (a) Membrane filterpress stack. (b) Reservoirs and associated electrolyte-flow systems. (Courtesy: Reilly Tar and Chemical Corp.)

Another methoxylation process recently commercialized by Otsuka in Japan is a stage in the manufacture of the food additive maltol. The electrode reactions are:

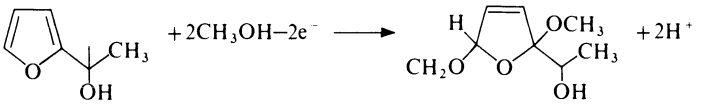

(6.17)

$$2CH_3OH + 2e^- \longrightarrow 2CH_3O^- + H_2O \qquad (6.18)$$

In this electrolysis, the electrolyte is a 20% solution of the furan in methanol containing sodium bromide. The bromide ion plays an essential role since bromine and brominated furans are probably important intermediates in the anode chemistry. The cell is a 1 mm gap, plate and frame design with carbon anodes and steel cathodes; the current density lies in the range 0.1–0.2 A cm^{-2}. The organic yield is 97% and the current efficiency 80–95% provided the electrolyte is cooled so as to maintain its temperature below 10° C.

The several reductions at lead cathodes in sulphuric acid media may be illustrated by the process developed by Reilly Tar and Chemical in the USA. The conversion of interest was:

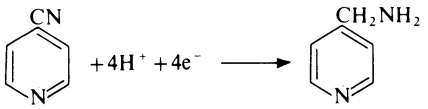

(6.19)

and the electrolysis was run in aqueous sulphuric acid with methanol added as a cosolvent. With a current density of 20 mA cm^{-2}, the organic yield was 93% (a small amount of a dimer was identified, approximately 1%) while the current efficiency was typically 106% (this could arise if methanol acted as reducing agent for some intermediates). Moreover, a clever product isolation procedure was found; beyond 50% conversion of the substrate, addition of further substrate led to precipitation of the product! A membrane cell stack in a filterpress was designed and developed within the company. Because of the rather low current density for this process, it was desirable to increase the space–time yield of the cells by incorporating a high-surface-area cathode. This was based on a bed of lead shot within the catholyte chamber. The anode reaction was oxygen evolution on a planar PbO_2 electrode. The economics of this process were reported to be very favourable; the costs of the electrochemical conversion were estimated as one-half that of a catalytic hydrogenation on a similar scale. Figure 6.7 shows photographs of the plant employed.

6.3 INDIRECT ELECTROSYNTHESIS

During an indirect electrode reaction, a redox couple is used as a catalyst or 'electron carrier' for the oxidation or reduction of another species in the system. In other words, the electrode is used to continuously reconvert the redox reagent

to an oxidation state where it is able to react with an organic compound in a desirable reaction. Although there are a few exceptions (e.g. $\phi_3N/\phi_3N^{+\cdot}$) most suitable redox couples are inorganic and examples of those which have been discussed include:

For oxidations: Ce^{3+}/Ce^{4+}, $Cr^{3+}/Cr_2O_7^{2-}$, Mn^{2+}/Mn^{3+}, Mn^{2+}/MnO_2, Br^-/Br_2, Cl^-/ClO^-, $Ni(OH)_2/NiOOH$

For reductions: Sn^{4+}/Sn^{2+}, Cr^{3+}/Cr^{2+}, Ti^{4+}/Ti^{3+}, Zn^{2+}/Zn, $Na^+/NaHg$

It has been proposed that indirect electrosynthesis may be carried out:

1. In-cell, i.e. the reaction between the organic substrate and the redox reagent in its active oxidation state occurs within the cell.
2. Ex-cell, i.e. the chemical reaction is carried out in a reactor separate to the cell. This approach has the advantages that the conditions for the electrode reaction and the chemical step may be optimized separately and also that the electrolyte may be conditioned/purified between the reactor and the cell. On the other hand, more unit processes are necessary and economic driving forces will encourage the process designer to combine the cell and reactor as closely as possible.

It should be noted also that the redox couple may be solution-soluble or may be immobilized within an electrode coating and that, in the former case, the chemical step may be carried out: (1) with the organic substrate dissolved within the electrolyte; (2) at the interface between the electrolyte and the substrate present as a separate phase or dissolved in a solvent immiscible with the electrolyte; (3) within a solvent immiscible with the electrolyte, the redox reagent in its active oxidation state being extracted into the other solvent (maybe by phase-transfer catalysis); and (4) at the interface between the electrolyte and the organic substrate present as a solid.

Hence, it may be seen that there is a multitude of possibilities for a chemical transformation by indirect electrolysis. In general, there are several possible advantages:

1. The chemical step is entirely equivalent to a chemical oxidation/reduction and it is therefore possible to use the literature to select the redox catalyst and reaction conditions as well as the chemical reactor.
2. The redox catalyst can have a high solubility in water, allowing the electrochemistry to be carried out at high current density in an aqueous electrolyte. On the other hand, it can often be actually advantageous for the organic substrate to be insoluble in water since then the conditions for the chemical step may be quite different, permitting a better selectivity.
3. The multiphase procedures can lead to very straightforward product isolations.
4. Since it is an essential feature of indirect electrosyntheses that the redox reagent is recycled, the problems of using toxic reagents are reduced and large

volumes of unwanted solids or solution effluent are not produced. This is in contrast to, for example, reductions with zinc powder or permanganate oxidations which lead to large volumes of heavy metal ion solution and solid manganese dioxide respectively.

One example of an indirect electrolysis – the methoxylation of the substituted furan – has already been described. The anode reaction was the oxidation of bromide ion to bromine which subsequently reacted with the furan. Here, two further examples will be presented. The first is the conversion of anthracene to anthraquinone via electrogenerated chromic acid. A concentrated solution of chromium(III) in aqueous sulphuric acid is partly oxidized to chromic acid at a lead dioxide anode:

$$2Cr^{3+} + 7H_2O - 6e^- \longrightarrow Cr_2O_7^{2-} + 14H^+ \tag{6.20}$$

and the dichromate is then reacted with anthracene:

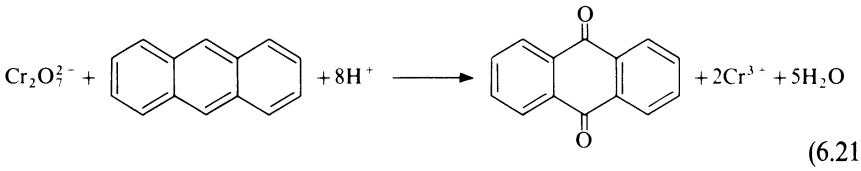

(6.21)

in a separate reactor. This indirect process has been carried out for over 50 years. In the most recent plant, the electrolysis is performed in a membrane cell while the chemical step is carried out by allowing the chromic acid to trickle through a column of solid anthracene. The product – anthraquinone – is also insoluble in the aqueous acid so that the organic conversion is effectively completed solid → solid. The reaction goes to completion provided the particle size of the anthracene falls within a suitable range. The spent redox reagent is then passed through an activated carbon bed to remove traces of organic material which otherwise lead to loss in current efficiency and the chromium(III) solution is recycled to the cell. The process is summarized in Fig. 6.8. The final example concerns the oxidation of a sorbose derivative, 2,3:4,6-*di*-O-isopropylidene-L-sorbose to the corresponding acid (four of the alcohol groups are protected with acetone in order to ensure selective oxidation at the desired site).

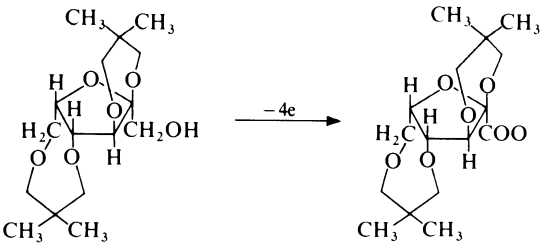

(6.22)

The reaction is part of a method for the manufacture of ascorbic acid (vitamin C). The medium for the oxidation is aqueous 0.3 mol dm^{-3} sodium hydroxide and the anode is nickel. In this situation, the nickel is covered by an oxide/hydroxide

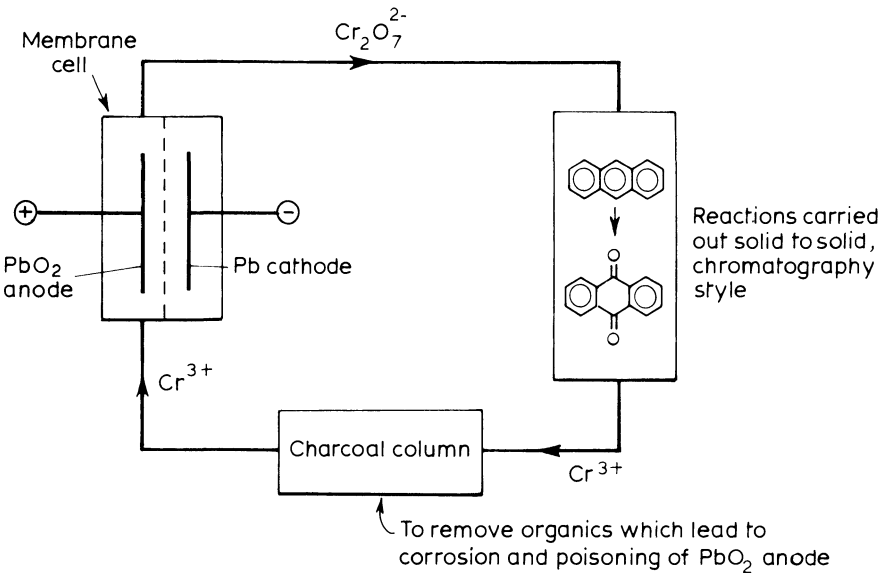

Fig. 6.8 Indirect electrosynthetic process for the oxidation of anthracene → anthraquinone.

layer which behaves as a trapped redox catalyst, i.e. the mechanism of the reaction is:

$$Ni(OH)_2 + OH^- - e^- \longrightarrow NiOOH + H_2O \tag{6.23}$$

$$4NiOOH + RCH_2OH \longrightarrow RCOO^- + 4Ni(OH)_2 \tag{6.24}$$

where the electrochemistry is maintaining the nickel within the electrode coating in the active, higher oxidation state. Since the current density for the oxidation of the protected sorbose is very low, maybe 10 mA cm^{-2}, it is essential to use a cell configuration with a high surface area of anode. An undivided Swiss roll cell was selected and the nickel gauze anode is also subjected to a pretreatment to enhance its roughness. The cathode is made from a steel gauze. Hoffman la Roche have reported that the process has been carried out on a 2 ton day^{-1} scale in Swiss roll cells with an anode area of 200 m^2. The reaction was carried out to 99% conversion in a cascade of cells with decreasing current density from 20 mA cm^{-2}. The selectivity was >90% and the current efficiency about 70%. It was necessary to develop a system to overcome the safety hazard from explosion due to the mixing of the hydrogen gas formed at the cathode with the oxygen evolved as a by-product at the anode. This was achieved with a catalyst which recombines the gases within the off-gas.

6.4 THE FUTURE OF ELECTROSYNTHESIS

The future for organic electrosynthetic processes must now be very bright. Compared with even 10 years ago, there is now much greater realism about the

targets which might be achieved electrochemically and there are successful examples relevant to most branches of the chemical industry. Moreover, there are far fewer obstacles to scale-up with the availability of cells from several suppliers and an increasing experience of integrating electrolytic cells into complete industrial processes. Additionally, there is a growing awareness of electrochemical techniques amongst synthetic organic chemists and chemical engineers.

It is to be expected that an increasing number of fine-chemicals companies will learn to consider electrolysis in the solution of their synthetic problems.

FURTHER READING

The hydrodimerization of acrylonitrile:

1 M. M. Baizer and D. E. Danly (1979) *Chem. Ind. (London)*, 435 and 439.
2 F. Beck (1972) *Angew. Chem.* **11**, 760.
3 D. E. Danly (1984) *J. Electrochem. Soc.*, **131**, 435C.
4 D. E. Danly (1981) *Hydrocarbon Processing*, 161.
5 M. M. Baizer and J. P. Petrovitch (1970) *Prog. Phys. Org. Chem.*, **7**, 189.
6 D. E. Danly and C. R. Campbell (1982) in N. L. Weinberg and B. V. Tilak, (Eds), *Techniques of Electroorganic Chemistry*, Part III, Wiley, Chichester.
7 M. M. Baizer (1983) (Ch. 25) and D. E. Danly (Ch. 30) in M. M. Baizer and H. Lund, (Eds), *Organic Electrochemistry*, Marcel Dekker.

Organic electrosynthesis:

1 N. L. Weinberg (Ed.) (1974 and 1982) *Techniques of Electroorganic Synthesis*, Part I, II and III, Wiley, Chichester.
2 M. M. Baizer and H. Lund (Eds) (1983) *Organic Electrochemistry*, Marcel Dekker, New York.
3 F. Beck (1974) *Elektroorganische Chemie*, Verlag Chemie Berlin.
4 D. E. Danly (1984) *Emerging Opportunities for Electroorganic Chemistry*, Marcel Dekker, New York.
5 T. Shono (1984) *Electroorganic Chemistry as a Tool in Organic Synthesis*, Springer-Verlag, Berlin.
6 S. Torri (1985) *Electroorganic Synthesis*, Part I, *Oxidations*, Kodansha-VCH.
7 H. L. Chum and M. M. Baizer (1985) *The Electrochemistry of Biomass and Derived Materials*, ACS Monograph, No. 183, American Chemical Society, New York.
8 S. Torri, (Ed.) (1987) *Recent Advances in Electroorganic Synthesis*, Kodansha-Elsevier, Amsterdam.

7 Water purification, effluent treatment and recycling of industrial process streams

There is now a great awareness of the dangers to ourselves and the environment from many effluents in industry and other activities of modern life. Certainly, it is no longer acceptable to indiscriminately discharge gases into the atmosphere or liquids, solids and solutions into waterways or landfill sites. This is reflected by the legislation introduced by many governments which, for example, prescribes legal limits for toxic materials such as carbon monoxide in car exhausts, metal ions and cyanide ion in water from chemical plants and organic compounds in water from sewage works, chemical plants or food factories. For such laws to be enforced, methods must be available both for treating the effluent to meet the standards and for monitoring the effluent to ensure that the legal limits are not exceeded. Moreover, in many cases the legal requirements are becoming steadily harsher and implemented more rigorously, and methods must therefore continue to develop. At the same time, with the increasing costs of raw materials and the threat of depletion of world reserves of many resources, it should become more attractive to reuse or recycle materials. Examples of this trend are described elsewhere and include: (1) the electrorefining and electrowinning of metals (Chapter 4); (2) electrolytic recycling of traditional redox reagants used in organic synthesis reactions (Chapter 6); and (3) metal removal from, and regeneration of, etchants in the printed circuit industry (Chapter 9).

The provision of water suitable for drinking is another essential to life. The quality of naturally available water varies greatly from site to site and in many places it may be necessary to remove bacteria, salts, heavy-metal ions and organics; desalination and chlorination are the most common processes. Moreover, it is again advantageous to monitor the water quality continuously or, at least, routinely.

Effluent and water treatment, therefore, are essential technologies which are likely to expand and develop considerably in the future. While such processes have a variety of objectives, a common feature is the need to handle a highly variable feed. Typical are the local-authority sewage works to be found in every town. Each person produces $200\,dm^3\,day^{-1}$ of sewage which, although

varying with season and location, will, on average, contain organic material equivalent to a biochemical oxygen demand (BOD) of 400 mg dm^{-3}. To this is added a component of industrial and commercial effluent, the nature of which will depend strongly on time and location, but the overall treatment process must aim always to reduce the BOD to below 20 mg dm^{-3}, to reduce suspended solids to below 30 mg dm^{-3} and to reduce to safe levels toxic and other undesirable species, e.g. NO_3^-, detergents.

What is the role of electrochemistry in water and effluent treatment? One answer would be, 'relatively small', since there are many competitive methods and these are cheaper on a large scale and use less energy; Table 7.1 summarizes the main processes used in the three stages of treatment of urban sewage. The mechanical and biological methods are very effective on a large scale and the physical and chemical methods are used to overcome particular difficulties such as final sterilization, odour removal, the removal of inorganic chemicals and breaking oil or fat emulsions. Normally, no electrochemical processes are used. On the other hand, there are particular water and effluent-treatment problems where electrochemical solutions are advantageous. Some such processes will be discussed in this chapter and it will be seen that the electrochemical processes are based on quite diverse principles. A general feature is that, whenever possible, the duty (and hence the size) of the electrochemical reactor is minimized by incorporating it as close to the source as possible. In this fashion, small volumes of electrolyte containing relatively high concentrations and having a reasonable electrolytic conductivity may be treated. The examples in this chapter are intended to illustrate the range of possibilities for electrochemical processes and are in no way exhaustive. Indeed, a large number of companies now market

Table 7.1 Principal types of processes used in local-authority sewage works

Stage	BOD range/mg cm^{-3}	Mechanical or biological processes	Physical or chemical processes
Primary	400–250	Comminution, sedimentation, sludge digestion or incineration	Flocculation by chemical additives, flotation
Secondary	250–40	Percolation through activated sludge filters, biological oxidation, nitrification	Flotation, coagulation by additives, precipitation (e.g. phosphate, fluoride, heavy metals), filtration
Tertiary	40–< 20	Filtration, oxidation ponds, disinfection	Treatment with Cl_2 or O_3, adsorption on high-surface-area carbons, osmosis, ultraviolet sterilization

electrolytic devices and it is beyond the scope of this book to more than 'scratch the surface' of available technology.

In addition, although electroanalysis has never been very popular in the laboratory, electrochemical devices for on-line monitoring and fieldwork are more attractive. They can be small, have low power requirements easily met by a small battery and give a readout which can easily be read on a meter, be displayed digitally, fed into a microprocessor or be used to operate an alarm. The principles of some of these devices will be discussed in Chapter 12.

7.1 METAL ION REMOVAL AND METAL RECOVERY

7.1.1 General considerations

Electroplating, electrorefining and electrowinning are described in other chapters and all use electrolytes in which the concentration of metal ions is greater than 50 g dm^{-3}. The processes described in this section aim to strip metal ions from dilute solutions, 1–1000 mg dm^{-3}, and in some cases there may not be a high concentration of inert electrolyte, i.e. the solution has a low total ionic strength. The feeds to the cell may arise from a wide range of sources, including:

1. Primary ore leaching.
2. Mine-dump leaching or runoff water.
3. Liberator cells in electrowinning and electrorefining.
4. Electroplating, including spent and contaminated baths, static rinses (drag-outs) and rinse waters.
5. Etching solutions and rinse waters.
6. Metal-cleaning solutions.
7. Scrap reprocessing and refining.
8. Catalyst liquors.
9. Chemical-processing reagants.
10. Photographic processing solutions, particularly fixers and rinse waters.
11. Effluents.
12. Reprocessing of spent batteries.

Hence, the liquor to be treated may have diverse properties regarding the types (and number of) metals, solution composition, pH and conductivity. Therefore, preconditioning of the feed may be required prior to the electrolytic treatment in order to, for example: (1) increase conductivity; (2) remove particulate matter; (3) remove aggressive or corrosive components; and (4) correct pH.

It should be recognized at the outset that the driving forces for the installation of metal-ion stripping equipment may also be quite diverse, namely:

1. It may be necessary to comply with legislation barring the discharge of effluent into a river or the sea unless a metal ion concentration is below a proscribed limit.

2. The local water authority may charge an excess for water from industrial sites to the community sewage installation which increases with the metal ion content.
3. One may need to condition a process stream for recycle.
4. It may be worthwhile for the value of the metal recovered.

Clearly, if the metal recovered rapidly returns the investment in the new cell and also covers the running costs, the extraction process is likely to be attractive. This is most likely when the metal is silver, gold or other precious metal although, as their prices increase, it may be economically worthwhile to recover others. Certainly, a major advantage of certain electrochemical processes is that the metal can be recovered directly, in its most valuable form, i.e. solid, pure metal. The competitive processes (i.e. precipitation of the metal ion as a hydroxide with sodium hydroxide, solvent extraction and ion exchange) essentially only lead to a precipitated salt or another metal ion solution of increased concentration, while cementation leads to very impure metal. On the other hand, treatment with sodium hydroxide or lime is undoubtedly the cheapest of the various technologies, even if sometimes messy. It is a well-established technique and, when correctly controlled, can precipitate a wide range of metals in the form of oxide and hydroxide sludges.

Of all the fields of application for electrochemical reactors, the removal and recovery of dissolved metal has provided the greatest spectrum of cell designs. This diversity is true not only in terms of the cell geometry, but also regarding the scale of operation, e.g. in terms of total cell current, the reactors range from modular bench-top precious-metal recovery cells (<50 A) through to large, purpose-built electrowinning tank houses involving, perhaps, 100 kA.

In the case of precious metals, optimization of the electrolytic cell is not usually critical. Indeed, a number of radically different types and size of reactor compete satisfactorily for a given application, especially when the concentration of dissolved metal is relatively high. Cell voltage (and, hence, the electrolytic power requirement) and electrolyte agitation costs are not usually critical; rather, security of the deposited metal from theft and the need to produce a relatively pure metal in a form suited to refining (or reuse) is paramount.

In the case of more base metals, power costs may become a significant factor, particularly on a large scale.

During the treatment of dilute solutions, the cathodic deposition of metal is often under mass transport control, either initially or during longer batch-processing times (section 2.5.2). In such cases, it was seen in Chapter 2 that the maximum duty of the reactor may be expressed in terms of the limiting current (which is proportional to the rate of metal deposition). From the definition of the mass transport coefficient:

$$i_L = k_L A n F c^{\infty} \tag{7.1}$$

where c^{∞} represents the bulk concentration of dissolved metal in the process

liquor. For a given metal level (and, hence, c^{∞}) the reactor duty is therefore dependent upon the mass transport coefficient k_L and the active electrode area A. Hence, it is desirable to use a cell having a high value of $k_L A$. The fractional conversion over the reactor has also been shown to depend upon the same factor. A number of cell designs incorporating high k_L, high A or both, have already been discussed in Chapter 2, cells having been classified according to the nature of their electrodes (two- or three-dimensional; static or moving).

An obvious strategy is to operate the reactor under limiting current conditions at the cathode. As will be seen in Chapter 8, this may have important consequences regarding the production of roughened or powdery deposits. Indeed, this feature may be exploited as a means of producing a metal product which is dislodged easily from the cathode (hence recovered as a powder) perhaps continuously. The difficulty in maintaining a uniform (limiting) current density over the entire cathode area has been highlighted earlier, particularly if the reactant concentration varies over the reactor or potential, and flow distribution are problematic.

The form and nature of the metal product are often of paramount importance. It is often necessary to choose the type of cell and the electrolysis conditions in order to produce the desired material, at a reasonable purity and in a suitable form:

1. Compact or powdered metal for resale.
2. Compact metal for reuse, possibly as a soluble anode material in electroplating.
3. An aqueous metal concentrate, which is recycled as a process liquor.

It is noteworthy that, while cells are capable of recovering metal directly, few can achieve continuous product extraction. Other cells are only capable of concentrating the dissolved metal; a deposition cycle is necessarily followed by chemical (or anodic) dissolution of the deposit in a small volume of a suitable leaching liquor.

The importance of the electrode potential and its distribution throughout the electrode has already been stressed in Chapter 2. Ideally, it might be controlled such that the entire cathode operates at maximum current efficiency for the desired, metal deposition reaction:

$$M^{n+} + ne^- \longrightarrow M \tag{7.2}$$

An excessive current density will normally lead to secondary reactions. In a simple case, this may be hydrogen evolution (which may create safety problems):

$$H^+ + e^- \longrightarrow \tfrac{1}{2}H_2 \tag{7.3}$$

or codeposition of a second metal:

$$M_1^{n+} + ne^- \longrightarrow M_1 \tag{7.4}$$

In some cases, however, the side reaction adversely affects the kinetics of metal-deposition reaction and the form of the product, e.g. in the recovery of silver from thiosulphate-based photographic fixing solutions, the desired reaction may be represented by:

$$Ag(S_2O_3)_2^{3-} + e^- \longrightarrow Ag + 2S_2O_3^{2-} \tag{7.5}$$

If the cathode potential becomes too negative, reduction of bisulphite, also present in spent fixing solutions, may occur:

$$6H^+ + HSO_3^- + 6e^- \longrightarrow HS^- + 3H_2O \tag{7.6}$$

as well as reduction of free thiosulphate ion:

$$S_2O_3^{2-} + 8H^+ + 8e^- \longrightarrow 2HS^- + 3H_2O \tag{7.7}$$

or:

$$S_2O_3^{2-} + 2e^- \longrightarrow SO_3^{2-} + S^{2-} \tag{7.8}$$

Due to rapid mixing of reaction products, silver sulphide may form on the cathode:

$$S^{2-} + 2Ag^+ \longrightarrow Ag_2S \tag{7.9}$$

Precipitation of Ag_2S has several adverse consequences:

1. Contamination of the silver deposit.
2. Contamination of the fixer by colloidal Ag_2S which is difficult to filter.
3. A reduction of cathode current efficiency for silver deposition.
4. Interference with the kinetics of silver removal.
5. Catalytic chemical decomposition of the fixer.

Such complexities of the electrode and solution chemistry are, moreover, typical of the problems met in the recovery of metal from industrial process liquors.

There are many variants for the mode of operation of a reactor, in addition to those discussed in Chapter 2, section 2.5, e.g. one strategy is to use a primary cell to extract the majority of metal from the process liquor, while a secondary cell performs the final stages of metal recovery (Fig. 7.1). In this fashion, the primary cell may involve a modest mass transport rate and operate with a small fractional conversion per pass. The secondary cell may scavenge metal effectively by virtue of, for example, a high electroactive area per unit volume. In some cases, metal leached as a concentrate from the secondary cell may be recycled to the primary one; all the metal recovered might then be obtained as solid material.

7.1.2 Typical cell designs

Some of the above comments are illustrated by considering a number of cell designs which are (or have been) used at a reasonable scale or in relatively large numbers (Table 7.2).

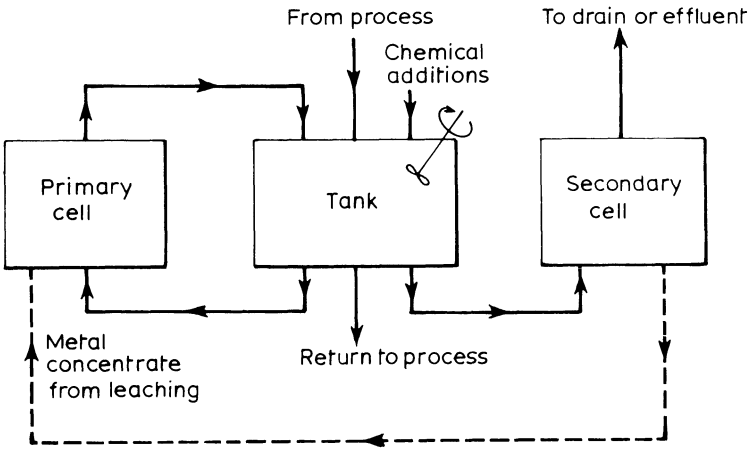

Fig. 7.1 A possible mode of operation for metal-extraction cells. The majority of the duty is met by the primary cell which is part of a batch-recycle loop incorporating the storage tank. The secondary, or 'tailing', cell is used as a single-pass (or cascade) reactor to reduce the metal to a level suitable for discharge.

(*a*) *Plate-in-tank cells*

Perhaps the simplest cell geometry is based on vertical, parallel plates in a tank. In practice, electrolyte agitation (usually air-sparging) is normally provided in order to enhance mass transport, although pumped flow or even mechanical stirrers have been used. The Recowin system (Table 7.2) provides an example of such an air-agitated cell in which permanent stainless-steel cathode plates are used. Metal may be recovered by manually stripping the deposit as a foil, and close spacing of the electrodes maintains a reasonably low cell voltage together with a moderate electroactive area per unit volume.

Rather than using plate electrodes, a much higher surface area is obtained by using reticulated (foam) cathodes (Chapter 2, section 2.4.2). This principle is exploited in the patented RETEC cell which employs one of three types of cathode: (1) Copper foam is standard for many applications; (2) Nickel foam used for special applications; and (3) Carbon foam, particularly for precious metals (this aids subsequent refining operations, and minimizes contamination by base metals).

Electrolyte is recirculated through the electrodes and air agitation may be provided. Typically, the undivided, monopolar cells utilize as few as six to as many as fifty vertical foam cathodes (Fig. 7.2), with interspersed, inert anodes (typically O_2-evolving DSA coated titanium mesh). The cathode foams have an electroactive area approximately 15 times the projected, geometric area and are held in place by a series of grooves on the inside tank walls, maintaining an evenly spaced, parallel arrangement.

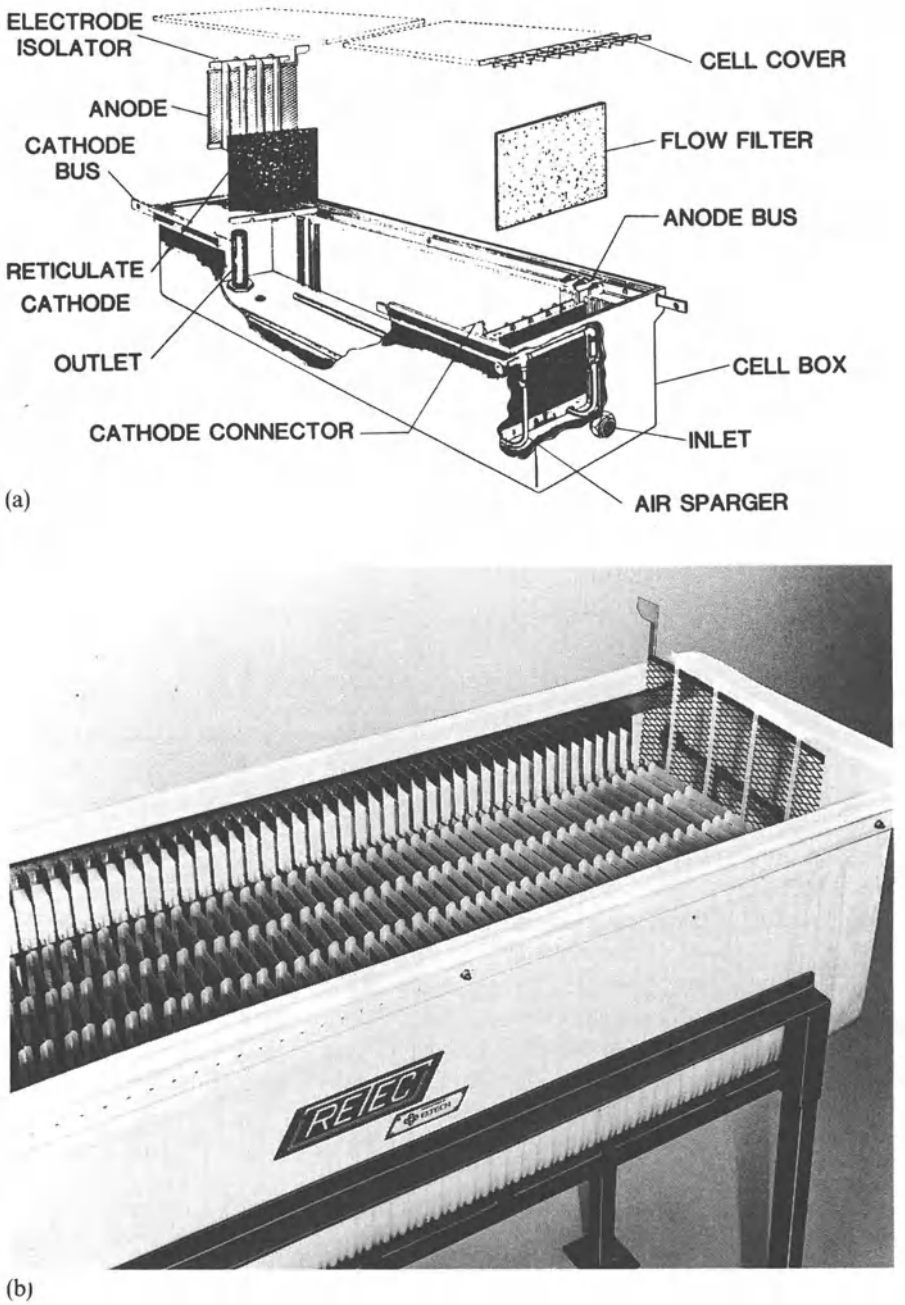

Fig. 7.2 The RETEC-50 cell. (a) The major components. (b) The RETEC-50 cell assembled. (Courtesy: EES Corporation. RETEC is a trademark of ELTECH Systems Inc.)

Table 7.2 Examples of electrochemical reactors for metal removal and recovery*

Reactor	Company	Type of cathode	Frequency and method of product removal	Performance enhancement mainly via:			
				Cell normally divided?	Electrolyte movement	Electrode movement	High electroactive area
ER cell	ElectroCell AB	For example, packed bed of carbon particles within a parallel plate and frame	Discontinuous via anodic or open circuit leaching	Yes	✓		✓
Envirocell	Deutsche Carbone	Contoured packed bed of carbon, possibly with non-conductive particles	Discontinuous via anodic or open-circuit leaching or vacuum removal of bed	Yes	✓		✓
FBE† reactor	(Originally AKZO) Billiton Research b.v.	Fluidized bed of metal particles in a tube-and-shell-type geometry	Continuous via withdrawal of grown particles	Yes	✓	✓	✓
Eco-cell†	(Originally Ecological Engineering) Steetley Engineering Ltd	Outer surface of a rotating cylinder with powdered-metal deposit	May be continuous via automatic scrapping and fluidization of metal powder	Maybe		✓	✓

Table 7.2 (*continued*)

Reactor	Company	Type of cathode	Frequency and method of product removal	Performance enhancement mainly via:			
				Cell normally divided?	Electrolyte movement	Electrode movement	High electroactive area
Chemelec cell	BEWT (Water Engineers) Ltd	Vertical mesh (or plate) in an electrolyte with fluidized glass beads	Discontinuous by manual scraping or reuse as anodes in plating	No	✓		
Concentric cell	Wilson Process Systems	Inner surface of a cylindrical foil (copper or stainless steel)	Discontinuous: cathode may be furnace-refined in the case of gold	No	✓		
Rotating electrode cell	Wilson Process Systems	Rotating cylindrical foil (usually stainless steel) or static cylindrical foil with rotating anode (larger cells)	Discontinuous by manual scraping or flexing	No	✓	✓	
Recowin	Eco-tec	Vertical plates in tank, air agitatation possible	Discontinuous via manual stripping of metal as sheet	No	✓		

Goecomet reactor	Goema AG	Rotating tubular bed or impact rod	Contiuous as settled powder via a sludge cone	No	✓	✓
Retec cell	Eltech	Vertical metal (or carbon) foam electrodes in a tank	Discontinuous: cathode may be steel (which may be chemically stripped for reuse) or carbon for precious metals – cathode may be reused as an anode in plating	No		✓

* All of these cells are (or have been) in commercial use at a reasonable scale.
† These cells are not readily available at present.

As an example of performance, a pilot-scale RETEC cell containing seven cathodes and operating at 35 A may be used to recover copper from an acid sulphate liquor, in a single-pass operation. At the 500 mg dm^{-3} Cu level, 84% metal removal is achieved with a current efficiency of 46%. A lower Cu level of 100 mg dm^{-3} results in 90% removal with 10% current efficiency. At very low Cu levels (*c.* 30 mg dm^3 min^{-1}) the fractional conversion is still high at 93%, albeit with a low (*c.* 3%) current efficiency. The data was obtained using standard pore cathodes and a flow rate of 0.75 dm^3 min^{-1}. Metal removal efficiencies are greater at low flow rates, but the amount of metal recovered is less than can be achieved at high flow rates with lower efficiencies.

The 50 cathode cell has overall dimensions of approximately 180 × 60 × 50 cm with a cross-sectional area for flow of *c.* 1530 cm^2; it has provision for an air-sparging system to improve mixing and promote turbulence within the electrolyte. A porous filter plate is built into the cell at the inlet in order to diffuse liquid flow through the cell to prevent localized metal accumulation on the cathodes which could lead to short circuiting. When the foam cathodes are fully loaded, they are replaced with fresh ones. In single pass operations, the cathodes nearest the inlet require most frequent replacement. The RETEC-50 cell is primarily aimed at electroplating wastes and typically operates at 400–500 A and from −2 to −6 V.

(*b*) *Plate-and-frame cells*

In order to achieve a high electrolyte velocity through a porous or packed-bed electrode, it is often desirable to seal the cell. Indeed, one of the present trends in cell design is the incorporation of 3-dimensional electrodes into the plate-and-frame geometry. The electrode material may be, for example, foam, a mesh or a

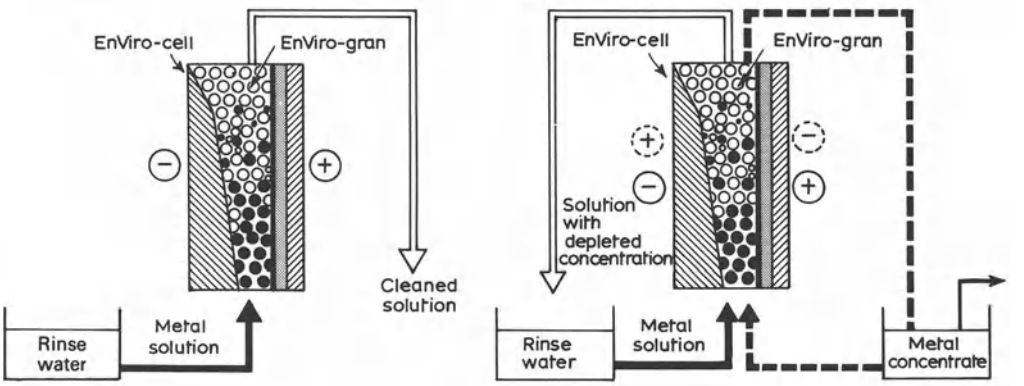

(a)

Continuous mode of operation
Regeneration by exchanging the granular graphite filling

Intermittent batch operation with electrical regneration via pole reversal

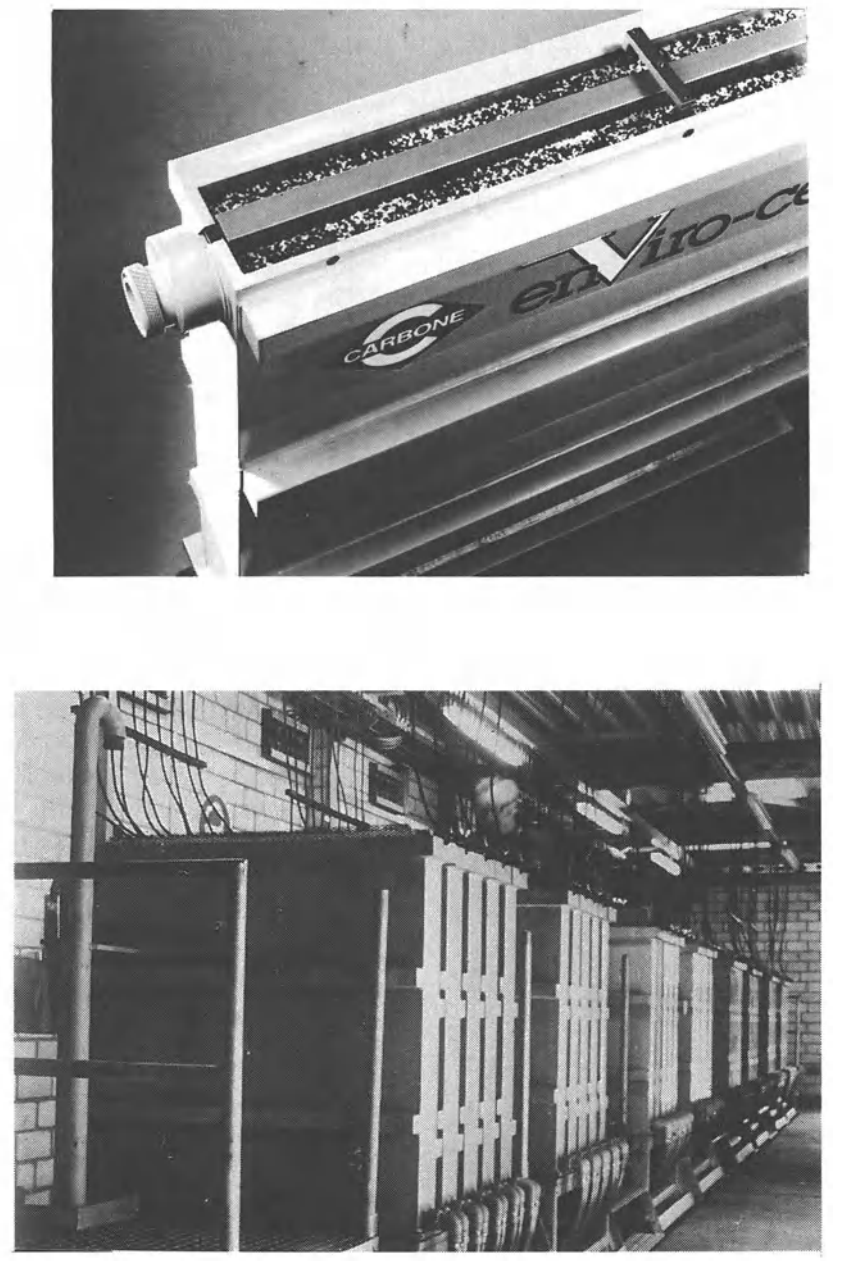

Fig. 7.3 The Enviro-Cell which uses a profiled, packed-bed cathode for metal removal. (a) modes of operation. (b) View from above of a single Enviro-Cell (approximately 1 m high) (c) A number of cell modules banked together. (Courtesy: Deutsche Carbone.)

packed bed of particles or fibre. As an example, it has been reported that an ElectroProd Cell (Chapter 2, section 2.7.3) with a packed bed of carbon particles has been developed to the pilot-plant stage and used commercially to control the level of Zn^{2+} ions in an acidic, ferric chloride solution used in pickling operations. Successful recovery of Cu, Zn and Ag from synthetic electrolytes of diverse conductivity has also been achieved, satisfactory cathode efficiency being achieved at conductivities as low as $1 \times 10^{-3}\ \Omega^{-1}\ cm^{-1}$.

The above version of the ElectroProd cell uses a thin (< 1 cm), porous-bed cathode, which has a constant thickness. In order to maximize the cathode current efficiency and achieve a high conversion in a single pass, one strategy is to increase the cathode area (hence, decrease the current density) towards the reactor outlet. In this fashion, the packed bed may be profiled in order to achieve a reasonable overall cathode-current efficiency. This principle is used in the Enviro-cell (Fig. 7.3; see also Chapter 2, section 2.7.6) which employs a tapered, packed bed of carbon granules. The cell module may be used singly for small applications or a number of modules may be banked together in series or parallel flow to provide a wide range in terms of capacity and fractional conversion. Each module is fabricated in a polymer such as polypropylene, having overall dimensions 102 cm (high) $\times$ 15–26 cm (deep) $\times$ 103 cm (wide).

A central, vertical anode (e.g. a graphite plate) is surrounded by the special particulate carbon bed. Electrolyte flows into the cell at the bottom via a dispersing tube and exits via an outlet near the top; the cell is unsealed.

Metal which has deposited on the packed bed may be recovered in two possible ways (Fig. 7.3(a)). The carbon packing plus metal may be removed from the cell by a vacuum cleaner. Fresh packing granules may then be added, most conveniently on a weight basis. Alternatively, the metal may be removed as a concentrated solution by recirculating a stripping solution and reversing the cell polarity to assist dissolution of the metal; in this fashion, regular removal of the packed bed is avoided.

(*c*) *Turbulence-promoted electrolytes*

In the case of filterpress cells, it was mentioned in Chapter 2 that the most common, practical method of enhancing mass transport is the use of plastic-mesh turbulence-promoters. It is rarely convenient to use such devices in metal-recovery cells due to the problems of the mesh being incorporated into the deposit or else promoting non-uniform deposits. One possibility is to utilize a porous electrode, such as a packed bed or a metal mesh or foam; in these cases, the electrode itself acts as a turbulence promoter (in addition to providing a high electrode area per unit volume).

Another practical approach is to promote electrolyte turbulence via the use of an expanded-mesh electrode in a solution containing fluidized inert particles (typically $\leqslant 1$ mm glass ballotini). This is the principle of the Chemelec cell (Fig. 7.4) which has been widely applied to metal finishing, photographic silver-recovery and precious metal reclamation processes.

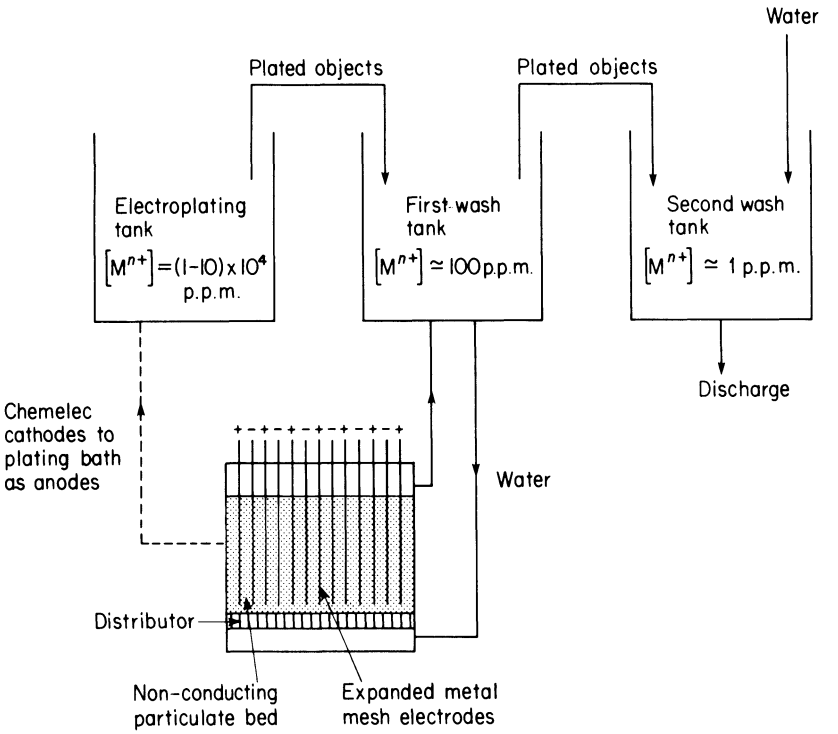

Fig. 7.4 The Chemelec cell installed as part of a batch recycle loop on a static electroplating rinse tank. (Courtesy: The Electricity Council.)

The Chemelec cell consists of a series of closely spaced gauzes or expanded-metal electrodes, alternately anode and cathode, separated by beds of non-conducting beads. The solution to be treated disperses via a flow distributor into the cell so that the particulate glass bed becomes partly fluidized, typically with a bed expansion of around 100%. Electrolyte exits at the top of the cell via an overflow weir. The standard cell has the dimensions $0.5 \times 0.6 \times 0.7$ m and contains up to six cathodes and seven anodes to give a total cathode area of 3.3 m^2. Quarter- and half-size modules are also available. Its main application has been in the treatment of washwaters from the electroplating industry where it is suitable for the recovery of copper, nickel, nickel/iron, zinc, cadmium, cobalt, gold and silver. At the normal operating current density of 5–30 mA cm^{-2} it can recover metal at the rate of 70–400 g h^{-1}. Cells like the Chemelec cell are not well-suited to solutions with very low concentration of metal; the limit of effective metal removal is about 50 mg dm^{-3}. It is therefore generally employed in the mode shown in Fig. 7.4 whereby the water in the first static rinsetank (dragout) of the plating line is cycled continuously through the cell to maintain

the metal ion at a relatively low level, say 100–250 mg dm^{-3}. This water can then be used for an extended period and the metal is recovered. The water in subsequent washtanks will only be contaminated to a very small extent and may be discharged without treatment. The metal recovered may be stripped from the cathode, or the cathode may be transferred to the electroplating bath and used directly as a dissolving anode. An example illustrating the use of the Chemelec cell for silver recovery is shown in Fig. 7.5.

(*d*) *Moving-cathode cells*

One of the most popular cells for small, modular recovery of precious metals is the rotating-cylinder electrode. Indeed, this cell geometry is perhaps the most common choice for photographic silver recovery applications. Whilst a rotating electrode requires more stringent engineering design and necessitates a slipring–brush electrical contact, adequate maintenance and housekeeping precludes serious problems. Moreover, such cells are capable of high rates of mass transport, and are relatively compact. The majority of rotating-cylinder



Fig. 7.5 A Chemelec P cell for photographic silver removal. (Courtesy: BEWT Water Engineers Ltd.)

cells are undivided, utilizing a static outer anode, which may be in the form of a circular metal mesh (e.g. platinized Ti) or a series of carbon plates or rods.

The hollow cathode is usually a thin sheet of stainless steel, curved into cylindrical form and, in some cases, extra anodes are located inside the cathode, improving the electroactive area of the cell.

In the majority of cases, metal is removed from the cathode at intervals, usually by manual peeling or scrapping the deposit. A rotating-cylinder cell for photographic silver recovery is shown in Fig. 7.6. Such cells are available with rotating cathodes (small-scale) or rotating anodes (on a larger scale).

The Eco-cell process is based on a rotating-cylinder cathode, which may be surrounded by a cation-exchange membrane and a concentric anode. This cell geometry gives a uniform cathode potential and allows the cathode potential to be controlled by a crude potentiostat, thus avoiding a waste of charge and unnecessary power consumption and also introducing the possibility of separating a mixture of metal ions. The process was designed to convert the metal ions in solution to metal powder to be collected outside the cell and if necessary the cathode surface is scraped with a blade to facilitate removal of the powder. Figure 7.7 illustrates the complete process.

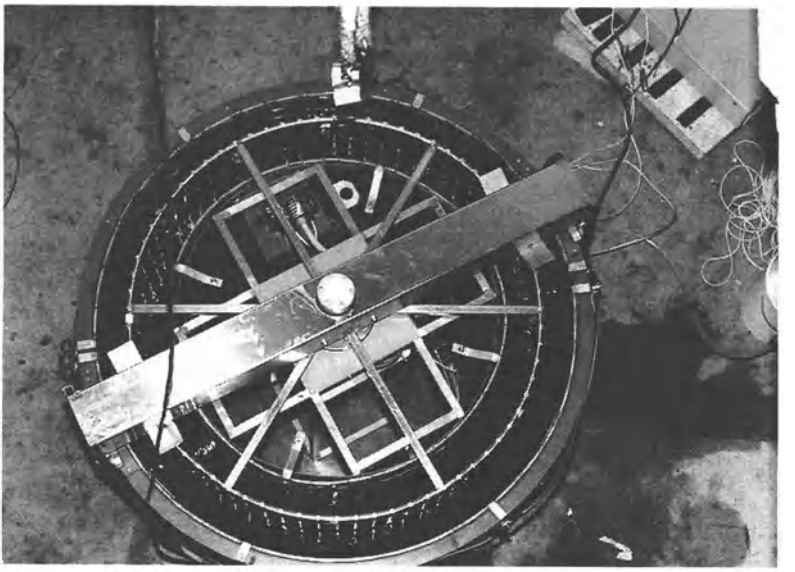

Fig. 7.6 A 300 A rotating-anode reactor for photographic silver recovery. A view of the top of the cell. The 6.5 m^2 cathode is surrounded by 72 carbon rod anodes mounted on rotating rings inside a glass-reinforced plastic tank. (Courtesy: Wilson Process Systems Ltd.) The anode mounting rings which lie inside and outside the cathode rotate at 30 rev min^{-1}. Cell liquor capacity is 750 dm^3; the tank has an approximate diameter of 1.4 m and is 1.2 m high. The electrolyte is pumped around the cell.

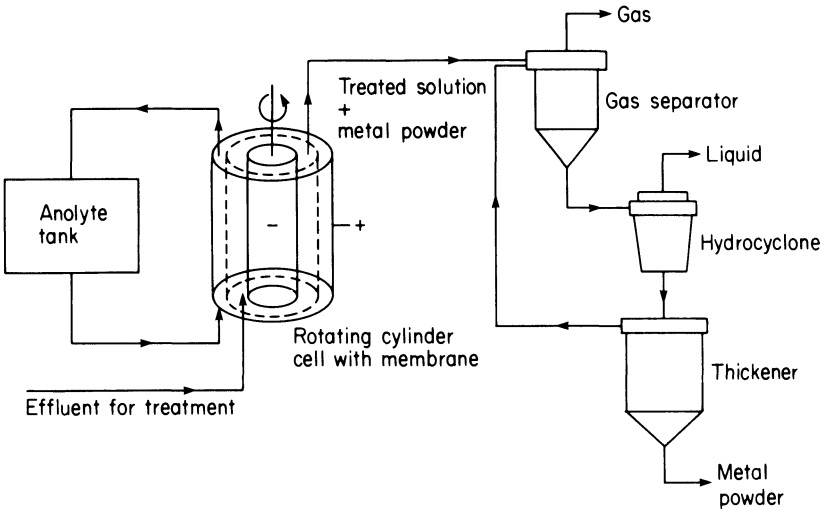

Fig. 7.7 The Eco-Cell process for continuous removal and production of metal in powder form.

An acceptable rate of metal removal is obtained by designing the cell with a high ratio of electrode surface area to catholyte volume and, more importantly, by using conditions which are highly turbulent. The turbulence is introduced by the rotation of the cathode, the peripheral velocity of this electrode commonly being 10–20 $m\,s^{-1}$, and is further enhanced by the roughness of the rotated surface resulting from the growing metal centres. These particles are very effective turbulence promoters and the mass transfer coefficient in such conditions can (in a large cell) be more than 50 times that in the cell with a hydrodynamically smooth rotating cathode. To ensure controlled hydrodynamics in the larger cells, the electrolyte enters and leaves the cell through dispersion manifolds placed parallel to the axis of rotation.

A typical 5 kA Eco cell has a cathode drum of radius 0.37 m and height 0.74 m, and the cathode–membrane gap is about 1 cm. The cathode is rotated at 100–200 rev min^{-1}. Such a cell can recover several kilograms per hour of copper powder from a 100–200 mg dm^{-3} Cu^{2+} solution. For applications where complete stripping of the metal ion is advantageous (i.e. pollution control) it is necessary to operate a number of cells in series (Fig 7.8(a)). It can be seen that the last two cells in the series are only responsible for the removal of 10% of the metal ion, while costing the same as the first two cells to install and operate. This clearly causes a high capital investment and running costs, but fortunately the same effect can be achieved in a single cell by dividing the catholyte compartment into several segments with baffles, e.g. the cell with dimensions given above but divided into twelve cathode compartments and operated at 1 kA can reduce the copper content of 8 $m^3\,h^{-1}$ of solution from 100 mg dm^{-3} to 1–2 mg dm^{-3} This concept is described as the Eco Cascade cell (Fig. 7.8(b)).

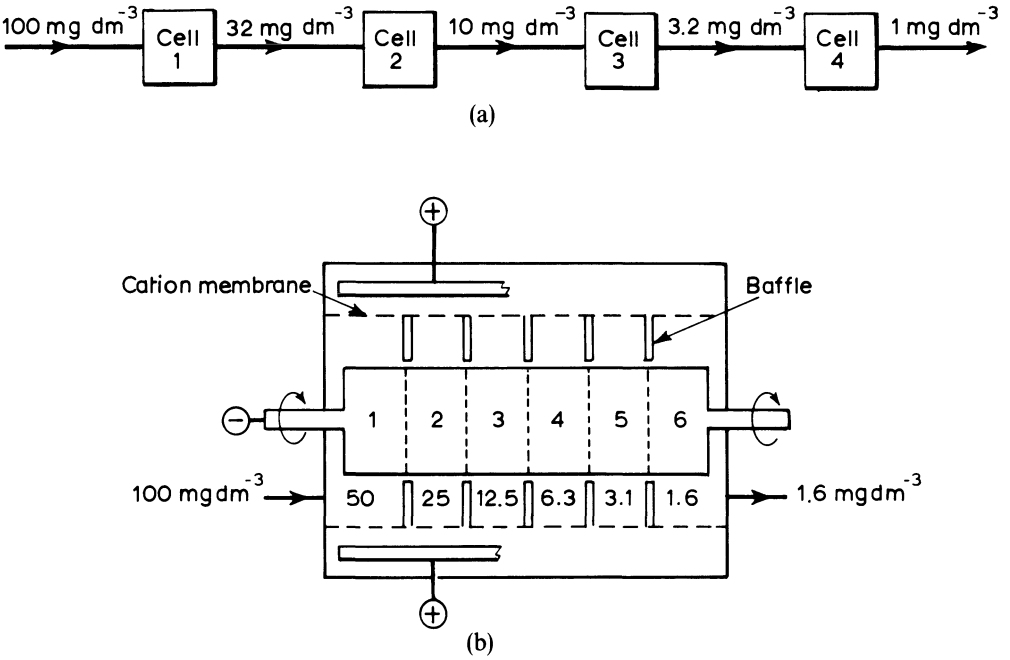

Fig. 7.8 Treatment of a 100 mg dm^{-3} Cu^{2+} solution by four 2 kA Eco cells in series and operating under identical conditions. In rotating-cylinder electrode cells, high fractional conversion may be obtained by: (a) employing a number of separate reactors in hydraulic series or more practically (b) by the Eco Cascade cell.

An Eco-cell plant operating in Denmark contains a 4 kA Eco cell followed by a 1 kA Eco cascade cell and this treats 200 m^3 day^{-1} of copper phthallocyanine pigment effluent, reducing the Cu^{2+} concentration from 400 mg dm^{-3} to 2–3 mg dm^{-3} and recovering about 80 kg of metal per day. While the majority of developments have concerned copper containing liquors, the process has been applied on a scale of 20 A–10 kA, to the recovery of the platinum group metals.

In the case of precious metals, it has already been mentioned that power requirements are not critical. Therefore, mechanical movement of electrodes is often practised and is one method of continously dislodging metal from the cathode, particularly when the metal deposit is particulate. An example is provided by the 'impact rod' reactor (Fig. 7.9). The ends of metal rods are agitated via cathodic guide rails in such a way that the rods frequently strike each other. This intermittent contact helps to achieve high rates of deposition in addition to continuously removing the deposit. The metal sediments to the conical bottom may be removed at intervals as a sludge by opening a drop valve. Moving particle-bed reactors, similar to the above concept, have also been developed.

A much smaller and simpler example of a moving-particle-electrode reactor is provided by a barrel cell (Fig. 7.10). Such devices are used routinely to

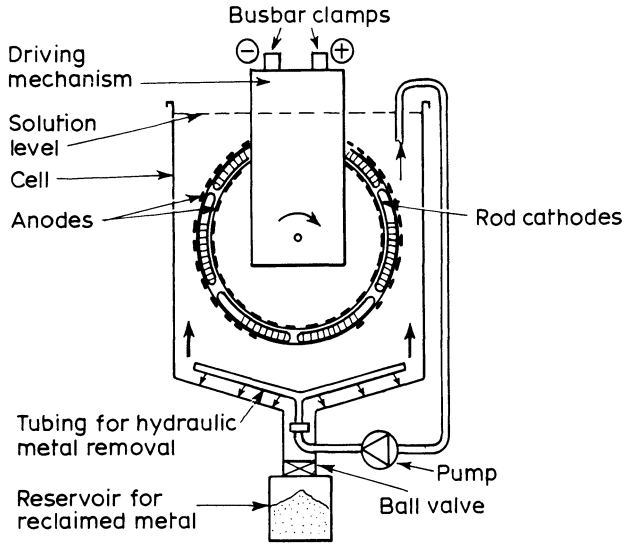

Fig. 7.9 The principle of the impact rod reactor (the Goecomet reactor.)

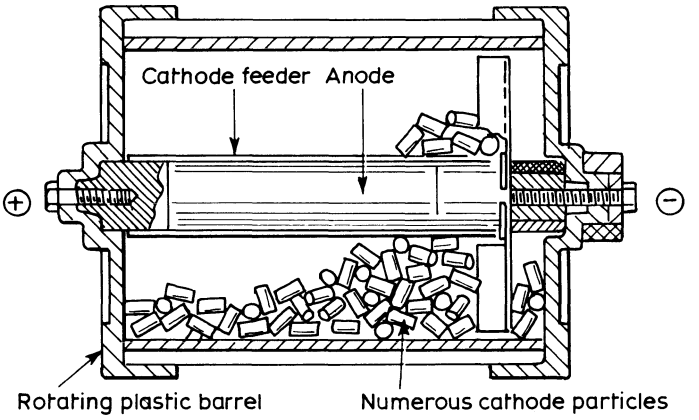

Fig. 7.10 A rotating-particle barrel cell for metal removal.

electroplate many small items and may be adapted for metal scavenging by charging them with a dummy load of regular, blank workpieces, e.g. small rods. The mass transport rates and electroactive area per unit volume are both relatively small, but the equipment is often available to the electroplating industry and represents familiar technology.

(*e*) *Fluidized-bed electrodes*

A continuous metal-extraction process developed by AKZO Zout Chemie based on the fluidized-bed cathode has the cathode itself as the turbulence promoter.

Such electrodes are capable of maintaining high apparent-current densities and rate of metal removal because of their very high surface area per unit volume and effective introduction of turbulence. The main problem is the tendency for the particles of metal to agglomerate, especially if there are stagnant zones in the cell, and careful cell design is essential to avoid the rapid loss of performance which results. The design of the AKZO cell is shown in Chapter 2 (Fig. 2.36) and has been discussed in section 2.7.7. The potential distribution within the fluidized electrode is made as uniform as possible by placing multiple anodes within the bed. Each anode is placed inside a tubular diaphragm and the anolyte and catholyte are controlled separately and may be different. The specially developed diaphragms have high mechanical strength and resistance to chemical attack but a low hydrodynamic permeability and electrical resistance. Their surfaces are also very smooth in order to avoid the commencement of bed agglomeration at this interface.

A typical unit will be up to 0.5 m in diameter and the bed may be 1 m high (plus 10–30% expansion on fluidization). The number of anodes will depend on the diameter of the cell. A 0.35 m diameter cell with seven anodes and operating at 1000–2000 A handles 10–20 $m^3\ h^{-1}$ of solution. The bed is made of metal particles 0.5 mm in diameter and these are allowed to grow to 1 mm (a tenfold increase in weight); the particles gradually sink down the bed during the growth so that the process can be operated continuously by adding small particles at the top and removing the heaviest from the bottom of the bed.

Several examples of the application of this technology have been described; the fluidized bed cells have been used:

1. To remove copper from the effluent of a hydrocarbon chlorination process which contained both solids and chlorocarbons as well as copper(II) in an acidic chloride medium, the copper content being reduced from 100 to 1 mg dm^{-3} with a 70% current efficiency.
2. To strip mercuric ion from effluent resulting from the chlor-alkali mercury cell process, the concentration being reduced from 5 to 0.06 mg dm^{-3}.
3. To recover copper and cadmium and to purify a zinc electrolyte. Using sequential cells, the copper and cadmium were removed to 0.1 mg dm^{-3} and 1 mg dm^{-3} with current efficiencies of 70 and 40% respectively. Moreover, the purities of the metals were greater than 99% for copper and greater than 90% for cadmium. It is understood that the AKZO technology is being further developed for hydrometallurgical applications by Billiton Research b.v.

(*f*) *Concentric cathode cells*

One of the simplest cell geometries is the concentric cylindrical one. This is a relatively common choice for metal removal on a small scale; it provides uniform electrode potential and freedom from moving parts, albeit with a low space–time yield. The mass transport may be enhanced by appropriate design of the

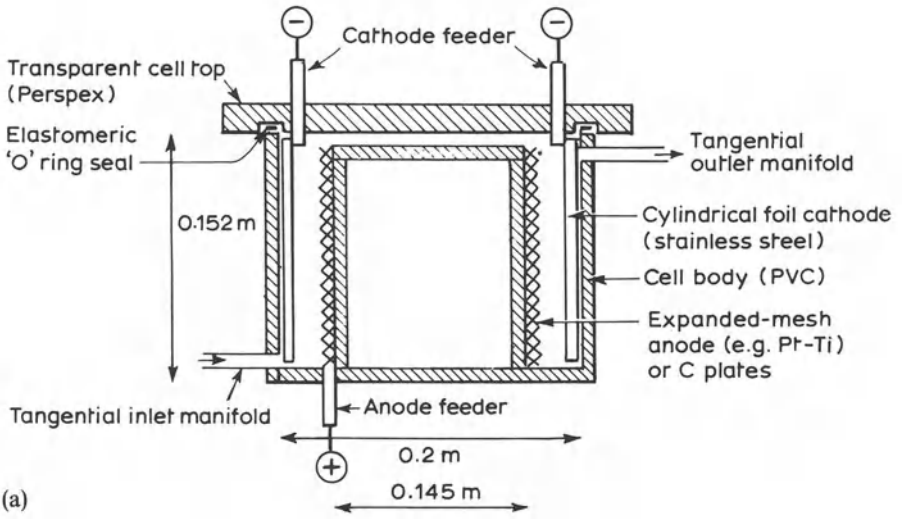

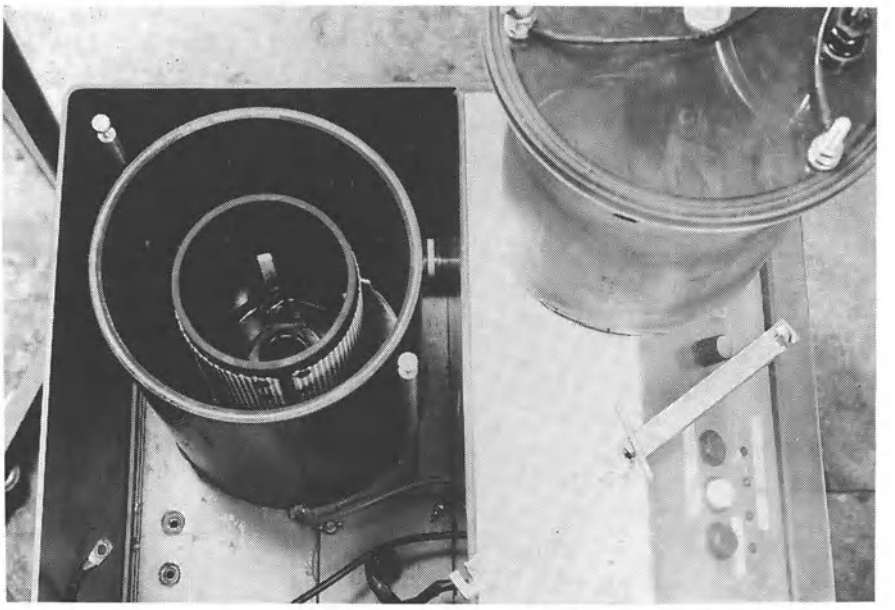

Fig. 7.11 A concentric, flow-through cylinder cell. (a) The cell section. (b) A typical cell, showing the cathode removed. (Courtesy: Wilson Process Systems Ltd.)

manifolds together with a sufficient volumetric flow rate of electrolyte, in order to provide turbulent flow.

Figure 7.11 shows a typical example of a concentric cell which is used for photographic silver recovery and removal of precious metals from electroplating and refining wastes. Following deposition of the metal, the cell is designed for rapid and convenient removal of the cathode (Fig. 7.11(b)) in order to inspect the deposit or replace the cathode. In the case of silver removal, for example, the deposit may be manually scraped from a stainless-steel cathode. For gold removal, a copper cathode is preferred as this promotes good adhesion and aids the subsequent furnace-refining of the gold.

7.1.3 Conclusions

The overall future for electrochemical removal of metal from solution seems bright and several established cell designs are helping to provide a maturing technology.

New cell designs for metal-stripping continue to be developed and may find commercial application. Their performances in terms of ability to remove metal ions is similar and, indeed, the difficulty with all cells lies in the chemistry when complexing agents may be present. Differences are, however, claimed in respect of investment cost and ease of both use and maintenance. Due to the number of existing cell designs on the market, competition is often severe and practical considerations such as reliability, convenience in operation, ease of automation and the capability of operation by unskilled personnel are important factors. Indeed, such considerations may assume greater importance than the cell geometry and its electrochemical performance, as expressed by figures of merit.

7.2 HYPOCHLORITE AND LOW-TONNAGE CHLORINE ELECTROLYSERS

A number of electrochemically generated oxidants may be used to purify water streams. In Chapter 5, cells for hydrogen peroxide (section 5.7) and ozone (section 5.8) generation were described in some detail. The most traditional oxidizing agent in these circumstances, however, is undoubtedly hypochlorite or chlorine.

The last decade has seen the introduction of a number of small electrolysis cells for the generation of either hypochlorite or chlorine gas; in many applications, either type of cell could, in principle, be employed and the choice will then depend on technological factors. In the water and effluent-treatment industry, the common applications of on-site chlorine and hypochlorite cells will include the treatment of sewage (particularly at remote sites), the sterilization of water for food processes and hospital laundries, the treatment of water on board ships and for swimming pools, the treatment of cooling water at coastal power stations to prevent the growth of shellfish and seaweed in the pipes and the enhanced

oxidation of cyanide ion in effluents. In addition, the same cells are used to provide chlorine gas for power stations and to provide bleaching agents in the paper and textile industries. Traditionally, all these markets have been satisfied by liquid chlorine, tanked from the large chlor-alkali plants, but avoidance of the potential hazards associated with the transport and storage of chlorine is now important.

The low-tonnage chlorine electrolysers are small versions of the membrane cells described in Chapter 3, although the anolyte will usually be a concentrated brine prepared from solid sodium chloride. Indeed, the development of membrane technology was a big boost to on-site chlorine generation since membrane cells, unlike mercury or diaphragm cells, are well suited to small-scale and intermittent production and units producing as little as a few kilograms per day are now available. The major disadvantage of such chlorine generators in the water treatment industry is the very high purity of brine which is necessary in membrane cells; the Mg^{2+} level must be low and this makes a seawater feed possible only if the process is complicated by a purification unit to precondition the electrolyte.

At one time, sodium hypochlorite was manufactured electrolytically on a substantial scale. Now it is regarded as a by-product of the chlor-alkali industry; the tail gases (containing only a low concentration of chlorine and resulting from dechlorination of the brine leaving the cell) are reacted with sodium hydroxide. On the other hand, there are many situations where low volumes of hypochlorite may be required or the requirement is irregular. Examples include suppression of algae and mollusc growth in cooling systems, sterilization of potable water, sterilization of injection water for oilwell drilling operations, sewage treatment, conditioning of swimming pools, disinfection of equipment in the food and dairy industries and deodourization of air from, for example, sewage- or tobacco-treatment plants. Aqueous solutions of sodium hypochlorite are much safer than chlorine gas but contain $\leqslant 15\%$ wt active chlorine. Hence, storage and transportation costs are relatively high. Indeed, the cost of aqueous NaOCl is nearly double that of the equivalent amount of Cl_2 gas. Often, the most convenient and cost-effective solution is to electrolytically generate OCl^- as required, using filtered sea water or a neutral brine liquor produced from solid sodium chloride solution, as appropriate.

A wide range of cell designs and sizes have been described. The cells do not require a separator, since cathodically formed hydroxide:

$$2H_2O + 2e^- \longrightarrow H_2 + 2OH^- \tag{7.10}$$

is consumed in the hydrolysis of anodically produced chlorine in the electrolyte:

$$2Cl^- - 2e^- \longrightarrow Cl_2 \tag{7.11}$$

$$Cl_2 + 2OH^- \longrightarrow H_2O + OCl^- + Cl^- \tag{7.12}$$

In practice, the current efficiency may be reduced and specific energy consumption increased by several factors. At high OCl^- levels, elevated temperature

and in turbulent-flow conditions, the mass transport controlled reduction of hypochlorite becomes important:

$$OCl^- + H_2O + 2e^- \longrightarrow Cl^- + 2OH^- \quad (7.13)$$

The reaction rate may also be increased by cathodically generated hydrogen gas which will improve mass transport.

If the NaCl content is low, at low temperatures or in the presence of too small an electrolyte movement, the rate of reaction (7.11) may be too low and oxygen evolution can occur:

$$2H_2O - 4e^- \longrightarrow O_2 + 4H^+ \quad (7.14)$$

At high hypochlorite concentrations and high temperature, loss of OCl^- product may also occur by anodic oxidation:

$$6OCl^- + 3H_2O - 6e^- \longrightarrow 2ClO_3^- + 4Cl^- + 6H^+ + 3/2O_2 \quad (7.15)$$

Finally, if seawater electrolyte is used, precipitation of group (II) metal hydroxides, particularly $Mg(OH)_2$, may occur on the cathode surface, due to the localized increase in pH.

These potential problems can usually be prevented or minimized by adequate attention to cell design and control of electrolysis conditions. In particular, care

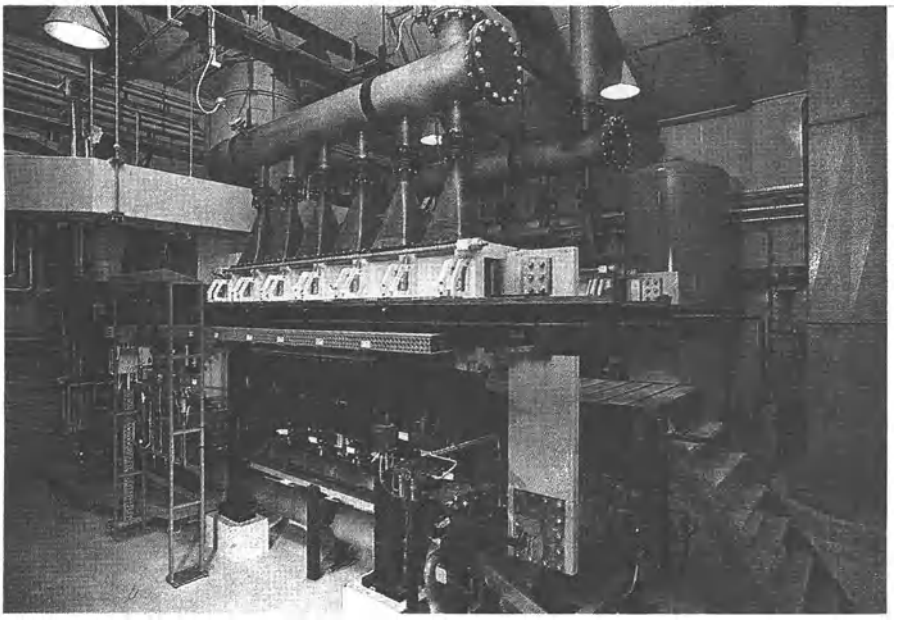

Fig. 7.12 Cells for hypochlorite production. Four units each producing 160 kg h^{-1} at a nuclear power plant at Paluel, France. The installation provides sterilization of the seawater coolant. (Courtesy: Krebs.)

must be taken to preclude stagnant electrolyte zones within the cell, or localized extremes of temperature. Some manufacturers have utilized a periodic reversal of the cell polarity in order to prevent the build-up of insoluble hydroxide films on the electrode, but care must then be taken to avoid corrosion of the electrodes.

For the majority of applications, the electrolyte contains 0.01–1% wt OCl^- when it leaves the cell, although higher levels are preferred for some applications.

For small-scale electrolysis units, energy consumption will be much less important than in a chlor-alkali process; ease of operation with a minimum of

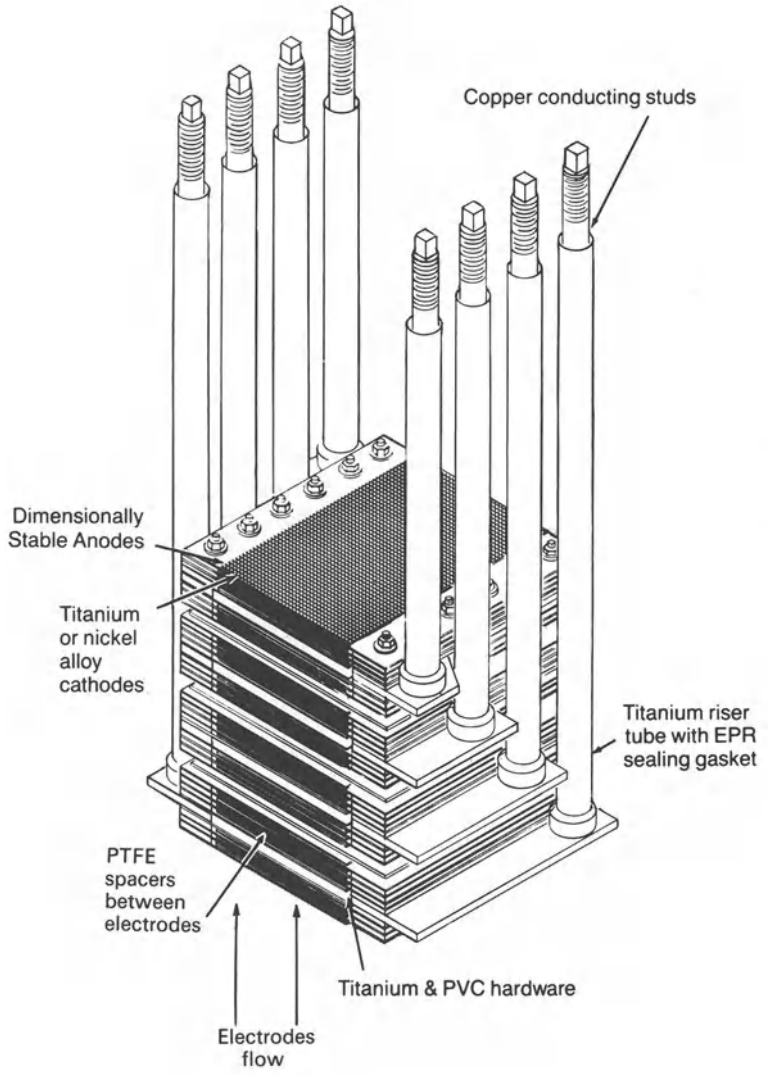

(a)

maintenance and replacement of components and the initial cost of the total unit will more often determine the choice of the cell. Particularly in the case of sea water electrolytes, the cell design should allow rapid and convenient disassembly for cleaning and removal of hydroxide deposits. The cathode material is usually stainless steel, a nickel alloy or titanium. A wide range of anode materials including graphite, lead dioxide and platinized titanium have been used as well as dimensionally stable anodes. Hence, the quoted energy consumptions of hypochlorite cells lie in the range 3.7–7.0 kWh kg^{-1}, considerably above those for a chlor-alkali cell. The current densities vary between 0.1 and 0.5 A cm^{-2}.

Several examples of cell designs may be considered in order to illustrate the range of cell types and sizes, together with typical applications. While diverse types of electrode geometry have been used, particularly on a small scale, the majority of hypochlorite cells use the parallel-plate type of geometry. The electrodes may be monopolar or bipolar and both mesh and solid plates are used. Indeed, some of the modular filterpress cells described for general electrosynthesis in Chapter 2 are used in the undivided mode for hypochlorite generation. Typical cell designs and installations are shown in Figs 7.12 and 7.13.

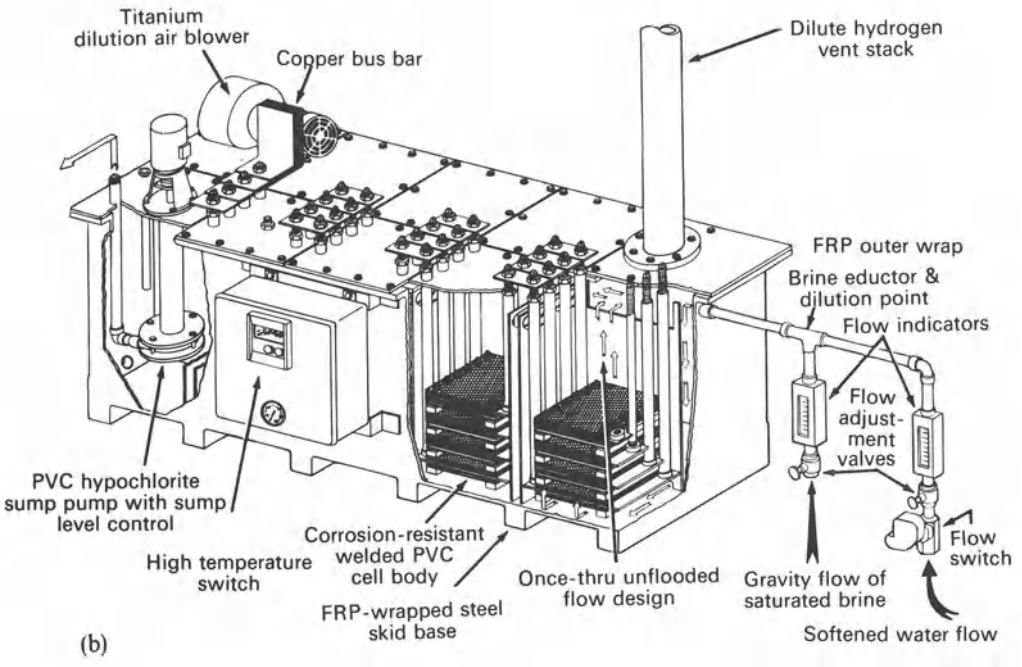

Fig. 7.13 The 'Sanilec' cells producing hypochlorite from brine. (a) A four-cell electrode pack with once-through, unflooded electrolyte flow. (b) Up to 32 electrode packs may be incorporated into a common PVC cell body, with provision for safe dilution of the hydrogen gas by air and automatic dispensing of the brine. (Courtesy: Eltech Systems.)

7.3 ELECTRODIALYSIS

The principle of an electrodialysis cell is shown in Fig. 7.14. Anion and cation exchange membranes are arranged alternately in a stack and a potential field sufficient to force current through the stack is applied between two electrodes placed at each end of the stack. In order for current to pass between the electrodes, ions must be transported through each of the membranes and, by arranging the feeds to the various intermembrane compartments, it is possible to force ionic salts to pass from the dilute stream to the concentrated stream. In fact, using a stack containing N pairs of anion + cation membranes, the passage of 1 F of electricity will allow the transfer of N mol of salt.

Clearly, the electrodialysis can be used for concentrating ionic solutions, deionizing salt solutions and separating ionic and non-ionic species. In the context of this chapter, electrodialysis has applications for the following:

1. The desalination of brackwish water (Table 7.3) in order to produce drinking water. Typically sea water or well-water is treated to reduce the total salt concentration from 1000–3000 mg dm^{-3} to less than 500 mg dm^{-3}. In most cases, the major ionic component is sodium chloride but this is not always so, e.g. in some well water the chief salt is calcium sulphate.
2. The recycling of transition-metal ions, e.g. the rinse waters from nickel plating containing perhaps 1 g dm^{-3} nickel sulphate can be concentrated to 60 g dm^{-3} and recycled directly to the plating bath. The removal of Cr(VI) is discussed in section 7.4.
3. Salt removal from effluent waters prior to reuse in industrial processes. Reduction in the concentration of ionic species is often necessary if the water is to be recycled through a chemical process, e.g. to reduce corrosion.

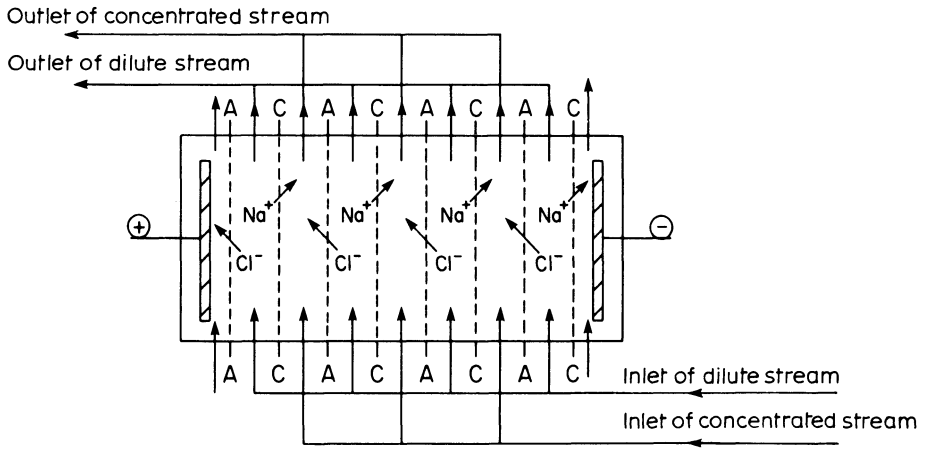

Fig. 7.14 The principle of an electrodialysis stack. Each A denotes an anion-exchange membrane; each C, a cation-exchange membrane.

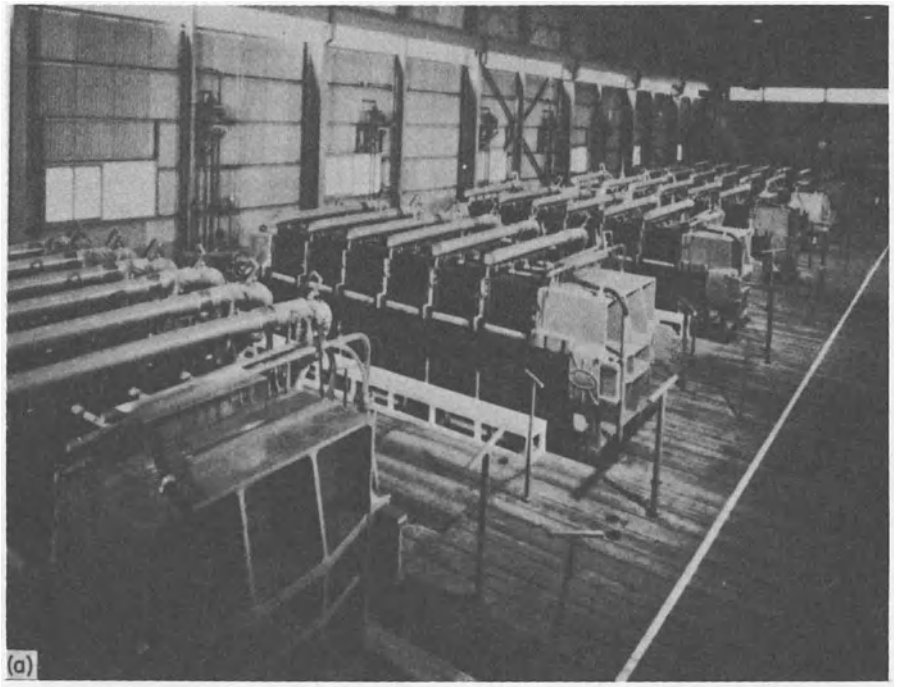

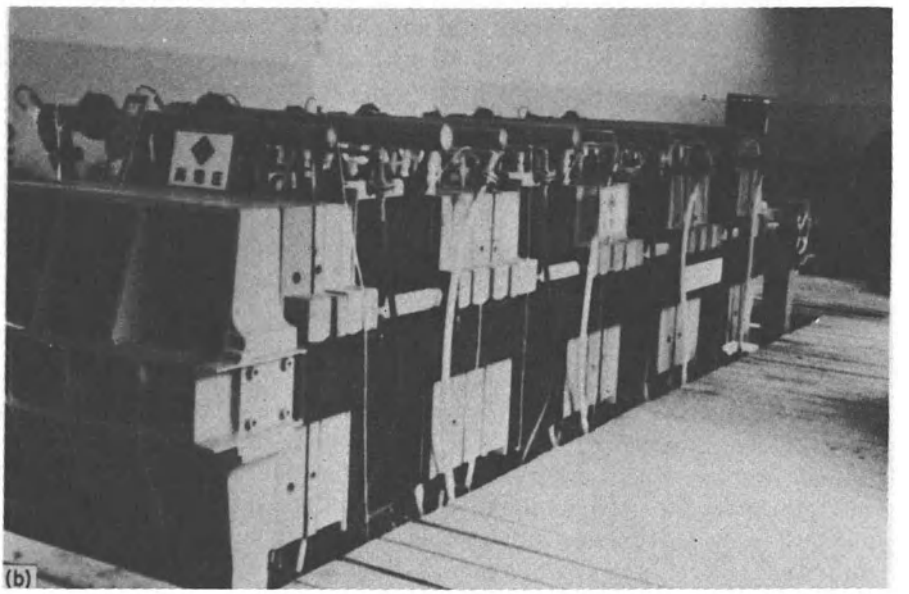

Fig. 7.15 Electrodialysis cells. For the concentration of sodium chloride in sea water. (Courtesy: Asahi Chemical Industry Co. Ltd.)

Table 7.3 Data* for three electrodialysis plants for the desalination of well water

	Webster, USA	Shikine, Japan	Oshima, Japan
Capacity/m^3 day^{-1}			
raw water	1660	227	1540
purified water	954	200	1340
Salinity of feed/mg dm^{-3}	1500–1800	1145	2900
Salinity of product/mg dm^{-3}	350	< 500	< 500
Major ionic species	$CaSO_4$	NaCl	NaCl
Operation	Continuous, four stacks in series	Batch, one stack	Continuous, one stack
Membrane pairs per stack	216	150	250
Membrane size/m × m	1.11 × 1.11	1.11 × 0.57	1.11 × 1.11
Power consumption/kWh m^{-3}	1.4	1.3	1.0

* Data from advertising literature, Asahi Chemical Industry Co. Ltd.

4. Salt splitting, i.e. the recovery of acid and alkali from a neutral salt solution, e.g. the formation of NaOH and H_2SO_4 from Na_2SO_4. For this purpose it is essential to have one pair of electrodes for each pair of membranes; the acid is formed in the anode compartment, the alkali in the cathode compartment and the stream between the membranes is depleted in the neutral salt.

Electrodialysis has a number of other large-scale applications and these would include the manufacture of pure sodium chloride for table salt (in Japan, electrodialysis is the principal method, production exceeding 10^6 ton $year^{-1}$), the demineralization of cows' milk (for baby food), cheese whey and sugar solutions, the removal of excess acid from fruit juice, the isolation of organic acids from reaction streams, and the production of low-salt foodstuffs.

As in all electrochemical cells, the energy consumption of an electrodialysis cell is determined effectively by the cell voltage and the current efficiency. In electrodialysis, these quantities are, however, determined by quite different factors from electrolytic processes. The current efficiency is determined solely by the properties of the membrane (see later in this section) and the faradaic processes occurring at the electrodes are unimportant except to the extent to which they introduce hazards or unwanted problems into the cell. In practice, the cathode reaction is almost always hydrogen evolution and the anode reaction is the evolution of oxygen or in chloride media an oxygen/chlorine mixture. The cathode reaction, of course, increases the pH of the solution in this compartment and this can lead to precipitation of hydroxides if the feed is anything but very pure, e.g. seawater contains Mg^{2+} which may precipitate as $Mg(OH)_2$ on the cathode; hence, the catholyte is commonly acidified. The distribution of voltage in a cell containing N pairs of membranes is given by:

$$E_{\text{CELL}} = E_e^C - E_e^A - |\eta_A| - |\eta_C| - Ni(R_{\text{CATION MEMBRANE}} + R_{\text{ANION MEMBRANE}}) - NiR_{\text{DILUTE SOLN}} - (N\text{-}1)iR_{\text{CONC.SOLN}} \quad (7.16)$$

and it will be apparent that the largest term will be the iR drop in the dilute streams, particularly towards the end of the process when the total ion concentration will be very low. Hence, the cell must be designed to minimize this term, i.e. the gap between the membranes must be as small as possible (typically 0.7–1.5 mm). Particularly when $N = 100$–2000, the terms associated with the electrode reactions are negligible. Indeed, in electrodialysis, the selection of electrode material will be based on stability and cost rather than overpotentials; common electrode materials are platinized titanium or dimensionally stable coatings as anodes with steel considered as the cathode metal.

Clearly, the performance of an electrodialysis cell is largely controlled by the properties of the membranes. Both the anion and cation membranes should have a low resistance and high chemical, mechanical and dimensional stability. While immunity to chemical attack is essential, it should be noted that, with the exception of those adjacent to the electrodes, the membranes are not subjected to extreme pH conditions or the presence of strong oxidizing agents (cf. the membrane in a chlor-alkali cell). The requirement for high mechanical and dimensional stability arises because a large area of membrane and an even gap between neighbouring membranes are essential. In some applications it would be advantageous for the membrane to be selective to particular anions or cations, although in general it is only necessary for the transport number for anions in the anion exchange membrane and cations in the cation exchange membranes to be close to one.

Very large areas of membrane are used in an electrodialysis cell and, hence, they should be as cheap as possible. Thus, while the perfluoropolymers have excellent properties, they are generally too expensive and the membranes used are more commonly copolymers of styrene and divinylbenzene. The cation-selective materials are activated by sulphonation while the anion-selective membranes are substituted with quaternary ammonium centres. To give the membranes the required mechanical and dimensional stability, the copolymerization reaction is initiated around a reinforcing mesh or within a porous polyethylene or thermoplastic sheet; the first method is generally preferred since it gives membranes of lower resistance. The ratio of styrene to divinylbenzene determines the extent of cross-linking and, hence, after activation, the amount of water absorbed into the polymer. The water creates channels across the membrane through which the ions can diffuse and the quantity of water controls the maximum size of ion which can be transported.

Such styrene–divinylbenzene copolymer membranes can be prepared with a wide variation of properties but the best anion exchange membranes give an anionic transport number greater than 0.98 (i.e. less than 2% of the current is carried by cations in the wrong direction) in typical operating conditions although the transport number will have some dependence on the concentrations of salt in the dilute and concentrated streams. The cationic transport number for the corresponding cationic membrane is commonly lower, typically 0.90, and this controls the current efficiency of the process.

The maximum useful current density through the membrane is normally determined by a phenomenon known as 'polarization' – in this context, depletion of the transported ion at the membrane surface. This is a mass transport problem and it is therefore necessary to avoid stagnant layers at the membrane–solution interfaces by operating the cell at a high-enough Reynolds number or with turbulence promoters. This will clearly be most necessary as the dilute stream becomes depleted in ionic species. Electrodialysis cells are usually operated with a current density in the range 20–200 mA cm^{-2}.

Membranes also suffer from a susceptibility to poisoning and fouling. Thus, certain ions have a high affinity for the active centres that they become irreversibly absorbed. An example is Mn^{2+} at cation-exchange materials. This is poisoning and can only be controlled by removal of the offending ion before it contacts the membrane. Fouling is a similar but less serious problem caused by phenols, detergents and large organic acids (all common species in industrial effluents) at anion membranes; it can be minimized by controlling the pore structure of the membrane.

Electrodialysis cells are invariably mounted in a filterpress and constructed on the plate-and-frame principle. The membranes are typically 0.5–2 m^2 in area and very thin to minimize their resistance; hence, they are supported by inert polymer separators placed in each space between membranes. These separators also serve to maintain the membranes a fixed distance apart (0.5–2 mm) to guide the electrolyte flow and to act as turbulence promoters. The number of membrane pairs will depend on the volume of solution to be processed, the total ion concentration in the feed and the level of ions desired in the solution leaving the cell. For the desalination of water, 100–300 membrane pairs are typical, while for the recovery of solid salt, the units may have 1000–2000 pairs. The operation of the cells is dependent on very good gasketing to prevent leaks, particularly from the concentrated to the dilute stream, and the design must permit a good, even solution flow through the cells. The hydraulic pressure must be the same on either side of each membrane and fairly uniform to each membrane gap. It is also necessary to prevent significant current leakage between adjacent membrane gaps through the common solution feeds since this will contribute to the current inefficiency.

A critical path length through the cell, dependent on the current density and flow rate, will be necessary to achieve the desired amount of ion transport from the dilute to the concentrated stream. Several strategies for the solution flow are possible (Fig. 7.16) but all designs must recognize that the current through each membrane will be the same. Hence, for example, in the case shown where 400 p.p.m. salt is removed for each pass through the cell, the ion concentration cannot be reduced below 400 p.p.m. Further reduction in this concentration would require passage through a further cell where the current density is lower and, say, 100 p.p.m. per pass is removed. The choice between the flow patterns shown will be based on the volume of solution to be treated and other local conditions. With each flow pattern, the path length can, however, be increased by

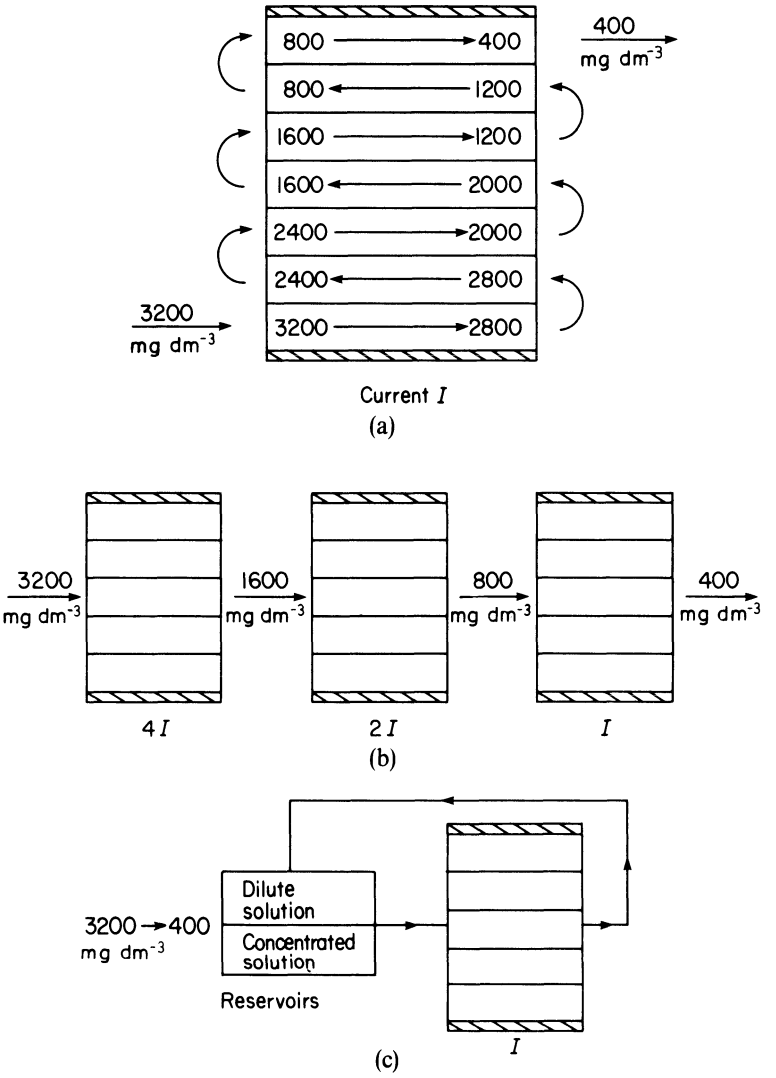

Fig. 7.16 Three flow patterns for electrodialysis cells to reduce salt concentration from 3200 mg dm^{-3} to 400 mg dm^{-3}. The relative currents in each stack are shown. (a) Eight pairs of membranes in series in one stack. (b) Three stacks in series, each stack with N pairs of membranes. (c) Batch process with recycle through one stack.

using the separator between each of the pairs of membranes to direct the solution in a labyrinth pattern across the cell. Several modern cell stacks utilize internal manifolding of the electrolyte flow (Fig. 7.17).

The energy consumption in electrodialysis plants is very dependent on local factors and the objectives of the process but for modern plant it normally lies in the range 1–2 kWh dm^{-3} of solution treated. The number of electrodialysis

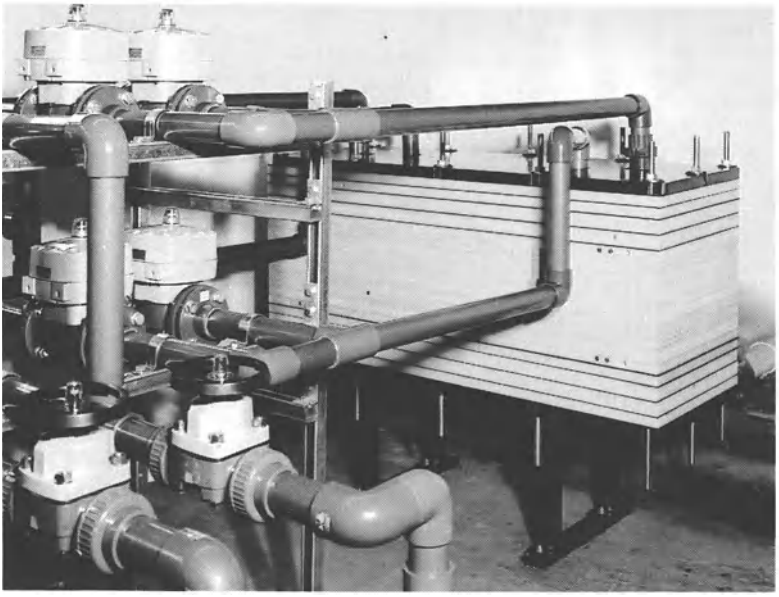

Fig. 7.17 An electrodialysis cell stack. The approximate dimensions are 1580 mm long and 580 mm wide. A typical application is the preliminary purification of raw water (roughing) prior to treatment by a deionizer column. The lifetime of the deionizer, between regenerations, is greatly extended in this manner. (Courtesy: Portals Water Treatment Ltd.)

plants is presently on the increase. The competitive processes for the concentration of ionic solutions and for desalination are evaporation and reverse osmosis (another process based on membranes but using pressure to push solvent through the membrane). Electrodialysis is likely to be the process of choice where the ion concentration of the dilute stream is relatively low, the scale of operation is large and the cost of electric power is low.

7.4 THE TREATMENT OF LIQUORS CONTAINING DISSOLVED CHROMIUM

Soluble chromium species (particularly Cr(VI)) are used in many sectors of industry, as shown by the following examples:

1. Electroplating of chromium from chromic acid baths, leading to spent or contaminated baths and rinsewaters.
2. Pickling, etching and stripping solutions in metal finishing.
3. Plastic surfaces may be etched, prior to electroplating, by Cr(VI) in order to improve adhesion.

4. Chromate conversion coatings (section 8.3.3) for aluminium and magnesium alloys.
5. In the production of sodium chlorate (section 5.3), Cr(VI) may be added to the NaCl-based electrolyte. It is believed that hexavalent chromium helps to prevent cathodic reduction of OCl^- and provides an optimum pH of 6.6 due to the chromate or dichromate buffering system.
6. Cooling waters often have additions of Cr(VI) in order to provide corrosion inhibition.
7. Oxidizing agents used in organic synthesis include Cr(VI).
8. Reducing agents used in synthesis and hydrometallurgy include Cr(II).
9. Cr(II)/Cr(III) electrolytes have also been utilized in flow-through redox batteries.

Despite increasing environmental pressure, including legislation, to minimize the discharge of toxic Cr(VI) species in effluent, the above processes continue to operate using chromium liquors. Indeed, in specific applications, it is often difficult to replace the chromium-containing liquors with alternative process solutions. Hence, it has become increasingly attractive to recycle these liquors or to find suitable treatments prior to disposal.

In the case of liquid wastes, several general treatment methods are available:

1. Physical concentration by evaporation, reverse osmosis or freezing.
2. Chemical concentration using ion exchange, liquid–liquid (or solid–liquid) extraction or electroflotation.
3. Chemical precipitation of chromium oxides or hydroxides.
4. Electrodialysis, which serves to concentrate liquors or to remove contaminant metals.
5. Electrolysis, including oxidation of Cr(III) to Cr(VI) in order to regenerate solutions or cathodic removal of contaminant metals.

Electrodialysis and electrolytic treatments are providing an important contribution to the recycling and safe disposal of chromium containing wastes. A wide range of process strategies and cell designs have been considered at the laboratory and pilot-plant level. In this section, we will consider a number of industrial-scale processes and devices to illustrate some of the possibilities.

7.4.1 Anodic oxidation of Cr(III) to Cr(VI)

Acidic, Cr(VI) solutions may be used as cleaners or etchants for metals (e.g. Cu) and plastics, e.g. ABS: acrylonitrile/butadiene/styrene. In the case of metals, the Cr(VI) may be used in order simply to clean the metal, etch the surface or completely remove a metal coating. The etching of plastic substrates is a key step prior to metallizing epoxy-based laminates during the production of printed circuit boards.

The solution composition depends upon the process requirements but may, for example, utilize $<900\ g\ dm^{-3}$ chromic acid. As the solution is used, the

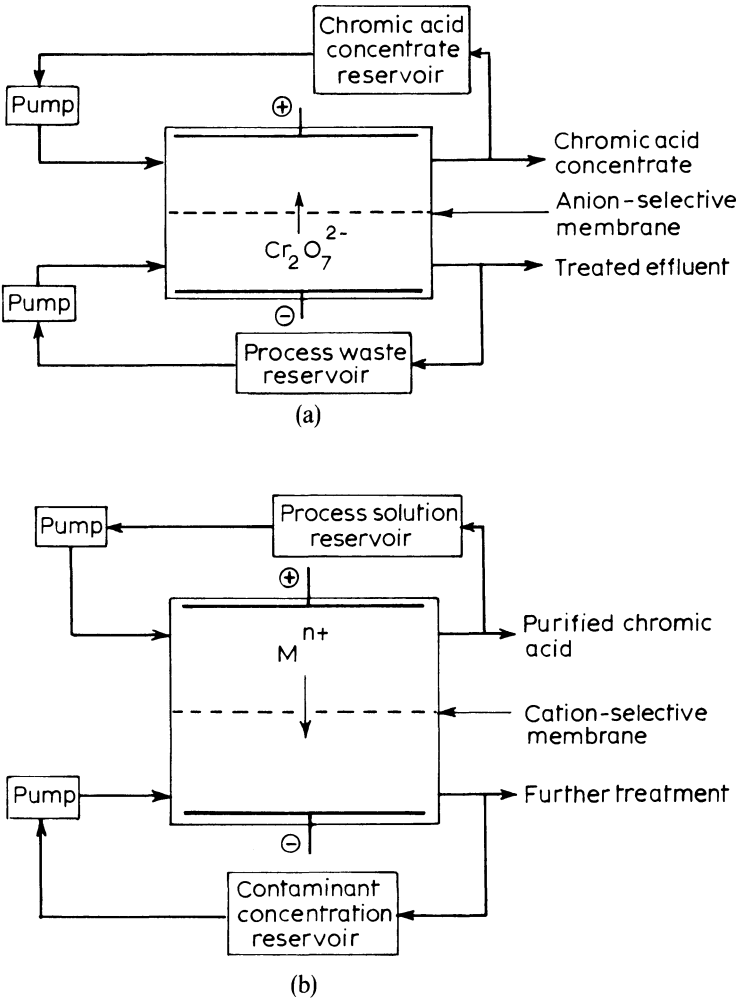

Fig. 7.18 (a) Electrodialysis used to concentrate chromic acid liquors. (Chromate ions migrate through anion-selective membrane to form chromic acid in the anolyte.) (b) Electrodialysis used to remove ionic contaminants.

Cr(III) level builds up, both in the etchant and in any dragout or rinse sections which follow. The rinses can be concentrated by physical techniques such as evaporation, but Cr(III) rapidly accumulates to a level where the liquor is no longer effective as an etchant. Loss of etchant due to drag-out and carry-over on the workpiece is relatively high with these viscous liquors.

Processes have been developed which use an electrochemical cell to oxidize Cr(III) to Cr(VI), regenerating the etchant in a convenient manner by recycling the

Table 7.4 Typical operating conditions for the regeneration of a Cr(VI) etchant for plastics. (*Courtesy*: General Motors Research Laboratories)

Temperature	68° C
Anode current density	21 mA cm^{-2}
Cathode current density	630 mA cm^{-2}
Anode/cathode area	30
Cell voltage	−4.5 V
Initial solution composition	(a) 900 g dm^{-3} CrO_3
	or (b) as (a) + 57 g dm^{-3} H_3PO_4

liquor through the anode compartment of a cell. The reactions are as follows:

Anode (PbO_2 covered lead alloy):

$$2Cr^{3+} + 7H_2O - 6e^- \longrightarrow Cr_2O_7^{2-} + 14H^+ \quad (7.17)$$

Cathode (nickel): $6H^+ + 6e^- \longrightarrow 3H_2$ (7.18)

Overall: $2Cr^{3+} + 7H_2O \longrightarrow Cr_2O_7^{2-} + 8H^+ + 3H_2$ (7.19)

Table 7.4 provides typical operating conditions. The cell is divided by a separator in order to prevent reduction of Cr(VI) at the cathode. In order to maintain a reasonable anode current efficiency, it is advisable to operate with a high (> 5 g dm^{-3}) Cr(III) level and the conversion is stopped short of 100%; indeed, effective surface etching often requires a certain, low level of Cr(III).

Chromic oxide/hydroxide sludges resulting from chemical precipitation processes may be dissolved in chromic acid, which is then treated, as above, to obtain a high-concentration Cr(VI) liquor:

$$6H^+ + Cr_2O_3 \longrightarrow 2Cr^{3+} + 3H_2O \quad (7.20)$$

7.4.2 Combined Cr(III) oxidation and cation removal

Electrodialysis offers two alternative processes for chromic acid liquors:

1. Dilute solutions (e.g. rinsewaters or cooling-water streams) can be concentrated (Fig. 7.18(a)).
2. Ionic impurities can be selectively removed from contaminated chromic acid (Fig. 7.18(b)).

An increasingly common strategy is to combine the regeneration of Cr(VI) (via anodic oxidation of Cr(III)) with removal of contaminant cations which are picked-up during processing. Such cations may arise from dissolution of the workpiece, surface contaminants, or carry-over from other process liquors. By using a cation-exchange membrane, such anolyte impurities will transport via the separator to the catholyte. Here, the cations may be removed regularly, either

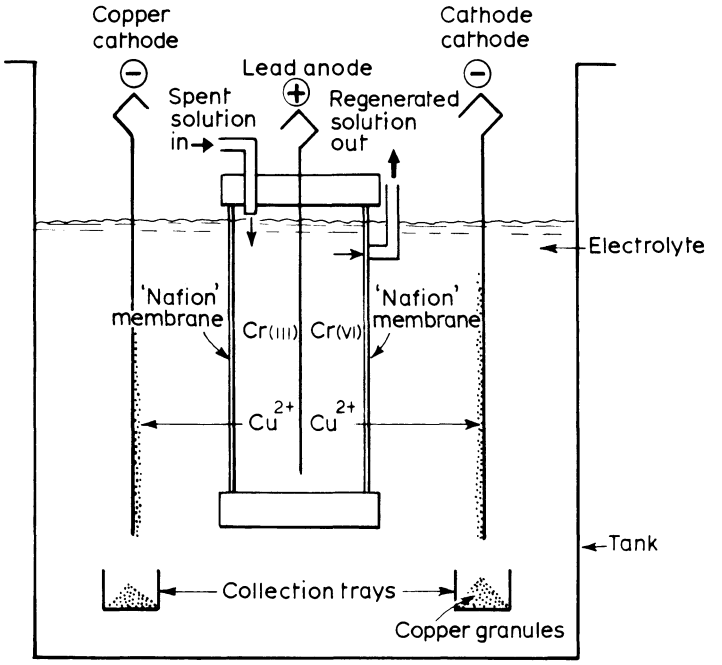

Fig. 7.19 A cell design for regeneration of chromium (VI) solutions. (Courtesy: Chromium Oxidation and Purification System (COPS), Scientific Control Laboratories, Inc. based on US Bureau of Mines Technology.)

by replacing the catholyte or more simply by electrodeposition of the corresponding metals (Fig. 7.19).

As discussed in section 7.4.1, the desired anode reaction (7.17) is Cr(III) oxidation. The anode material and conditions must be chosen to minimize oxygen evolution:

$$2H_2O - 4e^- \longrightarrow 4H^+ + O_2 \tag{7.21}$$

Hence, the anode is usually lead or a lead alloy which develops an oxide or chromate film in use; its area may be significantly larger than the cathode, allowing a low anodic current density.

The most popular cell geometry has been the parallel plate. Both plate-in-tank and filterpress designs have been utilized. Figure 7.19 shows a design concept which incorporates a number of anolyte 'box' sections (containing the cationic membrane) into a catholyte tank. Such cells have been used to treat a wide variety of liquors including a chromate dip for brass forgings, etching and passivating solutions together with stripping solutions used to remove copper plating from aircraft bearings (the selective copper coating being used to selectively prevent carburization of the underlying steel).

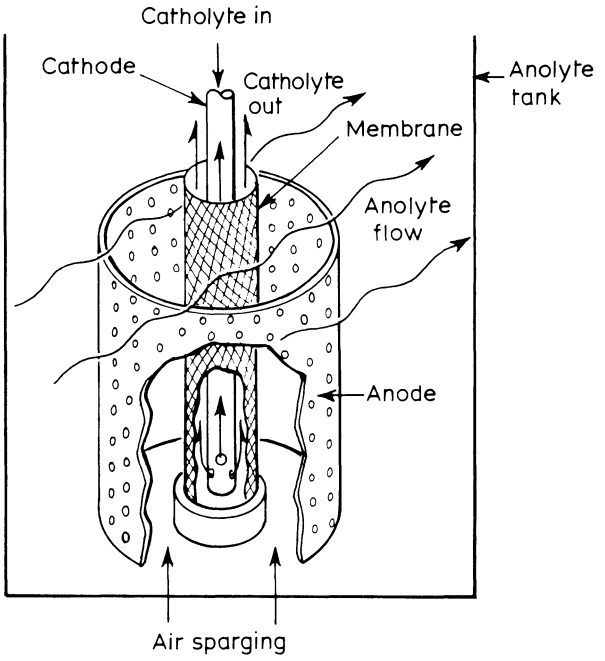

(a)

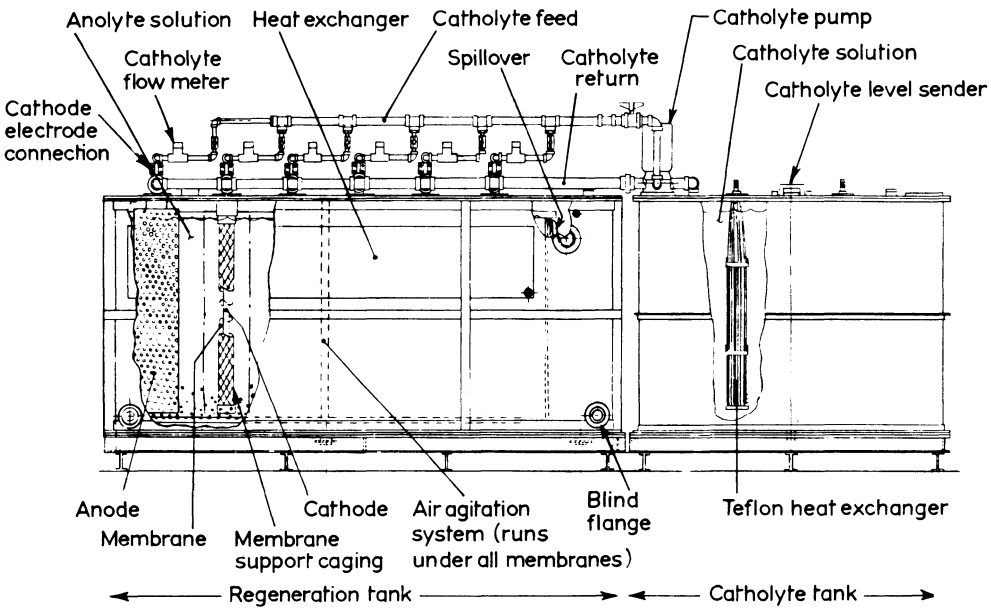

(b)

Fig. 7.20 A divided, concentric-cell design for Cr(III) oxidation. (a) A unit cell. (b) The overall reactor concept. (Courtesy: Ultrasonics, Inc., the Pure-Tec System, Heat Systems.)

The divided, flow-through, concentric cylindrical geometry is preferred by some manufacturers. The inner electrode may be a hollow cathode rod, surrounded by a cylindrical cation-exchange membrane, and an outer, perforated tubular anode (Fig. 7.20(a)). This arrangement provides a relatively large anode area while minimizing the area of the membrane and the size of the cathode. In practice, a number of cell modules are incorporated into a common anolyte tank (Fig. 7.20(b)), with air-sparging to provide improved anolyte flow.

Critical features of this design are a satisfactory, cylindrical membrane support and a secure, efficient membrane-to-cell seal.

7.4.3 Electrolytic techniques involving precipitation of chromium species

In some cases, it is necessary to remove chromium levels in a process stream to very low values, in order to reuse or safely discharge the water. In such cases it is sometimes possible to precipitate the dissolved chromium as oxide or hydroxide species by means of anodically generated Fe^{2+}, the simplified scheme being:

Anode: $$Fe - 2e^- \longrightarrow Fe^{2+} \quad (7.22)$$

Cathode: $$2H_2O + 2e^- \longrightarrow H_2 + 2OH^- \quad (7.23)$$

Cell: $$Fe + 2H_2O \longrightarrow Fe^{2+} + H_2 + 2OH^- \quad (7.24)$$

Electrolyte: $$3Fe^{2+} + CrO_4^{2-} + 4H_2O \longrightarrow 3Fe^{3+} + Cr^{3+} + 8OH^- \quad (7.25)$$

then, e.g.: $$Cr_2O_7^{2-} + 6Fe(OH)_2 + 7H_2O \longrightarrow 2Cr(OH)_3 + 6Fe(OH)_3 + 2OH^- \quad (7.26)$$

The undivided cell design (Fig. 7.21(a)) involves a number of bipolar, cold-rolled

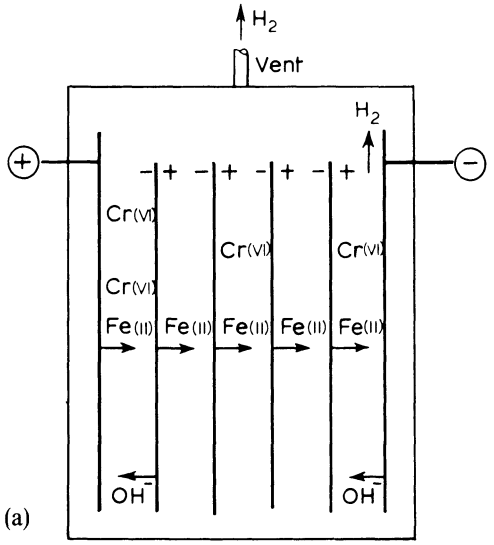

(a)

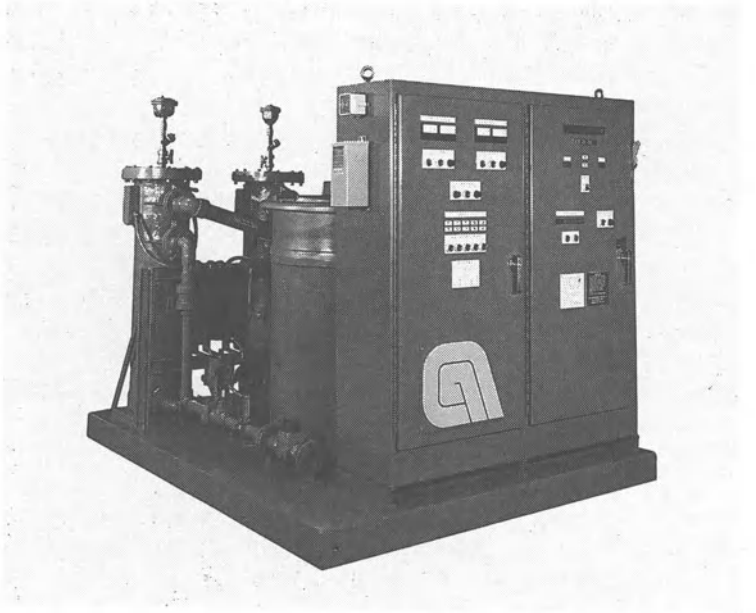

(b)

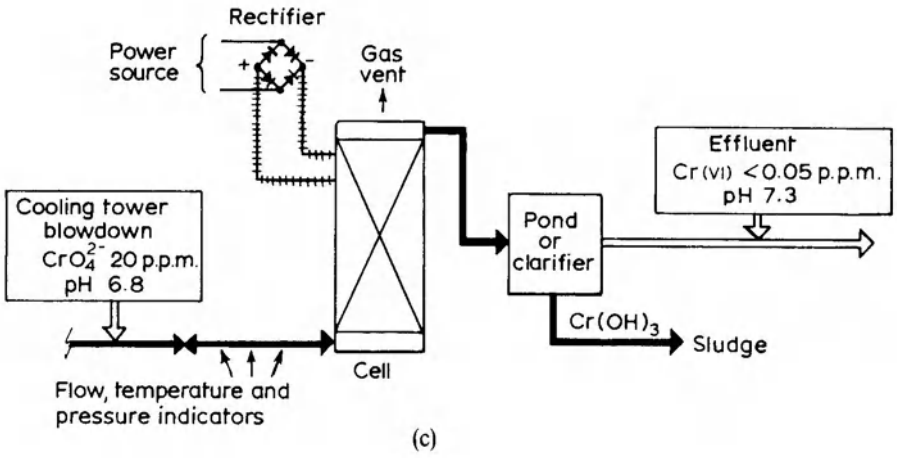

(c)

Fig. 7.21 The removal of chromate and other toxic metal species from cooling water and metal-finishing liquors. (a) The cell concept. (b) A typical automated process plant. (c) A simplified flow diagram for the treatment of cooling water. (Courtesy: Andco Environmental Processes, Inc.)

steel plates, the anodic sides slowly dissolving to form Fe^{2+}. The maximum duty of the cell (according to the above equations) corresponds to reduction of 0.45 kg of Cr(VI) by dissolution of 1.46 kg iron.

In practice, the mixture of ferrous, ferric and chromium hydroxides which precipitates is partly colloidal and gelatinous. Such precipitates, together with other solids, tend to collect on the electrodes, producing an insulating film. To alleviate this problem, intermittent washing with dilute H_2SO_4 may be used. In order to provide a uniform dissolution of the steel electrodes, the cell current may be reversed at regular intervals, e.g. daily. The consumable electrodes are changed at suitable intervals (e.g. once a month) when typically 75% has been consumed.

Following the electrolytic treatment, a pH correction stage may be used to optimize the effluent pH, while suspended solids may be removed by settlement or use of a lagoon clarifier.

The cell currents are relatively small, typically 10–50 A and the power consumption is approximately 11 kWh kg^{-1} of heavy metal removed. It is important to realize that a wide variety of metals may be coprecipitated in this process, providing a versatile treatment method. While the process produces sludge, this is in common with chemical precipitation methods and is often classified as non-hazardous landfill. Moreover, the electrolytic process is convenient, being easily controlled and automated; it is capable of discharging particularly low levels of toxic metals ($\leqslant 1$ mg dm^{-3}) often without pH adjustment. The technique has been developed for both cooling-tower blowdown waters and metal-finishing process streams. Over 100 units have been installed, ranging from 45 to over 7000 dm^3 min^{-1} volumetric flow rate.

As mentioned in Chapter 5, Cr(VI) is added to the sodium chloride electrolyte during sodium chlorate production, in order to improve the current efficiency. Whilst the resulting solid $NaClO_3$ contains only minute traces of Cr(VI), $NaClO_3$ is also marketed as a liquor, which typically contains 600 g dm^{-3} $NaClO_3$, *c.* 100 g dm^{-3} NaCl and *c.* 3–4 g dm^{-3} $Na_2Cr_2O_7$ on exit from the cell. The major markets for this liquor are the pulp and paper producers.

Chemical reducing agents (such as sodium dithionite) has been employed to precipitate chromium ions as $Cr(OH)_3$, but they are relatively expensive and the colloidal $Cr(OH)_3$ is difficult to separate. Recently, an electrolytic process has been developed in which the $Cr(OH)_3$ is formed by direct reduction at a high surface area, three-dimensional, cathode:

$$CrO_4^{2-} + 4H_2O + 3e^- \longrightarrow Cr(OH)_3 + 5OH^- \qquad (7.27)$$

The $Cr(OH)_3$ is effectively removed from solution in the electrode matrix, avoiding filtration. A regeneration step follows in which a suitable reagent (e.g. OCl^-, Cl_2 or HCl) is circulated through the cathode bed under zero current conditions. The $Cr(OH)_3$ is substantially removed from the cathode in the form of a Cr(VI) or Cr(III) liquor which can be recycled to the chlorate cell. The process is shown schematically in Fig. 7.22 and can utilize a variety of 3-dimensional cathode materials including carbon particles, felt or cloth.

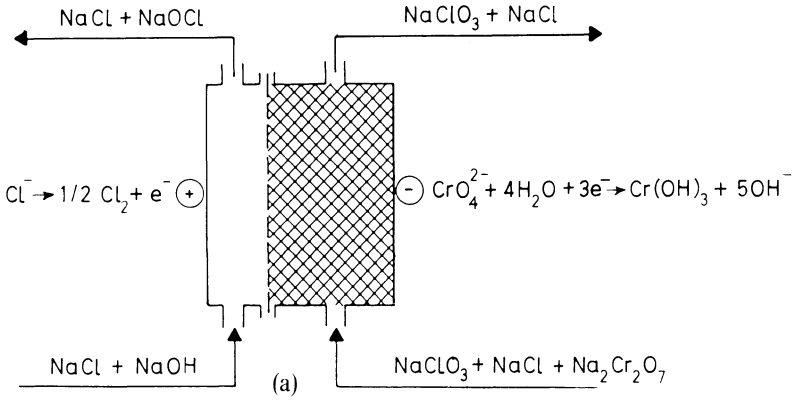

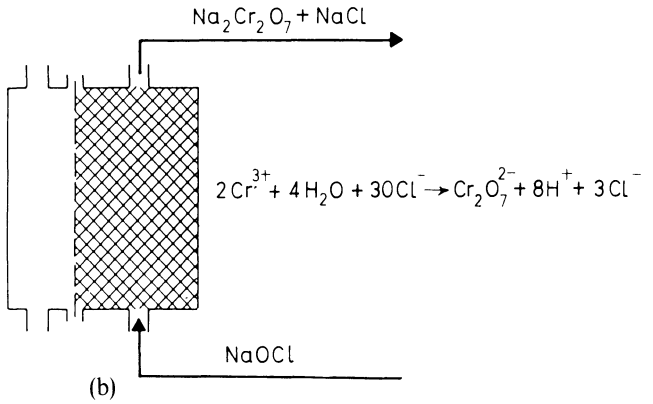

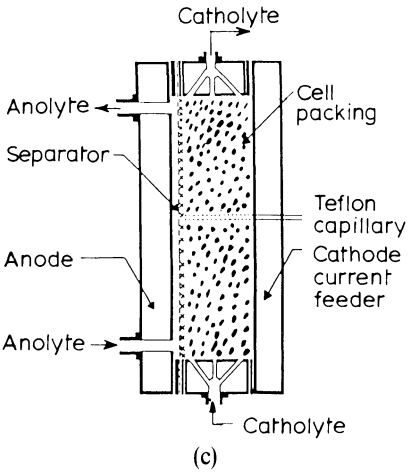

Fig. 7.22 Electrochemical removal of Cr(VI) from chlorate solutions. (a) The electrolytic removal of Cr(VI) as $Cr(OH)_3$. (b) The regeneration of Cr(VI). (c) The development cell. (Courtesy: Albright and Wilson Americas.)

7.5 ELECTROLYTIC METHODS OF PHASE SEPARATION

7.5.1 Electroflotation

A recurrent problem in effluent treatment is the separation of solid suspensions and emulsions or colloidal particles of oil or other organic compounds in water. Such separation is essential to lower the BOD of the effluent to an acceptable level before the water is discharged. Such effluents arise in the oil industry, from engineering, printing and paint workshops, in the food-processing industry, in paper-mills and in fibre and glass manufacture. The traditional approach to the solution of these problems is to allow the effluent to stand in holding tanks until separation into two phases occurs. Such methods can be expensive when large volumes of liquid have to be stored for extended periods of time. Hence, it has become common: (1) to add flocculating agents, commonly highly charged inorganic ions (Al^{3+}, Fe^{3+}), to the mixture; or (2) to use dissolved air flotation. A flocculating agent, however, represents an additional cost and can constitute an environmental hazard, so that its addition requires a reliable dosing procedure; its concentration must be monitored. In method (2), small bubbles of air are allowed to rise through the effluent and float the suspended matter to the surface where it can be removed by a scraper or a paddle into a collection hopper. This method requires a source of compressed air and a well-designed air-sparger to give a uniform supply of very small air bubbles throughout the tank. There are electrochemical versions of both (1) and (2) which are attractive in some circumstances.

In electroflotation, the gases are generated electrolytically in a cell such as that shown schematically in Fig. 7.23. A pair of closely spaced (0.2–2 cm), horizontal-gauze or expanded-metal electrodes are placed towards the base of the tank and

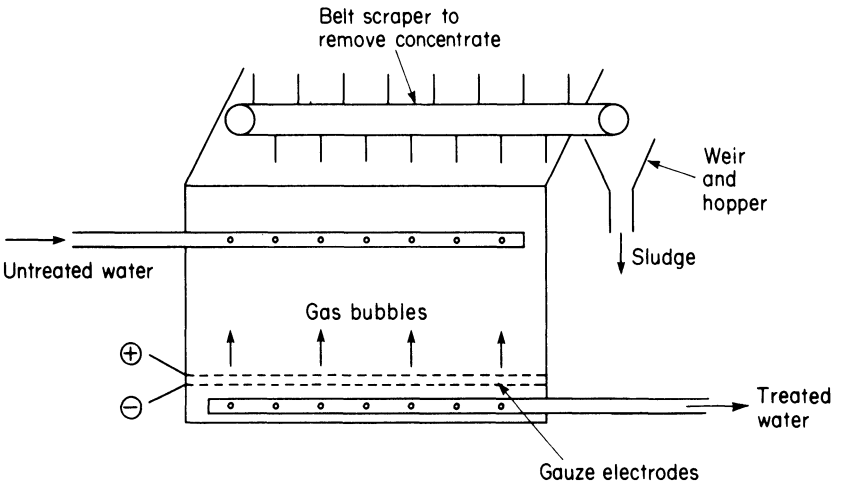

Fig. 7.23 The construction of an electroflotation cell.

cover the whole tank area. The water containing suspended liquid or solid organic particles is flowed slowly (convection should be minimized) into the top of the cell and the gas bubbles rising through the water capture the organic matter and lift it to the surface. The resulting scum, a much more concentrated form of the organic, is skimmed off for disposal and the purified water leaves the base of the tank.

It is generally considered that the mechanism is, as in dissolved air flotation, purely mechanical; as the bubbles of gas rise, they capture the organic particles and carry them upwards. In electroflotation it is also possible that there is an electrostatic contribution to the mechanism. If the gas bubbles leaving the electrodes carry small charges, then they can neutralize the electrical charges known to exist on colloidal particles and cause them to coalesce.

In almost all applications of electroflotation, the cell reaction is simple water electrolysis, so that the gases are oxygen and hydrogen. The size of the gas bubbles is critical in determining the efficiency of the separation process, and this is presumably a function of current density as well as the properties of the effluent and the electrode surfaces. Moreover, a major difficulty in the treatment of some effluents is the deposition of scale on the cathode surface and a consequent increase in the bubble size – the scale arises from the pH increase at the cathode surface leading to precipitation of magnesium and other metal hydroxides. The current density employed is low (0.1–10 mA cm^{-2}) but even then, and despite using a small interelectrode gap, the cell voltage may need to be as high at 5–10 V because the effluents, in general, contain little electrolyte. An overall energy consumption of 0.2–0.4 kWh m^{-3} of water is typical. This can be improved, and at the same time the problem of scaling can be overcome, by dosing the effluent with a low concentration of acid, but this may be undesirable because of the cost and the influence on the environment after disposal.

Electroflotation cells vary in capacity between 1 and 50 m^3, the largest size giving the capability of dealing with up to 150 $m^3 h^-$ of H_2O. In a typical specification, the plant will reduce 1000 mg dm^{-3} solids and 600 mg dm^{-3} oils to 30 and 40 mg dm^{-3} respectively. The components of the cell will be selected mainly for durability and low cost. The tank will be steel or a cheap plastic depending on size; the cathode will be a steel and the anode platinized titanium or lead dioxide on titanium.

Electroflotation is unlikely to challenge air floatation in its larger-scale applications in mineral ore concentration and oil–water separation in the petroleum industry. Moreover, a major disadvantage of an undivided electroflotation cell is the intimate mixing of finely dispersed hydrogen and oxygen. In the possible presence of electrical sparking, this represents a significant fire and explosion hazard.

In electroflocculation or electrocoagulation, the flocculating agent is introduced as a result of an electrode reaction and such processes permit a careful control of the amount of the reagent introduced into the effluent. Thus, for example, Al^{3+} or Fe^{3+} can be introduced by using an aluminium or iron anode and it is

also possible to use such an anode in an electroflotation cell. Also, magnesium hydroxide, or even hydroxide ion produced at the cathode of chlorine or hypochlorite cells, can act as flocculating agents, again allowing the combination of coagulation with chlorination.

7.5.2 Electrophoretic separation of biochemicals

The electrophoretic deposition of organic paints onto steel is considered in Chapter 8. A much smaller-scale ($\leqslant 100$ A) use of electrophoresis is the separation of biochemical species from natural sources including body fluids (such as blood plasma or muscle tissue extract).

Electrophoresis also provides a useful technique in biosynthesis for protein and enzyme purification and production.

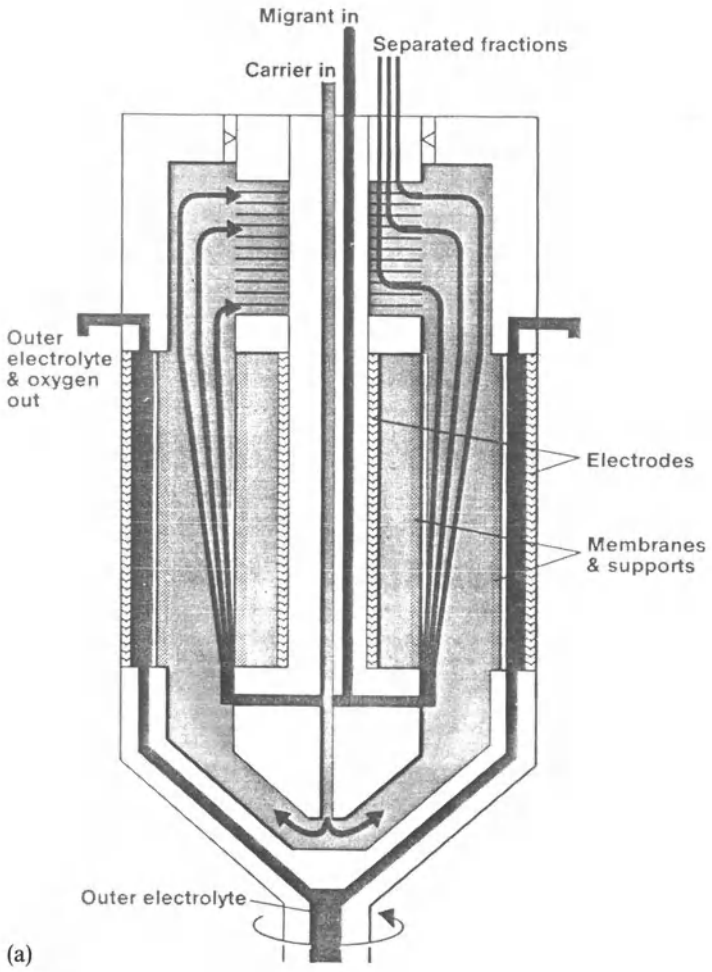

The majority of electrophoresis units are operated batchwise, on a small bench-top scale (0.1–1.0 A) involving gelled electrolytes, which minimize disruption of the separating species due to natural convective mixing. Such mixing may occur even in a static system as thermal gradients (set up by Joule heating in the electrolyte) and may give rise to significant thermal motion.

Recently, a device has been introduced for continuous electrophoretic separation of biochemicals in free solution. In order to prevent mixing of separated fractions, laminar-flow conditions are maintained using flow through the annulus of a divided, concentric cylinder geometry, the outer cylinder being rotated (typically at 150 revs/min) (Fig. 7.24(b)). The use of a buffered free solution permits the processing of suspensions, a wider range of fluids and reduces work-up compared to gel electrophoresis.



(b)

Fig. 7.24 (a) The principle of the Biostream process for continuous electrophoretic separation of proteins. (Courtesy: Harwell Laboratory, UK Atomic Energy Authority.) (b) The Biostream continuous electrophoretic separator showing the outer rotating-cylinder electrode unit and the arrangement for sample collection. (Courtesy: CJB Developments Ltd.)

The structure of this 'Biostream' electrophoretic separator is shown in Fig. 7.24(a) while Table 7.5 indicates typical conditions.

Electrophoresis take place in an annulus (typically 3 mm wide) between the inner and outer cylinders of the separator. A buffer electrolyte (the carrier solution) flows upward through the annulus. Stable laminar flow of the carrier solution is maintained by rotation of the outer cylinder (rotor). This overcomes the problem of convective turbulence which would otherwise be caused by resistive heating. The inner cylinder (stator) is held stationary.

Concentric with the annulus are compartments formed in the rotor and stator which contain the electrodes (stainless steel) and their electrolytes. These are isolated from the carrier solution by dialysis membranes of regenerated cellulose which are supported on inert porous tubes. An electric field is applied across the electrodes, typically 30 V at 60 A.

The mixture to be fractionated (the migrant) is injected into the carrier solution through a thin slot around the base of the stator. The components of the migrant mixture separate under the force of the electric field by moving at different rates towards the outer wall of the annulus. They thus form concentric bands within the annulus.

At the top of the stator is an assembly of discs (maze plates). Each pair of maze plates form at their edge a thin circumferential slot through which a layer of solution flows into a maze of channels precisely formed in each disc. The maze of channels ensures that the flow of solution through the slot is uniform and also guides the solution to a single collection point. Up to thirty maze plates are used and provide for the electrophoresis solution to be divided into as many fractions without remixing.

Table 7.5 Typical conditions for the BIOSTREAM electrophoretic separator

Nominal throughput	100 g h^{-1} protein or 10^{12} cells h^{-1}
Carrier electrolyte flow	2 dm^3 min^{-1}
Anolyte flow	0.1 dm^3 min^{-1}
Catholyte flow	0.1 dm^3 min^{-1}
Migrant flow	< 3 dm^3 h^{-1}
Migrant concentration	< 50 g dm^{-3} protein
Rotor speed	130–160 rev min^{-1}
Cell voltage	$\leqslant -40$ V
Cell current	$\leqslant 100$ A
Temperature increase in the carrier	0–25° C
Diaphragm material	for example, synthetic cellulose tube
Carrier electrolytes	ammonium acetate (pH 9.6–11.5) tris citrate (pH 7–9) tris acetate (pH 4–6) or ammonium formate (pH > 3)

Applications of the device include fractionation of blood plasma, isolation of enzymes from muscle extracts and the separation and concentration of platelet cells from red blood.

7.6 FLUE-GAS DESULPHURIZATION

One of the major atmospheric pollutants is sulphur dioxide, which is released during combustion of sulphur-containing fuels, particularly at coal- and oil-fired power stations. Sulphur dioxide has been associated with 'acid rain' which attacks building materials, steelwork and possibly woodland. It is obviously important to substantially remove sulphur dioxide from flue gases prior to discharge.

Traditional treatment has largely involved treatment with lime, producing gypsum. Unfortunately, such a process involves large quantities of both chemicals which then require disposal; a considerable amount of waste water is also produced.

Following research under the European Economic Community's hydrogen programme (1977–1980), a more attractive treatment technique, the 'ISPRA Mark XIII A' process, has been developed. This process (Fig. 7.25) involves removal of SO_2 via reaction with bromine in the solution phase:

$$SO_2 + Br_2 + 2H_2O \longrightarrow H_2SO_4 + 2HBr \qquad (7.28)$$

The bromine is generated from hydrobromic acid via electrolysis:

$$2HBr \longrightarrow H_2 + Br_2 \qquad (7.29)$$

The overall result of the process is conversion of sulphur dioxide and water into concentrated sulphuric acid and hydrogen, these products having market value. The intermediate, bromine, is completely recycled.

Figure 7.25 shows a simplified flow diagram of the process. Flue gas containing SO_2 is contacted at 50–70° C with a concurrent stream of 10–20% wt H_2SO_4 and 10–20% wt HBr plus 0.3–0.9% wt Br_2. The SO_2 is absorbed and rapidly converted into H_2SO_4 (reaction 7.26). The Br_2 should be completely converted in this step. Bromine is generated as a 1–2% wt solution, together with hydrogen by electrolysis of part of the main HBr stream (reaction 7.29).

The outlet solution from the electrolysis cell is mixed with the main reactor circulation stream and pumped to the top of the reactor where reaction (7.28) occurs. During pilot-plant studies, electrolytic hydrogen was simply vented-off for safety; in larger plants, it will be considered as a by-product.

The desulphurized flue gas exits from the bottom of the reactor and droplet separator, still containing some reactor liquid and HBr vapour. These species are removed by water scrubbing and returned to the reactor. The water inventory is maintained either by condensing water vapour from the flue gas or by fresh additions of water.

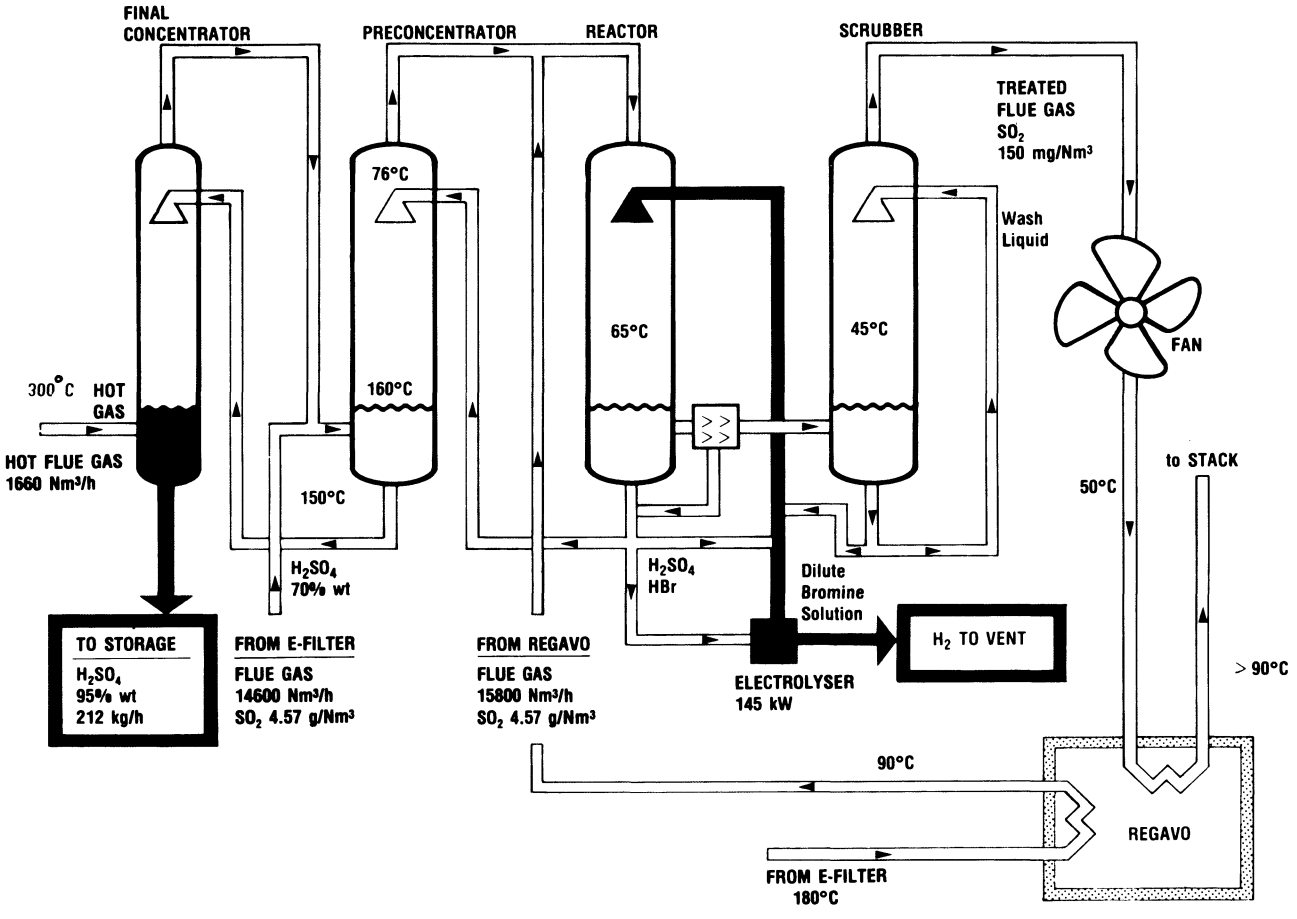

Fig. 7.25 The ISPRA Mk XIIIA pilot plant flue-gas desulphurization process at the Saras refinery, Sardinia. (Courtesy: Centro Commune di Ricerca, ISPRA.)

The sulphuric acid produced in the reactor is bled to a pre-concentrator where the majority of the water and all of the HBr are evaporated by the hot (110–150° C) flue gas which enters the reactor.

Further water removal from the acid is accomplished by a small stream of hot gas in the final concentrator, improving the concentration of the acid.

Fly ash in the flue gas largely ends up in the H_2SO_4 product. However, the amount is minimized by passing the flue gas through a dust-filter. The sulphuric acid produced is then suitable for use in the fertilizer industry. Following successful feasibility trials, a large pilot-plant facility is now being built in Sarroch, Sardinia, where flue gases with a minimum SO_2 content of 0.16% vol are treated. The design capacity of this plant is 32 000 $m^3\,h^{-1}$ flue gas with SO_2 levels up to 4.5 mg dm^{-3}, the degree of desulphurization being $\geqslant$ 90%.

Hydrobromic acid electrolysis is carried out in two different separate reactors supplied by different companies and run in parallel. Both reactors use undivided, vertical, parallel-electrode cells.

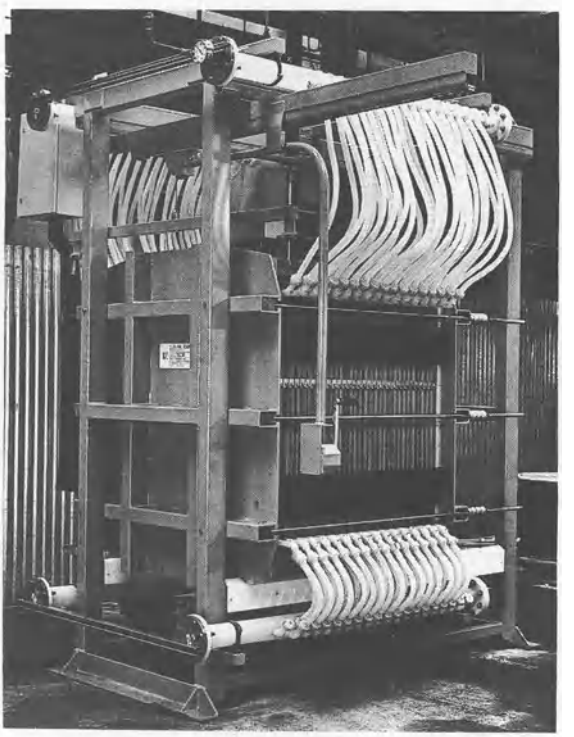

Fig. 7.26 A dished-electrode cell stack for use in flue-gas desulphurization. Each cell is undivided and the stack contains 34 cathodes, each of 1 m^2. The electrical connections are monopolar with external electrolyte manifolding to each compartment. (Courtesy: Steetley Engineering Ltd.) (Note: The Dished-Electrode Membrane cell has recently been acquired by Electrocatalytic Ltd.)

One of the reactors uses the dished electrode membrane concept (section 2.7.3) (Fig. 7.26). It employs thirty-four cathodes, each 1 m^2 in area and fabricated from Hastelloy C276; the plate anodes are DSA (RuO_2/TiO_2)-coated titanium. The other reactor is a Deutsche Carbone cell, which utilizes graphite anodes and cathodes.

Both types of cell have already undergone extensive laboratory trials. Typical operating conditions are: temperature 50° C; electrolyte composition, 15% wt HBr, 15% wt H_2SO_4; linear electrolyte velocity, 5 cm s^{-1}; current density, 200 mA cm^{-2}; cell voltage, −1.3 V; and current efficiency, 90%.

The large pilot-plant electrochemical reactors will each produce 169 kg h^{-1} Br_2 (as a 1–2% wt solution) at a total cell current of 64 kA. According to this data, the electrolysis section of the ISPRA Mark XIIIA plant will probably be the largest-scale example of HBr electrolysis.

7.7 OTHER ELECTROCHEMICAL PROCESSES

Many other applications of electrochemistry in pollution have been proposed and some of the more likely will be discussed briefly in this section.

The use of electrolysis for precise dosing has already been mentioned in Section 7.6; a major advantage is the ability to vary the dosing rate rapidly by controlling the current in the cell. This can be achieved in a particularly elegant manner if a minicomputer is used to control a system combining, with the electrolysis cell, a fast-response monitor to determine the dosing level required. An example is the control of effluent pH – a glass electrode may be used to determine pH and a divided cell used to introduce OH^- or H^+ by water electrolysis. An application might be in the chlor-alkali industry for readjusting the pH of the brine leaving the main cells from pH 4 to pH 7. The use of an inert (e.g. platinum) electrode to monitor the redox potential of etchant solutions (and, hence, the state of regeneration) is mentioned in Chapter 9.

Anodic oxidation has long been discussed as a method of removing organic molecules from effluents. In most cases this is quite impracticable because the complete oxidation of organic species to carbon dioxide is not a facile reaction; it only takes place for some species and only at a low rate in special conditions, e.g. at a platinized platinum electrode in concentrated acid or alkali at 80° C. Such conditions are clearly unsuitable for pollution control where it would be inappropriate to use large quantities of reagents, energy for heating or expensive electrodes. Moreover, complete oxidation of large molecules requires the transfer of many electrons and inevitably a high energy consumption. Occasionally, however, a small transformation of molecular structure leads to a large reduction of toxicity, or complete oxidation is possible at a high-surface-area carbon or the species to be removed is an inorganic molecule requiring a $1e^-$ or $2e^-$ oxidation. Then anodic oxidation seems more feasible. Reversible electrochemical adsorption has also been considered as a method of removing large organic molecules;

the electrode potential could be held at a value where the molecule adsorbs and periodically the electrode would be cleaned by changing the potential to a different region where the molecule desorbs. This would then only be a concentration procedure but it would consume little power. Indirect oxidation by an electrogenerated oxidant seems a more promising technique, e.g. while direct oxidation of cyanide ion is possible, the process is catalysed by the presence of chloride ion and most practical devices involve the intermediate formation of chlorine or hypochlorite (section 7.2). While chlorine and hypochlorite are, at the present time, very widely used, there is some concern that they may themselves lead to toxic, chlorinated species in the environment. Hence, there is interest in alternative oxidizing agents such as hydrogen peroxide and ozone; both can be prepared on site in small electrolyzers, hydrogen peroxide by oxygen reduction or via the persulphate route, and ozone by oxidation of acidic water at low temperature (Chapter 5). These are active research areas at the present time and commercial devices are now available.

Methods for the removal of low concentrations of species from effluent which involve either oxidation or adsorption will clearly require a cheap but high-surface-area electrode structure, and several particulate carbon and carbon fibre electrode cells have been described. The latter are prepared from 5–15 μm diameter carbon which has a specific area of 260 $m^{-3}\,g^{-1}$ and, hence, permits a high throughput of effluent. Such a cell has been used for treatment of paper-mill effluent and a 70% reduction of BOD with a 95% removal of highly toxic chlorinated phenols has been claimed.

The treatment of waste streams containing halogenated organics is receiving increasing attention, due to the persistent and toxic nature of many of these compounds. Electrochemical methods of dehalogenation have been developed and show promise in the particular case of waters containing polar or ionic compounds. One approach is to reduce the dilute halogenated compound:

$$R-Cl + H^+ + 2e^- \longrightarrow R-H + Cl^- \qquad (7.30)$$

Unfortunately, the cathode potential required is usually rather negative, substantial hydrogen evolution occurring as a secondary reaction and suspended particles may clog or foul the electrode. For these reasons, a cheap high-surface area, carbon electrode is a preferred choice, carbon fibre being especially suitable.

As an example of the technique, we may consider the reduction of pentachlorophenol (PCP). The reactor consisted of two compartments, each 10 cm long, 2 cm wide and 0.5 cm deep, the cathode being a packed bed of carbon fibre, which was separated from the anode by a cation-exchange membrane (Nafion 426). In the batch-recycle mode, constant current (10 A) electrolysis of 1 dm^3 of 50 mg dm^{-3} PCP in 0.1 mol dm^{-3} Na_2SO_4 plus 0.1 mol dm^{-3} NaOH removed PCP to a level < 0.5 mg dm^{-3} within 30 min. The overall current efficiency for complete dechlorination was approximately 1%, the energy consumption being 36 kWh m^{-3}.

FURTHER READING

1 C. F. Simpson and M. Whittaker (Eds) (1983) *Electrophoretic Techniques*, Academic Press, London.
2 D. van Velzen (1988) in H. Wendt (Ed.) *Electrochemical Techniques for the Production and Combustion of Hydrogen*, (Chapter 5), Elsevier, Amsterdam.
3 J. O'M Bockris (Ed.) (1972) *Electrochemistry of Cleaner Environments*, Plenum Press, New York.
4 P. Meares (Ed.) (1976) *Membrane Separation Processes*, Elsevier, Amsterdam.
5 A. T. Kuhn (Ed.) (1971) *Industrial Electrochemical Processes*, Elsevier, Amsterdam.
6 R. J. Marshall and F. C. Walsh (1985) *A Review of Some Recent Electrolytic Cell Designs, Surface Technol.*, **24**, 45.
7 D. S. Flett (Ed.) (1983) *Ion-exchange Membranes*, Ellis Horwood, Chichester.

8 Metal finishing

Metal finishing is the name given to a wide range of processes carried out in order to modify the surface properties of a metal, e.g. by the deposition of a layer of another metal or a polymer, or by formation of an oxide film. The origins of the industry lay in the desire to enhance the value of metal articles by improving their appearance, but in modern times the importance of metal finishing for purely decorative reasons has decreased. The trend is now towards surface treatments which will impart corrosion resistance or particular physical or mechanical properties to the surface (e.g. electrical conductivity, heat or wear resistance, lubrication or solderability) and, hence, to make possible the use of cheaper substrate metals or plastics covered to give them essential metallic surface properties.

A large fraction of the metal objects which we see in everyday life (e.g. car components, kitchen utensils, cans for food, screws and metal window frames) have undergone a metal-finishing process. Moreover, similar processes are an essential part of modern engineering and of the manufacture of electronic components, e.g. printed circuit boards, capacitors and contacts. As a result, the practice of metal finishing extends to many electronics, engineering and metal-processing companies as well as to both large and small specialist firms, resulting in a particularly diverse industry. In general, however, the industry tends to be labour-intensive and dependent on personal experience; the majority of processes have developed empirically and operator skill is often paramount. It should be emphasized that not all surface finishing is carried out using electrochemical methods, but electroplating, anodizing and other conversion-coating processes, together with electrophoretic painting, represent a large portion of the industry.

This chapter will consider five techniques: (1) electroplating metals, alloys and composites; (2) electroless plating of metals, alloys and composites; (3) immersion plating of metals; (4) chemical conversion coatings based on metal compounds; and (5) electrophoretic painting.

8.1 ELECTROPLATING

Electroplating is a very widely used and diverse technology. In principle, the choice of substrate and coating metals may encompass a large number of single metals and alloys; in fact, the substrate may also be a polymer, a ceramic or a composite. The coating may be a single metal, an alloy or, indeed, a metal–polymer or metal–ceramic composite. In practice, the choice is restricted severely by the technical constraints, the possibilities for electrodeposition and the desired deposit properties as well as economic factors. An obvious trend may be noted towards the use of relatively cheap substrates as bulk constructional materials. The more expensive metals are usually encountered as thin coatings. Intermediate metals, such as nickel, may be used either as substrates or coatings. It is noteworthy that aluminium-coated steel would offer a formidable combination of properties, but the development of electroplated aluminium surfaces is severely restricted by the need to utilize fused salts or non-aqueous solvents as electrolytes.

8.1.1 Fundamentals of electroplating

The objective of an electroplating process is to prepare a deposit which adheres well to the substrate and which has the required mechanical, chemical and physical properties (section 8.1.5). Moreover, it is of overriding importance that the deposit properties meet their specification on all occasions, i.e. the process is both predictable and reproducible. On the other hand, many metals may (by modification of the bath and plating conditions) be deposited with different properties. It is for this reason that it is not possible to define a single set of conditions for electroplating each metal; the bath, current density, temperature, etc. will depend to some extent on the deposit properties required.

It is important that the plating bath is stable for a long period of time because of the importance of reproducibility of the deposit. It is also necessary that the quality of deposit is maintained over a range of operating conditions, since some variations in concentrations and current density are bound to occur, particularly when different objects are to be plated. Tolerance of the bath to carry over from previous process liquors or mishandling during operation on the factory floor is an additional advantage.

The principle components of an electroplating process are shown schematically in Fig. 8.1. The essential components include:

1. An electroplating bath containing a conducting salt and the metal to be plated in a soluble form, as well as perhaps a buffer and additives.
2. The electronically conducting cathode, i.e. the workpiece to be plated.
3. The anode (also electronically conducting) which may be soluble or insoluble.
4. An inert vessel to contain (1) → (3), typically, e.g. steel, rubber-lined steel, polypropylene or polyvinylchloride.
5. A d.c. electrical power source, usually a regulated transformer/rectifier.

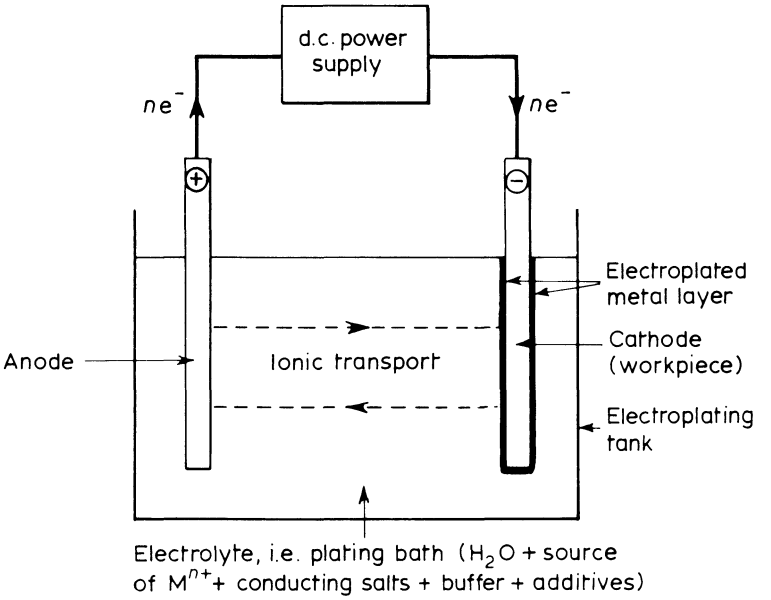

Fig. 8.1 Principle of electroplating.

Electroplating is the process of electrolytically depositing a layer of metal onto a surface. The object to be plated is made the cathode in an electrolyte bath containing a metal ion M^{n+} so that the simplest reaction at the cathode is:

$$M^{n+} + ne^- \longrightarrow M \tag{8.1}$$

In the general case, M^{n+} may be a simple aquo ion such as hydrated Cu^{2+} or it may represent a metal complex such as $[Au(CN)_2]^-$.

Where possible, the preferred anode reaction is the dissolution of the same metal to its precursor in solution.

$$M - ne^- \longrightarrow M^{n+} \tag{8.2}$$

and, ideally, the electrolysis conditions are controlled in such a way that the current efficiencies of reactions (8.1) and (8.2) are the same and, hence, the concentration of M^{n+} in the bath remains constant. In a few cases, the metal ion has to be added as a solid salt and then an inert anode† is employed; the main anode reaction is oxygen evolution.

For a successful electroplating process, the correct pretreatment of the cathode and careful selection of the anode material, plating bath, current density and

† The choice of insoluble anode is very dependent upon the process, e.g. platinized titanium is sometimes used in acid electrolytes, while stainless steel is stable in certain alkaline solutions.

other electrolysis conditions, are essential. All these factors will be discussed below.

The following types of layer may be electroplated:

1. *Single metals*: the most important are Sn, Cu, Ni, Cr, Zn, Cd, Pb, Ag, Au and Pt.
2. *Alloys*: including Cu–Zn, Cu–Sn, Pb–Sn, Sn–Ni, Ni–Co, Ni–Cr and Ni–Fe.
3. *Composites*: i.e. metals containing dispersed solids such as PTFE, Al_2O_3, WC, diamond, SiC, Cr_3C_2 and graphite.

The mass of electroplated metal w may be expressed in terms of Faraday's laws of electrolysis as follows

$$w = \frac{\phi M q}{nF} \tag{8.3}$$

where M is the molar mass of metal, q is the electrical charge and ϕ ($\leqslant 1$) is the cathode current efficiency for metal deposition. The majority of electroplating processes are carried out batchwise, at a constant current density I for a measured time t. The averaged rate of mass deposition per unit area is then given by:

$$\frac{w}{At} = \frac{\phi I M}{nF} \tag{8.4}$$

where the factor M/nF is traditionally called the 'electrochemical equivalent'. This expression can also be written in terms of the useful current density.

$$\frac{w}{At} = \frac{I_M M}{nF} \tag{8.5}$$

Thus, the rate of deposition depends upon the molar mass of the metal M, the number of electrons n per mole of M^{n+} and the prevailing current efficiency ϕ. For some metals, choice of different soluble metal species gives a choice of n, e.g. in the case of copper solutions, in an uncomplexed acid solution, the copper is present as the cupric ion:

$$Cu^{2+} + 2e^- \longrightarrow Cu \tag{8.6}$$

while in alkaline cyanide liquors it is present as a copper (I) complex:

$$[Cu(CN)_2]^- + e^- \longrightarrow Cu + 2CN^- \tag{8.7}$$

Obviously, the choice of a low oxidation state source of metal provides a higher deposition rate for a given useful current (or alternatively a given deposition rate can be achieved at a lower current).

The current efficiency depends greatly upon the actual process. The majority

of electroplating baths operate in the range $0.9 < \phi < 1$. Chromium deposition from chromic acid is an important exception, yielding very low values, typically $0.05 < \phi < 0.20$. The most common secondary reaction at the cathode is hydrogen evolution (which may present a safety hazard via spray/mist formation or the build-up of explosive gas mixtures). The averaged rate of deposition may be estimated on a thickness x basis by a consideration of equation (8.4) and assumption (or measurement) of a mass density ρ value for the plated metal:

$$x/t = \frac{\phi iM}{\rho AnF} = \frac{\phi IM}{\rho nF} \tag{8.8}$$

The quality of an electroplated finish is dependent upon a wide range of process variables, including electrolyte composition and purity, addition agent level, pH, temperature, current density, electrode–anode–cell geometry and flow conditions. Thus, quality-control procedures must consider the track record of both the electrolyte and the deposit. One of the most important parameters is the acceptable or optimum current density range; in this range, the electroplated layer must show satisfactory properties such as brightness, freedom from rough deposits, uniform texture, etc. In order to assess the behaviour of a plating bath, comparative tests may be made in a number of available test cells, the Hull cell (Fig. 8.2) being the most common.

The inclined cathode of the Hull cell enables a controlled variation of the current density over the cathode surface to be achieved in a single experiment. Typically, a constant cell current in the range 2 to 5 A is used; for chromium plating or high-speed processes, 10 A may be preferred. A nomogram is often used to estimate the local current density I_x, which varies with the distance x along the cathode (measured from the end nearest the anode) in the following manner:†

$$I_x = 10i(a - b \log_{10} x) \tag{8.9}$$

where a and b are constants depending on the cell size.

With an applied current of 2 A, the variation in cathode current density is from approximately 2.5 to 85 mA cm^{-2} which covers the working range of most electroplating baths. The Hull cell is also useful as an empirical development tool, e.g. for rapid screening tests on addition agents. The fundamental cell has been modified, for special purposes, in numerous ways, e.g. a bottomless cell may

† In the case of the 267 cm^3 cell, equation (8.9) takes the empirical form:

$$I_x = 10i(5.1 - 5.24 \log_{10} x)$$

where i is in A, x is in cm and I_x is in mA cm^{-2}

R.O. Hull (1939) *Proc. Amer. Electropl. Soc.*, **27**, 52.

H. M. Heiling (1956) 'Die Hullzelle', *Jahr. Oberflaechentech.*, **12**, 805.

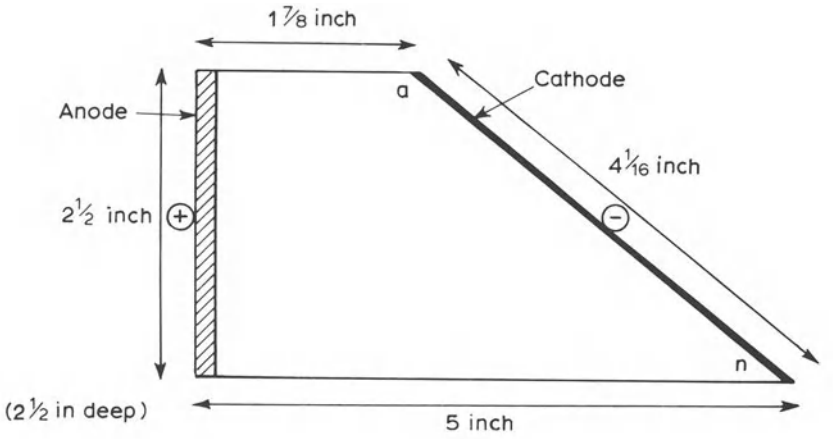

(a)

Applied current /A	Current density/A dm^{-2}													
	Position of Hull cell panel													
	a	b	c	d	e	f	g	h	i	j	k	l	m	n
1	5	4	3	2	1.5	1.25	1	0.75	0.5	0.4	0.3	0.2	0.1	0.05
2	10	8	6	4	3	2.5	2	1.5	1	0.8	0.6	0.4	0.2	0.1
3	15	12	9	6	4.5	3.75	3	2.25	1.5	1.2	0.9	0.6	0.3	0.15
5	25	20	15	10	7.5	6.25	5	3.75	2.5	2.0	1.5	1.0	0.5	0.25

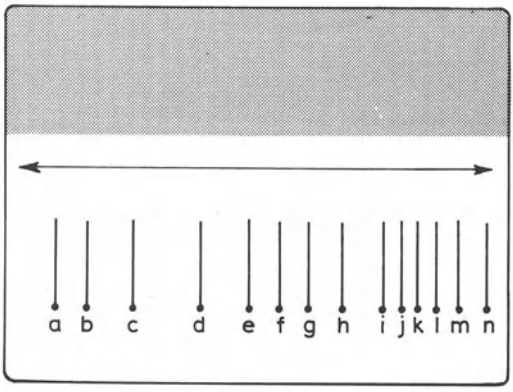

(b)

Fig. 8.2 The Hull cell. Various standard sizes are available, a common version being the 267 cm^3 cell; a 2 g addition of chemicals corresponds to 1 oz/US gallon in the process bath. (a) Plan view showing the internal dimensions of the American version. (b) Current density ranges along the cathode.

be immersed directly into the plating tank, or the cathode may be segmented to facilitate d.c. density-distribution measurements. In practice, the device is normally used on a laboratory bench with a simple magnetic stirrer or air agitation. The Hull cell is perhaps best utilized empirically as a simple tool allowing comparative checks to be made on plating baths in order to aid process control (e.g. additive replenishment) and troubleshooting operations.

In practical electroplating systems, it is clearly desirable that the deposit should have an even thickness over the whole of the surface to be electroplated. This requires the potential to be the same at all points over the surface of the cathode; this is impossible to attain when the object has a complex shape. To some extent the evenness of the deposit can be improved by introducing auxiliary anodes (usually platinized titanium electrodes where the reaction is oxygen evolution) at various positions in the electrolyte, the objective being to increase the cathode current density at points where it would otherwise be very low (i.e. at points on the cathode furthest from the normal anodes, e.g. in holes or recesses in the object being plated). Areas prone to excess deposition or high current density 'burning' may be treated by the use of auxiliary, dummy cathodes ('robbers' or 'burners') or the use of current shields to increase the solution path between anode and cathode. This approach is still limited, being very dependent on the skill and experience of the operator, involving a specific exercise for a particular workpiece–plating bath combination. Hence, in general, we are dependent on the properties of the plating bath to give a good, even deposit of metal. The ability of a plating bath to give an even deposit is measured by its throwing power which may be determined in the Haring–Blum cell (Fig. 8.3). Two cathodes are placed at markedly different distances from a single anode and electroplating is carried out. The weight of metal plated on the two cathodes w_1 and w_2 and the thickness of electroplate on them, x_1 and x_2 will be different because the iR drops in the two electrode gaps are not the same; electrode 1 must be a lower overpotential and, hence, less metal will deposit at this cathode. Several formulae have been

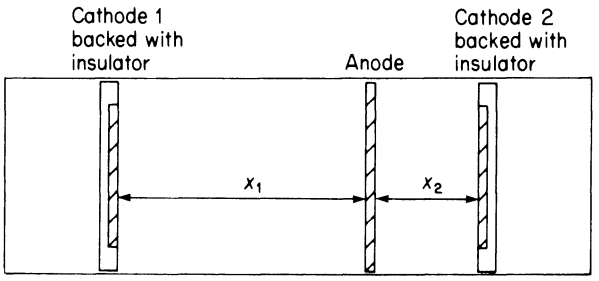

Fig. 8.3 The Haring–Blum cell for the determination of the throwing power of a plating bath (plan view).

used to express throwing power but that proposed by Field has some general acceptance†. The Field* formula is:

$$\% \text{ throwing power} = \frac{100(K-B)}{K+B-2} \tag{8.10}$$

where $K = x_1/x_2$ and $B = w_2/w_1$. This equation is designed to give throwing powers between $+100$ (very good) and -100 (very poor). If the cathodes both have a current efficiency near 100%, the deposit weights, w_1 and w_2, may be replaced conveniently by the corresponding currents to each cathode, i_1 and i_2.

Factors which determine the throwing power of an electroplating bath include:

1. *Conductivity of the electrolyte*: a high conductivity will minimize the iR drops in the bath which cause differences in potential over a complex cathode surface and therefore cause the rate of deposition to be more uniform at a given temperature and dissolved-metal concentration.
2. *The Tafel slope for the deposition reaction*: it will be seen from the curves in Fig. 8.4(a) that for any variation of potential the difference in deposition rate will be smaller when the Tafel slope is high (curve (ii)). Experimentally it is generally found that Tafel slopes are higher when complexing agents and additives, which adsorb on the cathode, are present in solution. Some additives known as 'levellers' and 'brighteners' have the role of ensuring an even deposit on a microscale; their mode of action will be discussed later.
3. *Competing electrode reactions*: although gas evolution may be a problem (Chapter 2) the throwing power may be enhanced by the occurrence of side reactions, e.g. hydrogen evolution. In the situation shown in Fig. 8.4(b), hydrogen evolution will occur only at points on the surface where the potential is high. The current for hydrogen evolution will then contribute to the iR drop without leading to metal deposition. Hence, it causes a reduction in the local overpotential, and leads to a more even deposit.

It can be seen that the main process parameters which affect the throwing power are the composition of the plating bath (i.e. total electrolyte concentration, complexing agents, pH, additives), temperature and current density.

From the viewpoint of energy efficiency, it is attractive for the electrodeposition process to have a high current efficiency and the plating cell to be designed to have a low anode–cathode voltage. In practice, the energy used in the electrolysis itself is commonly low compared with that required to heat the bath and to prepare the surface prior to plating. Moreover, the charge consumed

* S. Field, *Metal Ind.* (London) 1934, **44**, 614.

† A useful alternative formula due to D. A. Luke (*Trans. Inst. Metal Finish*, **61**, 64, (1983)) gives throwing power values in the range 0 to 100% and when $K = B$, the throwing power approaches 50% for reasonably high K values:

$$\% \text{ throwing power} = \frac{100\,K}{K+B-1}$$

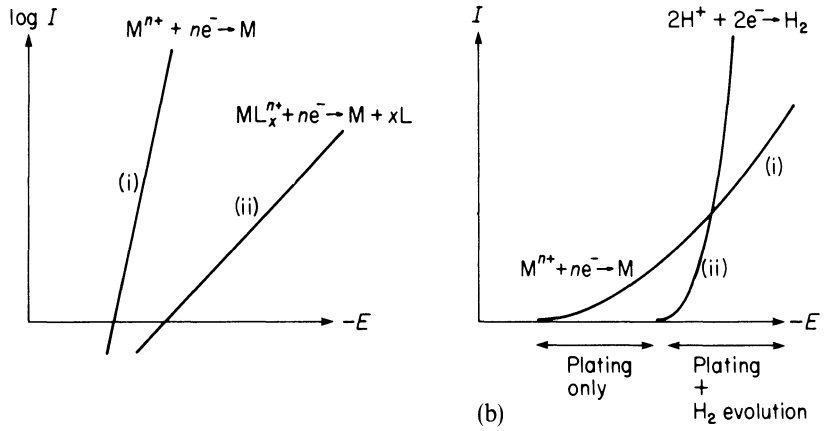

Fig. 8.4 (a) Tafel plots showing the common effects of the addition of a complexing agent to a plating bath on the reduction of the metal ion. (b) *I–E* plots for a metal ion and proton reduction in a plating bath.

during plating is low (1–10 C cm^{-2} for a 10 μm layer) and the value added during the process may be very high. Hence, energy efficiency is not as important as in the large-scale electrolytic processes and this (together with convenience in processing and versatility) accounts for the relatively simple cells employed.

It should be noted that the major requirement of any electroplating plant is that satisfactory deposit quality should be achieved, with due regard for costs and convenience in processing.

It is, of course, unavoidable that electroplating processes employ solutions containing high concentrations of heavy-metal and transition-metal ions. There is, however, an increasing awareness that the environment must be protected and that particularly toxic solutions should be avoided. Thus, all large electroplating facilities will have a plant for the removal of metal ions and other toxic species from effluent water before it is discharged. Moreover, the trend is towards recovery of the metal in a useful form (Chapter 7) and it is a long-term aim of the industry to employ plating baths which avoid the most toxic chemicals such as chromium (VI), cadmium metal and cyanide ion; some concern is also expressed about the toxicity of certain of the organic additives used to improve the product quality.

8.1.2 The mechanism of electrodeposition of metals

In discussing the mechanism by which an electroplate is formed, it must first be recognized that the deposition process has two distinct phases. At the start of the plating process, the deposition of the metal will occur on an electrode surface of a different material, that of the object to be plated. Hence, the first step will be the formation of nuclei of the new phase and their growth into crystals with the characteristic lattice of the electroplating metal. Then, once the electrode is fully covered by a few atomic layers of this metal, one is dealing with a M/M^{n+}

electrode and the thickening of the layer into a macroscopic deposit. In terms of time or charge, the plating process consists almost entirely of the latter process, but the initial stages are also important, since they determine the structure of the primary layer (such factors as the shape and number of growing crystallites) and thereby influence adhesion together with the structure of the final electroplate and its properties.

Nucleation and the early stages of phase growth were mentioned briefly in Chapter 1. It may be noted that nucleation is always an improbable event and is achieved at an electrode surface by the application of a large overpotential. The density of nucleation is dependent on the plating bath and is extremely sensitive to the electrode potential (therefore also, of course, the current density). The nuclei, once formed, grow quite rapidly at comparatively low overpotentials, and in a constant-current situation the potential will decrease substantially once nucleation has occurred.

The growth of the crystals occurs by incorporation of the individual metal atoms into the crystal lattice. The newly incorporated metal atom is only likely to be stable when it enters the lattice at a site where it interacts with several other atoms already in the lattice. Of the sites which are possible in a perfect crystal lattice (Fig. 8.5), incorporation will be most favourable at a kink site (where the atom can interact with three neighbours) although some incorporation will also take place at edge sites (two neighbours); adatoms (one neighbour) are likely to diffuse to more favourable sites or to redissolve, although a very small number will expand into new nuclei. Clearly, the overall phase growth is a sequence of at least three steps:

1. Mass transport in solution (this may be diffusion, convection or migration) of the metal-bearing species to the electrode surface.
2. Electron transfer to form an adatom.
3. Diffusion of the adatom across the surface into a position in the lattice.

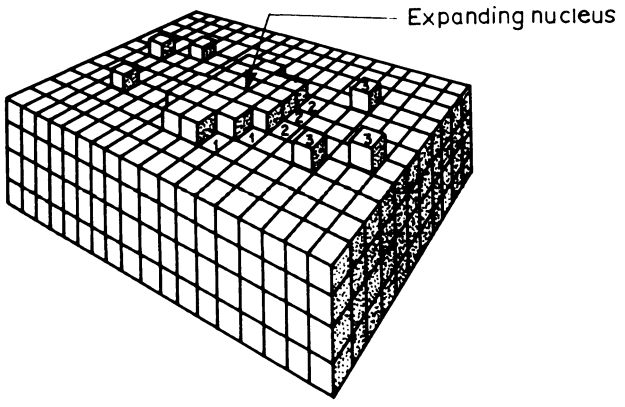

Fig. 8.5 Types of surface site on a perfect crystal. Kink sites are denoted by (1), edge sites by (2) and adatoms by (3).

The structure of the growing layer will be determined largely by the relative rates of processes (2) and (3) and, in a plating process, the electrolysis conditions, including the current density. At low current density, the surface diffusion is fast compared with electron transfer and the adatom is likely to end up in a favoured position in the lattice. At higher current densities, surface diffusion is no longer fast compared with electron transfer and further nuclei must form; the layer will be less ordered. Moreover, the presence of suitable bath additives may radically modify the growth process.

During most of the electroplating process, the primary metal layer is thickening from a few atomic layers to the desired thickness, perhaps 1–10 μm. In this period the metal deposition reaction occurs effectively at an electrode of the electrodeposited metal. The rate of this process may generally be estimated by an equation of the type:

$$I = nF\vec{k}\, c_{M^{n+}} \exp\left(-\frac{\alpha nF}{RT}\eta\right) \tag{8.11}$$

although this does not necessarily infer that the electrode reaction is simple. In some cases, the electroplating reaction will involve the reduction of a complexed metal species and then the electrode reaction may involve chemical steps, e.g.:

$$[Zn(CN)_4]^{2-} + 4OH^- \longrightarrow [Zn(OH)_4]^{2-} + 4CN^- \tag{8.12}$$

$$[Zn(OH)_4]^{2-} \longrightarrow [Zn(OH)_2] + 2OH^- \tag{8.13}$$

$$[Zn(OH)_2] + 2e^- \longrightarrow Zn + 2OH^- \tag{8.14}$$

Electrochemical experiments tell us little about the thickening process. Instead, information about thick deposits comes from empirical studies and from techniques such as optical microscopy, scanning and transmission electron microscopy (Fig. 8.6) and electron diffraction. On the other hand, the structure and properties of the deposit are totally determined by electrochemical parameters combined with the properties of the plating bath. Electrodeposits are almost invariably polycrystalline with many grain boundaries and imperfections such as screw dislocations (Fig. 8.7). Screw dislocations provide an edge which does not grow out; rather it rotates around the centre to form a pyramid of stacked rows of edges, the radius of curvature of the emerging dislocation controlling the step spacing on the pyramid.

Again, during the thickening stage a key parameter is the current density. At low current densities, the surface diffusion process is fast compared with electron transfer and both the crystal lattice and structures such as screw dislocations can be well formed and may be observed by electron microscopy. The predominant orientations of surface planes can also be determined using electron diffraction.

As the current density is increased, surface diffusion is no longer fast compared with the discharge process and adatoms no longer reach their equilibrium position in the lattice. Furthermore, at the increased overpotential, nucleation of additional growth centres remains a more frequent event. Hence, the lattice

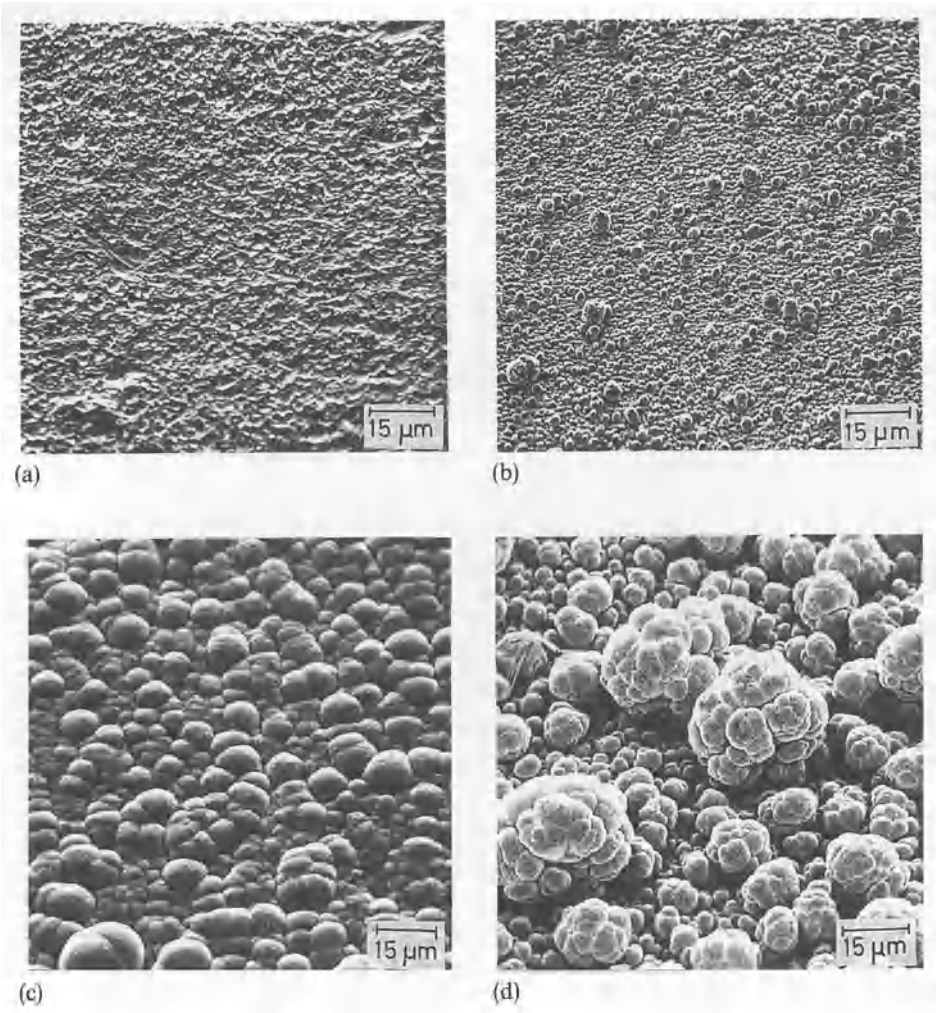

Fig. 8.6 Scanning electron micrographs of a copper electrodeposit from an acid sulphate solution at various times, illustrating the development of nodular growth at the limiting current. Nominal deposit thicknesses are as follows. (a) 10 μm. (b) 15 μm. (c) 20 μm. (d) 30 μm. (0.07 mol dm^{-3} $CuSO_4$; 1 mol dm^{-3} H_2SO_4; 22 °C and with a rotating-cylinder cathode.) (Courtesy: Dr D. R. Gabe, Loughborough University of Technology.)

formed will be less ordered and macroscale features, steps, ridges and poly-crystalline block growth (Fig. 8.8) become more likely. With further increase in current density, outward growth of the layer becomes of increasing importance and problems arising from mass transport control in solution can arise. For example, dendrite (Fig. 8.9) (or whisker growth) can occur and once this form of growth commences, it predominates totally because of the enhanced rate of mass

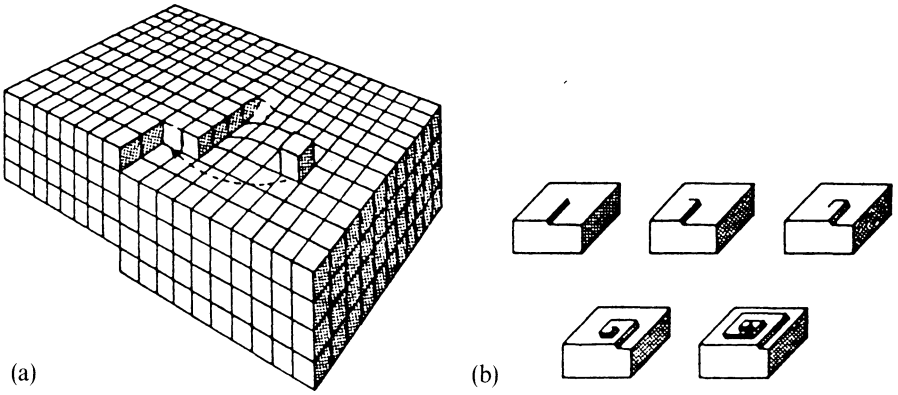

Fig. 8.7 A screw dislocation (a) and its propagation (b) leading to a spiral feature. Note that, as the screw dislocation extends, the kink site is never lost.

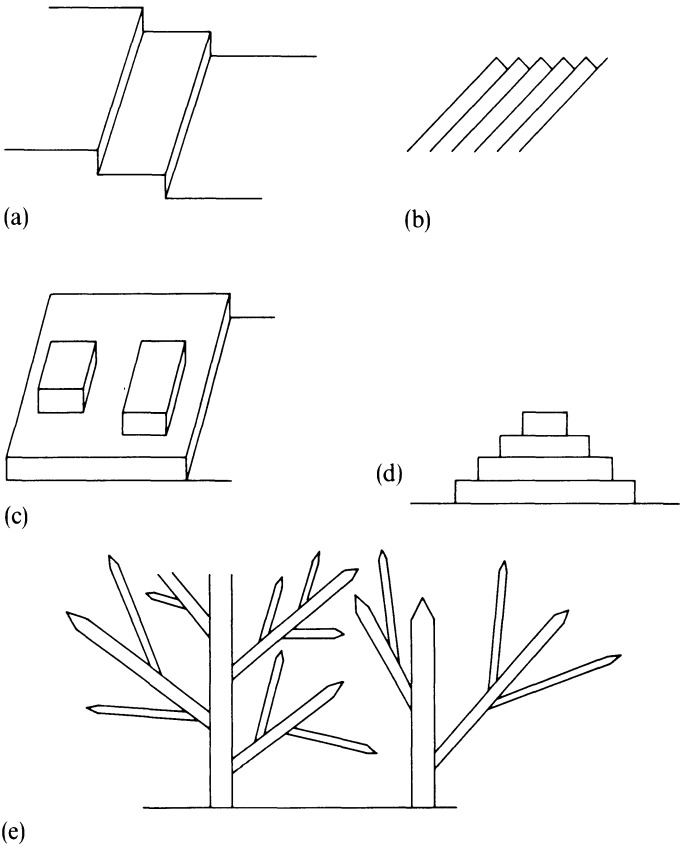

Fig. 8.8 Representation of various growth forms observed in metal deposition. (a) Layer growth. (b) Ridge growth. (c) Block growth. (d) Pyramidal growth. (e) Dendritic growth.

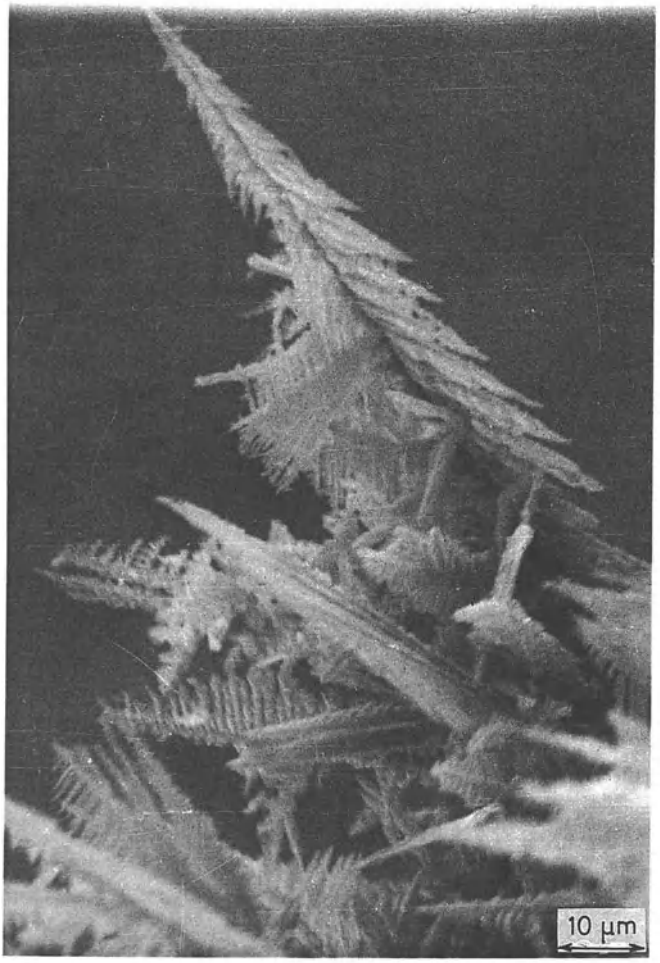

Fig. 8.9 Scanning electron micrograph showing dendritic growth of tin during its electrodeposition from a phenolsulphonate solution. (Courtesy: Dr. D. R. Gabe, Loughborough University of Technology.)

transport to the tip (spherical diffusion to the microscale tip) and because the iR drop to the tip is also a minimum as this is the closest point to the anode. In the completely mass transport controlled potential region, the deposit often exhibits a powdered texture. The formation of a roughened deposit is generally catastrophic for metal-finishing operations.

The way in which the structure depends on current density is summarized in Fig. 8.10. The above discussion should not, however, be taken to imply that the best electrodeposits are necessarily formed at the lowest current density; the correct conditions must be sought experimentally. Even when a perfect lattice is

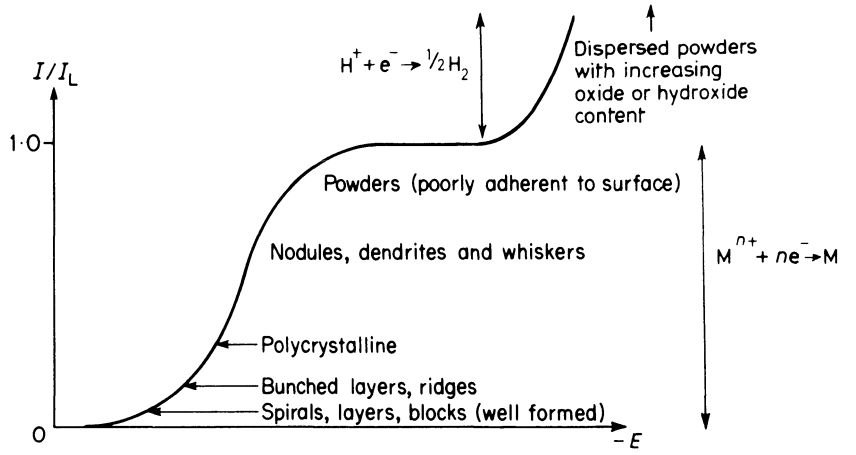

Fig. 8.10 The variation of characteristic growth modes with normalized current density I/I_L.

grown on a substrate with similar lattice dimensions (epitaxial growth), a good adhesive deposit is not always obtained. In many applications, the most durable deposits are often the even, polycrystalline type.

The vast majority of electroplating processes are carried out using relatively smooth, direct current (d.c.) power supplies to achieve a constant current flow to the cathode. The useful range of current density which produces satisfactory deposits is much lower than the limiting current density but related to it. Therefore, for a given electrolyte, higher rates of deposition are favoured by increasing I_L by the use of, for example: (1) high dissolved-metal concentrations; (2) high temperatures; and (3) relative movement between the cathode and the electrolyte. (1) and (2) are limited in practice. The metal concentration is restricted by solubility, cost (for precious metals) and disposal/effluent treatment considerations. Elevated temperatures can aggravate problems associated with corrosion of process equipment, evaporative losses, chemical decomposition (e.g. of addition agents), prolonged start-up times from cold, not to mention increased power costs for heating. Thus, in practice, there is often considerable scope for considering the cathode–electrolyte flow environment. Quite aside from allowing the use of an increased current density and, hence, increased production rate, improved flow may aid the removal of entrapped air or generated hydrogen gas from the workpiece or provide a more stable, local cathode pH and temperature environment.

The common methods of introducing electrolyte–electrode movement are:

1. *Cathode movement*: e.g. reciprocation of a cathode busbar (either horizontally, vertically or in both directions), rotation (particularly in the case of cylindrical objects when the current density distribution is time-averaged), or the use of barrel plating (section 8.1.7). A special case is provided by

continuous, reel-to-reel plating of wire or strip. This technique is assuming increasing importance in the electronics industry, where rapid and automated processing of components is facilitated by mounting them on a strip.

2. *Forced electrolyte flow via air sparging, pumping or jet flow*: in certain cases, a special closed cell may be used or the workpiece itself may function as a flow-through cell (as in the case of plating the internal surface of cylinders). In a very few, specialized, applications, ultrasonic stimulation of the electrolyte is used.

   Another specialized method is the use of various alternating current (a.c.) power supplies, the wide spectrum of possible waveforms being referred to as 'pulse' or 'period current reverse' – plating which has been commercially practised since 1965, particularly for certain gold-plating applications in the electronics industry. A general version might include the following sequence:
   (a) a forward (cathodic) current for a certain 'on' time;
   (b) a reverse (anodic) current for a certain 'on' time;
   (c) an 'off' time when no external current is applied;
   (d) repetition of this sequence.

The majority of practical power supplies are (nominally) square wave in form, the technique being applied in a largely empirical fashion. It is clear, however, that periodic current reversal may generally affect charge transfer, mass transport and surface electrocrystallization processes.

The effects of pulsed waveforms are extremely complex and poorly understood, but the following effects are generally accepted. During the 'off' period of a pulse, no net electron transfer can take place and the cathode surface is refreshed with metal cations as a result of convective diffusion. During the 'on' period, the surface metal ion concentration will initially approach the bulk solution value but will decay with time, i.e. the technique involves non-steady state diffusion. A limiting case is a surface metal ion concentration of zero, i.e. complete mass transport control. The reverse (anodic) current may lead to selective dissolution of high points on the deposit due to their enhanced current density, producing a more compact or smooth surface.

The following favourable effects of pulsed current on the deposit quality are generally accepted: higher density, lower porosity, reduced stress, better adhesion to the substrate, improved ductility and reduced incidence of H_2 embrittlement. However, the wider adoption of the technique is hindered by a lack of fundamental knowledge, inconsistent results, and the need for more complex and expensive power supplies.

8.1.3 Anodes

The performance of the anode is of considerable importance in determining the success of an electroplating process. Where possible the anode is made from the same metal as that being plated at the cathode and the conditions are selected so

that the concentration of the metal ion in solution remains constant. This requires the anode and cathode current efficiencies to be matched (usually with values approaching 100%) over the whole service life of the anode. In particular, the electrolytes in the plating bath must be chosen so that the anode does not passivate. A common type of polarization curve for the dissolution of a metal is shown in Fig. 8.11. In the active region, the electrode reaction is the desired metal dissolution but, on increasing the current density or the overpotential above a critical value, the surface becomes covered with an oxide film which passivates the anode, i.e. causes the current for the corrosion reaction to drop to a low level. In a constant-current electrolysis the potential of the anode will shift into the transpassive region where oxygen evolution is a major component of the current. Hence, in a plating process, it is essential to maintain the anode potential in the active region to ensure smooth and uniform dissolution. This may be achieved by using a large anode surface area and, hence, maintaining a suitably low current density at the anode (the anode is frequently in the form of small pellets to increase surface area). Additions of complexing agents, which prevent passivation, or halide ions, which generally cause sufficient pitting of the oxide film for dissolution to continue, are made to many baths. The metal must also dissolve to form the correct oxidation state. Thus, in acid solution, tin may dissolve as tin(II) or tin(IV) but only the former may be reduced to the metal at a potential positive to the hydrogen evolution reaction and therefore the anode current density must be controlled to form only tin(II).

The anodes are designed to produce the minimum of anode sludge. This is insoluble solid material which leaves the anode surface and can contain the metal as oxide or hydroxide or even the metal itself if physical disintegration of the anode accompanies dissolution. In addition, impurity elements in the anode which do not dissolve, collect in the sludge. The mode of fabrication and the purity of the anode metal affect its performance, particularly with regard to physical disintegration – rolled metal is frequently better than case metal. For

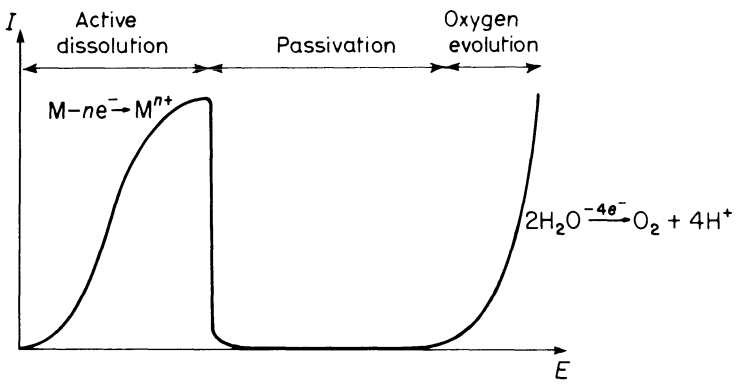

Fig. 8.11 Typical current-potential curve for an anode in an electroplating bath.

several metals, particular forms have been developed for electroplating anodes; examples are 'nickel carbonyl' and 'S-nickel' pellets which combine a high surface area with smooth dissolution and a minimum of sludge.

Chromium passivates strongly in acid sulphate media. Hence, an inert anode is always employed in chromium plating. It is generally a lead alloy which immediately covers with lead dioxide on positive polarization in the electrolyte. The alloying elements are tin, antimony and silver which are added to the lead to improve its mechanical properties and to reduce the overpotential for oxygen evolution. In addition to the main anodes, auxiliary anodes of platinized Ti are sometimes also used to improve the current distribution at the cathode.

8.1.4 The plating bath

The plating bath is normally a complex mixture of soluble species of the metal being plated, electrolytes and various additives to ensure that the electroplate has the desired properties and quality. In this section we shall consider the role of each of the components.

(a) The metal ion

The metal to be plated is present in solution either as the simple hydrated ion or as a complex but normally in high concentration, typically 1–3 mol dm^{-3}.† This high concentration is essential because, while it is necessary to use a reasonable current density, the quality of the plate suffers badly if the deposition occurs under conditions where the electrode reaction is even partially mass-transfer-controlled (Fig. 8.10). A non-complexing medium is frequently used for rapid plating on objects of simple shape while complexing media are employed when a high throwing power is important.

(b) Electrolytes

Various electrolytes are also added in high concentration to give the bath maximum conductivity. They may also have the role of controlling the pH and buffering the solution particularly if hydrogen or oxygen is evolved at the cathode or anode respectively, since these reactions will tend to change the pH. An increase in pH may lead to deposition of metal hydroxides. This is a particularly difficult problem when the metal depositing is a good H_2 evolution catalyst and also easily hydrolysed (e.g. Ni). Hence a Watts bath contains boric acid. A pH above 2 may be essential to decrease H_2 evolution, with a consequently reduced tendency for H_2 embrittlement or hydride formation in certain metals.

† An important exception is in precious-metal baths, where the inventory of metal is kept as low as possible to lower initial investment costs and losses via carry over of process liquor. For example, some gold baths operate at gold levels $\ll 10$ g dm^{-3}

(*c*) *Complexing agents*

Complexing agents are used to make the deposition potential more negative when it is necessary to prevent a spontaneous chemical reaction between the cathode and the plating ion, e.g. plating copper onto iron or steel:

$$Cu^{2+} + Fe \longrightarrow Cu + Fe^{2+} \tag{8.15}$$

This chemical reaction would lead to a very poor copper deposit, both porous and badly adherent, so a complexing agent is added to make the potential of the Cu^{2+}/Cu couple negative to that for the Fe^{2+}/Fe couple; reaction (8.15) is then no longer thermodynamically favourable. Complexing agents are also used to modify the Tafel slope for the metal ion reduction and, hence, to improve the throwing power of the bath. The most common complexing agents in electroplating are cyanide, hydroxide and, more recently, sulphamate ion.

Complexing agents also have a role at dissolving anodes; they can prevent passivation and therefore loss of current efficiency in the corrosion reaction and it is for this reason that a low concentration of chloride ion is a common constituent of many baths.

(*d*) *Organic additives*

A wide range of organic molecules are added in relatively low concentration to the electroplating bath to modify the structure, morphology and properties of the cathode deposit. Their development has been almost totally empirical and details of their mode of operation are seldom known. Indeed, it is not always clear whether their effect is due to the additive itself or to decomposition products formed in electrode reactions. Several generalizations concerning their operation are, however, possible.

Certainly, additives are usually capable of adsorption on the cathode surface, and in some cases organic matter is occluded into the deposit, especially when the plated metal has a high surface energy (high melting point). Many additives also increase the deposition overpotential and change the Tafel slope. This may be due to the need for electron transfer to occur through the adsorbed layer or due to complex formation at the electrode surface.

While the additives may affect more than one property of the deposit – and there is clear evidence that when several additives are present in the electrolyte their effect is synergistic – they are often considered in the following classification:

1. *Brighteners.* For a deposit to be bright, the microscopic roughness of the deposit must be low compared with the wavelength of the incident light so that it is reflected rather than scattered. Brighteners are commonly used in relatively high concentration (several $g\,dm^{-3}$) and may result in substantial organic matter in the deposit. They usually cause the formation of an even, fine-grained deposit and, hence, may act by modification of the nucleation process.

For nickel deposition from a Watts bath (a weakly acidic bath containing sulphate and chloride), two types of brightener are recognized: (1) aromatic sulphones or sulphonates leading to bright deposits without lustre and reduced stress; (2) molecules containing $-C\equiv N$, $-N=C=S$ or $>C=O$ entities (e.g. thiourea and coumarin), which produce deposits with a high lustre but also raise the stress and brittleness in the metal. In practice both types are used in combination. The aromatic sulphonates are also brighteners for tin or copper.

2. *Levellers.* These produce a level deposit on a more macroscopic scale and act by adsorption at points where otherwise there would be rapid deposition of metal. Thus, adsorption of additives occurs preferentially at dislocations because of a higher free energy of adsorption and at peaks because the rate of their diffusion to such points is enhanced; the adsorbed additive will reduce the rate of electron transfer. In practice, many addition agents act as both brighteners and levellers.
3. *Structure modifiers.* These additives change the structure of the deposit and maybe even the preferred orientation or the type of lattice. Some are used to optimize particular deposit properties, and others to adjust the stress in the deposit (stress is due to lattice misfit). The latter are often called 'stress relievers'.
4. *Wetting agents.* These are added to accelerate the release of hydrogen gas bubbles from the surface. In their absence, the hydrogen which is often evolved in a parallel reaction to metal deposition can become occluded in the deposit causing, for example, hydrogen embrittlement.

8.1.5 Typical application areas for electroplating

Electroplated coatings may confer one or more of the following surface properties:

1. Corrosion protection.
2. Build-up of material or restoration.
3. Decorative appeal.
4. Wear resistance.
5. Hardness.
6. Optical or thermal reflectivity.
7. Electrical conductivity.
8. Ease of cleaning.
9. Oil retention.
10. Solderability.
11. Thermal conductivity.

The usual compromise in choosing the thickness of electroplate is that of obtaining acceptable properties at a minimum, guaranteed thickness. Electroplating is rarely used for coatings thicker than 75 μm as competitive processes

(a)

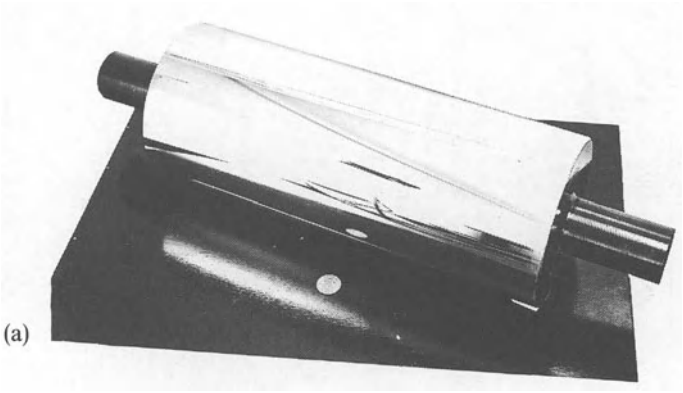

(b)



Fig. 8.12 Examples of 'hard chromium' electroplating for engineering applications. (a) A printing roll; following grinding and polishing, a smooth and highly reflecting surface finish is possible. (b) An injection moulding tool used to produce plastic water tanks (Photographs courtesy: Ionic Surface Treatments; Plating by Hilton and Tuck Division, Manchester.)

Table 8.1 Some typical electroplating conditions

Metal	Electrolyte composition/g dm^{-3}	T/°C	I/mA cm^{-2}	Current efficiency /%	Additives	Anode	Applications
Cu	(a) $CuSO_4$ (200–250) H_2SO_4 (25–50)	20–40	20–50	95–99	Dextrin, gelatin, S-containing brighteners, sulphonic acids	P-containing rolled Cu	Not suitable for iron and iron alloy substrates. High I but low throwing power. Additives essential
	(b) CuCN (40–50) KCN (20–30) K_2CO_3 (10)	40–70	10–40	60–90	Na_2SO_3	O_2-free, high-conductivity Cu	Good throwing power, deposits adhere well and are bright. Used as undercoat. Cyanide decomposes at anode
Ni	(a) $NiSO_4$ (250) $NiCl_2$ (45) H_3BO_3 (30) pH 4–5	40–70	20–50	95	Coumarin, saccharin, benzenesulphonamide acetylene derivatives	Ni pellets or pieces	H_2 evolved with deposition. Additives depend on purpose of deposit. Medium throwing power
	(b) Ni sulphamate (600) $NiCl_2$ (5) H_3BO_3 (40) pH 4	50–60	50–400	98	Not essential. naphthalene-1,3,6-trisulphonic acid	Ni pellets or pieces	Good throwing power. Some H_2 with additives, mirror finish at 400 mA cm^{-2}
Ag	$KAg(CN)_2$ (40–60) KCN (80–100) K_2CO_3 (10)	20–30	3–10	99	S-containing brighteners	Ag	Good throwing power. Functional or decorative

Sn	(a) $SnSO_4$ (40–60) H_2SO_4 (100–200)	20–30	10–30	90–95	Phenol, cresol	Sn	Poor throwing power. Additives essential
	(b) Na_2SnO_3 (50–100) NaOH (8–18)	60–80	10–20	70		Sn (control I)	Good throwing power but uses twice charge (Sn(IV) rather than Sn(II))
	(c) $SnCl_2$ (75) NaF (37) KF (50) NaCl (45) pH 2.5	65	50–200	90	SCN^-, disulphono-naphthalinic acid	Sn	Reasonable throwing power. More stable than (a). Rarely used.
Zn	(a) NH_4ZnCl_3 (200–300) NH_4Cl (60–120) pH 5	25	10–40	98	Dextrin, organic additives	Zn	Poor throwing power. Additives essential
	(b) ZnO (20–40) NaCN (60–120) NaOH (60–100)	15–30	10–50	70–90	Glycerin, organic additives	Zn	Good throwing power
	(c) ZnO (6–10) NaOH (70–100)	20–40	10–30	60–80	Organic additives	Zn	Medium throwing power. Non-toxic. Additives essential
Cr	(a) CrO_3 (450) H_2SO_4 (4)	45–60	100–200	8–12	Complex fluorides to increase efficiency	Pb–Sb or Pb–Sn coated with PbO_2	Need to reoxidise Cr^{3+} formed. Decorative finish. Poor throwing power
	(b) CrO_3 (200) H_2SO_4 (2)	40–55	100–200	10–15		Pb–Sb or Pb–Sn coated with PbO_2	Hard, wear-resistant deposit

may be faster and cheaper. Exceptions do exist however, particularly in heavy engineering; e.g. chromium plating (Fig. 8.12) may be carried out up to perhaps 500 or even 1000 μm thickness because alternative methods of coating are not available. Such heavy deposits require considerable skill and effective post-plating operations such as grinding and honing in order to improve the surface finish.

The likelihood of an unacceptable porosity increases markedly for thin coatings, and this may be catastrophic for noble coatings (as noted in Chapter 10), such as copper on steel. The upper limit on deposit thickness is influenced by such factors as an excessive process time, too high an internal stress or development of irregular deposit growth, e.g. nodules or dendrites (Figs. 8.8–8.10).

A particular application will require its own deposit characteristics (including thickness) and, hence, a different bath formulation and electrolysis conditions. Table 8.1 therefore sets out some typical plating conditions for six metals which are extensively electroplated. For several metals there is a choice of an acidic, non-complexing bath which is used for rapid plating of simple shapes (e.g. flat surfaces and wires) and a complexing medium which gives a lower plating rate but the additional throwing power essential for intricate surfaces. Moreover, only a range is given for several parameters since the value will depend on the deposit properties sought.

From Table 8.1 it can be seen that most plating processes operate at a current density between 10 and 70 mA cm^{-2}, a range which is low compared with that for the preparative electrolytic processes. Since, in general, the thickness of the deposit required will range between 0.01 and 100 μm, depending on the application, the electroplating procedure will last from only a few seconds to perhaps several hours. The current density for silver deposition is particularly low while those for nickel in sulphamate media and tin in the chloride or fluoride bath are markedly higher. The value for chromium is deceptive because of the low current efficiency; most of the current is hydrogen evolution. For most metals (chromium being an exception), the table also shows that the current efficiencies are good and that the use of additives and temperatures slightly above ambient is normal.

The plating of some alloys is possible although the limitations are greater and the control of the conditions more critical. It is essential to use a complexing bath selected to make the deposition potentials of the components of the alloy the same, although the *I–E* curves for the individual metals are not always good guides for suitable baths. The alloy deposited clearly depends on the electrolyte, bath temperature, current density and the ratio of the metal ions in solution. The latter is often critical, the exceptions being deposits which are intermetallic compounds (e.g. SnNi) although the deposit composition is not the same as that of the solution. Also, the current densities are towards the low end of the metal-plating range and many of the alloys do not dissolve anodically so that it is necessary to use anodes of both metals. The conditions for plating four alloys are summarized in Table 8.2.

Table 8.2 Typical conditions for plating alloys

Alloy	Electrolyte composition/g dm^{-3}	T/°C	I/mA cm^{-2}	Current efficiency/ %	Anode	Comments
70% Cu–30% Zn (brass)	$K_2Cu(CN)_3$ (45) $K_2Zn(CN)_4$ (50) KCN (12) Sodium tartrate (60)	40–50	5–10	60–80	Brass	Additives essential. Close control of bath + plating conditions essential
40% Sn–60% Cu (bronze)	$K_2Cu(CN)_3$ (40) Na_2SnO_3 (45) NaOH (12) KCN (14)	60–70	20–50	70–90	Bronze or mixture of Sn and Cu anodes	Additives essential
65% Sn–35% Ni	$NiCl_2$ (250) $SnCl_2$ (50) $NH_4F \cdot HF$ (40) NH_4OH (30)	60–70	10–30	97	Separate Ni and Sn plates	Good throwing power. Deposit composition not dependent on electrolysis conditions over a wide range
80% Ni–20% Fe	$NiSO_4$ (300) $FeSO_4$ (20) H_3BO_3 (45) NaCl (30) pH 3–4	50–70	20–50	90	Ni + Fe as pieces	Close control of $[Ni^{2+}]/[Fe^{2+}]$ in bath essential

In the mechanical engineering sectors of industry, electrodeposition has a well-established position as a coating technique (Table 8.3), the following advantages being important:

1. Operating temperatures generally lie in the range 20–70° C; thus, extreme temperatures (which may lead to distortion or adverse metallurgical changes) are avoided.
2. Under suitable conditions, the coating adhesion is very strong.
3. In many cases, a relatively thin coating produces a radically improved surface, with respect to its engineering performance.
4. Process automation is often possible.

Limitations include:

1. The speed of deposition is usually much lower than 75 $\mu m\, h^{-1}$ (although forced electrolyte convection may improve this).
2. The physical size of the plating bath may limit dimensions of the workpiece.
3. In some cases, the plating bath (or pretreatment liquors) may be toxic and require adequate treatment before discharge as effluent.

The plating of composites is a recent development but one which is likely to be of increasing importance because it is found that the inclusion of solid particles into the metal deposit can greatly enhance the wear resistance and friction properties of the deposits. Solids such as Al_2O_3, TiO_2, SiO_2, WC, TiC, SiC, Cr_3N_2, diamond, graphite, MoS_2 and PTFE, present in solution as particles 0.5–5 μm in diameter, are entrapped in a deposit under suitable electroplating conditions. They are usually present in 2–10 vol % and are codeposited by one or both of the following mechanisms:

1. Physical dispersion in the electrolyte and adequate agitation facilitates mechanical entrapment; special pumped electrolyte flow and plate plungers have been used.
2. The particles are dispersed in the electrolyte and electrically charged, courtesy of surfactant adsorption; electromigration can then occur towards the cathode; usually a combination of non-ionic and cationic surfactants are used.

The applications for hard particle composites lie, for example, in internal combustion engines, textile machinery and gas turbine compressors, where combined properties can include resistance to wear, fretting, scuffing and heat and chemical attack. The softer particles display an advantageously low coefficient of friction and effective self-lubricating properties.

8.1.6 Electroplating in the electronics industry

The applications of electroplating are legion within the electronics industry and the technique is used on a scale ranging from the minute, for the lead-in

Table 8.3 Typical engineering applications for electroplated metals

Deposited metal	Typical hardness/HV	Characteristics of coating	Typical applications
Cr	800–1000	Hard and wear-resistant; low friction and non-stick; corrosion-resistant; brittle	Reclamation of worn or oversize components; rolls for printing or steel rolling; plastic moulds; hydraulic rams
Ni	150–450	Softer; more ductile than Cr; corrosion-, heat-, and wear- resistant; solderable; can be machined by cutting tools	Reclamation of worn or oversize parts; food processing machinery; electroforming; hydraulics
Cu	60–150	Softer than Ni; ductile; resistant to fretting; good electrical and thermal conductivity	As a resist for selective case hardening of steel; electroforming; surface lubrication in metal working
Fe	150–350	Low cost; tough and easily heat treated; poor corrosion resistance	Anti-scuffing in internal combustion engines; soldering iron tips; reclamation of worn parts; electroforming of foil
Sn	8–12	Soft and ductile; low melting point; resistant to fretting, scuffing and adhesive wear	Overlay coatings for pistons in internal combustion engines; corrosion protection
Ag	60–120	Excellent electrical conductivity; resistant to fretting	Specialized anti-seizure of threaded parts at high temperature
65 Sn–35 Ni	650–700	Hard; low friction, retains oil film, corrosion resistant; brittle; temperature limit $\simeq 360^\circ$ C	Hydraulic braking systems in automobile engineering

conductors in large-scale integration (LSI) chips, to a wide variety of printed circuit boards used in the majority of electronic hardware. Alternative methods of metal deposition (including vacuum deposition or conductive paints and lacquers) have their niche but electroplating has provided the most favourable route, especially for large-scale processing. In general, the electrolytes and electroplating conditions used are similar to those for decorative or engineering

plating. The critical and ever-increasing performance of both printed circuit boards and components demanded by the electronics industry means that cleanliness and process control are much more stringent. The choice of metal depends on the nature of the component or device, service conditions, cost and required lifetime. Copper, silver and gold are primarily selected for their high electrical conductivity. Palladium and rhodium find use where hardness and enhanced corrosion resistance are important. Tin and tin–lead are utilized for their low melting points and solderability (tin–nickel deposits are also becoming increasingly important in this area).

Typical application areas of the metals are given in Table 8.4. In order to illustrate the utilization of electroplating in the electronics industry, two areas may be briefly described: (1) fabrication of printed circuit boards; and (2) electrical contacts.

(*a*) *Printed circuit boards*

The major technique used to manufacture printed circuit boards is the 'subtractive' method, where the desired pattern of copper tracking is formed by etching away unwanted copper (Chapter 9) from the glass fibre/epoxy (or phenolic) base. The base ranges from thick (< 5 mm), rigid boards for heavy power circuitry and components down to thin (< 0.15 mm) flexible materials.

The adoption of double-sided, copper clad laminates together with plated-through-holes permits a much higher packing density of components. A circuit pattern is produced via etching on both sides of the board followed by interconnection of the two sides via plated-through-hole fabrication.

It may be noted that the printed circuit board laminate is produced by using electroformed copper foil, nodular deposition of copper and surface anodic oxidation to Cu_2O providing greatly improved bonding to the insulating substrate. More sophisticated circuits employ multiple layers of copper tracking, interconnected by through-hole-plating.

Figure 8.13 shows schematically the steps involved in fabrication: etching, electroplating, electroless plating (section 8.2) and, occasionally, immersion plating are all involved, on an integral basis with mechanical, physical and optical techniques.

The manufacturer of printed circuit boards requires plating-through-holes; ideally, the electroplated layer should have a uniform thickness within the hole and on the flat laminate 'land' areas; this presents a challenge to the throwing power of the electrolyte (section 8.1), the racking of the printed circuit board and effective control over the electroplating process.

(*b*) *Electrical contacts and connectors*

The electronics industry relies upon effective contacts for the connection of:

1. Semiconductor wafer-to-chip connection.
2. Chip to package.

Table 8.4 Typical application areas and special properties of electroplated metals used in the electronics industry

Metal or alloy	Special characteristics	Application areas	Electrolyte type
Ag	High electrical conductivity; low contact resistance	Heavy-current busbars and tracks; switchgear; fuse holders; cable	Alkaline cyanide
Cu	Relatively low cost; good electrical conductivity	Printed circuit boards	Acid sulphate; alkaline cyanide; pyrophosphate
Au	Corrosion resistance; high electrical conductivity; low contact resistance	Printed circuit board edge connectors; reed relays; semiconductor lead-out connections	Neutral cyanide; acid cyanide; sulphite
Rh	Very hard, but can be highly stressed	Open contacts	Acid sulphate
Pd	Hard; corrosion resistant	Heavy-duty open contacts;	Sulphamate; halide; diamminodinitrite; ammino
Sn	Solderability; reasonable contact resistance	Pretinning of contacts; electrical contacts	Acid fluoroborate; acid sulphate
60:40 Sn–Pb	Solderability	Printed circuit board tracks	Acid fluoroborate
65:35 Sn–Ni	Solderability superior to Sn–Pb, especially after prolonged storage	Printed circuit board tracks	Acid chloride
80:20 Pd–Ni	Resistance to sliding wear; lower cost than Au	Sliding wear contacts	Ammine sulphate
Ru	Good wear resistance; oxide is electrically conducting	Reed switches	Nitrosyl sulphamate

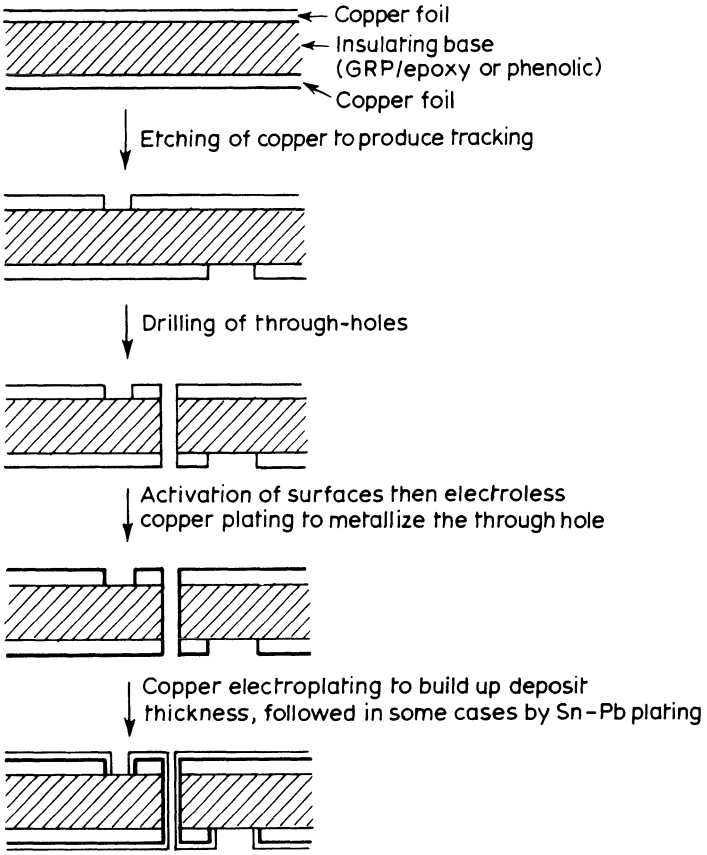

Fig. 8.13 The steps involved in the subtractive technique for the manufacture of printed circuit boards. A very simplified schedule is shown to obtain a double-sided board, i.e. one which has copper tracks on each side interconnected by 'plated-through' holes.

3. Package to substrate or printed circuit board.
4. One board to another or to the rest of the circuitry.
5. Switches, which may be of open or sealed construction.

In the case of printed circuit boards, edge connectors are required at the extremities of the panel for interboard connections. The connectors are of the mechanical pressure type, due to the need for intermittant board replacement. Gold is deposited either directly onto the copper pad or an intermediate, electroplated nickel layer (which provides a diffusion barrier). 'Acid' gold cyanide is a common electrolyte, the deposit containing small amounts of cobalt to provide hardness.

For contact applications, the surface preparation is often critical and the co-depositions of other materials are often of paramount importance to the reliability and service life. For many applications, especially those involving high currents,

the bulk contact is fabricated from copper or a copper alloy. In an open atmosphere, corrosion protection, wear/spark resistance and effective electrical conductivity are provided by a number of precious-metal deposits. Its high electrical conductivity finds silver numerous low-noise or high-current applications, particularly in plug and socket arrangements, switchgear, fuseholders, and copper cable. Gold and its alloys (pure gold is soft and costly) have been traditional choices, due to their favourable combinations of electrical conductivity together with corrosion and wear resistance. The selection and adoption of alternative methods have proved difficult but attract increasing attention. Palladium and rhodium layers provide considerably enhanced wear resistance, while palladium–nickel has introduced a cheaper alternative to gold.

A common form of closed contact is the reed relay, where the sealed capsule consists of two Ni–Fe blades, coated in the contact area with a precious metal and sealed into a glass envelope filled with, for example, a N_2–H_2 mixture. The capsule is positioned within, or close to, a coil which induces the blades to contact magnetically when energized. The blades are usually gold-plated using a continuous belt-feed system, the cathode contact area being limited by judicious control of electrolyte level.

A wide range of applications are found in semiconductor manufacture, e.g.:

1. In transistors, the base of the encapsulating can and lead wires are gold plated.
2. Integrated circuits (ICs) are generally packaged as discrete integrated packages (DIPs) or flat packs ('cerpaks'). The basic conductor pattern is a Mo–Mn alloy coating on a Ni–Fe (Kovar) lead frame. Gold is electrodeposited ($\simeq 1$ μm thick) onto this substrate (usually from a neutral cyanide solution) to reinforce the conductor pattern and provide improved conductivity.

The brazed ceramic base is gold plated with 0.5 to 1 μm pure gold, while the external leads may be electroplated with tin or tin–lead to improve solderability.

There remain several problematic factors in the development of palladium electrodeposits. Useful current densities (and hence deposition rates) are low, typically $< 50\,\text{mA cm}^{-2}$; baths have tended to show chemical instability and etching of base metal substrates. Moreover, evolution of hydrogen and its incorporation into the metal lattice, a facile process on active Pd, may result in β-PdH_2 producing high stress levels in the deposit.

Whilst problematic in electroplating, hydrogen absorption in palladium provides an effective method for the sensing of hydrogen gas (Chapter 12). Palladium surfaces are also prone to adsorption of organic contaminants, leading to catalysis of oxidation/reduction and, subsequent polymerization, in service, leading to unreliable contact resistance.

8.1.7 The overall plating process and the importance of component design

It is essential for the surface to be correctly prepared in order to obtain a good electrodeposit. A typical simple procedure will have the following steps.

1. Cleaning with organic solvents and/or aqueous alkali. In some situations the aqueous cleaning is assisted by making the surface cathodic (30–100 mA cm^{-2}) at 60–80° C; this has the effect of increasing the pH locally at the surface and catalysing the hydrolysis of fats while the evolved hydrogen also removes organics by electroflotation (Chapter 7).
2. Where the surface is covered by oxides as a result of corrosion, it is cleaned by immersion in acid; again electrochemical enhancement is possible by making the surface anodic ($\simeq$ 100 mA cm^{-2}).
3. Rinsing with water.
4. Electroplating.
5. Rinsing and drying.
6. Quality control prior to packing and despatch.

Where the surface is particularly bad, these steps may be preceded by an abrasive or ultrasonic clean.

Various approaches are used for electroplating, depending on the number, size and shape of the articles.

1. *Jig or rack mounting.* Jig or rack mountings (Fig. 8.14) are used for large-scale routine jobs and for improving the current distribution at the cathode (Fig. 8.18). The jig is either a general-purpose or tailor-made assembly, often with appropriate spring contacts to mount the workpieces. Deposition on the jig surface is minimized by a plastisol coating. Specialized jigs may be provided with essential auxiliary anodes (Fig. 8.14(a)). A compact manual plating line based on a modular concept is shown in Fig. 8.15.
2. *Barrel plating.* Barrel plating (Fig. 8.16) is used for the routine processing of large batches of small objects such as fasteners or certain electronics contacts. The barrel fabricated from, for example, perforated acrylic or polypropylene, is normally rotated (5–20 rev/min) horizontally in the plating bath and contains integral cathodes. Specialized barrels, including vibrating devices, are occasionally used for delicate components (Fig. 8.16a).
3. *Individual mounting.* This is necessary for large, single specialized workpieces, e.g. a one-off computer frame which may need multiple cathode contacts and auxiliary anodes to distribute current.
4. (*Copper*) *wire mounting.* This is the most versatile technique but requires an excessive labour component both before and after plating.
5. *Continuous cathode transfer.* Techniques such as *reel-to-reel plating* (Fig. 8.19) offer a high degree of automation and rapid throughput.

A wide spectrum of process operations is seen in electroplating. Both jig and barrel plating may be carried out in a 'line plating' operation (where the workpiece is moved automatically in a predetermined fashion from one tank to another, including precleaning and postplating operations) or a more flexible (and labour-intensive) 'vat plating' may involve manual movement of the workpiece between the tanks.

In barrel plating, the components are usually weighed before loading; deposit uniformity is usually assured due to the random orientation of components with respect to the anode. This technique is carried out on a wide range of scales and levels of automation (Fig. 8.16).

The electroplating step is normally carried out in a simple rectangular tank of volume between 20 and 2000 dm^3, which should be thermally insulated and have provision for heating the electrolyte. It is also frequently advantageous to introduce convection into the plating tank and, where oxygen does not interfere with the metal deposition, bubbling air through the electrode is the cheapest procedure. The jigs are mounted in the tank with anodes, in bags of cotton or plastic to retain anode sludge, placed symmetrically about the cathode jig; the positioning of the jigs, main and auxiliary anodes may be based on experience or a detailed computer optimization depending on the cost of the product and the scale of the operation.

In larger facilities, the tanks will have a loop for continuous filtering of the electrolyte and the bath temperature, pH and current will be monitored. The concentration of metal ions will be determined by external analysis on a regular basis. The most modern plants will also have an effluent-control plant to deal with liquids resulting from washing and spillages and sludges removed from the tanks. The heavy metals are still commonly precipitated with caustic soda and the solids then allowed to settle, although the modern trend is towards direct electrolytic metal recovery from the effluent (Chapter 7). The control units for the electroplating baths generally operate at a current between 100 and 10 000 A and a voltage of -8 to -12 V.

There are presently very few electroplating processes which utilize a divided cell, primarily due to the increased cell voltage (and, hence, power costs), constructional complexity and increased maintenance requirements. One example is the 'Envirochrome' process for decorative chromium plating which has been trial-manufactured during the last five years. This utilizes a Cr(III) electrolyte which avoids problems associated with the use and disposal of Cr(VI) solutions.

It is important to design the workpiece, wherever possible, to minimize the degree of masking required in those areas which must not be plated. In addition, care should be taken to avoid recesses which may serve to trap cleaning or plating liquors. Another important consideration is electrical conductivity; the workpiece should, when possible, have continuous conductivity across any welds, joins, etc. In general, irregularly shaped objects cause many problems, particularly if they feature sharp edges, abrupt changes in cross-section, perforations, recesses or box sections. The problems arise particularly from poor current density distribution and gas entrapment.

Figure 8.18 illustrates some problems associated with the geometry of the substrate, and low throwing power of, for example, a chromium electrolyte, together with suggested solutions. Whenever feasible, the design engineer should consider likely problems in the electroplating step during the early stages in the

design of the component. Failure in this respect inevitably results in a tedious, difficult (even impossible), unsatisfactory or expensive electroplating process. Any special preparation or replating procedures applied by the electroplater undoubtedly appear as increased overheads for the electroplating operation.

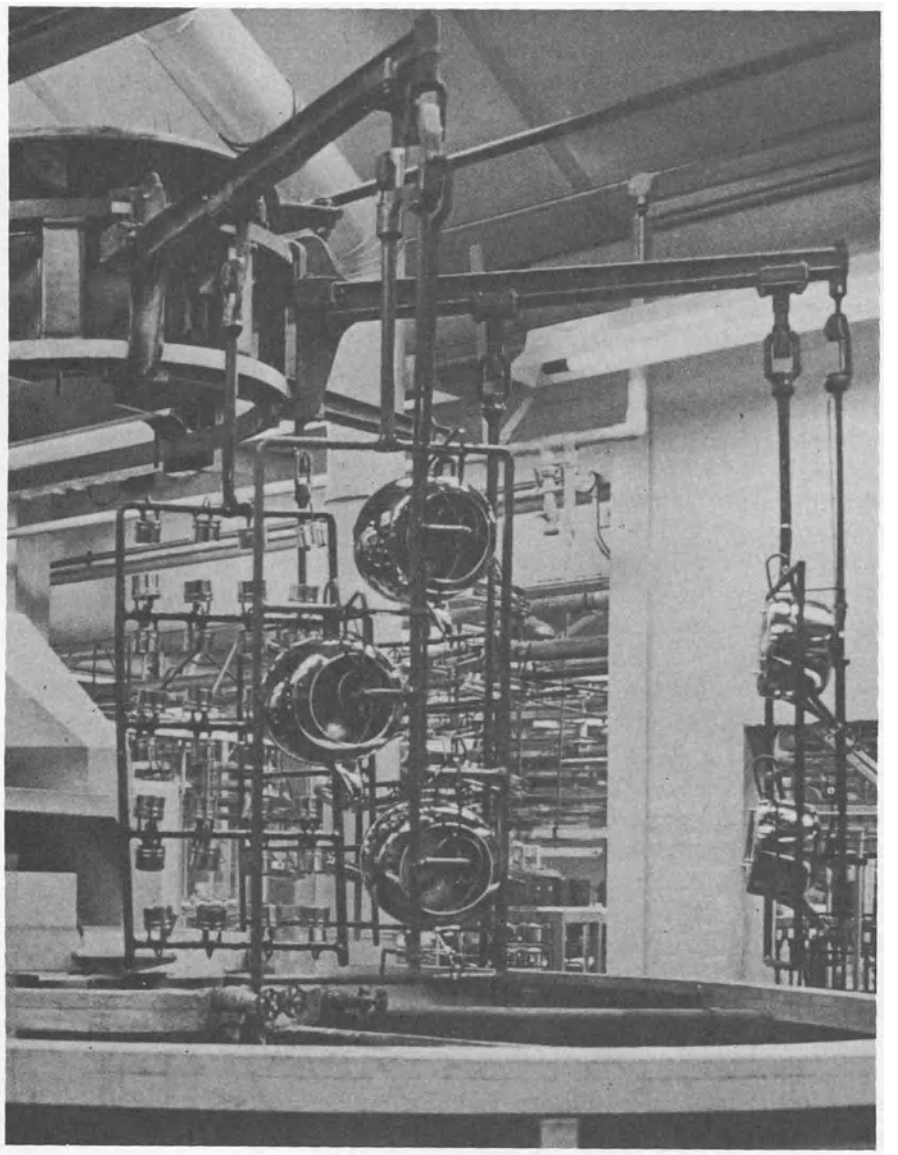

(a)

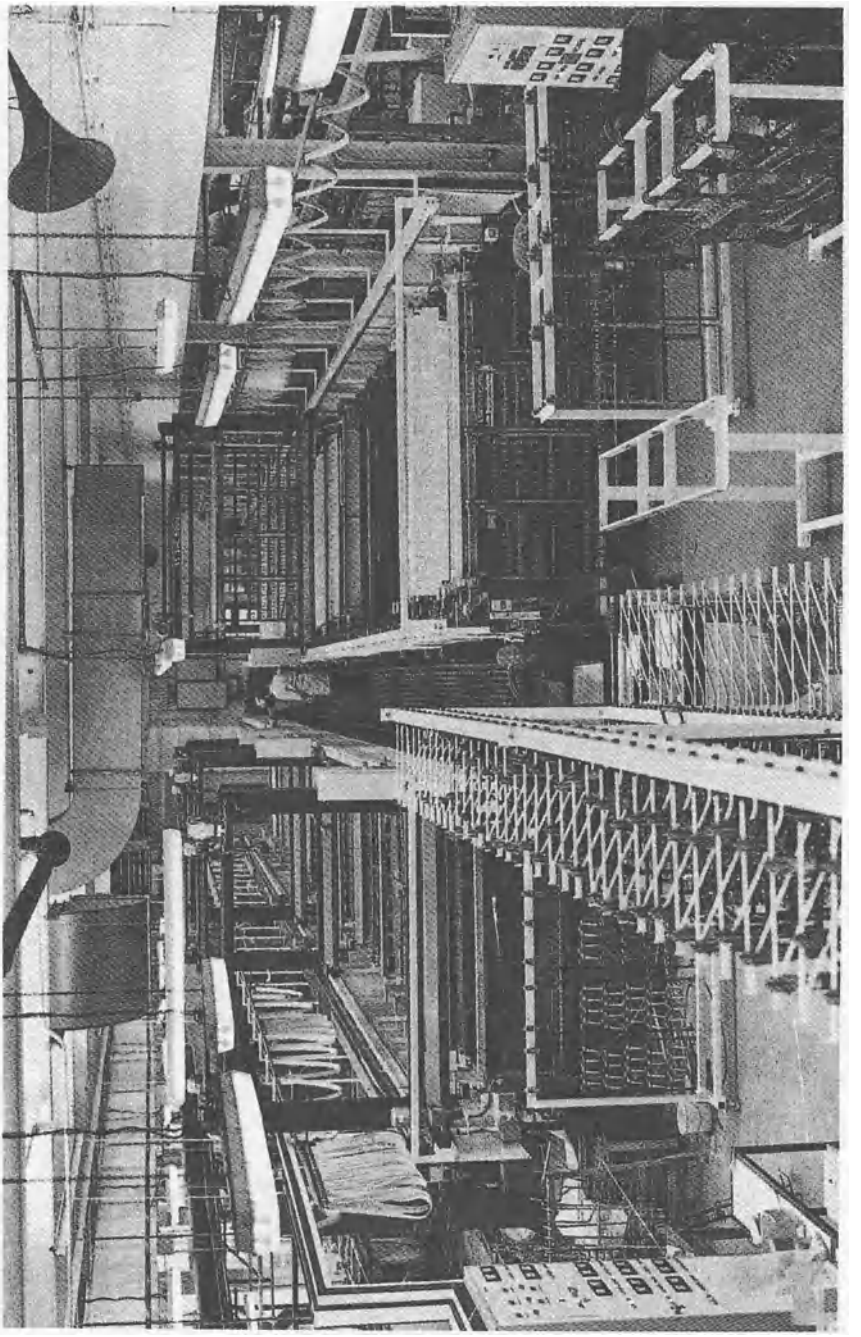

(b)

Fig. 8.14 Jig-rack mounting of electroplated articles. (a) A jig for nickel-plating the interiors and exteriors of kettle bodies. Note the use of platinized titanium auxiliary anodes inside the kettle to provide improved current distribution. (Courtesy: W. Canning Materials Ltd.) (b) A transported-serviced electroplating system, which may be semi- or fully automatic in operation and which utilizes rack- or jig-mounting of components. (Courtesy: Electroloid Ltd.)

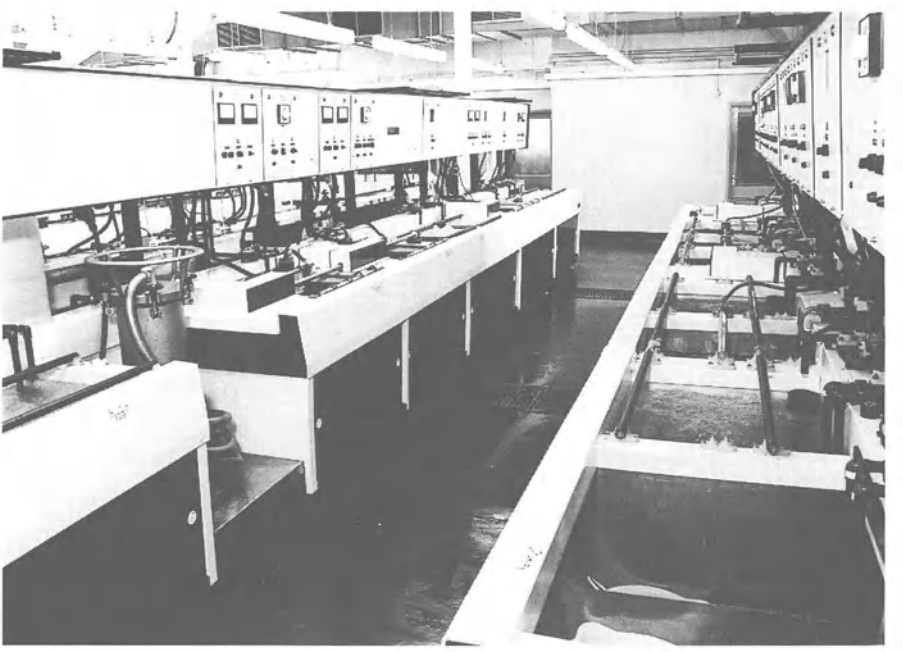

Fig. 8.15 A facility for manual electroplating. The modular equipment is suitable for both rack- and barrel-plating. Construction materials include corrosion-resistant PVC-clad steel and stainless steel. Applications include precious-metal plating in the electronics industry. Power supply and control circuitry are located above the tanks. (Courtesy: PMD Chemicals Ltd.)

Of the many modern developments in electroplating technology, several trends may be highlighted.

1. Electrodeposition of alloys having a controlled composition (e.g. Ni–Fe or Pd–Ni) as cheaper alternatives to single metal coatings.
2. Codeposition of metals with either polymers ('polymets') or ceramics ('cermets') to provide unique wear-resistant or 'tribomet' coatings, e.g. Ni–PTFE, Ni–diamond, Co–carbides.
3. Increasing consideration of less toxic plating baths; in particular cyanide solutions for gold and cadmium have partly been replaced by non-cyanide liquors.
4. Electroless (zero current) plating of an increasingly wide range of single metals, alloys and composites, e.g. Ni–PTFE (section 8.2).
5. Continued development of non-aqueous baths, particularly for aluminium[†] and titanium. (Baths for Ta and Nb have also been developed.)

[†] Commercial aluminium plating processes, based on aluminium triethyl at 80–100° C are currently in operation on a production scale (up to 2200 dm^3 electrolyte volume), e.g. the Sigal process (Hegin Galvano-Aluminium bv).

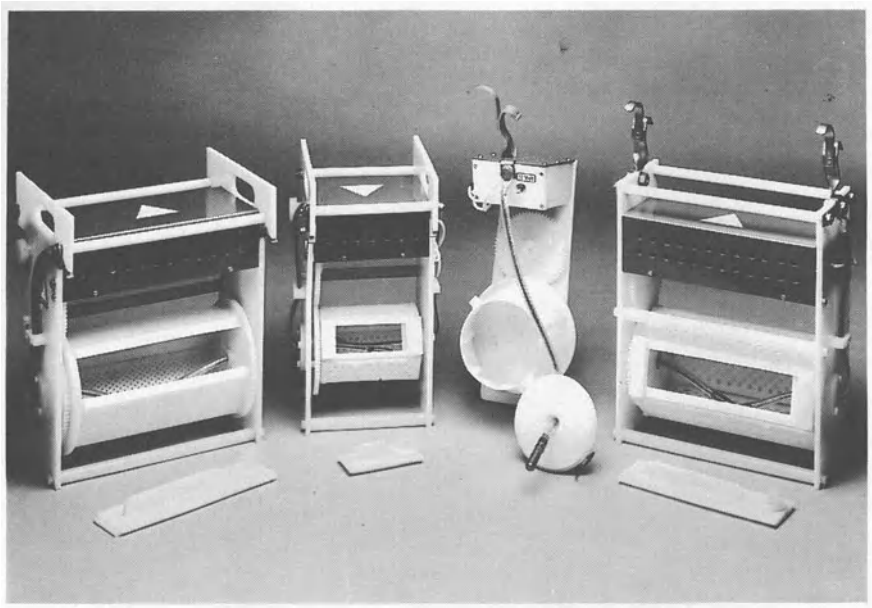

(a)

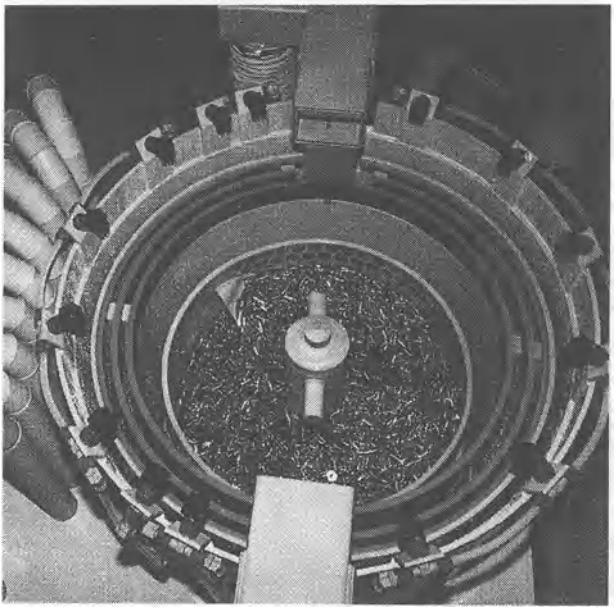

(b)

Fig. 8.16 Equipment for 'barrel-plating' small components. (a) A range of small electroplating barrels available in polypropylene (or Perspex) having 2.4 mm perforations as standard. (Courtesy: PMD Chemicals Ltd.) (b) A fully automatic vibrating barrel for bulk plating of numerous small parts such as electrode contacts which are too delicate for barrel plating. (Courtesy: Electroloid Ltd.)

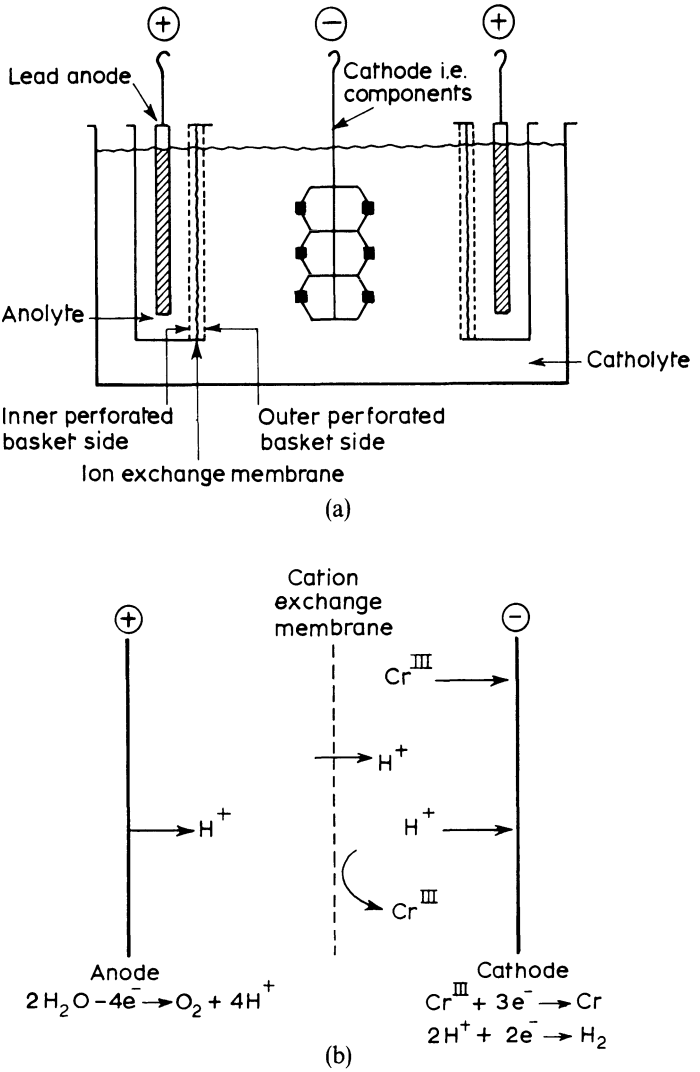

Fig. 8.17 A divided cell for decorative chromium electroplating (the Envirochrome process). (a) The cell design. (b) The electrode reactions. (Courtesy: W. Canning Materials Ltd and IBM UK.)

6. The use of programmed current waveforms (e.g. periodic current reversal) in order to produce thin, dense, pore-free coatings, particularly for demanding electronic applications (section 8.1.2).
7. Selective, high-speed, automated electroplating processes for reel-to-reel plating (Fig. 8.19) of electronics materials, e.g. by use of laser-stimulated deposition.

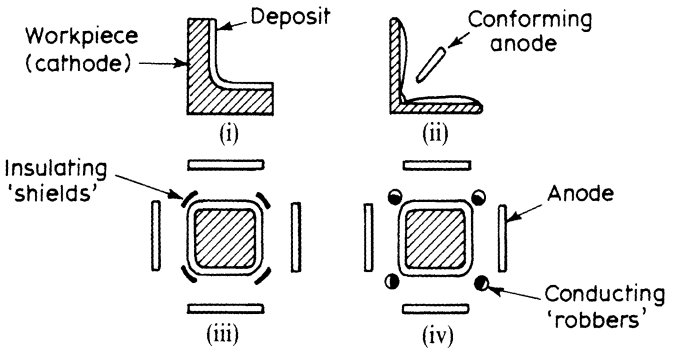

Fig. 8.18 Modification of extreme current densities to provide a more uniform current distribution. (i) use of a radiused corner to reduce throwing power deficiency in a recess; (ii) use of a conforming anode to overcome poor throwing power in a recess; (iii) use of inert shields to prevent build-up of deposits on edges; and (iv) use of cathodic 'burners' or 'robbers' to minimize edge build-up. (After: Ashby (1982) *Electroplating for Engineering Technicians*, National Physical Laboratory, London; and Courtesy: Ionic Plating Ltd.)

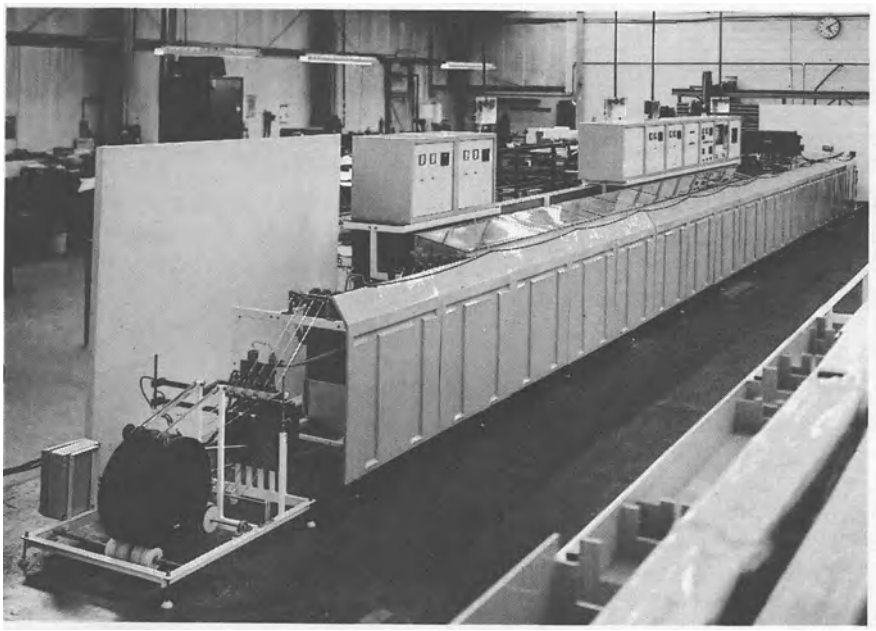

Fig. 8.19 A continuous reel-to-reel electroplating line. The machine is a four-strand device which incorporates pretreatment sections prior to electroplating. A typical application is the selective electroplating of gold spots onto nickel–iron lead frames, which is an important stage in the manufacture of integrated-circuit packages. (Courtesy: S. G. Owen (Northampton) Ltd.)

Table 8.5 Pros and cons of electrodeposition as a coating technique

Advantages	Disadvantages
Control of deposit thickness good	Only some metals may be deposited from aqueous solution
Control of deposit distribution fair	Rate of deposition limited to 20–100 $\mu m\, h^{-1}$
Variety of finishes possible	Thickness ranges limited in practice, e.g. <1 μm, too porous; >70 μm, too expensive
Technology readily available at reasonable cost and well-understood	Some substrates require special pretreatment
Most metals depositable	Throwing power variable with, for example, metal, electrolyte and process conditions
Most substrates coatable	
Deposits less porous, at equivalent thickness, than many competitive techniques	

In the light of the above, it is possible to summarize some advantages and drawbacks of electrodeposition as a coating technology (Table 8.5). It may be concluded that electroplating is vital in almost every branch of industry. The technique often provides a versatile and economic method of applying a thin (say 1–75 μm) metal coating which significantly improves the electrical or decorative properties of the substrate.

8.2 ELECTROLESS PLATING

8.2.1 Fundamentals of electrochemical deposition

It is important to distinguish between three types of electrochemical process for the deposition of metals: (1) electroplating; (2) immersion plating; and (3) electroless plating (Table 8.6). They differ in the nature of their anodic reaction. Considering the simple case of discharge of a metal ion, the common cathodic process is given in equation (8.1) as $M^{n+} + ne^- \longrightarrow M$. This is supported by a suitable anodic process (taking place at the same rate).

1. In electroplating dissolution of a separate anode, M_a occurs:

$$M_A - ne^- \longrightarrow M_A^{n+} \tag{8.16}$$

Table 8.6 Comparison of electrochemical methods for metal deposition

Property	Electroplating	Electroless deposition	Immersion plating
Driving force	Power supply	Autocatalytic redox reaction	Chemical displacement
Cathode reaction	$M^{n+} + ne^- \longrightarrow M$	$M^{n+} + ne^- \longrightarrow M$	$M^{n+} + ne^- \longrightarrow M$
Anode reaction	$M^n - ne^- \longrightarrow M$ or $n/2\ H_2O - ne^- \longrightarrow n/4\ O_2 + nH^+$	$R - ne^- \longrightarrow O$	$M_1 - ne^- \longrightarrow M_1^{n+}$
Overall cell reaction	$M_A \longrightarrow M_C$ or $n/2\ H_2O + M^{n+} \longrightarrow n/4\ O_2 + nH^+ + M$	$M^{n+} + R \longrightarrow M + O$	$M^{n+} + M_1 \longrightarrow M + M_1^{n+}$
Site of cathode reaction	Substrate (workpiece)	Substrate (workpiece) which must have a catalytic surface	Substrate (workpiece) which must remain partially exposed
Site of anode reaction	Separate anode	Substrate (workpiece)	Substrate (workpiece) which dissolves
Anode reactant	M or H_2O	R, reducing agent in solution	M_1, dissolving metal
Nature of deposit	Pure metal (or definite alloy)	Usually M contaminated by O/R derived species	Pure metal, but may be porous and poorly adherent
Thickness limit/μm	1–100	1–100	$\ll 10$

(or oxygen evolution takes place). The overall cell reaction is then:

$$M_A \longrightarrow M_C \tag{8.17}$$

In an ideal case, metal is simply transferred from anode to cathode.

2. In immersion deposition, simple displacement occurs as the substrate metal N dissolves:

$$M^{n+} + M_1 \longrightarrow M + M_1^{n+} \tag{8.18}$$

and M will deposit onto M_1, often in a porous and poorly adherent manner, at

a declining rate; the substrate metal, eventually will no longer be exposed to the electrolyte and deposition ceases.

3. In electroless deposition processes, the oxidation of a soluble reducing agent R

$$R - ne^- \longrightarrow O \tag{8.19}$$

occurs on some sites on the substrate surface such that the overall process is:

$$M^{n+} + R \longrightarrow M + O \tag{8.20}$$

The deposition of the metal is autocatalytic; once nucleation has occurred, further deposition is a very favourable process which occurs at a fast rate on the growing deposit.

The electroless process can be traced back to laboratory observations by Wurtz in 1844. Despite research by other workers in 1911 and 1931, industrial developments did not begin until 1946, when Brenner and Ridell devised an acid electroless nickel bath. Today, the majority of electroplated metals have been deposited successfully from electroless baths, but fundamental knowledge of the underlying chemical and electrochemical reactions is at an early stage. Moreover, considerable skill and research work is often necessary to formulate a practical electroless plating bath. Thermodynamically favourable but unwanted dropout of the metal in the bulk electrolyte or the plating tank walls is always a danger; the bath must deposit the metal at a high rate, but selectively onto the substrate!

By far the most important examples of electroless deposition in industry are deposition of:

1. Nickel onto steel substrates, largely for engineering applications, but also for uses in the electronics industry.
2. Copper onto printed circuit boards and plastics (section 8.1.6) (following surface activation).

These applications will be described in section 8.2.3, but first, the formulation and composition of electroless plating baths will be considered.

8.2.2 Composition of electroless plating baths

An electroless plating liquor in general will contain the following components: (1) a source of soluble, electroactive metal; (2) a reducing agent; (3) a complexant; (4) an exaltant, which may help to increase the rate of plating; (5) stabilizers to prevent bath decomposition; (6) other addition agents; and (7) a buffer to control pH.

Typical examples of electrolytes and operating conditions are given in Table 8.7.

Taking electroless nickel plating as an illustrative example, the reducing agent is often hypophosphite; the process may be represented by the much simplified

Table 8.7 Composition and operating conditions for selected electroless plating processes

Bath/Deposit	Formulation	
Acid nickel	Nickel chloride	20 g dm^{-3}
	Sodium hypophosphite	20 g dm^{-3}
	Sodium acetate	10 g dm^{-3}
	Sodium succinate	15 g dm^{-3}
	pH	4.5
	Temperature	93° C
Alkaline nickel	Nickel chloride	30 g dm^{-3}
	Sodium hypophosphite	10 g dm^{-3}
	Ammonium citrate	65 g dm^{-3}
	Ammonium chloride	50 g dm^{-3}
	pH	8–10
	Temperature	90° C
Alkaline cobalt	Cobalt chloride	30 g dm^{-3}
	Sodium hypophosphite	30 g dm^{-3}
	Sodium citrate	50 g dm^{-3}
	Ammonium chloride	40 g dm^{-3}
	pH	8.5
	Temperature	90° C
Copper	Copper sulphate	12 g dm^{-3}
	Formaldehyde	8 g dm^{-3}
	Sodium hydroxide	15 g dm^{-3}
	Rochelle salt	14 g dm^{-3}
	EDTA	20 g dm^{-3}
	pH	11
	Temperature	25° C

reactions:

Cathode $Ni^{2+} + 2e^- \longrightarrow Ni \qquad E^\ominus -0.25\ V$ (8.21)

Anode $H_2PO_2^- + H_2O \longrightarrow H_2PO_3^- + 2H^+ + 2e^- \qquad E^\ominus = -0.50\ V$ (8.22)

Overall cell $Ni^{2+} + H_2PO_2^- + H_2O \longrightarrow Ni + H_2PO_3^- + 2H^+$

$\Delta G = -48.3\ kJ\ mol^{-1}$ (8.23)

which take place on a single surface.

Several general points may be made.

1. The substrate metal (after surface preparation) and the deposited metal must support both reactions (8.21) and (8.22) for the electroless process to occur.
2. Substrates may be active upon immersion, or they may briefly be stimulated cathodically by, for example:
   (a) contact with a workpiece which is already plating;
   (b) an impressed current, courtesy of an external battery or power supply.

3. A pH decrease accompanies the overall cell reaction as in equation (8.23).
4. The reducing agent is depleted and its oxidation product accumulates.
5. The source of metal declines in concentration.

The exact mechanisms of the chemical and electrochemical reactions occurring during electroless plating are still obscure. In the case of electroless nickel, they are far more complex than those suggested by reactions (8.21) and (8.22). Other reactions are possible besides the formation of a metallic coating. For example, the hypophosphite bath can lead to the formation of phosphorus, resulting in a Ni–P alloy deposit.

The amount of phosphorous codeposition varies between 3% and 15%. When borohydride is used as the reducing agent, boron is incorporated in the deposit, while no codeposition is observed when hydrazine or formaldehyde are part of electroless formulations. Hydrazine is not very popular as a reducing agent owing to its potentially explosive nature and recent reports suggest that it may be carcinogenic.

The selection and concentration of the complexant must be considered very carefully, because if the metal is too-heavily complexed, insufficient free metal ions will be available for deposition. For instance EDTA, which has a high stability constant, requires very careful control if plating is not to cease.

As reactions in the bath involve the formation of either protons or hydroxyl ions, the pH of the solution will alter during plating and thus affect the rate of deposition and composition of the deposit (section 8.2.3 and 8.2.4). Buffers have to be added to stabilize the pH of the solution, and these include the carboxylic acids in acid media (which also act as complexants) and ammonia/ammonium chloride or organic amines in alkaline solutions.

Electroless plating formulations are inherently unstable and the presence of active nuclei such as dust or metallic particles can lead over a period of time to a process analogous to homogeneous reduction. Stabilizers, which adsorb onto these active nuclei and shield them from the solution, are added in small concentrations to overcome this problem. Typical examples are lead, calcium or thallium ions, thiourea and mercaptobenzthiazole. However, if they are used in excess, deposition will be completely prevented even on the substrate itself.

The rate of plating may be lowered drastically by the addition of complexants to the formulation. Additives which increase the rate to an acceptable level without causing bath instability are termed 'exaltants'. These are generally anions which are thought to function by catalysing oxidation of the anodic process. Common examples include sodium succinate, glycine and fluoride ions.

8.2.3 Operating conditions

The successful operation of an electroless process unfortunately does not end with the selection of the correct ingredients for the bath. The rate of deposition is markedly affected by temperature. This is clearly shown by the acid electroless

nickel formulation given in Table 8.7. Plating does not commence until a temperature of 70° C is reached. A further rise in temperature causes a dramatic increase in deposition rate with a value of over 20 $\mu m\, h^{-1}$ being obtained at 92° C. Temperatures above this value will make the bath very unstable and may cause metal deposition on the jigs and the walls of the tanks, or complete homogeneous reduction of the solution. The practical consequence of this experimental observation is that large objects to be coated have to be preheated to the operating temperature prior to immersion. This necessitates the use of accurate temperature controllers if consistent coating thicknesses are to be achieved without resorting to the use of test coupons in the bath for each batch of components plated. Current research is aimed at reducing the operating temperatures of the baths, and at present electroless copper baths for the printed-circuit-board industry are operated near room temperature.

As already stated, the pH of the solution alters the potential difference between the anodic and cathodic reactions and this is reflected in the plating rate which increases with pH. This is in agreement with the theoretical principles outlined earlier. The limit to which the pH can increase is determined by the value at which precipitation occurs. Large variations in pH may cause fine precipitates to form (e.g. nickel phosphite, cuprous oxide) and these may act as seed crystals for the complete reduction of the plating solution.

Some of the chemicals in the bath are consumed during operation (e.g. metal ions, reducing agent) and will produce by-products. Other chemicals will be unaffected but may be lost in dragout. The concentration of constituents will thus be changing continuously and will influence the plating rate. The rate increases sharply to reach a maximum of 20 $\mu m\, h^{-1}$ at 12 $g\, dm^{-3}$ of sodium hypophosphite for the acid electroless nickel process. Variations in the composition of other constituents will have effects on the speed of plating and therefore continuous analytical monitoring and make-up of the solution is required if consistent rates of deposition are to be attained.

8.2.4 Properties of electroless deposits

The cost of electroless coating a component is generally higher than that of conventional electroplating owing mainly to the use of more expensive chemicals and the necessity of heating the solutions. Moreover, the rates of deposition are rather low, ranging from a typical 25 $\mu m\, h^{-1}$ for acid electroless nickel baths down to 2 $\mu m\, h^{-1}$ for alkaline copper solutions at room temperature (although the recently developed 'heavy coppers' can plate at 6 $\mu m\, h^{-1}$). The use of electroless techniques is therefore restricted to those situations where the properties of the coating or the mode of application outweigh the overall cost of the process. A summary of the general properties is given in Table 8.8. One of the main advantages is its excellent throwing power. As no external current is employed, a uniform coating thickness will result provided the electrolyte is

Table 8.8 General characteristics of electroless deposition of Ni–P alloys

Deposition on non-conductors (e.g. plastics) is possible
Uniform thickness coating
Good throwing power
No levelling required
Coating is harder (480 HV) than electrodeposited metal (200 HV) as other elements (e.g. phosphorus, boron) are incorporated in the structure
The deposit can be further hardened to 1050 HV by heat treatment at 400° C for 1 h
The deposit has good wear resistance
Very low ductility (1–3% elongation)
Low porosity leads to good corrosion resistance
Solutions are expensive
Slow rate of deposition
Careful analytical control of the bath required

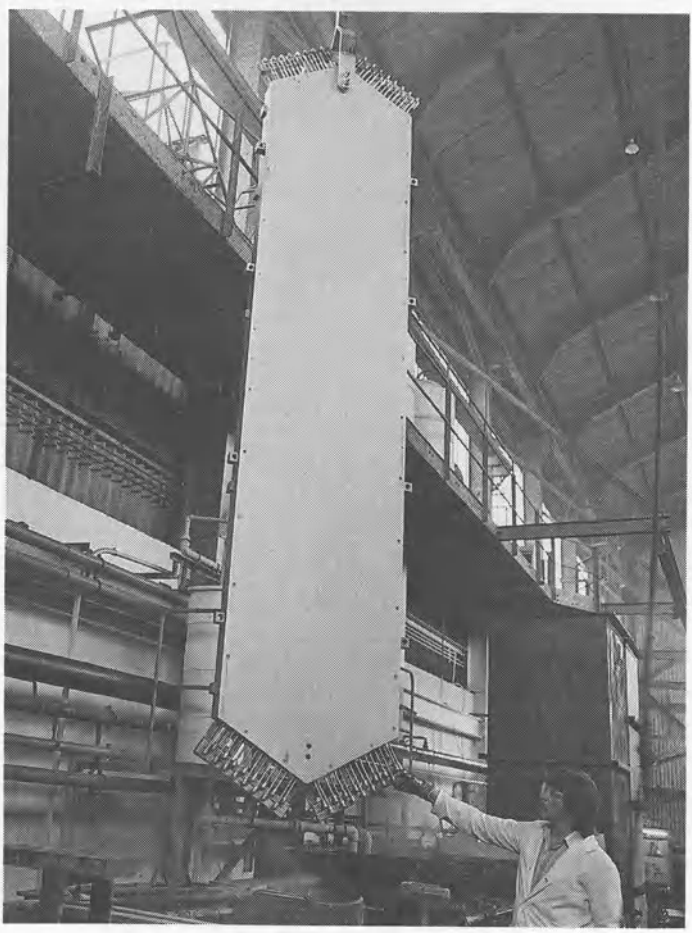

(a)

accessible to all areas of the component to be plated. This is very useful where it is necessary to plate inside tubes, recesses, threads, etc., the main concern being that hydrogen gas liberated is not trapped in blind holes. This even coating distribution, coupled with low porosity, imparts excellent corrosion resistance to the plated component, although some authors attribute this property to the presence of alloying elements (e.g. P or B) in the metallic film. Recent research has shown that the high temperature oxidation resistance of cobalt and nickel is increased by the presence of boron.

As already mentioned, electroless coatings are harder than conventional electroplated articles and as a result the wear resistance is increased. This property restricts the ductility of the deposit, with elongation values of 1–3% being found for electroless nickel. The residual stress is far higher than that of a sulphamate nickel electroplate and is generally tensile, which can be a serious hazard in certain industrial situations where crack propagation has to be avoided at all costs.

(b)

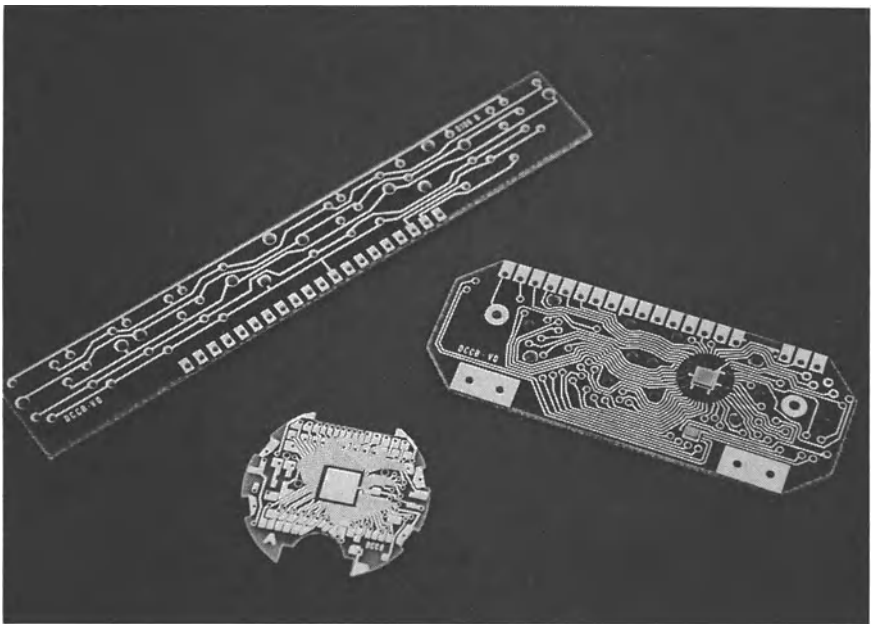

Fig. 8.20 Applications of electroless nickel plating: Ni–P deposits for wear-resistant and corrosion-resistant applications in engineering. (a) A cooling-coil assembly. (Photography courtesy: Ionic Surface Treatments; plating by Dudley Division.) (b) Printed circuit boards for a wrist watch and calculators. Electrically isolated areas of deposited copper may be built up by electroless nickel plating which also provides a corrosion-resistant and solderable finish. The deposits are various NIKLAD electroless nickels. (Photograph Courtesy: Lea Manufacturing.)

There is a divergence of opinion as to whether the nickel deposited from acid solution is amorphous or crystalline, although it is agreed that cobalt and copper coatings from alkaline electrolytes are crystalline. The phosphorus or boron is believed to be present in the film as a supersaturated solid solution. This causes the deposit to be hard, and in general electroless coatings are twice as hard (480 HV) as conventional electroplated metals (200 HV). This supersaturation allows the hardness to be increased further by a subsequent heat treatment which results in the formation of tiny precipitates of intermetallics, e.g. Ni_3P. This process is analogous to age-hardening aluminium alloys. Values of 1050 HV are observed after heat-treating electroless nickel coatings containing phosphorus at 400° C for 1 h, and even higher values (1300 HV) are obtained if nickel boron deposits are subjected to the same thermal treatment.

8.2.5 Applications of electroless deposition

Corrosion-resistant, light and resilient polymer substrates are electroless plated with metal for largely decorative and functional applications. Modern polymers which are decoratively plated (e.g. with Ni then Cr) include ABS (acrylonitrile/butadiene/styrene), PPO (polyphenylene oxide) and PAE (polyarylether). Following cleaning and etching procedures, the polymer surface is 'activated' by depositing an adsorbed Pd layer by immersion in a Pd-containing solution. The Pd surface acts as a catalyst for electroless copper or nickel plating. Subsequent electroplating by, for example, copper, nickel then chrome provides a visually pleasing finish which also protects against excess heat, ultraviolet degradation, wear and the build-up of static electricity. An extremely wide range of components are finished in this fashion for consumer, domestic, electronic and automative sectors of industry, examples including knobs on hi–fi equipment, tops on perfume bottles, costume jewellery and car trim.

Electroless nickel–phosphorous coatings are being used increasingly in electronics applications (Fig. 8.20(b))*, particularly as a means of increasing the solderability of aluminium, providing a non-magnetic underlay† in magnetic components, producing a reasonable electrical conductivity combined with ease of solderability (< 3% P) and as an intermediate diffusion barrier for gold plating on copper connectors.

* This is despite the rather high electrical resistivity which, at 60–70 μΩcm is some 10 times greater than pure nickel.

† Upon heat treatment, however, the weak coercivity can increase dramatically (by a factor of 30).

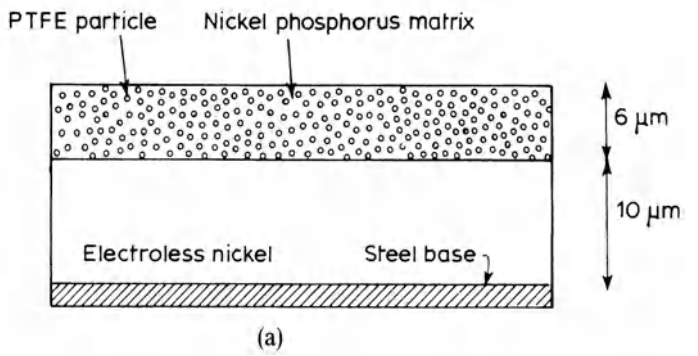

(a)



(b)

Fig. 8.21 Electroless nickel–PTFE deposition. (a) The deposit contains up to 23% by volume of PTFE as dispersed particles. The deposit has a typical composition of Ni 87%–P 7%–PTFE 6% wt. (b) Engineering applications utilize the low-friction corrosion resistance and self-lubricating properties. In addition to the threaded and grooved components shown, examples include ball and butterfly valves, pistons and moulds for plastics or rubbers. (Courtesy: Ionic Surface Treatments. Ionlube coatings by Dudley Division.)

The major field of application for Ni–P electroless coatings undoubtedly lies in engineering, due to its unique combination of good corrosion and heat resistance, wear resistance, high lubricity, higher hardness and uniform thickness distribution. The hardness of the deposit may be increased from approximately 400–600 HV to over 1000 HV by suitable heat treatment (typically 1 h at 400° C). Typical deposit rates for acid hypophosphite baths are 10–20 $\mu m\, h^{-1}$ at pH of 5 and 90° C.

8.2.6 Electroless deposition of composites

As in the case of electroplating, a range of dispersed inert particles may be codeposited with the electroless metal. There are two particular aspects which may cause process control problems, compared to electroplating.

1. The small dispersed particles may become active nuclei for autocatalytic deposition of metal, leading to bath instability.
2. Physical methods of particle entrapment (i.e. agitation) assume increased importance as the absence of a potential field precludes electromigration of charged particles.

An example of a developing coating is shown in Fig. 8.21 with applications for electroless Ni–PTFE coatings. These mimic their electroplated counterparts, but incorporate the advantages of electroless deposition (section 8.2.5). Diamond, SiC and graphite have also been incorporated into electroless Ni–P alloy deposits.

8.3 CONVERSION COATINGS

The presence of a suitable passive film on a metal can confer a high degree of corrosion resistance (Chapter 10), increased electrical insulation, an aesthetically pleasing surface finish, enhanced ability to key a subsequent paint film or the facility to absorb a dye or an oil.

A number of electrochemical treatments are used widely to produce inorganic 'conversion coatings' on a metal, the surface layers including oxides, chromates, phosphates and their mixtures. Depending upon the process, these treatments may be carried out under open circuit or they may be driven by an impressed current.

8.3.1 Anodizing

Anodizing is the process of forming a surface oxide film by electrochemical oxidation. It is used as a surface-finishing technique particularly for aluminium

but also for titanium, copper and steel, and for the manufacture of electrolytic capacitors based on aluminium, tantalum and niobium.

Aluminium is a very important metal. It is light, has a high conductivity and mechanical strength and is widespread in nature. Its extraction is, however, difficult and energy-intensive (section 4.1.1) and it is therefore fortunate that there is a simple and cheap way of surface-finishing aluminium which gives it both corrosion resistance and a pleasant appearance, i.e. anodizing. Indeed, as a finished product, aluminium compares well with steel as regards energy consumption per tonne. Perhaps 5–10% of the aluminium produced is anodized prior to sale for use in the construction of buildings, for household articles and for power transmission.

For these applications, aluminium is anodized in an acid electrolyte, usually 10% sulphuric acid although chromic acid and sulphuric acid/oxalic acid mixtures are also employed. Oxalic acid at low current density gives excellent results and is used for aluminium which is to be coloured. Chromic acid is preferred for the anodizing of complex shapes where thorough rinsing of the surface after oxidation is a problem; aluminium will corrode in sulphuric acid but not in chromic acid which passivates the surface.

A simple way of writing the electrode reaction in anodizing is:

$$2Al + 3H_2O - 6e^- \longrightarrow Al_2O_3 + 6H^+ \tag{8.24}$$

although, in practice, the outer surface oxide is hydrated, being primarily bohmite, $Al_2O_3 \cdot H_2O$ and (especially at high anodic potentials) significant oxygen evolution occurs:

$$2H_2O - 4e^- \longrightarrow O_2 + 4H^+ \tag{8.25}$$

At the inert cathode, hydrogen evolution is the main reaction:

$$2H^+ + 2e^- \longrightarrow H_2 \tag{8.26}$$

Anodizing is carried out in simple tanks very similar to those used for electroplating and the cathodes are steel or copper; the temperature is 20–25° C. The voltage is programmed to increase from 0 to 50 V so as to maintain an anode current density of 10–20 mA cm^{-2}; the increasing voltage is required to force the aluminium oxide to continue to thicken to the 10–100 μm layer needed to impart good corrosion resistance. Throwing power is not usually a problem since, once a partial layer of oxide is formed, that area will passivate and further oxide will be formed most readily on the parts of the surface as yet uncovered. In certain cases, (e.g. the internal structure of tanks) auxiliary cathodes are used, as in certain electroplating operations. Formation of the 2–100 μm layer will take from several minutes to one hour, depending upon the process.

The aluminium oxide formed in this process has a complex form. It is partly hydrated and has a two-layer structure. At the surface of the metal there is a thin (perhaps 0.025 μm), compact boundary layer and then a porous overlayer. The latter has a very open structure and structural techniques (Fig. 8.22) show it to

consist of a collection of parallel tubes perpendicular to the surface. After the anodic oxidation, the metal is dipped into a sodium hydroxide solution to precipitate aluminium hydroxide in the pores and, hence, produce a more robust layer. The thickness of the barrier layer and of the tubular cell walls depends on the cell voltage applied, but mainly upon the interrelated factors of electrolyte composition, temperature and applied current density. Hence, selection of the electrolyte and suitable control of the electrolysis can tailor the properties of the anodized film to suit the application. For example, in sulphuric acid solutions, dilute electrolytes and low temperatures give small pore size and a hard deposit, suited for engineering purposes. Higher H_2SO_4 levels and higher temperatures provide a more open cell structure more suited to dyeing prior to decorative applications.

Aluminium can also be produced in a number of coloured finishes. Two types of method are used: (1) an organic dye (which may be a traditional dye) is adsorbed on the freshly anodized surface and it is then sealed with boiling water; and (2) a metal, often nickel, cobalt or tin, is deposited into the pores using an a.c. power supply. The resulting colours resulting from this 'electrocolouring' process are due to interference effects, and a wide range of tints can be produced by variation of the plating time and conditions. The divalent tin process, often based upon proprietory addition agents in an acidic solution (20 g dm^{-3} H_2SO_4) of

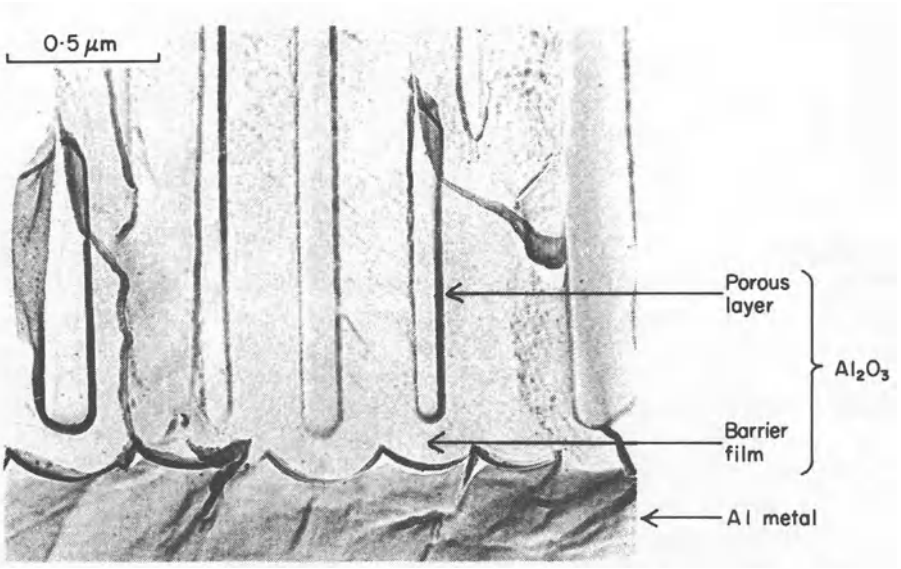

Fig. 8.22 Transmission electron micrograph of a carbon replica of a fracture section through an anodic film formed on aluminium. Anodizing conditions were 150 V for 70 minutes in 0.5 mol dm^{-3} phosphoric acid. (Courtesy: Dr. G. E. Thompson, Corrosion and Protection Centre, University of Manchester Institute of Science and Technology.)

stannous sulphate ($10\,g\,dm^{-3}$) with a.c. power, can produce a wide range of colours from pale gold through bronze to black, depending upon current density and time.

As with electroplating, the aluminium must be prepared and cleaned prior to anodizing. The pretreatment schedule depends upon the type of finish (and, hence, the application). The following sequence provides a typical example. Not all the steps are used in every process.

1. Mechanical treatments (e.g. wire-brushing, grit-blasting, abrasive-sanding or polishing) serve to remove minor surface imperfections and improve the surface finishing.
2. Chemical treatments (e.g. chemical polishing, electropolishing, or etching) may be used to control the surface texture.
3. Chemical cleaning by, for example, solvents or alkaline dips or electrocleaners, serve to remove oils and greases and detach oxide scale.
4. Chemical (or electrolytic) etching, often in an alkaline solution, predominantly fixes the surface texture.
5. Desmutting is the removal of surface smut (e.g. intermetallics, oxides, metal and carbon) together with the neutralization of residual alkalinity from (4); modern solutions, often based on iron salts, have partly replaced nitric acid liquors.
6. Anodizing.
7. Dyeing.
8. Sealing.

Sealing is usually accomplished by immersion in hot (sometimes boiling) water, or metal salt solutions. Hydration of the surface oxide occurs, the accompanying volume increase swells the cell walls and seals the pores.

The type of surface finish obtained in anodizing depends not only on the process conditions but also on the aluminium alloy concerned (and its pretreatment). Whilst a wide range of alloys can be anodized for corrosion protection, fewer can be colour-finished adequately and fewer still provide acceptable bright finishes. Careful selection and handling of aluminium is important, in addition to effective pretreatment.

Indeed, anodizing often exaggerates surface defects such as pits, cracks, inclusions, embedded soil or segregated phases. While this is an irritation in decorative or prestige architectural applications, anodizing provides a useful method of checking aluminium and magnesium alloy castings for surface flaws, e.g. cracks are sometimes revealed as darkened streaks bordered by yellow staining.

The majority of anodizing is performed using process equipment similar to that found in electroplating. Tanks are typically rubber, plastic or lead-lined steel (which may also serve as the cathode) in the case of sulphuric acid; mild steel tanks are preferred for chromic acid. The vigorous oxygen evolution during anodizing creates a fine acid mist which requires effective ventilation and/or

spray suppressants. Temperature control is often critical and cooling coils are usually provided to counteract heat generated by iR drop in the electrolyte and also the oxide film. Air agitation and forced flow of the electrolyte minimize concentration and temperatures gradients and prevent gas sticking to the workpieces.

The main cathode reaction is hydrogen evolution. Aluminium jigs have been used widely in anodizing but it is necessary to remove periodically the oxide film formed on unprotected areas. Titanium jigs are increasingly used as they do not anodize significantly in H_2SO_4 solutions. However, the jigs are appreciably more expensive and larger cross-sections are necessary because of its lower conductivity.

Table 8.9 provides examples of anodizing processes including electrolyte composition and typical applications.

The majority of aluminium anodizing processes utilize a sulphuric acid electrolyte. However, chromic acid anodizing may be preferred for the following reasons:

1. Minimum loss of metal and maximum corrosion protection are obtained from a thin ($\simeq$ 2.5 μm) opaque grey coating.
2. Minimum loss of fatigue strength upon anodizing.
3. Facile detection of flaws due to subsequent seepage of the yellow chromic acid liquor.
4. Components which have recesses, blind holes, crevices, etc. from which electrolyte is difficult to remove completely.
5. Anodizing of very thin (< 0.25 mm) material.

Anodizing is also employed in the fabrication of electrolytic capacitors, although the properties of the oxide film and the process conditions used contrast markedly with those described above. The oxide layer should be relatively thin for an electrolytic capacitor, but non-porous and very compact so as to act as an effective barrier to electron transfer, i.e. 'barrier' layers are required.

Thus, aluminium-based capacitors are manufactured by anodizing in a neutral medium, phosphate or borate, and a voltage source capable of an output of 500 V d.c. is required to thicken the layer to the 1 μm generally employed. High-stability capacitors often utilize tantalum or niobium anodized in this way.

The adoption of a particular metal-finishing treatment is often sensitive to fashion as well as technical and economic constraints. An example of this is provided by the recent introduction of anodized titanium jewellery, where the wide range of iridescent colours (dependent upon voltage and thickness) provide an aesthetically pleasing and durable item.

8.3.2 Phosphating

Phosphate coatings provide an underlayer for paint finishes on a wide variety of components. The principal substrate is steel, although zinc and aluminium may also be phosphated. The major advantages of phosphate coatings are improved

Table 8.9 Typical process conditions for aluminium anodizing and their applications

Electrolyte	Composition/ g dm^{-3}	Temperature/ °C	Cell voltage/V	Current density/ mA cm^{-2}	Cathodes	Deposition rate/μm h^{-1}	Nature of film (undyed)	Application
Sulphuric acid	175–250	20–25	10–24	10–15	Al or Pb	25	Transparent and near-colourless	General use; architectural cladding; window frames
	175	−5–5	22–80	20–50	Al or Pb	16	Transparent and near-colourless	Hard anodizing for engineering applications, e.g. cylinder linings; boat winches
Sulphuric/ oxalic acid	175 H_2SO_4 + 50 oxalic acid	20–30	10–16	10–15	Al or Pb	20–30	Transparent and near-colourless	Normal anodizing (as above)
		7–10	25–80	20–30	Al or Pb	40–60	Transparent and near-colourless	Hard anodizing (as above)
Chromic acid	50	50–55	Raised from 0 to 30, then maintained	10–15	Stainless steel or mild steel	13–20	Opaque grey-white, possibly enamel	High corrosion resistance; aircraft assemblies; military work; flaw detection in castings or forgings; as a paint primer; decorative uses, e.g. knitting needles

corrosion resistance and paint adhesion. In special applications (e.g. wire-drawing), the anti-seizure properties of phosphating are important, and in these circumstances heavy films may be overcoated with protective oils or greases.

The most important applications utilize a relatively thin coating of mixed iron and zinc phosphates on steel sheet as a standard pretreatment before painting of automotive bodies and other sheet-steel fabrications, e.g. refrigerators and washing machines. In the case of car bodies, electrophoretic priming (section 8.4) usually follows the phosphating stage.

Traditionally, phosphating has been applied by a high-temperature (60–90° C) immersion, the process taking between perhaps 10 min to several hours. Modern phosphating solutions contain a number of additives to accelerate the process; temperatures may be as low as 35° C and spray or combined spray–dip operations are used increasingly.

A modern phosphating bath often has a complex composition, but contains three essential components: (1) free phosphoric acid; (2) a primary metal phosphate; and (3) an accelerator. The pH is usually within the range 1.8 to 3.2; lower pHs are favoured for immersion deposits while spray processes often employ a high pH. The majority of routine phosphating processes involve open-circuit processing, but cathodic and (especially) anodic stimulation of the process is receiving increasing attention due to the possibilities of shorter process times and improved control over the deposited film.

The chemical and electrochemical reactions taking place during phosphating are complex; the combined substrate and electrolyte conditions exert a great influence on the structural characteristics of the phosphate layer. A greatly simplified version of the chemical reactions would envisage the dissolution of the metal (M = Fe, Zn, Mn) and its oxides, followed by the deposition of an insoluble phosphate layer.

In the case of zinc phosphate baths applied to steel substrates, the major phosphates deposited are hopeite ($Zn_3(PO_4)_2 \cdot 4H_2O$) = H and phosphophylite ($Zn_2Fe(PO_4)_2 \cdot 4H_2O$) = P. While there is considerable debate over its usefulness, the ratio P : P + H (obtained from X-ray diffraction measurements) has been applied as a quality-control method.

The quality of the phosphate layers on steel are classified crudely according to coating weight per unit area. Heavy weight (Fe-, Zn-based) coatings ($< 7.5\ g\ m^{-2}$) tend to be used for maximum protection under oils and greases. Medium-weight ($< 4.3\ g\ m^{-2}$) coatings are usually based on zinc and may be overpainted or covered in oil for general protection. Lightweight (1.1–4.3 $g\ m^{-2}$) phosphate layers are usually employed under paint and lacquers for routine metal finishing of sheet steel.

8.3.3 Chromating

Despite their toxicity, chromate solutions are widely used to provide protective and decorative conversion coatings on aluminium and magnesium–aluminium alloys, zinc and cadmium.

Application areas for chromate coatings include the following:

1. Aluminium or magnesium–aluminium alloy castings and extrusions are chromated to provide a decorative and protective finish.
2. Aluminium strip is chromated in order to provide an intermediate, adhesion-promoting coating prior to painting and lacquering in the canning industry.
3. Zinc- or cadmium-electroplated steel articles are frequently passivated with a chromate coating in order to enhance corrosion resistance, improve solderability and provide a pleasing (e.g. iridescent) finish.

8.4 ELECTROPHORETIC PAINTING

Paint coatings are perhaps the most versatile and widely applied method of corrosion protection, offering a wide range of decorative colours and textures and the ability to coat complex structures. While the formulation and chemistry of paints is complex, the cured paint film consists, in essence, of a cross-linked organic polymer film (or 'binder') containing a dispersed filler (pigment) together with additional solids and inhibitors. A broad spectrum of application methods is used but the vast majority of paint is applied by brush, spray or roller.

When the substrate is conducting, electrophoretic deposition of paint may be carried out. Indeed, in the case of steel automobile bodies, almost all factory-based primer coating is performed by electrophoretic painting.

8.4.1 Principles of electrophoretic painting

The medium for the electropainting process is water, sometimes containing a low percentage of an organic cosolvent such as cellosolve. The paint is a polymer containing: (1) acidic or basic groups which may be solubilized, usually to give micelles by the addition of base or acid respectively; (2) some inorganic solids such as copper chromate, titanium dioxide or carbon black; and (3) an organic pigment to give the desired colour. The bath contains about 10% solids. When a voltage is applied between two electrodes, deposition will occur at one of them; depending on the charge on the polymer, one will observe anodic or cathodic electrocoating. The following steps in the mechanism are important: (Fig. 8.23).

1. Migration of the charged micelles to the electrode of opposite polarity.
2. Neutralization of the charge at the electrode.

   The major process in anodic electrocoating will be the evolution of O_2, leading to an increase in pH and consequent deposition of the paint in its acid form, i.e.:

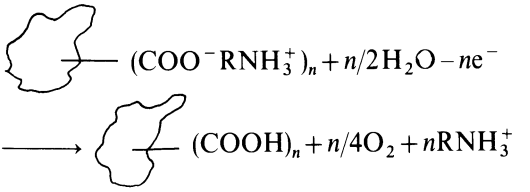

(8.27)

although some corrosion of iron-based materials may also occur, i.e.:

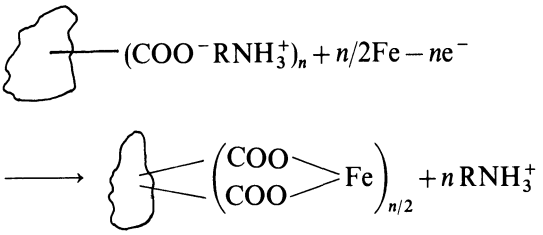

$$\text{(COO}^-\text{RNH}_3^+)_n + n/2\text{Fe} - ne^- \longrightarrow \left(\begin{matrix}\text{COO}\\ \text{COO}\end{matrix}\!\!>\!\text{Fe}\right)_{n/2} + n\,\text{RNH}_3^+ \qquad (8.28)$$

and there is also the possibility of neutralization of the micelles by the Kolbe reaction.

The main reaction in cathodic electrocoating will be the hydrogen evolution with deposition now resulting from formation of a neutral polymeric amine.

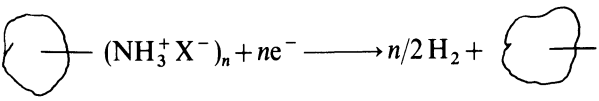

$$\text{(NH}_3^+\text{X}^-)_n + ne^- \longrightarrow n/2\,\text{H}_2 + \text{(NH}_2)_n + n\text{X}^- \qquad (8.29)$$

3. Precipitation of the neutralized polymer with occlusion and adsorption of the inorganic solids and the organic pigments.
4. Removal of water from the polymer layer by electroosmosis in the strong potential field across the non-conducting layer.

Polarity of car body	Anodic (+)	Cathodic (−)
Manufacture of the resin	$\text{R–C(=O)–OH} + \text{KOH} \longrightarrow \text{R–C(=O)–O}^- + \text{K}^+ + \text{H}_2\text{O}$	$\text{R–N:(R)} + \text{R–COOH} \longrightarrow \text{R–N}^+\text{H(R)} + \text{R–COO}^-$
	Insoluble → Soluble	insoluble → soluble
Electrode reactions	$1/2\text{H}_2\text{O} \longrightarrow \text{H}^+ + 1/4\text{O}_2 + e^-$	$\text{H}_2\text{O} + e^- \longrightarrow 1/2\text{H}_2 + \text{OH}^-$
Deposited paint film	R–C(=O)–OH insoluble	R–N:(R) insoluble

Fig. 8.23 A simplified comparison of the reactions during anodic and cathodic electrophoretic painting.

The product of the electrophoretic painting process is a paint layer which adheres strongly to the metal, contains over 90% solids and cures very rapidly on removal from the bath. Again, throwing power is not a problem because the deposit is non-conducting; deposition will occur naturally at uncovered surfaces and a high voltage is required to force the polymer layer to grow to the required thickness.

8.4.2 Principles of electrophoretic priming in the automotive industry

The electrophoretic priming of motor vehicles was introduced in 1963, some years after the principles of electrodeposition of paint were first established. The process is now widespread; indeed, almost all mass-produced, steel car bodies are pretreated in this manner.

The first versions of the process employed anodic deposition, primarily due to the relatively straightforward resin chemistry. Some typical paint formulations would contain: (1) polycarboxylic acids based on acrylic acid as monomer solubilized by an organic amine; (2) alkyds (i.e. branched polyesters) based on naturally occurring long-chain carboxylic acids and polyalcohols, e.g. glycerol; and (3) epoxy resins based on phenols, e.g.:

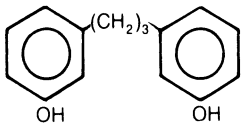

and ethylenechlorohydrin, $ClCH_2–CH_2OH$. The latter two will be dissolved using potassium hydroxide. The anodic process gives a good, reproducible finish but causes some corrosion of the underlying metal (equation (8.28)).

There have been several fundamental problems associated with the in-service behaviour of anodic electroprimers including:

1. Disruption of the phosphate coating, resulting in poor adhesion, chipping and 'scab' corrosion.
2. Poor saponification resistance, giving rise to lower adhesion, general corrosion (particularly with mixed metals, e.g. Zn–Fe substrates).
3. Inadequate protection of bare steel surfaces in zones such as internal box sections, which may lead to pitting, perforation and structural corrosion.

Cathodic electroprimers offer an overall performance superior to any known priming system, particularly at low film thicknesses. Their particular advantages compared to anodic systems include:

1. Improved throwing power and coating uniformity, even for thin films.
2. Better paint stability.
3. Freedom from substrate disruption or dissolution during electropaint application.

Cathodic electrodeposition tends to be more costly and involve complex resin chemistry but its increasing adoption since the mid 1970s reflects the ability to offer major advantages in corrosion protection at a justifiable premium. Indeed, the majority of electropriming is performed currently by cathodic deposition.

The main advantages of electrophoretic painting may be summarized.

1. The paints are water-based, non-toxic and present no fire risk. Moreover, because they have relatively low concentrations of solids and owing to the nature of the process (tanks vs. spray), effluent disposal problems are minimal.
2. The throwing power is good and it is easy to obtain complete coverage of even the most complex surface, e.g. in deep recesses or the insides of pipes.
3. It is well suited for automation.

On the other hand, it is only possible to electropaint conducting surfaces and, hence, the process is limited to a single coat. Also, the colour range is more restricted than with conventional painting. It should also be noted that electrolyte purification and conditioning is critical to the electrophoretic deposition process. Hence, ultrafiltration is widely applied to remove unwanted solids and microparticulates and to maintain electrolyte conductivity at a relatively low level.

8.4.3 The technology of electropriming

Two factors simplify the technology of electrophoretic painting: (1) the high throwing power which removes the need for complex cell geometry; and (2) the low charge and, hence, energy consumption compared with other

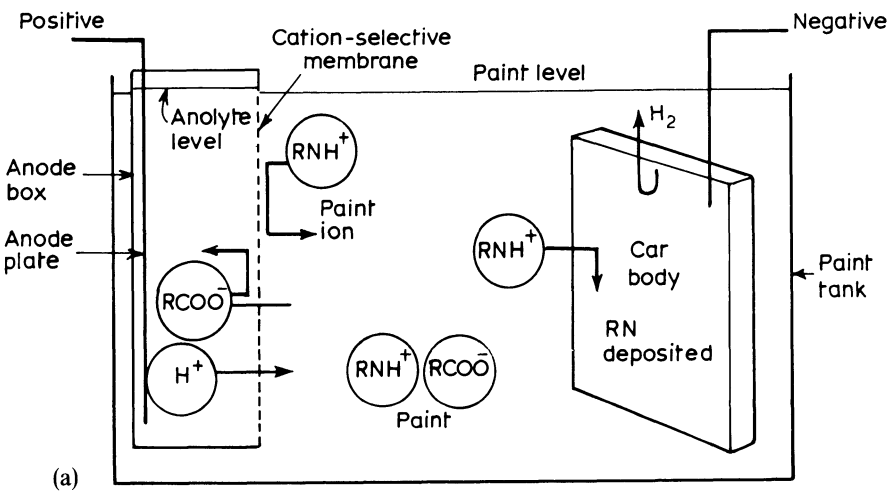

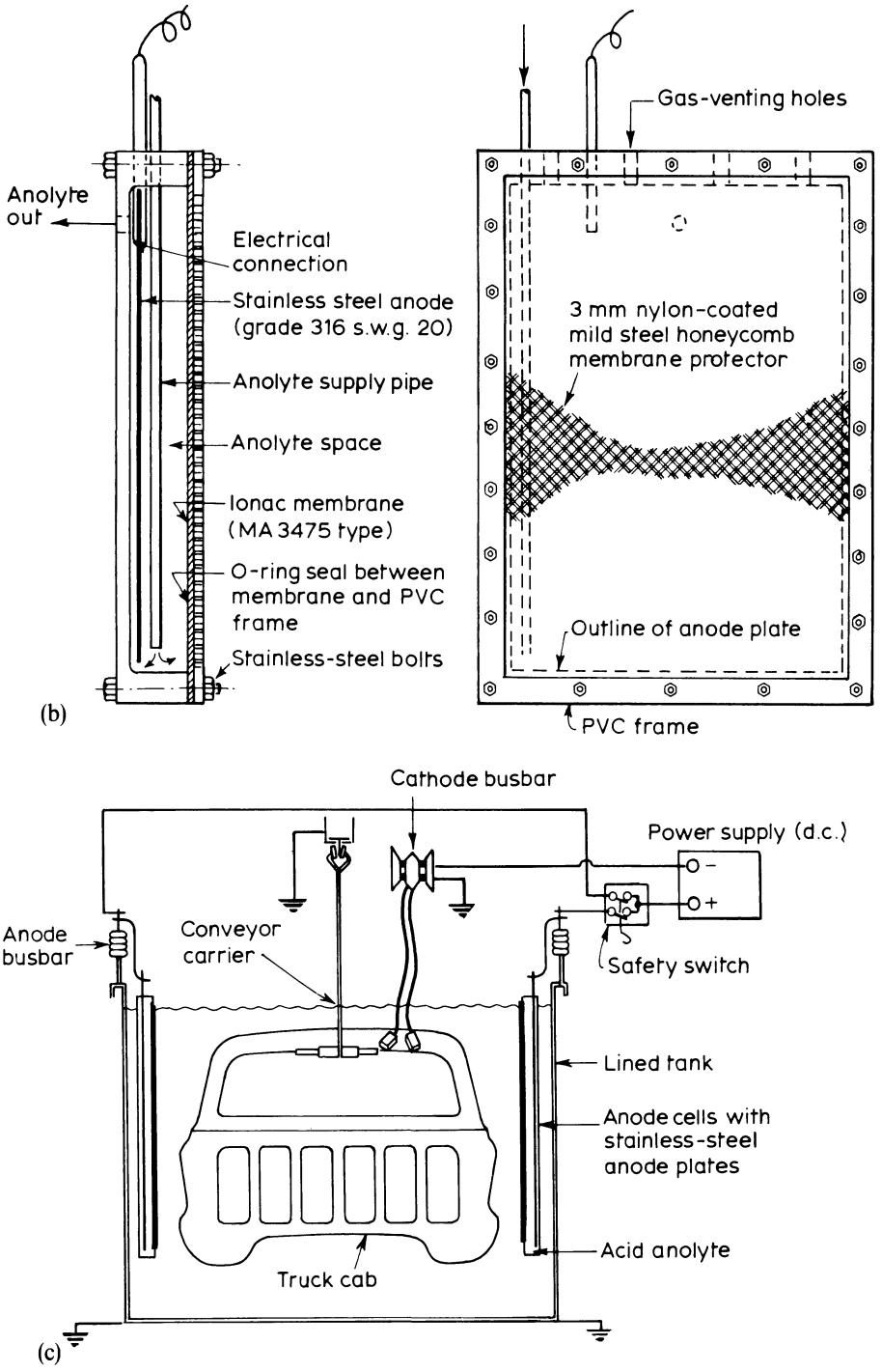

Fig. 8.24 The principles of cathodic electropainting. (a) A divided cell. (b) Detail of the anode box. (c) A general arrangement, showing the electrical connections. (Courtesy: ICI Ltd, Paints Division.)

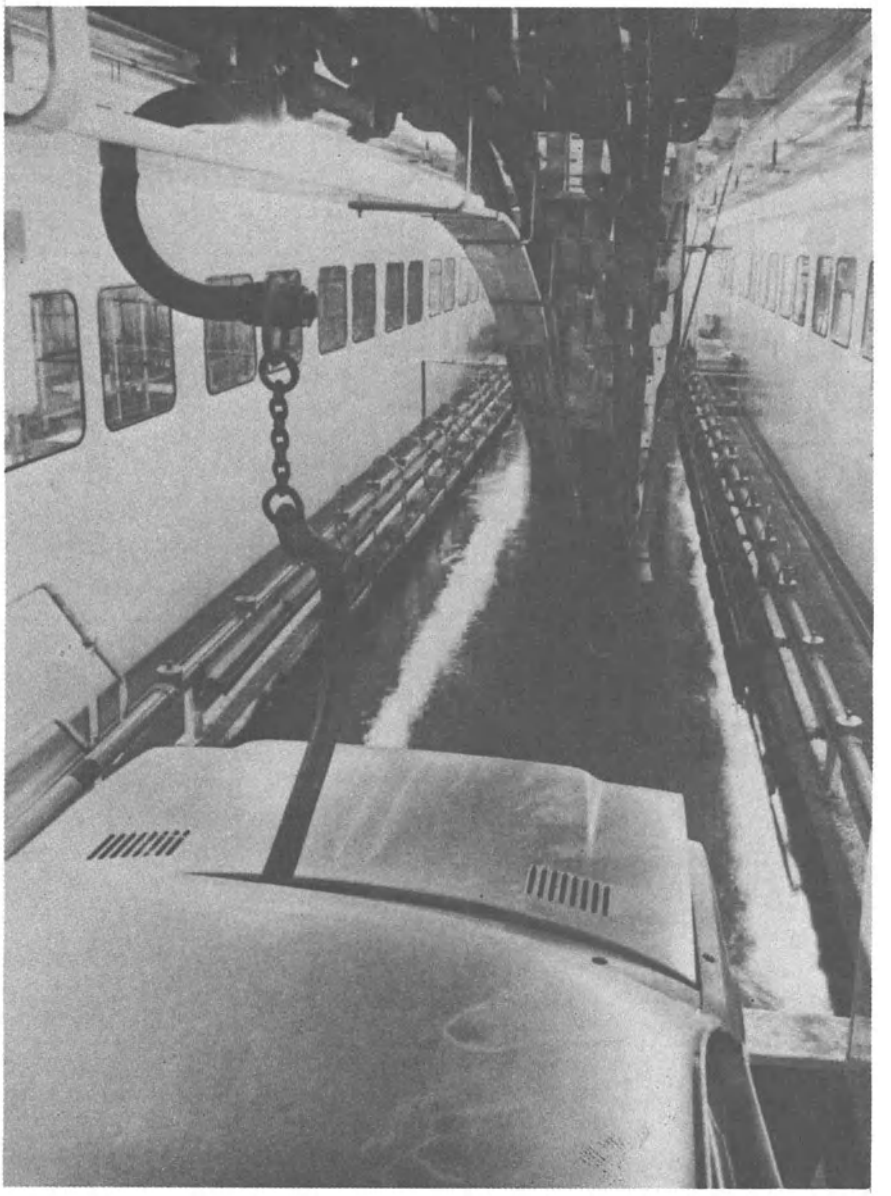

Fig. 8.25 Electrophoretic painting of a car body. (Courtesy: ICI Ltd, Paints Division.)

steps in the overall surface treatment of steels. Hence, many anodic processes use a simple rectangular tank which also acts as the cathode.

The more modern cathodic processes tend to employ more sophisticated engineering. Typically, graphite, steel, or stainless steel anodes are used in an

'anode box' containing cation exchange membranes (Fig. 8.24). Both anodic and cathodic electrodeposition processes will lead to a dilution of the polymer as paint is deposited and it is, therefore, necessary to remove water. This is accomplished continuously using ultrafiltration (i.e. pressure to force the water through a membrane). Plants for undercoating car bodies are usually fully automated and the car body will move slowly through the paint tank with the appropriate voltage applied between it and the tank wall (Fig. 8.25).

Typically, -200 to -300 V are used and the current at a stationary surface will drop from 70 mA cm^{-2} to 5 mA cm^{-2} in the steady state after a few seconds. It then takes 2–5 min to build up a paint layer of 20 ± 5 μm. Application techniques vary but the most common strategy is to dip, sometimes aided by simultaneous spraying of the electrolyte.

As in electroplating, the electrolysis step in electrophoretic painting is only one of a complex sequence which makes up the total surface protection sequence. Thus, for example, the steel in a car body may be treated by: (1) degreasing, cleaning and drying in an oven; (2) spraying zinc phosphate and drying; (3) electropainting, then curing at low-temperatures; and (4) spraying on top coat and curing in an oven.

8.5 OTHER RELATED SURFACE-FINISHING TECHNIQUES

Electrochemical variations of several other surface-finishing methods are used to a limited extent:

1. Electropolishing.
2. Electrochemical cleaning.
3. Electrochemical pickling.
4. Electrochemical stripping.
5. Metalliding.

8.5.1 Electropolishing

Electropolishing is a process used to produce metal articles with a highly reflective mirror finish; it is closely related to anodizing.

The most common metal to be electropolished is aluminium, but the procedure is also used for steel, brass, copper and nickel/silver alloy.

The article to be polished is made at the anode with a current density in the range 100–800 mA cm^{-2} in a bath of phosphoric acid at 60° C for a period of 5–10 min. The cathode material is not critical and may be steel, copper and lead. The mechanism of electropolishing is thought to involve both selective anodic dissolution (the potential distribution will favour corrosion of the surface at peaks rather than in troughs) and oxide film formation. The conditions are somewhat more forcing than those used in anodizing.

Electropolishing leads to extremely reflective surfaces which, unlike mechanically polished surfaces, are stress-free. Before the process can be carried out

successfully, however, the surface must already be smooth since macroroughness cannot be removed.

8.5.2 Electrochemical cleaning

This technique is used to remove grease and oil from metal surfaces. The medium is generally 5–10% caustic soda at 60–80° C and the surface is made cathodic (30–100 mA cm^{-2}). The principles of operation include: (1) a local increase in pH where the grease is sited and, hence, an increase in the rate of hydrolysis to water-soluble products; (2) the evolution of hydrogen gas bubbles which rise to the surface and take organic particles with them, i.e. electroflotation.

8.5.3 Electrochemical pickling

The objective in electrochemical pickling is to rapidly remove rust and other oxides and sometimes to produce a mild, uniform etch to enhance the adhesion of deposits. The surface is usually made anodic in an acid medium, e.g. H_2SO_4 or $FeCl_3$.

8.5.4 Electrochemical stripping

A deposit may be removed rapidly and selectively from the substrate by immersion in a suitable electrolyte, particularly in the reclamation of damaged or faulty electroplated workpieces. The technique may be carried out under open-circuit conditions or metal dissolution may be accelerated by anodic stimulation. The electrolyte may be chosen such that the substrate is immune or passive under the process conditions. In some circumstances, the rate of formation of this layer is enhanced by carrying out the coating electrochemically with the surfaces as the anode. Commonly, however, the layer is sprayed on and dried.

8.5.5 Metalliding

Metalliding is a deposition process carried out at elevated temperatures in a molten salt medium so that the deposited element diffuses into the lattice of the substrate. Elements of interest include nitrogen, boron, titanium and chromium, since the surfaces which result can be very hard and both wear- and corrosion-resistant. There have been extensive trials of electrochemical metalliding and it may be practised commercially to a limited extent.

FURTHER READING

1 R. Greef, R. Peat, L. M. Peter, D. Pletcher and J. Robinson (1985) *Instrumental Methods in Electrochemistry*, Ellis Horwood, Chichester.
2 J. O'M. Bockris and G. A. Razumney (1967) *Fundamental Aspects of Electrocrystallization*, Plenum Press, New York.

3 F. A. Lowenheim (Ed.) (1974) *Modern Electroplating*, 3rd Edition, Wiley, New York.
4 D. R. Gabe (1978) *Principles of Metal Surface Treatment and Protection*, 2nd Edition, Pergamon Press, Oxford.
5 A. T. Kuhn (Ed.) (1971) *Industrial Electrochemical Processes*, Elsevier, Amsterdam.
6 W. H. Safranek (Ed.) (1986) *The Properties of Electrodeposited Metals and Alloys: a Handbook*, 2nd Edition, American Electroplaters and Surface Finisher Society, Orlando, Florida.
7 D. J. Ashby (1982) *Electroplating for Engineering Technicians*, National Physical Laboratory, London.
8 A. Brenner (1963) *Electrodeposition of Alloys: Principles and Practice*, Academic Press, New York.
9 W. Canning and Company Limited (1982) *The Canning Handbook: Surface Finishing Technology*, 23rd Edition, W. Canning in association with Spon, Birmingham.
10 V. E. Carter (Ed.) (1982) *Corrosion Testing for Metal Finishing*, Butterworth, London.
11 J. K. Dennis and T. E. Such (1986) *Nickel and Chromium Plating*, 2nd Edition, Butterworth, London.
12 W. G. Foulke and F. E. Crane (1963) *Electroplater's Process Control Handbook*, Van Nostrand Reinhold, New York: Chapman and Hall, London.
13 J. A. von Fraunhofer (1976) *Basic Metal Finishing*, Elek, London.
14 D. R. Gabe (Ed.) (1983) *Coatings for Protection: A Guide for Production Engineers*, I. Prod. E., London.
15 W. Goldie (1968, 1969) *Metallic Coating of Plastics*, Vols 1 and 2, Electrochemical Publications, Hatch End, Middlesex.
16 G. Muller and D. W. Baudrand (1971) *Plating on Plastics: Practical Handbook*, 2nd Edition, Draper, Teddington, Middlesex.
17 E. Raub and K. Muller (1967) *Fundamentals of Metal Deposition*, Elsevier, London.
18 K. N. Strafford, P. K. Datta and C. G. Googan (Eds) (1984) *Coatings and Surface Treatment for Corrosion and Wear Resistance*, Ellis Horwood, Chichester.
19 J. M. West (1970) *Electrodeposition and Corrosion Processes*, 2nd Edition, Van Nostrand Reinhold, London.
20 R. Weiner (1977) *Electroplating of Plastics*, Finishing Publications, Teddington, Middlesex.
21 G. Rudzki (1983) *Surface Finishing Systems*, Finishing Publications, Teddington, Middlesex.
22 G. Lorin (1974) *Phosphating of Metals*, Finishing Publications, Teddington, Middlesex.
23 H. Silman, G. Isserlis and A. F. Averill (1978) *Protective and Decorative Coatings for Metals*, Finishing Publications, Teddington, Middlesex.

24 J. Edwards (1983) *Electroplating: A Guide for Designers and Engineers*, Finishing Publications, Teddington, Middlesex.
25 W. Machu (1978) *Handbook of Electropainting Technology*, Electrochemical Publications, Hatch End, Middlesex.
26 T. Biestek and J. Weber (1976) *Electrolytic and Chemical Conversion Coatings*, Portcullis Press, Redhill.
27 L. J. Durney (Ed.) (1984) *Electroplating Engineering Handbook*, 4th Edition, Van Nostrand Reinhold, New York.
28 F. A. Lowenheim (1978) *Electroplating – Fundamentals of Surface Finishing*, Wiley, New York.
29 A. W. Brace and P. G. Sheasby (1979) *The Technology of Anodising Aluminium*, 2nd Edition, Technicopy, Stonehouse, Gloucester.
30 A. T. Kuhn (Ed.) (1987) *Techniques in Electrochemistry, Corrosion and Metal Finishing – A Handbook*, Wiley, Chichester.

9 Metals and materials processing

Several electrochemical methods are employed in the metals-processing industry because of their ability to manufacture or surface-finish metal articles, fabrications and components which are difficult or impossible to produce by traditional mechanical workshop techniques. The most important methods are electrochemical forming, machining, grinding, deburring and etching.

The principles of electrochemistry are foreign to industries based on mechanical engineering and the electrolytes necessary for an electrochemical process cause corrosion in the workshop. Therefore, electrochemical methods have generally been developed by specialist companies or sections. This situation has minimized their impact on the engineering industry as a whole and their full potential has yet to be realized.

Rapid and diverse advances in semiconductor fabrication have also provided an incentive for the development of electrochemical etching of some such materials.

9.1 ELECTROFORMING

Electroforming is the complete manufacture of an article or component by electrodeposition. An early application of the method was the production of thin foils. Their cost when manufactured by conventional rolling is inversely proportional to thickness; in direct contrast the cost of producing the foil by electrodeposition is expected to increase with the weight of metal and therefore the thickness of the foil and it is therefore not surprising to find that it is economic to produce thin foil by electroforming. Electroforming is now used to produce a range of foils and gauzes, seamless perforated tubes (for printing materials) and endless plain or perforated bands as well as objects of more complex shape such as waveguides, audio and video stampers, moulds and dyes. Figure 9.1 illustrates the complex shapes which may be electroformed.

As in electroplating, the physical, chemical and mechanical properties of the electrodeposited metal must be controlled (in electroforming, the hardness,

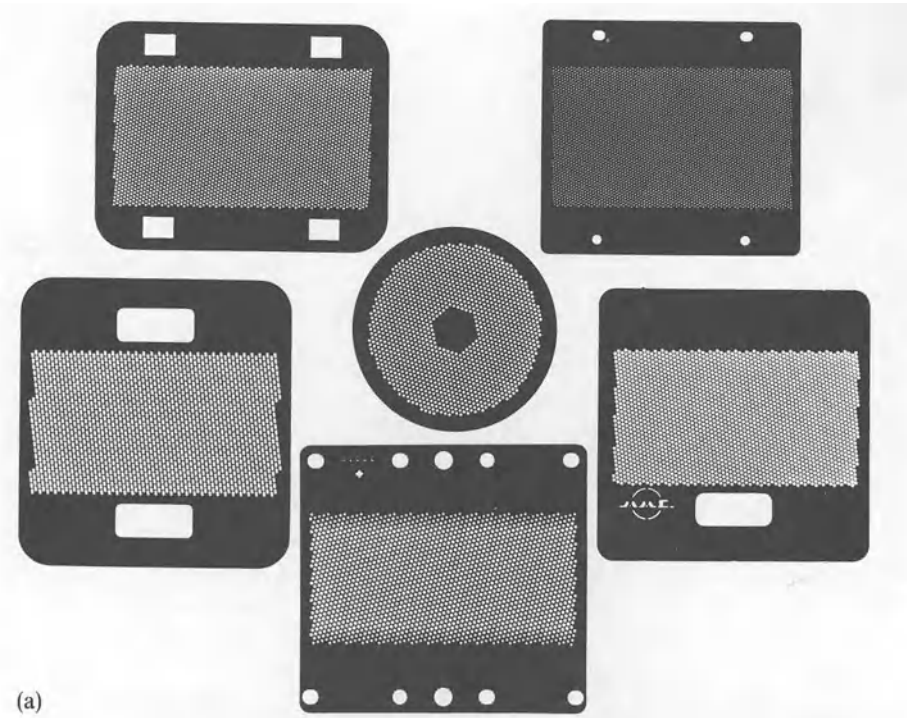

(a)

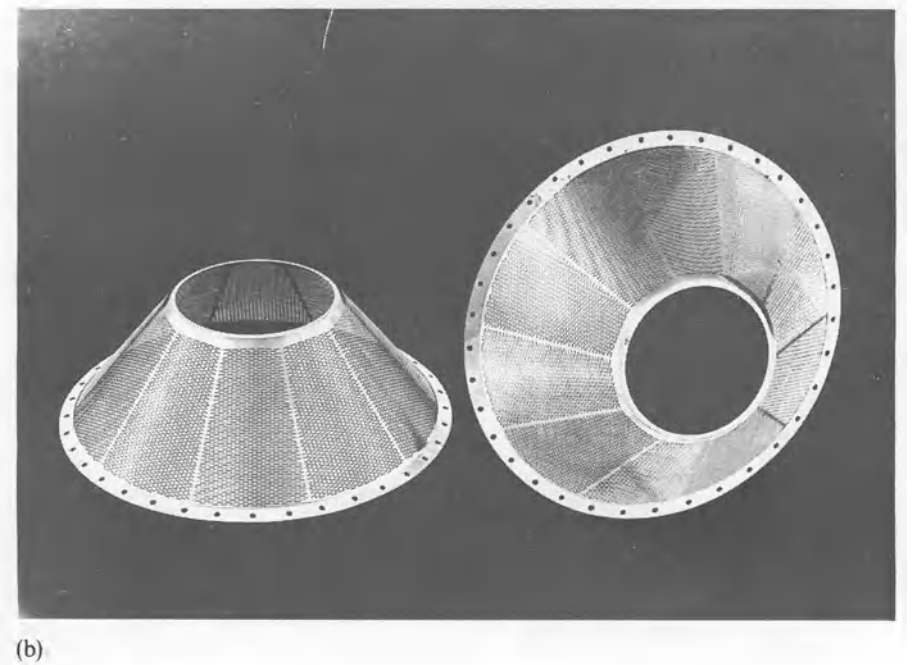

(b)

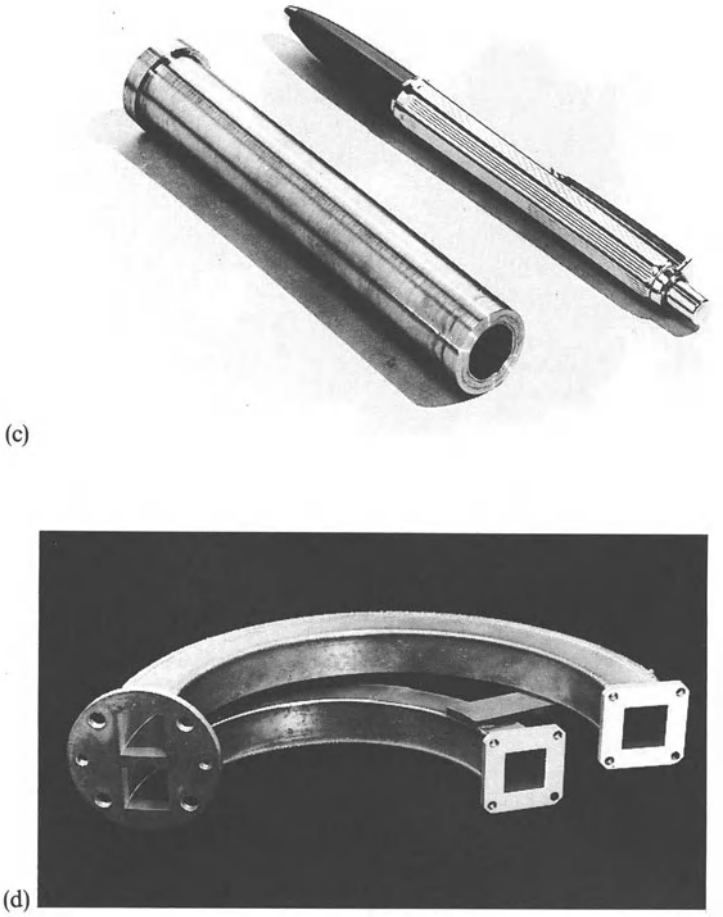

Fig. 9.1 Examples of objects that are electroformed commercially. (a) Electric razor foils. (Courtesy: Berec Components Ltd.) (b) Filter for a fruit-juice extractor (Société Buras-Sermoise). (c) Mould for a pen body, electroformed in a Ni-Co alloy (using the Ni-speed process from Galvanoform AG). (d) Twin track waveguide bend with a wall thickness of 0.25 mm Cu, 1.27 mm Ni. (Plessey Electronics Group). (Photographs b, c and d courtesy: the Nickel Development Institute.)

strength, stress and ductility will be of particular importance) and organic additives are used extensively for this purpose. It is necessary to have even greater control of the deposition bath and conditions. Moreover, the weight of metal deposited in electroforming greatly exceeds that in a plating process. The economics of the process are, therefore, governed to a greater extent by the

current density, the current efficiency and the cell design since these determine the rate of production, the energy needs and the required thickness profile of the deposit.

9.1.1 The electroforming process

The fundamental principles of electroforming are identical to those of electroplating and, hence, much of the discussion in Chapter 8 is again relevant. Rather than seeking an even deposit, however, the objective may be to plate the metal in an uneven but controlled manner so as to produce the desired shape.

The metal is deposited onto a mandrel which for some products (e.g. gauzes) will be a mixture of conducting and non-conducting surfaces. For the forming of many products the mandrel will also be of a shape and size determined by the process designer who may further make use of other aids when producing complex shapes. These might include:

1. Shaped or conforming anodes.
2. Auxiliary anodes.
3. Non-conducting shields in the anode mandrel gap to modify the local current density and, hence, the distribution of metal.
4. 'Robber' cathodes, i.e. cathodes which will not be part of the formed product and which act so as to reduce deposition at the part of the mandrel close to them. Their use will cause loss of both current and metal efficiency and, hence, should, whenever possible, be avoided.

It can be seen that the initial design of electroforming processes for complex-shaped products will be difficult. The electrodes and shields were originally designed and positioned on the basis of experience and 'trial and error'. Now computer-aided design (CAD) techniques have greatly shortened this approach and complex shapes can be formed reproducibly and to very close tolerances in a single stage.

It is clearly essential to separate the formed product from the mandrel without damage to the product and, if possible, to the mandrel since it can then be reused. This is generally accomplished by using a polished cathode which is covered by a natural or chemically induced thick oxide layer. Suitable materials include titanium, chromium and steel. For some products, their shape predetermines that a permanent mandrel cannot be used. Non-permanent mandrels have to be constructed of a material which can be removed from the inside of the product and several techniques have been used. The non-permanent mandrel may be made from a low-melting point metal (e.g. Zn, Al or their alloys), a metal which may be removed by chemical etching or a non-metallic material (e.g. Perspex, PVC or epoxy resins) soluble in organic solvents and plated by electroless deposition (Chapter 8) with a layer of silver or copper to make it conducting.

Mandrels for perforated products and gauzes must be made so that the surface has the necessary arrangement of conducting and non-conducting zones. This is

usually achieved by photoresist techniques. The prospective mandrel is covered with a thin layer of a liquid which may be hardened by a photochemical reaction and then exposed to the appropriate pattern of light of the required wavelength. The remaining unreacted liquid is washed away to leave a metal surface partly covered by a resistive film. This patterned mandrel may then be modified by etching and machining.

9.1.2 Electroforming of foil

The simplest electroforming process is that for manufacturing metal foil (Fig. 9.2). The mandrel is a slowly rotating metal cylinder and the cell has a conforming anode so that the interelectrode gap is constant. The anode may be dissolving pellets or rods or may be an inert electrode. The foil is separated from the mandrel by a knife system and is then passed through rollers which keep it taut.

The thickness of the foil will depend on the current density and the rotation rate of the drum. A system designed to produce nickel foil, 0.5 mm thick and employing a strongly stirred, concentrated sulphamate electrolyte so that a current density of 0.5 A cm^{-2} may be used, will produce about 1 m h^{-1} of the foil. The width may be up to 1 m.

The process for mesh or gauze is similar, except the mandrel must have the correct pattern of conducting and non-conducting zones.

9.1.3 Electrolytes for electroforming

The metal most used for electroforming is nickel, sometimes as an alloy with iron or cobalt, but the use of iron is increasing and copper is used extensively in the manufacture of components for the electronics industry. Electroforming with silver or gold is also carried out but only for the production of medals and in the jewellery trade.

It is essential, for production on any scale, to have a plating bath which is capable of deposition at high current density without loss of throwing power or quality. The control of stress is particularly important in electroforming because the product will later change shape if the metal is deposited with a high stress. It is the success of the concentrated sulphamate electrolyte for plating nickel at current densities in the range 0.25–0.75 A cm^{-2} without stress in the deposit that has led to the predominance of nickel in forming processes. Additives are used extensively to obtain the properties of metal required and air agitation, electrolyte flow or stirring is used universally to increase the rate of transport of metal ions to the mandrel and, hence, the maximum current density.

The deposition bath depends, as in electroplating, on the deposit characteristics necessary in the product, and typical baths for three metals are shown in Table 9.1. Solution purity, including freedom from particulate matter, is essential, particularly for electroforming.

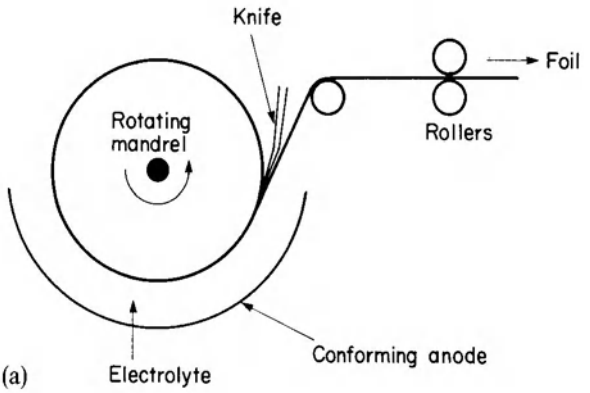

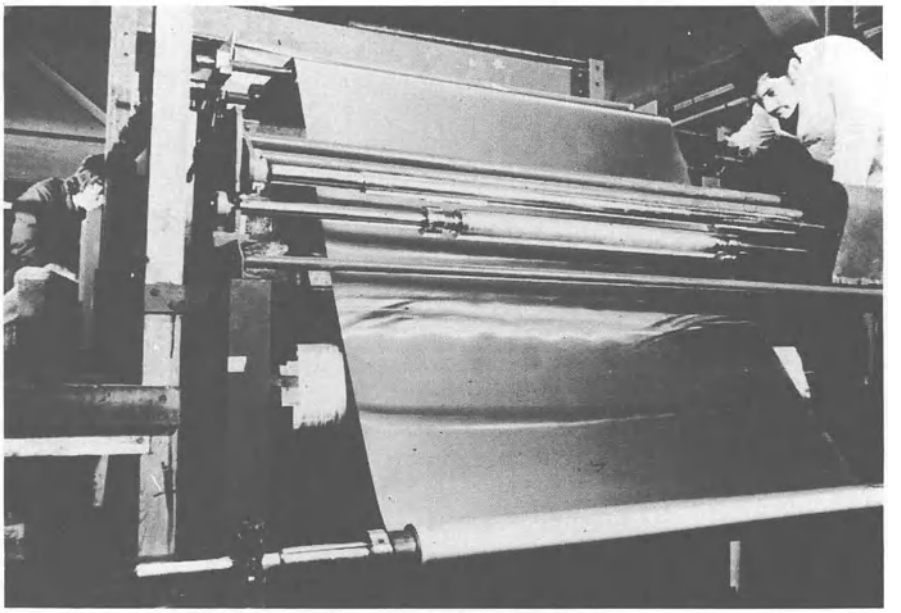

Fig. 9.2 The electroforming of metal foil. (a) The principle of the process. (b) The reeler end of a machine for continuous electroforming of nickel foil (Electrofabrication and Engineering Co.) (Photography courtesy: Nickel Development Institute, European Technical Service Centre.)

9.1.4 Applications of electroforming in the printing industry

An early application of electroforming which is declining in importance is in the printing industry. It is used in a number of processes for forming or strengthening

Table 9.1 Typical electroforming baths for three metals

Metal	Bath	Maximum current density/mA cm^{-2}
Ni	Standard Watts bath	85
	Conventional sulphamate	160
	Concentrated sulphamate	750
Cu	Cyanide	100
	Acid sulphate	100
	Pyrophosphate	40
	Fluoroborate	140
Fe	Acid chloride	150

printing blocks, and a typical procedure is that for the duplication of printing blocks in letterpress printing. An impression of the block is taken in plastic; this is then given a conducting surface by an electrodeless process and electroplated with nickel to form a plate 20 μm thick which may be detached from the mould and given a backing of a Sn–Pb–Sb alloy to produce a block with the required rigidity. Other related processes use copper or tin–lead as the metal for the forming process.

9.2 ELECTROCHEMICAL MACHINING

In electrochemical machining, the removal of the metal to form a hole or to contour the surface is by anodic dissolution (Fig. 9.3). Clearly, for the process to have sufficient accuracy to be useful in engineering, the metal removal must occur under totally controlled conditions. This is possible to good tolerances but requires the design of a cathode, known as the tool, for each job.

Electrochemical machining is a recent innovation, the practice dating back less than 35 years. Much of the driving force for its development has come from the aerospace propulsion and power generation sectors of industry with their requirement to machine very hard and tough alloys (e.g. those based on Ti and Fe–Co–Ni–Cr) to produce components able to perform a function reliably but also having minimum weight. This specification often leads to components of very complex shape. The alloys which must be employed cause problems in conventional machining because of the low rate of metal removal, the short tool life and overheating. There are two general strategies for metal removal which do not depend directly on hardness or toughness: (1) thermal; and (2) chemical techniques. Thermal methods concentrate energy over a small area causing local melting or vaporization of the workpiece. The energy input may be as heat from a flame, laser light, an accelerated electron beam or an electrical discharge. Of

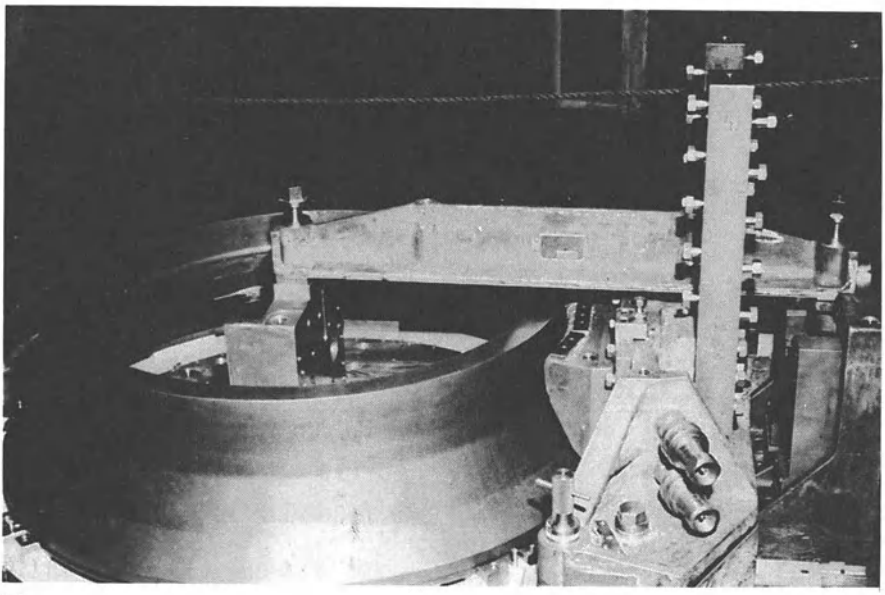

(a)

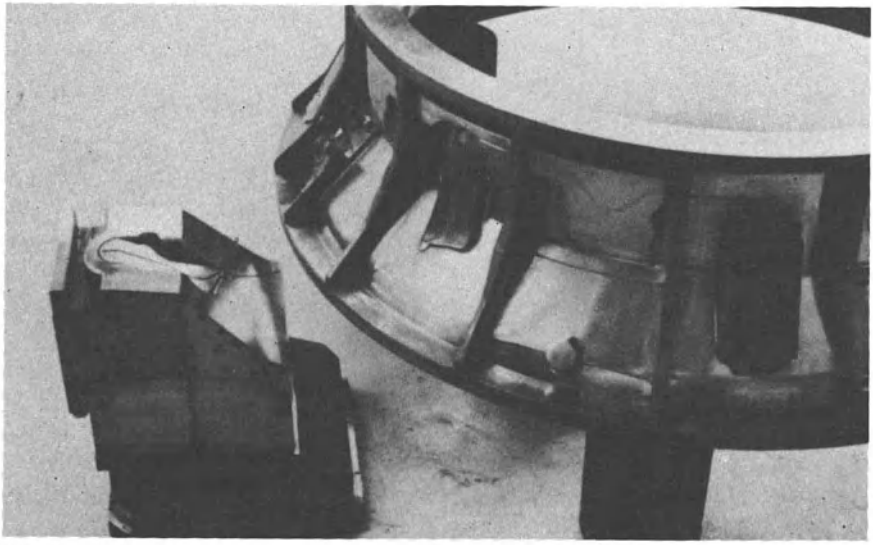

(b)

Fig. 9.3 An aircraft engine casing. (a) Before electrochemical machining. (b) After electrochemical machining. (The cathode tool is also shown in (b).) (Courtesy: Rolls-Royce Ltd, Aero Division.)

these, electric discharge machining (EDM) or 'spark machining', has found the widest acceptance as a means of producing cavities, narrow slots and holes.

Electrochemical machining (ECM) relies upon a high local current density and control of the anodic dissolution such that passivation (Chapter 10) does not

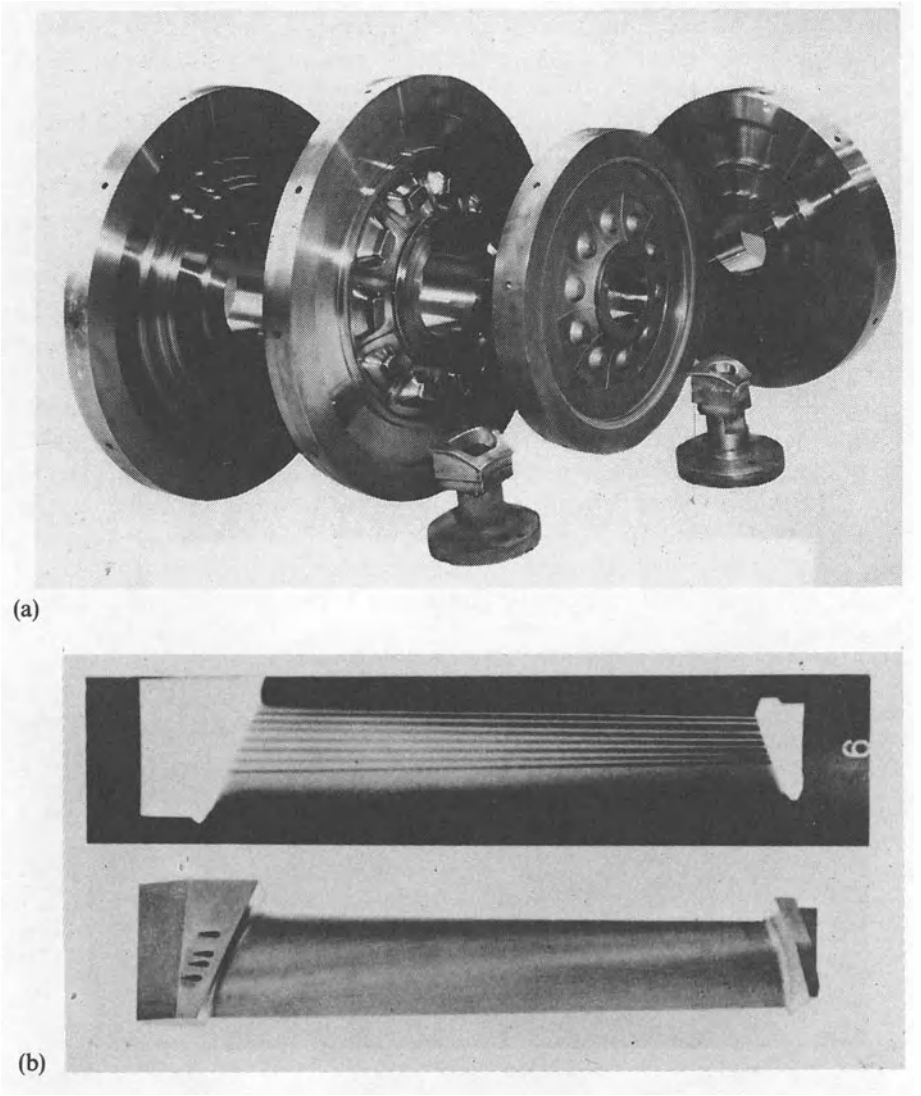

Fig. 9.4 Components manufactured by electrochemical machining. (a) Turbine discs (the cathode tools to form the complex features are also shown). (b) Turbine blade with longitudinal cooling holes formed by machining (the holes are seen on the X-ray photograph of the blade). (Courtesy: Rolls-Royce Ltd, Aero Division.)

occur. These requirements result in the use of highly conducting electrolytes containing depassivating species (Cl^- or complexants), a small interelectrode spacing (typically 0.10–1.5 mm), and a high flow rate of electrolyte. The last feature is also important in transporting insoluble compounds away from the workpiece and in cooling it. Ideally, the metal will dissolve at 100% current efficiency, the rate of removal being described by (and limited by) Faraday's laws. Electrochemical machining current densities on the workpiece are typically in the range 25–180 A cm^{-2}; a current of 10 kA may support a removal rate of approximately 15 cm^3 min^{-1}.

Electrochemical machining has other attractive features (Figs. 9.4–9.5). It may be used to machine many complex features and complicated contoured shapes (e.g. fine holes, angled holes, non-round holes, engine casings and turbine components) in a single operation to close tolerances and with good repeatability. It is also used to carry out sensitive operations such as the cutting of hypodermic syringe needles without causing distortion. Moreover, in contrast to conventional metalworking, electrochemical machining leaves the metal without scratches, tears, unwanted sharp edges or burrs and the surface is almost free of induced stress.

The main drawback to electrochemical machining lies in the need to design a tool (cathode) for each new job. Moreover, the design process to select a suitable electrolyte and obtain the correct current density distribution remains a skilled art rather than a science. It is often necessary to test the tool and to modify it by trial and error. In addition, the need to use large volumes of electrolyte solutions does not fit in well to a mechanical workshop because, however carefully they are handled, corrosion and chemical degradation in the environment are potential hazards.

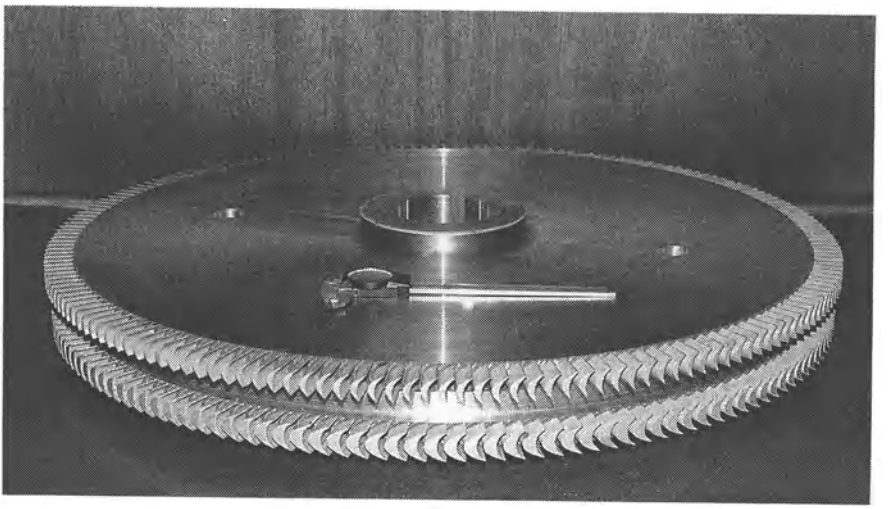

(a)

(b)



Fig. 9.5 A two-stage, steam turbine wheel produced by electrochemical machining. (a) The steam turbine wheel comprises two rows having 181 and 159 blades respectively. Each blade has a positional tolerance of less than $\pm 25\ \mu m$. Electrochemical machining offers the ability to machine blades from a material in a final hardened condition; no significant change in mechanical properties takes place on machining. (b) The above wheel is shown partly machined at an early stage of manufacture. The blade shape is integral with the original disc, resulting in high strength. (Courtesy: Anodic Machining Technologies Ltd.)

9.2.1 An electrochemical machining system

In the electrochemical cell the workpiece is the anode and the tool is the cathode. The electrolyte is fed through the tool at a rapid flowrate (9–60 m s^{-1}) in such a way that the supply of electrolyte is uniform over the surface. The electrolyte flow pattern is as important in practice as the arrangement of conducting surfaces on the tool in determining the current density distribution and both factors must be considered in the design of the tool.

Large volumes of electrolyte are required and, hence, it is normal to use an aqueous solution with a cheap electrolyte (i.e. NaCl or $NaNO_3$) or where essential to obtain metal dissolution, NaBr or NaF; the workpiece must not passivate. The electrode reactions are, at the anode:

$$M - ne^- \longrightarrow M^{n+} \tag{9.1}$$

and at the cathode, typically:

$$2H_2O + 2e^- \longrightarrow H_2 + 2OH^- \tag{9.2}$$

so that the metal ion will often precipitate in the interelectrode gap:

$$M^{n+} + nOH^- \longrightarrow M(OH)_n \tag{9.3}$$

Thus, the electrolyte leaving the gap is three-phase, containing both solids and hydrogen gas. It is to sweep away these products and to remove the heat that a high electrolyte flowrate must be used.

The control system typically should be capable of giving a total current of between 100 and 10 000 A at a voltage of from -8 to -30 V and the machining process will use a high current density, in the range 5–400 A cm^{-2}. The control system must also be capable of maintaining a constant, small gap between the workpiece and the tool and this will require the tool to move into the workpiece as the machining proceeds. A circuit to detect sparking and shut down the electrolysis within 20 ms is also necessary if damage to the tool is to be avoided under dry conditions.

Electrochemical machining uses a large volume of electrolyte and produces large volumes of effluent. It is therefore normal to recycle the electrolyte. The scale of the electrolyte system required is perhaps best seen by noting that the removal of 1 kg of steel produces 40 dm^3 of sludge containing about 20% solids. The electrolyte purification loop will contain a settling tank and filter as well as a

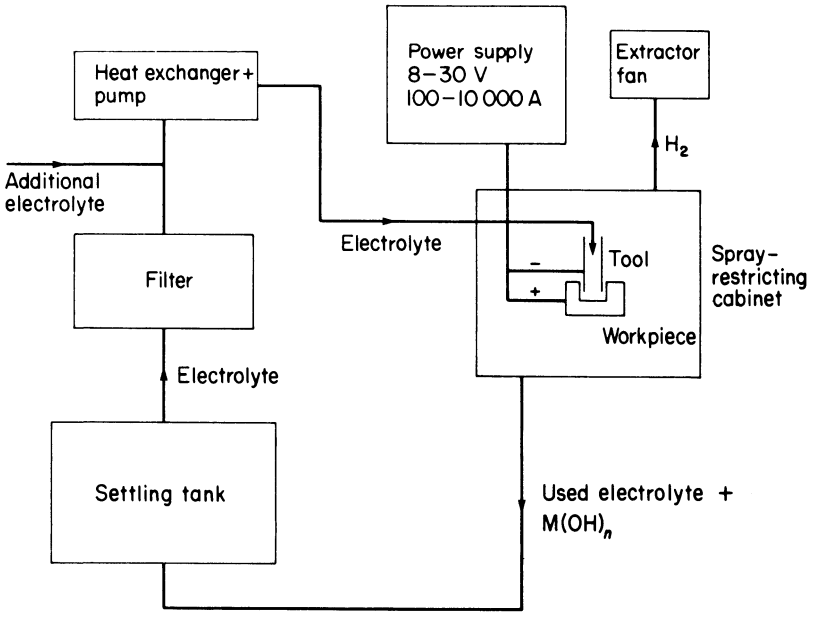

Fig. 9.6 The essential system components for electrochemical machining.

heat exchanger, to remove excess heat, and a pump. There will also be a facility for the continuous addition of new electrolyte since some is inevitably lost. The workshop environment must be protected from electrolyte spray and the hazards of hydrogen gas and, hence, the machining is carried out in an enclosed spray-restricting cabinet with an extractor fan (similar to a fume cupboard).

A typical system is shown in Figs 9.6 and 9.7 and it can be seen that the cell (tool plus workpiece) is but a small part of the equipment necessary for electrochemical machining (as is generally the case in electrochemical processing).

The following factors may be considered as contributing to the scarcity of electrochemical machining techniques in practice:

1. The technology is multidisciplinary and significantly different to conventional mechanical or thermal techniques of fabrication; it is poorly understood in industry.
2. There is insufficient experience of the technique to provide a comprehensive database.
3. Theoretical treatments are implemented poorly.

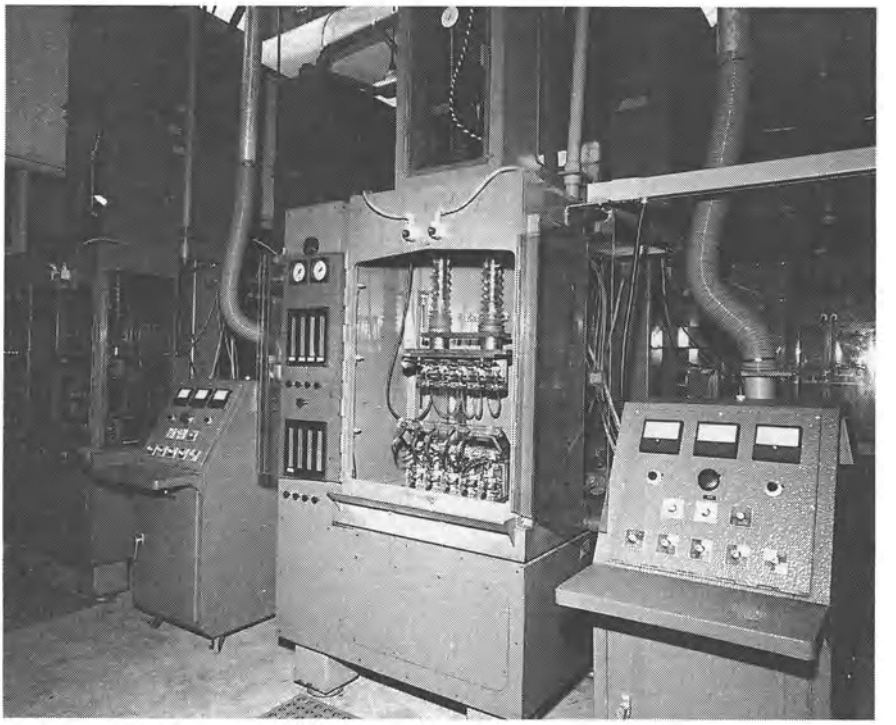

Fig. 9.7 A spray cabinet and control unit for electrochemically machining the longitudinal holes into a turbine blade. (Courtesy: Rolls Royce Ltd, Aero Division.)

4. Electrochemical machining equipment is specialized, and has high capital and maintenance costs compared to conventional machine-tooling.
5. The electrolytes used are often corrosive and require effective conditioning (including filtration, temperature control and maintenance of composition).

9.2.2 Tool design

The design of the tool determines the current density distribution and, hence, the shape of the feature being machined although, in general, the tool will not be exactly the same shape as the feature.

The tool will be constructed of both conducting (copper, copper–tungsten alloy or steel) and non-conducting (epoxy resins and rubber materials) surfaces and the positioning of the holes for electrolyte entry will determine the electrolyte flow pattern between the workpiece and the tool. In order further to ensure an even flow of electrolyte it is also common to use restrictors, particularly when forming a feature in a flat surface.

Figure 9.8 illustrates the principles of tool design using the example of machining a square hole. The cathode is a thin, square, plate of copper with a

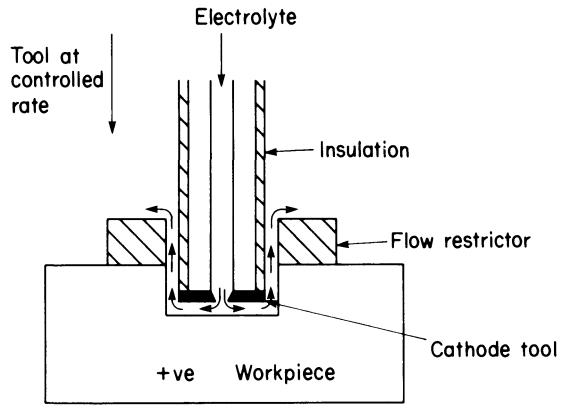

(a)

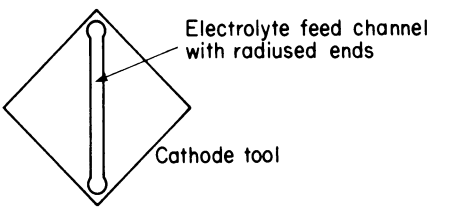

(b)

Fig. 9.8 A cathode tool for electrochemically machining a square hole. (a) Side view. (b) View from below.

diagonal electrolyte feedslot through which the electrolyte is pumped; the slot extends as far as possible into the corners of the tool and at both ends broadens out slightly to a circular finish so that electrolyte flows right into the corners. The sides of the tool are insulated so that metal dissolution takes place only at the base of the hole; if the sides were conducting, the hole would broaden towards the top. An electrolyte restrictor is placed on the surface of the workpiece and around the tool to assist uniform electrolyte flow; this is particularly necessary at the start of the machining operation. Using a current density of 10 A cm^{-2}, the tool must be fed at 0.3 mm min^{-1}. The tool design is particularly dependent upon the category of electrochemical machining being practised. For convenience, the type of application and process mechanics, suggest four (interrelated) categories of electrochemical machining: (1) electrochemical grinding; (2) electrochemical deburring; (3) electrochemical contour machining; and (4) electrochemical forming.

9.2.3 Electrochemical grinding

This modification of electrochemical machining has been widely used for grinding carbide tools, since conventional methods can produce burrs, poor-quality finish and even cracking. It is also used to grind stainless steel and titanium honeycomb material and other surfaces.

In electrochemical grinding (Fig. 9.9), the tool is a rotating and conducting circular stone or wheel composed of diamond abrasive bonded to copper. The electrolyte is pumped more slowly than in machining over the whole surface of the wheel which is moved slowly across the surface of the workpiece with a gap as low as 0.025 mm. The workpiece is again the anode and the wheel, the cathode. The process is operated at 50–3000 A cm^{-2} and requires a source with a voltage of from -4 to -8 V. In addition, all the ancillary equipment shown in Fig. 9.6 for electrochemical machining will again be required but generally on a smaller scale. In electrochemical grinding (Fig. 9.10), it is thought that perhaps 90% of

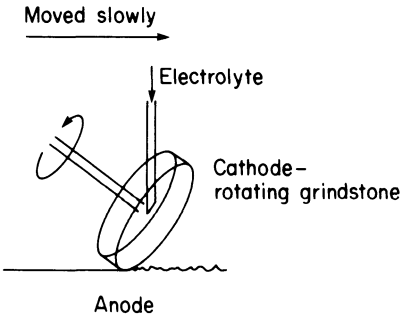

Fig. 9.9 The principle of electrochemical grinding.

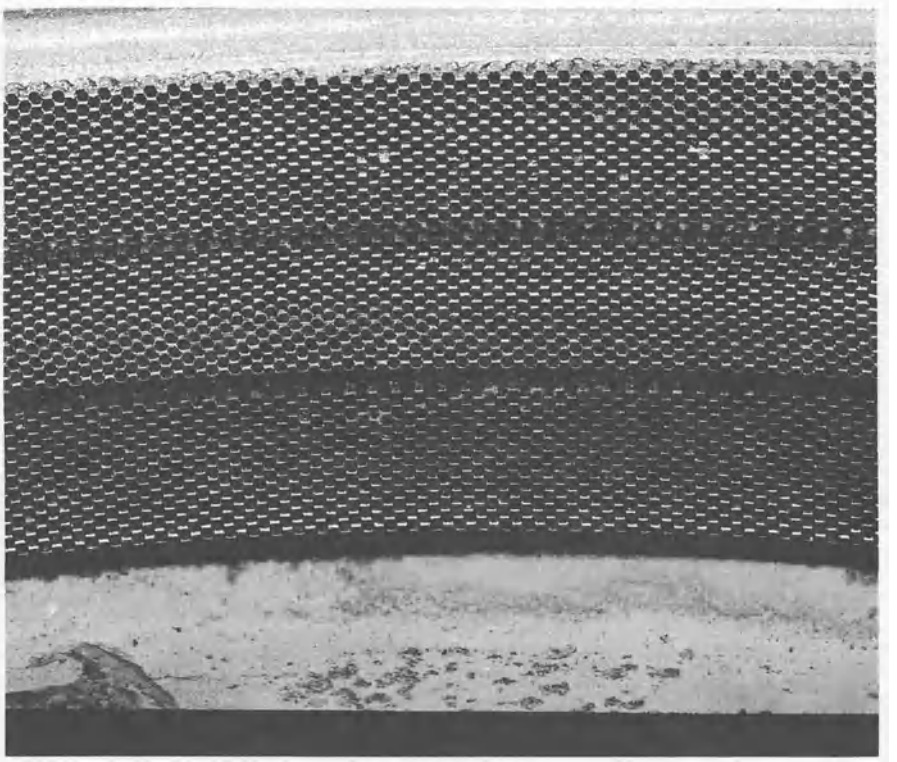

Fig. 9.10 An aero engine component constructed partly from a nickel alloy with a honeycomb cellular structure (cell size 2 mm). The top surface is smoothed via electrochemical grinding. (Courtesy: Rolls Royce Ltd, Aero Division.)

the metal removal is due to electrolysis while the balance is due to the abrasive action of the grinding wheel.

9.2.4 Electrochemical deburring

Electrochemical deburring is another modification of electrochemical machining carried out with smaller-scale ancillary and control equipment. It is used essentially to remove sharp corners, points and other raised imperfections which have been left by mechanical machining. The projecting areas have a locally high positive potential and are selectively removed by the high prevailing anodic current density. Applications lie particularly in the manufacture of components for engineering and include the finishing of pistons, power steering shafts, connecting rods and fuel injector nozzles. It requires the design of only a simple cathode tool and generally the currents do not exceed a few hundred amperes. A

particular advantage of electrochemical machining is the highly selective nature of removal, which does not adversely affect other features such as thread forms.

9.2.5 Electrochemical contour machining

A stationary tool is used here, producing a shallow recess whose shape corresponds closely to the reverse shape of the tool. As no tool or workpiece movement occurs, metal removal is limited to a depth of approximately 1.5 mm. Attempts at machining to a greater depth incur the problems of an increased electrolyte resistance which greatly restricts the current density and, hence, the metal removal rate. Additionally, at a lower current density, the quality of surface finish and the fidelity of recess-tool conformity degrade.

Typical applications include the production of recesses on the internal faces of pump housings, ring grooves on the internal face of cylindrical pressure chambers and a burr-free radius on 1.5 mm diameter holes in hydraulic components.

9.2.6 Electrochemical forming

Static electrode electrochemical machining techniques are limited in the form and accuracy of their machined products; as metal is removed from the workpiece, the interelectrode gap increases and the metal removal rate falls. This problem may be overcome by continuously moving the tool (or the workpiece) in order to maintain a constant gap. This is the principle behind electrochemical forming (sometimes called electrochemical sinking), which is perhaps the most important and versatile application of electrochemical machining.

The gap size is limited in practice by the need to provide an effective flow of cool, clean, pressurized electrolyte at all times. This requires adequate manifolding to avoid variations in the flow around the workpiece with time. Moreover, the hydraulic losses which occur within the entry manifold and across the machining gap may be large ($\leqslant 30$ bar) and the tooling and associated plumbing must be designed adequately and constructed to withstand the high resultant forces. Equally, the drive system to move the tool (or workpiece) must overcome large hydraulic forces, which may approach $300\ \mathrm{N\,cm^{-2}}$. These considerations mean that interelectrode gaps below 0.12 mm are uncommon; 0.25 mm may be regarded as a typical condition. The tool feed system should normally be capable of a smooth movement rate of 0.5–5 mm $\mathrm{min^{-1}}$. Adoption of a complex-shaped tool may allow a three-dimensional cavity to within ± 0.05 mm, together with low induced stress, no thermal damage and a surface finish in the range, for example, of 0.12 to 1–2 μm. It is interesting to note that it is difficult to produce sharp edges by electrochemical forming; bulk removal of material by electrochemical machining may be followed by final, profile milling as a complementary technique. Such an approach is, indeed, used to produce complex vane forms from blank nickel alloy castings.

9.2.7 Features of electrochemical machining

The major advantages may be summarized:

1. Machining rate is not affected significantly by metal hardness or toughness.
2. Burr-free machining is possible.
3. Negligible induced stress.
4. No thermal or mechanical damage.
5. Complex shapes may be created by a continuous single-axis movement.
6. Reasonable surface finish and dimensional accuracy.
7. No hydrogen embrittlement.
8. Relatively high metal-removal rates.

9.3 ELECTROCHEMICAL ETCHING

The deliberate (selective) and controlled removal of an electrically conducting (or semiconducting) material in an electrolyte may be practised for several important purposes, including the following:

1. Selective attack of active zones and phases on a metal surface (e.g. grain boundaries) to provide suitable contrast for microscopic techniques; the principle of metallographic etching.
2. Metal samples may be 'thinned' prior to transmission electron microscopy.
3. Controlled surface roughening in order to promote adhesion of a coating via more direct chemical bonding, as in the mild etching of metals prior to electroplating or anodizing (Chapter 8).
4. Aluminium alloys may be 'electrograined' in order to enhance their capacity for receiving and retaining the image of a printing ink (section 9.3.3).
5. Solid silver busbars, as specialized high-current conductors, are sometimes produced by etching-away unwanted material by $FeCl_3$.
6. Selective, patterned removal of a metal clad onto an insulator is an essential technique for the fabrication of printed circuit boards.
7. Selective etching of semiconductors, particularly silicon is a critical step in the manufacture of microelectronic devices.

Etching of the material may be carried out either chemically under open-circuit conditions (i.e. controlled 'corrosion' (Chapter 10)) or it may be electrochemically driven by applying a potential. The former case is more common. It requires no power supply or auxiliary electrodes; the electrolyte conditions are chosen such that the species to be removed is dissolved at a reasonable rate, courtesy of a simultaneous cathodic process. Taking the case of the dissolution of a metal M, the anodic process in reaction (9.1) is supported by a suitable electroreduction:

$$X + ne^- \longrightarrow X^{n-} \tag{9.4}$$

to give an overall etching process:

$$M + X \longrightarrow M^{n+} + X^{n-} \tag{9.5}$$

(cf. Chapter 9, section 9.3). Thus, the etchant must permit active dissolution of M to M^{n+} while supplying a cathodic reactant X. In the general case, both M^{n+} and X^{n-} may affect the rate of etching, i.e. the progress of reaction (9.5).

Anodic etching requires that the metal be driven to a convenient potential (positive of its open-circuit value), by means of a power supply and a suitable inert cathode such that reaction (9.1) proceeds at the desired rate.

The process conditions must be chosen carefully and controlled within limits to permit the etching to be sufficiently selective both chemically and physically, e.g. it may be required to etch one metal rather than another, one metallurgical phase rather than the whole matrix or an oxide rather than a metal or semiconductor. The profile or rate of removal may be critical (as in printed circuit board (section 9.3.1) or semiconductor etching (section 9.3.2).

Two different cases of etching deserve special attention due to their industrial relevance: (1) the etching of copper from printed circuit boards; and (2) selective etching of semiconductors in microelectronics fabrication.

9.3.1 Etching copper from printed circuit boards

In the subtractive process* for manufacture of printed circuit boards the plastic board is covered initially with a complete copper layer (5–100 μm but, typically, 17–35 μm thick). Selected areas are then protected by a photoresist or electroplated image and the resist of the copper is etched away.† The amount of copper removed depends considerably upon the design and type of board; it may be in the range 10–90% of the original, 50–70% being common. The direct anodic oxidation of the copper is difficult since the process must lead to a series of isolated copper areas to which it is difficult to maintain electrical contact. Hence, open-circuit chemical etching is usually employed. The copper clad board is printed with an etch-resistant negative pattern of the tracking required and is then introduced into the etching machine (Fig. 9.11). A conveyor belt is the usual method used to transport the boards horizontally for a controlled time through a spray chamber. Here, the surface is sprayed by the etchant at controlled

* The subtractive process has two main drawbacks: (1) possible wastage of copper removed by etching; and (2) the undercut can be severe, particularly with depleted etchants and fine, closely spaced, copper tracts. Additive techniques overcome these problems. The 'semi-additive' process involves electroless deposition of copper on a laminate (section 8.2.5).

The negative resist pattern is used to selectively build up the circuit by copper electroplating. When the required conductor thickness (typically 17 or 35 μm) is reached, it is plated with tin, tin–lead or gold as a positive resist. Removal of the resist is followed by rapid etching of the electroless copper layer. The remainder of the process is similar to that for subtractive methods. In the 'fully additive' method, the full conductor thickness may be built up in a single, long (24 h) electroless deposition stage.

Copper is etched at further stages in the manufacture of printed circuit boards including, after resist application: (1) removal of electroless and electroplated deposits before pattern plating with copper; (2) prior to electroplating gold onto edge contacts; and (3) final etching of all unwanted copper to leave the desired circuit pattern.

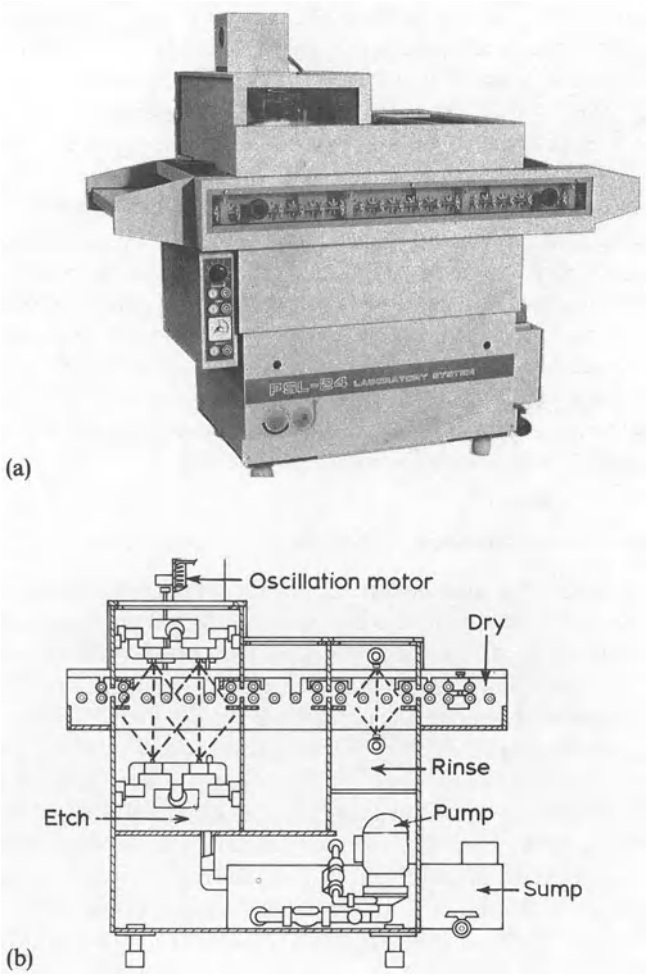

Fig. 9.11 A small-scale, modular system for etching printed circuit boards of overall dimensions 1490 × 860 × 1450 mm. (a) Photograph. (b) The main components. (Courtesy: Finishing Services Ltd.)

temperature. The same processing machine may then water-rinse the printed circuit board and remove the etch-resist ink followed by water-rinsing and air-drying.

A number of etchants are in use, depending upon the nature of the process and, to an extent, personal preference or tradition. These include: (1) ammonium persulphate; (2) sodium persulphate; (3) potassium peroxysulphate; (4) cupric chloride; (5) $FeCl_3$; (6) H_2CrO_4; (7) ammoniacal chlorite; and (8) hydrogen peroxide/sulphuric acid.

Elevation of the solution temperature enhances the etching rate but may produce problems of materials stability, non-uniform attack or etchant decomposition.

The overall etching process may be rationalized by considering the equilibrium:

$$Cu^{0}_{(s)} + Cu^{II}_{(l)} \rightleftharpoons 2Cu^{I}_{(l)} \tag{9.6}$$

which usually lies far to the left. If the soluble Cu^{I} species are stabilized by suitable co-ordination, then the equilibrium may be shifted to the right. As will be seen, $Cu^{I}_{(l)}$ may be stabilized as, for example, $CuCl_3^{2-}$ or $Cu(NH_3)_4^{+}$.

The use of persulphates is declining, partly due to their chemical instability and attack on tin-lead etch-resists (especially by ammonium persulphate). The oldest etchant is acidic ferric chloride, which is still used on a very small scale for batch processing and prototype development. The simplified reactions are:

Anode $$Cu - 2e^{-} \longrightarrow Cu^{2+} \tag{9.7}$$

Cathode $$2Fe^{3+} + 2e^{-} \longrightarrow 2Fe^{2+} \tag{9.8}$$

Cell $$Cu + 2Fe^{3+} \longrightarrow Cu^{2+} + 2Fe^{2+} \tag{9.9}$$

Cupric chloride in hydrochloride acid etchants are faster than the ferric chloride types and regeneration of the etchant is possible using chemical (H_2O_2 or Cl_2) or electrochemical treatments (see later). The overall etching process may be represented by:

$$Cu + Cu^{2+} + 6Cl^{-} \longrightarrow 2CuCl_3^{2-} \tag{9.10}$$

The etchant may be maintained in an active, oxidized state by chemical addition of chlorine gas or hydrogen peroxide.

$$2CuCl_3^{2-} + Cl_2 \longrightarrow 2Cu^{2+} + 8Cl^{-} \tag{9.11}$$

$$2CuCl_3^{2-} + H_2O_2 + 2HCl \longrightarrow 2Cu^{2+} + 8Cl^{-} + 2H_2O \tag{9.12}$$

Reactions (9.11) and (9.12) result in excess cupric chloride which must be removed from the etch machine and then disposed of by an economically and environmentally acceptable procedure.

Modern ammoniacal etchants are mildly alkaline solutions containing ammonium carbonate, cupric and chlorite ions together with proprietary additives. Metallic etch resists including tin–lead are not usually attacked but the pH and solution composition must be maintained in order to preserve the etch rate and prevent sludge formation. A possible set of reactions is:

Anode $$2Cu + 8NH_4OH - 4e^{-} \longrightarrow 2Cu(NH_3)_4^{2+} + 8H_2O \tag{9.13}$$

Cathode $$ClO_2^{-} + 2H_2O + 4e^{-} \longrightarrow Cl^{-} + 4OH^{-} \tag{9.14}$$

Cell $$2Cu + ClO_2^{-} + 8NH_4OH \longrightarrow 2[Cu(NH_3)_4]^{2+} + 4OH^{-} + 6H_2O + Cl^{-} \tag{9.15}$$

Certain ammoniacal solutions are operated without chlorite ions, dissolved oxygen maintaining the dissolved copper in the cupric state:

$$Cu + [Cu(NH_3)_4]^{2+} \longrightarrow 2[Cu(NH_3)_2]^{+} \tag{9.16}$$

and

$$2[Cu(NH_3)_2]^{+} + \tfrac{1}{2}O_2 + 4NH_4OH \longrightarrow 2[Cu(NH_3)_4]^{2+} + 2OH^{-} + 3H_2O \tag{9.17}$$

Perhaps the most versatile of the copper etchants is the hydrogen peroxide/sulphuric acid mixture, although these solutions require stabilizers to retard the spontaneous decomposition of peroxide to water and oxygen. The reactions occuring during etching are:

Anode $Cu - 2e^{-} \longrightarrow Cu^{2+}$ (9.18)

Cathode $2H^{+} + H_2O_2 + 2e^{-} \longrightarrow 2H_2O$ (9.19)

Cell $Cu + 2H^{+} + H_2O_2 \longrightarrow Cu^{2+} + 2H_2O$ (9.20)

A major advantage of this etchant is the simple nature of the products, which permit etchant regeneration via $CuSO_4.5H_2O$ precipitation on cooling or electrochemical methods. The latter approach has the advantage of retaining the sulphuric acid content.

The etching process (reaction 9.5) raises several problems in an untreated batch system:

1. Cu^{2+} builds up, which results in a declining rate of metal removal and a variable etching profile.
2. The oxidant X decays in concentration, which also causes a decline in the etching rate.
3. Both Cu^{2+} and the product of the oxidant's electroreduction, X^{n-} may cause effluent-treatment problems, particularly if the X^{n-} is a dissolved metal (e.g. Cu^{+} or Fe^{2+}). The problem is increased if the metal is highly complexed (e.g. $[Cu(NH_3)_4]^{2+}$ or $CuCl_3^{2-}$.

Therefore, it is often an attractive proposition to treat the used etchant (either batchwise or continuously) to remove the dissolved copper using reaction (9.18) and reoxidize the etchant species:

$$X^{2-} - 2e^{-} \longrightarrow X \tag{9.21}$$

Electrode reactions (9.18) and (9.21) may be conveniently carried out at the cathode and anode of a suitable, divided electrochemical reactor.

An example of such a recycling technology is illustrated in Fig 9.12(a) for the treatment of cupric chloride etchants. The relevant reactions may be simplified as

Anode $2CuCl_3^{2-} - 2e^{-} \longrightarrow 2Cu^{2+} + 6Cl^{-}$ (9.22)

Cathode $Cu^{2+} + 2e^{-} \longrightarrow Cu$ (9.18)

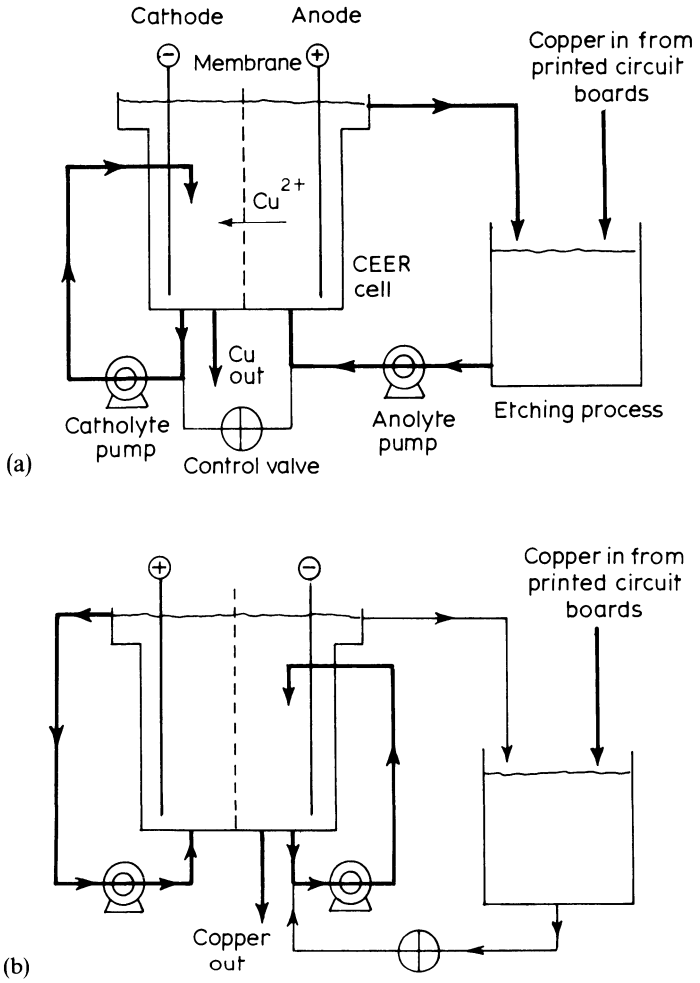

Fig. 9.12 The Capenhurst Electrolytic Etchant Regeneration (CEER) process. (a) Cupric chloride etchant. (b) Ammoniacal etchant.

$$\text{Cell} \qquad 2CuCl_3^{2-} \longrightarrow Cu^{2+} + Cu + 6Cl^- \tag{9.23}$$

The cathode reaction (9.18) may be subdivided into two processes. The desired cathode reaction is:

$$CuCl_3^{2-} + e^- \longrightarrow Cu + 3Cl^- \tag{9.24}$$

but this is accompanied by the unwanted side reaction:

$$Cu^{2+} + e^- + 3Cl^- \longrightarrow CuCl_3^{2-} \tag{9.25}$$

In principle, the overall cell reaction (9.23) is a complete reversal of the overall etching process.

The cell design employed (Fig. 9.13) is based on a simple parallel-plate design. The anodes and cathodes are divided by a perfluorosulphonic acid exchange membrane which prevents an otherwise drastic loss of current efficiency due to the parasitic redox shuttle:

$$2Cu^{2+} + 6Cl^- + 2e^- \underset{\text{anode}}{\overset{\text{cathode}}{\rightleftharpoons}} CuCl_3^{2-} \tag{9.26}$$

Etchant is pumped continuously from a sump in the etching machine (Fig. 9.13) (via a cooler) up into the anode compartment. The electrolyte flows over a weir to

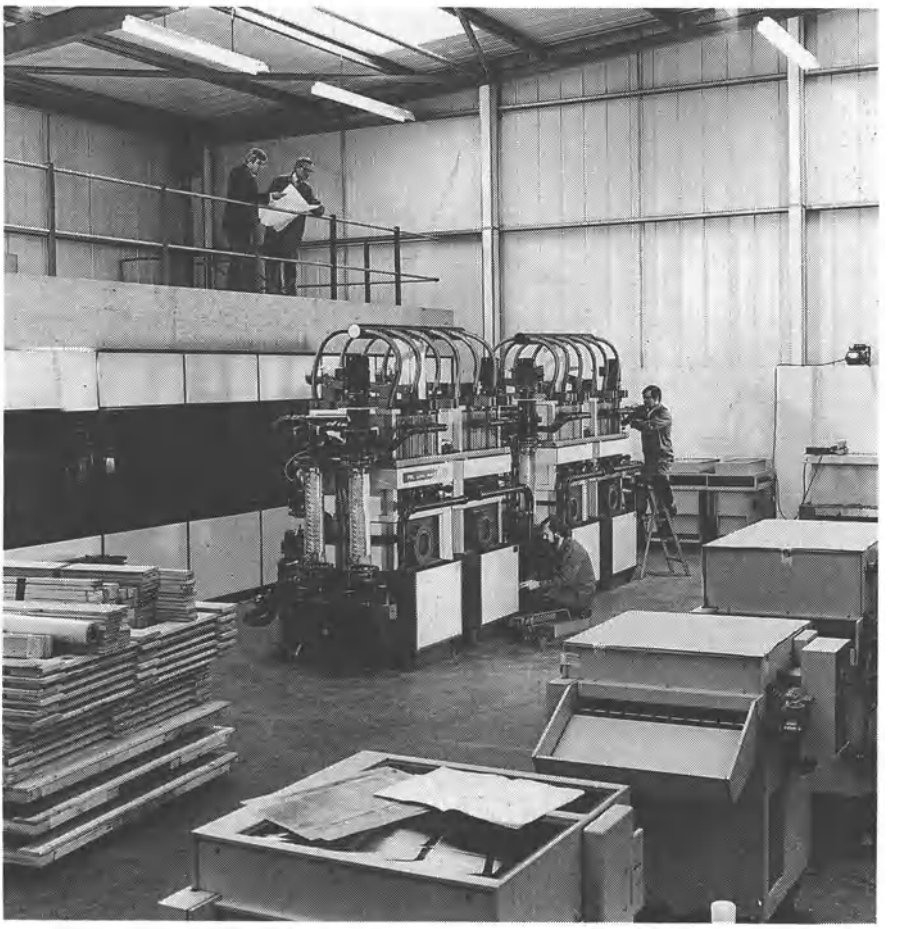

Fig. 9.13 Examples of the Capenhurst electrolytic etchant regeneration cell. Two cell units being assembled; an etchant machine is shown in the foreground. (Courtesy: Electricity Council Research Centre and Finishing Services Ltd.)

return to the etching machine. The catholyte (essentially a cuprous chloride solution) is pumped around a loop which incorporates the cathode compartment and a cooler. The 5 kA (Fig. 9.13) cell typically operates at a voltage of -7 V and a current density of 0.36 A cm^{-2} for recovery of up to 5 kg h^{-1} copper. Cuprous species are oxidized rapidly at the anode in order to regenerate the etchant. Copper ions pass through the membrane into the cathode compartment where they electrodeposit as dendritic metal. The copper falls from the cathode to collect in a settling pot at the bottom of the cell; metal is withdrawn through a port at suitable intervals (2–3 weeks) after the cell is drained. Transfer of copper ions through the membrane is supplemented by a small, deliberate flow of etchant into the catholyte in order to maintain the dissolved copper level in the catholyte within the range 10–20 g dm^{-3}. The overall cathode current efficiency is approximately 85%. The cell body is constructed in polyvinylchloride while graphite electrodes are used.

The CEER process has also been used for ammoniacal etchants (Fig. 9.12(b)), when a sulphuric acid anolyte is preferred together with platinized titanium anodes;* graphite cathodes are retained. In this case the anode reaction is oxygen evolution; etchant oxidation readily takes place chemically via dissolved oxygen in the etching machine:

$$\text{Anode} \quad H_2O - 2e^- \longrightarrow \tfrac{1}{2}O_2 + 2H^+ \tag{9.27}$$

$$\text{Cathode} \quad Cu(II) + 2e^- \longrightarrow Cu(0) \tag{9.28}$$

$$\text{Cell} \quad Cu(II) + H_2O \longrightarrow Cu(0) + \tfrac{1}{2}O_2 + 2H^+, \tag{9.29}$$

$$\text{Etchant machine} \quad 2Cu(NH_3)_2^+ + \tfrac{1}{2}O_2 + 4NH_4OH \longrightarrow 2Cu(NH_3)_4^{2+} + 2OH^- + 3H_2O \tag{9.17}$$

Another example of combined metal removal and electrolyte regeneration is provided by the removal of copper, zinc and cadmium from chromic acid stripping and etching solutions (Chapter 7).

In all of the above cases, etching of copper is carried out without the application of an external current. In certain cases, however, electrochemical processes have been introduced. An example is shown in Fig. 9.14. While it is effectively a form of 'low-power electrochemical machining', it is based on quite different principles. A slurry of high-surface-area graphite particles (15%) in sulphuric acid (10–15%) is charged positively by contact with a carbon or lead anode and is then pumped through nozzles onto the printed circuit board. The copper is etched by contact with the charged particles and the carbon particles are then returned to the anode for recharging. Moreover, the copper ions formed in the etching process may be passed to the cell cathode and recovered as the metal. Hence, the process notionally has following chemistry: at the anode the

* Some Cl^- passes from catholyte to anolyte and some Cl_2 is evolved at the anode.

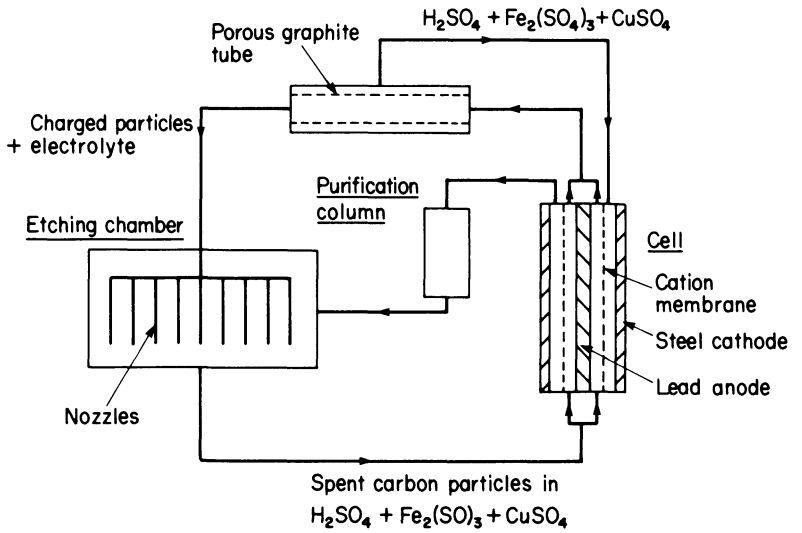

Fig. 9.14 An electrolytic etching process for the manufacture of printed circuit boards.

carbon is activated by oxidations:

$$C_x - 2ne^- \longrightarrow C_x^{2n+} \tag{9.30}$$

at the printed circuit board:

$$C_x^{2n+} + nCu \longrightarrow C_x + nCu^{2+} \tag{9.31}$$

at the cathode:

$$nCu^{2+} + 2ne^- \longrightarrow nCu \tag{9.32}$$

and overall:

$$(Cu)_{p.c.b.} \longrightarrow (Cu)_{cathode} \tag{9.33}$$

i.e. the process only transfers copper from the printed circuit board to the cathode for reuse or resale.

The mechanism for storage of the charge on the carbon particles is not yet proven and in principle could be a mixture of double-layer charging, reversible oxidation of surface redox systems or intercalation of sulphate species into the graphite lattice. The first is thought to be the major method because of the low potential used at the anode (< 1 V vs. NHE). Even so, it is possible to store $100\ C\,g^{-1}$ carbon on the high-surface-area material used.

It is found that the etching rate increases with the conductivity and storage capacity of the carbon, particle surface area and concentration, spraying pressure and temperature, and the process is also catalysed by the presence in solution of a soluble redox species. Hence, the process solution generally contains $30\ g\,dm^{-3}$ of ferric sulphate.

Figure 9.14 shows the principal components of the process. In the cell, both of the surfaces of the plate anode are used and the steel cathodes are separated from the anode by a cupric-ion-conducting cation-exchange membrane. The anode current density is 20–100 mA cm^{-2} and the cell voltage is from -2 to -4 V. In addition to the etching chamber, the circuit contains a porous graphite tube for bleeding-off a clear solution to the anode compartments and a tower for purifying the electrolyte. Electrodes of 1 m^2 will permit the etching of approximately 2 m^2 of printed circuit board (70% removal of 35 μm copper layer on both sides of the board).

The ever-present trends to miniaturization and increased density of components in microelectronic fabrication are placing increasing pressure on the dimensional accuracy of etching processes. Electrochemical etchants suffer from undercut and, partly for this reason, they are tending to be superseded by plasma-etching techniques.

Despite increasing competition from dry-etching techniques, wet etching continues to be used, particularly for fast removal of material.

9.3.2 Etching of semiconductors

Several processes in semiconductor manufacture and microelectronics fabrication involve wet electrochemical steps, including electrodeposition of metals (Chapter 8), electropolishing and etching.

Both 'chemical' (open-circuit) and 'electrochemical' etching are practised, the former being more important. These chemical processes involve concurrent anodic and cathodic half-cell reactions. The dissolution of the semiconductor M occurs via release of electrons e^- or acceptance of holes h^+:

$$M - ne^- \longrightarrow M^{n+} \tag{9.34}$$

$$nh^+ + M \longrightarrow M^{n+} \tag{9.35}$$

and this oxidation is supported by the reduction of an electrolyte species X via acceptance of electrons (electrochemical dissolution) or release of holes (chemical dissolution):

$$X + ne^- \longrightarrow X^{n-} \tag{9.36}$$

$$X \longrightarrow X^{n-} + nh^+ \tag{9.37}$$

The overall cell process is, in either case:

$$M + X \longrightarrow M^{n+} + X^- \tag{9.38}$$

Reaction (9.35) may be written for the three most common semiconductors:

$$Si + 4h^+ \longrightarrow Si(IV) \tag{9.39}$$

$$GaAs + 6h^+ \longrightarrow Ga(III) + As(III) \tag{9.40}$$

$$InP + 6h^+ \longrightarrow In(III) + P(III) \tag{9.41}$$

The actual products of dissolution depend upon conditions; e.g. in acid fluoride solutions, SiF_6^{2-} is the predominant species from reaction (9.39).

Electrolytes must be chosen to give a uniform and high rate of etching which implies the prevention of passivation. In the case of silicon, fluoride serves not only to prevent oxide formation but also to solubilize the silicon as the SiF_6^{2-} $NaF–H_2SO_4$, KF–HF and NH_4HF_2 mixtures. Electrochemical dissolution provides good control over the rate of etching and shows reasonable anisotropy. Its main disadvantages are a tendency to produce micro defects (such as pits), slowness and the need to illuminate *n*-type semiconductors; intrinsic material cannot be etched due to its high resistivity.

For chemical etching, the most common oxidizing agents are HNO_3, H_2O_2 or Br_2. In the case of silicon, HF/HNO_3 mixtures are the most common. For GaAs, H_2O_2 solutions containing H_2SO_4, H_3PO_4, or NH_3 are common, while Br_2/HBr or Br_2/CH_3OH are preferred for InP. Chemical etching is widely used for pattern etching and wafer thinning.

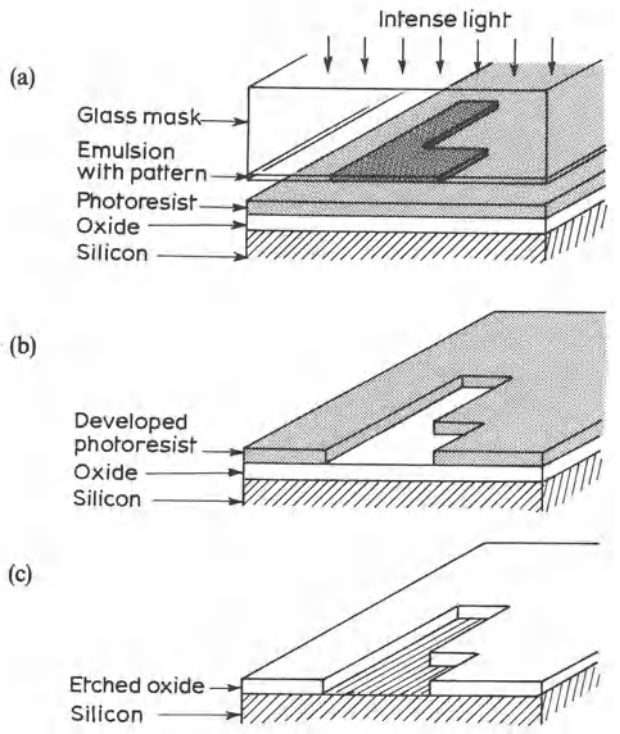

Fig. 9.15 A simplified drawing of the selective removal of silica dioxide from silicon wafers during the fabrication of metal-oxide silica semiconductor devices. (a) Photoresist exposure. (b) Patterned photoresist. (c) Etched pattern.

A number of modifications to the etching process are possible, e.g. heavy doping of silicon by boron (10^{20} atoms cm^{-3}) acts as an effective barrier to stop the etching process in ethylene-diamine and pyrocatechol-based etchants.

Silicon dioxide layers may also be removed from silicon substrates for metal oxide-silicon devices.

A simplified version of the process (Fig. 9.15) serves to illustrate the principles. A patterned mask is used to deposit a photosensitive, etch-resistant, negative pattern of the desired etch pattern on the silicon wafer. This photoresist prevents specific areas of the wafer being attacked when it is immersed in the etchant. The solution used is based on a buffered stabilized hydrofluoric acid which is scrupulously clean to prevent wafer contamination.

The selective removal of the silicon dioxide surface layer in this fashion has several applications, e.g. to provide an active Si site for: (1) further chemical diffusion reactions (with As, P or B species); and (2) electrical contacts.

9.3.3 Electrograining of aluminium

Lithographic printing is based on the controlled production of an oil-receptive positive image area and a water-receptive negative image area on a near-planar printing surface. One type of lithographic plate is based upon a light-sensitive polymer coating which is formed as a positive image on an aluminium surface. The hydrophilic nature of the aluminium is an important factor in the printing process; it may be predetermined by controlled roughening of the surface via 'electrograining'. This technique typically utilizes a.c. (usually mains-frequency etching) at current densities of 20–100 mA cm^{-2} for 5–20 min in aqueous HCl (0.5–3% vol) at *c.* 20° C. The treatment, when properly controlled, provides a uniform array of pits in the ($\geqslant$99.5% purity) aluminium surface, the depth and spacing being functions of the process conditions. Additionally, a micro-roughening of the general surface takes place. The electrograining is very sensitive to the metallurgy and surface preparation of the aluminium; in particular, pitting often takes place preferentially at grain boundaries or near intermetallic phases.

Since the first patented process using 0.5–2% vol HCl in 1960, a number of proprietary developments have taken place including improved electrolytes, e.g. HCl/H_3PO_4, HNO_3, CH_3COOH and H_3BO_4. Modified electrolysis conditions include improved electrolyte agitation and a wide range of a.c. waveforms to improve the speed and uniformity of graining.

FURTHER READING

1 W. Canning (1982) *The Canning Handbook: Surface Finishing Technology*, 23rd Edition, E. and F. N. Spon, Birmingham.

2 A. T. Kuhn (Ed.) (1971) *Industrial Electrochemical Processes*, Elsevier, Amsterdam.

3 J. A. McGeough (1974) *Principles of Electrochemical Machining*, Chapman and Hall, London.
4 A. E. de Barr and D. A. Oliver (Eds.) (1968) *Electrochemical Machining*, MacDonald, London.
5 P. Spiro (1971) *Electroforming: a Comprehensive Survey of Theory, Practice and Commercial Applications*, 2nd Edition, International Publications Service, Draper, Teddington, Middlesex.
6 A. F. Bogenschutz (1974) *Surface Technology and Electroplating in the Electronics Industry*, Portcullis Press, London.
7 G. Leonida (1981) *Handbook of Printed Circuit Design, Manufacture, Components and Assembly*, Electrochemical Publications, Ayr.
8 W. M. Macleod Ross (1975) *Modern Circuit Technology*, Portcullis Press, London.
9 A. F. Bogenschutz and U. George (1985) *Analysis and Testing in Production of Printed Circuit Broads and Plated Plastics*, Finishing Publications, Teddington, Middlesex.
10 S. R. Morrison (1980) *Electrochemistry at Semiconductor and Oxidized Metal Electrodes*, Plenum Press, New York.

10 Corrosion and its control

Corrosion may be defined as the process (or result) of unwanted attack on a metal by its environment.* At first sight, it may be surprising to find a chapter on corrosion control in a book on industrial electrochemistry. It is important to realize, however, that the majority of corrosion processes are (partly or wholly) electrochemical in nature. The relevance of corrosion to society lies in the widespread use of metals which may be exposed to a diverse range of aggressive environments (Fig. 10.1). Thus, the incidence of corrosion includes attack upon cars, household goods, buildings and their services (e.g. plumbing and central heating), shipping, oilrigs and chemical plant.

In practice, corrosion is an insidious process which is often difficult to recognize until deterioration is well advanced; it may have the following interrelated results:

1. Damage to process plant, structural assemblies and other equipment.
2. Consequent shutdowns for repair or replacement work.
3. Risk of injury to personnel due, for example, to leakage or mechanical fractures.
4. Contamination of process products.
5. Loss of product.
6. Loss of operating efficiency.
7. The need to redesign or to over-engineer.
8. Unfavourable publicity.
9. Environmental contamination.
10. Customer alienation.

Whatever the results of corrosion, remedial work may be costly in terms of

* The treatment here is restricted to an 'aqueous' environment which includes atmospheric condensates, fresh water, sea water, soils, etc. It should be realized, however, that other types of corrosion are of great practical importance including gaseous oxidation and corrosion by molten salts.

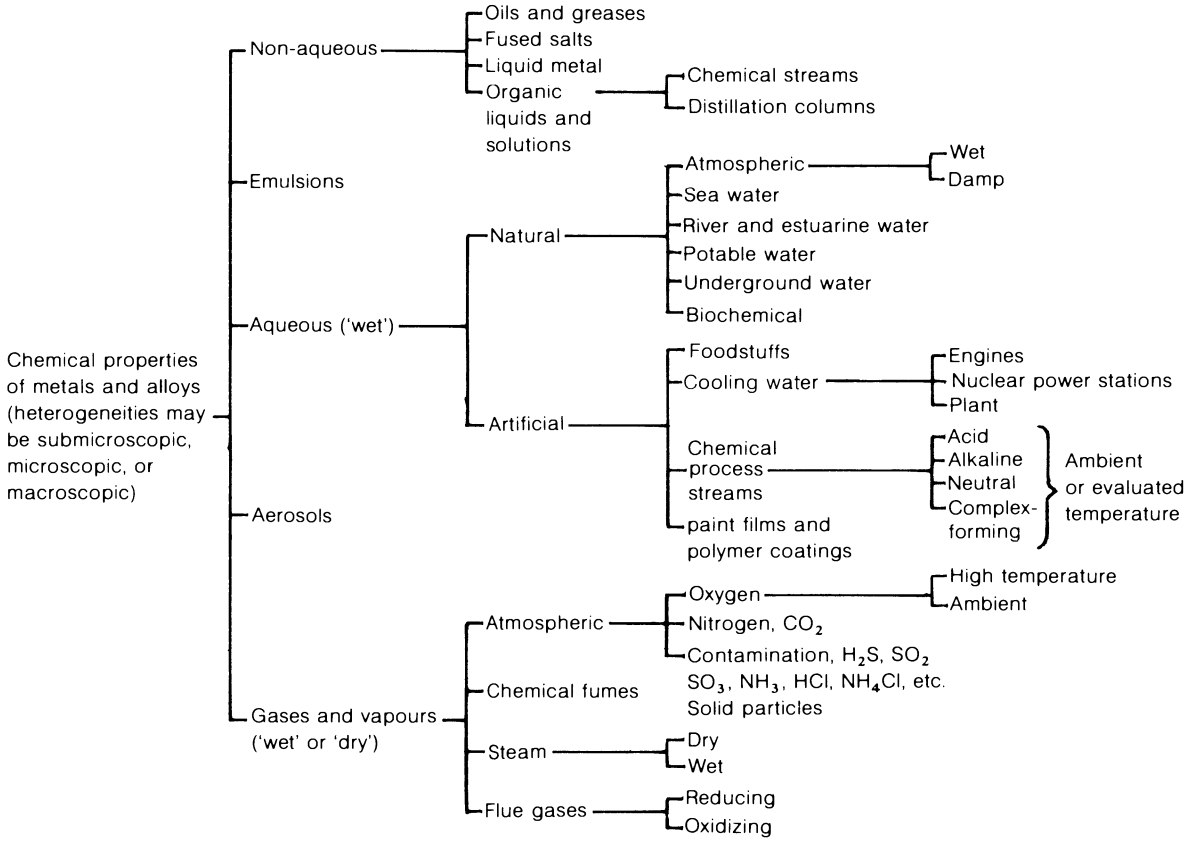

Fig. 10.1 Environments causing corrosion.

finance, time and manpower; extensive redesign, fabrication, materials replacement and treatment, or increased maintenance may be required.

Over the past two decades, increasing attention has been given both to an understanding of corrsion processes and to the development of methods of prevention. There are several possible reasons for this, including the following:

1. The extent and diversity of the use of metals has increased; new alloys continue to be developed.
2. Increasingly specialized applications of metals in particularly aggressive media as in the fields of aerospace, offshore oil and atomic energy.
3. The existence of more corrosive environments due to increasing air and water pollution.
4. Economic incentives sometimes result in the reduction of metal structures to slimmer dimensions; the impact of corrosion is thus made more rapid and/or severe.
5. The increasing trend towards longer periods between maintenance, faster remedial work and the desire to monitor processes automatically.
6. The cost of corrosion to industry (and, hence, to society) is very large. A sizeable fraction of these costs could be saved by a wider appreciation of known techniques for corrosion prevention, coupled with the development of more effective methods of protection.

This chapter aims to provide an understanding of the electrochemical principles of corrosion, in order to provide an appreciation of the techniques for corrosion protection. While an electrochemical approach is evident in the treatment, it should be remembered that corrosion is an interdisciplinary science combining, in addition, aspects of metallurgy and materials science, chemical engineering and mechanical engineering.

10.1 FUNDAMENTALS OF CORROSION

The vast majority of metals occur naturally in the combined state (commonly as oxides or sulphides). They are only won from these ores by a high energy input. Thermodynamically, the return of a metal to the combined state by corrosion is therefore expected to be a spontaneous process. Hence, the corrosion of most metals is almost inevitable but fortunately the rate of the process is often slow and there are several methods of further moderating the rate of reaction to acceptable limits. Several methods of control will be explored in section 10.5.

First of all, we must consider the 'corrosion cell', then its thermodynamics and kinetics in order to provide an understanding of corrosion processes.

The 'corrosion cell', which is shown as a highly schematic, instantaneous snapshot of the metal surface (Fig. 10.2) has five essential components: (1) anodic zones; (2) cathodic zones; (3) electrical contact between anodic and cathodic zones; (4) an (ionically) conducting solution; and (5) a cathodic reactant.

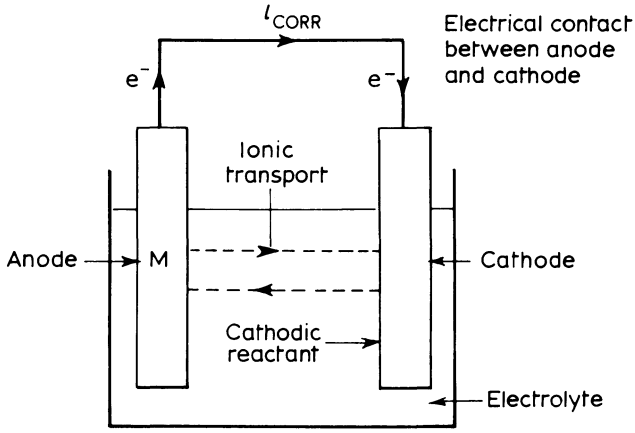

Fig. 10.2 The essential components of a corrosion cell.

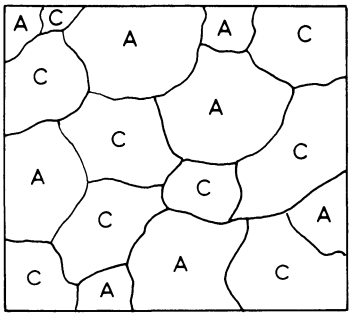

Fig. 10.3 Localized anodic (A) and cathodic (C) zones on the same metal surface covered by an electrolyte. This is a 'snapshot' of a dynamic situation; the anodic and cathodic zones may change in shape, size and position. The zones may arise due to differences in, for example, constituent phases, stress levels, thermal history, surface coatings and imperfection levels (such as grain boundaries, dislocations, kink sites, etc). These features tend to become anodic.

The corrosion cell may be viewed as a short-circuited electrolysis cell, whose cell voltage provides the driving force for materials wastage. In practical situations, the actual anodes and cathodes may be entirely separate and macroscopic or may occur locally on a heterogeneous metal surface. The latter case is more common (Fig. 10.3); numerous, discrete microcells may arise due to differences in the constituent phases of the metal (possibly due to heat treatment or welding), from variations in stress, from natural-coating (e.g. oxides) or protective-coating variations, or from ionic conductivity changes or compositional differences in the electrolyte, e.g. differential aeration. The electrolyte may

be in bulk form (as in immersion conditions or flow through a pipe) or be present only as a thin condensed or adsorbed film (as in atmospheric corrosion).

The wide range of electrolyte types may be classified according to their nature and location (Fig. 10.1). Attention will be focused on aqueous electrolytes in this chapter.

The overall corrosion process is a chemical reaction representing spontaneous dissolution of the metal (M) by reaction with the environment. This can be described schematically by one of the following processes:

$$M + n/4O_2 + n/2H_2O \longrightarrow M^{n+} + nOH^- \tag{10.1}$$

$$M + nH_2O \longrightarrow M^{n+} + n/2\,H_2 + nOH^- \tag{10.2}$$

$$M + nH^+ \longrightarrow M^{n+} + n/2\,H_2 \tag{10.3}$$

$$M + nH^+ + n/4\,O_2 \longrightarrow M^{n+} + n/2\,H_2O \tag{10.4}$$

In fact, these chemical reactions do not occur by direct interaction between the metal and oxidizing agent in the environment (e.g. O_2, H_2O or H^+). Instead, each of these cell reactions is the result of an anodic and a cathodic reaction occurring simultaneously at identical rates on the corroding surface, i.e.:

Anode: $$M - ne^- \longrightarrow M^{n+} \tag{10.5}$$

Cathode: $$O_2 + 2H_2O + 4e^- \longrightarrow 4OH^- \tag{10.6}$$

Or cathode: $$O_2 + 4H^+ + 4e^- \longrightarrow 2H_2O \tag{10.7}$$

Or cathode: $$2H_2O + 2e^- \longrightarrow H_2 + 2OH^- \tag{10.8}$$

Or cathode: $$2H^+ + 2e^- \longrightarrow H_2 \tag{10.9}$$

Thus, the corrosion processes represented by reactions (10.1)–(10.4) are overall cell reactions, each being the sum of the anode reaction (10.5) and an appropriate cathode reaction, e.g.:

Anode: $$M - ne^- \longrightarrow M^{n+} \tag{10.5}$$

Cathode: $$n/4O_2 + n/2\,H_2O + ne^- \longrightarrow nOH^- \tag{10.6}$$

Cell: $$M + n/4O_2 + n/2\,H_2O \longrightarrow M^{n+} + nOH^- \tag{10.1}$$

This simplified treatment indicates some of the factors influencing corrosion; the following points are noteworthy:

1. The anodic process results in dissolution of metal from the 0 to the $n+$ oxidation state; M^{n+} may be a simple, hydrated metal ion or it may represent a more complex soluble or insoluble species.
2. The rate of the anodic process may be significantly altered if M^{n+} builds up in solution or if M^{n+} undergoes further reactions, e.g. hydrolysis.
3. The same anodic process (reaction (10.5)) may be supported by one or more of the four different cathode reactions (10.6)–(10.9).

4. The cathodic process may determine the nature of the corrosion products (as well as the rate of reaction), e.g. the local increase in pH due to reactions (10.6)–(10.9) may result in the metal being coated by an oxide of hydroxide film.
5. The corrosion products are varied; they include dissolved species or dissolved ions (e.g. M^{n+}, OH^-); insoluble solids (e.g. M_2O_n, $M(OH)_n$ and gaseous (e.g. H_2) species.
6. The reactants for corrosion may include a solid (e.g. M), solvent or dissolved ions (e.g. H_2O, OH^-, H^+) and dissolved gases, e.g. O_2.
7. The cathodic process (and, hence, the corrosion reaction) depends upon the supply of a cathodic reactant. Hence, reaction (10.6) involves dissolved oxygen and the solvent, water; reaction (10.8) requires only water; reaction (10.9) necessitates protons; and reaction (10.7) involves protons and dissolved oxygen. This has at least two further implications: (1) dissolved oxygen is often supplied by convective diffusion resulting in the possibility of mass transport control; and (2) the electrolyte composition (in particular pH) is very important as it determines the cathodic reaction which occurs and its rate.
8. The progress of a corrosion process usually results in compositional changes in the electrolyte; in particular, the local pH near the cathodic zones usually experiences an increase in pH (due to reactions (10.6)–(10.9). The significance of this effect depends upon the electrode and electrolyte conditions; possible implications are the saponification of paint films or the precipitation of basic metal oxides or hydroxides.
9. So far, reactions between the corrosion products themselves and between the metal and the corrosion products have been ignored. It will be seen later that the formation of metal oxides and hydroxides via chemical reaction may be critical in determining the thermodynamics (section 10.2) and kinetics (section 10.3) of corrosion processes. Additionally, in the case of acid electrolytes, hydrogen evolution (reaction (10.9)) may result in the blistering of paint films or hydrogen embrittlement.

In general, these points serve to illustrate the heterogeneous nature of corrosion reactions and indicate the need, whenever possible, to identify the component electrodes and electrode reactions of the 'corrosion cell'. Furthermore, it can be seen that compositional changes in the electrolyte are always involved both in facilitating corrosion and as a result of the process.

In practice, more than one cathode process may occur: (1) in aerated, near-neutral solutions, both reactions (10.6) and (10.8) may take place; and (2) in aerated, acid electrolytes, both reactions (10.7) and (10.9) may occur. Dissolved oxygen is a very common cathodic reactant and its removal can significantly reduced overall corrosion rates by removal of reactions (10.6) or (10.7).

In the above treatment, only the ubiquitous species O_2, H_2O, and H^+ have been considered as cathodic reactants. In particular systems, other processes can

occur, e.g. the following reactions may be noted:

1. A lowering of the oxidation state of a metal ion:

$$M^{n+} + e^- \longrightarrow M^{(n-1)+} \tag{10.10}$$

e.g. $$Fe^{3+} + e^- \longrightarrow Fe^{2+} \tag{10.11}$$

The Fe(III) species may be present in the solution phase or it may exist in previously formed rust. Another possibility is:

$$Cu^{2+} + e^- \longrightarrow Cu^{+} \tag{10.12}$$

Particularly in solutions containing high levels of Cl^-, the Cu(I) product may be stabilized as chloro-complexes such as $CuCl_2^-$.

2. Electrodeposition of a metal:

$$M^{n+} + ne^- \longrightarrow M \tag{10.13}$$

e.g. $$Cu^{2+} + 2e^- \longrightarrow Cu \tag{10.14}$$

An example is provided by the deposition copper onto the surface of ferrous pipework and radiator surfaces in central heating or boiler systems containing dissolved copper. The immersion deposit of copper is cathodic and porous, allowing access to the underlying anodic steel.

3. The reduction of oxidizing acids and their anions may also be considered, particularly in the case of nitric acid and nitrate solutions:

$$NO_3^- + 2H^+ + e^- \longrightarrow NO_2 + H_2O \tag{10.15}$$

The reduction of chromate films is an important method of corrosion inhibition by passivation (section 10.2.2):

$$CrO_4^- + 8H^+ + 7e^- \longrightarrow Cr + 4H_2O \tag{10.16}$$

4. A special and important class of cathodic reactants is provided by microbial infections. In the case of soils containing water and in water storage tanks, for example, the growth of sulphate-reducing bacteria (such as 'desulphovibrio desulphuricans') is especially dangerous as these bacteria can readily metabolize sulphate to produce aggressive sulphide species, the (very simplified) reactions being:

Anode: $$4Fe - 8e^- \longrightarrow 4Fe^{2+} \tag{10.17}$$

Cathode $$8H_2O + 8e^- \longrightarrow 8H_{ads} + 8OH^- \tag{10.18}$$

$$8H_{ads} + SO_4^{2-} \longrightarrow 4H_2O + S^{2-} \tag{10.19}$$

Cell: $$4Fe + 4H_2O + SO_4^{2-} \longrightarrow 4Fe^{2+} + S^{2-} + 8OH^- \tag{10.20}$$

Followed by: $$S^{2-} + Fe^{2+} \longrightarrow FeS \tag{10.21}$$

The most important step (reaction (10.19)) is the utilization of adsorbed hydrogen by hydrogenases in the bacteria. In practice, microbial corrosion often involves the subtle interplay between many types of microorganism, metallurgical factors, electrolyte composition and flow conditions, e.g. a significant presence of aerobic bacteria or fungi may cause local oxygen depletion. Aside from promotion of differential aeration or deposit corrosion, conditions are then rendered more favourable for anaerobic bacteria such as sulphate-reducing species. Microbial contamination may also promote emulsification in water or oil media and produce an aggressive microenvironment due, for example, to metabolic generation of acid. It is noteworthy that microbial corrosion may be particularly severe due to the localization and speed of attack. In addition to

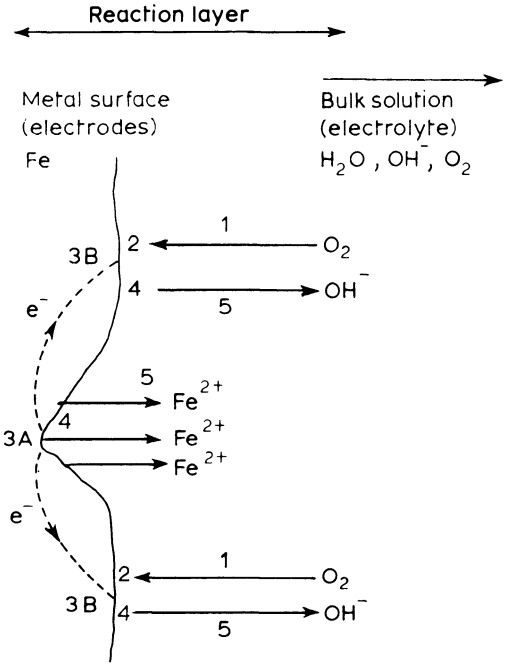

Fig. 10.4 A simplified summary of the steps involved in a corrosion process. The corrosion of iron via oxygen reduction in an alkaline medium is considered. (1) Mass transport of reactant O_2 to the surface via convection and diffusion. (2) Adsorption of reactants O_2 and H_2O.

(3) electrochemical reactions:

3A anode $Fe - 2e^- \longrightarrow Fe^{2+}$

3B cathode $\frac{1}{2}O_2 + H_2O + 2e^- \longrightarrow 2OH^-$

Cell $Fe + \frac{1}{2}O_2 + H_2O \longrightarrow Fe^{2+} + 2OH^-$

(4) Desorption of products (Fe^{2+} and OH^-) or reaction between products: e.g.

$2Fe^{2+} + 4OH^- \longrightarrow 2Fe(OH)_2$ then

$2Fe(OH)_2 + O_2 + (n-2)H_2O \longrightarrow Fe_2O_3 . nH_2O$

(5) Mass transport of products Fe^{2+} and OH^- away from the surface by migration and convective diffusion.

corrosion, problems may include spoilage of engineering materials (fuels, lubricants, polymers) and blocking of filters and pipelines due to microbial sludge, together with health and safety objections.

It will now be evident, from consideration of possible cathodic reactions, that corrosion cells may arise because of localized compositional differences in the electrolyte with respect to, for example, pH, dissolved O_2, metal ions, oxyanions and the metabolism of microbial infections.

The overall corrosion process may be subdivided schematically into a number of simplified steps (Fig. 10.4). Any one of these may become rate-determining under appropriate conditions. Again, this serves to underline the complexity of corrosion.

10.2 THE THERMODYNAMICS OF CORROSION

10.2.1 Simple electrode potential series

An appreciation of equilibrium thermodynamics is essential both to an understanding of corrosion and to the answer of the question: can corrosion occur in particular circumstances? It must be stressed, however, that a thermodynamic treatment alone is extremely limited and the conclusions are often misinterpreted. There are many reasons for this but the major ones include the stringent, idealized conditions for much reported thermodynamic data (e.g. data commonly to be found considers pure metals in pure water at 25°C and atmospheric pressure, no complexing ligands, unit activity of species) and a failure to consider the rates of reaction (i.e. kinetics) or the physical and mechanical stability and ionic properties of surface oxides. Moreover, corrosion reactions are inherently heterogeneous and non-equilibrium.

If a corrosion reaction is to be spontaneous, the Gibbs free energy associated with the cell reaction must be negative $\Delta G_{\text{CELL}} < 0$. These free-energy changes may be related to the relevant equilibrium potentials:

$$\Delta G_{\text{CELL}} = -nF\,E^{\text{e}}_{\text{CELL}} < 0 \tag{10.22}$$

i.e.: $E^{\text{e}}_{\text{CELL}} > 0$ and: $E^{\text{C}}_{\text{e}} - E^{\text{A}}_{\text{e}} > 0$

i.e. the cathode process must have a more positive equilibrium potential than that of the anode process for corrosion to occur.

Values of the equilibrium potential, for known redox couples under *standard* conditions may be conveniently listed, in order, as an electrochemical series (Table 10.1). From this table it can be inferred that, *under standard conditions only and considering only the listed equilibria*, certain corrosion processes may be feasible, e.g. the copper dissolution reaction (10.23) has a more positive potential than that of the hydrogen evolution reaction (10.9) and therefore spontaneous corrosion (reaction (10.24)) is not possible in deaerated uncomplexed, acid

solution under standard conditions:

		$E_e^{\ominus}$/(V)	
Cathode:	$2H^+ + 2e^- \longrightarrow H_2$	0.00	(10.9)
Anode:	$Cu^{2+} + 2e^- \longleftarrow Cu$	0.34	(10.23)
Cell:	$Cu + 2H^+ \longrightarrow Cu^{2+} + H_2$	−0.34	(10.24)

$\Delta G = +66\ \text{kJ mol}^{-1}\ \text{Cu}$

Similarly, the spontaneous corrosion of gold via hydrogen evolution is not feasible. In contrast, spontaneous corrosion of iron (reaction (10.25)) is, however, feasible as the potential of the iron dissolution reaction (10.17) is negative to that of hydrogen evolution (10.9):

		$E_e^{\ominus}$/(V)	
Cathode:	$2H^+ + 2e^- \longrightarrow H_2$	0.00	(10.9)
Anode:	$Fe^{2+} + 2e^- \longleftarrow Fe$	−0.44	(10.17)
Cell:	$Fe + 2H^+ \longrightarrow Fe^{2+} + H_2$	0.44	(10.25)

$\Delta G = -85\ \text{kJ mol}^{-1}\ \text{Fe}$

Evidently, zinc may also corrode via hydrogen evolution, the driving force being greater than for iron, due to the more negative potential of the Zn/Zn^{2+} couple. If the acid electrolyte at pH = 0 was saturated with O_2 at unit partial pressure, oxygen reduction is then an alternative process and zinc, iron and copper would all corrode; indeed, of the metals listed in Table 10.1, only gold would not, e.g.:

		$E_e^{\ominus}$/(V)	
Cathode:	$\frac{1}{2}O_2 + 2H^+ + 2e^- \longrightarrow H_2O$	+1.23	(10.7)
Anode:	$Cu^{2+} + 2e^- \longleftarrow Cu$	+0.34	(10.23)
Cell:	$\frac{1}{2}O_2 + 2H^+ + Cu \longrightarrow H_2O + Cu^2$	+0.89	(10.26)

$\Delta G = -172\ \text{kJ mol}^{-1}\ \text{Cu}$

Thermodynamically, metals can only corrode by anodic dissolution if an associated cathodic reaction with a more positive equilibrium is available. As noble metals such as gold have particularly high electrode potentials, they have excellent corrosion resistance. However, if an alternative cathodic reaction which has a more positive potential becomes available, or if the potential of the metal dissolution reaction is reduced by complex formation, corrosion again becomes possible, e.g. gold may corrode in concentrated hydrochloric acid, courtesy of the

Table 10.1 Electrochemical series for reactions important in corrosion. Standard conditions (25° C; 1 atm; H_2O; unit activities, metals present in their standard states)

Electrode reaction			$E_e^\ominus$ / V (SHE)
$Au^{3+} + 3e^-$	$\rightleftharpoons$	Au	1.50
$2O_2 + 4H^+ + 4e^-$	$\rightleftharpoons$	$2H_2O$	1.23
$Pt^{2+} + 2e^-$	$\rightleftharpoons$	Pt	1.20
$Ag^+ + e^-$	$\rightleftharpoons$	Ag	0.80
$\frac{1}{2}Hg_2^{2+} + e^-$	$\rightleftharpoons$	Hg	0.79
$Cu^{2+} + 2e^-$	$\rightleftharpoons$	Cu	0.34
$H^+ + e^-$	$\rightleftharpoons$	$\frac{1}{2}H_2$	0
$Pb^{2+} + 2e^-$	$\rightleftharpoons$	Pb	−0.13
$Sn^{2+} + 2e^-$	$\rightleftharpoons$	Sn	−0.14
$Ni^{2+} + 2e^-$	$\rightleftharpoons$	Ni	−0.23
$Co^{2+} + 2e^-$	$\rightleftharpoons$	Co	−0.28
$Cd^{2+} + 2e^-$	$\rightleftharpoons$	Cd	−0.40
$Fe^{2+} + 2e^-$	$\rightleftharpoons$	Fe	−0.44
$Cr^{3+} + 3e^-$	$\rightleftharpoons$	Cr	−0.74
$Zn^{2+} + 2e^-$	$\rightleftharpoons$	Zn	−0.76
$V(II) + 2e^-$	$\rightleftharpoons$	V	−1.18
$Mn^{2+} + 2e^-$	$\rightleftharpoons$	Mn	−1.18
$Al^{3+} + 3e^-$	$\rightleftharpoons$	Al	−1.66
$Ti^{3+} + 3e^-$	$\rightleftharpoons$	Ti	−1.80
$U(III) + 3e^-$	$\rightleftharpoons$	U	−1.80
$Mg^{2+} + 2e^-$	$\rightleftharpoons$	Mg	−2.36
$Na^+ + e^-$	$\rightleftharpoons$	Na	−2.71
$Ca^{2+} + 2e^-$	$\rightleftharpoons$	Ca	−2.87
$K^+ + e^-$	$\rightleftharpoons$	K	−2.92
$Li^+ + e^-$	$\rightleftharpoons$	Li	−3.04

following reactions:

		$E_e^\ominus$ / V	
Cathode:	$3O_2 + 12H^+ + 12e^- \longrightarrow 6H_2O$	+1.23	(10.7)
Anode:	$4AuCl_4^- + 12e^- \longleftarrow 4Au + 16Cl^-$	+1.00	(10.27)
Cell:	$4Au + 3O_2 + 16Cl^- + 12H^+ \longrightarrow 4AuCl_4^- + 6H_2O$	+0.23	(10.28)

$\Delta G = -22\ \text{kJ mol}^{-1}\ \text{Au}$

The most important restrictions regarding the electrochemical series are the assumptions of highly idealized (and unrealistic) conditions involving single, pure metals and simple, pure solutions at pH 0. It does not, therefore, consider the following:

1. Films of corrosion products which may be formed on the metal surface.
2. Complex reactions which occur and produce H^+ or OH^- ions (and are therefore pH-dependent) are not considered.
3. Any factors which lead to non-ideality, i.e. an activity coefficient not equal to one or the presence of a complexing agent for M^{n+}.
4. The value of the electrode potential when the metal is first immersed is indeterminate due to the absence of an oxidized metal species.

When a finite amount of metal dissolution has occurred, the equilibrium electrode potential of the metal is given by the Nernst equation:

$$E_e^M = E_e^\ominus + (RT/nF) \ln a_{M^{n+}}/a_M \tag{10.29}$$

where $a_M = 1$ as the metal is present in its standard state. The increasing value of the activity of metal ions $a_{M^{n+}}$ results in a change in the electrode potential to more positive values.

The shortcomings of the electrochemical series are readily illustrated, e.g. aluminium has a very negative standard potential yet it exhibits particularly good corrosion resistance in many environments. This is because the electrochemical series considers only Al metal and Al^{3+} while in practice Al_2O_3 films determine the properties of the system. Hence, a much more sophisticated thermodynamic treatment is necessary to predict the behaviour of aluminium. This is a general situation in corrosion.

A more practical collection of electrode potentials is provided by a galvanic series of metals based on practical observations in a specific electrolyte under known conditions. As an example, Table 10.2 shows a galvanic series for metals in sea water at 25° C. In contrast to the electrochemical series, a metal can have more than one electrode potential if it contains different impurities or when it is subjected to different pretreatments or solution conditions. Moreover, the relative position of some metals depends greatly on the electrolyte composition and temperature e.g. types 304 and 316 stainless steels show high positive potentials in aerated sea water at 25° C due to their protective passive film. In deaerated conditions, these alloys become most active; the passive film is unstable, resulting in a high negative potential. Such dramatic 'potential reversals' are also known for galvanic coatings, e.g. steel is effectively protected in tap water at 20° C by a sacrificial coating of zinc, i.e. by galvanizing. At elevated temperatures (> 60° C), the zinc may become negative to the steel and the steel starts to corrode. Despite its practical derivation, the galvanic series still does not consider the nature of the corrosion products, including solubility restrictions.

Table 10.2 Galvanic series of metals in sea water at 25°C, 1atm

Least likely to corrode:	
Platinum	
Gold	
Graphite	
Titanium	
Silver	
Chlorimet 3 (62% Ni, 18% Cr, 18% Mo) (passive)	
Hastelloy C (passive)	
18% Cr–8% Ni-3% Mo steel (passive)	
18% Cr–8% Ni, steel (passive)	
13% Cr–Fe (passive)	
Inconel (passive)	
Nickel (passive)	
Ag solder	
Monel	
Copper–Nickel	E_{CORR} more negative ↓
Bronzes (Cu–Sn)	
Copper	
Brasses (Cu–Zn)	
Chlorimet 2 (66% Ni, 32% Mo, 1% Fe)	
Hastelloy B (65% Ni, 30% Mo, 5% Fe)	
Hastelloy A (60% Ni, 20% Mo, 20% Fe)	
Inconel (active) (80% Ni, 13% Cr, 7% Fe)	
Nickel (active)	
Tin	
Lead	
Lead–Tin solders	
Hastelloy C (active) (62% Ni, 18% Cr, 15% Mo)	
18% Cr–8% Ni–3% Mo steel (active)	
18% Cr–8% Ni steel (active)	
Ni-resist	
13% Cr–iron (active)	
Cast iron	
Steel or Fe	
Aluminium 24S-T	
Cadmium	
Aluminum 2S	
Zinc	
Magnesium alloys	
Magnesium	
Most likely to corrode	

10.2.2 Extended thermodynamics

(a) Potential – pH (Pourbaix) diagrams

In order to extend the thermodynamic treatment, it is necessary to consider other types of equilibria, particularly formation of metal hydroxides and oxides:

$$M + nH_2O \longrightarrow M(OH)_n + ne^- + nH^+ \tag{10.30}$$

and:

$$M + 2nOH^- \longrightarrow MO^{n-} + nH_2O + ne^- \tag{10.31}$$

Both of these reactions are electron transfer processes and therefore are potential-dependent but they are also clearly pH-dependent. Other reactions occur, including purely chemical but pH-dependent ones:

$$M^{n+} + nOH^- \longrightarrow M(OH)_n \tag{10.32}$$

and:

$$MO_n^{n-} + nH^+ \longrightarrow M(OH)_n \tag{10.33}$$

The Pourbaix (phase) diagram is a plot of redox potential (ordinate) as a function of pH (abcissa) for a given metal under standard, thermodynamic conditions (usually water at 25° C). The diagram takes account of electrochemical and chemical equilibria and defines the domain of stability for the electrolyte (normally water), the metal and selected compounds, e.g. oxides, hydroxides and hydrides. The following criteria are often adopted regarding dissolved metal-ion levels:

$< 10^{-6}$ g dm^{-3}: protection (via immunity or passivation)

$> 10^{-6}$ g dm^{-3}: corrosion

and the Nernst equation may be used to calculate the corresponding electrode potential.

There are three general types of solid line on the Pourbaix diagram, each representing an equilibrium between the metal and other species:

1. Horizontal lines indicate reactions which are only potential-dependent.
2. Vertical lines indicate reactions which are only pH-dependent.
3. Sloping lines indicate reactions which are both potential and pH-dependent.

A particular case of (3) is seen in the dotted lines in Fig. 10.5 which relate to the electrolysis of water. The lower dotted line describes the equilibrium:

$$2H^+ + 2e^- \rightleftharpoons H_2 \tag{10.9}$$

The Nernst equation for this equilibrium is:

$$E_e^H = E_e^\ominus + (RT/2F) \ln a_{H^+}^2 / p_{H_2} \tag{10.34}$$

or, at unity partial pressure of hydrogen ($p_{H_2} = 1$):

$$E_e^H = E_e^\ominus + (2.3RT/F) \log a_{H^+} \tag{10.35}$$

By convention, $E_e^\ominus = 0$ V for the H_2 electrode and at 298 K, $2.3\,RT/F = 0.059$ V, giving:

$$E_e^H = 0.059 \log a_{H^+} \tag{10.36}$$

But pH is defined as:

$$pH = -\log a_{H^+} \tag{10.37}$$

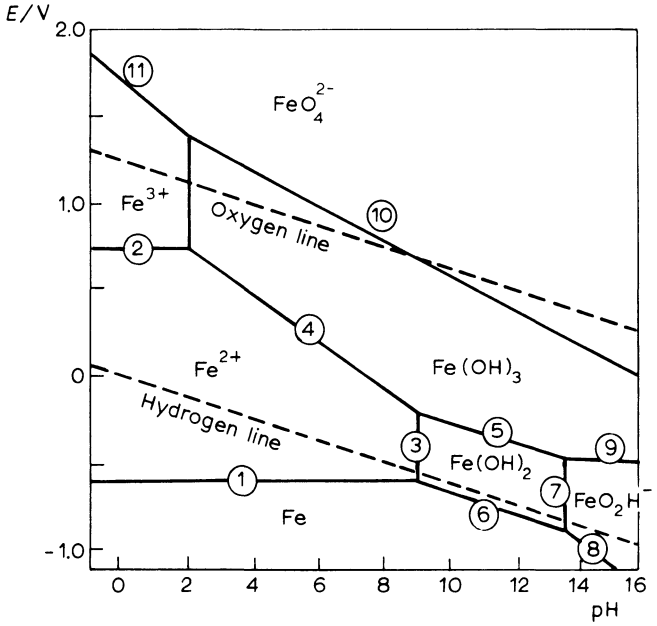

Fig. 10.5 A simplified Pourbaix diagram for iron in water at 25° C. Dissolved iron concentration: 10^{-6} g dm^{-3}. The following equilibria are considered:

1. $Fe^{2+} + 2e^- \rightleftharpoons Fe$
2. $Fe^{3+} + e^- \rightleftharpoons Fe^{2+}$
3. $Fe(OH)_2 + 2H^+ \rightleftharpoons Fe^{2+} + 2H_2O$
4. $Fe(OH)_3 + 3H^+ + e^- \rightleftharpoons Fe^{2+} + 3H_2O$
5. $Fe(OH)_3 + H^+ + e^- \rightleftharpoons Fe(OH)_2 + H_2O$
6. $Fe(OH)_2 + 2H^+ + 2e^- \rightleftharpoons Fe + 2H_2O$
7. $FeO_2H^- + H_2O \rightleftharpoons Fe(OH)_2 + OH^-$
8. $FeO_2H^- + H_2O + 2e^- \rightleftharpoons Fe + 3OH^-$
9. $Fe(OH)_3 + e^- \rightleftharpoons FeO_2H^- + H_2O$
10. $FeO_4^{2-} + 5H^+ + 3e^- \rightleftharpoons Fe(OH)_3 + H_2O$
11. $FeO_4^{2-} + 8H^+ + 3e^- \rightleftharpoons Fe^{3+} + 4H_2O$

Note: variants are possible which consider other oxides, hydroxides and soluble oxyanions.

Therefore, equation (9.35) may be written:

$$E_e^H = -0.059\ \text{pH} \tag{10.38}$$

which describes the lower dotted line. The upper dotted line relates to the equilibrium:

$$O_2 + 4H^+ + 4e^- \rightleftharpoons 2H_2O \tag{10.7}$$

which is described, at 298 K and unity partial pressure of O_2, by:

$$E_e^O = (1.23 - 0.059\ \text{pH}) \tag{10.39}$$

Here, equation (10.39) describes the upper dotted line on the Pourbaix diagram. The region between the two dotted lines represents a zone where water is stable. Above the upper dotted line, oxygen evolution is possible; below the lower dotted line, hydrogen evolution can occur.

The following types of zone exist in Pourbaix diagrams:

1. *Immunity* refers to the metal as a thermodynamically stable phase.
2. *Corrosion* occurs if a compound of the metal is the thermodynamically stable state unless (3) below applies.
3. *Passivity* occurs when a sparingly soluble metal compound forms a thin, protective film (usually an oxide or hydroxide) on the surface, resulting in a negligibly small corrosion rate. The protective properties of a surface film of corrosion products are best established by practical experience, guided by a knowledge of reaction kinetics.

Pourbiax diagrams provide compact means of summarizing data for the following types of equilibria:

1. Redox couples involving the metal as a function of pH.
2. Hydrolysis and proton-exchange reactions of each metal-oxidation state.

Hence, they indicate the most stable species at a particular pH and potential as well as the conditions where spontaneous change becomes thermodynamically favourable.

At a given pH, for example, the diagram shows the potential where (kinetics permitting) oxidation will occur; it also shows the nature of the species formed. As previously discussed, the stability of water as a function of pH is also indicated.

The Gibbs free energy change for reactions (10.1)–(10.4) will be negative if the potentials for the cathodic reactions (10.6)–(10.9) respectively are more positive than for the anodic reaction (10.5). Hence, corrosion is possible at pH values where the dotted lines for oxygen reduction (reactions (10.7) and (10.39)) or hydrogen evolution (reactions (10.9) and (10.38)) lie above the line for the M/M^{n+} couple.

Figure 10.5 shows a simplified Pourbaix diagram for iron, in water at 25° C. The potential of the hydrogen electrode lies above the immunity region, over the entire pH scale. This means that iron may dissolve with hydrogen evolution at all pH values. In the pH interval 9.4–12.5, however, passivation due to $Fe(OH)_2$ occurs. At a lower pH, $Fe(OH)_2$ dissolves to give Fe^{2+} ions; at higher pH, dissolution of $Fe(OH)_2$ yields $HFeO_2^-$ ions. At sufficiently positive potentials, the passive layer consists of Fe_3O_4 or $Fe_2O_3.nH_2O$. In very strongly oxidizing, alkaline electrolytes, corrosion may occur via formation of FeO_4^{2-}.

Consider an iron sample immersed in an oxygen-free solution at pH 6. The potential of the metal is a so-called 'mixed potential'; it lies between the equilibrium potentials for $M - ne^- \rightleftharpoons M^{n+}$ and for $nH^+ + ne^- \rightleftharpoons n/2\,H_2$ (see

below). The corrosion potential established in this fashion is determined by two simultaneous and electrically coupled electrode reactions.

The following thermodynamic predictions can be made regarding the stability of iron; protection is possible by any of the following strategies:

1. The electrode potential may be lowered into the region of immunity by making the specimen the cathode in a suitable galvanic cell (in which dissimilar metals are in electrical contact) or an electrolytic cell. This is the basis of cathodic protection (section 10.5.3). A lowering of the potential from the FeO_4^{2-} zone into the passive zone is an example of incomplete cathodic protection.
2. The electrode potential may be raised into the passive region. This may be achieved by making the specimen the anode in a galvanic or electrolytic cell (as in anodic protection, section 10.5.3). More commonly, an oxidizing agent may be added to the solution to form a passive layer on the metal (section 10.5.2).
3. The pH of the electrolyte may be increased to bring the sample into a passive zone.

The different thermodynamic behaviour of two other common metals is illustrated in the Pourbiax diagrams of Fig. 10.6. It must be emphasized that these diagrams consider only solutions in the absence of complexing agents and, for any other combination of metal and medium, it is necessary to construct a separate diagram.

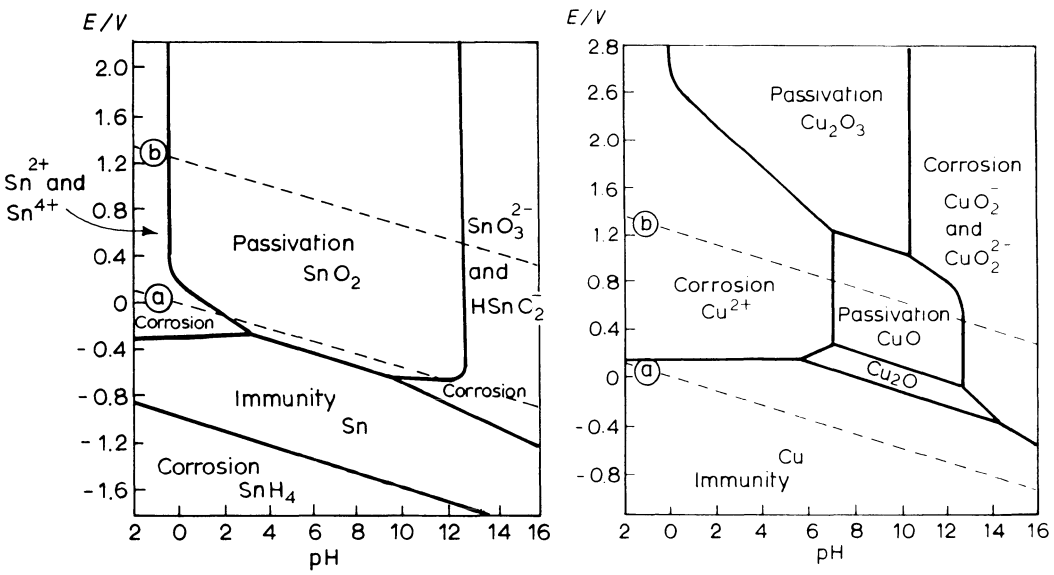

Fig. 10.6 Pourbaix diagrams for pure metals in water at 25° C. (a) Tin. (b) Copper. Potential axes are with respect to NHE.

It is very important to exercise care in the use of Pourbaix diagrams for predicting the likelihood of corrosion because:

1. The diagrams are thermodynamic; no information (or even indication) of the corrosion *rate* (i.e. kinetics) is given. Neither are the physical stability, porosity or adhesion of passive films indicated.
2. There is no consideration of even low levels of extraneous ions. For example, SO_4^{2-} may enhance passivity by formation of insoluble sulphates; CrO_4^{2-} may either passivate by insoluble film formation or promote corrosion by acting as an alternative cathodic reactant (reaction (10.16)); CN^- may promote corrosion by facilitating $M(CN)_x^{y-}$ complexes; Cl^- may break down passivity or form complexes (reaction (10.27)), etc.
3. The diagrams usually refer to 25° C and atmospheric pressure. In-service conditions may correspond to much higher (or lower) temperature and pressure.
4. Only pure metals are considered. In practice, all metals are either impure, or are used in an alloyed form.
5. Localized pH changes are not considered.
6. The data used to compile the diagrams may sometimes not be reliable or precise.

Potential-pH diagrams may be modified, to an extent, in order to consider other simple electrolytes (e.g. NaCl), contaminants (e.g. SO_4^{2-}), elevated temperatures and pressures and even metal alloys. They are perhaps best used as an introductory guide and as a means of rationalizing corrosion processes. The conclusions drawn from a Pourbaix diagram may sometimes be shown to be quite incorrect when the kinetics of the reactions are defined. It is therefore important to exercise care in the application of such diagrams.

10.3 THE KINETICS OF CORROSION REACTIONS

Consideration of the Pourbaix diagrams for the metals familiar in everyday life will lead to the conclusion that the metals have little stability; almost all the metals should react with oxygen and many should also dissolve to give hydrogen, particularly in acid solution. Fortunately, many metals corrode only very slowly in a normal environment and, hence, it is clear that kinetic factors are often dominant in determining the stability of metals. This should not be surprising since it was shown in Chapter 1 that both oxygen reduction and hydrogen evolution can be slow processes and their rate varies greatly with the metal of the cathode. In fact, the kinetics of metal dissolution reactions also vary and it is also necessary to consider passivation.

It is important to realize that metal corrosion is a non-reversible and non-equilibrium situation. The metal takes up a 'mixed-potential' which depends on the thermodynamics and kinetics of both metal dissolution and the balancing cathodic process. Considering a simple corrosion reaction:

$$M + nH^+ \longrightarrow M^{n+} + n/2\ H_2 \tag{10.3}$$

Several obvious points may be made:

1. The reaction continuously leads to the production of M^{n+} and H_2 and also consumes H^+, i.e. the process is non-equilibrium.
2. No charge build-up occurs; the rate at which electrons are produced in the metal dissolution reaction is balanced by their rate of consumption by the hydrogen evolution reaction.
3. The M^{n+} is electrochemically equivalent to $n/2$ H_2.

Figure 10.7 shows an *i–E* curve recorded for a metal, M, in an oxygen-free aqueous electrolyte. Suitable analytical experiments have confirmed that the cathodic current is due to hydrogen evolution and that the anodic current is due to metal dissolution. On open circuit, or if a lump of the metal is dropped into the same aqueous solution, the metal must take up the corrosion potential E_{CORR}, the potential where no net current flows, because the anodic and cathodic partial currents are equal, i.e.:

$$i_{M/M^{n+}} = i_{H^+/H_2} = i_{CORR} \tag{10.40}$$

i_{CORR} is called the corrosion current and the rate of corrosion estimated from this

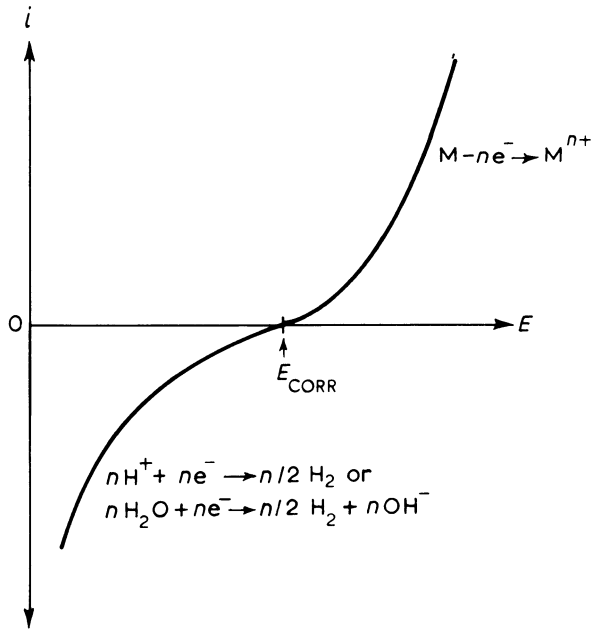

Fig. 10.7 Current–potential curve for a metal M corroding in an aqueous, non-oxidizing, deoxygenated acid.

current and Faraday's laws (section 10.4.1) should be the same as that from weight-loss experiments where the rate of metal dissolution is determined by weighing a sample of metal before and after standing in the electrolyte for a period. It should be noted that the corrosion potential is a, so-called, mixed potential since it is determined by the kinetics and thermodynamics of two electron transfer couples, M/M^{n+} and H^+/H_2 (cf. the equilibrium potential for a single couple, Chapter 1). If the attack is of a uniform, general nature, the entire surface may be considered to be both anode and cathode. If the metal was not corroding but was placed in a solution of M^{n+} so that its only reaction was the reversible electron exchange:

$$M \rightleftharpoons M^{n+} + ne^- \tag{10.5}$$

it would assume the equilibrium potential E_e^M for the M/M^{n+} couple. On the other hand, if the non-corroding metal was instead placed in an acid solution saturated with hydrogen gas, only the reversible electron transfer reaction:

$$2H^+ + 2e^- \rightleftharpoons H_2 \tag{10.8}$$

will occur at its surface and the equilibrium potential E_e^H would be assumed.

In practice, the metal takes up an intermediate value during corrosion, the corrosion potential E_{CORR} (Fig. 10.7). i_{CORR} is the corrosion current. E_{CORR} and i_{CORR} appear at the point of intersection of linear polarization curves for metal dissolution and hydrogen evolution on a semilogarithmic plot (Fig. 10.8). In order to make the diagram applicable to localized attack (when the anode and cathode sizes are disparate) it is necessary to strictly plot *log current** rather than *log current density*.

The *i–E* curves used in this chapter are related to the Evans diagram, beloved by corrosion chemists, but follow the conventions used throughout the rest of this book. While they are greatly simplified polarization diagrams, their usefulness lies in their ability to predict and rationalize the kinetics of corrosion processes. The figures show, in a diagnostic fashion, the following features:

1. The role of the anode and cathode reactions in the corrosion process.
2. Whether the electrode reactions are under charge transfer, mass transport or mixed control, or if resistance polarization is appreciable (see later); in Fig. 10.8 the linear, Tafel regions on the E–log $|i|$ plot signify activation control, i.e. charge transfer predominates.
3. The relative values of the Tafel slopes for the anodic and cathodic processes.
4. The overall driving force for the corrosion (cell) reaction, as represented by $E_{CELL} = E_e^C - E_e^A$.
5. The individual anodic and cathodic polarizations, $\eta'_A = E_{CORR} - E_e^A$ and $\eta'_C = E_{CORR} - E_e^C$.

* For convenience in presentation, the algebraic sign of current is disregarded by taking its modulus. In contrast to corrosion technologists, it is an accepted convention amongst electrochemists that potential is the abcissa.

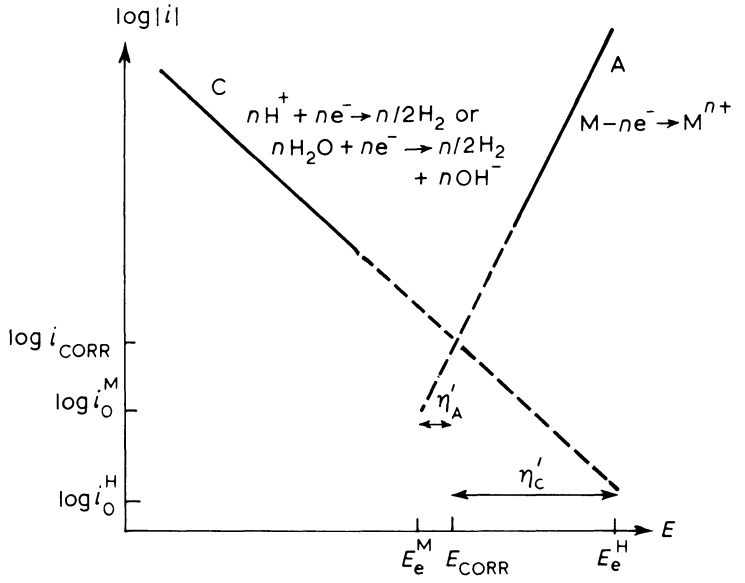

Fig. 10.8 Steady-state log (current)–electrode potential diagram for a metal M corroding via hydrogen evolution. Both electrode processes are under activation control. The diagram shows the definition of corrosion current i_{CORR} and the corrosion potential E_{CORR}. The reversible potential E_e^H and E_e^M corresponding to the exchange currents i_0^H and i_0^M for the single electrode reactions are also shown together with the cathodic polarization $\eta'_c = E_{CORR} - E_e^C$ and the anodic polarization $\eta'_A = E_{CORR} - E_e^A$.

6. The exchange current for the anodic and cathodic reactions i_0^M and i_0^C.
7. The corrosion potential, E_{CORR}.

The Tafel lines in Fig. 10.8 may be quantitatively described as follows. For the cathodic process (hydrogen evolution):

$$E - E_e^H = -\beta_H (\log I - \log I_0^H) \tag{10.41}$$

and for the anodic (metal dissolution) reaction:

$$E - E_e^M = \beta_M (\log I - \log I_0^M) \tag{10.42}$$

where $1/\beta_H$ and $1/\beta_M$ are the Tafel slopes. For both the anodic and cathodic processes, $I = I_{CORR}$ at $E = E_{CORR}$; substituting this information into equations (10.41) and (10.42), one obtains a pair of simultaneous equations which may be solved to give:

$$I_{CORR} = (I_0^M)^{\beta_1} (I_0^H)^{\beta_2} \exp\left(\frac{2.3(E_e^H - E_e^M)}{\beta_H + \beta_M}\right) \tag{10.43}$$

where $\beta_1 = \beta_M / (\beta_M + \beta_H)$ and $\beta_2 = \beta_H / (\beta_M + \beta_H)$ and

$$E_{CORR} = \frac{\beta_M E_e^H + \beta_H E_e^M}{\beta_H + \beta_M} + \frac{\beta_H \beta_M}{2.3(\beta_H + \beta_M)} \log\left(\frac{I_0^H}{I_0^M}\right) \tag{10.44}$$

It can be seen that both the corrosion current and potential depend on the equilibrium potentials for the hydrogen evolution and metal dissolution reactions calculated from the Nernst equation, as well as the kinetic parameters: the exchange currents and Tafel slopes. Table 10.3 shows the corrosion currents calculated for some typical values of these parameters; it is also important to note that even a corrosion current of 10^{-3} mA cm^{-2} corresponds to a metal loss rate of the order of 10 mg cm^{-2} y^{-1} (section 10.4.1). Clearly, the corrosion current has an appreciable dependence on both the reversible cell potential ($E_e^H - E_e^M$) and all the kinetic parameters. In most practical situations, the choice of metal is such that the reversible cell potential is seldom much in excess of 0.5 V. Even so, because of the large variations in exchange currents and mechanisms for the two electrode processes which are possible, the corrosion rate for different metals and environments can still vary by many orders of magnitude. The pronounced effect of the electrode material on the exchange current density for hydrogen evolution is indicated schematically in Fig. 10.9. This has an important consequence; contamination and alloying of zinc with metals having a high i_0^H (e.g. Cu or Fe) will greatly increase the corrosion rate. On the other hand, the addition of phosphorus to steel decreases i_0^H and hence the rate of corrosion. Equations (10.43) and (10.44) also emphasize the key role of pH in determining the rate of corrosion; it affects both the thermodynamic and kinetic terms. Both E_e^H and E_e^M change with pH, but shifts will have opposing effects on the rate of corrosion. E_e^H

Table 10.3 Influence of the electrochemical parameters for hydrogen evolution and metal dissolution on the corrosion current in oxygen-free solution

$E_e^H - E_e^M$/V	I_0^H/mA cm^{-2}	I_0^M/mA cm^{-2}	β_H/mV	β_M/mV	I_{CORR}/mA cm^{-2}
0.0	10^{-6}	10^{-4}	120	120	10^{-5}
0.5	10^{-6}	10^{-4}	120	120	1.2×10^{-3}
1.5	10^{-6}	10^{-4}	120	120	17
0.5	10^{-10}	10^{-4}	120	120	1.2×10^{-5}
0.5	10^{-10}	10^{-8}	120	120	1.2×10^{-7}
0.5	10^{-6}	10^{-4}	120	60	2.8×10^{-3}
0.5	10^{-6}	10^{-4}	30	120	8.5×10^{-2}

E_e^H = equilibrium potential for the hydrogen evolution reaction
E_e^M = equilibrium potential for the metal dissolution reaction
I_0^H = exchange current density for the hydrogen evolution reaction
I_0^M = exchange current density for the metal dissolution reaction
β_H, β_M = Tafel slopes for the hydrogen evolution, metal dissolution reaction respectively

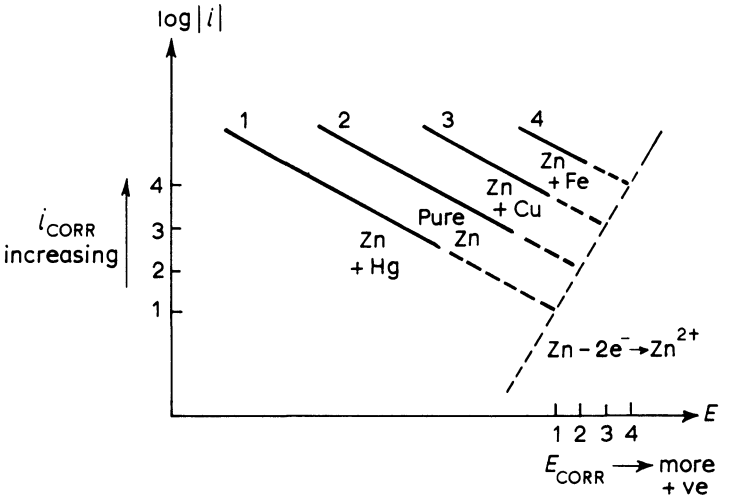

Fig. 10.9 Log $|i|$–E diagram showing cathodic control: the effects of impurities on zinc dissolution in acid. For simplicity, the following assumptions are made: (i) that the anodic process is not affected by the impurities (i.e. β_M and i_0^M remain constant); and (ii) the single cathodic process is always hydrogen evolution with constant E_e^H and β_H values. The only cathodic reaction is $2H^+ + 2e^- \longrightarrow H_2$.

will always change by 60 mV per pH unit so as to decrease the reversible cell potential and, hence, the rate of corrosion with increasing pH. E_e^M will only vary with pH if the oxidation of the metal leads to an oxide or hydroxide (Fig. 10.5) and, hence, the effect of pH depends on the metal and the pH range. Where a shift in E_e^M with pH occurs, the effect will be to make the potential more negative with increasing pH and thus to increase $(E_e^H - E_e^M)$; this will increase the corrosion current. The exchange currents, particularly that for hydrogen evolution, are very sensitive to pH and it is also possible that the mechanisms for hydrogen evolution and metal dissolution (and in consequence the Tafel slopes) will be a function of pH.

So far, the quantitative discussion of corrosion has only dealt with de-oxygenated solutions. In the real world, this is a very unusual environment; oxygen is almost always present. How does the presence of oxygen change our discussion of corrosion? In fact, two situations must be considered.

1. When there is a plentiful supply of oxygen to maintain the corrosion current, the argument will be similar to the above except that the cathode reaction is the reduction of oxygen. The corrosion current and potential are then determined by the intercept of the Tafel lines for oxygen reduction and metal oxidation (Fig. 10.10) and since E_e^O is more positive than E_e^H by 1.23 V, the thermodynamic driving force for corrosion $(E_e^O - E_e^M)$ will be larger and the rate of corrosion would be expected to be higher; an equation analogous to (10.43) will again give the corrosion current. To some extent, the rate of

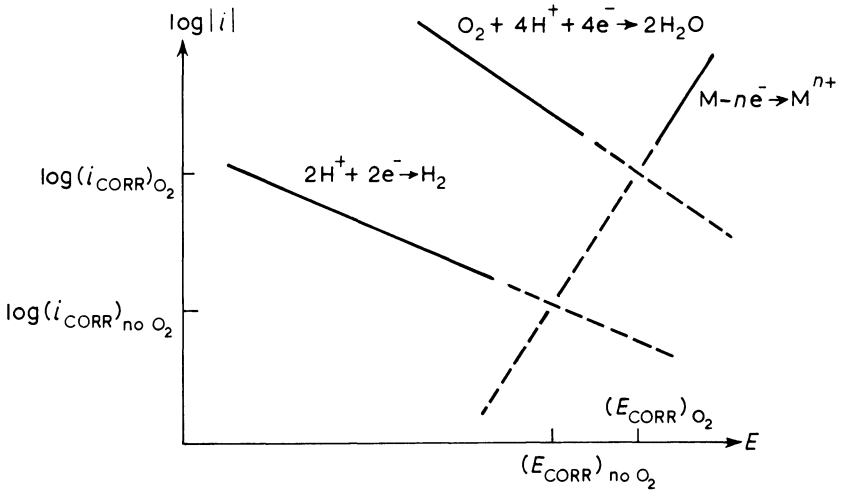

Fig. 10.10 Log $|i|$–E diagram for a metal corroding in acid in contact with air. The presence of oxygen increases substantially the rate of corrosion. (It is assumed that the oxygen reaction is under activation control.)

corrosion is commonly less than expected because of the extremely low exchange current for oxygen reduction at many surfaces. Even so, corrosion normally becomes more of a problem in the presence of oxygen.

In the presence of a high concentration of oxygen but at a metal where the exchange current for oxygen reduction is low, the rate of corrosion is also enhanced by the presence in solution of redox couples with an equilibrium potential in the range from 0 to + 1.23 V (at pH 0), e.g. in the presence of ferrous ions, the cathodic reaction in the corrosion process can be part of the catalytic cycle:

$$4Fe^{2+} + O_2 + 4H^+ \longrightarrow 4Fe^{3+} + 2H_2O \qquad (10.45)$$

$$Fe^{3+} + e^- \xrightarrow{\text{surface}} Fe^{2+} \qquad (10.11)$$

i.e. oxygen reduction is catalysed by such ions, effectively causing an increase in the exchange current for oxygen reduction.

2. In most practical situations, the dissolved oxygen concentration is relatively low.* In the presence of a lower concentration of oxygen, the corrosion current may be controlled by the rate of mass transport of the oxygen to the metal surface and the corrosion potential will occur at the intercept of the oxygen plateau with the Tafel line for metal dissolution. The log $|i|$–E curves for this simple situation are illustrated in Fig. 10.11. It is also possible for the

* For example, in pure water saturated with air, the dissolved oxygen content is approximately 40 mg dm^{-3} ($\simeq$ 1.2 mmol dm^{-3}) at 20° C. The concentration falls to *c.* 10 mg dm^{-3} at 5° C in sea water.

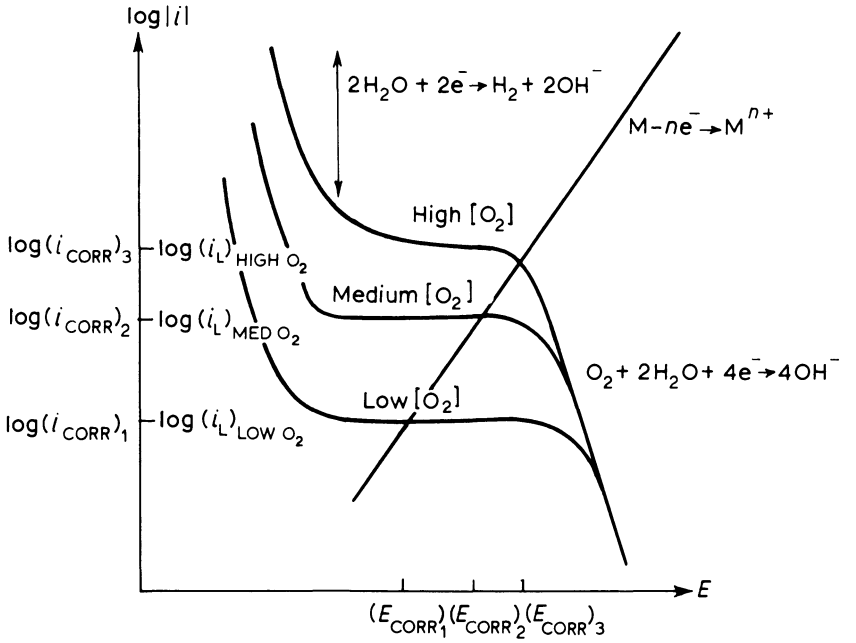

Fig. 10.11 Log $|i|$–E curves for a metal corroding via mass transport controlled oxygen reduction in a near neutral (pH $\simeq$ 7) electrolyte showing the effect of dissolved oxygen level*. An increased oxygen concentration results in an increased limiting current for oxygen reduction until a critical point is reached $(i_{CORR})_3$ when the cathodic reaction reverts to charge-transfer control. The cathodic reaction is oxygen reduction: $O_2 + 4e^- + 2H_2O \longrightarrow 4OH^-$.

cathodic current to be the sum of the limiting current for oxygen reduction and a contribution from hydrogen evolution.

In such systems, the rate of corrosion will depend strongly on the mass transport regime in the solution. This situation obviously arises in systems where the metal

* The corrosion rate in Fig. 10.11 is as expected from a fully mass transport controlled cathodic process (section 1.2.1):

$$I_L = I_{CORR} \tag{10.46}$$

and:

$$I_{CORR} = k_L n F c_{O_2}^{\infty} \tag{10.47}$$

where $c_{O_2}^{\infty}$ is the concentration of dissolved oxygen in the bulk solution and k_L is the mass transport coefficient, which depends on the relative velocity, v:

$$k_L \propto v^x \tag{10.48}$$

where x depends upon the electrode roughness, the electrode geometry and the type of flow (as described in Chapter 2).

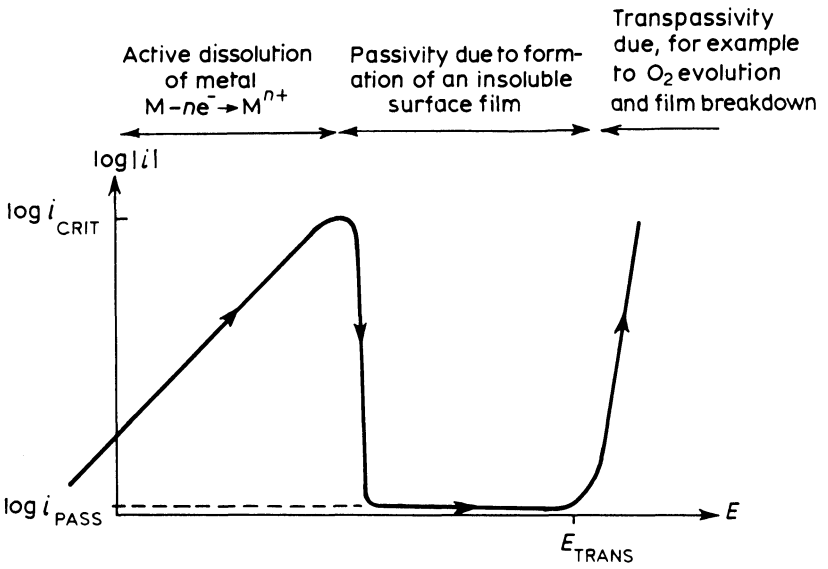

Fig. 10.12 Log $|i|$–E curve for a metal which shows classical passivity.

is moving or the electrolyte flowing. So far, our treatment of kinetics has considered the metal to freely dissolve anodically. Under appropriate pH, potential, composition and temperature conditions, the metal may become passive as already seen in section 10.2.

When metals are placed in a solution of certain oxidizing agents, it is common to find that corrosion does not occur although the oxidation of the metal is thermodynamically very favourable. Indeed, this phenomenon was first observed over 100 years ago when it was found that iron dissolved in dilute, but not in concentrated, nitric acid; it was suggested that in concentrated nitric acid, a thin layer of a non-porous and insoluble oxide film was formed. This protection by a surface film is termed 'passivation' and explains the apparent stability of metals such as Al, Cr, Ni, Ti and Pt in damp air.

Passivation is also observed in electrochemical experiments. Figure 10.12 shows a log $|i|$–E curve resulting from a potential sweep experiment commenced at a potential where the metal is immune from corrosion. At some potential the metal will begin to oxidize and initially the product is likely to be a soluble metal ion. Throughout this active region the current will increase with overpotential and at least during the early part of the rising i–E region, this increase will be exponential. As the potential is made more positive, however, a critical potential E_{CRIT}) is reached where the rate of dissolution drops sharply (often by several orders of magnitude) from i_{CRIT} to i_{PASS}, remaining at this latter value for an appreciable range of potential. When a sufficiently positive potential is reached

(E_{TRANS}) the electrode becomes 'transpassive' and the current once again rises due to:

1. Oxygen evolution and/or
2. Oxidation of species in the passive film.

The potential range where only a low current is observed is the passive region. Natural passivation therefore occurs if, in the solution, there is a species (e.g. oxygen or a redox reagent) capable of taking the surface potential into the passive region (the surface potential is calculated from the Nernst equation for the redox reagent couple).

While it is certain that in the passive region, the metal is covered by an adherent and non-porous film (usually considered to be 1–15 nm thick), the exact nature of this layer and its mechanism of formation remain a subject of controversy. The simplest model for the formation of the film would note that as the current increases through the active region, the surface concentration of M^{n+} will also increase and at some point the solubility product for a metal species (e.g. $M(OH)_n$) must be exceeded and a precipitate must result. The mechanism, however, cannot always be this straightforward since a surface layer often forms prior to passivation. This suggests that the surface layer is only passivating if it has certain properties. Thus, the critical current may correspond to a change in film composition (e.g. oxidation state) which causes a change in properties. This may be a reduction in porosity although it has been proposed that the change is

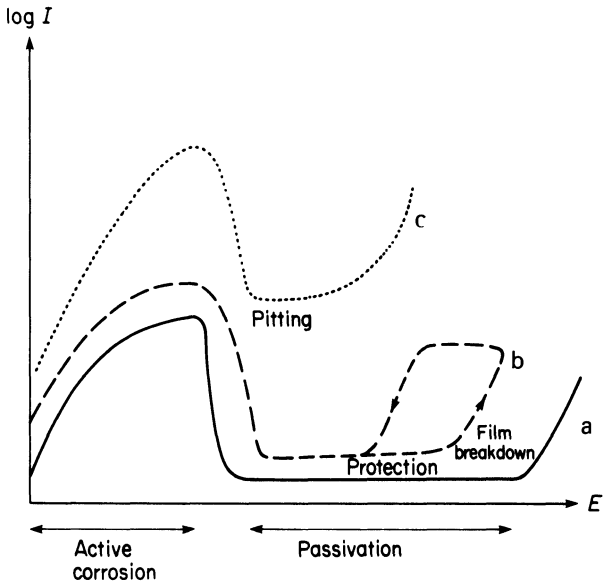

Fig. 10.13 Log $|i|$–E curve for nickel in acid solution, showing the effect of chloride ion. (a) 0 mol dm^{-3}. (b) 1×10^{-2} mol dm^{-3}. (c) 1×10^{-1} mol dm^{-3}.

from ionic to electronic conduction. If there is no mechanism for ions to travel through the film, corrosion must stop since the film cannot thicken.

The incidence and ease of passivation will depend on both the metal and the solution environment. Even when passivation is observed, however, there is the further phenomenon of pitting, a process which causes an increase in current in the passive region and which in its severest form causes complete breakdown of the passive film. It is commonest in media containing halide ion. The term derives from characteristic circular holes which appear in the passive film but their mechanism of formation is still poorly understood. Generally, pitting becomes worse with increasing halide ion concentration and as the potential is made more positive (Fig. 10.13) and it is thought likely that the pits arise by transport of the anion through the passive film and corrosion from beneath. This is said to create acid spots which locally dissolve the passive film and set up a situation akin to crevice corrosion (section 10.4) where the metal dissolves rapidly. Solutions containing ions which promote pitting are particular corrosion hazards.

Increasing the relative electrolyte velocity or dissolved oxygen concentration in a system exhibiting passivity may cause the corrosion rate to fall, as i_L may exceed i_{CRIT} (Fig. 10.14). This behaviour is in marked contrast to the case of active metal dissolution (Fig. 10.11).

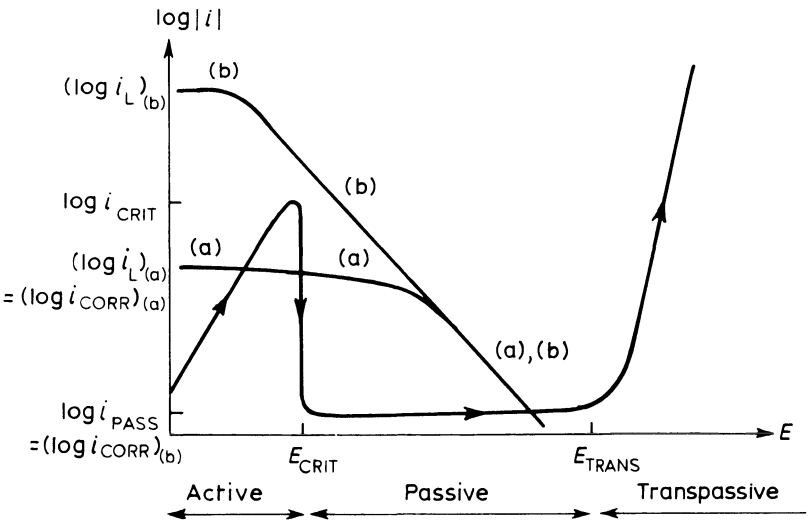

Fig. 10.14 Log|*i*|–*E* curve for a metal exhibiting passivity, showing how increased stirring or a higher oxygen concentration may cause the limiting current for oxygen reduction to exceed the critical current for the onset of passivity i_{CRIT} and, hence, reduce the corrosion rate i_{CORR}. (a) Low oxygen concentration or low electrolyte velocity. (b) High oxygen concentration or high electrolyte velocity.

10.4 CORROSION PROBLEMS IN PRACTICE

10.4.1 General Types of Corrosion

So far, the discussion has been limited to a consideration of homogeneous metals in a uniform environment where corrosion will occur at the same rate over the whole surface. This situation seldom constitutes a major corrosion hazard; it is often possible to plan remedial work when armed with a knowledge of the uniform averaged corrosion rate expressed as a weight loss (e.g. mg dm^{-2} day^{-1} : mdd) or a penetration rate, e.g. mm $year^{-1}$: mpy.

These data are estimated readily from a knowledge of the averaged corrosion current density $I_{CORR} = i_{CORR}/A$ in amperes and the application of Faraday's laws of electrolysis. The weight loss of metal Δw at the constant current i is given by:

$$\Delta w/M = it/nF \tag{10.49}$$

dividing by the electrode area and rearranging:

$$\Delta w/At = iM/nFA \tag{10.50}$$

Assuming 100% current efficiency for the anodic dissolution, and inserting:

$$i = i_{CORR} = AI_{CORR}$$

$$\frac{\Delta w}{At} = \frac{I_{CORR}M}{nF} \tag{10.51}$$

the average weight loss per unit area per unit time is often given in mg dm^{-2} day^{-1} (mdd).

The averaged penetration rate $\Delta x/t$ may be calculated from a knowledge of the density of the metal ρ, again with the assumption of uniform corrosion:

$$\frac{\Delta x}{t} = \frac{I_{CORR}AM}{\rho nF} \tag{10.52}$$

The most common units are mm $year^{-1}$ (mpy). As an example, consider the corrosion of an iron pipeline by an acid liquor. If the steady corrosion current density is 0.1 mA cm^{-2}:

$$\Delta w/At = 32 \text{ mg dm}^{-2} \text{ day}^{-1}$$

and:

$$\Delta x/t = 1.16 \text{ mm y}^{-1}$$

which is a relatively high corrosion rate.

General (uniform) corrosion is normally associated with spatially and temporally random cathode and anode zones on a 'homogeneous' metal surface (Table 10.4). In practice, the corrosion engineer is generally much more concerned with situations where corrosion is accelerated because it is limited to particular sites

Table 10.4 Comparison between general and localized electrochemical corrosion (see also Fig. 10.18)

Feature	General	Localized
Spatial distribution of anode and cathode	Not separated	Separated
Temporal distribution of anode and cathode	Fluctuates randomly	Constant
Relative area	$A_A = A_C = A_M$	$A_A \ll A_C$
Potential E	$E^A = E^C = E_{CORR}$	$E^A < E^C$
Corrosion current density I_{CORR}	$I_A = I_C = I_{CORR}$	$I_A \gg I_C$
Nature of corrosion products	*Can* be protective	*Rarely* protective
Type of attack	Uniform	Selective
Rate of penetration	Constant	May accelerate with time

(i.e. it is localized); the cathodic and anodic zones are recognizable, spatially distinct and constant in time on a 'heterogeneous' metal surface (Table 10.4). Some common types of localized corrosion are shown in Figs. 10.15 and 10.16. It is possible to contrast general and local attack by means of E–log $|i|$ diagrams (Fig. 10.17). In the case of general corrosion (Fig. 10.17(a)) the sub-microscopic anodic and cathodic zones have a negligible separation and iR drop in the electrolyte may be disregarded; the anodic and cathodic curves intersect at the corrosion potential E_{CORR}. For localized attack (Fig. 10.17(b)), the widely separated anodic and cathodic zones may have significantly different potentials, e.g. the (anodic) bottom of a pit may have a potential several hundred millivolts more negative than that at the (cathodic) surface; an appreciable iR drop exists in the electrolyte.

10.4.2 Examples of localized corrosion

In practice, one of the most common types of corrosion cell is that arising from differential aeration. To understand differential aeration one should first consider two pieces of the same metal placed in media identical except for their oxygen concentration, e.g. one is placed in unstirred solution below an air atmosphere and the other in a solution saturated with oxygen by a stream of gas as in Figs 10.18 and 10.19. The metal samples will take up different potentials and corrode at different rates; that in the oxygen-saturated solution must be more positive and the corrosion current will be higher (Figs 10.10 and 10.11). How does the situation change if the two pieces of metal are joined by a wire contact? Provided

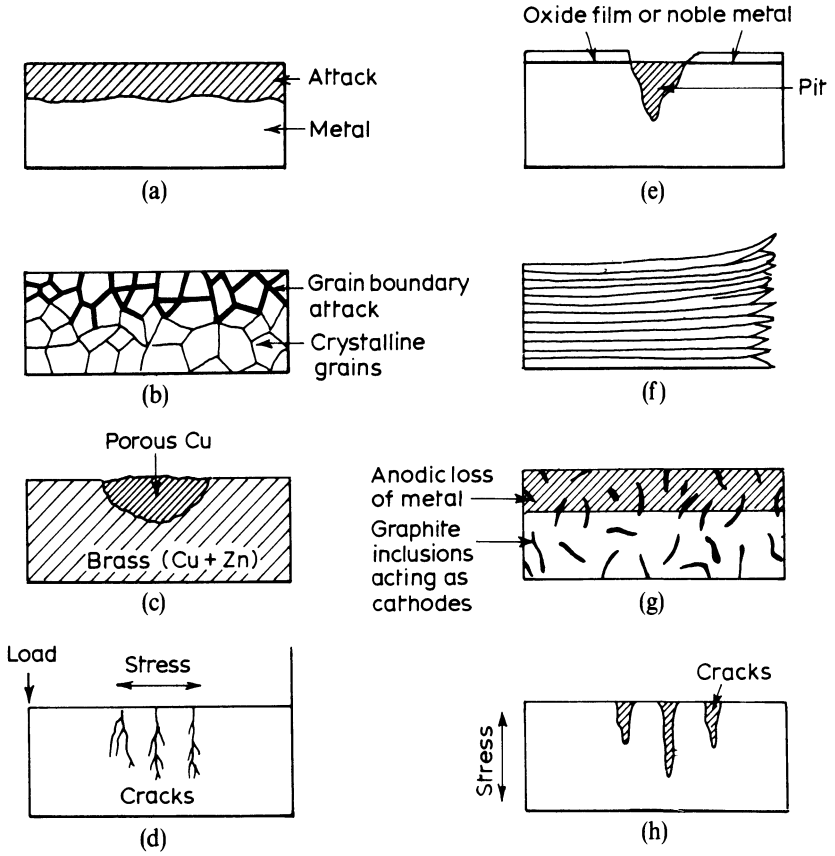

Fig. 10.15 Types of corrosion. (a) General, uniform attack corrosion. (b) Intergranular corrosion. (c) Selective corrosion, e.g. dezincification of brass. (d) Stress corrosion cracking. (e) Pitting. (f) Layer corrosion (exfoliation). (g) Graphitic corrosion. (h) Corrosion fatigue. Types (b)–(h) are initially associated with the nature of the metal.

the metal remains in the active corrosion region and the resistance of the medium is not very high, the two pieces must take up the same potential and therefore the rate of corrosion becomes uniform over both surfaces. The corrosion potential will take up an intermediate value between that of the two isolated pieces of metal. In order to allow an even corrosion rate, however, electrons must flow through the contact from the metal in the oxygen-deficient solution to the metal in the oxygen-rich solution and ions must move through the environment so as to maintain neutrality. Hence, if the resistance of the medium between two pieces of metal is not negligible there will be an iR drop and the rate of corrosion at the two pieces of metal will not totally equalize. In practice, this occurs on large metal structures particularly in poorly conducting media (e.g. underground pipes) but in this situation the highest rate of corrosion is always in the oxygen-rich region.

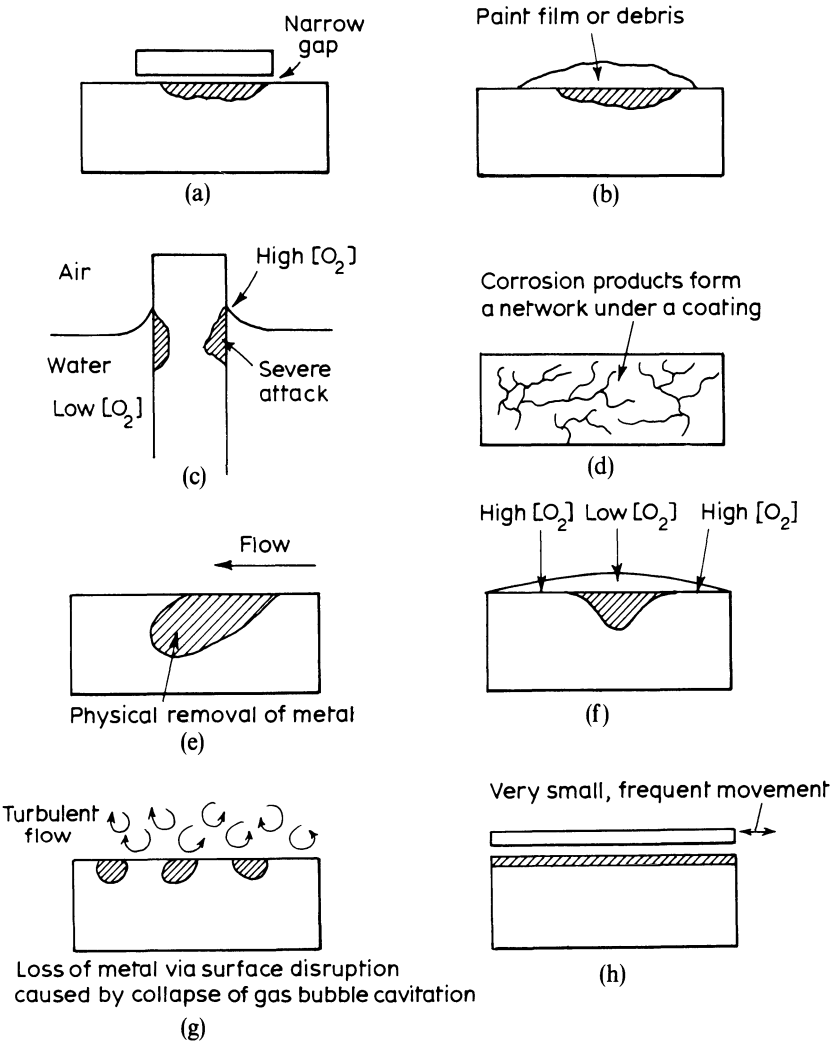

Fig. 10.16 Types of localized corrosion initially associated with the environment. (a) Crevice corrosion. (b) Deposit corrosion. (c) Waterline attack. (d) Filiform corrosion (e) Erosion corrosion. (f) Drop corrosion. (g) Turbulent-flow corrosion. (h) Fretting.

The real problem of differential aeration arises when it is combined with passivation. In the presence of a sufficient supply of oxygen, many metals will passivate. Consider the experiment in Fig. 10.18 with the contact closed; it is possible for the piece of metal in the oxygen-rich medium to take up a potential in the passive region and corrosion will then stop. If the film is an electronic conductor, however, oxygen reduction can continue to occur and in order for the metal oxidation and oxygen reduction currents to balance, the rate of corrosion at the metal in the oxygen-deficient solution must increase. The corrosion rate

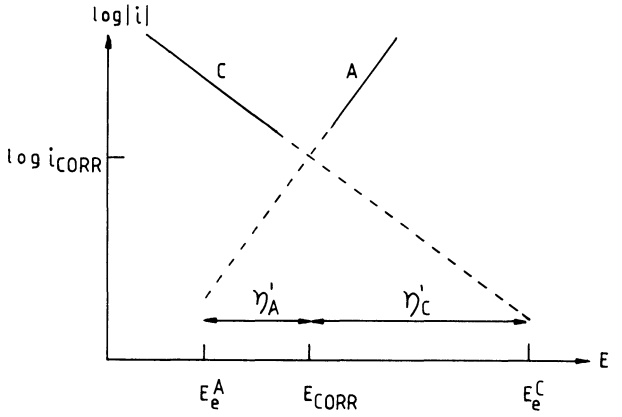

(a)

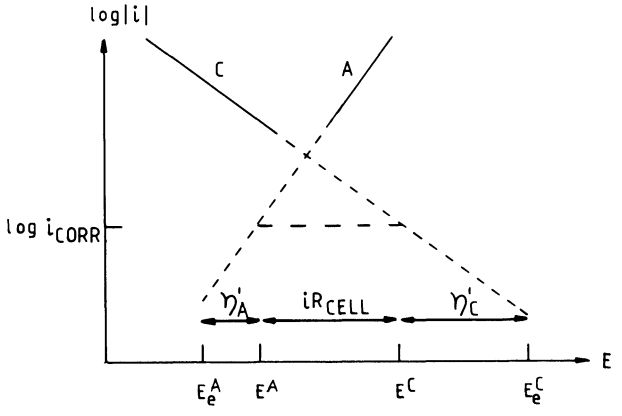

(b)

Fig. 10.17 Log$|i|$–E curves for uniform and localized attack.
(a) General corrosion, resulting in uniform attack:

$E_{CORR} = E^C = E^A$

$\eta'_C = E_{CORR} - E_e^C$

$\eta'_A = E_{CORR} - E_e^A$

$E = |\eta'_A| + |\eta'_C|$

(b) Local corrosion:

$\eta'_C = E^C - E_e^C$

$\eta'_A = E^A - E_e^A$

$E = |\eta'_A| + |\eta'_C| + iR_{CELL}$.

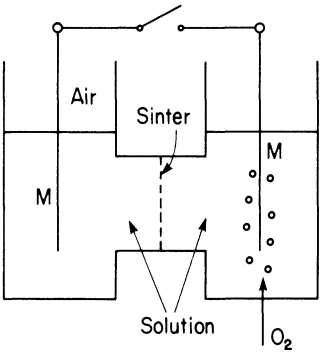

Fig. 10.18 An electrochemical cell to discuss the effect of differential aeration.

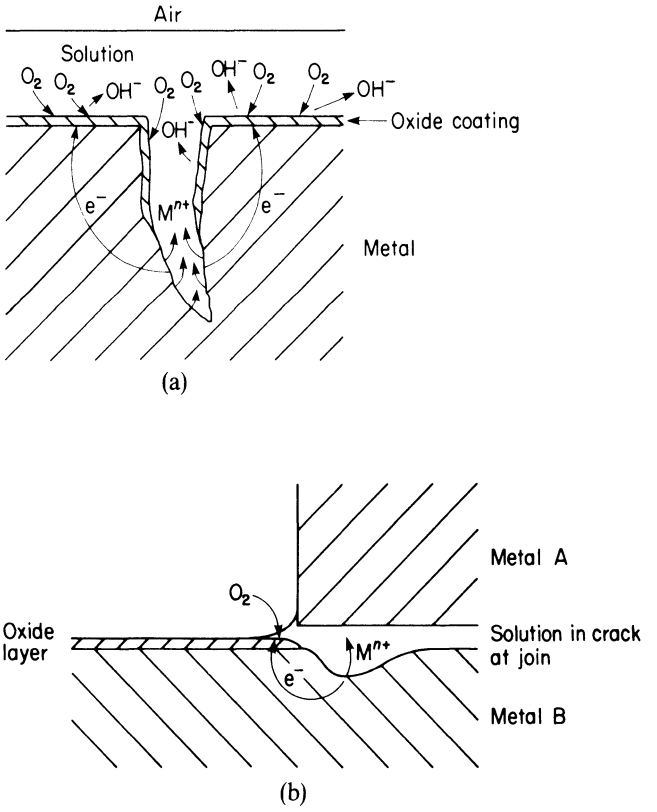

Fig. 10.19 An explanation of corrosion inside a crevice. The oxide acts as the cathode and only the bare metal at the bottom of the crevice (a) or between the plate (b) acts as an anode.

will become even higher if the piece of metal in the oxygen-rich solution is larger than the other where corrosion is occurring; the total current for oxygen reduction and metal corrosion must still balance.

There are many examples of the way in which differential aeration combines with passivation to produce difficult problems. Figure 10.19 illustrates the case of crevice corrosion. The outer flat surface (Fig. 10.19(a)) receives a plentiful supply of oxygen and, hence, passivates to produce a large protected area where oxygen reduction can occur. Only the inner part of the crevice is free of the film and it is in this small area that the metal oxidation is localized. Hence, once crevice corrosion has commenced, the depth of the crevice increases very rapidly. An identical argument applies to corrosion between two metal plates (Fig. 10.19(b)) while a similar situation at scratches in paint on metals leads to severe peeling (Fig. 10.20). In the latter example, the oxygen supply is highest to the exposed metal at the centre of the scratch and it is there that passivation occurs; the anodic part of the corrosion process takes place beneath the paint causing it to lift and peel.

Pitting is possibly the most common type of localized attack. It usually occurs on an oxide-covered surface due to the presence of an aggressive species, e.g. Cl^- which prevents complete passivation, together with a sufficiently high anodic potential (Fig. 10.13). In the case of plain carbon steels, pits are often initiated around sulphide inclusions. Pitting attack is often autocatalytic and self-stimulating in nature. The self-generating conditions for pit propagation may be summarized:

1. Within the pit, the following conspire to prevent repassivation:
   (a) enrichment of Cl^- due to electromigration;
   (b) generation of acidity by hydrolysis of metal ions may increase the critical potential for passivation;
   (c) electrolyte conductivity increases;
   (d) O_2 supply is limited, both by convention and diffusion and by low solubility in the concentrated electrolyte.

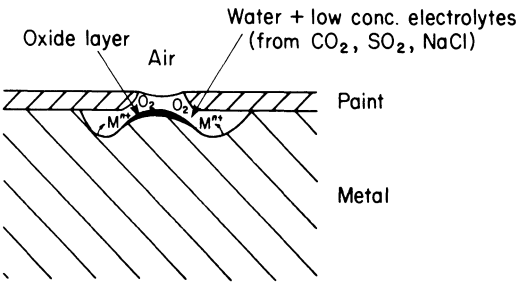

Fig. 10.20 A simplified case of atmospheric corrosion due to a break (e.g. a scratch or crack) in a paint film.

2. At the mouth of the pit a crust of hydrate may form. This tends to strengthen the factors in (1) by preventing dilution by the bulk electrolyte.
3. In the vicinity of the pit, general corrosion is opposed by:
   (a) cathodic protection;
   (b) passivation by OH^- formed at cathode sites, especially in the presence of Ca^{2+} and HCO_3^-;
   (c) deposition of more noble metals (e.g. Cu) provides more effective anode sites, keeping the anode potential above that needed for pitting;
   (d) noble precipitates (e.g. Al_3Fe, Si, and $CuAl_2$) also act as effective cathodes (cf. Fe_3C in steels).

Localized corrosion can also occur when two different metals are in contact, e.g. for different applications iron is protected by a layer of zinc or tin. The former is the better choice although it is potentially more prone to corrosion than tin. If a scratch or hole is formed in a tin layer, the corrosion of the underlying iron is rapid; again oxygen reduction can occur over the whole tin surface while the anodic oxidation is limited to the exposed area of iron. On the other hand, zinc is more electropositive than iron so even if the top layer is damaged, the iron does not corrode. The iron is protected at the expense of the zinc (Fig. 10.21). Tinplate is used largely for packaging foods because tin ions are non-toxic.

When two different metals are in contact there are always potential corrosion hazards. It is always likely that one of the metals will dissolve more rapidly and a

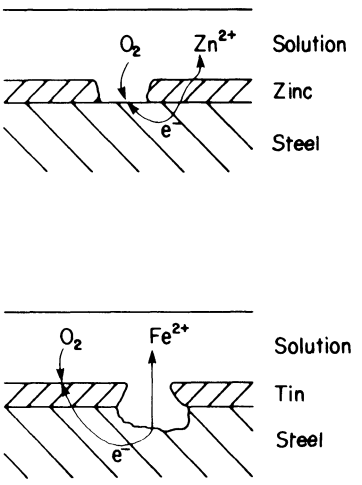

Fig. 10.21 Corrosion at damaged metal coatings on iron or steel. (a) The zinc coating is anodic with respect to the steel and dissolves preferentially. (b) The tin coating is cathodic; damage to the coating or the presence of imperfections in it may give rise to a small exposed area of steel. The resultant attack may be localized and rapid due to the adverse situation of a high ratio of cathode to anode area.

corrosion cell will be set up. This metal will become anodic while the more stable metal will become cathodic; as a result, all the metal loss will occur from the more susceptible metal.

The exact mechanism of stress cracking corrosion is not fully understood but it is thought to be related to hydrogen embrittlement and to the localized increases of stress followed by stress relief via cracking. It was seen in the earlier discussion that in many corrosion situations the cathodic part of the process is hydrogen evolution. We know from Chapter 1, however, that the mechanism for hydrogen formation will at many metals involve adsorbed hydrogen atoms. Also, hydrogen atoms are small and it is not surprising that they are able to enter the lattice of some metals; the classic example is palladium but it is also found with iron and alloys based on iron*. Of course, during proton or water reduction, hydrogen gas evolution is the dominant process but a small percentage of the hydrogen enters the lattice. Moreover, hydrogen absorption into the lattice is usually quite reversible up to a critical percentage; beyond this limit, however, the lattice is forced to change its structure with a consequent loss of mechanical strength and changes in other properties occur. Normally, the limit is only reached under conditions which by corrosion standards are quite extreme (e.g. at a current density well above the corrosion current) but it is found that the hydrogen tends to collect in areas in the metal where there is stress. Hence, the role of stress is to concentrate the hydrogen and this creates the conditions for hydrogen embrittlement and component failure. This may not be the only result of the hydrogen collecting in areas of stress; the build-up of hydrogen pressure in fissures and cracks may cause them to expand and, when they reach the surface, the conditions are ripe for crevice corrosion. Certainly, stress-cracking corrosion has led to sudden and catastrophic failure of components and has frequently contributed to, for example, plane crashes and the bridge collapses.

We must recognize that there are two quite different situations where corrosion arises: (1) in atmospheric corrosion, the electrolyte is normally a thin film or small pool of water rendered slightly conducting by CO_2, SO_2 or H_2S absorbed from the atmosphere (hence, its pH will not be extreme and the electrolyte will only be dilute) but it will contain a high concentration of oxygen; and (2) it is also necessary to restrict corrosion in containers (for foods, paints, oil, etc.) and in pipes and reactors carrying all types of plant streams. These streams, in general, will be less rich in oxygen but may contain concentrated electrolytes, be at any pH, contain redox species (which may be corrosion catalysts) and be based on non-aqueous solvents rather than water. It will be clear that these latter situations may produce even more difficult corrosion problems than are met in atmospheric oxidation and certainly each

* Titanium is also prone to hydrogen adsorption leading to the possibility of hydride formation; this limits the use of titanium as a cathode material in electrochemical reactors involving acidic electrolytes. Such conditions may not allow a stable passive film to be retained on the electrode surface.

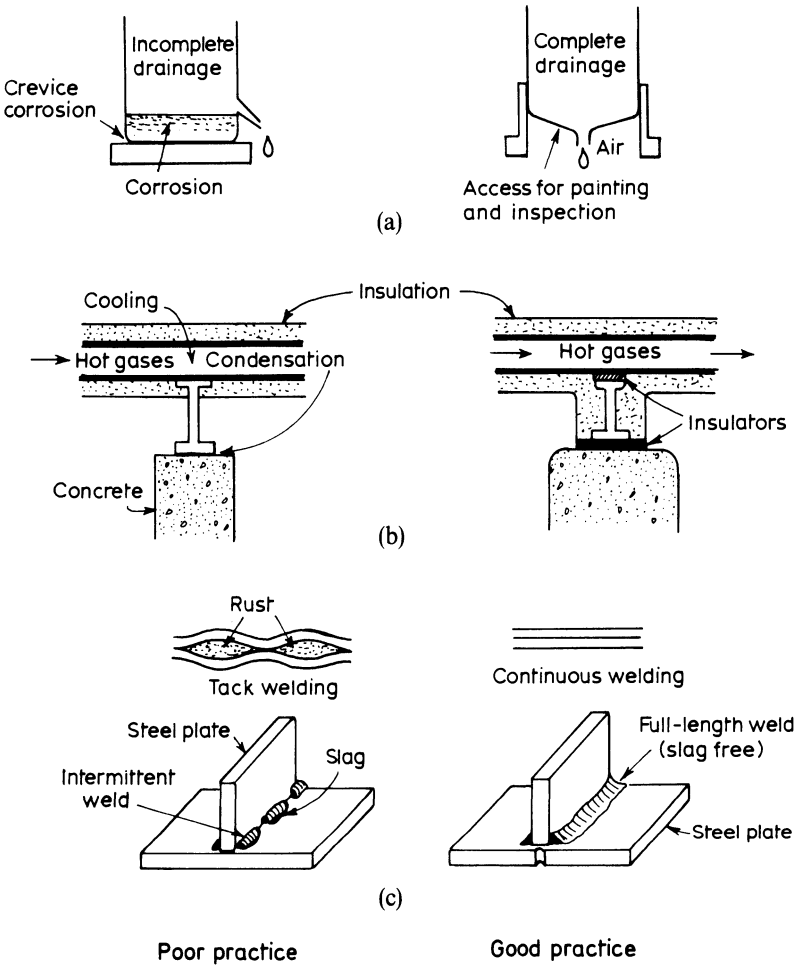

Fig. 10.22 The influence of design factors on corrosion. (a) Storage tanks should be fabricated to allow complete drainage and access to outside surface for painting. (b) The insulation of cool pipe supports may prevent internal or external condensation of an electrolyte film. Insulation may prevent bimetallic corrosion; tight insulation may prevent water ingress. (c) Full length, continuous welds are preferred to intermittent, tack ones. Slag and surface oxides must be removed prior to surface coating.

must be considered individually in the light of both fundamental knowledge and practical experience.

10.5 CORROSION PREVENTION AND CONTROL

The simple corrosion cell (Fig. 10.2) serves to illustrate possible strategies for the prevention of electrochemical corrosion; at least one of the following must be modified:

1. The anode, anode–electrolyte interface or anode reaction.
2. The cathode or cathode–electrolyte interface or cathode reaction.
3. The electrolyte.
4. The cathodic reactant, e.g. H^+, O_2.
5. The electrical connection.

It should also be noted that the components of real corrosion cells (and the electrochemical reactions) are not always easy to identify or to isolate.

A wide range of methods has been developed (largely in an empirical fashion) for the control of corrosion. For convenience, the methods for protection may be subdivided into selection of material and design considerations, modification of the electrolyte, change in the electrode potential, and surface coatings.

10.5.1 Materials selection and design

Corrosion control should always begin with a due regard for the choice of a suitable material (or coating) coupled with consideration of design factors (Table 10.5). Many of the types of corrosion referred to in section 10.4 may be diminished or even prevented via an awareness of undesirable design features. Figure 10.22 attempts to illustrate problem areas due to inadequate design, fabrication or joining techniques. These examples may appear simplistic and even trivial but it should be noted that each one can readily be found in practical

Table 10.5 A summary of design factors which are important in corrosion protection

Factor	Strategy
Materials (metals, alloys, non-metallic materials)	Selection of suitable materials (consistent with cost, availability, ease of fabrication, etc.) for given environmental conditions
Dissimilar metals in contact	Avoidance of designs in which the kinetics of attack on one metal are stimulated by another
Geometry	Avoidance of designs which lead to localized attack, erosion or cavitation
Mechanical factors	Avoidance of excessive stress (internal or applied) when using metals known to be susceptible to stress–corrosion cracking; avoidance of conditions leading to corrosion fatigue or fretting corrosion
Surface	Avoidance of conditions on surface which lead to localized attack, e.g. discontinuous films of oxides or metals, roughened surfaces, weld spatter, etc.
Protection by electrochemical methods	Provision in design for cathodic or anodic protection (section 10.5.3) and for application of protective coatings (Chapter 8)

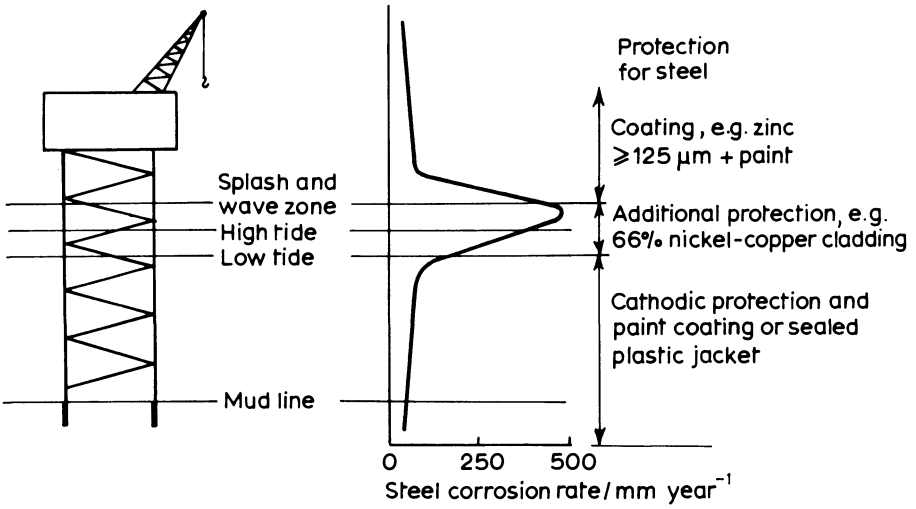

Fig. 10.23 The corrosion zones and methods of protection for an offshore platform.

corrosion situations and are best avoided by a consideration of corrosion in the early stages of design.

The importance of metallurgical phase composition may be illustrated by the layer corrosion (exfoliation) of aluminium, particularly in marine environments. In this case, selective grain-boundary attack can cause whole grains to fall away. This may be exaggerated by the stresses created when the high volume aluminium oxide forms. If a well-defined texture is present due, for example, to rolling or extension of the metal during fabrication, intergranular corrosion may be concentrated at $CuAl_2$ precipitates.

For certain, specific, applications, speciality alloys provide a useful means of corrosion prevention, e.g. the tidal and splash zones of offshore structures and jetties may be partly constructed (or clad) with a 66% Ni–34% Cu alloy (Fig. 10.23). This also reflects that:

1. Corrosion rates are very dependent on flow and aeration conditions.
2. Different methods of protection may be applied on various zones of the same structure.

10.5.2 Modification of the electrolyte

When electrolyte treatment is a feasible strategy, there are two (interrelated) strategies: (a) removal of the aggressive species; and (b) the addition of inhibitors.

(a) Removal of aggressive species

The following strategies may be considered:

1. Elimination of dissolved oxygen from solution by evacuation, N_2 saturation or by addition of oxygen scavengers, e.g. in the case of boiler waters,

hydrazine may be used:

$$N_2H_4 + O_2 \longrightarrow N_2 + 2H_2O \tag{10.53}$$

Typical concentrations depend strongly on the conditions but may be 100 mg dm^{-3}; sulphite has also been used:

$$2SO_3^{2-} + O_2 \longrightarrow 2SO_4^{2-} \tag{10.54}$$

2. Elimination of acid by neutralization, e.g. lime addition.
3. Elimination of dissolved salts by, for example, ion exchange or reverse osmosis.
4. Elimination of humidity, e.g. by silica gel.
5. Lowering of local relative humidity by an increase in temperature, typically about 6–7° C above the surroundings.
6. Elimination of solid particles may help prevent differential aerations and deposit corrosion.

(*b*) *Addition of corrosion inhibitors*

An approach which is attractive for the protection of metals in contact with aqueous solutions, particularly where the solution is part of a closed system (e.g. cooling and heating systems) is that based on corrosion inhibitors. These are organic or inorganic species, which slow down corrosion when added to the solution in low concentration.

There are several mechanisms whereby inhibition occurs. A major group of inhibitors function by adsorption on the metal surface. The adsorption must occur in the region of the corrosion potential and decrease the rate of either or both the anodic and the cathodic reactions by one of the mechanisms discussed in Chapter 1.

Inhibitors which operate mainly on the metal dissolution process would include aromatic and aliphatic amines, various sulphur compounds and carbonyl molecules; many phosphorus, arsenic and antimony compounds have a greater effect on the hydrogen evolution reaction. Additions to the metal can have a similar effect, e.g. phosphorous is added to some steels to inhibit H_2 evolution.

A second group of inhibitors promote the appearance of a precipitate on the metal surface and maybe catalyse the formation of a passivating layer. Examples would include phosphate and bicarbonate; the oxidation of the metal leads to an ion and commonly the phosphate and carbonate salts of multivalent ions are quite insoluble. Other inhibitors are redox reagents which are able to shift the potential of the surface into the region where cathodic or anodic protection takes place, e.g. dichromate will often lead to passivation of a surface.

Figure 10.24 shows the action of inhibitors on polarization behaviour. In practice, several inhibitors may be used together in a complementary (and often synergistic) fashion; each inhibitor may function in several of the modes shown in Fig. 10.24.

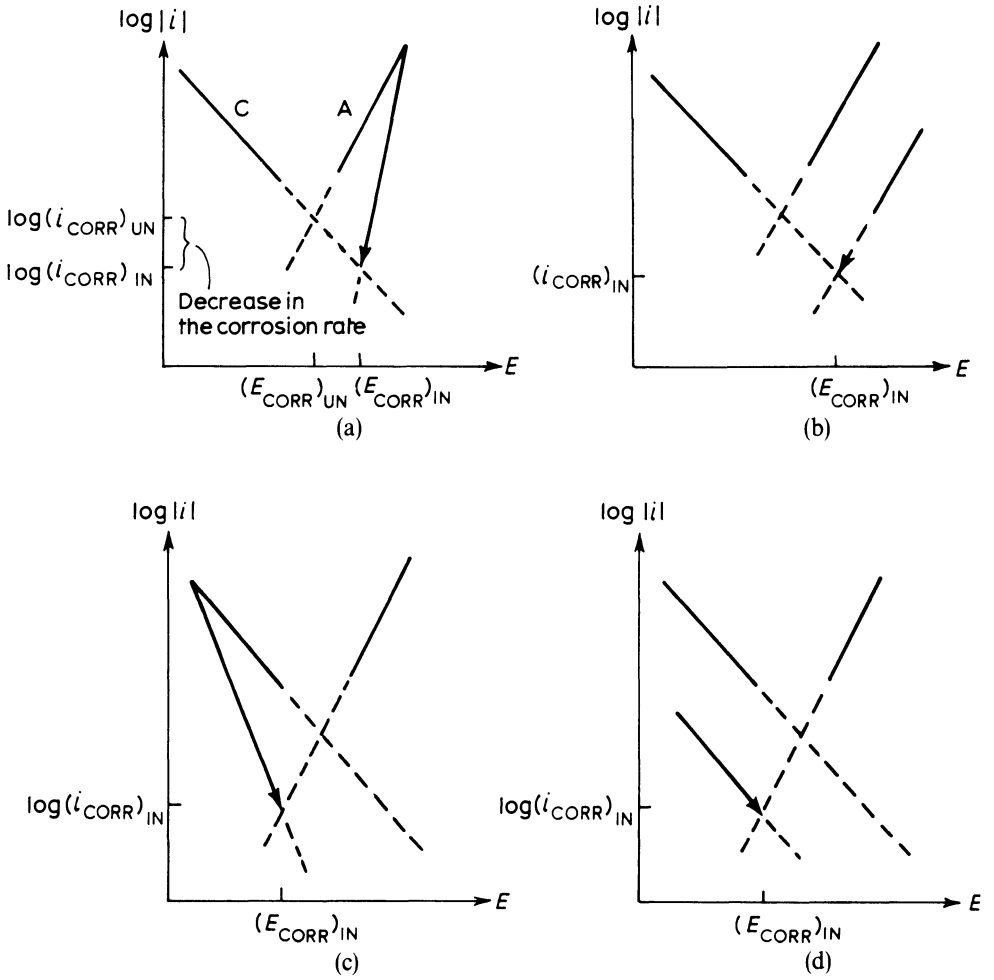

Fig. 10.24 Modes of inhibition, shown by the effect on polarization for charge-transfer-controlled electrode reactions. (a) Decrease in the apparent anodic Tafel slope. (b) Decrease in the anodic exchange current (in the case of anodic inhibitors, passivation may also occur). (c) Decrease in the apparent cathodic Tafel slope. (d) Decrease in the cathodic exchange current.
——— = uninhibited; ——→ = inhibited.

10.5.3 Changing the electrode potential

In many earlier chapters, the key to the success of an application of electrochemistry has been the ability to control the potential of a metal surface, either with a potentiostat or, more likely, by passing a calculated- and controlled-current density. The importance of electrode potential has been stressed earlier in this chapter, via thermodynamic (Pourbaix) and kinetic log $|i|$–E diagrams.

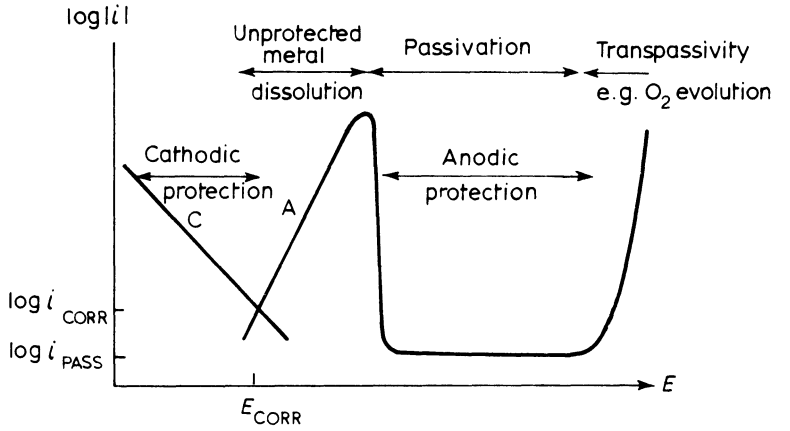

Fig. 10.25 Schematic $\log|i|$–E diagrams illustrating the principle of cathodic and anodic protection for a metal exhibiting passivity. The cathodic process (C) may be reduction of H_2O or O_2. The zones of electrode potential for protection are indicated.

It is possible, in principle, to depress the potential from its free corrosion value E_{CORR} to a value which lies within a stable zone of immunity (Fig. 10.5) in order to cathodically protect the metal. Alternatively, the potential may be elevated from E_{CORR} to a value such that stable passivity is achieved, the principle of anodic protection (Fig. 10.25).

(*a*) *Cathodic protection*

The principle of cathodic protection is shown in the polarization diagram in Fig. 10.26. There are two separate methods of applying cathodic protection (Fig. 10.27), namely the use of sacrificial anodes or impressed current.

In the former, a deliberate electrolysis cell is set up between the structure to be protected and a number of strategically positioned anodes of another metal. The essential property of a sacrificial anode is its ability to dissolve freely at a reasonably uniform rate at a potential negative to the corrosion potential of the metal to be protected in order to provide a consistent and sufficiently high protective current to the steel. Figure 10.27(a) illustrates the principle of cathodic protection using sacrificial anodes. The dissolution of the auxiliary metal will cause the equilibrium potential of the metal to be protected to shift to a more negative value. While both metals have almost the same potential (there will be an iR drop between sites) the auxiliary metal will function as an anode while the surface to be protected will become cathodic. It is apparent that the overall rate of metal loss will increase but it is the auxiliary metal that dissolves; the rate of metal loss from the protected surface decreases; hence, the term 'sacrificial' anode.

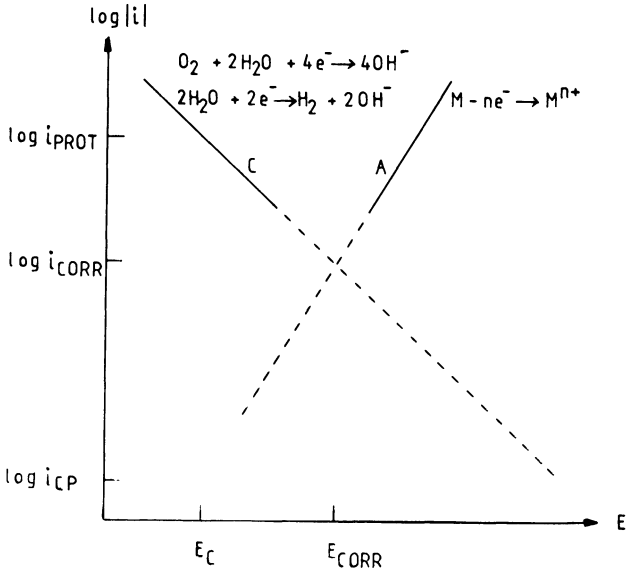

Fig. 10.26 Log $|i|$–E diagram showing the principle of cathodic protection. (The cathodic process may typically be oxygen reduction and/or hydrogen evolution; it is assumed to be under charge transfer control.) If the potential of the metal is lowered from E_{CORR} to E_C, the corrosion rate is reduced (from i_{CORR} to i_{CP}) and the rate of the cathodic reaction is increased (from i_{CORR} to i_{PROT}). i_{PROT} may be taken to correspond to a negligible rate of corrosion (i_{CP}). If $i > i_{PROT}$, 'overprotection' results; if $i < i_{PROT}$, only partial protection is conferred.

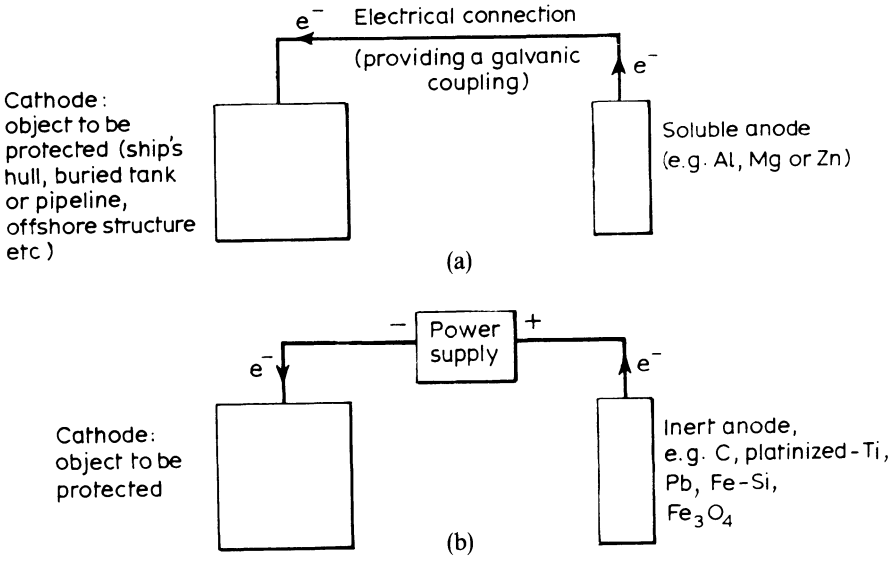

Fig. 10.27 Methods of applying cathodic protection. (a) Sacrificial anodes. (b) Impressed current.

The use of a sacrificial anode is electrochemically equivalent to cathodic protection since it causes the potential of the surface to become more negative. Hence, it must produce the same risks of hydrogen embrittlement. It is, however, a convenient procedure for reducing corrosion and has been widely used for protecting such metal structures as ships' hulls, (Fig. 10.28) oilrigs and pipelines. On large structures the anodes must be placed at intervals to ensure that the whole surface is protected. This is because, in practice, there will be an iR drop caused by the need for ions to move between anodic and cathodic zones and this must be provided by the sacrificial anode being at a more negative potential than indicated in the figure. In a poorly conducting medium the anodes must be closer together.

Traditionally, sacrificial anodes are made of zinc or magnesium although it is now increasingly common to use aluminium alloys because of their low density and the low molar mass of aluminium. It may be noted that if aluminium or, indeed, magnesium, were to dissolve anywhere near their equilibrium potential, and the metals remained in the active state, the simple argument of Fig. 10.27(a) would suggest that they would be unsuitable as sacrificial anodes; the anodes would dissolve too rapidly and much hydrogen would evolve from the protected surface. This does not happen because both metals passivate readily and as



Fig. 10.28 An example of cathodic protection using sacrificial anodes; A newly installed zinc anode on a bilge keel of a vessel in dry-dock. (Courtesy: Corrintec (UK) Ltd.)

sacrificial anodes they are probably in a state of controlled and partial passivation (which will vary with the medium). Indeed, pure aluminium cannot be used here as it almost totally passivates; the role of the alloying element (usually Mg, Hg or Tl: 1–5% wt) is to catalyse the anodic dissolution.

In the more versatile, impressed current method (Fig. 10.27(b)) a power supply is used to supply current to the protected metal, courtesy of an auxiliary electrode (anode).

Theoretically, it would be possible to hold the potential at a value where the metal is thermodynamically immune from corrosion. In practice, however, this is likely to be too expensive. The continuous passage of current requires the consumption of power ($iE_{CELL}t$) and, particulary if the medium between the protected surface and the anode is not highly conducting, the use of anything but a very low current will entail an unacceptably high energy consumption. The voltage required of the power supply also depends upon the active area of the structure, the nature of the electrode reactions and resistance of the anode. The cathode potential is kept within the desired limits by:

1. Current or cell voltage regulation, e.g. pipelines.
2. Large scale potentiostats, as in the case of offshore structures.

Moreover, if the electrode process initiated by the cathodic current is hydrogen evolution, the likelihood of hydrogen embrittlement and disbondment of paint coatings is greatly increased by a higher current density. The anode may be consumable (e.g. scrap iron or cast iron), semi-consumable (e.g. Fe–14Si–3Mo or resin-bonded graphite) or inert, e.g. Pb–6Sb–1Ag or platinized Ti or Ta). In the case of inert anodes, the electrode reaction is normally:

$$2H_2O \longrightarrow O_2 + 4H^+ + 4e^- \tag{10.55}$$

or in sea water, possibly:

$$2Cl^- \longrightarrow Cl_2 + 2e^- \tag{10.56}$$

Consumable electrodes are cheap but require regular replacement; they contaminate the environment with dissolution products and cannot sustain high current densities (being, therefore, bulky). Non-consumable anodes avoid many of these problems but incur a high capital-cost penalty.

Examples of impressed-current, cathodic protection are illustrated in Fig. 10.29. Each method of cathodic protection has its own strengths and weaknesses. Sacrificial anodes have the following advantages:

1. Operation is independent of a power supply.
2. Installation is simple.
3. Inadequate protection may sometimes be corrected by additional anodes.
4. Incorrect polarity connections are not possible.

5. Regulation and control of power-supply settings is not required.
6. Overprotection is easy to avoid; a spatially uniform electrode potential is relatively easy to obtain.

The most severe limitation is the small potential difference obtained which restricts its application to conductive environments, small anode–cathode spacing and, often, substantially coated structures.

The advantages of the impressed current method include:

1. The ability to achieve a wide range of potential difference.
2. The ability to exercise control over its value as conditions change.
3. Large (sometimes uncoated) structures may be protected in high-resistivity environments with wide anode–cathode spacings.
4. Few anodes are required.

The drawbacks include the need for a specialized, reliable, power supply, increased danger of overprotection, difficulty in achieving uniform potential distribution and the problem of inadvertent reversal of the connections causing an enhancement in corrosion rates.

The successful commissioning and effective use of a cathodic protection system is usually monitored by measuring the spatial distribution of the cathode potential on the structure. This may be achieved via regular ground stations in the case of a buried pipeline (Fig. 10.30) or a portable, heavy-duty reference electrode/digital voltmeter probe (Fig. 10.31) in the case of offshore rigs and platforms.

The current application of cathodic protection to steel reinforcing bars in concrete structures is illustrated in Fig. 10.32.

In practice, the application of cathodic protection requires skill and experience; at present it is difficult to predict the optimum arrangement and number of anodes for the optimum potential distribution. Whenever possible, the method is applied to a coated system, cathodic protection serving to prevent localized corrosion at flaws or degrading areas. The joint use of paint coatings can, however, cause problems. The cathodic reactions (10.6) or (10.8) result in a local rise in pH which may saponify or blister paint films. This is largely overcome by the most suitable bituminous, epoxy, chlorinated rubber and coal-tar epoxy, paints. Additionally, hydrogen generated at steel surfaces may cause embrittlement in high-strength steels or disbondment of paint films. Another problem which may arise is the existence of stray currents near impressed cathodic protection anodes. Aside from risks to divers and swimmers in marine environments, stray currents may result in significant localized attack in conductors which are rendered bipolar in the current path (Fig. 10.33). Related problems may occur in other situations, including current leakage or induction from railway traction, overhead power transmission, and welding operations.

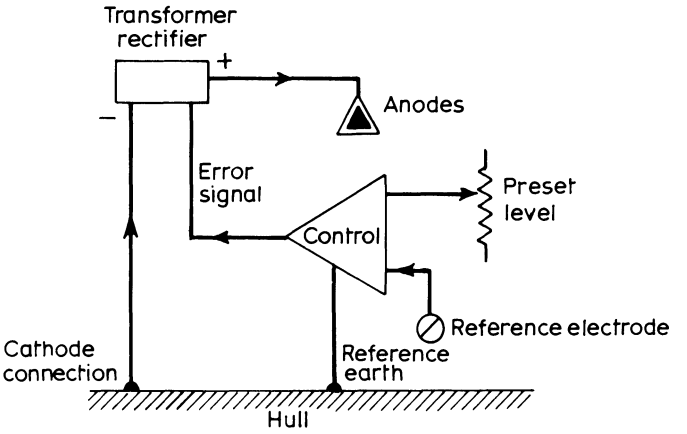
Transformer
rectifier
+
−
Anodes
Error
signal
Control
Preset
level
Reference electrode
Cathode
connection
Reference
earth
Hull

(a)

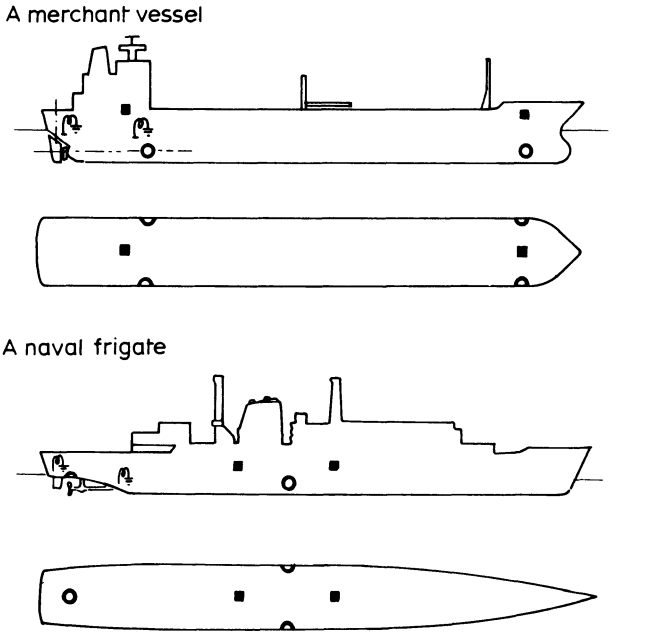
A merchant vessel
A naval frigate
Anodes
Power units
Reference electrodes
Bonding

(b)

(c)

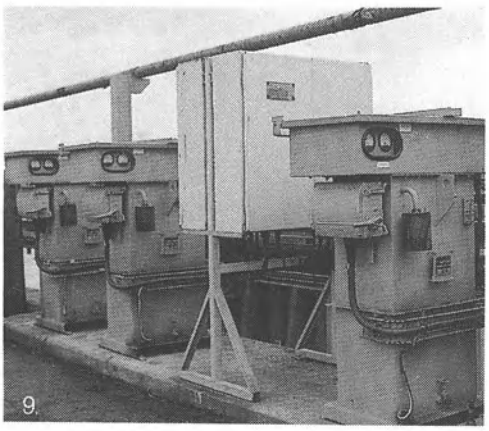

(d)

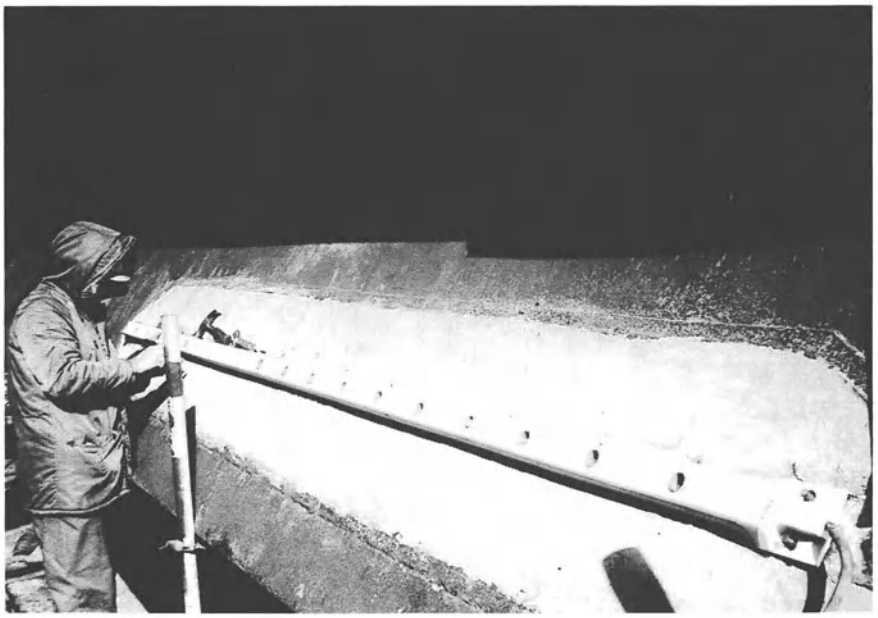

Fig. 10.29 Cathodic protection using impressed current. (a) A circuit showing the principles: the signal from the reference electrode is passed to a power-unit control where it is compared with a preset level. The resultant error signal is amplified and used to control semiconductor power devices which allow a controlled current to pass through the anodes. (b) A typical layout of components in various types of vessel. (c) Transformer/rectifier power units for marine use. (d) Platinized titanium or lead–silver alloy anodes being installed on a ship's hull. The anodes are insulated from the hull and have special insulating, backing shields which help to improve potential distribution and prevent over-protection, i.e. too negative a potential (Photographs courtesy: Corrintec (UK) Ltd.)

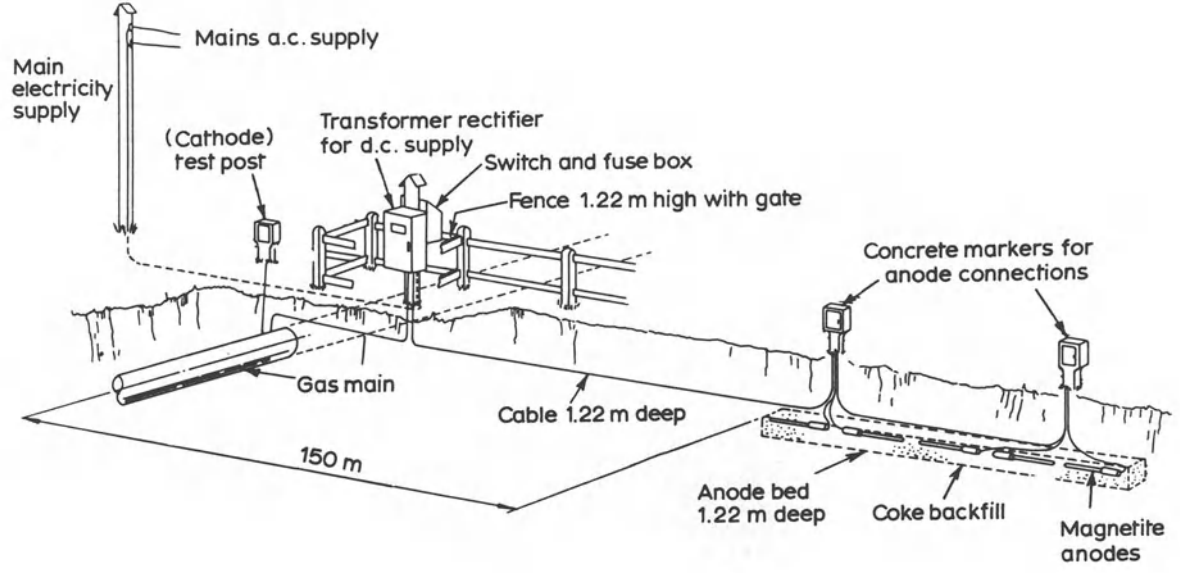

Fig. 10.30 An impressed-current cathodic protection station for a gas main with test points for monitoring of cathode and anode potentials.

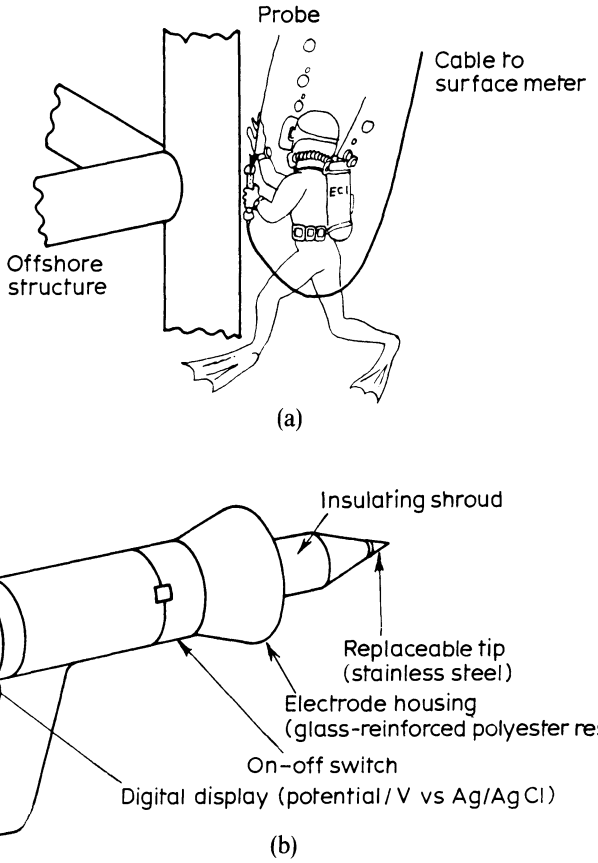

Fig. 10.31 Portable reference electrode probe. (a) Surveys of electrode potential distribution on ships' hulls, submerged offshore pipelines, oilrigs, platforms, jetties and docks are often carried out by manual diver-held probes. (b) These battery-powered devices usually incorporate a tip spike, a silver/silver chloride reference electrode and a digital voltmeter (dvm) within a tough, insulated and sealed pistol. The shroud surrounding the electrode element defines the sensing area. These probes are used to depths of approximately 300 m and are capable of measuring to a precision of $\pm$ 1 mV. Rechargeable Ni–Cd batteries are used. Sharpened tips may be used to penetrate coatings. (Courtesy: Corrintec (UK) Ltd.)

(*b*) *Anodic protection*

It will be evident from the underlying thermodynamics and kinetics (Fig. 10.25) that successful anodic protection of a metal relies upon the maintenance of a stable passivating film. A simple example of galvanic anodic protection is the addition of alloying elements (0.1% Pd or 1% Cu) to stainless steel which form local cathodes (Fig. 10.34).

Impressed current anodic protection is of little importance in comparison to cathodic protection. It has been applied successfully to the protection of stainless steel and titanium alloys in the presence of acidic electrolytes. As in the case of impressed-current cathodic protection, it is essential to control the electrode potential within suitable limits. Figure 10.35 indicates the application of anodic protection to a simple tank and to a more complex tube-and-shell heat exchanger. When anodic protection is commissioned, the current must be large enough to exceed i_{CRIT}, in order to passivate the surface. The current then falls to i_{PASS} and current is increasingly deflected to more remote parts of the structure which passivate in turn. Once established, the current drain is minimal and is approximately equal to i_{PASS}.

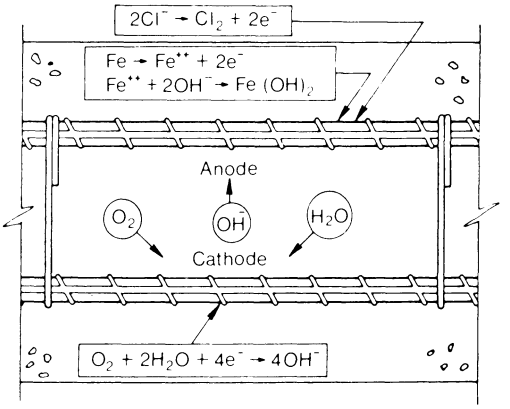

(a)

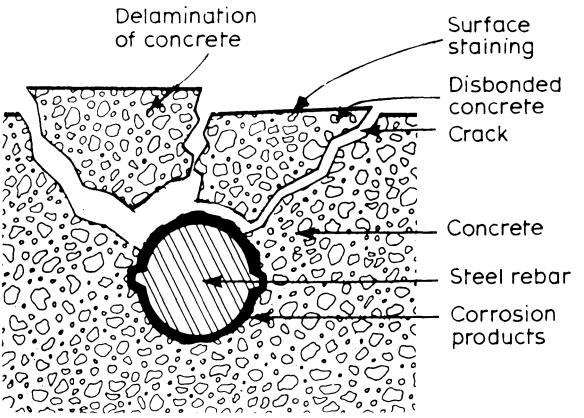

(b)

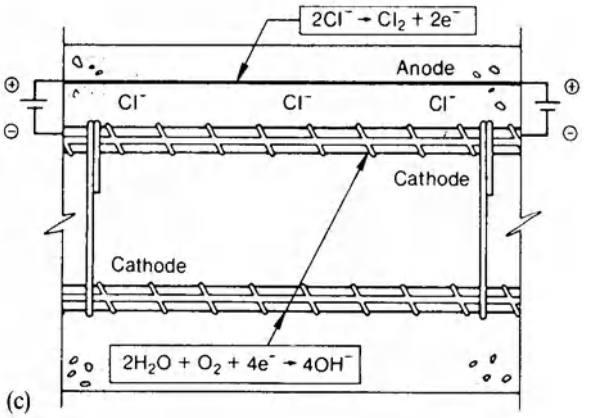

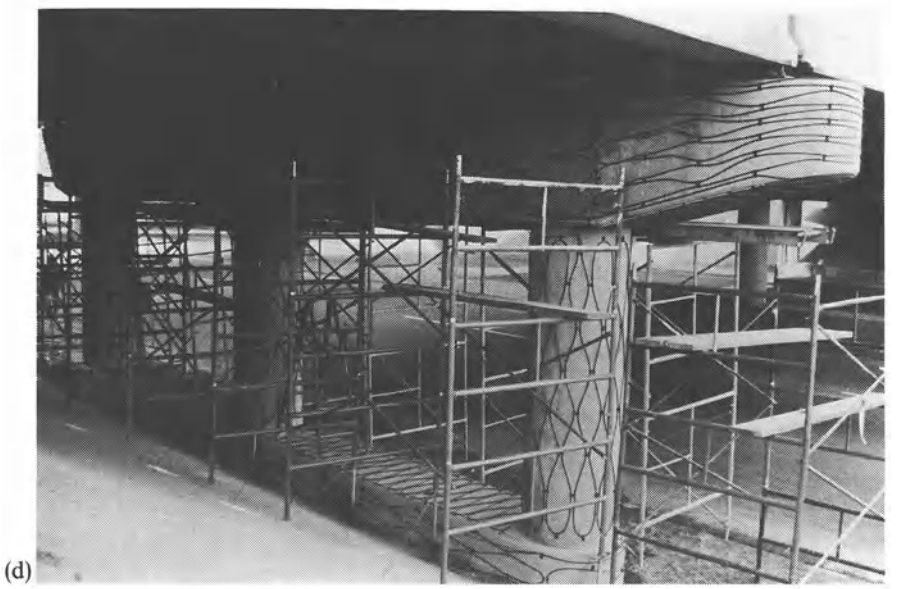

Fig. 10.32 Corrosion of steel reinforcing bars (rebars) in a concrete bridge head. (a) The corrosion cell which arises due to water penetration and chloride pick-up from the concrete or from deicing salts. (b) The expansive corrosion products may cause cracking of the concrete. In severe cases, delamination results. (c) Impressed current, cathodic protection may be applied. (d) A flexible anode mesh may be installed (which is then covered with a concrete overlay). Power usage is $\leqslant 10\ W\,m^{-2}$ of the concrete surface. (Courtesy: Raychem Ltd.)

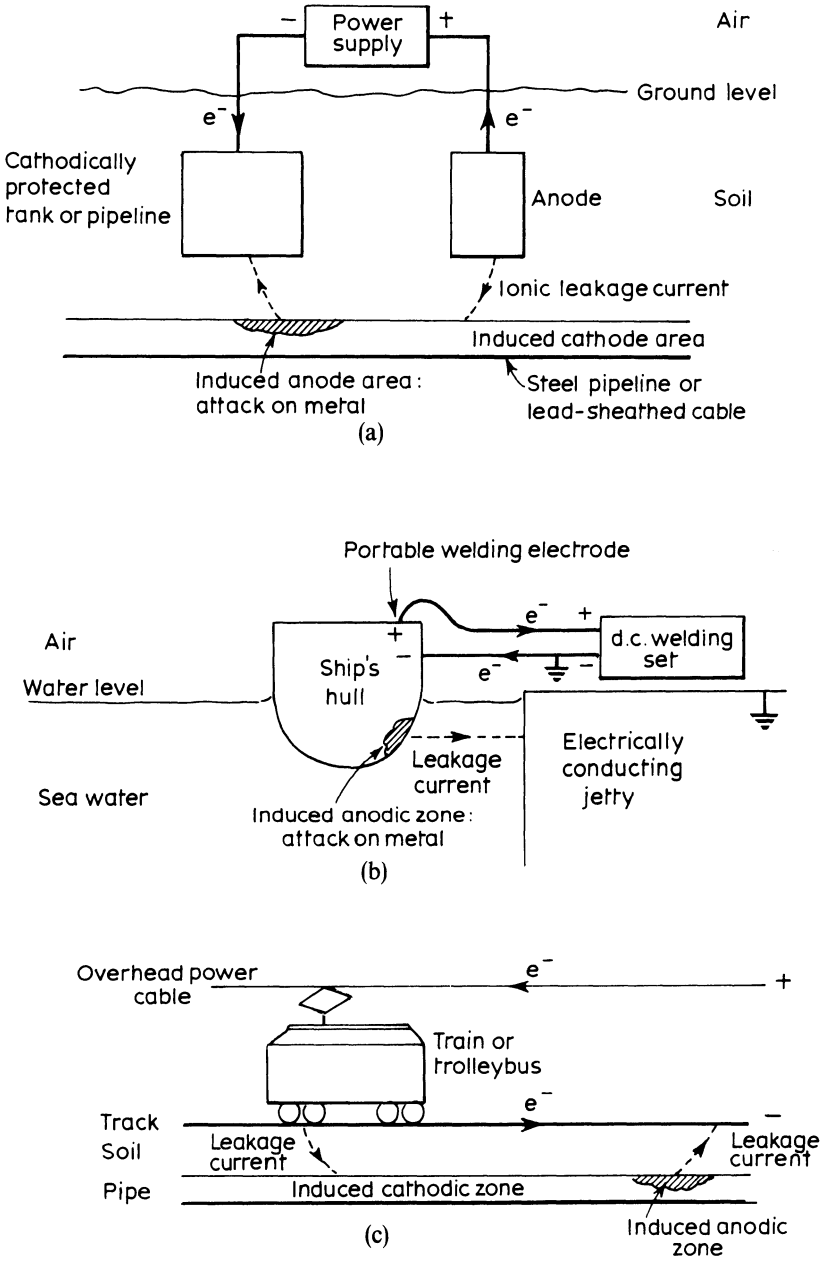

Fig. 10.33 Stray current corrosion. (a) A pipeline or cable may provide a lower resistance path than the soil. (b) Welding operations on a ship may give rise to stray currents if the earth bonding is insufficient. (c) Leakage currents may be induced by an overhead train cable.

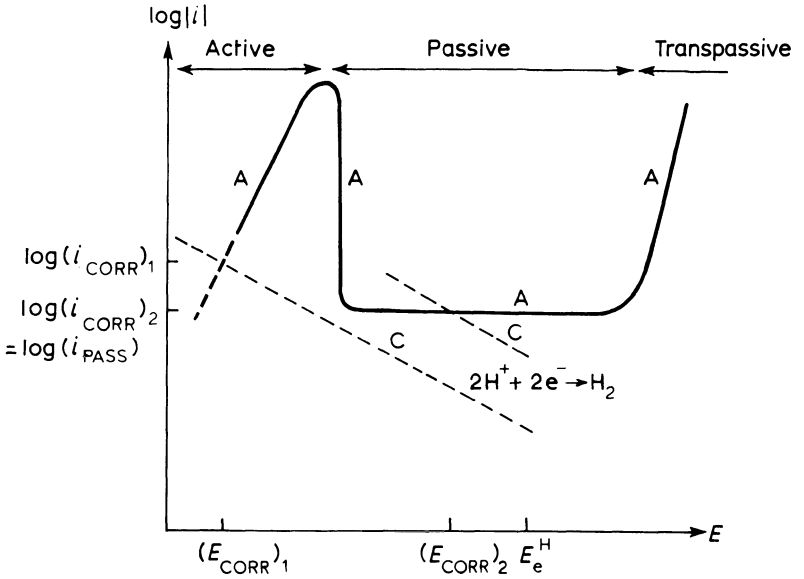

Fig. 10.34 Anodic protection of stainless steel by additions of noble metals which form local cathodes for hydrogen evolution. The alloying element (palladium or copper) has a high exchange-current density for hydrogen evolution which effectively raises E_{CORR} from an active to a passive region on the anodic curve of the metal. Note the shift in the corrosion potential to more positive values due to the passivation which occurs upon alloying.

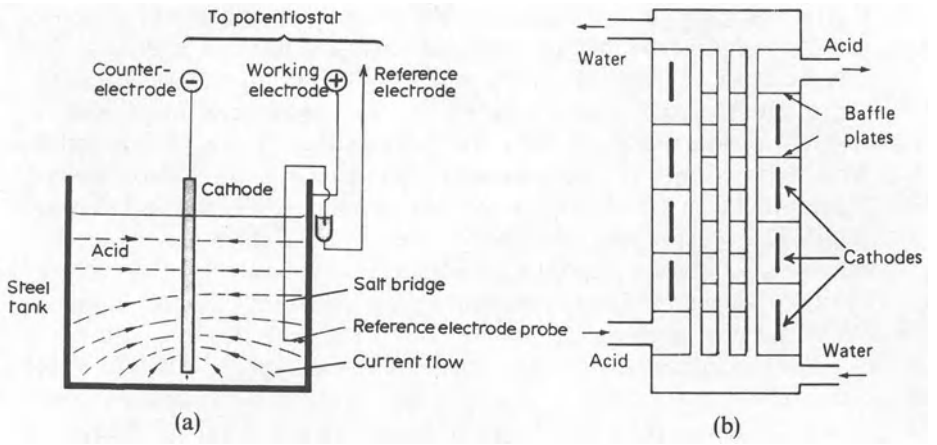

Fig. 10.35 The application of (impressed current) anodic protection. (a) Protection of a steel tank storing acid using a reference electrode and potentiostatic control. (b) Protection of a tube-and-shell heat-exchanger. (after: West (1980).)

10.5.4 Surface coatings

A wide range of protective coatings may be applied, as indicated in Chapter 8. In practice, care must be taken in the choice, production and utilization of such coatings in order to avoid localized damage followed by intense attack on the substrate (section 10.4).

10.6 CORROSION PROBLEMS IN ELECTROLYTIC PROCESSING

Special mention may be made of cases of corrosion damage associated with processes utilizing electrolytic cells or reactors. Possible effects include the following:

1. Corrosion of the anode or cathode under 'standby' or 'open-circuit' conditions. On open circuit the electrodes are at a quite different potential from when on load and may be shifted from the immune or passivated state to an active one. Moreover, heterogeneities in the electrode, discontinuous surface coatings which are cathodic with respect to the substrate, or the presence of an unusually high concentration of cathodic reactant, may aggravate this situation. For example, oxygen may be provided by aeration in a flow cell (or a dynamic-electrode reactor) or produced at the anode in an undivided reactor. Also in a chlor-alkali diaphragm cell, it is on open circuit that catalytic cathode coatings are particularly prone to corrosion; during cell operation they are cathodically protected but on open circuit the potential is more positive and the environment contains both hypochlorite and chloride.
2. 'Current on' dissolution of 'inert' anodes or unwanted attack on electrode feeders due to aggressive species in the electrolyte, a.c. ripple from the power supply, or poor electrode/feeder design.
3. 'Current on' cathode dissolution, particularly due to combination of electroreduction of protective surface films and active generation of hydrogen. This may be especially marked in the case of titanium, due to facile hydride formation. The result may be pitting, embrittlement or exfoliation of the electrode surface. Electrode corrosion may significantly alter electrocatalytic properties (resulting in a reduced selectivity); contaminate electrolytes (and, hence, products); block cells, dividers or manifolds; cause electrical shorting, or provide parasitic redox couples (e.g. Fe^{3+}/Fe^{2+}) which decrease current efficiency; or promote deposit or bimetallic corrosion efficiency elsewhere.
4. Current leakage, particularly from a bipolar cell stack (Chapter 2) via the electrolyte flow circuits, may induce stray current corrosion in a range of electrically conducting, ancillary equipment. Components which suffer attack may include tanks, pumps, heat-exchanger plates, measurement probes, heaters, agitators, rotameter floats, valves and piping or the cell body (Fig. 10.36). In addition to the choice of stable electrode and cell materials, consideration should be given to the following:
   (a) restricting the use of electrically conducting components to the electrodes themselves;

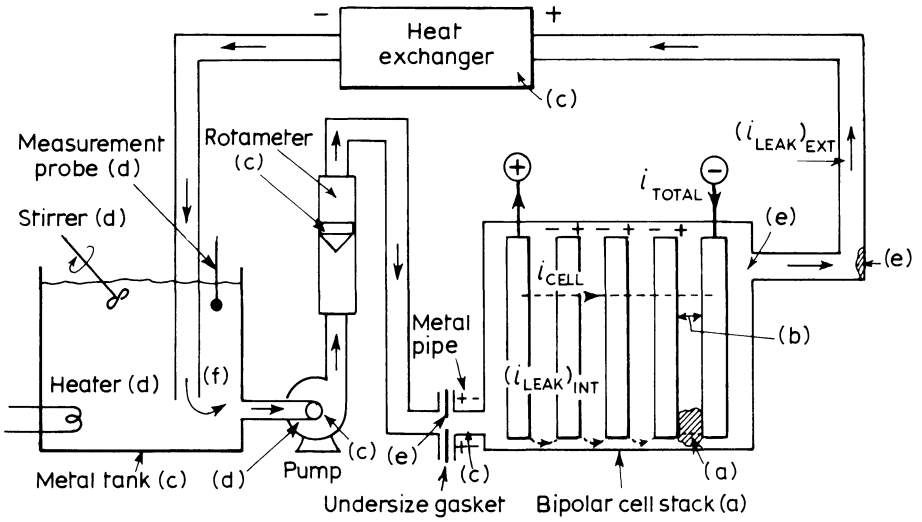

Fig. 10.36 Corrosion problems in electrochemical process plant: $i_{TOTAL} = i_{CELL} + (i_{LEAK})_{INT} + (i_{LEAK})_{EXT}$. (a) In the bipolar cell stack, internal current leakage $(i_{LEAK})_{INT}$ may cause blockage of internal manifolds, interelectrode shorting or membrane damage due to conductive anode debris. In an undivided cell, noble metal from anode dissolution may deposit via cementation or electroplating of the cathode, causing bimetallic or deposit corrosion. (b) Extensive metal dissolution may provide a reduction in current efficiency due to the establishment of parasitic redox shuttles, e.g. $Fe^{3+} + e^- \rightleftharpoons Fe^{2+}$. (c) Any conductive components such as a pump, tank, heat-exchanger, rotameter float, pipes or coupling, etc. may become bipolar; an induced potential difference may arise due to stray current corrosion caused by bypass current leaking from the cell stack $(i_{LEAK})_{EXT}$. (d) Leakage of a.c. mains supply to components such as heaters, stirrers, measurement probes and pumps may also result in stray-current corrosion. (e) Flow restrictions or rapid changes in flow direction may induce erosion corrosion. (f) Cavitation may result from the recycling of electrode gases or air to the pump inlet.

(b) draining/washing cells after use;
(c) leaving a small polarizing current flowing through a flooded, vented cell during standby periods;
(d) dividing cells to prevent anode corrosion via aggressive catholyte species (Chapter 2);
(e) designing the cell and its ancillaries to facilitate inspection and maintenance;
(f) avoidance of high external leakage currents in bipolar cells (Chapter 2);
(g) avoid cavitation by appropriate design of the electrolyte plumbing (e.g. allow effective gas separation to occur); separate reservoir feed and return pipes to prevent recycling of gas.

A number of the above comments also apply to, for example, electroplating cells, which may have other specific corrosion problems (Fig. 10.37).

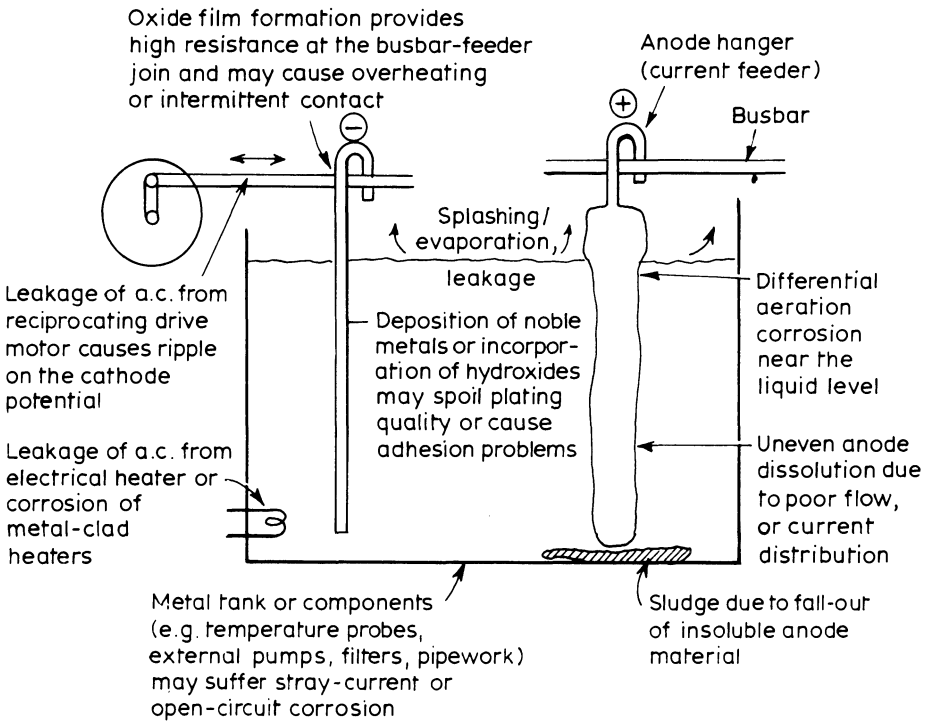

Fig. 10.37 Corrosion-related problems in electroplating baths.

10.7 CORROSION MEASUREMENT AND MONITORING

The possible benefits of corrosion monitoring may be enumerated:

1. Problems may be highlighted and advance warning obtained.
2. Inspection and maintenance schedules may be organized efficiently, with minimal down-time.
3. Improved usage and reliability of materials and plant are achieved.
4. A continuous and dynamic record of metals stability is available.

Apart from increased cost and complexities, drawbacks may include:

1. The qualitative nature of the data.
2. The need to obtain confirmatory or complementary data from laboratory tests and non-destructive testing.
3. The skill and experience necessary for valid interpretation.

While an extremely diverse range of laboratory techniques exists for the measurement of corrosion rate, a relatively small number of methods have found an accepted, routine industrial use.

In addition to classical methods such as weight loss (via coupons), solution analysis for dissolved metal, monitoring of gas evolution (in the case of H_2) and change in metal resistance, a select number of electrochemical techniques are widely accepted. This section briefly describes these methods. Weight-loss coupons are still the traditional, accepted baseline for comparisons; electrical resistance (ER) and linear-polarization resistance (LPR) are the most widely used electrical and electrochemical techniques. Electrode potential monitoring is sometimes a valuable way of following active/passive transitions. There continues to be an emphasis on the use of non-destructive testing (NDT) techniques (particularly ultrasonic types).

10.7.1 Electrical resistance (ER)

The electrical resistance of a sacrificial electrode is measured during exposure to the environment. The decrease in cross-sectional area ΔA due to corrosion results in an increase in resistance ΔR. If the material has a constant resistivity κ and length l, then:

$$\Delta R = \kappa l / \Delta A \tag{10.57}$$

This change in area may be related via Faraday's laws (section 10.4.1) to a corrosion rate, assuming uniform corrosion. In practice, measurements are made relative to an identical non-corroding sample within the probe body in order to compensate for temperature effects and terminal resistances. A wide range of probe types are available, the older 'wire loop' type having given way to the tubular-element probe as the most popular type. Preference is increasingly given to flush-mounted probes to avoid turbulence effects.

10.7.2 Linear polarization resistance (LPR)

This is perhaps the singly most important technique; it arises from the Stern–Geary equation which describes a linear overpotential – current relationship in the vicinity (typically ± 20 mV) of the corrosion potential where the linear polarization resistance is:

$$R_p = dE/di = \beta_A \beta_C / 2.3(\beta_A + \beta_C) i_{CORR} \tag{10.58}$$

where β_A and β_C are the anodic and cathodic reciprocal Tafel slopes, which must be established by prior laboratory work, retrieved from the literature or estimated. For a given electrode reaction (i.e. a known metal under constant electrolyte conditions) β_A and β_C are constant and:

$$1/R_p = K \cdot i_{CORR} \tag{10.59}$$

i.e. the polarization conductance $(1/R_p)$ is directly proportional to corrosion rate i_{CORR} the constant of proportionality being:

$$K = 2.3(\beta_A + \beta_C)/\beta_A \beta_C \tag{10.60}$$

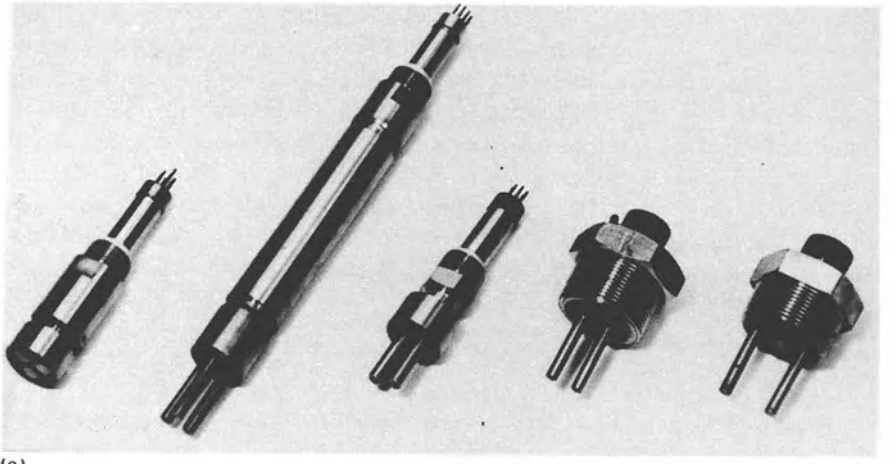

(a)



(b)

Fig. 10.38 Typical linear polarization resistance (LPR) equipment. (a) Probe designs, including 2- and 3-electrode types, protruding or flush mounted. (b) Instrumentation. The device shown is a battery-powered, portable probe, capable of use in hazardous environments with dimensions 23 × 15 × 21 cm and weighs 2 kg. (Courtesy: Cormon Ltd.)

In its simplest form, the probe uses two electrodes, with a 10–20 mV polarization between them (typically maintained by a square wave E–t signal). The resultant current flow is measured to give i_{CORR} or millimetres per year directly via equation (10.52). Complications arise due to the electrolyte resistance, and three-electrode systems attempt to minimize this by introducing a reference electrode adjacent to the test (corroding) electrode. Unfortunately, this renders the probes susceptible to bridging between the reference and working electrode. In an attempt to overcome operational limitation, four-electrode probes have recently been designed. These utilize two reference electrodes positioned between two working electrodes. The potential gradient between the two reference electrodes represents the iR drop in solution.

Thus, iR drop may be allowed for. This type of probe is seeing continued development, especially in high-resistance media. Figure 10.38 shows instrumentation for linear-polarization-resistance monitoring.

The field of corrosion monitoring is advancing rapidly and several trends are noteworthy:

1. The laboratory development of sophisticated electrochemical methods, including impedance, zero resistance ammetry (ZRA) and electrochemical noise.
2. The increasing use of computers for control and data logging/retrieval.
3. The development of remote and robot transducers for offshore or hazardous environments.
4. The application of several techniques, in parallel, to 'fingerprint' corrosion.
5. Attempts to develop techniques suitable for detecting the initiation and progress of localized attack.

FURTHER READING (see also Further Reading for Chapter 8)

1 U. R. Evans (1963) *An Introduction to Metallic Corrosion*, Edward Arnold, London.
2 N. D. Tomashov (1966) *Theory of Corrosion and Protection of Metals*, Macmillan, London.
3 H. L. Logan (1966) *The Stress Corrosion of Metals*, Wiley, New York.
4 M. G. Fontana and N. D. Greene (1967) *Corrosion Engineering*, McGraw-Hill, New York.
5 L. L. Shreir (Ed.) (1976) *Corrosion and Corrosion Control*, Vols 1 and 2, 2nd Edition, Butterworth, London.
6 G. Wranglen (1985) *Introduction to Corrosion and Protection of Metals*, Chapman and Hall, London.
7 M. Pourbaix (1966) *Atlas of Electrochemical Equilibria in Aqueous Solution*, Pergamon Press, Oxford; *Corrosion Science* (1965), **5**, 677.
8 E. Heitz, J. C. Rowlands and F. Mansfield (Eds) (1986) *Electrochemical Corrosion Testing with Special Consideration of Practical Applications*, Dechema-Monograph 101, Dechema, Frankfurt.

9 V. Ashworth and C. J. L. Booker (Eds) (1986) *Cathodic Protection: Theory and Practice*, Ellis Horwood, Chichester.
10 C. G. Munger (1984) *Corrosion Prevention by Protective Coatings*, NACE Publications, Houston, Texas.
11 H. Leidheiser Jr (Ed.) (1981) *Corrosion Control by Organic Coatings*, NACE Publications, Houston, Texas.
12 C. P. Dillon (Ed.) (1982) *Forms of Corrosion Recognition and Prevention*, NACE Publications, Houston, Texas.
13 R. Baboian (1977) *Electrochemical Techniques for Corrosion*, NACE Publications, Houston, Texas.
14 J. M. West (1971) *Electrodeposition and Corrosion Processes*, 2nd Edition, Van Nostrand Reinhold, London.
15 H. H. Uhlig (1971) *Corrosion and Corrosion Control: An Introduction to Corrosion Science and Engineering*, 1st Edition, Wiley, New York.
16 J. M. West (1986) *Basic Corrosion and Oxidation*, 2nd Edition, Ellis Horwood, Chichester.

11 Batteries and fuel cells

A battery is a device which can store chemical energy and, on demand, convert it into electrical energy to drive an external circuit. The importance of batteries to modern life surely requires no emphasis. Even so, there may be a tendency to overlook their diversity and the scale on which they are used; e.g. in size they range from a small fraction of a cubic centimetre for a hearing aid battery, to many cubic decimetres for some industrial and military versions, while in the Western world we manufacture some four to ten batteries per year per head of population.

The electrical energy results from a spontaneous chemical change (i.e. a redox reaction with a negative free energy) within the battery. The redox reagents must not react directly but are consumed at different sites in the battery, at the anode and the cathode, and it is this which causes electrons to flow through the external circuit between the battery terminals. The electrochemistry of the three battery systems that are by far the most widely manufactured is summarized in Table 11.1. In practice, a battery is always designed and manufactured for a particular duty, e.g. to power a torch, to start a car engine or to supply emergency power for a hospital or a computer. For each application, a set of battery characteristics will be essential and these will, in turn, place requirements on the electrode reactions and determine the design of the cell. Figure 11.1 shows a battery which recognizes that, in general, the electroactive species and the products of the electrode reactions are solids. The performance of the battery will depend on the cell geometry and on the design and composition of all the components labelled in the figure, in addition to the choice of electrode reactions and their kinetics. The multitude of battery specifications is met by the manufacture of a number of battery systems (see later) and also by the production of the same system in various sizes, e.g. a lead–acid battery for a car is typically 50 A h while for industrial use it may exceed 1000 A h. The range of Leclanché cells manufactured by a UK company is illustrated in Fig. 11.2.

Battery characteristics and their relationship to the thermodynamics and kinetics of the electrode reactions and to cell design will first be discussed. Later,

Table 11.1 Electrochemistry of the three most common battery systems

1. *Lead–acid*: Chemistry during discharge:
   +ve (cathode):

$$PbO_2 + 4H^+ + SO_4^{2-} + 2e^- \longrightarrow 2H_2O + PbSO_4$$

   −ve (anode):

$$Pb + SO_4^{2-} - 2e^- \longrightarrow PbSO_4$$

   overall reaction:

$$PbO_2 + Pb + 4H^+ + 2SO_4^{2-} \longrightarrow 2PbSO_4 + 2H_2O$$

   Electrolyte: aqueous H_2SO_4.
   Current collectors: both Pb.
   Reversible cell potential = 2.05 V:
   $\Delta G = -394\ \text{kJ mol}^{-1}$.

   Applications: cars, standby supplies, industrial, traction.

2. *Nickel cadmium*: Chemistry during discharge:
   +ve (cathode):

$$NiO(OH) + H_2O + e^- \longrightarrow Ni(OH)_2 + OH^-$$

   −ve (anode):

$$Cd + 2OH^- - 2e^- \longrightarrow Cd(OH)_2$$

   overall reaction:

$$2NiO(OH) + Cd + 2H_2O \longrightarrow 2Ni(OH)_2 + Cd(OH)_2$$

   Electrolyte: aqueous KOH.
   Current collectors: Ni and Cd.
   Reversible cell potential = 1.48 V.
   $\Delta G = -283\ \text{kJ mol}^{-1}$.

   Applications: standby supplies, industrial, plane engine starting, railway lighting.

3. *Zinc–carbon*: Chemistry during discharge:
   +ve (cathode):

$$2MnO_2 + H_2O + 2e^- \longrightarrow Mn_2O_3 + 2OH^-$$

   −ve (anode):

$$Zn - 2e^- \longrightarrow Zn^{2+}$$

   overall reaction:

$$2MnO_2 + Zn + H_2O \longrightarrow Mn_2O_3 + Zn^{2+} + 2OH^-$$

   Electrolyte: moist NH_4Cl–$ZnCl_2$–MnO_2–C powder.
   Current collectors: graphite and Zn.
   Reversible cell potential = 1.55 V:
   $\Delta G = -257\ \text{kJ mol}^{-1}$.

   Applications: small (but not miniature) portable power sources (torches, radios, toys).

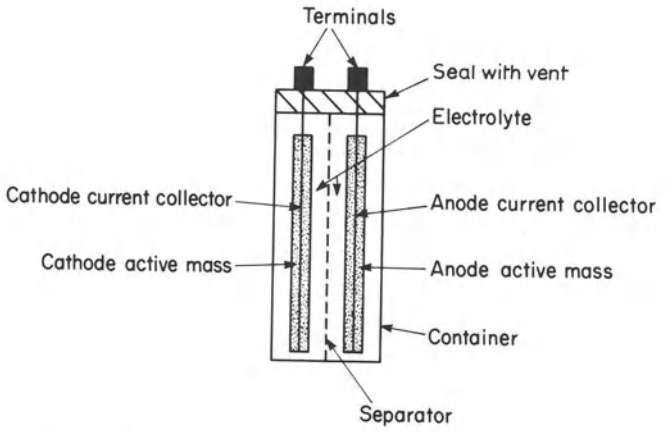

Fig. 11.1 The principal components of a battery.



Fig. 11.2 The Ever Ready range of Leclanché cells. (Courtesy: Berec Ltd.)

some battery specifications, the evaluation of battery performance and the design, manufacture and performance of some practical batteries will be described. The discussion will emphasise batteries presently manufactured but some under development will also be mentioned.

Fuel cells will be considered briefly in section 11.7. In principle, a fuel cell differs from a battery only in that the reactants are fed from outside the cell, but the nature of the electrode reactions requires totally different technology based on catalytic, gas-diffusion electrodes. Fuel cells were conceived as a method of converting primary fuels, particularly hydrocarbons, and oxygen into electrical energy in a way that would avoid the well-known Carnot inefficiencies of conventional power generation based on burning the fuel. It has, however, proved impossible to obtain meaningful cell potentials and current densities because of the poor performance of the available electrocatalysts. Hence, at the present time, fuel cells would only be considered for very specialist applications. Moreover, the anode fuel is more likely to be hydrogen, methanol or carbon monoxide.

11.1 BATTERY CHARACTERISTICS

A certain performance is necessary for a battery to perform satisfactorily in any duty and we therefore need to define characteristics which may be measured and used to judge whether a battery is suitable for a particular application. Moreover, in some cases (e.g. a car traction battery) no battery system presently available has all the essential properties. It is important, therefore, to understand how the characteristics depend on the choice of electrode reactions and on the design of the cell. It will also be clear that the various battery characteristics are not independent of each other and commonly a change of design to improve one will have an adverse effect on another.

11.1.1 Voltage

The terminal voltage of the battery will depend on the free-energy change in the overall cell reaction and, hence, the choice of electrode reactions, the kinetics of the electrode reactions and the cell resistance, i.e.:

$$E_{\text{CELL}} = E_{\text{e}}^{\text{C}} - E_{\text{e}}^{\text{A}} - |\eta_{\text{A}}| - |\eta_{\text{C}}| - iR_{\text{CELL}} \tag{11.1}$$

This equation has been used in other chapters but, in contrast to its application in electrolytic processes, the battery designers' concern is to make the voltage large and positive. Hence, the electrode reactions will be selected so that the active mass at the positive electrode reduces very easily and the active mass at the negative electrode oxidizes readily. Then, the free energy for the overall battery reaction will be large and negative and $E_{\text{e}}^{\text{C}} - E_{\text{e}}^{\text{A}}$ is a high positive quantity. Moreover, both electrode reactions should occur at the required rate without significant overpotentials and the cell should, as always, be designed to minimize

voltage drop, i.e. the electrodes should be closely spaced and the electrolyte should have a high conductivity.

Clearly, the voltage will decrease as the current drawn from the battery is increased, since η_A, η_C and the iR_{CELL} term will all increase with current density. The cell voltage, excluding the iR_{CELL} of a practical battery, can be estimated from i–E data for the anode and cathode processes (Fig. 11.3).

In principle, the polarization at each electrode may have a contribution from charge transfer, mass transport, nucleation and passivation overpotentials. The major contribution will normally be from the charge transfer overpotential since mass transport control has a catastrophic effect on the battery voltage (Fig. 11.3) and one would not normally design a battery to operate in such conditions. Examples of nucleation and passivation overpotentials do occur, the former when the electrode reaction requires the formation of a new phase, although the nucleation overpotential is normally a transitory phenomenon since, once nuclei of the new phase are present in numbers, the overpotential will disappear. The nucleation overpotential therefore occurs as a dip on the discharge curve at the commencement of discharge (Fig. 11.4); such a dip is seen in the discharge curve of Zn–HgO cells since the cathode reaction requires formation of mercury nuclei on the graphite powder current collector. Passivation can contribute a substantial overpotential as, for example, in the Mg–AgCl sea-water battery; this is a reserve battery stored dry and activated by addition of sea water. The magnesium anode does not take up the potential of the Mg/Mg^{2+} couple because it corrodes with the formation of a passive layer in the sea-water medium. The polarization due to the passive layer can exceed 1V, although this can be reduced by alloying the magnesium. Lithium anodes in aprotic medium, increasingly common because of their high theoretical energy density, also suffer

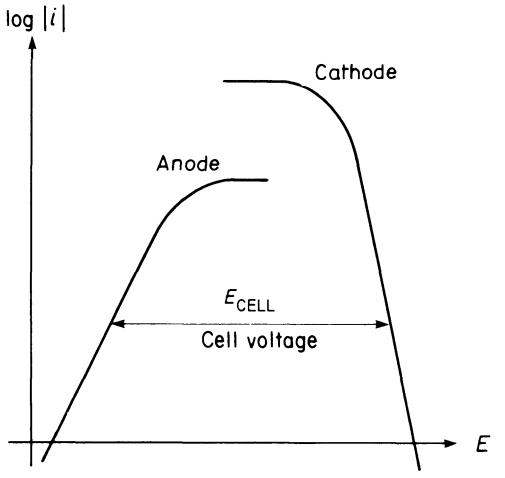

Fig. 11.3 Plot of $\log|i|$ vs. E (vs. a reference electrode) for the cathode and anode of a battery.

to some extent from passivation effects; in this case, however, the passivation overpotential generally decreases when the battery is operating.

Generally, a high cell potential is sought and this is favoured by: (1) the selection of electrode reactions which lead to an overall cell reaction with a high negative free-energy change; (2) electrode reactions without large overpotentials in the range of current to be drawn from the cell (i.e. the electrode reactions should be fast); and (3) designing the cell with a low resistance, i.e. with a high-conductivity electrolyte, low-resistance separator and small interelectrode gap.

11.1.2 Current

Current is a measure of the rate at which the battery is discharging. Current and voltage are, of course, always interlinked (Fig. 11.3) but the ability to deliver a high current without an excessive voltage penalty is dependent on rapid electron-transfer reactions and correct design of the active material to ensure a plentiful supply of electroactive species to the site where electron transfer is occurring. The active material generally behaves as a porous electrode but it should be noted that its composition and structure can change during discharge, e.g. PbO_2 to $PbSO_4$ during discharge of the lead–acid positive. This involves the conversion of an electronically conducting species to a very poor conductor and, hence, the current which can be drawn from the cell may depend on the state of charge and on the rate at which it has been discharged; both factors will determine the distribution of the $PbSO_4$ in the porous structure.

11.1.3 Capacity

The capacity is the charge that may be obtained from the battery; it is usually quoted in ampere hours and clearly depends on the size of the battery. The nominal capacity of each electrode may be calculated from the weight w of active material via Faraday's law, i.e.:

$$C = wnF/\mathrm{M} \tag{11.2}$$

where M is the molar mass of the active material. The capacity of the battery will be determined by the electrode of lowest capacity.

The practical capacity of each electrode and, hence, of the battery, will depend on how much of the active materials can actually be consumed during discharge and this must be determined by experiment. Certainly the capacity will depend on the discharge conditions (e.g. current) and commonly it is measured by monitoring voltage vs. time during a fixed current discharge (Fig. 11.4). The capacity is then it' where t' is the time at the fixed current i for the voltage to reach a value $E_{\mathrm{CELL}}^{\mathrm{min}}$ where the battery is no longer useful. The flatness of the discharge curve (i.e. the variation of the battery voltage during discharge) and the ability of the cell to continue to deliver the expected capacity at increased discharge rates, are important battery properties. The positive electrode of a lead–acid battery is

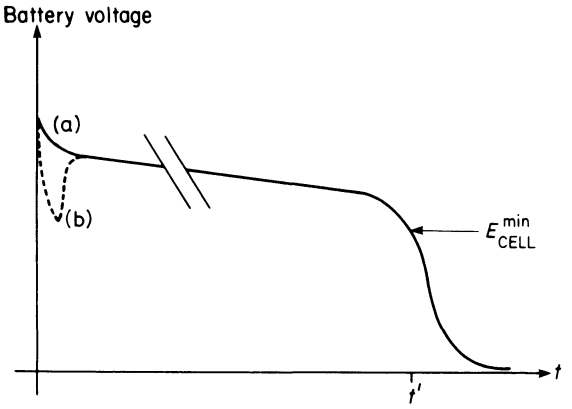

Fig. 11.4 Discharge curves at constant current i for (a) a simple battery and (b) a battery in which one electrode reaction has a nucleation overpotential. t' is the time for the battery voltage to reach a limiting value E_{CELL}^{min} where the cell is no longer useful. The capacity of the battery is then it'.

an example where the practical capacity is well below the theoretical value. The major cause is the formation of poorly conducting $PbSO_4$ in the discharge reaction which can form a barrier between the electroactive PbO_2 and the current collector and prevent continuation of the reduction.

11.1.4 Electricity storage density

This is a measure of the charge per unit weight stored in the battery, i.e. it is the capacity per unit weight. Hence, it is measured as in Fig. 11.4 but it applies to the whole battery and hence, the weight is that of the complete battery including electrolyte, current collectors, terminals, the case, etc.

Therefore, a high storage density depends on good battery design (minimizing the weight of all subsidiary elements) and also the correct selection of electrode reactions. The popularity in recent years of lithium anodes is due partly to the low weight of a mole of the metal; $1F$ of charge is obtained from the dissolution of only 7g of lithium. Of the other possible anode materials, only Al and Mg are comparable – the corresponding weights are 9 and 12 g respectively (cf. Pb 104 g).

For some applications, the battery volume is more important than its weight. Then the electricity storage density and, indeed, energy and power density (sections 11.1.5 and 11.1.6) are normally determined and quoted per unit volume rather than per unit weight.

11.1.5 Energy density

Energy density is the energy obtainable per unit weight of battery, (in, for example, kilowatt hours per kilogram) and is defined by:

$$\text{Energy density} = \frac{it' E_{CELL}^{ave}}{w} \tag{11.3}$$

Hence, it is measured by determining the capacity (Fig. 11.4) and noting the average potential during discharge and the total weight of the battery. It depends on the cell voltage (i.e. the choice of electrode reactions) and the factors which determine the storage density.

11.1.6 Power density

Some battery applications require defined capability to deliver power iE_{CELL} per unit weight of battery. This is the power density. The requirement may be for a continuous power density above a certain value or for a high value for a short period, i.e. pulse capability. The power density will decrease during discharge.

11.1.7 Discharge rate

The discharge rate is, as is current, a measure of the rate at which charge is drawn from the cell. It is normally quoted as the C/n or n-hour rate, which is the current to discharge the nominal capacity C of the battery in n hours.

11.1.8 Cycle life

Primary batteries are designed only for a single discharge but a secondary battery is expected to be capable of repetitive charge/discharge cycles. The cycle life is the number of charge/discharge cycles that are possible before failure occurs.

For a secondary battery, it is essential for the discharge/charge cycle to reform the active material in a suitable state for further discharge. The active material must have the correct chemical composition, morphology and distribution in the cell (with respect to current collectors). The cycle life will often depend strongly on the depth of each discharge, attempts to discharge totally the battery often being particularly damaging to the electrodes. The most common forms of failure include: (1) corrosion of the current collectors or contacts; (2) shedding of the active material from the plates; (3) shorting due to dendrites growing between the electrodes; or (4) changes in morphology. The battery may show a gradual decline of performance as it is cycled or the failure can occasionally be quite sudden.

11.1.9 Energy efficiency

With secondary batteries for energy storage on a large scale, the energy efficiency (in per cent) defined by:

$$\% \text{ Energy efficiency} = \frac{\text{energy released on discharge}}{\text{energy required for charge}} \times 100 \qquad (11.4)$$

will be important. This will depend on the current efficiency of the electrode processes and the overpotentials involved in both discharge and charge reactions

as well as the battery resistance. Again, it will depend on the rate of charge and discharge.

11.1.10 Behaviour on overcharge

With secondary batteries, it is not always possible to stop charging at exactly the correct moment. If the battery is overcharged, new electrode reactions must occur (e.g. electrolysis of water) and it is important that these reactions do not represent a hazard (e.g. the possibility of fires or explosion) or damage to the active material.

11.1.11 Shelf life

It is essential for most batteries to be stored, sometimes for many years, without self-discharge (i.e. reaction between the anode and cathode active materials or between either and the solvent or electrolyte) or corrosion of current collectors causing a significant loss of performance.

11.1.12 Tolerance to service conditions

The battery duty may require that it provides power continuously, intermittently or at an irregular rate. It may also be expected to perform its duty or be stored under a range of conditions, e.g. a car battery in the USA must operate between temperatures of from -30 to $+50\,^{\circ}C$ if it is to be successful in the extreme conditions of winter and summer. The battery may also have to be tolerant to various types of misuse, including occasional shorting, vibration and shock.

11.1.13 Reliability

This is the ability to perform to specification reproducibly and without failure. It will normally be expressed as a failure rate within a given period.

11.1.14 Economic factors

Two factors must be considered: (1) the cost of manufacture; and (2) the cost of servicing during the working life of the battery. Clearly, the components of the battery must be cheap enough for the final product to be competitive (although not all batteries need be cheap – it again depends on the application) and the raw materials must be available on the scale required. In duties which require long service lives, the extent and cost of maintaining the batteries in prime condition will, however, also be important in determining the choice of battery system.

11.2 BATTERY SPECIFICATIONS

It has already been noted that a battery is always manufactured for a specific duty. On the other hand, batteries are used to provide a wide variety of power

requirements and, prior to the design of a battery system, it is essential to write an accurate specification. In this section three examples will be discussed.

Table 11.2 shows a specification for a car traction battery. A battery to power a car will clearly require a substantial power and energy output and by necessity will contribute substantially to the weight and volume of the vehicle; hence, the emphasis is on energy and power density in order to minimize the weight and volume of the battery. Moreover, the capacity must be large to permit an acceptable range and, of course, the battery must be rechargeable. Moreover, unlike the duty of present car batteries, the battery is likely to be almost fully discharged on a regular basis to obtain the maximum range. Hence, the specification must call for a large number of charge/discharge cycles to deep discharge (this is much more difficult than cycling, say, to 50% discharge). Energy efficiency is also important since any value below 100% will represent a proportionate increase in running costs. The other specifications recognize the way in which a car is used – it must cruise at an acceptable speed, accelerate periodically and be driven intermittently with periods parked or garaged (a few minutes to several weeks) and be able to operate over a wide range of climatic conditions. It may also be involved in accidents, when it must present no additional hazards. In order to give confidence to the driver, a high reliability and a measurement of the state of charge of the battery will additionally be necessary. At the present time, no system can meet this specification, but the potential market is so large that such a battery remains a very active research

Table 11.2 A specification for a car traction battery

Voltage	90–400 V
Capacity	10–20 kA h
Size	0.1–0.5 m^3
Cycle life	> 600 deep discharge cycles
Energy density	> 50 Wh kg^{-1}
Power density	
constant	> 20 W kg^{-1}
for 20s period	> 100 W kg^{-1}
Energy efficiency	> 60%
Temperature	253–313 K
Vibration	> 5g*
Shock	> 30g*
Usage	Intermittent with uneven demand during use. Must store and withstand overcharge
Maintenance	Low
Reliability	Very high
Cost	Battery cost + power for charging equivalent to petrol cost over mileage during battery life. Say $600–1500
Market	Many millions per year

*Here g is the acceleration due to gravity.

goal. Possibilities include improved lead–acid, nickel–zinc, nickel–iron, sodium–sulphur, and aluminium–air (see section 10.6).

The requirements for a heart pacemaker power supply are quite different (Table 11.3). A primary cell will suffice and it need only have a power output of a few microwatts but this must be supplied continuously for several years without maintenance and with absolute reliability. It must also be compatible with the body and operate at 37.4° C. Lithium–iodine cells are presently used for this application.

The final specification (Table 11.4) is for an emergency power supply for a computer memory; this is again a relatively small battery and the prime need is a long shelf life and the ability to work promptly on demand. Possible batteries would include secondary Ni–Cd, sealed Pb–acid, a long-life primary cell such as HgO–Cd or certain lithium cells.

Table 11.3 Specification for heart pacemaker battery

Voltage	1–3 V
Capacity	0.5 A h
Size	Few cubic centimetres
Cycle life	Primary
Power density	1–5 mW kg^{-1}
Temperature	310 K
Usage	Almost constant demand for many years
Maintenance	None
Reliability	Extremely high
Cost	Relatively unimportant
Market	10^5 per year

Table 11.4 Specification for standby supply to volatile computer memories

Voltage	1–3 V
Capacity	0.1–0.5 A h
Size	Few cubic centimetres
Cycle life	Some advantage in ability to recharge; never deeply discharged
Power density	1–4 W kg^{-1}
Temperature	273–313 K
Usage	Long shelf life. Operational for a few milliseconds to hours at infrequent intervals (to cover mains failure or deliberate disconnection)
Maintenance	Low
Reliability	High
Cost	Relatively unimportant
Market	Few millions per year

11.3 EVALUATION OF BATTERY PERFORMANCE

It is important to evaluate the performance of a battery (i.e. to determine the characteristics described in section 11.1) in conditions which relate closely to those in which it will be used. Traditional methods would include measurement of capacity, energy density and power density and, for secondary batteries, the determination of cycle life and energy efficiency during:

1. *Discharge into fixed resistances.* This is the test which is least critical of the battery. It is necessary to monitor both voltage and current as a function of time.
2. *Discharge (and charge) at constant currents.* This permits simple and direct measurement of capacity, cycle life, etc.
3. *Discharge (and charge) at constant voltages.* This method gives the maximum power output directly and allows the determination of the capacity at fixed voltage.
4. *Discharge at constant wattages.* This most closely imitates the duty of many batteries to power instrumentation but it is the most difficult test to carry out; it requires complex electronic equipment. For this reason, it is often easier to test the battery with the instrumentation that it is designed to power.

Following developments in computers and electronic instrumentation, it is now possible to automate battery testing. Such evaluation facilities are also capable of much more complex test procedures. It is, for example, common to test using a variable current, voltage or wattage demand which seeks to imitate more closely the battery duty. Thus, car traction batteries are evaluated using a standard programme cycle defined by the US Department of Energy. It represents the demands on the battery during a typical day in urban driving conditions, i.e. start–stop driving at 30–50 m.p.h., regular acceleration, parking and recharge overnight.

A complete test programme must consider many other factors including:

1. The effect of ambient conditions – particularly temperature and pressure, both during duty and storage – on performance. The length of shelf life before use must also be varied.
2. The effect of mechanical shock, acceleration and perhaps radiation.
3. The dangers arising from various types of misuse including overcharge, shorting, spillage of the electrolyte and damage by fire.
4. The eventual recycle or disposal of cell components in the battery.

Table 11.5 shows a comparison of some primary and secondary batteries, the data being obtained for R20 size (50 cm^3) by constant current discharge at the 100-h rate, i.e. $C/100$ rate. It can be seen that, while there is a wide variation of performance, the primary cells do, in general, give higher capacities and energy densities. Moreover, they are much cheaper, by at least a factor of 10.

Table 11.5 Performance data for R20 size (50 cm^3) batteries during discharge at 100 h rate at 20° C

Battery	Average voltage/V	Capacity/A h	Weight/g	Energy density/Wh kg^{-1}
1. *Primary systems*:				
Zn–C	1.2	6	90	80
Mg–C	1.5	8	100	120
Alkaline MnO_2	1.2	10	120	100
Zn–HgO	1.2	12	170	85
Zn–air	1.3	22	85	340
Li–$SOCl_2$	3.4	12	100	410
Li–MnO_2	2.9	10	100	290
2. *Secondary systems*:				
Sintered plate Ni–Cd	1.25	4	150	33
Spiral wound Pb–acid	2.1	2.7	185	30
Zn–AgO	1.5	5	105	70

The Leclanché cell (Zn–C) has the advantage of cheapness, although it can be seen that other primaries have a considerable advantage in terms of performance, particularly the cells with a lithium anode or an air cathode, and the reasons for this can readily be understood. It was noted above that the performance depends on the mode of discharge. As an example, it may be noted that the Zn–C battery gives higher performance on intermittent discharge; the capacity increases to about 10 A h.

11.4 BATTERY COMPONENTS

11.4.1 The container

The battery case must be resistant to corrosion from both inside and outside and, hence, must be stable to chemical attack by the electrolyte, active materials and the environment at the operating temperature. In addition, it must have the required mechanical strength, be cheap and light and have a simple method of sealing.

For alkaline batteries, the case is generally steel, while for systems with an acid electrolyte, polypropylene is rapidly replacing materials such as hard rubber. For a few batteries, the case also acts as one of the active materials, e.g. the zinc can in a Leclanché cell.

11.4.2 Separators

Again, the separator must be stable chemically to the electrolyte and to the active materials at the temperature of operation. It is also necessary for the membrane

to have the correct qualities of wetability, selectivity, resistivity and flexibility for the particular battery system. The cost is very variable: in lead–acid batteries the target would be a few pence per square metre while for some Ni–Cd batteries, £1 per square metre may be acceptable.

In practice, a wide range of materials are used as battery separators. Even with one system, different materials may be used for batteries designed for different discharge rates or, indeed, manufactured by different companies. An example of the former is the Ni–Cd battery; for high-discharge-rate pocket-plate cells the separator is generally only a series of thin plastic pins, while for sintered plate cells it will be one to three layers of nylon or cellulose-based felt reinforced for vented cells by a membrane (to act as an oxygen barrier). The most common materials are microporous (pore size 0.01–10 μm) or macroporous (30–70 μm pores) polymer sheets a fraction of millimetre thick; these generally have a porosity of 50–80% and a resistance of 0.05–0.5 ohm cm^2. An example is the microporous polyethylene material normally used for lead–acid car starter batteries. With more expensive systems, ion exchange membranes are considered. The sodium-β-alumina developed for the sodium–sulphur battery and the Nafion membrane in redox batteries are examples.

11.4.3 Current collectors

In order for the battery to have an acceptable capacity, the active material is almost always a thick layer of a porous, particulate paste and the electronic conductivity of this material is seldom very high. Hence, it is necessary to have a current collector, which is usually a metal grid or sheet, to provide a conducting path through the paste and thereby minimize the resistance of the battery. The current collector also acts as a physical support for the active mass which otherwise would be a very brittle structure.

In early batteries, the current collector was generally a plate or a closely spaced grid. These, however, contributed susbstantially to the total battery weight and have proved to be not always essential; hence, the current collector is now designed to minimize weight, e.g. by using very thin metal sheet or expanded metal without loss of performance . The optimum grid sometimes contains little metal. In the lead–acid negative, the paste always contains sufficient lead to make a current collector superfluous and the modern design is more of a contact to the external circuit. In contrast, the positive electrode paste is poorly conducting and a close grid is essential. In some pastes (e.g. the Leclanché electrolyte) a carbon powder is added to improve conductivity to the central carbon rod current collector.

Clearly, the current collector must be stable to chemical attack by both electrolyte and active material and this limits the choice of material, e.g. lead is the only widely used material in a lead–acid battery. Corrosion of the collector and shedding of the active paste are the two major causes of battery failure.

11.4.4 Electrolyte

The selection of the electrolyte is determined by the electrode reactions and its concentration is also important. This will control the plate potentials, the electrolyte resistance and viscosity and, by its effect on the rate of diffusion, the differences in concentrations of species between the inside and the outside of the pores of the active paste.

Temperature has a great effect on electrolyte properties and both viscosity and resistance increase by more than an order of magnitude as the temperature drops from ambient to $-30°$ C. This largely accounts for the poorer performance of the battery at lower temperatures.

The weight of the electrolyte is a major contribution to that of the complete battery and, hence, must be minimized. In any case, the electrode spacings should be small to minimize battery resistance.

11.4.5 Active materials

For a battery with a reasonable discharge rate and capacity, the electroactive species must be readily available at the sites of electron transfer and be present in large quantities. In most batteries these requirements are met using solid reactants and, at least in secondary batteries, the product of the electrode process is also a solid; the anion of the electrolyte and sometimes the proton are also participants in the chemical change during the charge or discharge process. Hence, if the change is to be accomplished at a reasonable rate, intimate contact and a high-area surface between the solid reactants and the electrolyte are essential. This is accomplished by using the electroactive materials in the form of a paste on the current collector.

Such structures are known as porous electrodes and they behave quite differently from the effectively planar electrodes used in most other areas of applied electrochemistry. The porous electrode is a mass of particulate reactants (sometimes with additives) with many random and tortuous electrolyte channels between. Real porous electrodes cannot be modelled but their behaviour can be understood qualitatively using a simplified model shown in Fig. 11.5; in fact, there are two distinct situations which arise. In the first (Fig. 11.5(a)) the electroactive species is a good electronic conductor (e.g. a metal or lead dioxide); here, the electrode reaction will occur initially on the face of the porous electrode in contact with the electrolyte but at the same time, and probably contributing more to the total current, the reaction will occur inside the pore; not, however, along the whole depth of the pore because of the iR drop in solution. The potential and current distribution will depend on both the kinetics of electron transfer and the resistance of the electrolyte phase. A quantitative treatment of the straight, circular pore approximation allows a calculation of the penetration depth (the distance down the pore where reaction occurs to a significant extent) and it is found to increase linearly with electrolyte conductivity and the radius of

the pore but to be inversely proportional to the exchange current density. It should also be noted that the active mass material and its structure change during discharge (and, of course, charge). For example, in the lead–acid negative electrode, the lead is oxidized to lead sulphate and this change causes an increase in volume of the active mass and the interconversion of a good electronic conductor to a bad one. Since this change will occur at the highest rate, initially at the pore–electrolyte interface, a consequence is pore blocking and a loss of capacity compared with that calculated from the weight of active material. In pore blocking, the non-conducting material seals the head of the pore, preventing contact between the electrolyte and active material down the pore. Insufficient transport of ions throughout the porous layer can also lead to unexpected pH gradients, e.g. although the lead–acid positive electrode operates in strong sulphuric acid, the pH at the lead/lead dioxide interface can became as high as 9.

A different situation can arise during recharge (Fig. 11.5(b)). Here, the active mass in the discharged state would largely be poorly conducting material, e.g. lead sulphate in the lead–acid positive electrode. Now the electrolyte is more conducting than the solid structure and it is perhaps more helpful to discuss a 'porous electrolyte'. The behaviour of such electrodes should be quite different. Certainly, the oxidation of lead sulphate to lead dioxide must occur first at the current collector–paste interface and the reaction zone will move out through the paste towards the electrolyte. This is in sharp contrast to the case where the porous paste is conducting; then the reaction occurs initially at the electrolyte side and the reaction zone will tend to move through the paste towards the current collector.

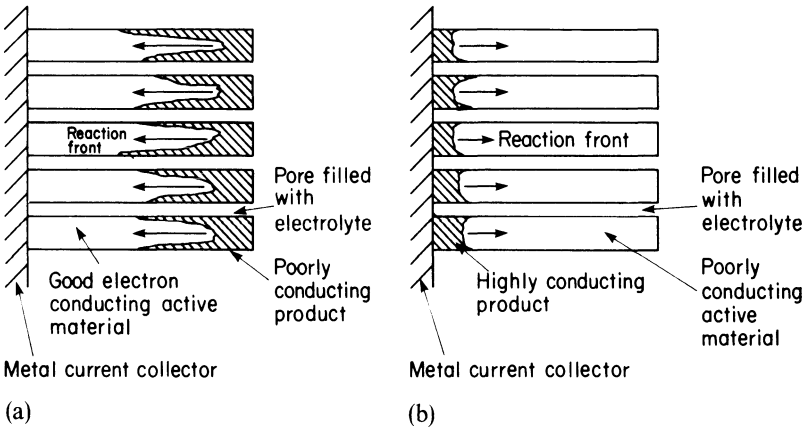

Fig. 11.5 Simple models for a porous electrode in a battery. (a) Active material highly conducting, e.g. a metal or PbO_2. (b) Active material poorly conducting, e.g. $PbSO_4$.

Table 11.6 Effect of paste loading on performance

Battery	Capacity/A h		
	Discharge time	10 h rate	30 h rate
13 plates 4.8 mm thick		40	152
26 plates 2.4 mm thick		67	182

The electroactive species at the negative electrode is generally a metal. For secondary batteries, the porous-metal electrode is usually prepared by electrochemical reduction of a paste containing the metal ion, e.g. PbO–$PbSO_4$ for the lead–acid and ZnO–Zn–KOH for the zinc electrode. The preparation is carried out *in situ* in the battery in a process known as 'forming' because the high-area metal would not be stable to oxidation by air. With many primary batteries the negative electrode can be a plate which develops porosity during discharge. The positive electrode paste can also be formed *in situ* (e.g. PbO_2 from PbO–$PbSO_4$, NiO(OH) from $Ni(OH_2)$) or prepared by chemical oxidation (e.g. CuO from Cu) or precipitation methods, e.g. AgO by addition of KOH to $AgNO_3$.

In secondary batteries, metal electrodes are not area-stable. During cycling, an undesirable decrease in surface area occurs (i.e. ball-up) and additives known as 'expanders' are added to avoid this. For example, lignin sulphates and barium sulphate are added to the lead–acid negative. While their mode of action is not fully understood, it may be significant that $BaSO_4$ is isomorphous with $PbSO_4$ and therefore able to act as nuclei for $PbSO_4$ formation during lead oxidation. On the other hand, positive electrodes are normally area-stable and additives are not necessary.

Clearly, the sizes of the particles and the pores (i.e. the porosity of the paste) are important in determining the performance of the battery. In practice, porosity should be about 50%. Below this value, the utilization of the active material suffers due to pore-blocking, and above it the mechanical stability becomes a problem. Hence, there is a trade-off between capacity and cycle life.

The loading of the paste and the thickness of the porous layer, also affect performance (Table 11.6). Thin plates improve capacity, particularly at high discharge rates and also give a higher power density.

11.5 PRESENT BATTERY SYSTEMS

11.5.1 Lead–acid batteries

While all are based on the same electrochemistry, the PbO_2–$PbSO_4$ positive electrode and the Pb–$PbSO_4$ negative electrode in aqueous H_2SO_4 (Table 11.1) a number of technologically quite different Pb–acid batteries are manufactured

to obtain the various performances demanded by the many applications. Some of the more important types will be described here.

The most important market remains the car battery for starting, lighting and ignition with approximately 50×10^6 units per year being sold in the USA. Lead–acid batteries are, however, also used on a very large scale for traction (e.g. delivery vans, milk floats, forklift trucks, industrial trucks; there are more than 100 000 such vehicles in the UK) and for stationary back-up or emergency power supplies. More recently, small lead–acid cells to compete with high-quality primary and nickel–cadmium cells for instruments, radios, etc. have also become available.

(*a*) *Car batteries*

A starting, lighting and ignition battery will be a 6 or 12 V (three or six cells in-series) battery with the following characteristics: (1) a capacity of 100 A h at the 20-h rate; (2) a high-pulse capability to permit engine starting, typically 400–450A for 30s without the voltage dropping below 7.2 V; (3) the ability to provide a lower current for an extended period (e.g. 25 A for 3 h without the voltage dropping below 10.5 V; and (4) multiple charge/discharge cycles, although not necessarily to deep discharge.

Invariably, starting, lighting and ignition car batteries are designed for each cell to have parallel pasted electrodes and a separator, and Fig. 11.6 shows a cutaway diagram of a typical battery. Conventionally, the current collectors are die-cast grids, say 10×15 cm, made from an alloy of lead usually Pb–5% Sb. The alloying element is present to improve the die casting and mechanical properties of the metal. More recently, it has been found possible to reduce the weight of lead in the current collectors by using expanded metal. Moreover, with the negative electrode, the active mass always contains lead powder and is therefore relatively conducting. Hence, it is found possible to use grids with greatly reduced amounts of lead. Such changes in grid design are not possible with the positive electrode because the paste has a lower conductivity and shedding the active mass is also a common difficulty.

The electroactive pastes are prepared from pure lead. Lead ingots are air-oxidized under controlled conditions to give a powder mixture of lead oxide and lead (approximately 50 : 50). To the paste to be used for the negative electrode are added various additives, most commonly carbon powder ($\simeq 0.25\%$), lignin sulphonates ($\simeq 0.2\%$) and barium sulphate ($\simeq 0.35\%$). The carbon improves the conductivity of the final plate while the latter compounds prevent the reduction in surface area of the lead and other changes in morphology of the plate, i.e. they are expanders. Usually, no additives are used in the positive electrode paste. The positive and negative pastes are then made by addition of aqueous sulphuric acid, and spread uniformly on the grids (the thickness of the final electrodes will be 0.1–0.5 cm). At this stage, the electrodes are allowed to dry and stand for several days in air and the oxidation of the lead in the paste goes to completion. At this stage both electrodes are fully discharged. The pastes contain

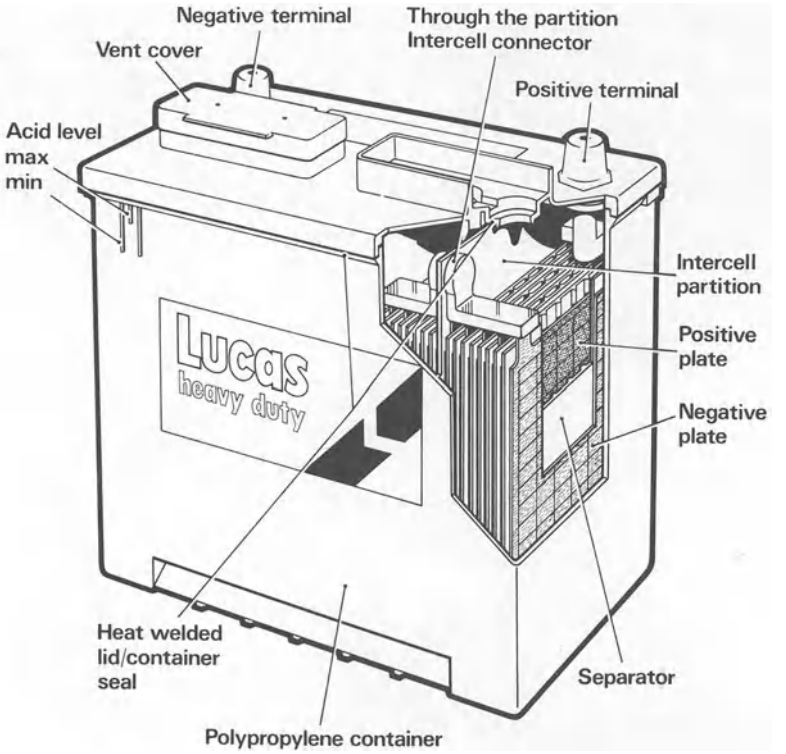

Fig. 11.6 A cutaway drawing of a starting, lighting and ignition lead–acid battery. (Courtesy: Lucas Batteries Ltd.)

a mixture of PbO and $PbSO_4$ while the negative electrode paste also contains the additives. The pasted grids and separators – usually microporous polyethylene or resin-impregnated paper – are placed in the battery container and the intercell connectors and terminals are welded into place. The battery is filled with sulphuric acid and sealed before the electrodes are charged slowly, e.g. at constant current at the 20 h rate.

The design of lead–acid batteries develops continuously. The major changes in the last 20 years have been to reduce the weight of the grids, to change the case from hard rubber to the lighter polypropylene and to improve slightly the use of active material, reducing that necessary in the battery. These combined have improved the energy density from 24 to 32 $Wh\,kg^{-1}$ without loss in other performance. More recently, the trend has been towards totally maintenance-free sealed batteries and this requires protection against overcharge; on overcharge, water electrolysis will occur and oxygen and hydrogen will be formed. This increases the pressure inside the battery and the mixture of gases presents an explosion hazard. The approach is to build a catalyst for the recombination of hydrogen and oxygen into the cell.

The performance of SLI (starting, lighting and ignition) batteries has been characterized extensively and data are available in several of the texts mentioned at the end of this chapter, e.g. the capacity–discharge rate characteristics will be known as a function of temperature, plate thickness, type of separator and

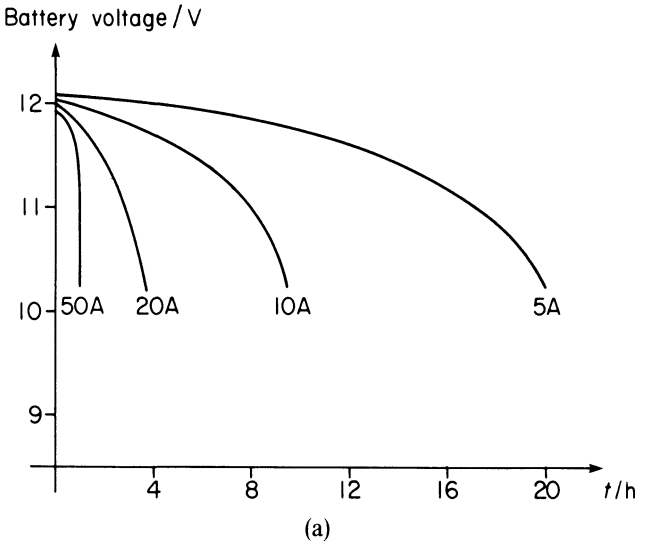

(a)

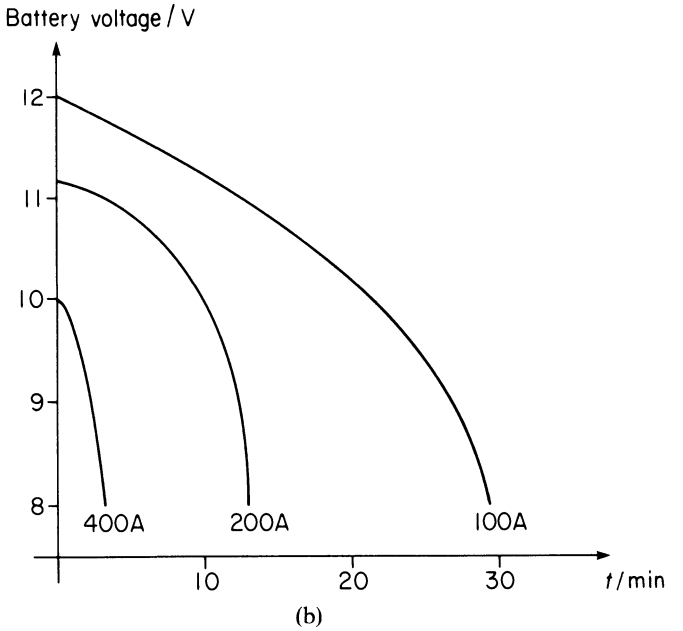

(b)

Fig. 11.7 Constant-current discharge curves for a 12 V, 100 A h starting, lighting and ignition lead–acid battery at 25° C.

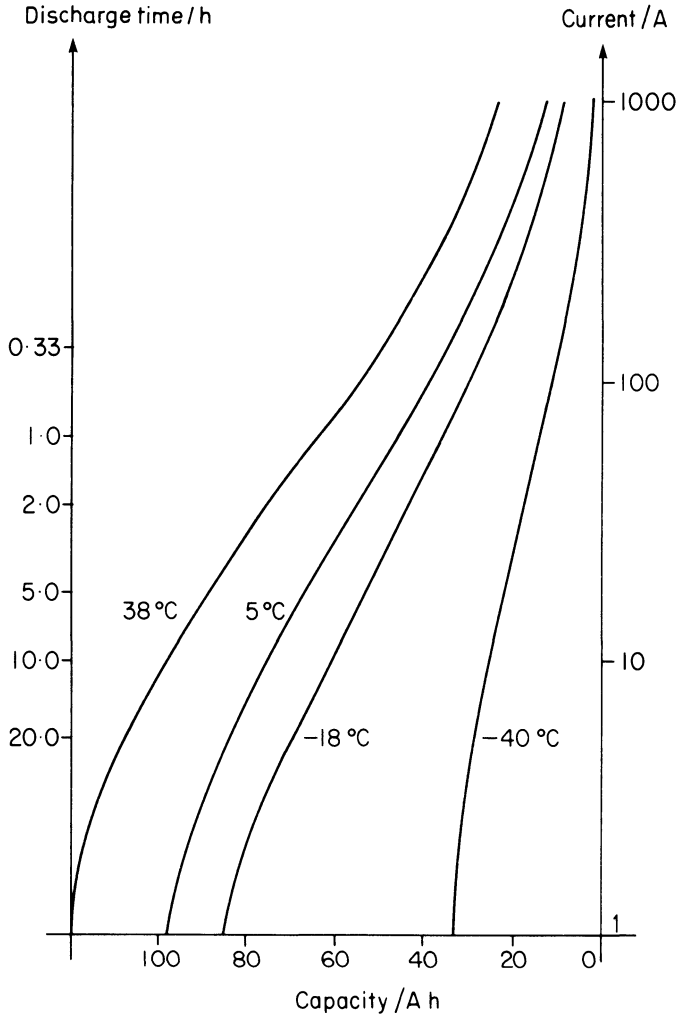

Fig. 11.8 The dependence of the capacity on the discharge rate for a 100 A h starting, lighting and ignition battery.

sulphuric acid concentration as will the variation of voltage and power as a function of current at various stages of charge. Figures 11.7–11.9 show some typical data.

(*b*) *Traction and industrial power supplies*

These batteries differ from the starting, lighting and ignition type in that they often have a larger voltage (48–96 V) and a higher capacity, obtained by using larger and thicker electrodes. They are also required to cycle to a much higher percentage of total discharge. The grids, therefore, must be more robust and care must be taken that the active material remains available and is not shed during

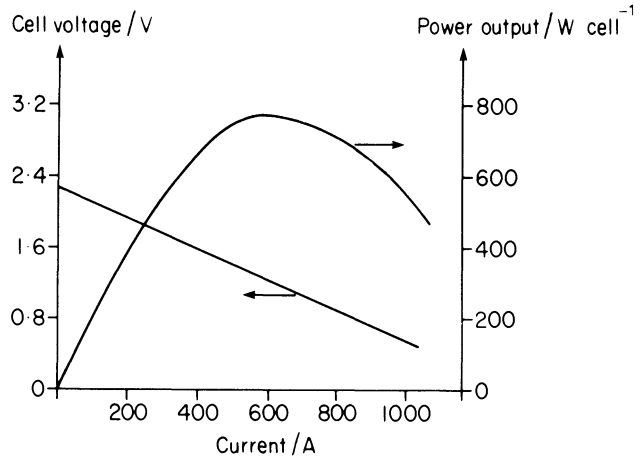

Fig. 11.9 Cell voltage and power output as functions of current for a starting, lighting and ignition lead–acid battery.

repeated cycling. The complete discharge of the electrodes may result in a volume increase of over 50% and this clearly presents a potential problem. In practice, shedding is a greater problem at the positive electrode and in this class of lead–acid battery, it is normal to protect this electrode physically in some way.

Traction batteries are constructed with both the flat plate and the tubular positive plate design. The former are very similar to the starting, lighting and ignition design except that they may be larger and constructed more robustly; the major addition is a second separator – a thick matted glass-wool felt is placed against the positive plate to support the active material. The design of a tubular positive plate is shown in Fig. 11.10. Each plate consists of fifteen to twenty-three tubes, diameter 8 mm, originally made from perforated indiarubber but now from woven glass wool or a plastic. An example of the latter is the Chloride gauntlet type which is manufactured by stitching at intervals two layers of woven or non-woven, felt Terylene cloth; tubular mandrels are placed in each 'tube' and the cloth is then impregnated with a thermosetting resin to give it rigidity. The current collector is a Pb–Sb rod placed at the centre of each tube and the tubes are filled with positive paste. This is generally done by packing with dry oxide and then standing the plate in H_2SO_4. The negative plate is pasted, as the starting, lighting and ignition battery, and the conventional separator is also present. The advantage of these tubular anode cells is that shedding of the positive active material is not possible and, hence, the cycle life is likely to be improved.

Energy densities for these larger batteries normally lie in the 20–30 Wh kg^{-1} range although the contractors in the US Department of Energy car traction battery programme now claim values of 37–42 Wh kg^{-1} for test Pb–acid units.



Fig. 11.10 A cutaway of a lead–acid motive-power cell showing a Gauntlet-type non-woven Terylene tubular-plate positive electrodes (cf. Fig. 11.6). (Courtesy: Chloride Technical Ltd.)

(*c*) *Stationary and standby power supplies*

Lead–acid batteries are used for many diverse remote and standby duties and, hence, are manufactured with a wide range of voltage and current capabilities and capacities. Lead–acid batteries do self-discharge slowly because of some reaction between the active materials and water; as a result they are often left on constant trickle charge.

Flat-plate and tubular-positive plate cells are produced for stationary duty, but where reliability is a prime consideration, Planté cells are used. In a Planté cell, the positive electrodes are manufactured by a quite different process. The oxide is formed by electrochemical oxidation (say, 10 mA cm^{-2} for 20 h) of a lead baseplate or grid, often shaped to increase its surface area, in an electrolyte which contains sulphuric acid and an anion (perchlorate or nitrate) which forms a

soluble Pb^{2+} salt. This leads to a layer of thick porous oxide; the nitrate or perchlorate is present to prevent total passivation of the lead surface. The resulting plate (thickness 6–12 mm) is then reduced to form spongy lead metal, is washed thoroughly, and is recharged when in a fabricated cell. The active material formed in this way adheres to the base lead better than pasted materials and therefore cycles more reliably. Against this, there is less active material on each plate and, inevitably, the energy density of the battery will suffer; 7–12 Wh kg^{-1} is typical.

(d) Sealed cells without free electrolyte

Cells with the electrolyte gelled by the addition of sodium silicate or sulphuric acid absorbed into a felted glass-fibre mat or thick paper have been manufactured for many years; such cells avoided the hazards of acid spillage and were sold mainly for aircraft or motor cycles. Now, cylindrical lead–acid cells, typical capacity 2 A h and without free electrolyte, are produced to compete with small Ni–Cd and primary cells for the consumer market. These cells are spirally wound (as a Swiss roll) with electrodes of thin, pure lead sheet perforated to increase the amount of pasted active material adhering to the metal and an adsorbent glass-fibre paper separator, packed into a metal can.

11.5.2 Nickel–cadmium batteries

The basic electrochemistry of the Ni–Cd battery was given in Table 11.1; once again, however, the equations are misleading in that the reactions are not nearly as simple as indicated particularly at the positive electrode. In the nickel oxide paste, the oxidation state of the oxidized nickel species is uncertain and varies between +2 and +4; both the oxidized and reduced species exist in several crystal modifications and the important roles of water and potassium ions are not included in the table.

Nickel–cadmium batteries are manufactured in very large numbers in two basic types; (1) pocket-plate cells; and (2) sintered-plate cells. Pocket-plate designs are known for their reliability and very long shelf life (>20 yr) without any significant maintenance; hence, they are ideal for emergency power supplies and are also used for train lighting, switchgear and engine starting. Where there is direct overlap in applications with Pb–acid batteries, the Ni–Cd alternative often gives better performance but is also more expensive. Sintered-plate cells give higher discharge rates and are capable of good performance at low temperatures; they are particularly attractive for many military applications.

(a) Pocket-plate batteries

The active material for the positive electrode typically contains nickel hydroxide (80%), cobalt hydroxide (2%), graphite (18%) and maybe a trace of a barium compound. The graphite is present in two forms (powder and flake) to improve conductivity; the cobalt and barium compounds increase the percentage usage of

the active material during discharge and also increase the cycle life. The nickel hydroxide is prepared by precipitation with sodium hydroxide from aqueous nickel sulphate. The precipitate is filtered, dried, rewashed to ensure complete removal of Na^+ and SO_4^{2-} ions and finally redried. The active material for the negative electrode is cadmium hydroxide (78%), iron (18%), nickel (1%) and graphite (1%) and is prepared by dry-mixing; the iron, nickel and graphite are present to reduce ball-up, i.e. changes in morphology leading to loss in active surface area of cadmium.

The electrodes are made from perforated, nickel-plated steel strip and the active material in the form of long briquettes. The process is illustrated in Fig. 11.11, the final stage being to compress the structure into a thin plate. The size of the final plate is determined by the number of strips interlocked together. Figure 11.12 shows the complete design of the battery, the electrodes being alternately positive and negative plates and the plates being kept apart by thin insulating rods. All the metal components are nickel-plated and this cell is assembled in a plastic or steel case. The batteries are completed by filling with the electrolyte, 6 mol dm^{-3} KOH, and then charging.

Pocket-plate batteries are manufactured with capacities between 10 and 1200 A h. Their chief advantages are: (1) the ability to retain charge during long periods of storage; (2) to deliver all their rated charge; and (3) to maintain a steady voltage over a wide range of discharge rates and temperatures. In addition they have long cycle lives. The energy density is, however, only moderate and lies in the range 15–25 Wh kg^{-1}.

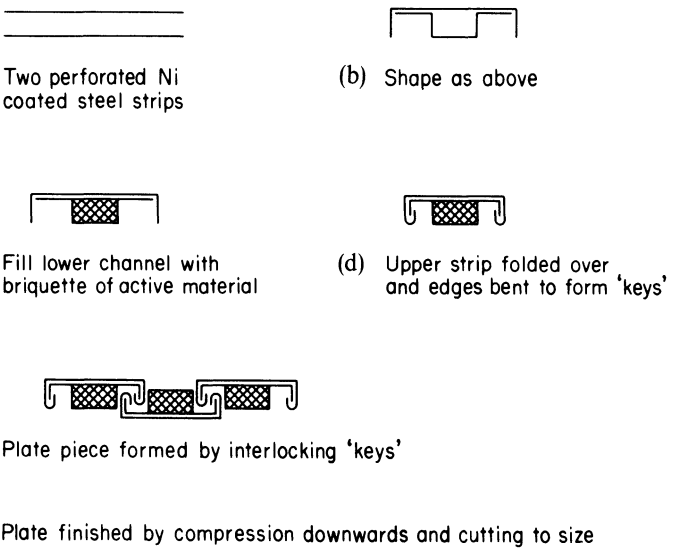

Fig. 11.11 Procedure for the manufacture of pocket-plate electrodes for a nickel–cadmium battery.

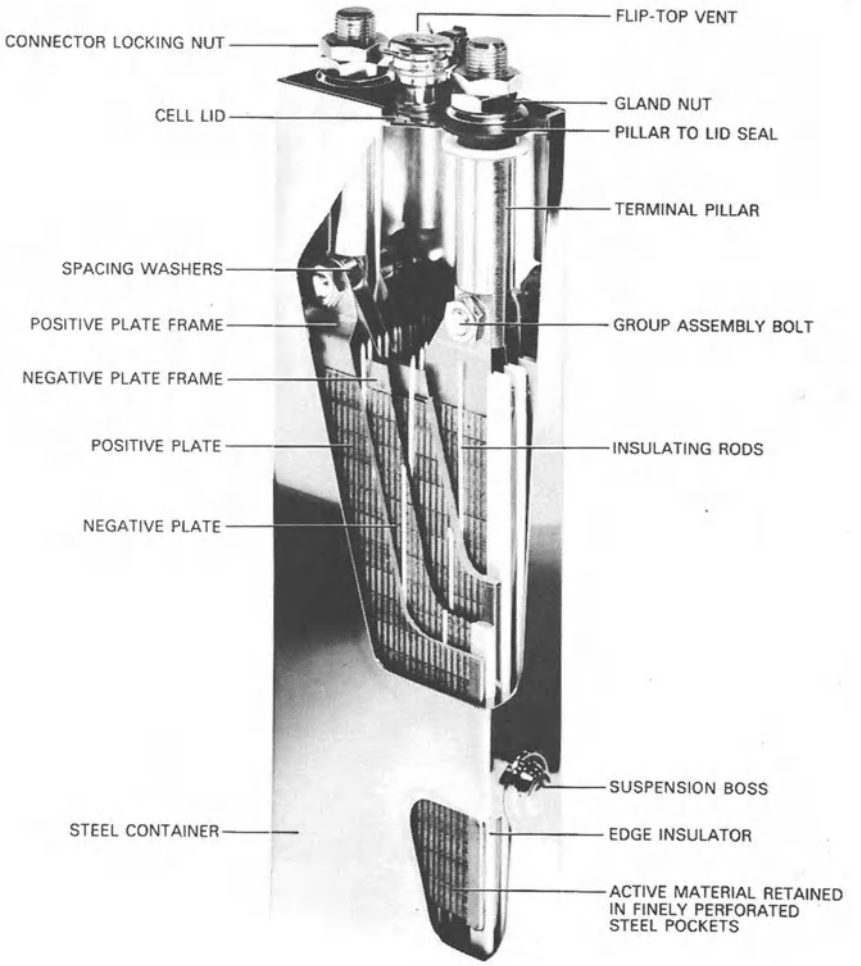

Fig. 11.12 A cutaway of a nickel–cadmium pocket-plate battery. The battery shown has a nominal capacity of 100 A h. (Courtesy: Chloride Alcad Ltd.)

(*b*) *Sintered-plate batteries*

In these cells, the electrodes are manufactured from sintered metal, thickness 0.5–1 mm, and with a high porosity (80–85%) and surface area of 0.25–0.50 $m^2 g^{-1}$. The active material is impregnated into the sintered metal in a series of steps. The sintered metal is first dipped into a solution of the nickel or cadmium ions (usually present as nitrates) and a vacuum is used to draw the

solution into all the pores. Then the sintered metal containing the solution is treated (chemically, thermally or electrochemically) to cause the ions to precipitate, nickel as the hydroxide and cadmium as a mixture of metal, oxide and/or hydroxide. The cycle is completed by washing and drying and then the complete procedure is repeated three to ten times to obtain a high loading of active material. The solution for the positive electrode sometimes contains cobalt ($< 10\%$) to help maintain capacity when the battery is cycled. The electrodes are generally charged after the cell is assembled.

In vented cells, the sintered metal is cut to the final plate size and, after conduction tabs are welded, the cell is put together in a similar way to the pocket plate cells except that the separator is a thin sheet of low-resistance, small-pore plastic often with a second layer to prevent oxygen transport. These membranes may be cellophane and a non-woven polyamide respectively.

Sealed cells are made in three different designs where the sintered electrodes are vertical rectangular plates, horizontal discs (button cells) and spirally wound, cylindrical cells. In the sealed cells, the problem of oxygen evolution during overcharge is overcome by using an excess of active material at the negative electrode and a separator which allows transport of any oxygen formed at the

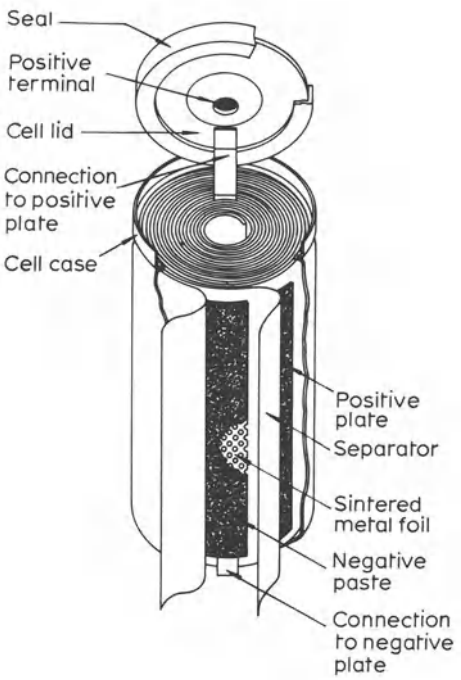

Fig. 11.13 The construction of a cylindrical nickel–cadmium battery. (Courtesy: Berec Ltd.)

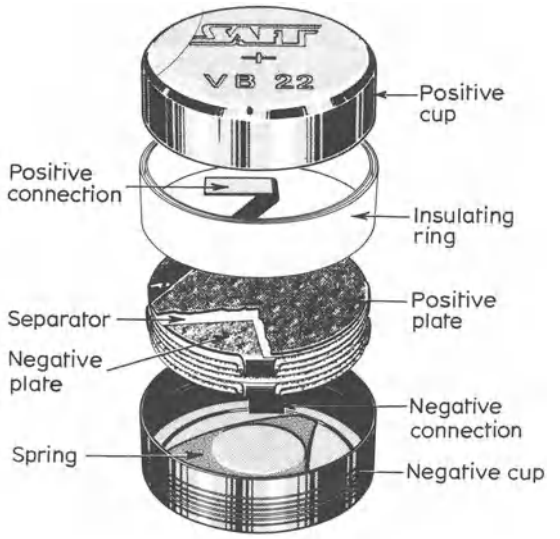

Fig. 11.14 The construction of a nickel–cadmium sintered-plate button cell. (Courtesy: SAFT Ltd.)

positive electrode (by oxidation of water) to the negative electrode. At the negative plate it reacts chemically with cadmium metal:

$$2Cd + O_2 + 2H_2O \longrightarrow 2Cd(OH)_2 \qquad (11.5)$$

and this forms further material for the charging reaction. Hence, the negative electrode never becomes fully charged. Suitable separator material can be non-woven polyamide or polypropylene.

Cells with rectangular electrodes are very similar to the battery in Fig. 11.12 except that the pins are replaced by a thin membrane, thus reducing the interplate gap and aiding the rapid discharge of the cell. Figures 11.13 and 11.14 show the designs of a spirally wound cylindrical cell and a button cell.

Sintered-plate cells are also made in a variety of sizes, i.e. rectangular plates 1–1000 A h, cylindrical cells 0.1–10 A h and button cells 0.04–1.75 A h. The energy density of sintered plate cells is considerably better than their pocket-plate counterparts because the electrodes are closer together, and with the high porosity of the plates there is also more active material per unit volume; with a 100 A h cell, an energy density of over 50 Wh kg^{-1} has been achieved. The major advantage is, however, that a high capacity may be obtained at high currents; even at the 10 *C* rate (1000 A from a 100 A h cell) 75% of the rated capacity can be obtained. Moreover, the sintered-plate design has the ability to remain charged (70% after 6 months) and has good cycle characteristics; 1000–2000 cycles to 50% discharge is a reasonable expectation.

11.5.3 Leclanché cells

Unlike the Pb–acid and the Ni–Cd systems, Leclanché batteries cannot be recharged effectively and, hence, are primary cells. Even so, Leclanché cells are produced in many shapes and sizes (Fig. 11.2) and the total world production probably exceeds 10^{10} per year; they are truly the workhorses amongst consumer batteries. Their replacement by higher-performance or secondary batteries has frequently been predicted but the market has always held up because of their comparative cheapness, e.g. a Leclanché cell is typically a twentieth of the cost of a Pb–acid battery or a fiftieth of that for a Ni–Cd battery to provide the equivalent power supply. Much of this cost difference lies in the materials of construction, but the battery also benefits from the scale of manufacture since Leclanché cells are produced by fully automatic processes.

Despite the long history of manufacture (the dry Leclanché cell dates from the 1880s) its detailed electrochemistry is again far from understood. Indeed, the open-circuit potential measured for the completed cell is frequently higher than that estimated on the basis of the reactions in Table 11.1 or the more complex:

$$2MnO_2 + 2NH_4Cl + Zn \longrightarrow 2MnO(OH) + Zn(NH_3)_2Cl_2 \qquad (11.6)$$

and, hence, it is clear that they do not faithfully represent the reaction which occurs. Moreover, the current–voltage characteristics depend on the source of the MnO_2 and more directly the exact oxidation state of the manganese, the

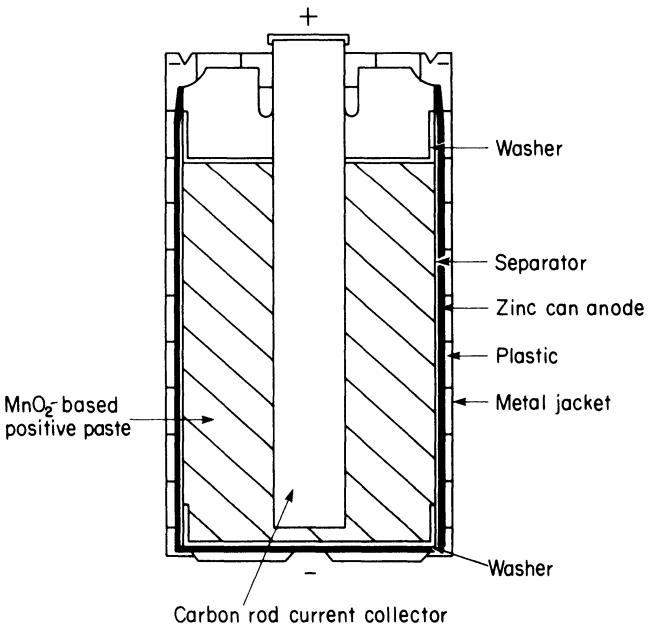

Fig. 11.15 The construction of a cylindrical Leclanché battery.

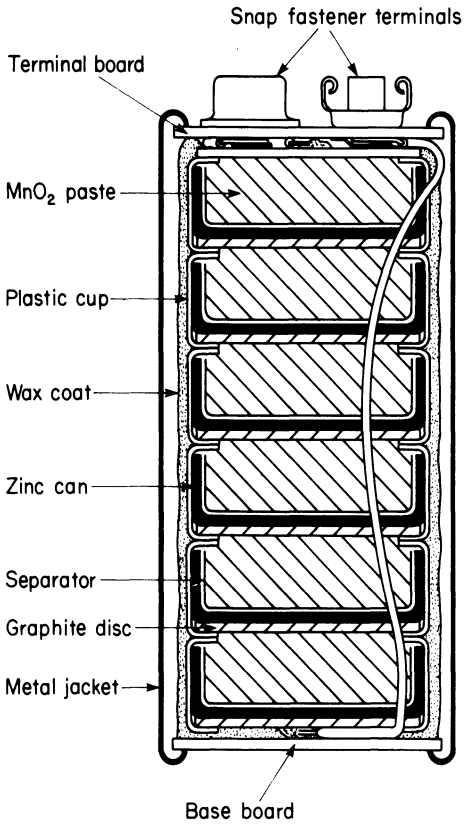

Fig. 11.16 The construction of a flat-cell Leclanché battery.

density of the lattice imperfections, the crystallite size and the extent of hydration.

Figures 11.15 and 11.16 illustrate two designs of Leclanché battery. The first shows the traditional cylindrical design. The negative zinc electrode is a zinc lining to the metal can which is amalgamated with mercury to minimize hydrogen gas formation by reaction of the metal with water; the separator is a paper stiffened with cellulose or starch placed adjacent to the zinc can. The positive current collector is a carbon rod at the centre of the can, while most of the volume is taken up by the positive paste. This is a mixture of powdered manganese dioxide, ammonium chloride and acetylene black (carbon) to increase the conductivity; the pores are filled with an aqueous electrolyte ($NH_4Cl + ZnCl_2$) gelled by addition of starch. The can is totally sealed.

The second battery (Fig. 11.16) is a series of six cells with bipolar (or duplex) electrodes. Each cell has the same components as the first cell, i.e. zinc can, separator, positive paste and carbon current collector. The latter is not a carbon rod but the bottom face of the duplex electrode. The whole set of cells is sealed in

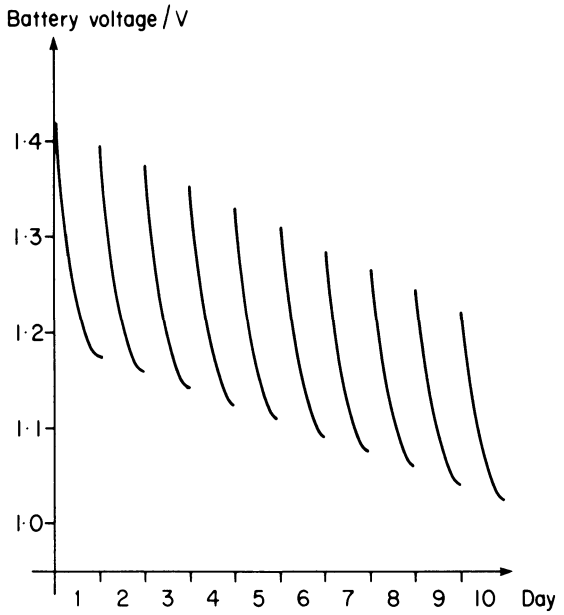

Fig. 11.17 Discharge characteristics for a commercial Leclanché battery. The battery was discharged into a 5 Ω resistance for 1 h each day.

wax. In both cells, the zinc electrode rapidly develops porosity as the corrosion process occurs while the performance is largely determined by the quality of manganese dioxide. Cells constructed from electrolytic manganese dioxide have a significantly better performance than those which use MnO_2 from natural ores or prepared chemically. Electrolytic MnO_2 is, however, more expensive.

Leclanché cells are produced with nominal capacities ranging from 0.05 to 500 A h, consumer batteries usually falling in the more restricted range of 1–10 A h. The practical capacity depends very much on the discharge regime. On constant discharge at high currents (0.1–1.0 A) only perhaps 25% of the rated capacity is obtained. On the other hand, when used only for a few hours a day, almost all the capacity is obtained with a current of 1–150 mA cm^{-2} and these conditions correspond more closely to the normal applications of the battery. On drawing current, the cell voltage always drops with time and, although it recovers on standing at open circuit (Fig. 11.17), the absence of a stable voltage is a disadvantage. It may also be noted that the energy density (70 Wh kg^{-1}) is high compared with that for the secondary systems.

11.5.4 Lithium batteries

For the last quarter century, almost every battery company in the world has conducted an R and D programme targeted to the development of batteries with a lithium negative electrode. This very high level of activity resulted from the

dual recognition that all the traditional batteries fall well short of their theoretically attainable performance and that a lithium negative electrode could have a unique combination of properties.

Amongst the important advantages envisaged for a lithium electrode were: (1) the formal potential of the Li/Li^+ couple is very negative and, hence, in combination with suitable positive electrodes, batteries with an unusually high voltage should be possible; (2) the electricity storage density of lithium batteries is potentially high because of the low atomic mass of lithium (1 F is released by the dissolution of only 7 g of the metal); (3) the discharge of a lithium electrode can be achieved at high current density; and (4) some lithium batteries could be rechargeable. Such properties would lead to both primary and secondary batteries with high energy and power densities.

In practice, it is the difficulty of obtaining the expected properties which has led to the intensity of the research activity. Many of the problems arise because of the extreme reactivity of lithium metal. It must be handled in the absence of moisture, oxygen and, perhaps, even nitrogen and is stable only in certain media. Hence, the study as well as the manufacture of lithium batteries requires the development of special techniques. In fact, in many lithium battery electrolytes the metal is clearly thermodynamically unstable and the lithium remains in the stored battery only because of films formed on its surface. Hence, it is the properties of these surface films which largely determine battery performance. It has been found that in several diverse media, films are formed that protect the metal on open circuit but still allow anodic dissolution at a reasonable rate (and even recharge of the electrode, i.e. deposition of lithium). There is no doubt, however, that the presence of the films degrade battery performance to some extent. Certainly, the film properties cannot be predicted and, hence, the search for battery electrolytes has been largely empirical.

The term 'lithium battery' is now used to describe a large family of batteries whose only common feature is the lithium negative electrode. The major differences involve the choice of the electrolyte medium and of the positive electrode chemistry but there is also a range of designs, sizes and materials of construction which use a variety of separators.

Five distinct types of electrolytes have been investigated:

1. An aprotic solvent containing a lithium salt. The organic solvents which have been studied in detail include propylene carbonate, dioxolane, tetrahydrofuran and other ethers. Mixtures of solvents have also found application and a popular combination has been a high dielectric constant solvent such as propylene carbonate with a low viscosity ether. Common lithium salts have included the perchlorate, hexafluoroarsenate and hexafluorophosphate.
2. Thionyl chloride, sulphuryl chloride or sulphur dioxide where the solvent is also the electroactive species at the positive electrode, made from a high surface-area, high-porosity carbon. In thionyl and sulphuryl chloride cells the electrolyte is usually lithium tetrachloroaluminate while sulphur dioxide is

often diluted with acetonitrile to lower the vapour pressure when the electrolyte is lithium bromide. It is implicit in the chemistry of these cells that the reaction of lithium metal with the solvent is thermodynamically favourable, indeed, highly exothermic (to give the large, observed battery voltage) and, hence, their existence is totally dependent on the presence of a surface film on the lithium. These films have unexpectedly favourable properties which lead to high cell voltages at high discharge rates.

3. A lithium ion conducting solid electrolyte such as lithium iodide or lithium iodide + alumina (33 mol%). The lithium iodide solid electrolyte is formed as a very thin film by directly contacting lithium metal with the positive electrode material, iodine, complexed with polyvinylpyridine. Such cells are only capable of discharge at a low rate ($< 100\,\mu A\,cm^{-2}$), at ambient temperatures but they perform excellently when only required to provide a low power, e.g. for a heart pacemaker. The lifetime in service can be many years and the shelf-life during storage is also long.
4. An organic polymer able to conduct lithium ions. The best-known example is polyethylene oxide. The polymer is, however, modified to lower the temperature where acceptable conductivity is obtained. The published literature suggests that about 373 K is the minimum temperature for such polymers to have the properties for a moderate current battery. The advantage of a polymer electrolyte lies in the possibility of a totally solid-state battery and, hence, great flexibility in the shape and packing of the battery as well as improved safety.
5. A molten salt. One such battery employing a lithium chloride + potassium chloride eutectic is described in section 11.6.2.

Similarly, there are a number of quite distinct types of positive electrode reactions which have been investigated for use in lithium batteries.

1. The reduction of an oxide, sulphide, metal salt or oxidizing agent, e.g. CuO, CuS, Ag_2CrO_4, PbI_2, I_2 in polyvinylpyridine.
2. The intercalation of lithium into a suitable material. These include TiS_2, V_6O_{13}, MnO_2, MoS_2 and certain neutral polymers such as polyacetylene. In an intercalation reaction, the lithium passes into the lattice and it may be written:

$$Li^+ + V_6O_{13} + e^- \longrightarrow LiV_6O_{13} \tag{11.7}$$

or:

$$Li^+ + V_6O_{13} + e^- \longrightarrow Li^+V_6O_{13}^- \tag{11.8}$$

The inorganic materials have lattice structures with channels of appropriate dimensions to allow the lithium species to move easily into the host lattice. Effectively, a solid solution of lithium in the host is formed and these reactions can be thermodynamically very favourable, sufficient for a lithium battery to have an open-circuit potential of around 3 V.

3. The reduction of an organic polymer. The polymer which has been most successful is poly(carbon monofluoride) $(CF)_n$ which can be manufactured as a high surface-area powder capable of being reduced at a high rate at a very positive potential. Oxidized polyacetylene, polypyrrole and polyaniline are other polymers which have been discussed.
4. The reduction of the solvent (e.g. thionyl chloride, sulphuryl chloride and sulphur dioxide) at a high surface-area carbon cathode which may also contain a catalyst. These cathodes give the highest battery voltages and energy densities but their behaviour and even their existence are dependent on the formation of a film on the lithium surface which stops the very exothermic reaction between the metal and the solvent.

Batteries based on most combinations of the above types of solvent–electrolytes and positive electrodes have been produced and tested. Naturally, only a fraction have reached the stage of commercial manufacture but the wide variety of primary lithium batteries which have reached the market-place during the last 15 years is impressive. Table 10.7 seeks to illustrate the chemistry and performance as well as the options as regards cells sizes and geometries for the most important lithium primary batteries now available for purchase.

Lithium–thionyl chloride battery technology has reached a mature state. Such batteries are manufactured in a very wide range of sizes which uniformly give a high battery voltage (3.6 V on open circuit and around 3.4 V during discharge) excellent energy density (up to 500 Wh kg^{-1}) a flat discharge curve (Fig. 11.18), acceptable performance over an unusually wide temperature range and a very long shelf-life for storage. Moreover, with a suitable cell design, the power density can be high. Their wider use is probably impeded only by fears over safety hazards associated with the exothermic nature of the lithium–thionyl chloride reaction and hazards from exposure to these chemicals. Hence, lithium–thionyl chloride batteries, although believed to be quite safe, are seldom sold to the public and the largest markets are the military and applications such as emergency supplies at remote sites. Note that some Li–$SOCl_2$ batteries are, by any standards, very large. Although their manufacture is limited to the smaller sizes, the same general comments are applicable to lithium–sulphur dioxide batteries.

Lithium batteries based on organic solvents are now made on a large scale for medical applications, back-up power for computer memories, power for small electronic gadgets and the general consumer market. Batteries based on four types of positive electrode (intercalation into MnO_2, reduction of poly(carbon monofluoride), cupric oxide and silver chromate) are listed in Table 11.7; note that the exact solvent–electrolyte is not specified because their selection is considered confidential. The exact composition may also vary from company to company. All these batteries give performances markedly better than the traditional batteries (Table 11.8). The better performance, however, is obtained

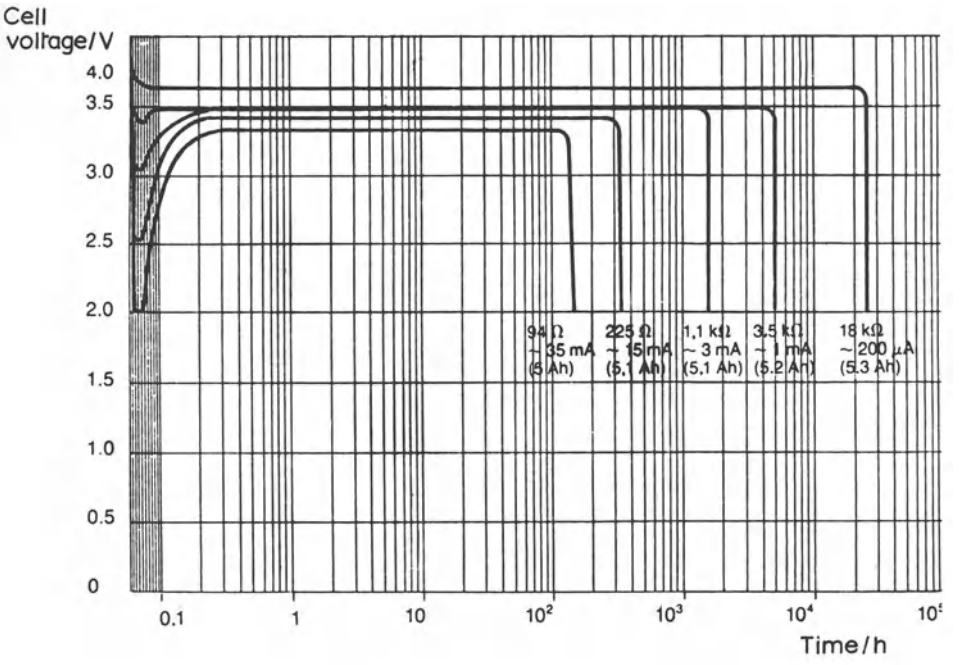

Fig. 11.18 Discharge curves for a 25 cm^3, 5.2 $A\,h^{-1}$, cylindrical Li–$SOCl_2$ battery after one year of storage.

only at a higher cost and, hence, these batteries find a market mainly where the superior properties merit the additional cost. The organic electrolyte batteries are manufactured in a variety of geometries, and this is illustrated in Fig. 11.19 which shows three different constructions for poly(carbon monofluoride) batteries. Lithium batteries are also now produced in a number of novel configurations particularly as very thin batteries. For example, Figure 11.20 shows an unusual 6V battery based on a MnO_2 positive electrode. Elsewhere, batteries as thin as 0.5 mm are being marketed.

Several batteries based on solid electrolytes are also made and the chemistry and characteristics of one are included in Table 11.7. Such cells can only be discharged at low currents and therefore give an extremely poor power density. On the other hand their great reliability make them well suited for low powered electronic circuitry and medical implants.

While there is now a wide variety of primary lithium batteries which have successfully reached commercial manufacture, the path to rechargeable lithium batteries has proved to be much more difficult. It was originally expected that

Table 11.7 The chemistry and characteristics of some commercially available primary lithium batteries

Battery chemistry				
Solvent/electrolyte	Positive electrode reaction	Cell voltage/V	Energy density/Wh kg^{-1}	Power density
$SOCl_2/LiAlCl_4$	Reduction of $SOCl_2$ at high-area carbon e.g. $2SOCl_2 \xrightarrow{4e^-} S + SO_2 + 4Cl^-$	3.4	250–500	Low to high
$SO_2/CH_3CN/LiBr$	Reduction of SO_2 at high-area C $2SO_2 + 2e^- \longrightarrow S_2O_4^{--}$	2.8	280	High
Organic solvent/LiX	$Ag_2CrO_4 \xrightarrow{2e^-} 2Ag + CrO_4^{--}$	3.2	280	Low
Organic solvent/LiX	Intercalation of Li into MnO_2	2.9	200–400	Low to medium
Organic solvent/LiX	$(CF)_n \xrightarrow{ne^-} F^- + nC$	2.6	200–450	Low to medium
Organic solvent/LiX	$CuO \xrightarrow{2e^-} Cu$	1.4	275	Low
Solid LiI matrix	$I_2 \xrightarrow{2e^-} 2I^-$ I_2 as complex with polyvinylpyridine	2.8	120	Very low

lithium battery technology would extend to large secondary batteries suitable, for example, for vehicle traction. These expectations have not yet been realized and, indeed, remain a somewhat distant hope. In practice, there are severe problems in cycling both the lithium electrode and most possible positive electrodes in all the media investigated. Hence, the only secondary lithium batteries to reach a production stage are relatively small ($< 50\ cm^3$) cells based on an intercalation positive electrode and an organic electrolyte carefully optimized to allow deposition as well as dissolution of lithium metal. It was possible, for a period to purchase miniature batteries (25 or 90 mA h capacity) based on a TiS_2 positive electrode and a LiAl negative electrode (to reduce problems of lithium recharging). They were not however, very successful and could not be scaled-up to larger cells and so were withdrawn from the market.

Other characteristics	Typical size/A h	Construction	Applications
Flat discharge curve from −55 to +100° C operation; long shelf-life	0.1–30	Spirally wound cylindrical or flat disc	Computer memory back-up; military; emergency supplies
	30–15 000	Spirally wound cylindrical, or rectangular flat plates	Military, missiles etc.
Very flat discharge curve; very long shelf-life; good low temperature performance	0.4–30	Spirally wound cylindrical	Military/civilian supplies for radios, sonobuoys, alarms
Excellent reliability on continuous drain	0.1–4	Button or rectangular plate	Pacemakers and other implanted devices; electronic memory small consumer, e.g. watches, microcomputers, instruments
Flat discharge curve; good shelf-life	0.05–2	Button, coin cylindrical or planar, thin sheet	
Excellent storage	0.001–5	Coin, cylindrical and thin sheet	Military and small consumer
Excellent storage	0.5–3	Cylindrical	Small consumer
Continuously falling voltage but operates many years	0.1–1	Button cells	Medical implants and small consumer

More recently, a battery based on a MoS_2 positive and Li negative electrode has become available and shows greater promise. The batteries are spirally wound cylindrical cells (up to 50 cm^3) with the organic electrolyte totally absorbed into the porous separator. Cycle lives above 50 cycles have been achieved. Morever, the high voltage and energy density and the ability to hold charge during prelonged storage mirror well the behaviour of the primary cells discussed above. On the other hand, the use of an intercalation electrode predetermines that the battery voltage will decrease during discharge (the potential of an intercalation electrode varies continuously with its composition, Li_xMoS_2). But even this effect can be used to some advantage, since the battery voltage is a simple state of charge indicator. It will be interesting to see whether this system can be scaled further.

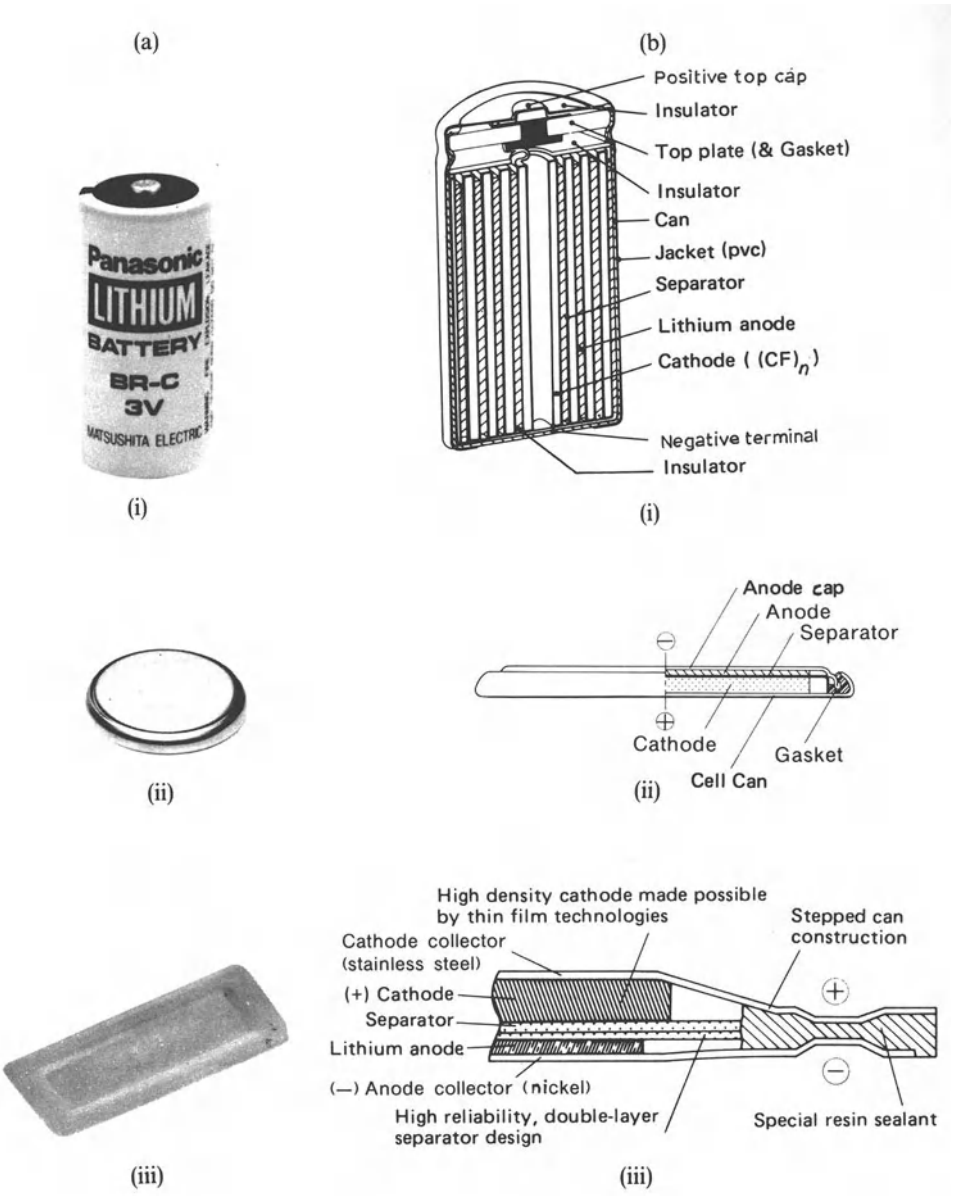

Fig. 11.19 Primary $(CF)_n$–Li batteries. (a) External views. (b) Cross-sections to show constructions of: (i) a cylindrical spirally wound cell; (ii) a coin-type cell; (iii) a paper-thin cell. (Courtesy: Panasonic Industries (UK) Ltd.)

Fig. 11.20 A thin-configuration 6 V Li–MnO_2 battery. (Note the bipolar connection to two cells in series). (a) Cross-section. (b) Components. (c) Exterior. (Courtesy: Gould Inc.)

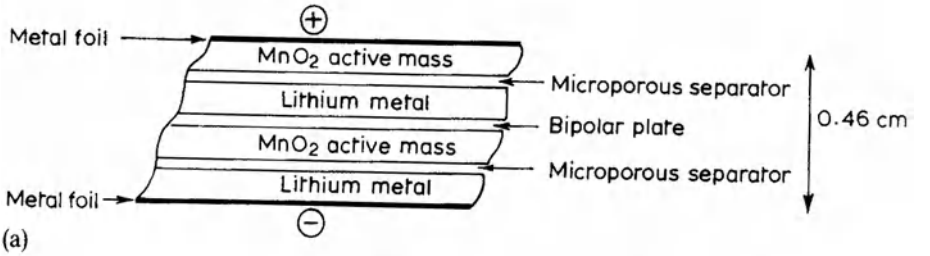
Metal foil
⊕
MnO_2 active mass
Lithium metal
MnO_2 active mass
Lithium metal
Metal foil
⊖
Microporous separator
Bipolar plate
Microporous separator
0.46 cm

(a)

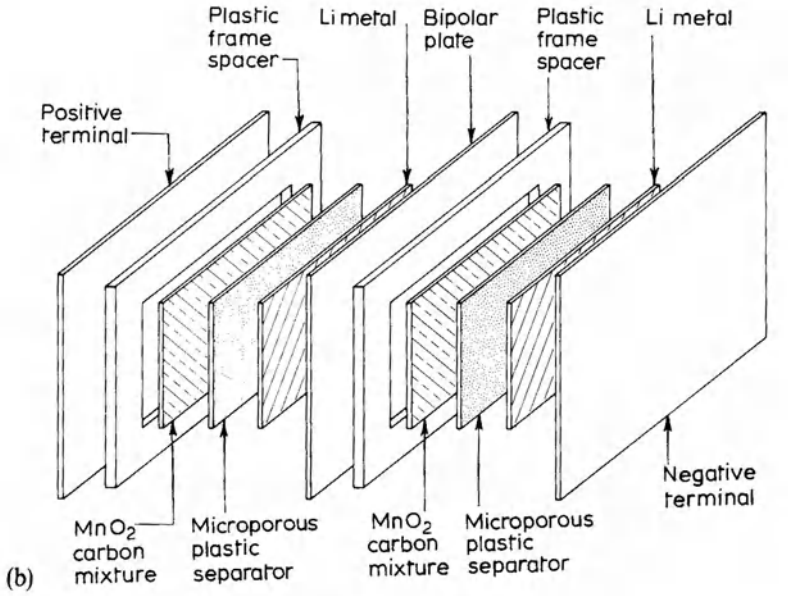
Plastic frame spacer
Li metal
Bipolar plate
Plastic frame spacer
Li metal
Positive terminal
Negative terminal
MnO_2 carbon mixture
Microporous plastic separator
MnO_2 carbon mixture
Microporous plastic separator

(b)

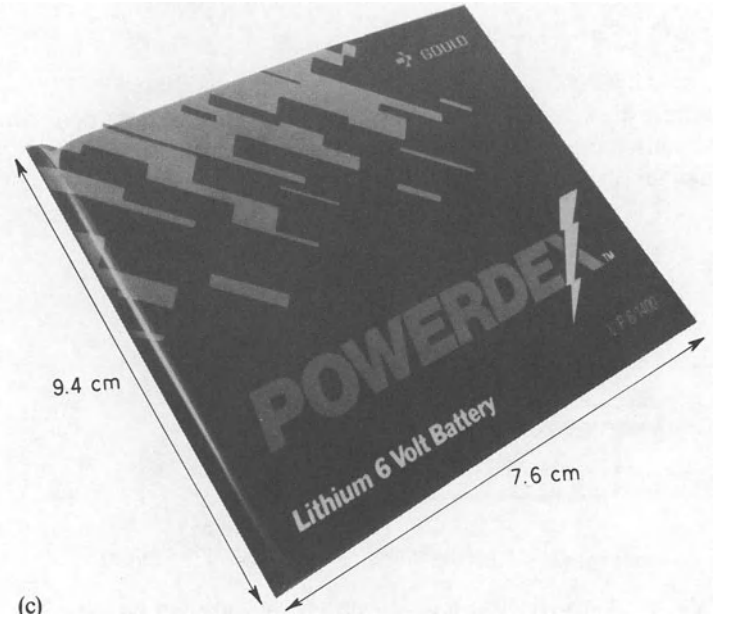
GOULD
POWERDEX
Lithium 6 Volt Battery
9.4 cm
7.6 cm

(c)

11.5.5 Other battery systems

Batteries based on a very wide range of electrode reactions are manufactured for military applications. The specifications for batteries in such applications are very diverse and suitable systems are produced in small numbers and often have no civilian market. Such batteries are well beyond the scope of this discussion but a few systems produced for more specialist civilian markets deserve some mention.

A number of batteries are based on modifications of the technology or the substitution of electrode reactions into either the Ni–Cd or Leclanché cells; the changes usually improve one characteristic of importance to a particular duty but usually only at an increased cost. In an alkaline manganese battery, the cathode is manganese dioxide and graphite in the form of compressed tablets, and the electrolyte is a strongly alkaline solution. The overall cell reaction is:

$$2MnO_2 + H_2O + Zn \longrightarrow 2MnO(OH) + ZnO \qquad (11.9)$$

It is also normal to use the highest grade manganese dioxide (inevitably more expensive) but in all respects the performance of such batteries is superior to the Leclanché cell. In the small (0.02–0.2 A h) button cells, the cathode active material is more commonly mercuric oxide + graphite or silver oxide + graphite pressed into pellets and the electrolyte is again aqueous potassium hydroxide (Fig. 11.21). The cell reactions are:

$$HgO + Zn \longrightarrow Hg + ZnO \qquad (11.10)$$

and:

$$Ag_2O + Zn \longrightarrow 2Ag + ZnO \qquad (11.11)$$

and these cells have the advantage compared with those based on MnO_2 in that their voltage is constant during most of the discharge and their performance on continuous discharge is good. They are therefore suitable for watches and hearing-aid supplies.

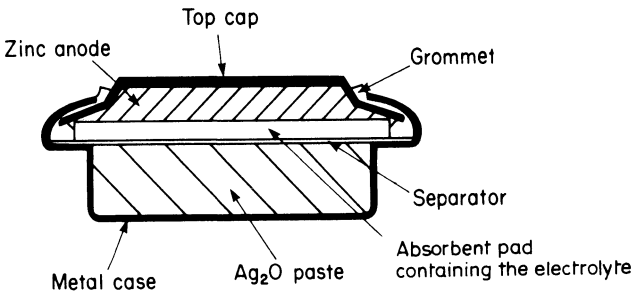

Fig. 11.21 The construction of a silver oxide–zinc button cell.

Silver oxide–zinc can be manufactured in rechargeable cells with free potassium hydroxide electrolyte and pasted rectangular electrodes. Such cells are expensive but have good energy density compared with Pb–acid or Ni–Cd (70 Wh kg^{-1}) and are also capable of high discharge rates for short periods. Other alkaline secondary batteries which have been manufactured include NiO(OH)–Zn, NiO(OH)–Fe and Ag_2O–Cd.

Metal–air batteries have received considerable attention because one of the active materials does not contribute to the mass of the battery, and this gives the possibility of a very high energy density. The systems have not yet been totally successful even as primary cells because of polarization of the air cathode causing a substantial loss of cell voltage. Moreover, attempts to recharge such cells have met problems at the negative metal electrode, e.g. with a zinc electrode the distribution of metal over the current collector changes with time. Commercially, the most successful primary batteries have been based on zinc–air with a neutral or alkaline electrolyte. Aluminium–air, iron–air and lithium–air with an aqueous electrolyte now have supporters as traction batteries. Lithium (in strong hydroxide solution to prevent spontaneous dissolution) and aluminium combine low density with a low electrochemical equivalent and such metal–air cells could in theory give rise to very high-energy densities of several kilowatt-hours per kilogram. Since aluminium cannot be plated from aqueous media, it is envisaged that the aluminium would be recycled external to the battery; aluminium would

Table 11.8 Performance of some D-size batteries (50 cm^3) when discharged at the 100 hour rate ($C/100$) at 293 K

	E_{CELL}^{AVE}/V	Capacity/Ah	Theoretical energy density/Wh kg^{-1}
Primary:			
Zn–carbon	1.2	6	80
Alkaline MnO_2	1.2	10	100
Zn–HgO	1.2	12	85
Zn–air	1.3	22	340
Li–$SOCl_2$	3.4	12	410
Li–SO_2	2.8	8	270
Li–MnO_2	2.7	10	225
Li–$(CF)_n$	2.3	8	230
Secondary:			
Pb–acid (spirally wound)	2.1	2.7	30
Ni–Cd (sintered plate)	1.2	4	33
Zn–AgO	1.5	5	70

be fed to the battery where it may be oxidized to alumina or aluminium hydroxide, which could be collected in an electrolyte flow system outside the battery and returned to the smelter. In the long term, this battery looks particularly attractive for a car traction battery since the intractable problem of battery replacement or recharging on long journeys is avoided (more aluminium could be added) and the battery is based on room-temperature aqueous electrochemistry.

11.6 BATTERIES UNDER DEVELOPMENT

For many years, the traditional batteries described earlier underwent slow evolutionary development. The 1970s saw a major expansion in the research efforts of the battery industry. The main driving forces were the microelectronics revolution (which had led to a situation where power supplies were the largest part of many devices and instruments) and the 'energy crisis'. In particular, in response to the greatly increased cost of oil and fears that the world's supply of oil would be insufficient to meet demand, the US Department of Energy sponsored a very large programme. The dual aims were to develop batteries for energy storage (load levelling and solar-derived electric power) and for an electric car. The programme was quite remarkable for the number of different systems which were investigated in some detail. While many argued that batteries were not the most likely way of solving the problems of energy storage or family transport, there is no doubt that the programme led both to significant improvements in the presently manufactured primary and secondary batteries, the introduction of the lithium batteries discussed above and the demonstration of several new systems with potentially much improved characteristics. The 1980s have seen a decrease in the cost of oil and at least a temporary abatement of fears that oil supplies are on the verge of running out. Hence, the political will to support further development of large batteries has, at least for the present, been much diminished. As a result, the scale of activity is much reduced and the rate of advancement has slowed greatly.

This section will briefly describe the principles and problems of three of the most successful systems under development in the USA and elsewhere. The demonstration of several new practical batteries based on quite different chemistry should be recognized as a considerable achievement. Many of the problems now relate to techniques of manufacture or materials compatibility over a long period of time. In the final part, we have attempted to summarize the status of secondary batteries in the mid 1980s.

11.6.1 Sodium–sulphur batteries

The sodium–sulphur system is being discussed for load levelling and car traction and is believed to be close to commercial production in the UK as a traction

battery for commercial vehicles. The overall cell reaction is usually written:

$$2Na + S \longrightarrow Na_2S \tag{11.12}$$

which leads to an open-circuit potential of +2.1V and a theoretical energy density of 756 Wh kg^{-1}. The electrode reactions during discharge can be written in the simplified form:

$$Na - e^- \longrightarrow Na^+ \tag{11.13}$$

$$S + 2e^- \longrightarrow S^{--} \tag{11.14}$$

although both the sulphur and sulphide are present as complex polysulphides. The cell is operated with a sodium-conducting solid electrolyte; in most cells sodium β-alumina although sodium-conducting glasses have also been investigated. The temperature of operation is 300–375° C so that the active materials are liquid and to increase the conductivity of the solid electrolyte.

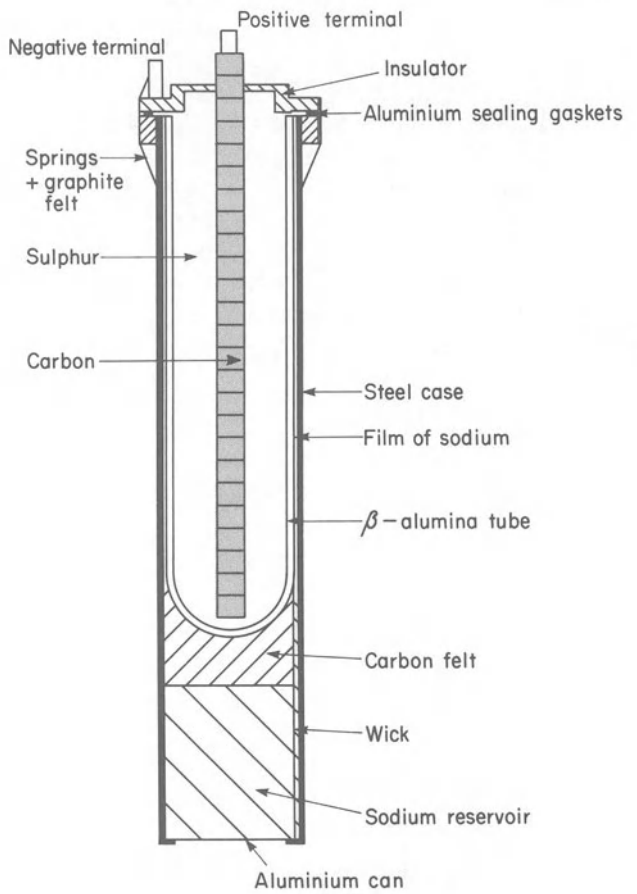

Fig. 11.22 The construction of a 38 A h sodium–sulphur battery.

The major problems with the cell are associated with safety (since contact between the sodium and the sulphur would cause a very exothermic reaction) and with the low conductivity and high corrosiveness of the sodium polysulphides. These factors determine the cell design. A typical design, based on a sodium β-alumina tube (the easiest form to seal), is shown in Fig. 11.22. The outer tubular case is made of mild steel and the β-alumina tube fits inside with a small gap between. The positive electrode is molten sulphur at all times except when 100% charged containing sodium sulphide, and this is placed inside the β-alumina tube so that it does not come into contact with, and then corrode, the outer case. The current collector is graphite felt which takes up all the volume inside the tube and there is also a central graphite rod which connects to the cell terminal. The negative current collector is the case and the molten sodium is stored below the cell and is only wicked-up into the gap between the tube and the case as the sodium film there is consumed; this arrangement reduces problems from the sodium–sulphide reaction if the β-alumina tube cracks or, more commonly, sodium dendrites grow through faults in the β-alumina.

Such cells with a β-alumina tube 60 cm long and 3.5 cm diameter have been thoroughly tested. They have a capacity of about 150 A h and have been shown to maintain 80% capacity after more than 1000 charge/discharge cycles. The practical energy density lies in the range 100–150 Wh kg^{-1} and they can maintain a peak power density (for 15 s) over 100 W kg^{-1}. As with all high-temperature systems, thought must be given to heat management; although cells have been cooled and reheated, this cannot be advisable and, hence, batteries are insulated to allow the system to remain molten during reasonable storage periods. Even so, such batteries are probably best used in duties which are regular and without long off-periods.

11.6.2 Lithium–iron sulphide batteries

The second molten salt battery to have received detailed attention is the lithium–iron sulphide battery. During discharge, the negative electrode reaction is the dissolution of lithium from a lithium–aluminium (10–20% lithium alloy), while the positive electrode reaction is the reduction of iron disulphide which occurs in stages:

$$3FeS_2 + 4e^- \longrightarrow Fe_2S_5^{4-} + FeS \tag{11.15}$$

$$Fe_2S_5^{4-} + FeS + 2e^- \longrightarrow 3FeS_2^{2-} \tag{11.16}$$

$$FeS_2^{2-} + 2e^- \longrightarrow Fe + 2S^{2-} \tag{11.17}$$

or the reduction of ferrous sulphide:

$$FeS + 2e^- \longrightarrow Fe + S^{2-} \tag{11.18}$$

The former gives a higher cell voltage but produces technological problems; corrosion of the current collector by iron disulphide always occurs unless it is made

of molybdenum, an unacceptably expensive metal. Hence, most practical cells have used iron sulphide as the active material and these batteries have now reached the stage of detailed engineering and testing.

Reaction (11.17) is not totally reversible and after the first discharge the positive electrode reaction is better represented by:

$$8S^{2-} + 7Fe - 14e^- \longrightarrow Fe_7S_8^{2-} \tag{11.19}$$

and the inability to reform iron sulphide causes a loss in capacity.

The electrolyte for the battery is LiCl–KCl mixture with a temperature of 430–490° C. Batteries are constructed on the parallel-plate principle with alternate anodes and cathodes, and in each interelectrode space there is a boron nitride cloth or felt separator. Commonly there is one extra negative plate because some lithium is lost during cycling. The plates, typically 5 mm thick, were initially prepared by cold-compaction techniques, the active material being compressed into a fine metal honeycomb material which also acts as the current collector. The negative electrode was just the Li–Al alloy in an Fe lattice while the positive electrode was a mixture of FeS + LiS + CuS (to improve use of active materials) in a nickel honeycomb. The positive electrode, when prepared in this way, tends to swell during discharge and the trend now is to assemble the cell in a half-charged state with the positive plate being produced by hot-compression methods with carbon and molybdenum as additives instead of copper sulphide which has led to copper dendrite shorting.

In the present state of the art, the energy density is about 80 Wh kg^{-1} and more than 300 cycles have been achieved; the peak power density is, however, rather low, indicating problems with the electrode kinetics. All these figures are likely to improve, however, as the programme proceeds.

11.6.3 Zinc–halogen batteries

Zinc–halogen batteries, with the electrode reactions during discharge:

$$Zn - 2e^- \longrightarrow Zn^{2+} \tag{11.20}$$

$$X_2 + 2e^- \longrightarrow 2X^- \tag{11.21}$$

seem attractive since they are based on low-cost chemicals, on aqueous electrochemistry at almost ambient temperature and pressure, and because the electrode reactions involved are fast. Moreover, they are capable of a high cell voltage and a good energy density. The problem has always been to store the halogens and this must almost certainly be done external to the cell so that the battery systems require storage tanks and pumps as well as the cell; this makes their success dependent on the engineering.

In the zinc–chlorine cell, the chlorine is stored as chlorine hydrate, $Cl_2 \cdot xH_2O$ ($x = 6$–10), which precipitates as a solid below 9.6° C. During charge, the electrolyte, aqueous zinc chloride, is cooled in a reservoir, while during discharge

Table 11.9 Comparison of data for batteries in the US DoE battery programme. Theoretical values in parentheses

	Open-circuit cell voltage/V	Energy density/Wh kg^{-1}	Power density/W kg^{-1}	Cycles to deep discharge	Energy efficiency on cycle/%
Near-term:					
Pb–acid	2.1	40(170)	100	400	82
NiO(OH)–Zn	1.6	65(380)	110	150	70
NiO(OH)–Fe	1.2	53(390)	110	> 1000	70
Advanced:					
LiAl–FeS	1.2	80(460)	80	350	80
Na–S	2.1	110(760)	100	> 600	80
Long-term:					
Al–air	2.7	—(4250)	—	0	—
Fe–air	1.2	84(698)	74	—	—
Zn–Br_2	1.8	65(430)	—	—	70

the reservoir is heated under controlled conditions. The cell itself, however, can be simple; the electrodes are graphite and can operate without catalyst and the cell can be constructed from PVC without a separator. There also remain some problems with the morphology of zinc deposits.

In the zinc–bromine cell the halogen is stored in the electrolyte as a polybromide (mainly Br_3^-) and, hence, a separator is essential; Nafion cation exchange membrane has again been used. The electrolyte is aqueous zinc, bromide with tetraalkylammonium bromide to aid the bromine complex formation.

Engineering of the chlorine battery is well advanced but zinc–bromine cells exist only as small laboratory modules.

11.6.4 Some comments on the various battery systems

The US Department of Energy programme was divided into near-term, advanced, and long-term batteries and emphasized the development of systems which fulfil the requirements for car traction, load levelling and the storage of solar-derived energy. The state of the art in the early 1980s with respect to some important performance characteristics is summarized in Table 11.9. It can be seen that efforts to modify the traditional battery systems ('near-term batteries') to meet the new challenges have met with some success, e.g. all the characteristics of the lead–acid battery show significant improvement compared with present commercial batteries – energy density 30–40 Wh kg^{-1}, power density 80–100 W kg^{-1}, cycle life to deep discharge 100–400 cycles. Even so, such improvements are unlikely to totally change the future of batteries, and the Ni–Zn system has a serious weakness with respect to cycling.

The advanced batteries represent an attempt to select systems which have potentially a large advantage, e.g. the theoretical energy densities are shown in Table 11.9. While these have little meaning since they make no allowance for cell components other than the active materials and are never, in practice, approached, a high theoretical energy density (cf. Na–S with Pb–acid) gives potential for improvement. On the other hand, the systems selected present difficult materials problems and operate well above room temperature. Even so, without the many years of evolutionary development, these cells still show energy densities and cycle lives well above those of some of the traditional systems.

The long-term batteries are notable for a return to ambient-temperature, aqueous-electrolyte cells. Particularly, the Al–air battery shows a huge theoretical energy density (10% of this value would be very acceptable). But this cell requires fundamental advances in the electrochemistry of both electrodes:

$$Al + 4OH^- - 3e^- \longrightarrow AlO_2^- + 2H_2O \tag{11.22}$$

$$O_2 + 2H_2O + 4e^- \longrightarrow 4OH^- \tag{11.23}$$

The major difficulty in reaction (10.22) is passivation which limits the rate of discharge and one approach to improving the performance is to use an Al alloy.

As elsewhere in electrochemical technology, the requirement at the cathode is an improved oxygen reduction catalyst.

When the world next begins to worry over the depletion of its oil resources, the advances resulting from the research on these systems during the last 15 years will be found to be of great value. Further improvements in energy and power densities as well as in the ability to maintain performance during many charge/discharge cycles will be the most important properties sought.

11.7 FUEL CELLS

The original concept of the fuel cell was that primary fuels could be reacted with oxygen in an electrochemical cell, e.g.:

$$CH_4 + 2H_2O - 8e^- \longrightarrow CO_2 + 8H^+ \tag{11.24}$$

$$O_2 + 4H^+ + 4e^- \longrightarrow 2H_2O \tag{11.25}$$

Since electrolysis cells are not necessarily subject to the inefficiencies associated with the Carnot cycle, it is possible, in principle, for a fuel cell to convert all the free energy of combustion of the fuel to electrical energy. This is in sharp contrast to thermal oxidation processes where such losses always accompany combustion of the fuel. Hence, fuel cells have a potential advantage over thermal processes and could offer a superior technology to thermal power stations and the internal combustion engine. Achievement of 100% efficiency in a fuel cell is, of course, quite unlikely because an overpotential at each electrode and iR_{CELL} losses in the electrolyte between the electrodes are inevitable. The serious question is whether it is possible to design a fuel cell where the efficiency is greater than the 20–40% usually achieved by modern thermal combustion processes. Moreover, the fuel cell must operate economically and, hence, must run with a current density $> 0.1\ A\,cm^{-2}$ and be constructed from materials which are cheap and stable.

Unfortunately, despite a substantial research effort over some 30 years since the possible applications of fuel cells in power generation and vehicle traction were first recognized, the progress towards a fuel cell operating on a primary fuel has not been rapid. In particular, it has not proved possible to design catalysts for the anodic oxidation of hydrocarbons which even approach the required performance. Even at extreme pH and elevated temperatures, such oxidations occur at only low current densities and at substantial overpotentials with all investigated electrode materials.

On the other hand, although the technology for oxygen-reduction cathodes is far from perfect, it is possible to obtain catalytic electrodes (based usually of dispersed Pt on carbon) which allow reduction of oxygen to occur with a current density $> 0.1\ A\,cm^{-2}$ at a cost of some 400 mV in overpotential (at least at elevated temperatures). Moreover, some intensive R and D has led to marked improvements in the design, manufacture, performance and stability of the porous electrodes essential to the operation of cells with low solubility, gaseous reactants.

In consequence, it has proved possible to design fuel cells based on secondary fuels – particularly hydrogen but also carbon monoxide, which merit serious consideration for commercial exploitation. Also systems have been constructed where the primary fuel has first been converted catalytically to hydrogen and/or carbon monoxide and these products fed to a fuel cell. Furthermore, in the laboratory, there has been some progress towards fuel cells based on methanol oxidation.

There are probably no economically viable applications of the available technology at the present time. This may, however, change if energy again spirals in cost or there are further advances in the technology. Certainly, there will always be periodic resurgences of interest in fuel cell technology because the rewards of success are high. Their attraction is not only in terms of potential energy efficiency; fuel cells also offer a method of energy conversion which is quiet and does not lead to pollution (cf. thermal power stations and present car engines!).

The following applications of fuel cells have frequently been discussed:

1. *Large-scale power generation.* Fuel cells are particularly well-suited to the job of power generation within the urban environment. In fact, phosphoric acid fuel cells have been tested for this application in both the USA and Japan; the cells operate on hydrogen produced on site from natural gas. The largest installation was a 4.8 MW plant in New York City which it is believed was run continuously for many months. The same technology was later used to construct a 200 kW plant in Tokyo and this was due to operate between May 1987 and September 1988. Also in Japan, several 10 and 40 kW fuel cell stacks have been run for periods between 6 months and 3 years. The latter are housed in a building $3 \times 1.6 \times 2$ m high including the catalytic reactor for conversion of the natural gas to hydrogen and are suitable for providing power to a small hotel or group of houses. It appears that such fuel-cell-driven power plants are now able to meet the required specification technologically but the economics remain unfavourable.
2. *Vehicle traction.* Fuel cells have been proposed for cars, buses and commercial vehicles and, indeed, several demonstration units have been built and tested. It is popular to build particularly the cars with a hybrid traction units containing both a fuel cell and a battery. The fuel cell would be used to provide the power for cruising and the battery for peaks in power requirements such as start-up or rapid acceleration. The hybrid power pack greatly reduces the strain on the battery since it need no longer be deep-discharged and the range of the vehicle is increased indefinitely. In this application the preferred fuel is probably 50% aqueous methanol which would be reformed to hydrogen in a small gas-phase reactor within the vehicle. Tanked hydrogen has also been considered.
3. *Small-scale power generation at remote sites.* Examples are fuel cells, which continue to play important roles in space exploration.

4. *Energy recovery in the chemical industry.* This is an application which considerably extends the range of fuels to be used, e.g. in the mercury process for the production of chlorine and sodium hydroxide (Chapter 3), sodium amalgam is reacted with water at a catalytic surface in the denuder; the reaction is highly exothermic but the free energy of reaction is obtained only as low-grade heat. If, on the other hand, the sodium amalgam were to be fed to the anode in a cell where the cathode reaction was oxygen-reduction or hydrogen evolution, the free energy of the reactions:

$$4NaHg + O_2 + 2H_2O \longrightarrow 4Hg + 4Na + 4OH^- \tag{11.26}$$

or:

$$2NaHg + 2H_2O \longrightarrow H_2 + 2OH^- + 2Na^+ + 2Hg \tag{11.27}$$

could be recovered as useful electrical energy. It should be noted that sodium hydroxide would still be produced. The equilibrium cell potentials would be approximately 2.3 and 1.05 V respectively and in the latter case no large overpotential losses are to be expected. A number of organic electrosyntheses which would give out electrical energy have been proposed, e.g. some hydrogenations when carried out in a cell with a catalytic cathode and the anode reaction is hydrogen oxidation give out electrical energy as the hydrogenation reaction has a negative free energy and have been called 'electrogenerative hydrogenations'.

Before discussing briefly the chemistry of the more successful fuel cell systems we should perhaps note that the development of fuel cells has led to a number of 'spin-off' ideas in other areas of electrochemical technology. Thus, for example, the catalysts and porous electrodes developed for the oxygen electrode in a fuel cell have been modified to produce the oxygen cathodes for metal–air batteries and trials in the chlor-alkali industry. Also, hydrogen anodes have been developed for energy-saving in zinc electrowinning and a device for converting air to pure oxygen has been built for use in remote hospitals (an air cathode is combined with an oxygen evolving anode to produce a cell with a low power requirement).

11.7.1 Phosphoric acid fuel cells

These cells operate only with hydrogen as the anode fuel and, moreover, the hydrogen must be pure since sulphur compounds and carbon monoxide adversely affect the performance of the Pt catalyst. Each cell consists of two Teflon-bonded gas-diffusion electrodes on a porous conducting support (Fig. 11.23). At both anode and cathode the catalyst is platinum particles dispersed on carbon and a recent success has been a reduction in Pt loading from 10 mg cm^{-2} to 0.75 mg cm^{-2}. The electrolyte is concentrated phosphoric acid absorbed into a solid matrix and the cell operates at 200° C to improve the electrode kinetics.

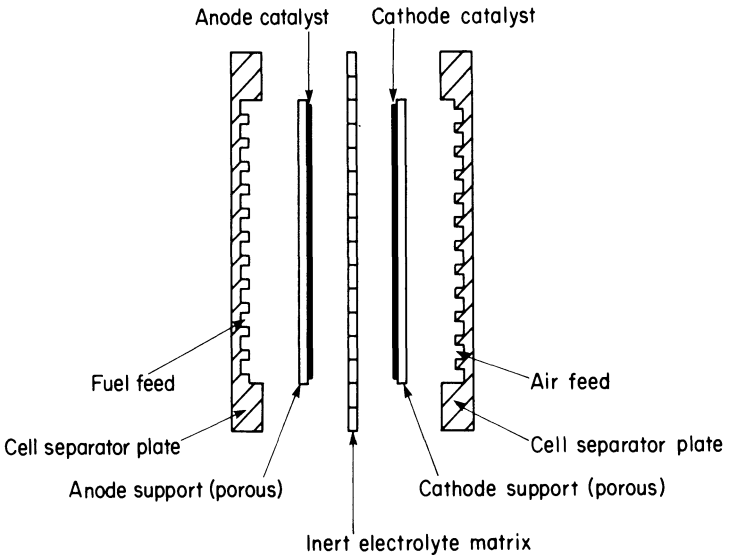

Fig. 11.23 The basic structure of the phosphoric acid fuel cell.

The cells are then mounted in stacks to increase the power output and care is taken to design an air-cooling system to maintain a constant temperature.

The cell voltage, with present technology, is typically 0.67 V (cf. a reversible potential of 1.16 V) at a current density of 0.15 A cm^{-2} and most of the voltage loss occurs at the air cathode. When combined with a catalytic reformer, the overall system energy efficiency (natural gas to electrical energy) of these fuel cells is 40%.

As noted above, this is the type of fuel cell which has been most extensively engineered and tested and several cells stacks up to 4.8 MW have been built and run for several months.

11.7.2 Alkaline fuel cells

The alternative, low-temperature system is based on a strongly alkaline electrolyte (KOH) and employs hydrogen and oxygen as fuels (carbon-containing fuels cannot be used because the final product is CO_2 which would convert the electrolyte to carbonate). The advantage of this system lies in the possibilities for non-Pt catalysts. Both Raney-nickel and silver-catalysed carbon materials are still being tested. A 1 kW hydrogen–air stack has been run for 3 months and now a 7.5 kW unit is being developed. The aim is a cheap and reliable unit for emergency or portable power generation.

11.7.3 Molten carbonate fuel cells

These cells operate at much higher temperature, which assists the kinetics of the electrode reactions. Also, the anode is capable of using either hydrogen or carbon monoxide as the fuel:

$$H_2 + CO_3^{2-} - 2e \longrightarrow CO_2 + H_2O \tag{11.28}$$

$$CO + CO_3^{2-} - 2e \longrightarrow 2CO_2 \tag{11.29}$$

while the reduction of oxygen in the molten carbonate medium is:

$$O_2 + 2CO_2 + 4e \longrightarrow 2CO_3^{2-} \tag{11.30}$$

so that the electrolyte must permit transport of carbon dioxide between the electrodes. The anode is porous nickel or a Ni–Cr alloy and the cathode is porous NiO. The electrolyte (40% $LiAlO_2$, 28% K_2CO_3 and 32% Li_2CO_3) is absorbed into a porous inorganic matrix. The cell is operated at 650° C.

In this cell, the voltage can be as high as +0.9 V with a current density of 150 mA cm^{-2}. This gives an overall energy efficiency, e.g. coal to electricity is in the range 40–45%. The major problem with this cell is the low tolerance of the electrode reactions to sulphur and chlorine. Several Japanese and US companies are involved in the construction and/or testing of 10 kW stacks and several are fully engineered including complex heat-management systems and components designed to be mass-produced.

11.7.4 The solid electrolyte fuel cell

A US company has been developing a fuel cell based on a ceramic oxide electrolyte to operate at about 1000° C. It is able to consume either hydrogen or hydrogen–carbon monoxide mixtures (reformed natural gas, etc.) as the anode fuel. Unlike all the other systems which are based on stacks of parallel porous electrodes, the design here is centred on a ceramic oxide tube and cylindrical electrodes. A number of 3 kW units with 144 cells are under test to check performance and to ascertain lifetime under practical conditions. A high electrical efficiency of > 50% has been achieved in early tests and very useful waste heat is available from this high-temperature cell.

11.7.5 Conclusions

Several fuel cell systems have reached advanced states of engineering and testing. They each are able to meet their scientific targets but are not able currently to capture clearly identifiable markets because of economic difficulties. Breakthroughs could happen simply from changes to the costs and availability of energy but the improvements in cell technology would still be very welcome. In particular, catalysts which led to a decrease in the oxygen-reduction overpotential and the development of components with a lower-cost and/or longer lifetime in

the very aggressive conditions (high temperatures, extreme pH) would be extremely beneficial.

FURTHER READING

1 M. Barak (ed) (1980) *Electrochemical Power Sources – Primary and Secondary Batteries*, Peter Peregrinus, Stevenage.
2 C. A. Vincent, F. Bonino, M. Lazzari and B. Scrosati (1984) *Modern Batteries*, Edward Arnold, London.
3 F. Beck and K.-J. Euler (1984) *Elektrochemische Energiespeicher*, VDE Verlag, Berlin.
4 D. Linden (Ed.) (1983) *Handbook of Batteries and Fuel Cells*, McGraw-Hill, New York.
5 H. Bode (1977) *Lead Acid Batteries*, Wiley, New York.
6 G. W. Heise and N. C. Cahoon (1976) *The Primary Battery*, Vols 1 and 2, Wiley, New York.
7 K. V. Kordesch (1974) *Batteries*, Vol. 1, 'Manganese Dioxide', Marcel Dekker, New York.
8 K. V. Kordesch (1977) *Batteries*, Vol. 2, 'Lead Acid Batteries and Electric Vehicles', Marcel Dekker, New York.
9 S. U. Falk, and A. J. Salkind (1969) *Alkaline Storage Batteries*, Wiley, New York.
10 J. P. Gabano (Ed.) (1983) *Lithium Batteries*, Academic Press, London.
11 J. O'M. Bockris and S. Srinivasan (1969) *Fuel Cells: Their Electrochemistry*, McGraw-Hill, New York.
12 T. C. Benjamin, E. H. Camera and L. G. Marianowski (1980) *Handbook of Fuel Cells*, Institute of Gas Technology, Chicago.

12 Electrochemical sensors and monitoring techniques

12.1 ELECTROCHEMICAL PROCEDURES

All analysts are familiar with the principles of potentiometry and polarography and, indeed, most analytical laboratories will contain a pH meter and a polarograph. However, electrochemical methods are, in general, not very important in modern analysis. In contrast, there are specific applications such as trace metal ion analysis in water and effluents and also some other aspects of environmental analysis for which electrochemical methods are particularly attractive. This is because: (1) some methods, especially anodic stripping voltammetry, have a very high sensitivity for heavy-metal ions and the lowest detection limit of from 10^{-10} to 10^{-12} mol dm^{-3} is well below that of other available methods; (2) electrochemical methods are well suited for modification to on-line and/or portable devices for analysis in the field. Whether the analysis is based on current, conductivity or the response of an ion-selective electrode, both the cell and the control electronics are readily miniaturized and operate on low power. Hence, this chapter considers the principles of the electroanalytical methods important in environmental and on-line analysis, together with biochemical applications of electrochemical sensors.

12.2 POLAROGRAPHY TO ANODIC STRIPPING VOLTAMMETRY

Direct-current polarography dates back some 60 years to the discovery by Heyrovsky that highly reproducible i–E curves could be obtained using a dropping mercury electrode (DME) (under natural convection) as the working electrode. Thus, in a polarographic analysis, an i–E curve is recorded using a slow linear potential scan and a DME with a droptime of 2–10 s; the i–E curve will, ideally, have the S-shape shown in Fig. 12.1(a). The half-wave potential $E_{\frac{1}{2}}$ can be used for qualitative analysis since it is a measure of how readily the electroactive species is reduced or oxidized and therefore is a reflection of its

molecular structure. In addition, the measurement of the mass transport limited current i_L can be used for quantitative analysis.

Polarographic analysis has considerable generality since a very wide range of both organic and inorganic species are electroactive within the potential range of the DME. For the same reason, when analysing mixtures, it is often difficult to obtain the necessary selectivity; the species to be determined must give a wave

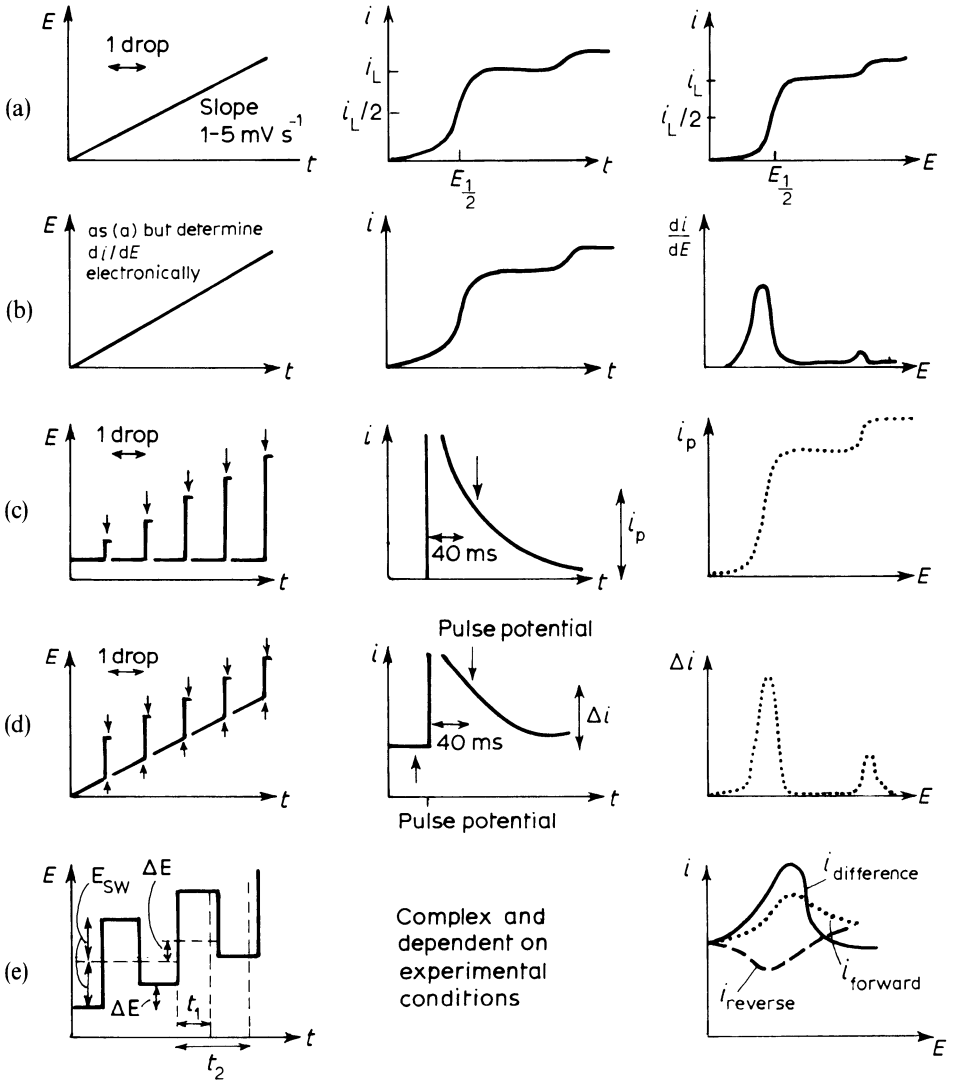

Fig. 12.1 Modern polarographic techniques. ↑ or ↓ indicate times when the current is measured. (a) Polarography. (b) Derivative polarography. (c) Pulse polarography. (d) Differential pulse polarography. (e) Square-wave polarography.

well separated from all others (in practice $\Delta E_{\frac{1}{2}} > 200$ mV) and if other electroactive species are present in excess they must be more difficult to reduce (it is not possible to determine accurately a small change in a large current). The order of the reduction waves and the separation of the waves can only be varied using pH and/or complexing agents and these are often insufficient when dealing with mixtures of similar species. Also, simple d.c. polarography is not a particularly sensitive technique.

These shortcomings led to modifications of the experiment to improve both the sensitivity and selectivity of analysis. It was found that the sensitivity could be improved by measuring the current under conditions of non-steady-state diffusion and increasing the ratio of the faradaic to the charging current. In pulse polarography this is achieved by constructing an i–E curve point by point where each point is the current measured a short time, typically 40 ms, after a potential pulse has been applied during the final stages of the lifetime of a mercury drop. The selectivity could be improved by differentiating the i–E curve since this led to

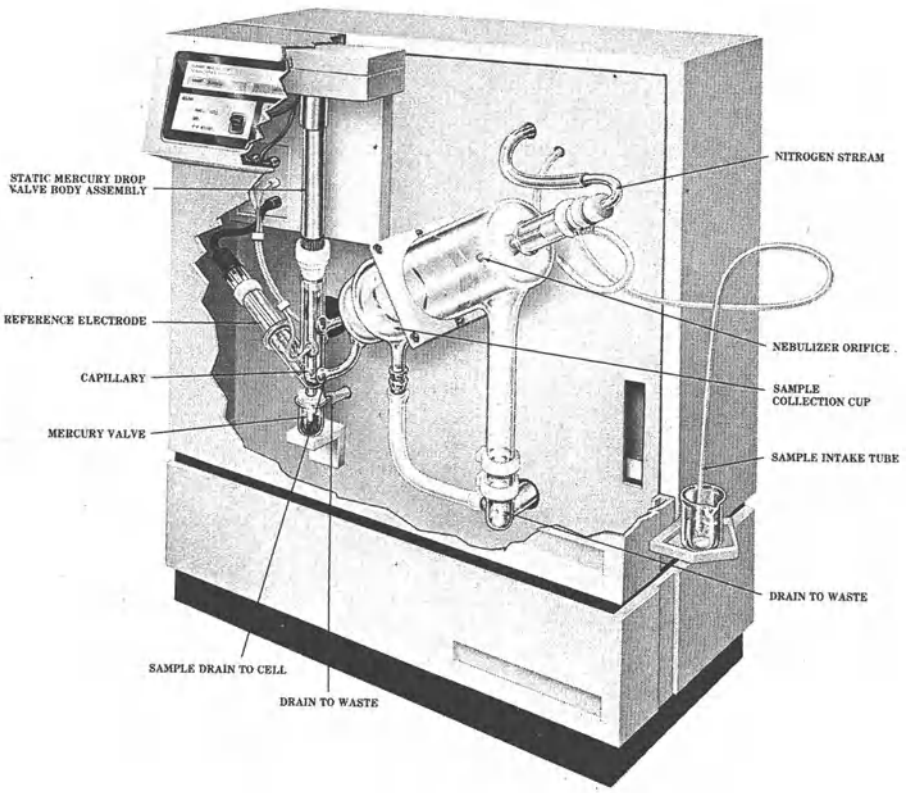

Fig. 12.2 An automated instrument for routine voltammetric analysis. (Courtesy: EG & G and PAR Electrochemical Instruments Division.)

separated peaks when $\Delta E_{\frac{1}{2}} > 50$–$80$ mV. The most successful techniques are differential-pulse polarography and square-wave polarography which employ a pulse profile which leads directly to a differentiated curve while giving the increased response due to non-steady-state diffusion. These modified polarographic methods are illustrated in Fig. 12.1 and compared in Table 12.1. Computer-controlled instrumentation for such analyses is now readily available.

In many sectors of industry, including process control, medical testing, pharmaceutical development and water analysis, there is an increasing pressure to process samples routinely, in a rapid, automated and consistent fashion. Conventional manual polarography usually requires 5–10 min per sample, a large fraction of this time (up to 4 min) being required for deaeration of the sample with nitrogen gas in order to remove troublesome oxygen reduction waves. Recently, a number of automatic, voltammetric analysis instruments have been introduced, capable of processing many samples (up to eighty in some cases) sequentially. An example is provided in Fig. 12.2. Rapid (< 50 s) deaeration is achieved by a nebulizer (similar to the type used in flame atomic absorption spectroscopy) and a small cell volume. Analysis time, using square-wave voltammetry, may be as low as 10 s, giving an overall sample time of 1 min. Built-in rinse cycles serve to prevent sample carry-over. A typical instrument process sequence is:

1. A mercury valve creates a slight vacuum, pulling the previous sample from the cell.
2. A fresh sample is transferred to the cell by a stream of nitrogen gas exhorting venturi action over the sample tubing orifice.
3. The sample is nebulized into small droplets to allow efficient and rapid removal of dissolved oxygen.
4. The sample droplets collect at the bottom of the nebulization chamber and the deaerated solution is transferred to the cell (sensing electrodes in the cell ensure that an appropriate volume is transferred).
5. Voltammetry is carried out on the sample, using a static Hg drop electrode, DME or vitreous carbon electrode as appropriate.

Such instruments greatly facilitate routine analysis of samples containing *c.* 50 μg dm^{-3} species and help remove the tedium and imprecision of manual transfer; they are not suitable, however, for solvents of high vapour pressure, high viscosity or high surface tension.

In anodic stripping voltammetry, additional sensitivity is obtained by preconcentrating the metal ion or ions to be determined in the mercury electrode in the form of an amalgam and the determination is carried out by measuring the current for the reoxidation of the amalgam. Hence the experiment has three parts:

1. In the first, a potential is applied to a mercury electrode such that one or all of the metal ions in solution is/are reduced to their amalgam at a mass-transfer-controlled rate. Clearly, the sensitivity of the analysis can be increased by

Table 12.1 Comparison of modern polarographic methods

Method	Measurable parameters		Selectivity Minimum $\Delta E_{\frac{1}{2}}$/mV	Sensitivity Minimum detection limit/mol dm^{-3}	Wave order important?
	Qualitative	Quantitative			
Polarography	$E_{\frac{1}{2}}$	I_L	200	5×10^{-6}	Yes
Derivative polarography	E_{max}	$(dI/dE)_{max}$	50–100	5×10^{-6}	No
Pulse polarography	$E_{\frac{1}{2}}$	I_L^P	200	10^{-8}	Yes
Differential pulse polarography	E_{max}	ΔI_{max}^P	50	10^{-9}	No
Square wave polarography	E_{max}	I_{diff}	50	10^{-9}	No

extending the period of formation of the amalgam, minimizing the volume of the mercury electrode and carrying out the deposition under conditions of forced convection. For the latter reasons, it is now common to use a rotating carbon disc plated with a thin film of mercury as the working electrode. The traditional working electrode is a stationary mercury drop. A more recent development involves the use of a mercury ultra-microelectrode where the very high rate of spherical diffusion during the deposition stage and the very low mercury volume combine to give excellent sensitivity.

2. After the period of deposition, the electrode is allowed to stand on open circuit for a short period so that the concentration of metal(s) in the mercury becomes uniform throughout the film or drop electrode.
3. Finally, the concentration of metal(s) in the amalgam is determined by programming the electrode potential to values where the metal(s) are reoxidized to their ions in solution. In practice, the optimum presentation is obtained using the potential–time profile of differential pulse polarography.

The potential–time profile for anodic stripping voltammetry and a typical experimental curve for the determination of a mixture of heavy-metal ions are shown in Fig. 12.3. The method is clearly limited to the determination of metals which form simple amalgams (intermetallic compounds must also be avoided). This limitation, however, introduces some desirable selectivity and most organic compounds will not interfere with the determination of the metals. Analysis of very low concentrations is possible using acceptable deposition times. Certainly for heavy-metal ions, the sensitivity of anodic stripping analyses compares well

Table 12.2 Comparison of lowest detection limits by anodic stripping voltammetry and atomic absorption spectroscopy

Metal ion	Lowest detection limit/10^{-9} g cm^{-3}		
	Anodic stripping voltammetry*	Atomic absorption spectroscopy	
		Flame	Non-flame
Bi^{3+}	0.01	46	3
Cd^{2+}	0.005	0.7	0.01
Cu^{2+}	0.005	2.0	0.3
Ga^{3+}	0.4	38	—
In^{3+}	0.1	38	—
Pb^{2+}	0.01	15	0.5
Sn^{4+}	2.0	30	0.1
Tl^{+}	0.01	13	1
Zn^{2+}	0.04	1	0.008

* Mercury film electrode. Plating for 120 s with rotation at 3600 rev min^{-1}. Analysis by differential-pulse polarographic waveform

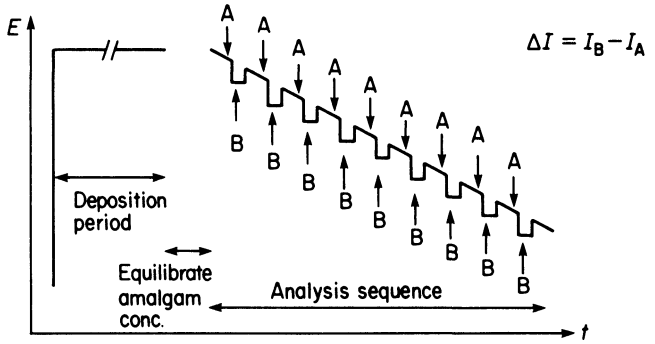

(a)

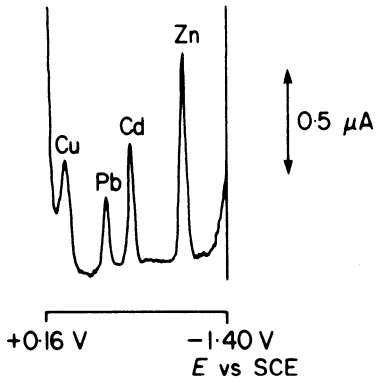

(b)

Fig. 12.3 (a) The *E–t* sequence for anodic stripping analysis. (b) An anodic stripping voltammogram of a solution of KCl (1 mol dm^{-3}) containing 1.5×10^{-7} mol dm^{-3} Zn^{2+}; 8.8×10^{-8} mol dm^{-3} Cd^{2+}; 4.8×10^{-8} mol dm^{-3} Pb^{2+} and 1.55×10^{-7} mol dm^{-3} Cu^{2+}, Hg drop electrode. Plating for 120 s at − 1.4 V. (Results supplied by J. D. Burton and A. M. Ortega, Department of Oceanography, University of Southampton.)

with that of atomic absorption spectroscopy even with non-flame atomization (Table 12.2). Moreover, these data do not represent the ultimate detection limit since the plating time can be extended or an ultramicroelectrode may be used. Hence, anodic stripping voltammetry is the method of choice for the analysis of very low concentrations of heavy-metal ions in water and effluents. Pulse, differential pulse- and square-wave polarography also have their advocates for particular analyses but they do not have the same general acceptance.

12.3 ION-SELECTIVE ELECTRODES

Glass electrodes sensitive to proton concentration were first introduced in 1909 and have long been the generally accepted way of determining pH. Similar electrodes which respond selectively to other ions are a much more recent development dating back only to the mid 1960s; even so, ion-selective electrodes now have many applications in water and environmental analysis, e.g. the determination of pH, F^-, CN^-, NH_3 and total hardness ($Ca^{2+} + Mg^{2+}$).

The cell for the determination of the concentration of an ion, M^{n+}, with an ion-selective electrode is shown in Figs 12.4 and 12.5, although in many cases the ion-selective electrode and the external reference electrode are mounted in a single (combination) probe. The measurement of the potential between the two reference electrodes allows the determination of the ion M^{n+} between the analyte and the internal reference solution. For application in analysis, the membrane potential E_M should be given by:

$$E_M = (2.3RT/nF) \log c/c_S \tag{12.1}$$

where c and c_S are the concentration of M^{n+} in the analyte and the internal reference solution respectively. The cell potential will be given by:

$$E_{CELL} = E_M + \Delta E_{REF} \tag{12.2}$$

where $\Delta_{REF} = 0$ if identical reference electrodes are used. Since c_S is a constant, the equation for the cell potential can be simplified to:

$$E_{CELL} = \text{constant} + (2.3RT/nF) \log c \tag{12.3}$$

so that concentration can be determined from a plot of E_{CELL} vs. $\log c$, a plot which should be linear with a slope of $60/n$ mV.

The success of an analysis with an ion-selective electrode is almost totally dependent on the properties of the membrane. The response of the membrane to changes in the concentration of M^{n+} should be given by equation (12.1), but on the other hand, it should be completely independent of the concentration of

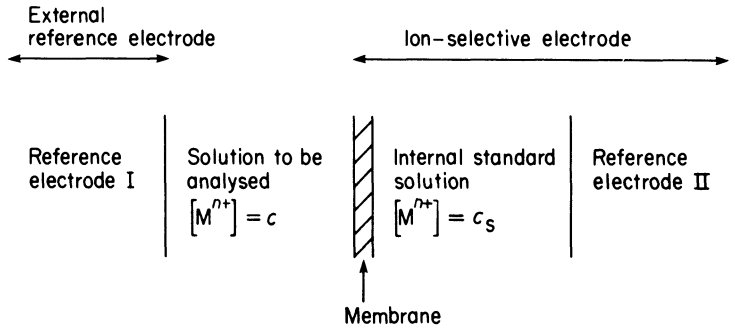

Fig. 12.4 Schematic of cell for analysis of M^{n+} in solution with an ion-selective electrode.

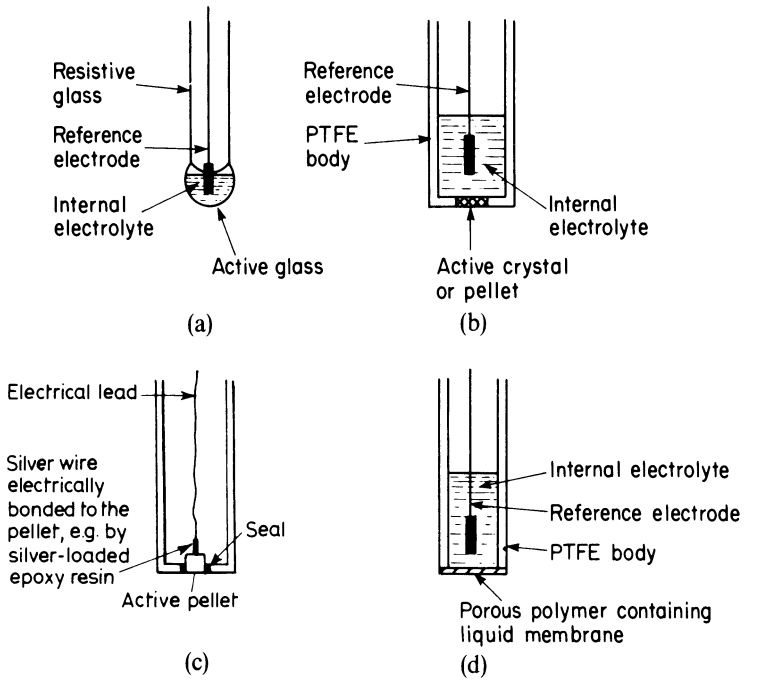

Fig. 12.5 Common constructions of ion-selective electrodes. (a) Glass electrode. (b) Crystal or pellet-membrane electrode with internal reference electrode. (c) Pellet membrane with direct electrical contact. (d) Liquid membrane electrode.

other species in the solution. Moreover, a stable potential should be reached rapidly. The design of membranes is largely empirical because, although it is thought that there is a contribution from both Donnan equilibria at the two membrane–solution interfaces and a diffusion potential within the membrane, the origin of the membrane potential is not fully understood. Certainly, the factors which introduce selectivity for a single ion and speed of response are unclear. In practice, the selectivity is discussed in terms of selectivity constants K_i, where

$$E_{\text{CELL}} = \text{constant} + (2.3RT/nF) \log (c + \Sigma_i K_i c_i^{n/n_i}) \tag{12.4}$$

where c_i is the concentration of the ion $M_i^{n_i+}$ and clearly K_i should be as small as possible. Some typical selectivity coefficients, in fact for a calcium electrode based on a liquid ion-exchange material $(RO)_2PO_2^-$, $R = C_8$ to C_{16} alkyl chains, in dioctylphenylphosphonate, are shown in Table 12.3.

Several quite different types of membranes have been used in the construction of ion-selective electrodes, namely: (1) glasses; (2) solid-state membranes; (3) heterogeneous membranes; and (4) liquid membranes.

Table 12.3 Selectivity coefficients for interferences to a Ca^{2+} ion electrode based on $(RO)_2PO_2^-$ in $(C_8H_{17}O)_2PO(OC_6H_5)$ where $R = C_8$ to C_{17} alkyl chains

Interfering ion	K_i
Mg^{2+}	3×10^{-2}
Ba^{2+}	2×10^{-2}
Zn^{2+}	7×10^{-2}
K^+	1×10^{-4}
Na^+	1.5×10^{-4}

12.3.1 Glasses

The selectivity of such membranes depends on the composition of the glass. Generally they are based on Na_2O–Al_2O_3–SiO_2 mixtures; those rich in SiO_2 but low in Al_2O_3 are selective to protons while those with a high content of Al_2O_3 respond more strongly to alkali metal ions. Unfortunately, selectivity between alkali-metal ions is not good with glass membranes. Two typical compositions are: $Na_2O(22\%) + CaO(6\%) + SiO_2(72\%)$ which responds to H^+ with no interferences below pH 13 and $Na_2O(11\%) + Al_2O_3(18\%) + SiO_2(71\%)$. In the latter case, at low pH, the glass responds to H^+; in neutral solution the response decreases, $Na^+ > Li^+ > K^+$.

The thin membrane of the active glass is sealed to an electrode body of non-responsive, high-resistance glass. The electrode is completed by filling with a buffered chloride solution which connects the inner membrane surface to a Ag/AgCl reference electrode.

For convenience in handling, the ion-selective electrode may be incorporated with the reference electrode (e.g. a calomel electrode) in a single package to form a combination electrode. The combination pH electrode is perhaps the best-known example (Fig. 12.6(a)). Conventional reference junctions in such devices generally utilize porous ceramic plugs, fabric wicks or possibly ground-glass joints as the ionic separator. After periods of (particularly intermittent) use, these junctions may become contaminated or clogged, resulting in restriction of electrolyte flow with a degraded response time and/or corrupted potentiometric response. There have been several attempts to improve the stability of reference junctions. One possibility (Fig. 12.6(b)) is to eliminate the porous reference junction and replace it with a free-flowing tube. The resultant liquid–liquid junction may be stabilized and the reference electrolyte refreshed when required. This is accomplished by a dispenser built into the pH meter which provides a pressurized flow of reference electrolyte to the combination probe.

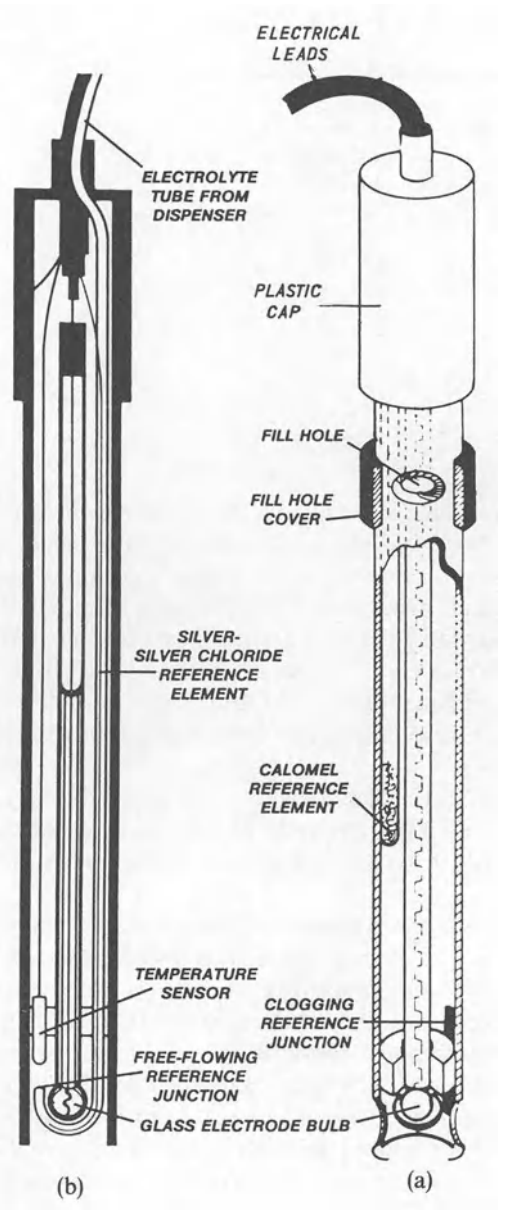

Fig. 12.6 Combination pH probe. (a) Conventional design. (b) Pressurized reference electrode solution. (Courtesy: Hach Co.)

12.3.2 Solid-state membranes

The most successful of these ion-selective electrodes is that for fluoride ion. It is based on a lanthanum fluoride crystal doped with EuF_2 to increase its conductivity) and is stable and reproducible with no interferences, provided the solution is approximately neutral (excess free OH^- and the formation of HF must be avoided). The electrode is usually manufactured with a PTFE body and the LaF_3 crystal is held in position with epoxy resin. The filling solution contains NaF + NaCl and the internal reference electrode is again Ag/AgCl.

In a related type of electrode the membrane is a pressed disc of $Ag_2S + AgX$ where X^- may be Cl^-, Br^- or SCN^- and the electrode responds to X^-. With such a membrane, it is a very low concentration of Ag^+ ions on both sides of the disc which determines the membrane potential and the selectivity is a function of the solubility product; any anion which forms a silver salt with a solubility product lower than the ion being determined will be a serious interference. Hence, the electrode responds strongly to Ag^+ and S^{2-} and for the determination of other ions their presence is catastrophic. Similarly, I^- and Br^- is a serious interference to the Cl^- electrode and I^- to the Br^- electrode. M^{2+} electrodes (M = Cu, Pb, Cd) may be prepared by making a pellet from a mixture of Ag_2S and MS. In these electrodes, the M^{2+} ion activity controls the S^{2-} activity and thereby the Ag^+ activity and, hence, the electrode response. The pellet is again positioned in an inert matrix with epoxy resin.

For convenience of handling and in order to facilitate replacement of the membrane and/or reference electrode element, certain ion-selective electrodes feature a detachable lead and provision for dismantling the probe components.

12.3.3 Heterogeneous membranes

The active component is deposited into the pores of an inert support such as silicone rubber instead of being pressed into a pellet. Otherwise, the systems used are similar to those discussed for pellet electrodes.

12.3.4 Liquid membranes

In these electrodes, the active material is a large organic molecule capable of interacting specifically with an anion or cation. Typical of these materials are the phosphate diesters $(RO)_2PO_2^-$, used for calcium ion electrodes, metal complexes used for anion electrodes and the neutral macrocyclic crown ethers which are suitable for alkali–electrodes. The active organic molecule is adsorbed onto an inert porous support or dissolved in an organic solvent, and indeed their selectivity can be affected by the choice of medium. Some typical electrodes are shown in Table 12.4.

While such electrodes can have acceptable selectivity they are not as robust as some of the other membrane electrodes and can only be used in certain

Table 12.4 Ion-selective electrodes based on liquid membranes

Active materials	Solvent	Ion electrode
tris-(1,10-phenanthroline)$Fe^{2+}(ClO_4^-)_2$	*p*-Nitrocymene	ClO_4^-
$(C_{12}H_{25})_3C_{16}H_{33}N^+NO_3^-$	n-C_8H_{17}–O–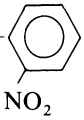	NO_3^-
Valinomycin	Hydrocarbon	K^+
$(C_{10}H_{21}O)_2PO_2^-$	$(C_8H_{17}O)_2PO(OC_6H_5)$ $C_{10}H_{21}OH$	Ca^{2+} $Ca^{2+}+Mg^{2+}$

Table 12.5 Typical specifications for some commercial ion-selective electrodes

Ion electrode	Membrane	Concentration range/mol dm^{-3}	Major interferences
H^+	Glass	10^{-14}–1	None
K^+	Valinomycin	10^{-6}–1	Cs^+, NH_4^+
Na^+	Glass	10^{-6}–sat.	Ag^+, H^+, Li^+
F^-	LaF_3	10^{-6}–sat.	OH^-, H^+
Cl^-	$Ag_2S/AgCl$	10^{-5}–1	Br^-, I^-, CN^-, S^{2-}
Br^-	$Ag_2S/AgBr$	10^{-6}–1	I^-, CN^-, S^{2-}
I^-	Ag_2S/AgI	10^{-7}–1	CN^-, S^{2-}
CN^-	Ag_2S/AgI	10^{-6}–10^{-2}	I^-, S^{2-}
S^{2-}	Ag_2S	10^{-7}–sat.	Hg^{2+}
Ag^+	Ag_2S	10^{-7}–1	Hg^{2+}
Cd^{2+}	CdS/Ag_2S	10^{-7}–1	Ag^+, Hg^{2+}, Cu^{2+}
Pb^{2+}	PbS/Ag_2S	10^{-7}–1	Ag^+, Hg^{2+}, Cu^{2+}
Cu^{2+}	CuS/Ag_2S	10^{-8}–sat.	Ag^+, Hg^{2+}, S^{2-}
Ca^{2+}	$(RO)_2PO_2^-/(RO)_3PO$	10^{-5}–10^{-1}	Zn^{2+}, Fe^{2+}, Pb^{2+}, Cu^{2+}
$Ca^{2+}+Mg^{2+}$ (hardness)	$(RO)_2PO_2^-/ROH$	10^{-7}–1	Cu^{2+}, Zn^{2+}, Fe^{2+}, Ni^{2+}, Pb^{2+}
NO_3^-	R_4N^+/ether	10^{-5}–1	ClO_4^-, ClO_3^-, I^-, Br^-

conditions where the solubility of the active organic molecule is very low. Their response times can also be undesirably long.

A wide variety of ion-selective electrodes are now available (Table 12.5) and the only essential instrumentation required is a high-impedance voltmeter to monitor the potential difference between the measuring electrode and the external reference electrode. The voltmeter must, however, be capable of

accurate measurement since an error of 0.1 mV in the measurement of potential introduces an inaccuracy of almost 1% in the ion analysis (a 1 mV error in potential leads to a concentration error of 4% and 8% for singly and doubly charged ions respectively).

Moreover, ion-selective electrodes can be manufactured in very robust probes and, provided they are protected from fouling and physical attrition, can often be used for continuous and on-line analyses as well as laboratory determinations. Their application is expected to increase substantially in the coming years as active electrode materials continue to be improved and instrumentation becomes increasingly automated, simplifying its use.

One of the most ambitious trends in ion-selective electrode design is the development of ion-selective membranes combined with a metal oxide semiconductor field-effect transistor (MOSFET) such as 'ISFETs' in a single package. Rapid advances are being made with these devices which would facilitate miniaturization.

12.4 PORTABLE AND ON-LINE DEVICES

The criteria used to judge an analytical device for fieldwork and on-line monitoring are often quite different from those for a procedure to be employed in a laboratory with full facilities. Clearly, portable devices should be small, light, robust, and auxiliary equipment such as gas supplies should be avoided; both the active components and the control electronics must be capable of miniaturization and not require frequent adjustment or calibration. On the other hand, the device need only have the selectivity, sensitivity and speed of response essential to the particular analysis. Thus, for example, the method need only discriminate against interferences likely to be found in the particular situation of the analysis. Electrochemical cells and their control circuits are much more able to meet these requirements than the other common analytical techniques (e.g. chromatography and spectroscopy) and their output is well-suited to continuous monitoring or as an input to a control loop or an automatic warning.

It will be apparent from the previous section that ion-selective electrodes can be made suitable for analysis in the field and that, in circumstances where the overall composition of the medium is not too variable, they may also be used directly to monitor metal ion and/or anions in plant streams, effluents, water supplies and even rivers. In such applications of ion-selective electrodes, however, it is necessary to avoid electrical pick-up and ground loops by correct placement and shielding of the electrodes. In some applications, electrolyte preconditioning may be necessary and in many cases, the flow environment must also be controlled via suitable design of the ion-selective electrode–reference electrode cell. There are also many other situations where the capabilities of electrochemistry and the characteristics of an analysis can be matched to allow the manufacture of on-line or portable devices. The actual measurement may be the potential of an ion-selective electrode, the mass transport controlled current

at an electrode held at constant potential, or even conductivity. This latter measurement, for example, remains the optimum way of estimating the total salt concentration in solution and may be used to monitor the quality of rinsing and washing operations in metal-finishing processes.

The analysis of industrial water involves an extremely wide range of samples, ranging from almost pure water to mixtures containing high levels of soluble and undissolved species. One of the most important examples of trace analysis of high-quality water is provided by conventional power stations (Figure 12.7). The continuing search for higher thermal efficiency has resulted in an increase in the size and operating pressure of steam-raising plant, necessitating close control of the water quality to prevent corrosion, deposition of thermally insulating scale or blockage. A range of species may be determined electrochemically (Table 12.6) using on-line sensors. As an example, Fig. 12.8 illustrates a sodium monitor, utilizing a sodium selective-glass electrode. Both chemical pretreatment of the sample and temperature stabilization are applied to the sample prior to its exposure to the probe. A sodium free, alkaline reagent (e.g. ammonia solution) raises the pH to approximately 11. The whole analytical system is thermostatted by controlling the air temperature and the system is calibrated automatically by periodic operation of a change-over valve which allows a calibrant to be substituted for the sample.

The fouling of sensors by, for example, scale, organic compounds or biofilms may cause serious problems in heavily contaminated samples. In certain cases, the sensor and its assembly are designed to incorporate a self-cleaning device, which may utilize mechanical jet flow or even ultrasonic methods. Mechanical

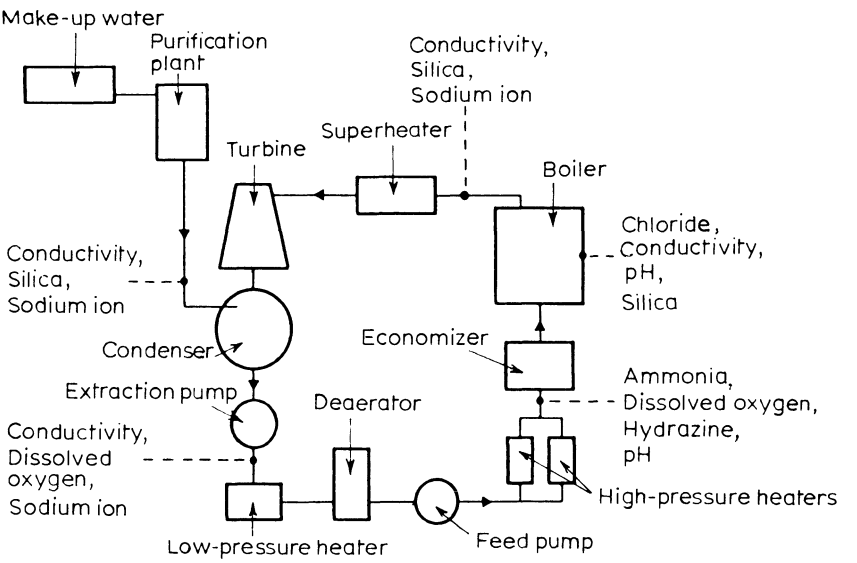

Fig. 12.7 The steam-water circuit of a conventional power station.

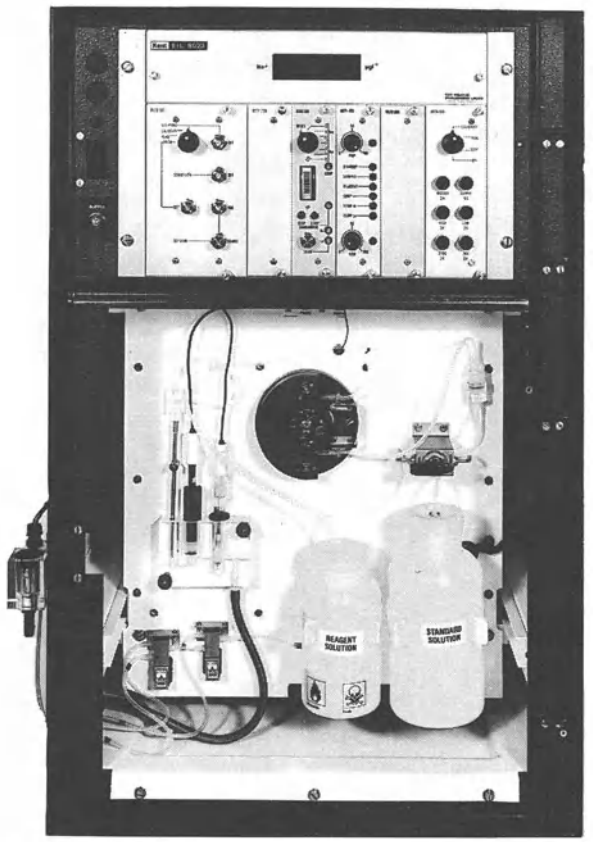

Fig. 12.8 A dissolved sodium monitor based upon an Na^+ ion selective electrode. (Courtesy: Kent Industrial Measurements Ltd.)

Table 12.6 Electrochemical sensors used for on-line monitoring in the power generation industry

Species	Range/$\mu g\,dm^{-3}$	Type of sensor	Type of membrane
H^+	(pH 6–11)	Potentiometric	Glass
Na^+	0.1–500	Potentiometric	Glass
Cl^-	0–2000	Potentiometric	Mixed inorganic salt
NH_3	50–10 000	Potentiometric	Gas-permeable
N_2H_4	0–200	Amperometric	(None)
O_2	0–2000	Amperometric	Gas-permeable

cleaning is useful for crusty, scaly deposits such as calcium salts while ultrasonic cleaning is often preferred to prevent deposition of organics and fine suspended matter. In either case, the probe must be designed specially to withstand the cleaning process (Fig. 12.9). A number of gas-sensing electrodes are manufactured which function by interposing a gas-permeable membrane between the test solution and the sensing element (see Fig. 12.10). The gas diffuses through the organic polymer membrane (e.g. PTFE, polyethylene, silicone rubber) into a thin film of electrolyte between the membrane and the ion-selective electrode. The electrolyte and the ion-selective electrode are chosen to introduce selectivity between gases and the film of electrolyte is as thin as possible so that it equilibrates rapidly following a change in the composition of the test solution. The probes are complete cells including a reference electrode. Some typical gas-sensing electrodes are described in Table 12.7.

Monitors for oxygen are again based on the diffusion of the gas through a permeable membrane but in this case the parameter often measured is the

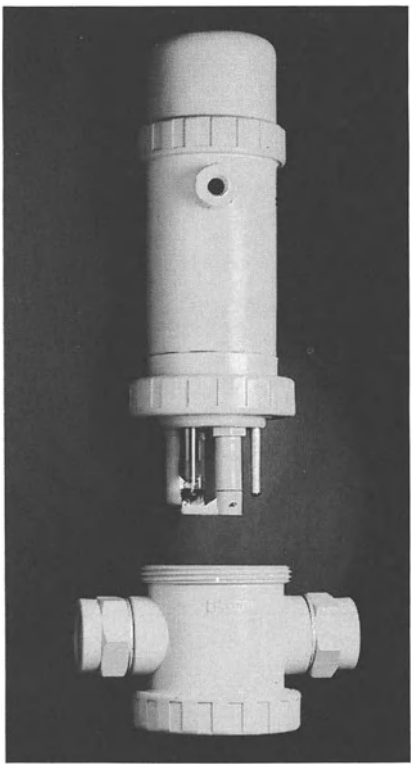

Fig. 12.9 A pH measurement system for industrial use. The robust assembly includes a pH electrode, reference electrode, temperature compensator and a mechanical cleaner. (Courtesy: Kent Industrial Measurements Ltd.)

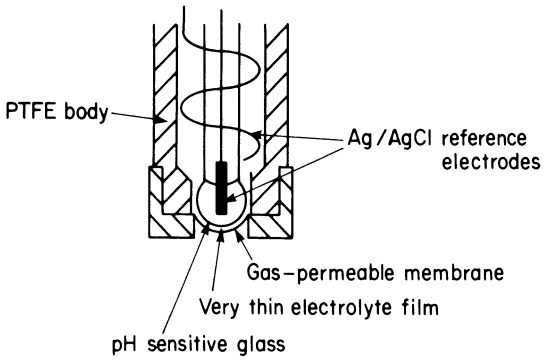

Fig. 12.10 The construction of a gas-sensing ion-selective electrode. This example has a pH-sensing electrode.

limiting current for the cathodic reduction of the oxygen. Devices for measuring oxygen in blood levels via the oxygen diffusing through the skin and atmospheric oxygen are also commercially available. This latter measurement is particularly favourable since the oxygen range normally of interest is 15–21% and there are no other gases which are reducible and present in significant concentration. Figure 12.11 illustrates the principles of design of two such oxygen meters, and portable units are shown in Fig. 12.12. In the first, a PTFE membrane is stretched across a head containing a gold disc-working electrode surrounded by a silver ring which acts as the counter and reference electrode since the electrolyte is a chloride solution. In the second, the metal for the working electrode is deposited by sputtering techniques directly onto the PTFE membrane; this minimizes the response time of the detector which can then be < 1 s. The metal

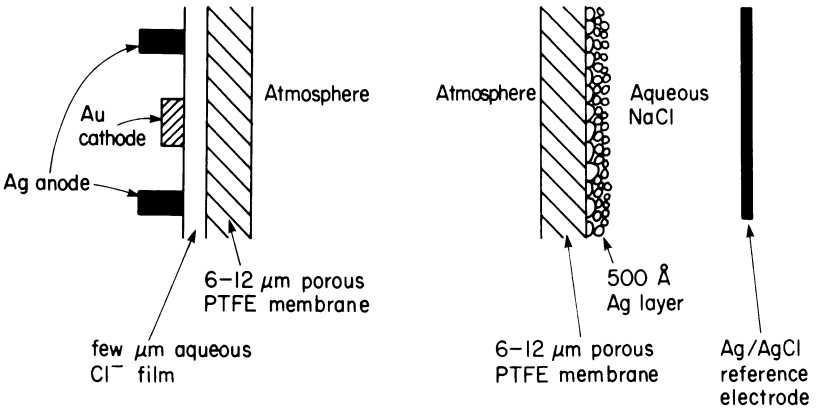

Fig. 12.11 Design principles of two amperometric atmospheric oxygen sensors.

Table 12.7 Construction and performance of gas sensing ion-selective electrodes

Gas	Ion-selective electrode	Electrolyte	Membrane	Concentration range/mol dm^{-3}	Serious interferences
H_2S	S^{2-}	Citrate buffer pH 5	Polypropylene	10^{-6}–10^{-2}	None
NH_3	pH	0.1 mol dm^{-3} NH_4Cl	PTFE	10^{-1}–1	Volatile amines
CO_2	pH	0.01 mol dm^{-3} $NaHCO_3$ + 0.1 mol dm^{-3} NaCl	PTFE	10^{-2}–10^{-4}	Volatile weak acids
NO_2	pH	0.1 mol dm^{-3} $NaNO_2$ + 0.1 mol dm^{-3} NaCl	PTFE or polypropylene	10^{-6}–10^{-2}	Volatile weak acids
SO_2	pH	0.1 mol dm^{-3} $K_2S_2O_5$ + 0.1 mol dm^{-3} NaCl	PTFE or silicone rubber	10^{-6}–10^{-2}	Volatile weak acids
HCN	Ag^+	10^{-2} mol dm^{-3} $KAg(CN)_2$	Polypropylene	10^{-7}–10^{-1}	Sulphide

(a)



(b)



Fig. 12.12 Portable (battery-powered) electrochemical sensors for gaseous oxygen. (a) A typical application for the device is monitoring the atmosphere during welding or cutting or grinding operations on metal in confined spaces. Other uses include atmospheric monitoring during inspection and repair of tanks (e.g. ballast tanks on-board ship) and pipelines, e.g. sewers. (b) Similar devices may be used to monitor a boiler system. (Courtesy: Neotronics Ltd.)

used is silver since this was found to give the best-formed reduction wave for oxygen. Similar cells are available for monitoring chlorine in atmospheres and in solution. Typically the cells including the control electronics are the size of a small torch and they may have analogue or digital readouts with provision for audible alarms corresponding to preset minimum and maximum levels.

In recent years there has been some success in modifying such membrane polarographic cells for monitoring toxic gases from car exhausts and industrial discharges, e.g. H_2S, SO_2, NO_2, NO and CO. These analyses are, however, much more challenging because: (1) the concentration range of interest is 1–100 p.p.m. (much lower than for oxygen); (2) the electrode reactions are subject to poisoning and vary in rate with the state of the electrode surface; and (3) there is an interference problem because all the gases mentioned may be oxidized. In general, sufficient sensitivity and selectivity can be obtained even if it is necessary to introduce gas filters into the gas feed to the cell. It does, however, remain necessary to calibrate the meters regularly, even daily, and this is often inconvenient.

Gas potentiometric sensing probes are now available for NH_3, amines, HCN and CO_2. Amperometric gas diffusion probes are preferred for H_2, HCl, ClO_2, H_2S, SO_2, CO, AsH_3, PH_3, SiH_4, F_2, Br_2, I_2, Cl_2, NO_2 and HF and combustible gases. Other. closely related devices based on diffusion of a gas through a membrane employ conductivity for the measurement technique; CO_2 and SO_2 are typical gases for which such sensors are available. This wide range of sensors finds use in fields including semiconductor manufacture, petrochemicals and mining as well as the treatment of water and effluents.

The application of portable electrochemical sensors to personal health and safety is of undeniable importance, e.g. portable oxygen monitors are an essential device during the inspection and maintenance of chemical reactors, ships' ballast tanks and sewers (Fig. 12.12). Portable CO and O_2 sensors are commonly used to monitor flue gases as an indicator of combustion efficiency while H_2S, SO_x and NO_x sensors serve to monitor flue-gas discharge levels.

There are several circumstances where the sensing and measurement of gaseous hydrogen is important. In particular, the monitoring of hydrogen in process plant for health and safety or process control reasons and of hydrogen penetration through steel vessels and pipework as an indication of corrosion are becoming increasingly important. An example of a process stream is provided by boiler feedwater or condensate. As described in Chapter 10, corrosion of iron or steel in acid or neutral media often proceeds, at least in part, via hydrogen evolution. The atomic hydrogen first produced is mobile, small and penetrating, giving rise to possible problems of hydrogen embrittlement, hydrogen blistering or hydrogen induced stress-corrosion cracking. Probes have recently been developed which monitor the current due to hydrogen penetration through, for example, a pipe wall. An example is given in Fig. 12.13. Following surface cleaning, a piece of palladium foil (thickness 250 μm) is attached to the pipe via a flexible seal around its edges. The 'patch probe' is then mounted over the foil and

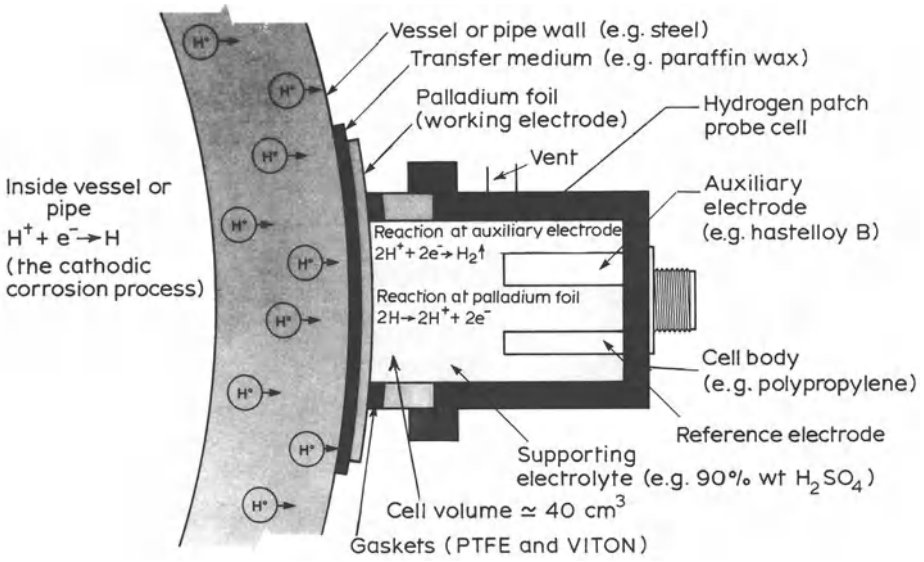

Fig. 12.13 An electrochemical 'patch probe' for the measurement of the hydrogen penetration rate through a process vessel or pipe. (Courtesy: Petrolite Corp.)

clamped in place over the foil via leak-tight gaskets. When the palladium foil is polarized anodically, it acts as an indicator electrode, quantitatively oxidizing hydrogen as it emerges. After an initial settling period, the current flowing between working and auxiliary electrodes is taken to indicate the real-time hydrogen penetration. The probe may be moved to another location relatively easily and will operate over a wide range of temperatures from -23° C to $+143^\circ$ C; hydrogen flux currents up to 5 mA may be measured. Other dissolved hydrogen sensors consist of a platinum anode and an Ag or AgCl cathode protected from the sample by a thin PTFE membrane. An aqueous HCl or KCl solution is retained in the sensor as the electrolyte. Hydrogen diffuses through the membrane to the anode where it is oxidized to H^+ with concurrent reduction of AgCl at the cathode. Typically, a potential of approximately 500 mV is applied between the electrodes, the observed current being proportional to the partial pressure of hydrogen in the liquid. Such devices are capable of measuring in the parts per million or even parts per billion range.

Other oxygen and toxic-gas monitors are based on fuel-cell technology, the current being measured between a porous fuel cell working electrode and a counter-electrode. The problems and successes of this approach are very similar to those of the membrane cells described above. An interesting variation has been used to manufacture a 'breathalyser' which has been accepted by several national and state police forces. It is based on two Pt-catalysed porous fuel cell electrodes (Fig. 12.14). The cathode is open to the atmosphere so that the reduction of oxygen can occur when a suitable fuel is present at the anode and to

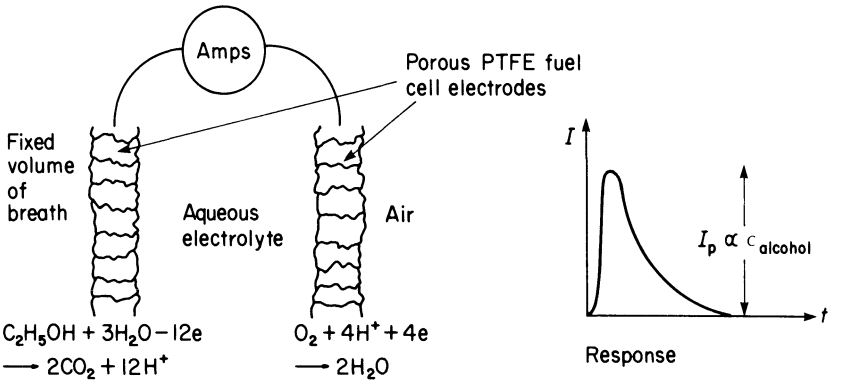

Fig. 12.14 The principle of an electrochemical breathalyser.

activate the cell a fixed volume (1 cm^3) of the suspect's breath is fed to the anode. No potential is applied across the electrodes so that the experiment can be considered as a form of coulometry at the open-circuit potential of the anode in the presence of ethanol, and the cathode in the presence of air. In fact, the current is measured as a function of time; the current goes through a peak and this peak current is found to have a satisfactory relationship with alcohol in breath (using the charge for the complete oxidation of the ethanol would be theoretically sounder but would substantially increase the measurement time). Carbon monoxide, hydrogen and acetone (found in the breath of, for example, smokers and diabetics) are found not to interfere.

12.5 ELECTROCHEMICAL BIOSENSORS

Undoubtedly, two of the biggest growth areas for electrochemical sensing devices and instrumentation lie in biochemical and biomedical applications. Laboratory developments have involved a remarkably wide range of species but we will restrict this section to those sensors which are available commercially and which have become acceptable to biochemists and biomedical practitioners.

While there is considerable overlap, the application areas for biosensors include:

1. Laboratory measurements of pH, pO_2, glucose, penicillin and certain enzymes in a range of media including tissue extracts and body fluids such as blood, saliva and urine.
2. Laboratory immunoassays in which the sensitivity of electrochemical detection is combined with the specificity of an antibody–antigen interaction.
3. 'In-vivo' measurements, where the sensor is inserted into the body or perhaps into a pumped recycle loop incorporating a body fluid.
4. Industrial process control of biochemical synthesis such as fermentation and other enzyme-driven reactions.

Electrochemical sensors offer several potential advantages in such applications including:

1. Rapid, selective analysis.
2. The facility of continuous monitoring in order to follow dynamic changes in biochemical kinetics or physiological state. This is often of critical importance in clinical and health-care applications.
3. They put out an electrical signal, which may be readily displayed, recorded, incorporated into a microcomputer database, or relayed to remote instrumentation, e.g. prenatal dissolved oxygen probes may be left attached to the foetus since they do not require direct connection to the instrumentation: a telemetry link allows the mother an improved freedom of movement.
4. Many electrochemical probes are easily miniaturized, encouraging their application to small or difficult zones in the body.

There are some special (and sometimes critical) requirements of electrochemical measurement devices for biomedical applications:

1. Reliability of the probe and its associated equipment and instrumentation.
2. Ease, speed and efficiency of calibration.
3. Health and safety conditions dictate that appreciable currents must not be induced in the body. Electrical isolation is therefore essential.
4. The probe must be biocompatible and rapidly sterilizable by, for example, gamma rays or gaseous ethylene oxide.
5. In some cases, a disposable sensor is required.

In practice, the electrochemical sensor often has a temperature probe associated with it. This facilitates concurrent monitoring of temperature and facilitates temperature compensation when needed.

The most commonly used biomedical sensors are the dissolved oxygen pO_2 and pH electrodes, although enzyme electrodes for glucose and penicillin are becoming more widely accepted.

12.5.1 Dissolved oxygen sensors

Many of the commercial probes are based on a Clark-type electrode (Fig. 12.15) which effectively responds to oxygen via its cathodic reduction under mass-transport control (section 12.4). The medical applications for dissolved oxygen include the following:

1. Comparison of pO_2 in the arteries and veins provides an indication of the efficiency of the cardiovascular system, e.g. cardiopulmonary bypass surgery uses an on-line sensor to monitor flowing blood in a 'T' piece (Fig. 12.16).
2. A special case of arterial pO_2 measurement is the monitoring of umbilical blood to prevent undue deficiency (hypoxaemia) or excess (hyperoxaemia) of oxygen.

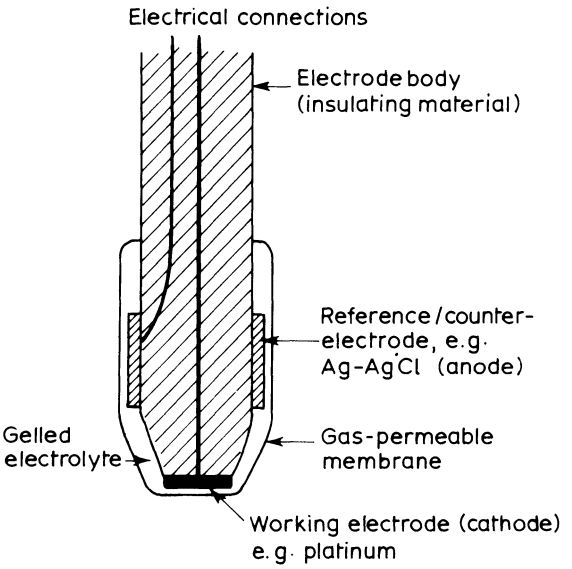

Fig. 12.15 A Clark-type electrode for amperometric dissolved oxygen measurement. (see also Clark, L. C., Wolf, R., Granger, D. and Taylor, Z. (1953) *J. Appl. Physiol.*, **6**, 189.)

3. Arterial pO_2 is often monitored during anaesthesia or intensive care.
4. Transcutaneous (tissue) pO_2, e.g. in the human eye, conjunctural tissue may be probed with a special (disposable) sensor (Fig. 12.17). This measures oxygen levels at the palpebral conjunctiva (a peripheral tissue supplied with O_2 by the internal carotid artery). Such non-invasive monitoring is helpful as an indication of tissue oxygenation in patients during surgery, in intensive care, on mechanical ventilation or with cardiopulmonary problems. The electrode consists of a Clark electrode (Pt cathode and Ag/AgCl anode), the cathodic reduction of oxygen giving a current which is proportional to O_2. An in-built thermistor provides automatic temperature measurement and compensation. The surface of the electrode is covered by a drop of electrolyte, a nylon mesh spacer and a porous polypropylene membrane, held in place by a retainer ring. This sensor, like many voltammetric O_2 electrodes, shows interference from halothane anaesthetic (although 70% N_2O, 2% halothane appears to cause little interference).

Fig. 12.16 The application of dissolved oxygen sensors to blood monitoring. (a) A heart bypass operation. (b) Blood gas analysis detectors and instrumentation (only the pO_2 sensor is electrochemical). (Photograph courtesy: Biomedical Sensors Ltd.)

(a)



(b)

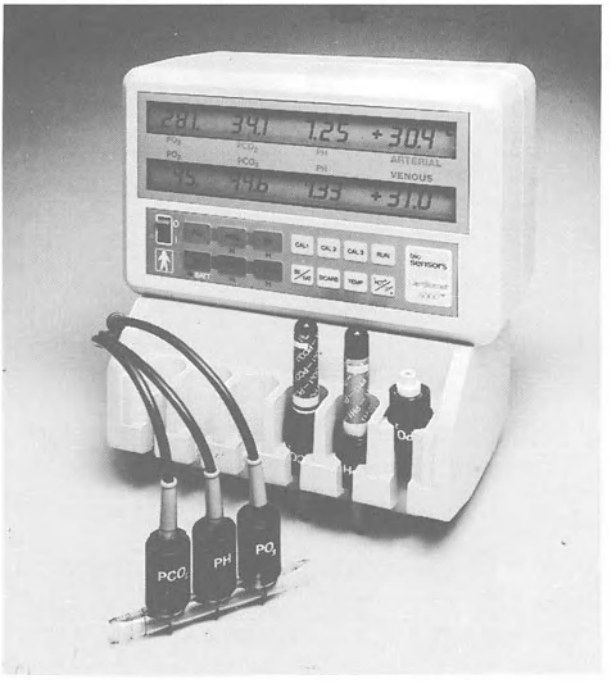

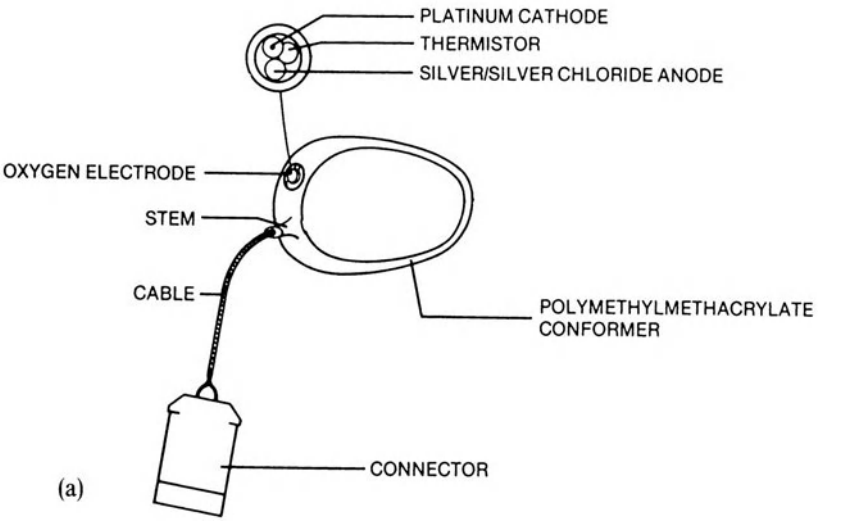

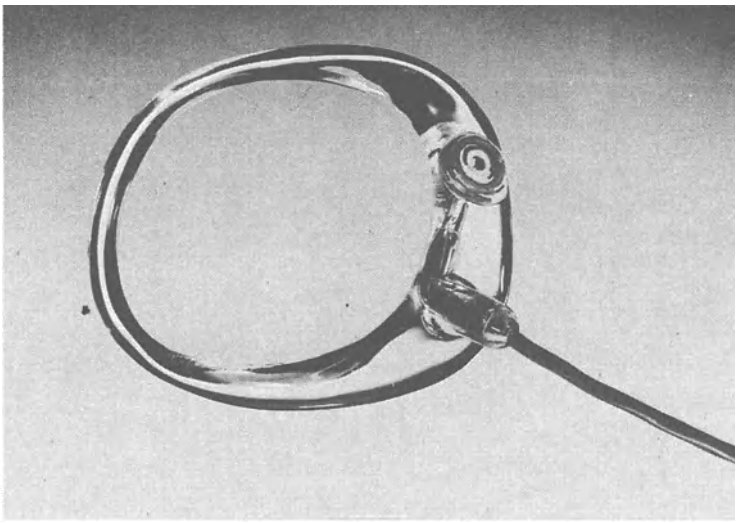

Fig. 12.17 A dissolved-oxygen electrode used to monitor conjunctival oxygen. The sensor is positioned under the patient's eyelid. (Courtesy: Biomedical Sensors Ltd.)

12.5.2 Enzyme electrodes

The chemical specificity of enzymes is increasingly being exploited in a range of electrochemical sensors. Simple enzyme electrodes result from the combination of an amperometric electrochemical sensor with a thin (10–250 μm) layer of enzyme. The most developed of these is the glucose oxidase electrode for glucose

analysis which is based upon:

$$\text{Glucose} + O_2 \xrightarrow[\text{oxidase}]{\text{glucose}} \text{Gluconolactone} + H_2O_2 \tag{12.5}$$

This reaction may be monitored by oxygen uptake or peroxide production. In principle, a large number of oxidoreductase enzymes are available, offering many possibilities for species determination. There are, however, several practical difficulties which require attention. One problem is oxygen limitation. When the concentration of unbound oxygen is sufficiently low, it restricts the rate of electron transfer; this is a particular problem during some *in vivo* measurements. The solutions include:

1. Design the sensor such that oxygen supply is no longer limiting.
2. Replacement of oxygen with an artificial electron transfer mediator, such as ferrocene-based molecules.

While both techniques have been described, the latter has received greater attention. The role of the mediator is to efficiently shuttle electrons between the electrode and the enzyme (Fig. 12.18). The most common mediators are based upon ferrocene (i.e. *bis*(η^5-cyclopentadienyl) iron and its derivatives or analogues. The mediator may be used to modify other molecules including proteins, while retaining the properties of a simple, one-electron redox couple. Ferrocene (and its derivatives) in their oxidized, ferricinium ion form, will act as electron acceptors to a number of flavoproteins including pyruvate oxidase, diaphorase, alcohol dehydrogenase and xanthine oxidase. However, the most successful application has been the amperometric enzyme electrode for glucose. Here, a water-soluble substituted ferrocene mediates electron transfer between an immobilised glucose oxidase (GOD) and a graphite electrode:

$$\text{Glucose} + \text{GOD}_{ox} \longrightarrow \text{Gluconolactone} + \text{GOD}_{red} \tag{12.6}$$

$$\text{GOD}_{red} + 2Cp_2Fe^+ \longrightarrow \text{GOD}_{ox} + 2Cp_2Fe \tag{12.7}$$

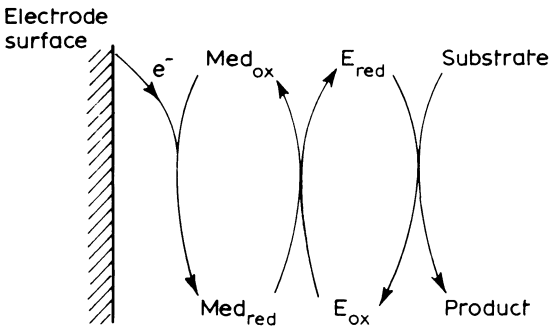

Fig. 12.18 The sequence of events in a mediated enzyme electrode. E_{ox} and E_{red} are the redox forms of the enzyme; Med_{ox} and Med_{red} are those of the mediator.

Once reduced, the ferricinium ion can be regenerated at the electrode:

$$2Cp_2Fe \longrightarrow 2Cp_2Fe^+ + 2e^- \tag{12.8}$$

A linear current response, proportional to the glucose level is observed over a useful (1–30 mmol dm^{-3}) range found in diabetic blood samples. The response is substantially free from oxygen interference.

Other, practically useful, enzyme electrodes include those based on urease and penicillinase. The penicillin electrode utilizes a pH electrode with immobilized penicillinase. It is widely used to monitor the penicillin content of fermentation reaction mixtures:

$$\text{Penicillin} \xrightarrow{\text{penicillinase}} \text{penicilloic acid} \tag{12.9}$$

the generated H^+ being sensed by a pH electrode. One versatile approach is to utilize a common Clark-type dissolved oxygen electrode which can be used with interchangeable immobilized enzymes. Each enzyme is bound into a gel matrix attached to the electrode tip and glucose, alcohol, lactic acid and lactose enzyme gels are supplied as a starter kit.

A general problem with enzyme sensors is the ease with which overloading can occur, e.g. the majority of sensors cannot be inserted directly into fermentation medium.

12.6 ELECTROCHEMICAL DETECTOR CELLS FOR HIGH-PERFORMANCE LIQUID CHROMATOGRAPHY (HPLC)

In specific circumstances where there happen to be no interferences, the simple voltammetric response of an electrode can be a very convenient monitor in process streams and effluents. Such applications, however, have little generality. An application of electrochemical cells of increasing importance is as a detector for high-pressure liquid chromatographs. Here, the chromatographic column should have already separated the components of the mixture and the ability to record complete i–E responses quite rapidly can be used to identify components and to confirm complete separation (does the i–E curve change through a peak?), while the i_L vs. t record may be used for quantitative analysis.

The available detectors for HPLC involve either bulk properties of the mobile phase (such as refractive index, conductance, dielectric constant) or specific properties of the solute, e.g. ultraviolet, visible or infra-red absorbance, fluorescence, or electrochemical characteristics. The latter class are generally more selective and have a wider dynamic range.

Ideally, an electrochemical detector must possess all of the following properties:

1. High sensitivity, facilitating low detection limits.
2. A wide dynamic response to a range of concentrations.

3. A reproducible and stable response.
4. Rapid response time.
5. Negligible volume and no dispersion to allow plug flow.
6. Similar sensitivity for all solutes.
7. Rapid and convenient change of electrodes, particularly the working electrode.
8. Cheap, inert, easily prepared and reproducible working electrodes.

In practice, no detector fulfils all of these properties and considerable skill and knowledge are often required to select the best compromise.

Electrochemical detectors have the following advantages:

1. High sensitivity and a low detection limits.
2. A broad, linear dynamic range.
3. The possibility of tuning the selectivity and detection signal by judicious control of the experimental conditions, e.g. solvent, flow rate or potential.
4. In certain cases, more than one species may be determined.

However, the species to be determined must be electroactive or capable of being transformed readily to one that is, and the solvent must be relatively conductive. If a compound is not directly electroactive, pre- or post-column reactions may be carried out, e.g. sugars can be oxidized by hexacyanoferrate(III) while unsaturated compounds can be brominated. Other problems with electrochemical detectors include the inexperience of many HPLC users (although this is changing rapidly) and the possibility of electrode poisoning by, for example, adsorbed organics or polymers. The basis of electrochemical detectors is a chemical reaction and therefore the selection/optimization of the design of the detector and its control is more critical than devices for measurement of bulk properties of the mobile phase. In particular, the electrical conductance, pH and solvent composition must be considered. If the required conditions for the electrochemical analysis differ appreciably from those required for the chromatography column, then post-column mixing may be practised. A relatively high conductance is required in order to minimize iR drop in the cell, and it is also advisable to provide a high level of indifferent electrolyte and to minimize background currents. In practice, electrolyte levels (>0.1 mol dm^{-3}) are often used. The importance of pH is illustrated by one of the most important applications of an electrochemical–HPLC, the assay of catecholamines (Fig. 12.19). In practice, pH buffers are frequently used.

12.6.1 Types of electrochemical (EC) detector

While potentiometric and coulometric detectors are used, various amperometric detectors provide the most common type of EC detector for HPLC. Early cell designs included a wide variety of polarographic (mercury) electrodes. While dropping mercury electrodes are still occasionally used, the majority of detectors employ solid electrodes.

Commonly, cells utilize three (working, auxiliary and reference) electrodes. It is desirable to site the reference electrode very close to the working electrode in order to control accurately the potential of the latter. The auxiliary electrode should be positioned sufficiently near to the working electrode to prevent excessive cell voltages. In practice, the reference electrode often has a gelled or microporous ceramic–polymer liquid junction for convenience of handling, while the auxiliary electrode is situated downstream so that its electrode reaction (e.g. gas evolution) does not interfere (chemically or hydrodynamically) with the working electrode reaction.

A multitude of cell designs, many of them interrelated, has been described. Figure 12.20 indicates some of the possible geometries. Of these, the two most common are the channel (including the thin layer type) and wall-jet detectors.

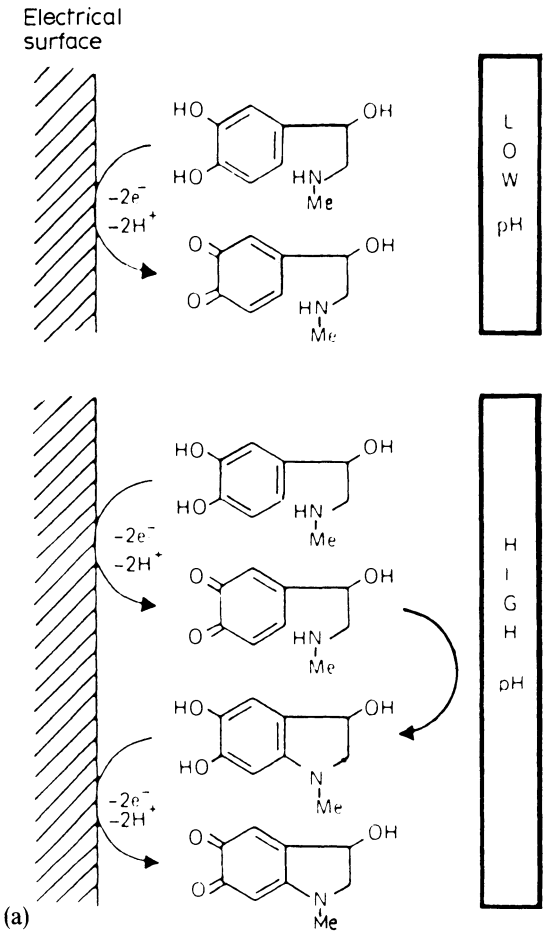

In practice, the detector cells are operated such that the working electrode reaction is under complete mass transport control. The mass transport may then be described by a generalized dimensionless correlation (see also Chapter 2) of the type:

$$Sh = KRe^{a}Sc^{b} \tag{12.10}$$

where the Sherwood, Reynolds and Schmidt numbers are defined in Chapter 2. K, a and b are numerical constants; the value of b may be assumed to be $\frac{1}{3}$, then:

$$Sh = KRe^{a}Sc^{1/3} \tag{12.11}$$

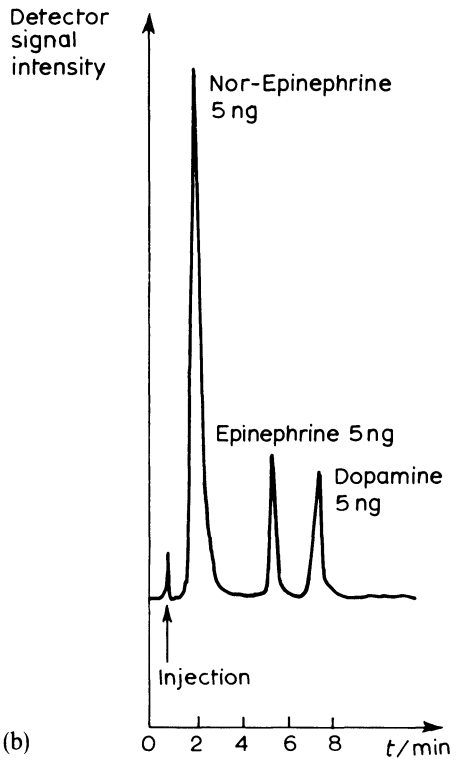

Fig. 12.19 (a) The effect of pH on the electrochemical oxidation of epinephrine during electrochemical–high-pressure liquid chromatography analysis. At high pH, the epinephrine signal is greatly increased; the other catecholamines, norepinephrine and dopamine do not follow this trend. (*After*: Kissinger, P. T., Bratin, K., Davis, G. and Pachla, L. A. (1979) *J. Chromatog. Sci.*, **17**, 137.) (b) Determination of catecholamines (in blood, plasma or urine). Chromatograph conditions: detection limit, 20 pg on column; potential, + 0.65 V; column, C_{18} reverse phase; mobile phase, 5% MeOH, citric acid, sodium acetate and sodium hydroxide; flow rate, 0.5 $cm^3\,min^{-1}$. (Courtesy: EDT Research.)

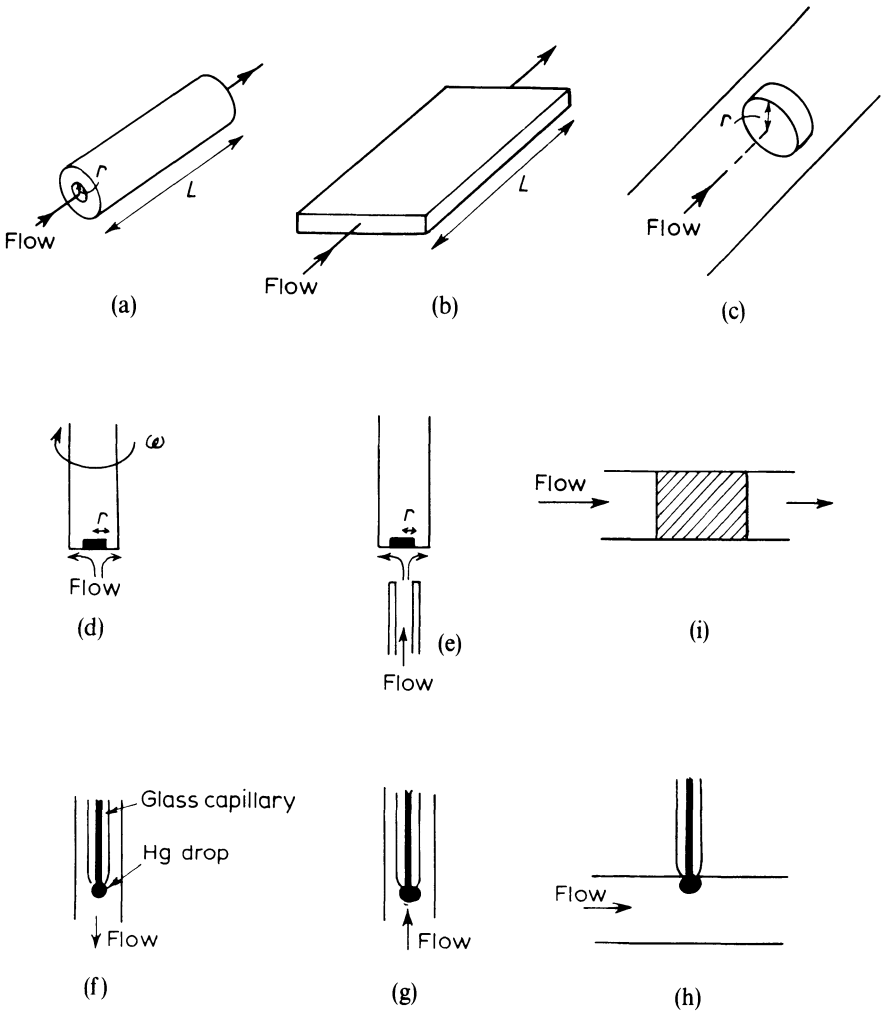

Fig. 12.20 Types of amperometric electrochemical detector used in high-pressure liquid chromatography. (a) Tubular electrode. (b) Thin-layer channel cell. (c) Disc electrodes. (d) Rotating-disc electrode. (e) Wall jet. (f) Polarographic detector; mercury flow parallel to, and in same direction as, electrolyte flow. (g) Mercury flow parallel to, and in opposite direction to, electrolyte flow. (h) Mercury flow perpendicular to electrolyte flow. (i) Porous electrode.

K and a will depend upon the nature of the flow and the electrode geometry. Expanding Sh and rewriting in terms of the measured limiting current:

$$i_L = \frac{KAnFc^{\infty}D}{l} Re^a Sc^{1/3} \tag{12.12}$$

For a given reaction, n is constant. Since the diffusion coefficient depends largely

upon the background electrolyte and solvent, it will also be constant, as will the characteristic length l for a given electrode. Therefore, equation (12.12) may be rewritten:

$$i_L = k' A c^{\infty} Re^{a} \tag{12.13}$$

where k' is a constant incorporating K, n, F, D, l and $Sc^{1/3}$.

Equation (12.13) indicates that the observed limiting current i_L depends directly upon the active electrode area A and the bulk concentration of electroactive species c^{∞}. The limiting current is also dependent upon the geometry and flow-sensitive parameters k' and a. If the Reynolds number is

Table 12.8 Limiting current expressions for EC–HPLC detectors

	Detector	Characteristic length in Re	Equation for limiting current i_L
(a)	Tubular electrode	L	$7.96\, nFc^{\infty} D L^{1/3} r^{2/3} \overline{Re}^{1/3} Sc^{1/3}$
(b)	Thin-layer channel cell	L	$0.83\, nFc^{\infty} D B \overline{Re}^{1/2} Sc^{1/3}$
(c)	Static-disc electrode with perpendicular flow	r	$3.27\, nFc^{\infty} D r \overline{Re}^{1/2} Sc^{1/3}$
(d)	Rotating-disc electrode (laminar flow)	r	$1.95\, nFc^{\infty} D r \overline{Re}^{1/2} Sc^{1/3}$
(e)	Wall jet cell (infinite container)	r	$1.15\, nFc^{\infty} a' \overline{Re}^{3/4} Sc^{1/3}$
	Mercury		(for $\bar{v} > 3.5\,\mathrm{cm\,s^{-1}}$; $t \simeq 1\,\mathrm{s}$)
(f)	Parallel Hg and fluid flow		$0.0605\, nFc^{\infty} D^{2/3} \bar{v}^{1/3} (m' t)^{4/9}$
(g)	Opposite Hg and fluid flow		$0.0154\, nFc^{\infty} D^{1/2} \bar{v}^{1/2} (m' t)^{1/2}$
(h)	Perpendicular Hg and fluid flow		$0.0178\, nFc^{\infty} D^{1/2} \bar{v}^{1/2} (m' t)^{1/2}$

l = characteristic length in $\overline{Re}$
m' = mercury mass flow rate
t = droptime
$\overline{Re}$ = Reynolds number based on mean linear velocity $\overline{Re} = \dfrac{\bar{v} l}{v}$

B = width of electrode
r = radius of electrode
L = length of electrode
a' = nozzle diameter
$\bar{v}$ = mean linear fluid velocity

Table 12.9 Summary of characteristic parameters for mass transport in EC–HPLC voltammetric detectors

	Detector	Characteristic width z	Characteristic length l	Numerical constant k''	Reynolds Number exponent a
(a)	Tubular electrode	$L^{1/3}r^{2/3}$	L	8.0	1/3
(b)	Thin layer channel cell	B	L	0.8	1/2
(c)	Static disc electrode with perpendicular flow	r	r	3.3	1/2
(d)	Rotating disc electrode (*laminar flow*)	r	r	1.95	1/2
(e)	Wall jet cell (infinite container)	a'	r	1.15	3/4

$i_L = k'' nFc^{\infty} Dz\, Re^a Sc^{1/3}$

l is the characteristic length used to define a mean Reynolds number $\overline{Re} = \bar{v}l/v$

defined in terms of the average velocity ($\overline{Re}$), equation (12.13) may be written in the form:

$$i_L = k'' nFc^{\infty} DB\, \overline{Re}^a\, Sc^{1/3} \tag{12.14}$$

where k'' is a constant which is primarily dependent on geometry and B is a characteristic electrode width. Table 12.8 lists limiting-current expressions in this form for certain detector geometries. Table 12.9 summarizes the values of k'', B, l and a for the electrodes of Table 12.8. Several comments may be made regarding the implications of Tables 12.8 and 12.9 for detector performance:

1. In the case of polarographic (mercury) detectors, the highest limiting currents are obtained when the mercury flow is perpendicular to the electrolyte flow. This is the preferred arrangement for practical detectors (Fig. 12.20(h)).
2. For all the detectors, the limiting current increases with Reynolds number. Therefore it is desirable to construct detectors with small cross-sectional areas (or high electrolyte speeds) in order to increase the mean linear fluid velocity, and to choose an electrode geometry with a high Reynolds exponent.
3. Equation (12.14) indicates that the limiting current is directly dependent on active electrode area A. Also, Table 12.8 shows that i_L may be significantly increased by enlarging the characteristic length of the electrode.

Fig. 12.21 Electrochemical detector cells for high-pressure liquid chromatography. (a) Porous-electrode cell for coulometric detection in high-pressure liquid chromatography (Courtesy: Coulochem). (b) Thin-layer amperometric detector for high-pressure liquid chromatography. (c) The Wall jet amperometric cell. (Courtesy: EDT Research.)

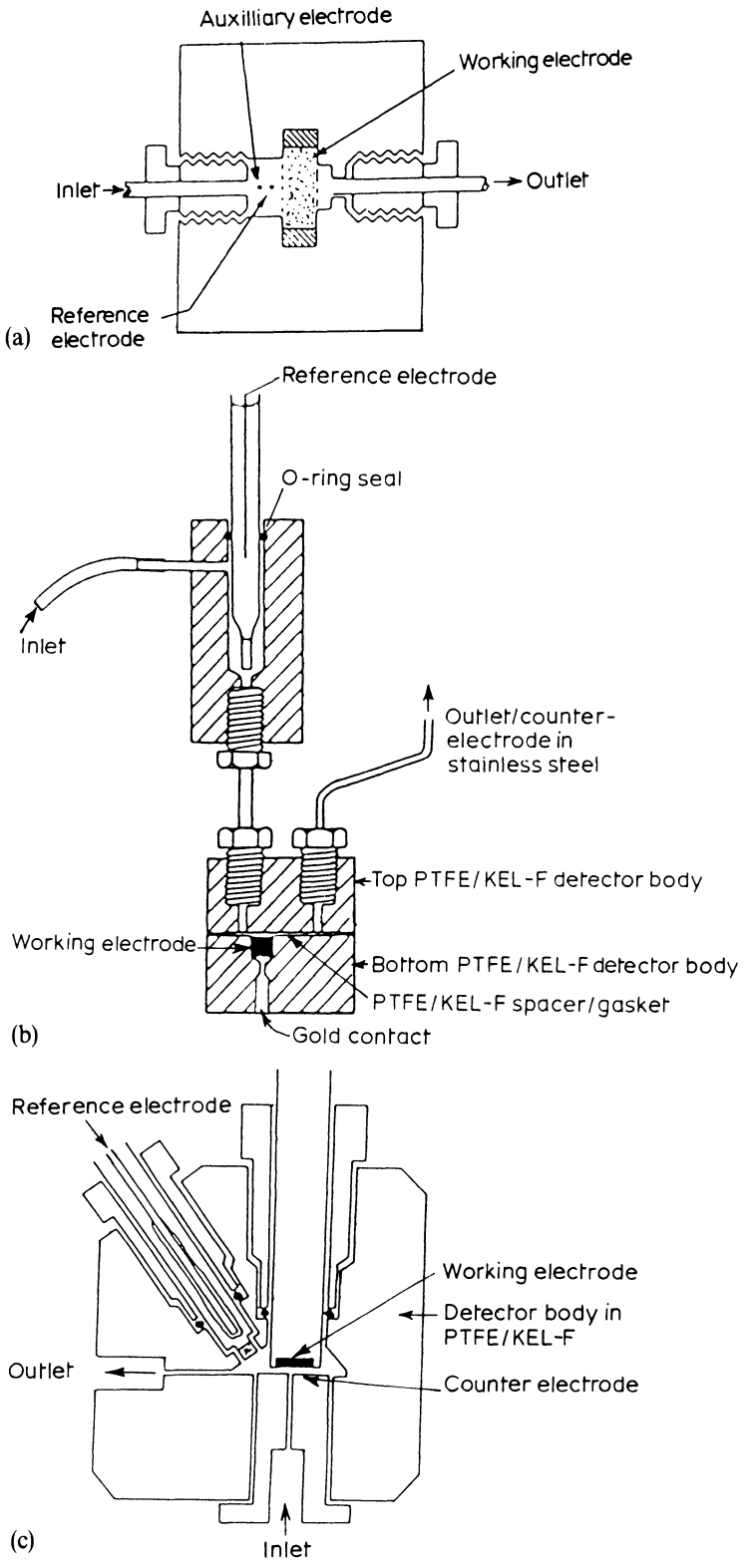
Auxilliary electrode
Working electrode
Inlet
Outlet
Reference electrode
(a)
Reference electrode
O-ring seal
Inlet
Outlet/counter-electrode in stainless steel
Top PTFE/KEL-F detector body
Working electrode
Bottom PTFE/KEL-F detector body
PTFE/KEL-F spacer/gasket
Gold contact
(b)
Reference electrode
Working electrode
Detector body in PTFE/KEL-F
Outlet
Counter electrode
Inlet
(c)

Increasing the electrode length may, however, result in a much poorer response, as the signal to noise ratio (S:N) is reduced. Recalling that the flow-through detector is on line to a HPLC column, the concentration time profile may be considered as a Gaussian distribution. The chromatographic plate number may be used to characterize the column:

$$N_C = (t_R/\sigma_c)^2 \tag{12.15}$$

where t_R is the retention time in the column and σ_c^2 is the peak variance. The detector performance may be related to that of the column by:

$$(\tau/\sigma_c)^2 = (1/\phi^2) - 1 \tag{12.16}$$

where τ is the detector time constant and ϕ is the peak fidelity. For the ideal case of $\phi = 1$, the peak is completely undistorted meaning $\tau = 0$. τ may be related to a response volume V_{res}* via

$$\tau = V_{res}/Q \tag{12.17}$$

where Q is the volumetric flow rate.

Equation (12.16) shows that, in order to limit peak distortion (i.e. maintain ϕ) the volume and, hence, the electrode length must be minimized. The detection limit may be defined as the quantity of electroactive species which causes 3 times the noise level. The noise N is proportional to active electrode area A:

$$N \propto A \tag{12.18}$$

and combination of equation (12.14) with equation (12.18) allows the S:N ratio to be expressed in terms of a characteristic length parameter y (Table 12.10). It is

Table 12.10 Idealized signal to noise ratio (S:N) for an electrochemical detector as a function of characteristic electrode dimensions. (*After*: H. B. Hanekamp and H. J. van Nieuwkerk (1980) *Analytica Chimica Acta*, **121**, 13)

	Detector	Electrode area A	Signal S varies as	Characteristic parameter y	Overall signal: noise ratio (S:N)y varies as
(a)	Tubular electrode	$2\pi rL$	$r^{2/3}L^{2/3}$	rL	$(rL)^{-1/3}$
(b)	Thin-layer channel cell	BL	$BL^{1/2}$	L	$L^{-1/2}$
(c)	Static-disc electrode with perpendicular flow	πr^2	$r^{3/2}$	r	$r^{-1/2}$
(d)	Rotating-disc electrode	πr^2	$r^{3/2}$	r	$r^{-1/2}$
(e)	Wall-jet cell	πr^2	$r^{3/4}$	r	$r^{-5/4}$

* The response volume is not necessarily equal to the geometrical volume but the two parameters are closely related.

clear from Table 12.10 that y should be as small as possible, its minimum value being determined by the gain of instrumentation amplifiers. In practice, miniature electrodes can be difficult to mount and to prepare, e.g. a small degree of roughness or adsorption will alter significantly the exposed area. Tubular electrodes should have a short and narrow bore; thin layer cells should be short but have wide electrodes in a narrow flow channel. Static-disc and wall-jet electrodes should each have small radii. To a first approximation, the radius of rotating disc is not critical but such devices may introduce electrical noise via eccentric rotation or drive motor interference.

12.6.2 Practical aspects

One of the most important detector design features is the ability to rapidly and conveniently extract the working electrode, in order to prepare its surface by polishing, etc. Tubular cells are somewhat inconvenient in that the electrode surface is curved and difficult to clean or inspect. For routine work, therefore, flat electrodes such as the various disc geometries are preferred.

The choice of electrode material is dictated by the potential range required in a given solvent. The most common electrode materials are mercury or gold amalgams (with high H_2 overpotential), platinum, gold and a wide range of carbons. Mercury exhibits very high hydrogen overvoltage and is well suited to many reductions. In suitable hanging or dropping mercury designs, the electrode may be renewed semicontinuously or continuously, providing a fresh electrode surface. The anodic range of mercury is severely limited, as oxidation of the metal takes place at approximately $+0.4$ V (vs saturated calomel electrode), giving rise to high background currents and surface problems.

Perhaps the single most versatile class of material is carbon. Pyrolytic graphite, glassy (vitreous) carbon, various polymers or oil-impregnated or paste electrodes have been used. There is a growing awareness of the complex surface chemistry of carbons, coupled to an appreciation of the great electrochemical differences between apparently similar forms of the material. In practice, mechanical, chemical and electrochemical pretreatment methods are usually essential if reproducible results are to be achieved.

While two-dimensional electrodes are simpler to prepare, a growing number of detectors utilize porous electrodes, including reticulated vitreous carbon. Three-dimensional electrodes are particularly suited to coulometric cells. (Fig. 12.21a)

Figure 12.21 (b) and (c) show some typical cell designs for amperometric detectors.

12.6.3 Applications

The number of HPLC applications using electrochemical detection continues to increase as the cells and methodology become more available and better

understood. The majority of applications involve the pharmaceutical, biochemical or biomedical fields.

12.7 MISCELLANEOUS

There are many specific examples of electrochemical devices which do not fit readily into the major areas considered above. An important example is the coulometric thickness gauge (Fig. 12.22) which is used routinely to measure the thickness of metal coatings,* particularly in the case of electroplating. A well-defined and precleaned area of the sample is exposed to a chosen electrolyte and under well-agitated conditions (provided by jet flow, or a stirrer) the coating is

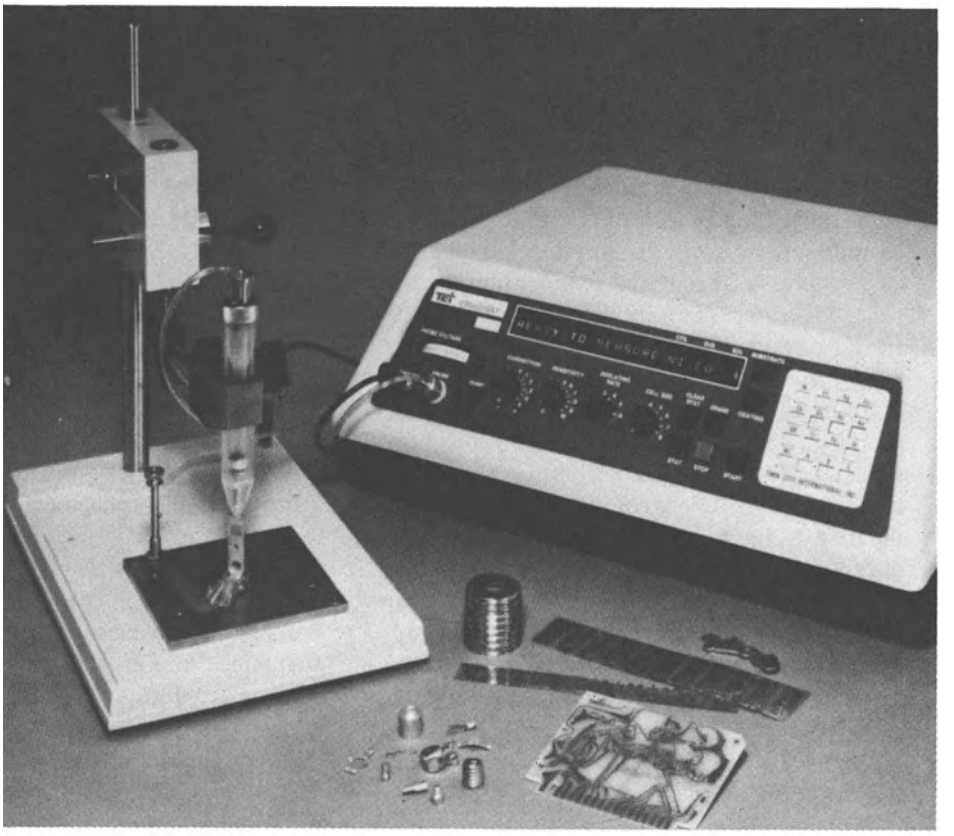

(a)

* For example, the method meets the requirements of standards ASTM B504–82, ISO 2177 and DIN 50032 and 50955.

anodically dissolved. Typically, a constant current is applied and the cell voltage changes abruptly when the substrate is exposed, providing a signal to terminate the electrolysis. The recorded time t may then be related to the metal thickness x via Faradays laws of electrolysis:

$$x = \left(\frac{\phi \mathrm{M} i}{nF\rho A} \right) t \tag{12.19}$$

Under suitable conditions, the current efficiency ϕ is a constant (which may be 1.0). For a given metal, the molar mass M, density ρ and number of electrons n are also constant. Here, if the area A is well-defined and a known, constant current i is applied, the thickness, x is proportional to time, t.

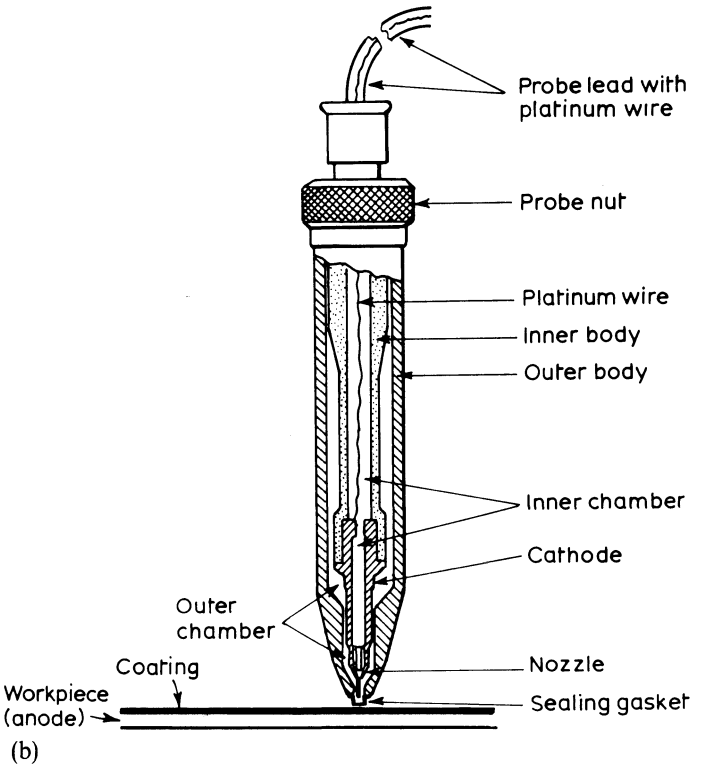

Fig. 12.22 Coulometric gauge for the measurement of metal coating thickness. (a) The Coulotest instrument, together with the measurement probe and typical applications. (b) A section of the probe. (Photograph, courtesy: Twin City International Inc.)

FURTHER READING

1 L. Meites (1965) *Polarographic Techniques*, Wiley-Interscience, New York.
2 A. Bond (1980) *Modern Polarographic Methods in Analytical Chemistry*, Marcel Dekker, New York.
3 A. J. Bard and L. R. Faulkner (1980) *Electrochemical Methods – Fundamentals and Applications*, Wiley, Chichester.
4 Southampton Electrochemistry Group, (1985) *Instrumental Methods in Electrochemistry*, Ellis Horwood, Chichester.
5 P. T. Kissinger and W. R. Heineman (Eds) (1984) *Laboratory Techniques in Electroanalytical Chemistry*, Marcel Dekker, New York.
6 K. J. Clevett (1986) *Process Analyzer Technology*, Wiley, New York.
7 Princeton Applied Research Corp. (1973) *Modern Analytical Polarography Workshop Manual*,: also PARC Application Notes.
8 F. Vydra, K. Stulik and E. Julakova (1976) *Electrochemical Stripping Analysis*, Ellis Horwood, Chichester.
9 E. Pungor, Z. Feher and M. Varadi (1980) 'Hydrodynamic Voltammetry', *CRC Critical Reviews in Analytical Chemistry*, **9**, 2, 97.
10 K. Stulik and V. Pacakova (1987) *Electroanalytical Measurements in Flowing Liquids*, Ellis Horwood, Chichester.
11 H. Freiser (Ed.) (1978) *Ion-selective Electrodes in Analytical Chemistry*, Vol. 1, Plenum Press, New York.
12 P. Bailey (1976) *Analysis with Ion-selective Electrodes*, Heyden, London.
13 K. Cammann (1979) *Working with Ion-selective Electrodes*, Springer-Verlag, Berlin.
14 A. K. Covington (Ed.) (1979) *Ion-selective Electrode Methodology*, CRC Press, Cleveland.
15 M. L. Hitchman (1978) *Measurement of Dissolved Oxygen*, Wiley, Chichester.
16 I. Fatt (Ed.) (1978) *The Polarographic Sensor; its Theory of Operation and its Applications in Biology, Medicine and Technology*, CRC Press, Florida.
17 H. Dietz, W. Haeker and H. Johnke (1977) 'Electrochemical Sensors for the Analysis of Gases', *Advances in Electrochem. & Electrochem. Eng.*, **10**, 1.
18 H. Thompson and M. Riley (1981) 'On line Sensors in Industrial Water Analysis', *Phil. Trans. Roy. Soc. (London)*, **A302**, 327.
19 D. E. Williams and P. McGeehin (1984) *Specialist Periodical Reports on Electrochemistry*, **9**, 246, Royal Society of Chemistry.
20 J. E. Frew and H. A. O. Hill (1987) 'Electrochemical Biosensors', *Analyt. Chem.*, **59**, 933A.
21 M. Akhtar, C. R. Lowe and I. J. Higgins (Eds) (1987) 'Biosensors', *Phil. Trans. Roy. Soc. (London)*, Series B, **316**.
22 D. Parker (1987) 'Sensor for Monitoring Blood Gases in Intensive Care', *J. Phys. E: Sci. Instrum.*, **20**, 1103.
23 H. B. Hanekamp and H. J. van Nieuwkerk (1980) 'Theoretical Considerations on the Performance of Electrochemical Flow Through Detectors', *Analytica Chimica Acta*, **121**, 13.

24 J. E. Giddings, E. Grushka, J. Coyes and P. R. Brown (Eds) (1984), *Advances in Chromatography*, Vol. 24, Marcel Dekker, New York.
25 J. Sibbolt and A. Carter (1985) *Med. Biol. Eng. Control*, **23**, 329.
26 A. Junter (Ed.) (1988) '*Electrochemical Detection Techniques in the Applied Biosciences*' Vols 1 and 2, Ellis Horwood, Chichester.

Index

ABB Membrel cell 284–6
Acrylonitrile hydrodimerization 298–311
Actimag process 229–30
Active mass in batteries 545, 557–9
Activity coefficient 53
Adatoms 394
Additives to
  battery electrolytes 559
  electroplating baths 402–4
  electrorefining baths 231
Adiponitrile production 298–311
Adsorption 7, 32–8
  equilibria in absence of electron transfer 34–6
  in presence of electron transfer 36
  in presence of neutral adsorbate 36
  isotherms 34–5
Air
  cathode 286–8, 590–4
  sparging 224
AKZO-Billiton fluidized bed electrode reactor 163–4, 339, 350–1
Albright and Wilson Americas chromate removal cell 372–3
Alcoa aluminium process 216–17
Alcohol meter 617–18
Alkaline fuel cells 593
Alkaline manganese dioxide batteries 582
Alloy electrodeposition 408–9
Aluminium
  anodizing 434–8, 439
  chromating 440–1
  colouring 436
  electrograining 479
  extraction 211–18
  oxide film 436
  production 211–18
  refining 244–5
Amalgam cell 184–8
Ammonia ion selective electrode 611, 614
Ammoniacal etchants 471–2
Amperometric detector cells 611, 613, 623, 628
Analysis via electrochemical sensors 596–637
Andco environmental processes for chromate removal 370–2
Anode
  auxiliary 391, 418, 423, 454
  cathode gap 77
  effect 214, 253–5
  for electroplating 400–2
  for electrowinning 225
  impurities 233, 401
  pellets 402
  reactions 1
  slimes 233, 238–40
  sludge 401
Anodic
  dissolution to produce metal salts 291–2
  electropainting 441–3
  film formation 49
  oxidation of Cr (III) 365–70
  protection 531–2, 535
  process in corrosion 485
  reactions 1
  stripping voltammetry 601–2
Anodizing 434–9
Anthraquinone synthesis 328, 329

Applications of
  chlorine 174
  electroless plating 432–4
  electroplating 404–15
  sodium hydroxide 174
Asahi chemicals
  adiponitrile process 305
  chloralkali cells 196–7
  electrodialysis cells 358, 359
Asbestos diaphragm cells 188–96
Atmospheric
  corrosion 481–3, 515, 517
  pollution 331, 379
Automotive industry electropainting 443–7
Auxiliary anodes 391, 418, 423, 454

Backmixed flow reactor 97, 101–4
Baffles in plate-and-frame cells 149
Balbach-Thum cell 241–2
Ball-up 559
Barrel plating 416, 421
Base generation 318
BASF adiponitrile process 305
Batch reactor 96–9, 105–8
Batch recycle (recirculation) 102–3
Baths for electroplating 402–4, 406–7, 409
Battery technology 543–90
  active materials 557–9
  capacity 548–9
  characteristics 546–51
  components 555–9
  container 555
  current 548
  current collectors 556
  electrolytes 557
  performance 554–5
  separators 555–6
  specifications 551–3
  voltage 546–8
Benzaldehyde plant 67
Benzene oxidation 321
BEWT Chemelec cell 340, 344–6
Bilayer membranes (chlor-alkali) 182–3
Biochemicals separation 376–9
Biosensors 618–24
Biostream process 377–9
Bipolar
  capillary gap cell 156, 325
  cells 136–41
  filterpress cell 147
  pump cell 158–9
  trickle tower reactor 138, 140
  water electrolysers 256–69
Bismuth ion analysis 601
Bleaching by
  chlorine 174, 354
  hydrogen peroxide 354
  hypochlorite 354
  ozone 288
Block growth of electrodeposits 397
Blood monitoring 619–21
Boundary layer
  concentration or diffusion 22–4
  hydrodynamic 25–6
Brass electroplating 409
Breathalyser 617–18
Brighteners in electroplating 403–4
Brine electrolysis 173, 353–7
Bromide ion selective electrode 607, 608
Bromine generation 379
Bronze electroplating 409
Busbars 91, 137
Butler–Volmer equation 11
Button cell Ni-Cd batteries 570

Cadmium ion
  analysis 601
  removal 345, 351
  selective electrode 607, 608
Capacitance of an electrode 35
Capacitor manufacture 438
Capacity of a battery 548–9
Capenhurst electrolytic etchant regeneration (CEER) cell 473–5
Capillary gap cells 143–4
  annular 157
  planar 156–7
Capital costs 65–6
Car battery
  (SL I) 560–3
  traction 552, 563–5
Carbon
  based anodes in ozone cells 286–8
Carbon dioxide sensors 614, 616
Carbon monoxide sensors 616
Carbon, PTFE particle electrodes 280–1
Carboxylic acid reductions 314–15
Carus cell 276–8
Cascade
  eco-cells 348–9
  mode of operation 104
Catecholamine assay 627

Cathode tool design for ECM 464–5
Cathodic
  cleaning 416
  cleavages 316–17
  coatings 179, 260, 307, 516
  electropainting 442–7
  hydride formation 415, 517, 536
  inhibitors 521–2
  protection 523–31
  reactant in corrosion 483–8
  reactions 1
Caustic potash production 208–9
Caustic soda production 173–208
Cell
  design 95–108, 247, 336–53
  house design 137, 183–4, 186, 214–15, 222–3, 233–7
  lifetime 89–90
  reaction 1, 34
  resistance 77–9
Cell voltage (actual) components 5, 54–5, 75–9
  batteries 546–8
  chlor-alkali 175–7, 195, 201, 205
  copper electrorefining 237
  fluorine production 255
Cell voltage (reversible) 4, 9
Cementation 228–31
Cerous ion oxidation 67
Channel flow 26–30, 112, 127
Characteristic
  length 26, 629–30
  velocity 26
  width 630
Charge transfer processes 3, 8–18
Chemelec cell 340, 344–6
Chemical reactions 7, 50
Chemical reactor types 95–6
Chloralkali industry 173–209
  diaphragm cell 188–96
  electrode materials 177–9
  membrane cell 196–202
  membranes 179–83
  mercury cell 184–8
Chloride ion
  additions to electrorefining baths 231
  breakdown of passivity 507–8
  pitting corrosion 515
  selective electrode 607, 608
Chlorides for aluminium production 216
Chlorinated pherol removal 383–4
Chlorine
  generators 353–5
  manufacture 173–208
  uses 174
Chromate removal 364–73
Chromating 440–1
Chromatographic
  plate number 632
  style electrosynthesis 329
Chromic acid
  conversion coatings 440–1
  electroplating bath 407, 411
  production 278–9
  removal 364–73
Chromium electroplating 402, 405, 406, 407, 408, 411, 417, 422
Chromium (III) oxidations 365–70
Circulating (fluidized) bed cathode 165
CJB developments
  biostream process 377–9
  high-pressure water electrolysers 263–9
Clark-type electrode 619–20
Classification of cells according to
  design criteria 143
  direction of current flow 127, 129
  electrical connections 136–41
  nature of energy transformation 63–4
  reactor geometry 80
  type of electrode 144
Coatings
  anodic (base) 516
  cathodic (noble) 516
  conversion 434–41
  electroplated 386–424
  paint 441–7, 515
Cobalt
  ion removal 345
  refining 233
Combination pH probe 605–6
Compact layer at the interface 16–17
Comparison of
  chlor-alkali cells 203–8
  metal deposition techniques 424–5
Complexing agents 403
Composite
  coatings 420, 433, 434
  electrodes 92, 280–1
Concentration
  determination 596–634
  expressions for reactors 97–108
  of electroactive species 94
  profile near electrode 21–4

Concentric
  battery cells 569, 571, 580, 585
  capillary gap cell 157
  cathode cell 340, 351–2
  cylinder cells 112
Concrete, corrosion in 532–3
Conduction of heat 135
Conjunctival oxygen sensors 620, 622
Continuous flow reactors 96–7, 99–105
Continuous product extraction 143, 335
Continuous stirred tank reactor (CSTR) 97, 101–4
  batch recycle 103
  cascade 104
  single pass 101–2
Convection
  in mass transport 19
  of heat 135
Convective diffusion 22
Convenience in operation 90–1
Conversion coatings 434–41
  anodized aluminium 434–9
  chromates 440–1
  phosphates 438, 440
Copper
  corrosion (Pourbaix diagram) 497
  electroplating 406, 411, 413
  electrorefining 232–7
  extraction 220–6
  ion analysis 601
  ion removal 342, 345, 348–9, 351
  ion selective electrode 607, 608
COPS system for Cr (VI) treatment 368
Corrosion 481–542
  cell 483–4
  control 518–36
  current 499–501
  design aspects 518, 519
  environments 482
  inhibitors 521–2
  kinetics 498–508
  measurement 538–41
  mechanisms 55–8, 488
  monitoring 538–41
  potential 490–3
  problems in electrolysis 536–7
  problems in electroplating 537–8
  rates 509
  thermodynamics 489–98
  types 509–18
Costs for an electrolytic process 64–70
  chloralkali 204–6
  general cost components 64–7
  process optimization 67–70
Coulometric thickness gauge 634–5
Coupled chemical reactions 7
  adiponitrile synthesis 298–300
  electroplating of zinc 395
Coverage by adsorbates 37
Crevice corrosion 514–17
Cryolite melt 211–14
Cumulative current efficiency 73
Cuprous chloride etchants 472–4
Cuprous oxide
  bonding in printed circuit boards 412
  production 290–1
Current
  collectors 544–5, 556, 560
  density 9–13, 399
  distribution 120, 122–33, 389–93, 417, 423
  efficiency 73–4
  limited process 106
Current (current density)–overpotential curves for
  cathodic reactions under mass transport control 115–17
  three-dimensional electrode 130
Current (current density)–potential curves for 12
  corrosion of a metal 499
  electrodeposition of a metal 399
  mixed control 31
  polarography 596–7
  reversible couple 33
  see also i–E curves
Cyanide ion selective electrode 608
Cycle life of a battery 550
Cylindrical Leclanché batteries 569, 572

Delamination of concrete 532–3
DEM cell 150–1, 381–2
Dendritic growth
  in batteries 550
  of electrodeposits 396, 397–8
Density
  of electrolyte 26
Denuder (chlor-alkali) 184–5, 592
Deposition
  of metals 49, 386–434
  of paints 441–7
  rates for metals 388–9
Depth of discharge 550
Derivative polarography 597, 600

Desalination 358, 359, 360
Design
  equations for mass transport control in reactors 97–108
  factors in corrosion 518, 519–20
  of components for electroplating 415–16, 417–18
  of electrocatalytic electrodes 45–8
Detectors
  for gases 613–18
  for HPLC 624–34
Deuterated water production 257, 258
Deutsche-Carbone
  Enviro Cell 162–3, 339, 342–3
  flue-gas desulphurization cell 382
Diaphragm 139–41
  cells 188–96
Differential
  aeration 511–15
  pulse polarography 597–602
Diffuse layer at the interface 16–18
Diffusion
  in mass transport 18
  layer 18–24
Dimensionally stable anodes (DSAs) 92, 178
Dimensionless group correlations 28, 173, 627–30
Disbonding of concrete 532
Disc electrode, HPLC detector cell 628–31
Discharge
  curves for a battery 549, 562, 573, 577
  rate 550
Dished electrode membrane (DEM) cell 150–1, 381–2
Disinfection by
  chlorine 174–5, 353–7
  hypochlorite 353–7
  ozone 284–8
Dissociative adsorption 33
Dissolution of metals
  anodes in electroplating 401–2
Dissolved oxygen
  in corrosion 503–5, 511–15
  sensors 619–22
Divided cells 143–5
Doré metal (copper refining) 239–40
Double layer 16–17
Dow-Huron cell 161
Down's cell 218–19
Driven cells 64
Driving force for electron transfer 14
Dropping mercury electrode (DME) 596–602
DSA electrode coatings 178–9
DuPont-Electrochem International cell 292
Dynamic electrodes 144
  three-dimensional 163–6
  two-dimensional 157–60
Dynamic viscosity 26

Eco-cell 339, 347–9
  cascade cell 348–9
Economics 64–70
  aluminium extraction 217–18
  batteries 551
  chloralkali industry 175, 204–6
  corrosion 483
Eco-Tec Recowin cell 337, 340
Edge site 394
Effluent treatment 331–84
Electrical connections and contacts
  plating of 412–15
  to cells 136–41
Electrical double layer 16–18
Electrical energy consumption 74–5
Electrical resistance of corroding metals 539
Electroactive area per unit volume 79–81, 82–3
Electroanalytical methods 596–637
Electrocatalysis 38–48
  and electrode design 45–8
  of hydrogen evolution 38–44
  of oxygen reduction 44–5
Electrocatalytic Ltd DEM cell 150–1, 381–2
Electrocell electrolysers 149, 152–3, 339, 344
Electrocell MP cell 152–3
Electrochemical
  cell 3
  cleaning 448
  contour machining 467
  deburring 466–7
  engineering 60–172
  etching 469–79
  forming 467
  grinding 465–6
  kinetics 4, 10–48
  machining 457–68

Electrochemical *cont'd*
methods of metal deposition pickling 448
pump cell 158–60
reactions 1, 55–8
reactors 62–4, 95–171
sensors 596–637
stripping 448
thermodynamics 4, 8–9
Electrocoagulation 375–6
Electrocrystallization of metals 394–400
Electrode
area 79–81
conductivity 93
design 45–8, 91–4, 144–5
electrolyte movement 95
geometry 80, 92–4, 144–66
grids/materials in batteries 91–4, 177–9
potential 4, 91, 176, 522
potential series 489–93
reactions 1–4, 6
structure 91–4
Electrodeposition
engineering applications for 410, 411, 432–4
for electronics industry 410–15
of alloys 408–9
of composite coatings 420, 433, 434
of metal powders 245–7
of single metals 406–8, 410–34
Electrodialysis cell 168, 358–64, 366–70
Electroflocculation 375–6
Electroflotation 374–5
Electroforming 451–7
Electrograining of aluminium 479
Electroless deposition 424–34
applications 432–4
baths 426–9
of composites 433, 434
of metals 424–34
Electrolyser Inc. (EI-) cells 258, 260–2
Electrolysis
medium 94
parameters 91–5
Electrolytes
for batteries 557
for electroforming 455, 457
for electroless deposition 426–8
for electroplating 402–4, 406–7, 409
properties 51–4
Electrolytic
cells 64
cleaning 416
conductivity 51–3
etching 475–7
power consumption 79
process development 61–2
Electronics, plated coatings for 410, 411–15
Electron transfer 6
kinetics 4, 9–49
thermodynamics 4–6, 8–9
Electropainting 441–7
Electrophoretic
deposition of paint 441–7
separation of biochemicals 376–9
Electroplating 386–424
alloys 408–9
baths 402–4, 406–7
composites 410
electronics applications 410, 411–15
engineering applications 405, 411
rates 388–9
trends 420, 422
Electropolishing 447–8
ElectroProd cell 152–3, 344
Electrorefining 231–44
ElectroSyn cell 152–3
Electrosynthesis of
inorganics 249–93
organics 294–330
Electrowinning 211–28
Eltech
RETEC cells 337, 338, 341–2
Sanilec cells 356, 357
Energy
of activation 14
consumption 74–5, 206–7
density of batteries 549–50
efficiency 5, 79, 550–1
storage density 549–50
Engineering applications of electroplating 410, 411
Enviro-Cell 162–3, 339, 342–3
Envirochrome process for chromium plating 417, 422
Environmental protection 331–76, 379–84
Enzyme electrodes 622–4
Epinephrine oxidation 626–7
Epoxidation of propylene 38, 322
Equilibrium potential 4, 9
of chlor-alkali electrodes 176

Equivalent (or hydraulic) diameter 29
ER cell 339
Etchant regeneration 472–5
Etching of
  metals 468–77
  semiconductors 477–9
Evans diagrams, *see* I–E curves for corrosion
Exchange current density 9
  hydrogen evolution 38–40, 502–3
  in corrosion 502–3
  metal dissolution 502–3
Exfoliation corrosion 511
Expanders in batteries 559, 560
Extended area electrodes 126–8, 144, 160–3
  see also Packed-bed electrodes; Porous electrodes
Extraction of metals 210–48
Eye (oxygen) sensors 620, 622

Faraday's laws of electrolysis 4
  batteries 548–9
  corrosion 509
  coulometric metal thickness gauge 634–5
  electroplating 388–9
  reactors 86
FBE reactor 339
  see also AKZO-Billiton fluidized bed electrode reactor
Ferric chloride etchants 468, 471
Fick's laws of diffusion 19–22
Field formula 392
Figures of merit 63, 70–89
Film breakdown 507
Film formation 48–9
Filterpress cell 146–55, 168, 170–1
  chlor-alkali 196–203
Flat-cell Leclanché battery 572
Flemion membrane 141, 181
Flow characterization
  by dye injection 27
  by marker (stimulus-response) 120–1
Flow patterns (in electrodialysis cells) 362–3
Flow segregation 29, 149
Flow sheets 66–7
  benzaldehyde production 67
  chlor-alkali mercury cells 187
  electrochemical machining 462
  refining of metal 234
Flue gas desulphurization 379–82
Fluid flow 21–2, 24–30
Fluidized bed electrode 163–6
  AKZO-Billiton reactor 163–4, 166, 339, 350–1
  chemelec cell 340, 344–6
  current and potential distribution 129–33
  for cementation 229–30
  parel cell 165
Fluid mechanics 24–7, 111
  at a flat plate 25
  at a rotating disc 21
  for flow through a tube 26–7
Fluoride ion selective electrode 607, 608
Fluorination of organics 319
Fluorine production 249–56
Flux in mass transport 20–1
FM-21 electrolyser
  HP version 201
  SP version 153–5, 202
FM01-LC laboratory reactor 170–1
Foam electrodes 93, 337–8
Foil manufacture 455, 456
Forced convection mass transport 117
Fouling of sensors 610, 612
Fourier's laws 135
Fractional conversion 72, 99–107
Free energy
  curves 15
  of adsorption 35
Frequency factor 14
Fuel
  cells 590–5
  efficiency monitor 615

Gallium ion analysis 601
Galvanic
  cells 64
  corrosion 492, 516
  series 491–3
Gaseous oxygen sensor 613, 615–16, 617
Gas
  main: cathodic protection 527, 530
  sensors 613–18
Gauntlet type battery electrodes 564–5
Gauze manufacture 452–5
General (uniform) corrosion 511
Glass electrodes 604, 605–6
Glucose electrode 622–4
Goecomet reactor 340, 349, 350

Gold
  electroplating 413, 415
  electrowinning 227–8
  ion removal 345, 353
  recovery 353
  refining 242–4
Grashof number 112–13
Growth of electrodeposits 394–400

Half wave potential 596–600
Hall-Héroult process 211–16
Halogenated phenols, removal 383–4
Hardness (of water) determination 603, 608
Haring-Blum cell 391–2
Harwell biostream process 377–9
Heart pacemaker battery 553
Heat
  balance 134
  transfer 133–6
  transfer coefficient 135–6
Heterogeneous membrane electrodes 604, 607
High pressure water electrolysers 263–5
HPLC detector cells 161, 624–34
Hull cell 389–91
Hydraulic (equivalent) diameter 29
Hydrazine
  corrosion inhibitor 521
  sensor 611
Hydride formation
  corrosion 517
  electroplating 402, 415
  nickel 402
  palladium 415
  titanium 517
Hydrobromic acid electrolysis 379–82
Hydrodimerization of acrylonitrile 298–311
Hydrodynamic boundary layer 26
Hydrodynamics 24–7
Hydrogen
  adsorption detection 415, 517
  economy 257, 259
  embrittlement 402, 525
  evolution 38–44, 499–503
  penetration probe 616–17
  production 256–69
Hydrogeneration of
  nitriles 314
  nitrogen heterocycles 313
  steroids 318
Hydrogen ion selective electrode, *see* pH measurement and control
Hydrogen peroxide production 279–82
Hydrogen sulphide
  corrosion 517
  ion selective electrode 614
Hydrometallurgy 219–28
4-Hydroxybenzaldehyde synthesis 324–5
Hypochlorite generation 353–7

ICI
  fluorine cell 250–1
  FM21 cells 153–5, 202–3
i–η curves, *see* Current–overpotential curves
i–E curves, *see* Current–potential curves
Immersion plating 425
Immunity to corrosion 494–7
Impact rod reactor 349, 350
Imperfections in metal coatings 516
Impressed current
  anodic protection 531–2, 535
  cathodic protection 527–34
IMT (Improved Mass Transport) cell 227–8
Inclined fluidized bed electrode reactor 165–6
Indirect organic processess 326–9
Indium ion analysis 601
Industrial lead/acid batteries 563–4
Inhibitors of corrosion 521–2
Inorganic electrolytic processess 249–93
In situ spectroscopic techniques 38
Intercalation of lithium in battery electrodes 575
Interface between electrode and electrolyte 16–18
Interferences in ion selective electrodes 604–5
Internal recirculation cells 271
Interval current efficiency 73
Iodideion selective electrode 607, 608
Ion
  activity 53–4
  exchange membranes 141, 179–83, 361–2
  transport in electrolytes 51–4
Interelectrode gap 77, 143–4
Ion selective electrodes 603–9
Iron
  corrosion 488, 495
  electroplating 411

Iron ion removal 345
ISFETs 609
ISPRA Mk XIII A process 379–82

Jig mounting for electroplating 416, 418
Joule heating 136

Kinematic viscosity 26
Kinetics
  in a chlor-alkali cell 176
  in the simple batch reactor 105–8
  of corrosion 499–508
  of electron transfer 8–18
  of hydrogen evolution 39–44
Kink site 394
Kohlrausch law 52
Kolbé coupling of half esters 323
Krebs
  chlorate cell 272
  hypochlorite cell 355, 357

Laboratory cells and scaleup 166–71
Laminar flow 26–7
  at a rotating disc 21–3
  between parallel plates 28
  in a rotating cylinder reactor 377–9
Langmuir isotherm 34
Laplace's equation 122–3
Layer growth of electrodeposits 397
Lead
  alkyls 161
  alkyl production 319
  electrorefining 232
  ion analysis 601
  ion selective electrode 607, 608
Lead–acid battery 4, 544, 558, 559–66
Leakage currents 138
  corrosion 534, 536–8
Leclanché battery 544, 545, 571–3
Levellers in electroplating 404
Liberator cells (copper refining) 236
Lifetime of reactors 89–90
Limiting current 81–2
  determination 114–20
Linear polarization resistance 539–41
Line plating 416
Liquid membrane electrodes 604, 607–9
Lithium batteries 573–81
  Li-$(CF)_n$ 580
  Li-iron sulphide 586–7
  Li-MoS_2 579
  Li-$SOCl_2$ 576–7
  primary 578–81
Lithium production 218
Lithium salts; electrolytic conductivity 52
Load levelling 589
Localized corrosion 484, 510–18
Log current (or log current density)–potential curves 12
  batteries 547
  for addition agents in electroplating 393
  for an electrolysis cell 55
  for an open circuit electrode 57
  for corrosion of metals
    anodic protection via alloying 535
    cathodic and anodic protection 523
    cathodic protection 524
    classical passivity 506
    effect of chloride on nickel dissolution 507
    effect of impurities in zinc 503
    effect of stirring and oxygen level on passivity 508
    modes of inhibition 522
    uniform and localized attack 513
    via charge transfer controlled cathode reactions 504
    via hydrogen evolution 501
    via mass transport controlled oxygen reduction 505
  see also Tafel plots

Magnesium extraction 218
Mandrel 454
Manganese dioxide production 288–90
Manual electroplating 420
Marker techniques for flow characterization 30, 120–1
Mass balance 62–3, 97, 99, 101, 103
Mass transport (transfer) 6, 18–32, 109–20
  coefficient 23, 81–2
  controlled oxygen reduction (corrosion) 505
  correlations 28–30, 111–13, 627–30
  effectiveness factor 82
  in electrowinning cells 224
  in HPLC detector cells 627–30
  in industrial electrolysis 24–30
  in laboratory experiments 19–24
  in metal recovery cells 334–5
  limited process 106–8
  regime 95, 111

Mass transport *cont'd*
to parallel plates 28–9, 112
to porous electrodes 112
to rotating cylinder electrodes 112
to rotating disc electrodes 21–3, 30, 112
Materials selection for
corrosion protection 519–20
electrodes 91–4
Material yield 72–3
Mathematical modelling 63
Mean flow velocity 26
Mean ionic activity coefficient 53–4
Mechanism of
electrodeposition of metals 393–400
hydrodimerization 308–11
hydrogen evolution 39–44
Mediated enzyme electrodes 623–4
Membrane
chloralkali cells 179–83
potential 603
sensors 603–24
Membranes for
chlor-alkali cells 179–83
electrodialysis cells 361–2
MEMBREL cell 284–6
Mercuric oxide/zinc battery 582
Mercury
cells 173, 184–8
detector cells 628–30
ion removal 351
pollution 207
ultra-microelectrodes 601
Metal-air batteries 583, 589–90
Metal
coating thickness gauge 634–5
deposition 386–434
dissolution
anodes 401–2
etching 468–77
extraction 210–48
finishing 385–450
hydrogen bonding 40
ion removal 333–53
polymer deposits 410, 433–4
powders 245–7
processing 451–79
recovery 333–53
refining 231–44
salts via anodic dissolution 291–2
winning 211–28
Metalliding 448
Methane oxidation in fuel cells 590
Methoxylations 319–20, 324–6
Methyl aromatics, oxidation 321
Microbial corrosion 487–9
Microelectrode arrays 119
Microflow cell (Electrocell AB) 152–3
Microprobes for localized measurements 30
Migration in mass transport 18
Mixed (i.e. combined electron transfer and mass transfer) control 30–2
Mixed potential 56
Mobility
of ions 53
of species 24
Modelling of reactors 63
Mode of operation for
electrochemical reactors 98, 102, 104
metal-extraction cells 336, 337
Moebius cell 238–40, 242
Molar
electrolytic conductivity 52–3
energy consumption 74
Molten carbonate fuel cell 594
Molten salt
metal extraction 211–19
metal refining 244–5
Monitoring
corrosion 538–41
techniques 596–637
Monopolar cells for water electrolysis 136–8
Monsanto adiponitrile process 298–310
Mark I 301–4
Mark II 305–8
reaction mechanism 308–11
MOSFET ion selective electrodes 609
Moving bed electrodes 165, 166, 350–1
Moving electrodes 144, 157–60, 346–50

Nafion membranes 141, 181
Nalco cell 161, 319
Natural convection mass transport 112
Nernst diffusion layer 22–3
Nernst equation 8
in corrosion 492
Neue-Bitterfelder cell 275–7
Nickel
electroplating 406, 411
electrorefining 232
ion removal 345
-PTFE electrodeposits 433, 434

Nickel-cadmium batteries 544, 566–70
Nickel-phosphorus alloy deposition 426–32
Nickel oxide/hydroxide catalysts 328–9
Nickel, PFTE electroless deposition 433, 434
Nitrate ion selective electrode 608
Nitrogen dioxide ion selective electrode 614
Nitrogroup reduction 317
Normalized
  space time yield 89
  space velocity 88–9
NO_x sensors 616
Nucleation of electroplated metal 394
Nylon-6,6 298

Offshore platform corrosion 520, 531
On-line analytical devices 609–18
Open circuit reactions 55–8
Operating costs 65, 204
Organic
  additives in electroplating 403–4
  electrosynthesis 294–330
Overall
  conversion related yield 73
  current efficiency 73
  operational yield 72–3
  selectivity 74
Overcharge behaviour 551
Overpotential 11, 75–8, 395
Oxide films
  anodized aluminium 434–8
  batteries 558–70, 580–2
  electrode materials 91–4, 178
  passivity 506–8, 514
Oxygen
  monitors 611, 613, 615–16, 619–22
  production 256–69
  reduction 44–5, 504–5, 511–15, 524, 590
  sensors 613, 615, 616, 619–22
OxyTech Systems chlorine cells 191–2, 198
OxyTech (UK) ozone cell 286–8
Ozone production 282–8

Packed bed electrodes 160–3, 280–1, 342–4
  current and potential distribution 129–33
Paint scratch corrosion 515
Palladium electroplating 413
  electroplating 413, 415
  hydride 415
Parallel plate
  cell, mass transport 28
  reactors 127, 146–55
Parel cell 165–6
Partial current density 9–11
Particulate electrodes 129–33, 160–3, 280–1, 342–4
  in electrowinning 226
  see also Packed-bed electrodes
Passivation
  of anodes in electroplating 401–2
  of battery electrodes 547
  of metals in corrosion 496, 506–8, 521–3, 535
Patch probe 617
Peak fidelity 632
Penetration rate in corrosion 509
Penicillin enzyme electrode 624
Perchlorate ion selective electrode 608
Perfluorinated ion exchange membranes in chlor-alkali cells 181–2
Performance of reactors 70–91
Periodic current reversal 400, 422
Phase
  formation 7, 48–9
  separation 374–9
pH measurement and control 605–6, 612
Phosphating 438, 440
Phosphoric acid fuel cells 592–3
Photoelectrolysis of water 259
Photographic silver recovery 336, 346, 347
Pilot plant
  cells 168–71
  organic electrosynthesis 311–29
Pinacolizations 315
Pipeline corrosion 530, 534
Pit growth 515–16
Pitting of metals 507, 511, 514–16
Planté lead/acid cells 565–6
Plate-and-frame cells 146–55, 168, 170–1
  chloralkali 196–203
  metal removal 342–4
Plate-in-tank cells 145–6
  for metal removal 337–8, 342
Plate loading 559
Plating 386–424
  see also Electroplating

Plug flow reactor 97, 99–100, 103–4
  batch recycle 103
  cascade 104
  single pass 99–100
pO_2 measurement 619–22
Pocket plate Ni/Cd batteries 567–8
Polarization
  batteries 546–7
  fluorine cells 244–55
Polarization resistance 539–41
Polarography 596–601
Pollution control 331–84
Polycrystalline growth 399
Polymer electrodes in batteries 576
Polynuclear aromatics, oxidation 320–1
Porous electrodes 160–3
  as coulometric detectors 628, 631
  for metal ion removal 337–44
Portable
  analytical devices 609–18
  reference electrode probes 531
Potassium
  dichromate production 278–9
  hydroxide production 208–9
  ion selective electrode 608
  permanganate production 275–8
  stannate production 291–2
Potential 195
  distribution 120, 122, 126–33, 139–40, 195
  field at the interface 17
  field strength 24
  -pH diagrams 493–8
  range for electrodes 633
  series of metals 489–93
Potentiometry 603–9
  see also Ion selective electrodes
Pourbaix diagrams 493–8
Power density 550
Power station monitoring 610–11
Power supplies 136–7
PPG electrolysers 193–4
Precious metal
  extraction 238–44
  removal from process streams 334, 346–7, 351–3
Pressure 94, 145
Primary batteries 550, 554–5, 578–9
Process
  control 139
  optimization 67–70
Primary current distribution 122–5
Printed circuit board
  etching 496–77
  manufacture 412, 414
Printing industry, electroforming applications 456
Product quality and form 90, 335
Properties of plated meals 411, 413
Protective coatings 536
PTFE-carbon chip electrodes 280–1
Pulse polarography 597–600
Pulsed
  magnetic fields 229–30
  plating 400, 422
Pump cell 158–60
Pure-Tec System 369–70
Pyramidal growth of electrodeposits 397

Rack mounting for electroplating 416, 419
Radiation of heat 135
Rate constant 10
  standard rate constant 13
Rate of
  corrosion 509
  discharge in batteries 550
  electron transfer 4, 9–18
  electroplating 388–9
Reaction engineering parameters 142
Reaction orders for H_2 evolution 43
Reactor
  design, practical consideration 89–91
  geometry 80–1
  modelling 63, 97–108
  performance 70–91
  types 95–102
  volume 82–3
Rebar corrosion 532–3
Recovery of metals 333–53
Recowin cell 337, 340
Rectifiers 136–7
Recycle loop, on a
  reactor/tank system 102–3
  single pass reactor 102
Recycling of process streams 331–84
  redox reagents 327
Reel to reel electroplating 416, 423
Reference electrode probe for corrosion surveys 531
Refining of metals 231–44
Regeneration of
  chromium (VI) solutions 365–70
  etchants 469–77

Reilly Tar & Chemical Corp, cell 297, 324, 325, 326
Reinforcing bar corrosion in concrete 532–3
Reliability of
  batteries 551
  reactors 89–90
Removal of
  chromate 364–73
  halogenated organics 383–4
  metal ions 333–53
Resistance of cells 5, 75–9
Resistivity probes 539
Retec cell 337, 338, 341–2
Reticulated electrodes 93, 337–8
Reversible
  cell potential 4
  electron transfer 32
Reynolds number 26
Rhodium electroplating 413
Ridge growth of electrodeposits 397
Rotating
  cylinder electrode 112, 241, 243, 340, 346–50, 376–9
  disc electrode 21–3, 112, 628–30
  electrodes 112
  particle barrel cell 350
Rough electrodeposits 245–7, 396–9, 403–4
Roughness of electrodes and current distribution 126, 128

Sacrificial anodes 523–7
Safety 90–1
Salt splitting 360
Sanilec cells 356, 357
Scale of electrochemical engineering 62
Scaleup and scaledown 62, 166–9
Scanning electron micrographs 396, 398
Schmidt number 28
Screw dislocations 395–7
Seawater
  batteries 547
  electrolysis 355–6
Secondary batteries 550
Secondary current distribution 124–6
Segmented electrodes 30, 119
Segregation of flow 29
Selectivity
  coefficient for ion selective electrodes 604–5
  in polarography 597
  in reactors 74
Self-driving cells 64
Semi-batch operation 104
Semiconductor
  contacts 415–21
  etching 477–9
Sensitivity
  anodic stripping voltammetry 601
  ion selective electrodes 603
  polarography 598
Sensors 596–637
Separators 139–41
  chlor-alkali 179–83
  voltage drop 77–8
Sewage treatment 332
Shelf life of batteries 551
Shell and tube type reactor 163–4, 339, 350–1
Sherwood number 27
Ships' hulls and corrosion 525, 529, 534
Signal to noise ratio in HPLC detector cells 632–3
Silver
  electroplating 406, 411, 413
  electrorefining 238–42
  ion removal 336, 345, 346, 347
  ion selective electrode 607, 608
Silver chloride reference probe 531, 607
Silver oxide/zinc battery 582
Silver sulphide formation 336
Simple batch reactor 96–9, 105–8
Single pass reactor 99–102
Sintered plate Ni/Cd batteries 568–70
Slurry electrodes 165
Sodium
  amalgam decomposition 173, 184–5
  bromate production 272–4
  chlorate production 269–72, 273
  extraction 218–19
  hydroxide production 173–208
  perborate production 274–5
  perchlorate production 274–5
  periodate production 274–5
  persulphate production 274–5
Sodium ion
  monitor 611
  selective electrode 608
Sodium/sulphur batteries 584–6
Solid electrolyte
  fuel cells 594
  ozone production cell 284–6
  water electrolyser 266–9

Solid state membrane electrodes 604, 607
Solution flow 24–7
Solvent properties 51–4
Space time 83
Space time yield 86–8
Space velocity 83–6
Specific energy consumption 75
  copper electrorefining 237
Spouting bed electrode 165
Square wave polarography 597
Standard
  potential 4, 491
  rate constant 13
Standby power supplies 553, 560, 566
Starter sheets 222
Static disc electrode 628–33
Static electrode reactors 144–57
Steam-water circuit monitoring 610
Steetley Engineering DEM cells (now acquired by Electrocatalytic Inc.) 150–1, 381–2
Stefan-Boltzmann law 135
Step growth 396–7
Stimulus-response flow characterization 120, 121
Storage density of batteries 549
Stray current corrosion 527, 534
Stress corrosion cracking 517
Stress relief in electrodeposits 404
Structure modifiers
  batteries 559, 560
  electroplating baths 404
Stuart cell 260–1
Sugar electrochemistry 318
Sulphate reducing bacteria 487–8
Sulphide ion selective electrode 607–8
Sulphur dioxide
  ion selective electrode 614
  removal from flue gases 379–82
Surface diffusion 394–5
Surface pretreatment prior to
  anodizing 437
  electroplating 416
  painting 439–41
Swiss-roll cell 162–3

Tafel
  equation 12
  plots 12–13, 31–2, 57, 393
    see also I–E curves
  slopes for H_2 evolution 43
  slopes in corrosion 501–4
Tank cells 145–6, 337–8, 342
Temperature 94–5
Tertiary current distribution 126–8
Thallium ion analysis 601
Thermodynamics
  of cells 4–5
  of chlor-alkali cells 175–6
  of corrosion 489–98
  of electron transfer 8–9
Thermoneutral cell voltage 79
Thin layer HPLC detector 628–31
Three-dimensional electrodes
  configurations regarding current flow 127, 129
  current and potential distribution 126–33
  for metal recovery 342–4
Throwing power 391–3
Tin
  corrosion (Pourbaix diagram) 497
  electroplating 407, 411, 413
  electrorefining 232
  ion analysis 601
Tissue (oxygen) sensors 620, 622
Titanium hydride formation 517
Tolerance of battery to service conditions 551
Tool design for ECM 464–5
Traction batteries 552, 563–4
Transcutaneous tissue oxygen monitors 620, 622
Transfer coefficient 10
Transition state theory 16
Transpassivity 506, 507
Transport number of ion 53
Trickle flow, packed bed cell 280–1
Trickle tower reactor 138, 140
Tritiated water 257
Tritium production 257, 258
Tubular detector cell 628–30
Tubular plates (lead/acid battery) 564
Turbulence 26–7
  promotion 82, 344–6
Two-dimensional electrodes 143–60
Types of
  cell 4–5, 64, 143–5
  corrosion 509–18

Uniform corrosion 511
Union Carbide (UCAR) fluorine cell 250–3

Urease electrode 624
US Bureau of Mines
  COPS cell for Cr (VI) 368
  modified Zadra cell 227
US Department of Energy Battery
    Programme 588–9

Vat plating 416
Velocity gradients 25
Vitreous carton electrodes 92–3, 283,
    337–8, 633
Volcano plot 40
Voltage components 5, 54–5, 75–9,
    546–8, 175–7, 195, 201, 205, 237,
    255
  see also Cell voltage (actual)
      components
Voltammetric techniques in analysis
    596–602
Volumetric energy consumption 75
'Volumetric' mass transport coefficients
    82–3

Wagner number 124
Wall-jet detector cell 628–31
Water
  analysis 596–612
  electrolysis 4, 256–69
  purification 331–84
Wetting agents 404
Wilson Process Systems cells 340, 347,
    352–3
Wire mounting for electroplating 416
Wohlwill cells 242–4
Workpiece
  electrochemical machining 461
  electroplating 416

Zadra cell 227–8
Zero-gap cells 143–4
  in chlor-alkali 177
Zero resistance ammetry 541
Zinc-air batteries 583
Zinc-carbon batteries 544, 545, 571–3
Zinc
  corrosion in acid 502, 503
  electroplating 407
  extraction 220
  halogen batteries 587–9
  ion analysis 601
  ion removal 344–5